NASA Conference Publication 3153

Types and Characteristics of Data for Geomagnetic Field Modeling

Proceedings of a symposium
held in Vienna, Austria
August 23, 1991

NASA

NASA Conference Publication 3153

Types and Characteristics of Data for Geomagnetic Field Modeling

Edited by
R. A. Langel
NASA Goddard Space Flight Center
Greenbelt, Maryland

R. T. Baldwin
Hughes STX Corporation
Lanham, Maryland

Proceedings of a symposium
held in Vienna, Austria
August 23, 1991

NASA
National Aeronautics and
Space Administration
Office of Management
Scientific and Technical
Information Program
1992

CONTENTS

INTRODUCTION

R.A. Langel
Geodynamics Branch
Goddard Space Flight Center
Greenbelt Md. 20771

A symposium entitled "Types and Characteristics of Data for Geomagnetic Field Modeling" was convened on Friday August 23 at the General Assembly of the International Union of Geodesy and Geophysics (IUGG) held in Vienna, Austria. The announced scope of the symposium was as follows: "Models of the geomagnetic field are only as good as the data upon which they are based and depend upon correct understanding of data characteristics such as accuracy, correlations, systematic errors and general statistical properties. This symposium is intended to expose and illumnate these data characteristics. Papers are invited which discuss the properties and availability of the various kinds of data."

Table 1 shows the final schedule of invited and contributed papers. Of these, the papers by McKnight and Herzog were withdrawn. In their place, the following papers were given: "Helsinki Magnetic-Meteorological Observatory Revisited - Numerical Magnetic Data Available from 1844 to 1908", presented by H. Navanlinna, and "Magnetic and Electromagnetic Induction Effects in the Annual Means of Geomagnetic Elements", presented by C. Demetrescu.

The talks presented, while not dealing with topics generally appearing in scientific journals, are yet of great interest to much of the geomagnetic community. It was, therefore, decided to collect the papers into a special report to be issued by the Goddard Space Flight Center. As a comparison of Table 1 with the Table of Contents of this volume will show, unfortunately not all speakers were able to submit written versions of their presentations for publication. On the other hand, in order to

make the resulting collection more complete, I invited those speakers who had to withdraw papers from the symposium to submit written versions of what they would have said and I also invited additional contributions which serve to complement the original papers. I would especially like to thank C. Williams, J. Verhoef, R. Mcnab, G.. Sharman and D. Metzger for agreeing to contribute. I would also like to thank W. Webers for his contribution. I am grateful for the support of NASA Headquarters RTOP 579-31-02 which made this work possible.

TABLE 1: Scheduled Papers for Symposium GAM 5.3.

Session 1: Chairman: C. Barton; 1100 - 1230

INTRODUCTION	R.A. Langel	1100
GAM 5.3-1 (Invited)	A. Jackson HISTORICAL DATA FOR GEOMAGNETIC FIELD MODELLING	1105
GAM 5.3-2 (Invited)	D.R. Barraclough SURVEY DATA FOR GEOMAGNETIC FIELD MODELLING	1130
GAM 5.3-3 (Invited)	R. Langel SATELLITE DATA FOR GEOMAGNETIC FIELD MODELING	1155
GAM 5.3-4	Panel: SPECIAL NEEDS FOR EARLY DATA	1120

LUNCH: 1230 - 1400

Session 2: Chairman: R. Langel; 1400 - 1530

GAM 5.3-5 (Invited)	S.C. Cande GEOMAGNETIC FIELD MEASUREMENTS AT SEA	1400
GAM 5.3-6	R.J. Coleman PROJECT MAGNET HIGH-LEVEL VECTOR SURVEY DATA REDUCTION	1430
GAM 5.3-7 (Invited)	P. Hood USE OF AEROMAGNETIC DATA IN GEOMAGNETIC FIELD MODELLING	1445
GAM 5.3-8	J.D. McKnight A SPHERICAL CAP HARMONIC MODEL OF THE NEW ZEALAND REGIONAL GEOMAGNETIC FIELD BASED ON VECTOR AND SCALAR DATA	1515

BREAK: 1530 - 1600

Session 3: Chairman: M. Sugiura; 1600 - 1730

GAM 5.3-9 (Invited)	C.E. Barton MAGNETIC REPEAT STATION DATA	1600
GAM 5.3-10	D.C. Herzog OBTAINING GEOMAGNETIC DATA FOR THE U.S. MAGNETIC OBSERVATORY SYSTEM	1625
GAM 5.3-11 (Invited)	J.-L. LeMouel OBSERVATORY DATA	1640
GAM 5.3-12	Panel: OUTSTANDING DATA PROBLEMS FROM THE VIEWPOINT OF THE MODELLER	1705

HISTORICAL DATA FOR GEOMAGNETIC FIELD MODELLING

Andrew Jackson
Department of Earth Sciences
Oxford University
Parks Road
Oxford, U.K.

Abstract

This paper describes the various types of historical data (by which we mean actual measurements of the field taken in the past) which are available for geomagnetic field modelling, concentrating exclusively on observations made prior to the 20^{th} century. These data take quite diverse forms, being derived from voyages of discovery or scientific expeditions, from surveys on land, or from observatories after the formation of the Göttingen Magnetic Union. Towards the latter part of the 19^{th} century declination was measured quite regularly by various Naval vessels for the purpose of constructing charts. Prior to the invention of a method for measuring field intensities by Gauss in 1832, all measurements were of declination or inclination. During the 19^{th} century over 40,000 observations are available, with over 2,000 observations being available in one year (the first International Polar Year 1882–83). Prior to 1800 there are only of the order of 12,000 measurements. We discuss measurement methods and the types of instruments used, as well as focussing on specific problems which have been noted, such as those associated with measurement of intensity on iron ships in the late 19^{th} century.

1 Introduction

The last twenty five years have seen renewed interest in studies of the secular variation of the magnetic field by using historical magnetic observations. Partly as a result of the increasing availability of modern computers, most of the available data collected since 1900 were put into machine-readable form by the U.S. Coast & Geodetic Survey for the 1965 world charts (e.g. Hendricks & Cain, 1963); discussion of these data can be found elsewhere in this volume. More recently, data collected prior to the 20^{th} century have been the subject of renewed attention in an effort spearheaded by Prof. David Gubbins (now at Leeds University), and this paper summarises the data which are now available in machine-readable form for geomagnetic analyses. I am endebted to David Barraclough, Jeremy Bloxham, David Gubbins and Ken Hutcheson for access to data that they have collected and for help in the preparation of this report.

2 Historical Perspective

This section gives a very brief overview of the development of geomagnetism, and does not purport to be comprehensive. Fuller treatments of the history can be found in various places; for example, relevant chapters of Merrill & McElhinny (1983) or Chapman & Bartels (1940), or Malin (1987). A detailed account of geomagnetism up to 1500 can be found in Crichton Mitchell (1932, 1937, 1939); recent articles on 19th century geomagnetism are those of Good (1985, 1988). Excellent discussions of geomagnetic instruments can be found in McConnell (1980) and Multhauf & Good (1987).

It is generally acknowledged that the Chinese were the first to discover the directive property of lodestone, almost certainly by the first century AD. Its development as a primitive navigational device was slow, though the declination had almost certainly been discovered by the 9th century and compasses were certainly in use by the 11th century; early observations of declination are given by Needham (1962) and Smith & Needham (1967). The first recorded observation of declination in Europe was by George Hartmann in 1510; inclination was discovered by Robert Norman in 1576. The fact that the field underwent slow changes with time (the secular variation) was not discovered until 1635: by comparing a series of records taken at London previously, Henry Gellibrand showed that secular variation was a real effect. Relative intensities of the field were made at the end of the 18th century by La Perouse, D'Entrecasteaux and Humboldt, by comparing the periods of oscillation of a magnetic needle at different places. Measurements of the absolute intensity of the field were not made until a method was devised by Gauss in 1832 (see e.g. Malin, 1982).

Whilst early observations of the field are extremely valuable, some problems do exist. For example before the discovery of SV, some observations are undated as the need to record the date was not apparent. The accuracy with which an observer's position was known is also a source of error. Although the measurement of latitude was precise even by late 15th century (for example, an accuracy of 10 minutes of arc was claimed by 1484 (John II's commission, 1509)), the measurement of longitude at sea remained a problem until approximately 1770 with the introduction of accurate chronometers by Harrison. The result of this poor knowledge of longitude lead to the practice of "running down the parallel", or sailing to the correct line of latitude before sailing due east or west along that parallel to the desired location. Although this practice meant that the ship's company often arrived at their desired destination, it does mean that large navigation errors could occur in the quoted positions of magnetic observations. For example, Bloxham (1986) found accumulated errors of up to 8° 45′ of longitude on the legs of Cunningham's voyage to China in 1700. To a certain extent these errors can be aleviated to a large extent by examination of the original ship's log and plotting the positions on a modern chart. This painful task has been performed for 16th, 17th and 18th century data by Bloxham (1985, 1986), Hutcheson (1990) (see also Hutcheson & Gubbins, 1990) and Barraclough (1985 and personal communication).

The Greenwich meridian was adopted as an international longitude standard only in 1884, and some national conventions remained in use later than that date. Consequently care must be taken as to which of the particular national conventions of Paris, the observatory at Pulkova (Leningrad), Washington or San Fernando was being used. One example of French marine data measuring longitude from Paris until at least 1895 has been given by Jackson (1989); this difference of 2° 13′ of longitude between Paris and Greenwich is difficult to detect. For intensity data, the conversion 1 B.U. = 4610.8 nT has been used to convert intensity measurements from British (or English) units to nanoTeslas (Barraclough, 1978).

3 Catalogues of Data

Many historical geomagnetic observations have been the subject of catalogues and compilations which vary in their completeness and usefulness; a discussion of compilations can be found in Barraclough (1982), Malin & Gubbins (1983) and Bloxham (1985). Unfortunately, some catalogues do not present original observations but only values averaged within a time-space window. Therefore, although catalogues such as that of Veinberg & Shibaev (1969) have been the subject of several analyses of the historical field, as has been stressed previously (e.g. Barraclough, 1982) these catalogues represent a severe degradation of the original measurements, which should be used in preference. A similar set of tables for fixed times and positions was published by Mountaine & Dodson (1757), whose tables were claimed to be based on 50 000 observations from 1700–1756. The original observations from Naval and merchant shipping were unpublished and their origin is presently unknown, representing a great loss to the geomagnetic community. One of the most useful catalogues of early observations is that of Bemmelen (1899), who gives original observations made between 1492 and 1741, some of which were extracted from manuscripts kept in British, Dutch and French maritime archives. Similar excellent catalogues which must be mentioned are those of Sabine (1868, 1872, 1875, 1877), containing over 10 000 measurements of declination, inclination and intensity made during the 19^{th} century, and those of Veinberg (1929–1933) which contain extensive original observations from the Soviet Union and adjacent countries. Data after approximately 1860 have not been the subject of a catalogue or compilation; a discussion of sources of data for this period can be found in Jackson (1989) and Bloxham, Gubbins & Jackson (1989).

4 Original Data

As a guide to the types and number of data available, we now give a brief indication of the sources and distribution of data from 1500 to 1900; for the purposes of discussion these are split into century time-windows. More comprehensive discussions of the data can be found in Bloxham (1986), Jackson (1989) and Hutcheson (1990).

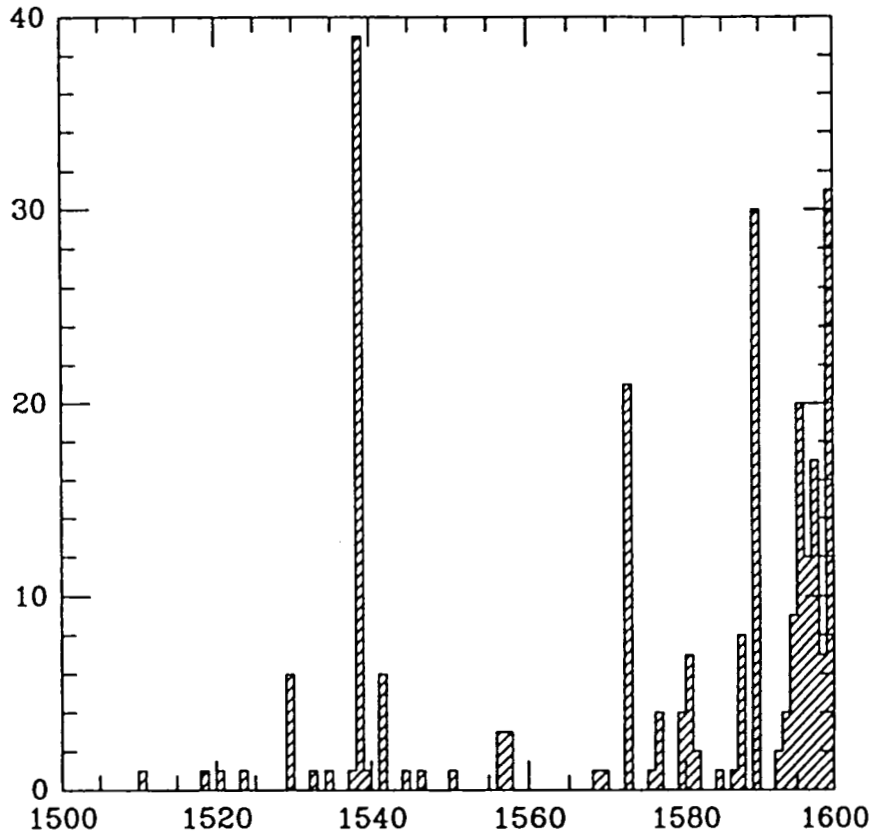

Figure 1: Temporal distribution of data for the period 1500–99.

4.1 The Period 1500–1599

The primary source of data for this period is the catalogue of Bemmelen (1899). Most of the data is taken from voyages of discovery, such as those of de Castro, Vicente Rodrigues, Frobisher, Edward Wright, Barents, Stevin, Wilkens and Drake. There are only 2 inclinations and 249 declinations. Figures (1) and (2) show the temporal and spatial distribution of the data.

4.2 The Period 1600–1699

Much of the data for this period can again be found in Bemmelen (1899) or the references therein. Most data is again taken from voyages of discovery, such as those of Hudson, Raleigh, Baffin and Tasman. The surveys of the Atlantic by Halley in the years 1698–1700 are an important source of data. Halley's measurements thought to have measurement error of 0.5° (Barraclough, 1985). The instrumental accuracy for declination measurements during most of this century was estimated as just over 1° from two compasses

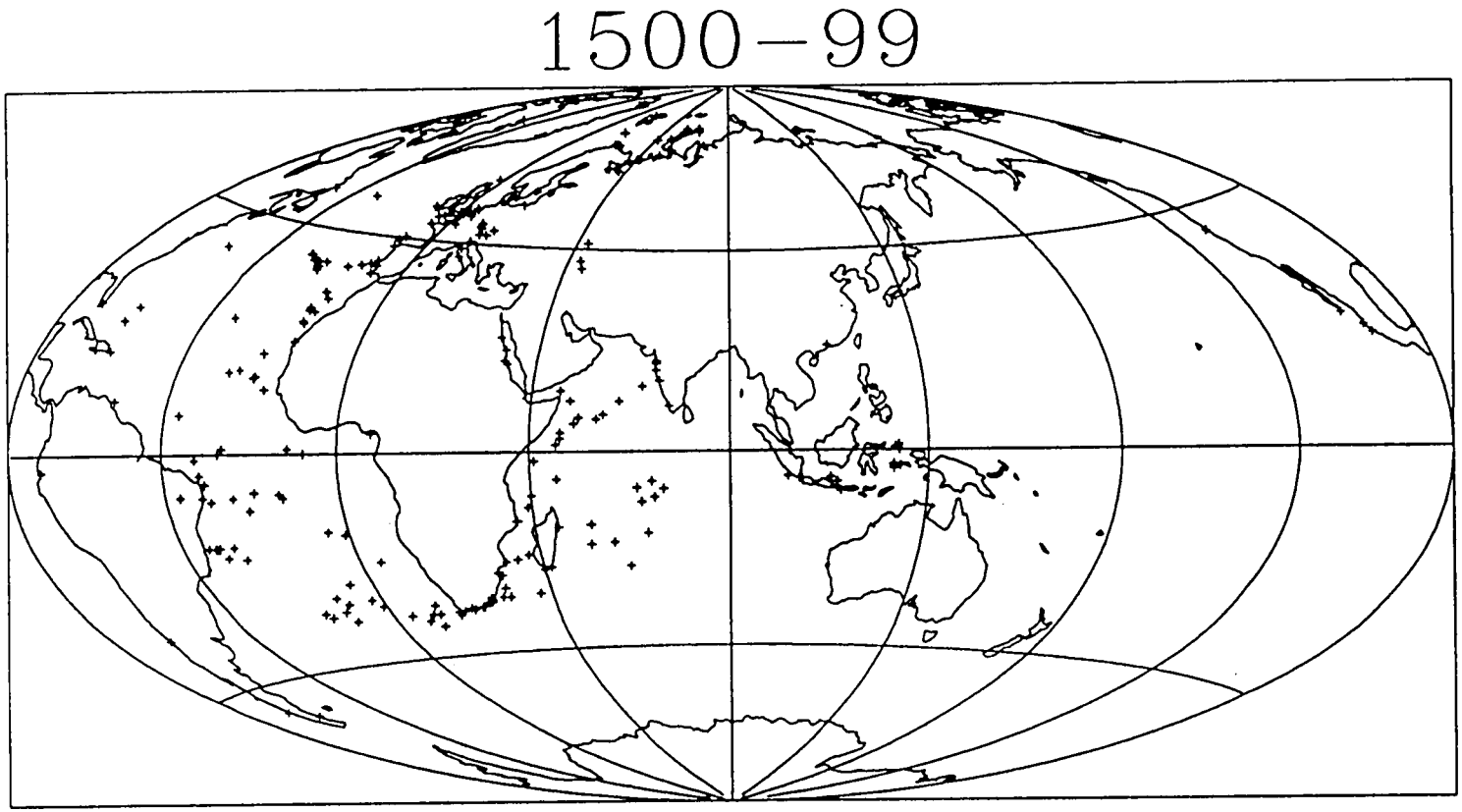

Figure 2: Spatial distribution of data for the period 1500–99. The projection is Aitoff equal area.

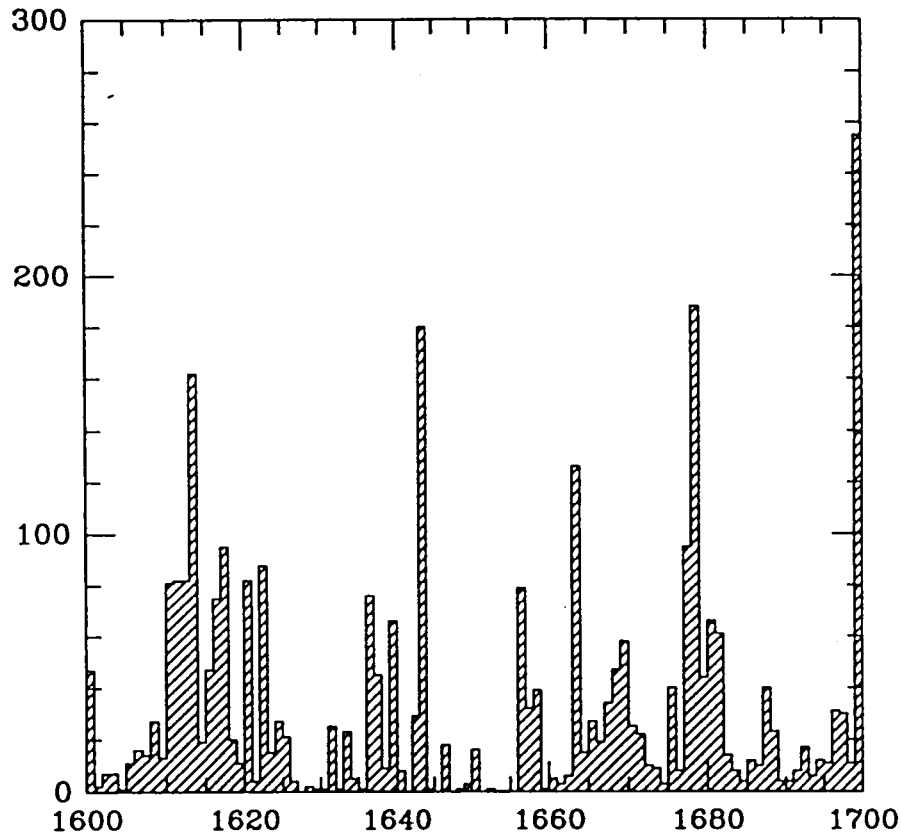

Figure 3: Temporal distribution of data for the period 1600–99.

carried by Jaques L'Hermite on a voyage in 1623 (Hutcheson, 1990). In this period there are 37 inclinations and 3 097 measurements of declination. Figures (3) and (4) show the temporal and spatial distribution of the data. In Figure (4) an example of the practice of "running down the parallel" can be seen in the Pacific.

4.3 The Period 1700–1799

For this period some of the most famous voyages of discovery which contribute data include those of Bering during the years 1725–30, Bligh in 1788, and the three expeditions of Cook during the years 1768–71, 1772–75 and 1776–80 measuring both declination and inclination. Care has again be afforded to correcting longitudes wherever possible, although post-1770 data have accurate longitudes because of the ability for accurate timekeeping after the introduction of the marine chronometer. Some relative intensity measurements were made towards end of the century (see §2). During this period there were 1 633

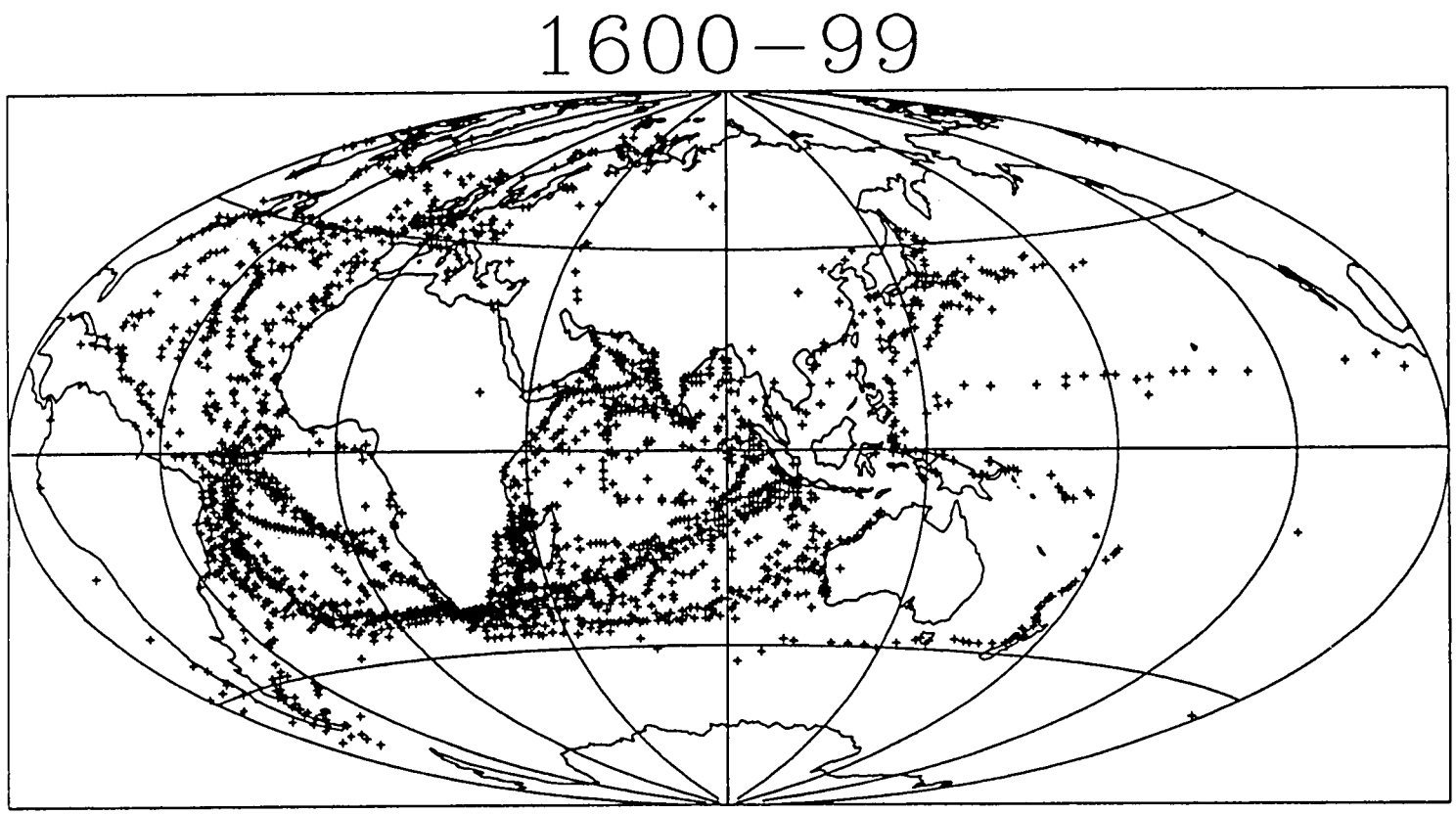

Figure 4: Spatial distribution of data for the period 1600–99.

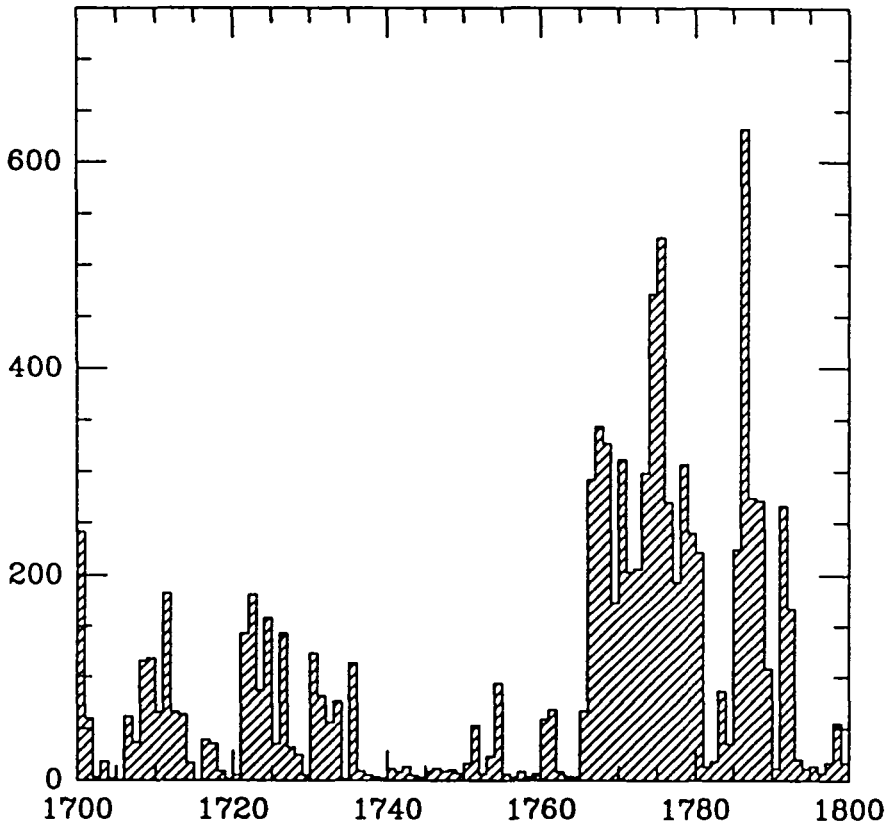

Figure 5: Temporal distribution of data for the period 1700–99.

measurements of inclination and 7 938 of declination. Figures (5) and (6) show the data distributions.

4.4 The Period 1800–1899

Many data (over 17 500) were catalogued by Sir Edward Sabine for the early part of this century; this represents a fine collection. As we mentioned before, no catalogue of data exists for the latter half of the century. During this period was the invention of a method for the absolute determination of intensities in 1832 by Gauss (1833). It was also due to Gauss's efforts that the Göttingen Magnetic Union was founded and permanent observatories were establishment in 1841. Colonial observatories were being established by the British government at the same time.

As a result of Gauss's invention, the measurement of intensities on land and at sea became commonplace. Typically horizontal intensity was measured on land with a unifilar magnetometer, whilst total intensity was often measured on ships using Fox's apparatus, a device also capable of measuring incli-

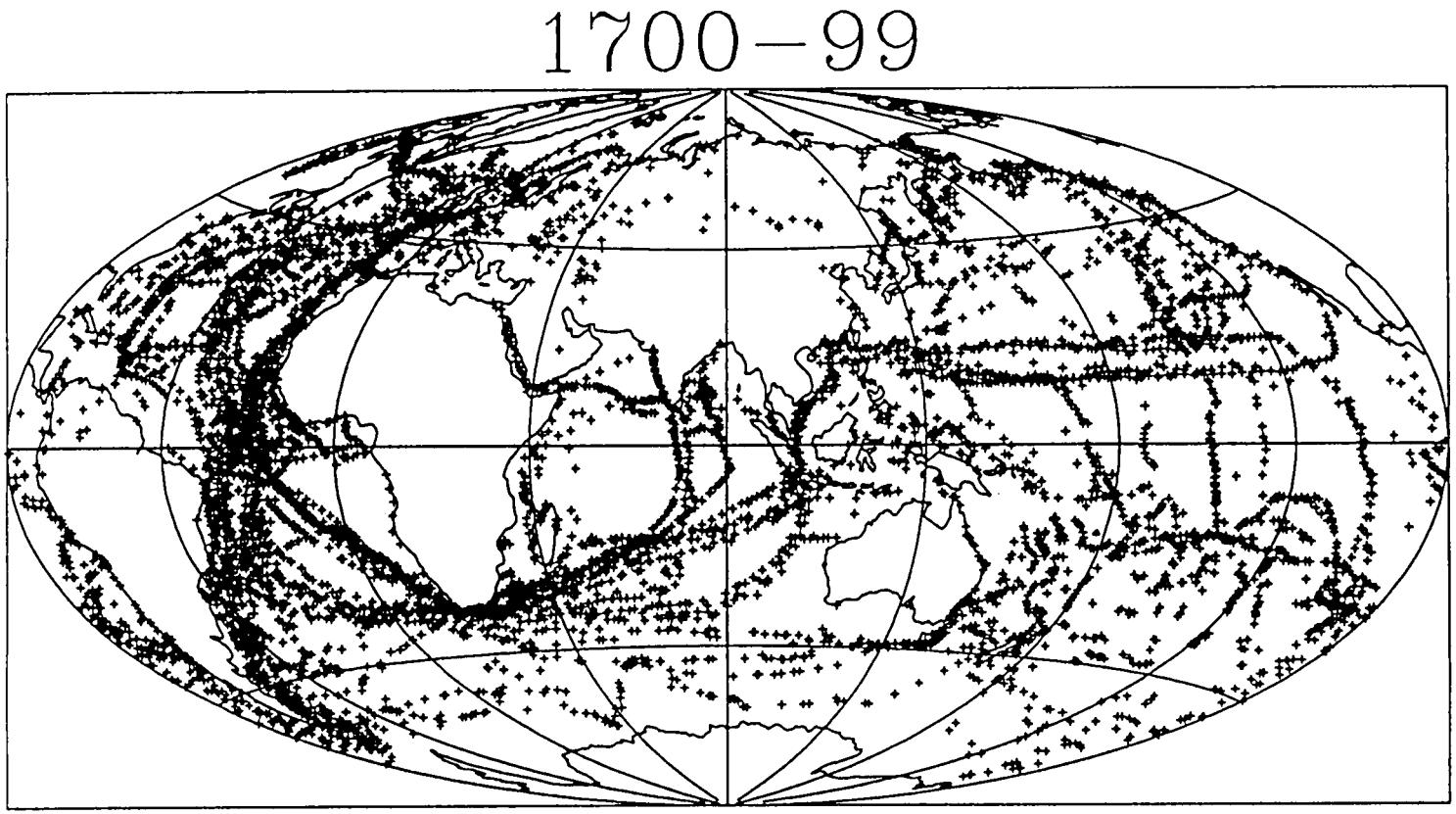

Figure 6: Spatial distribution of data for the period 1700–99.

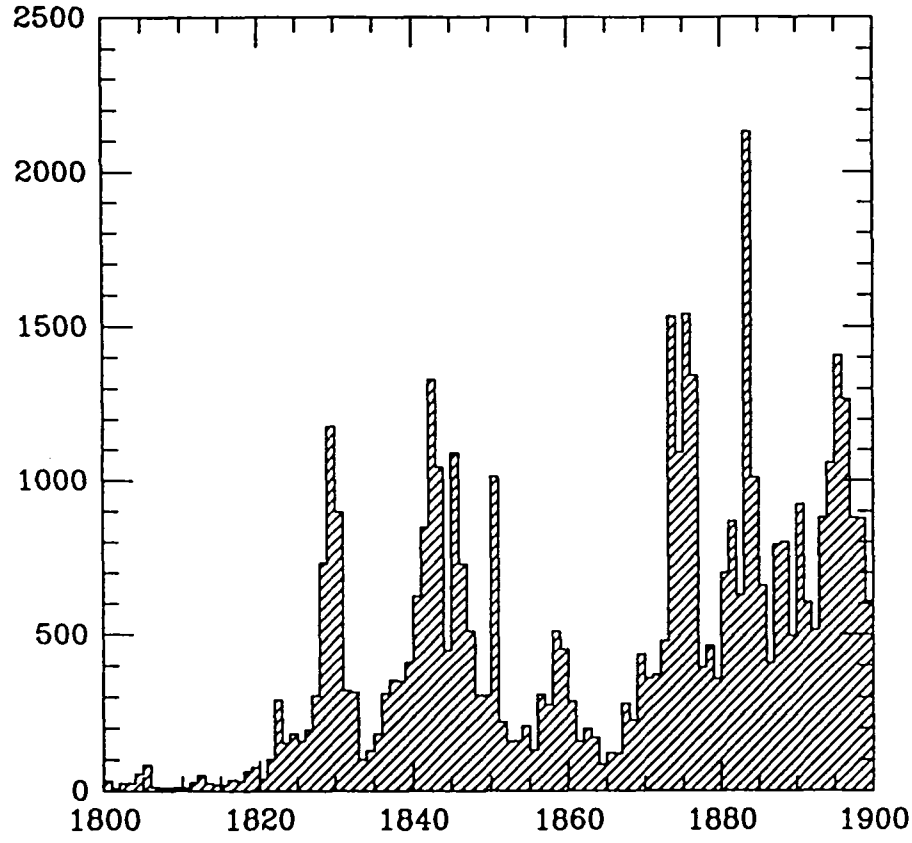

Figure 7: Temporal distribution of data for the period 1800–99.

nation (see McConnell, 1980). Thus the "Magnetic Survey of the South Polar Regions of the Globe", performed by Ross & Crozier in the ships *Erebus & Terror*, and Moore & Clerk in the *Pagoda* in the 1840's, included the measurement of inclination and intensity at sea. Similarly, in the latter part of the century the expeditions by *HMS Challenger* (in 1872-76), *SMS Gazelle* (in 1874-76) and the *Vanadis* (in 1883-85) were charged with the measurement of 3 components of the field. This century witnessed a massive surge in the number of surveys on land; some of the earliest were the surveys of N. America by John Franklin from roughly 1820 onwards. From the mid-19^{th} century onwards similar surveys were performed in Europe, USSR, Australia and Japan, some on a very fine scale. The temporal distribution of data is shown in Figure (7). Because of the size of dataset this century, the spatial data distribution has been divided into the two periods 1800–1849 and 1850–1899 (see Figures (8) and (9)).

The middle of the 19^{th} century saw increasing use of iron in ships, and great efforts were made to alleviate the effect on the compass (see §5). By the end of the century, charts of Declination were being

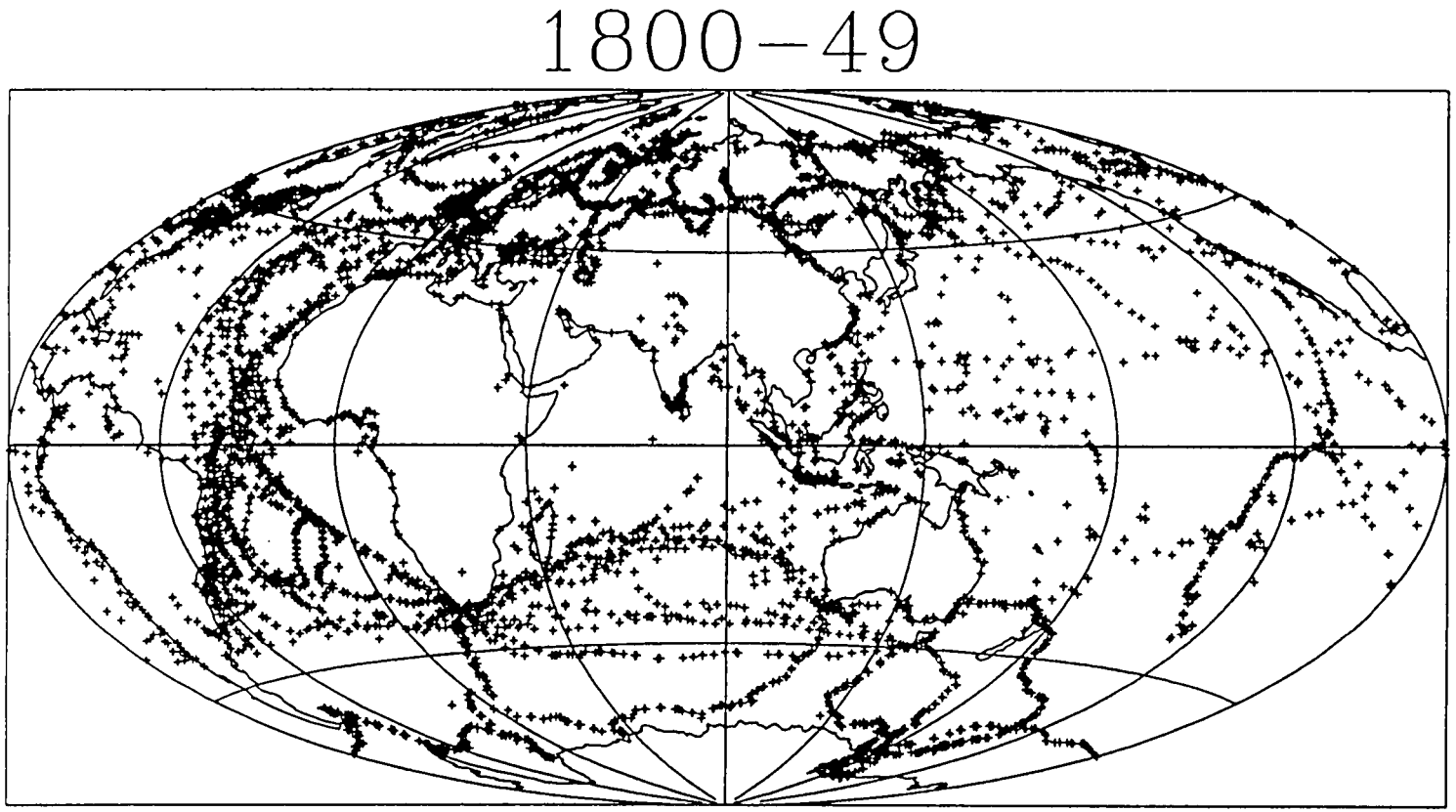

Figure 8: Spatial distribution of data for the period 1800–49.

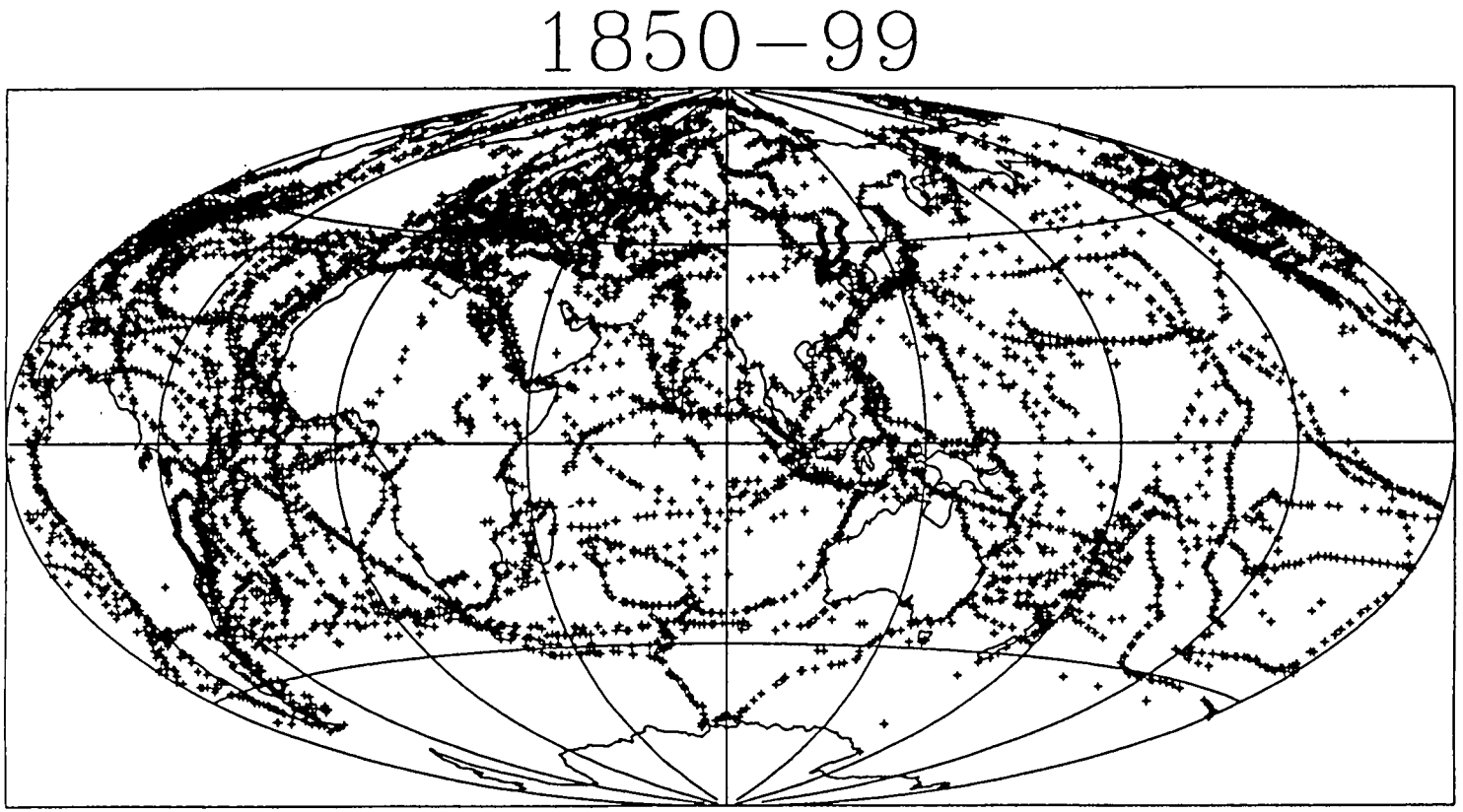

Figure 9: Spatial distribution of data for the period 1850–99.

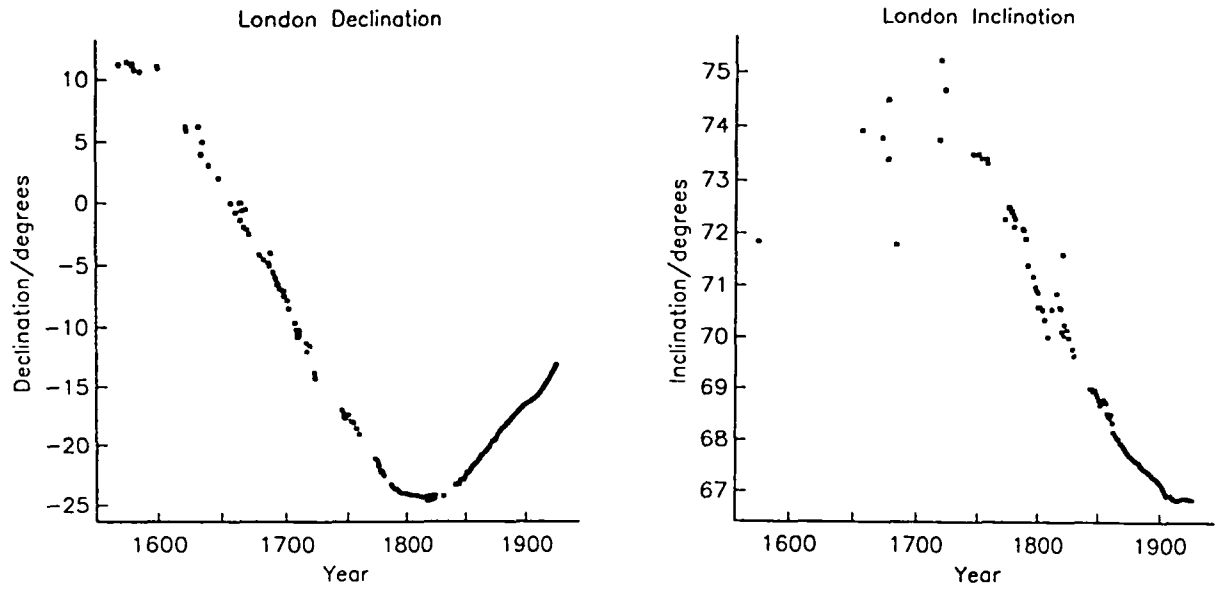

Figure 10: Observations of the magnetic field at London. (a) Declination. (b) Inclination.

routinely produced by various Naval authorities, such as those of the UK from 1858, Germany from 1880 and U.S.A. from 1882. The First International Polar Year was held during 1882–3 with 12 arctic stations and two southern stations augmenting the network of permanent observatories with observations throughout the year. The total data collected for this period comprises 5 588 horizontal intensities, 4 615 total intensities, 12 895 inclinations, 19 858 declinations and 2 538 observatory annual means.

4.5 Repeat Measurements

Long series of measurements are available at some specific sites. For example, Figure (10) shows the inclination and declination measured by various observers at London, firstly taken from Malin & Bullard (1981) and then from the values reported at the Greenwich observatory. The early observations of intensity show considerable scatter. Unfortunately, such time series are also often disrupted by changes of location. Indeed, the Greenwich observatory closed in 1925 and moved location to Abinger, which subsequently closed and moved to Hartland in 1957. These changes in location are an undesirable feature of many long time series. Similar long records exist at other places, such as Copenhagen, Paris and Rome (see e.g. Raulin, 1867).

5 Local disturbance of ships

Up to the middle of the 19th century the majority of ships were of wooden construction. Subsequently, iron became increasingly favoured in shipbuilding, and this change in material profoundly affected a great wealth of marine data within the time period of interest. Note that after the turn of the century most marine magnetic data were collected by non-magnetic ships such as the *Carnegie* and *Zarya*, or were taken from magnetometers towed behind the ship and away from its magnetic field; the problems associated with iron are therefore mostly confined to the particular time period which we are considering.

In 1801, Captain Flinders noted on his voyage to Australia that the compass direction was not always in the direction of the known declination at that place, and that the discrepancy depended on the direction of the ships bows. He found the effect to be opposite in southern latitudes to that in northern latitudes, and attributed it to the inductive effects of the vertical iron girders in the primarily wooden ships. The *deviations* (or differences between the measured declination and the true declination) were small, of the order of 2° to 3°, and his method of compensation, that of placing a vertical soft-iron bar close to the compass position, a so-called "Flinder's bar", was widely adopted. With the increased use of iron in the construction of ships in the mid-19th century for cladding, it was found that the deviation could be as large as 50°. In 1839 the Astronomer Royal, Airy, performed a series of experiments, and introduced a method of correcting the deviation using compensating magnets and bars. Two schools of thought developed on the subject of deviations: physical corrections, favoured by the merchant navy and advocated by Airy, and tabular corrections, promoted by Archibald Smith and favoured in the Royal Navy. In practice, when the deviations were large, the Royal Navy used a combination of physical and tabular corrections.

It was Poisson (1824) who first set forth the mathematical theory which related the magnetic field as measured locally on a ship to that of the Earth:

$$X_{\rm loc} = X' + aX' + bY' + cZ' + P \tag{1}$$

$$Y_{\rm loc} = Y' + dX' + eY' + fZ' + Q \tag{2}$$

$$Z_{\rm loc} = Z' + gX' + hY' + iZ' + R \tag{3}$$

or in modern matrix notation

$$\mathbf{B}_{\rm loc} = (\mathsf{I} + \chi)\mathbf{B}' + \mathbf{B}_{\rm perm} \tag{4}$$

Here $X_{\rm loc}$ etc. represent the components of the magnetic field as measured in a ship's local reference frame (with $X_{\rm loc}$ to head, $Y_{\rm loc}$ to starboard and $Z_{\rm loc}$ to keel for example). The primed symbols represent the Earth's field in the same directions, the matrix χ we shall call the susceptibility tensor with elements $\{a, b, \ldots i\}$, I is the identity matrix, and $\mathbf{B}_{\rm perm} = (P, Q, R)$ is the vector of permanent magnetic effects of the ship.

Equation (4) is a completely general formulation of the effects of induced and permanent magnetisation on the compass needle. In the 19th century mariners used the compass as an aid in navigation, using the charts of declination which were available, and thus they had to correct for the ship's magnetic effects by knowing the deviation. Our ability to solve (4) for the elements of χ and $\mathbf{B}_{\text{perm}}$ is limited by the fact that a ship has only one fully rotational degree of freedom around the vertical axis. By spinning the ship (a procedure termed "swinging") it is possible to measure deviation for many values of the ship's heading. We rewrite (4) in the form

$$\mathbf{B}_{\text{loc}} = (\mathsf{I} + \chi)\mathsf{T}\mathbf{B} + \mathbf{B}_{\text{perm}} \tag{5}$$

where $\mathbf{B}$ is the true field as measured in the Earth's coordinate system, and the rotation matrix T is of the form

$$\mathsf{T} = \begin{pmatrix} \cos\alpha & \sin\alpha & 0 \\ -\sin\alpha & \cos\alpha & 0 \\ 0 & 0 & 1 \end{pmatrix} \tag{6}$$

and α is the angle the ship is turned through, reckoned positive anticlockwise.

By considering (5) and (6) it can be seen that the elements c and f of (1) and (2) cannot be determined from deviations only, since "swinging" the ship does not change the local value of Z. Given this deficiency, the solution adopted at the time was that of Archibald Smith (published in Sabine, 1843, 1846, 1868) and further developed in the *Admiralty Manual on Deviations of the Compass* (Admiralty, 1863):

$$\delta \approx A + B\sin\xi + C\cos\xi + D\sin 2\xi + E\cos 2\xi \tag{7}$$

which is a good approximation for δ less than about 20°. Here δ is the deviation and ξ the compass course (the azimuth of the ship's head from the *disturbed* compass position), the coefficients A, D and E depending on non-linear combinations of the elements of χ, and B and C depending on elements of χ and also the dip and horizontal intensity. Thus by determining the values of A, B, C, D and E at a certain locality it was possible to correct for the deviation (by subtracting it from the measured declination) for all ship's headings. In fact, a frequent procedure was to measure the deviations for 16 compass points and to plot these graphically. Since (7) depends on the local values of H and I it was necessary to "swing" frequently, especially in the event of a large change in latitude. Correction for deviation for all ship's headings was performed at the Hydrographic Office by interpolation of the curves of deviation taken at adjacent spinning sites.

Experience showed that the elements of χ and $\mathbf{B}_{\text{perm}}$ were not in fact constant and regular re-determination of the so-called "sub-permanent" magnetism of a ship was necessary. For example, the ship *Royal Charter* lost 17° of deviation during its circumnavigation of the globe, an effect attributed to the battering of the new ship by rough seas (London Quarterly Review, 1865).

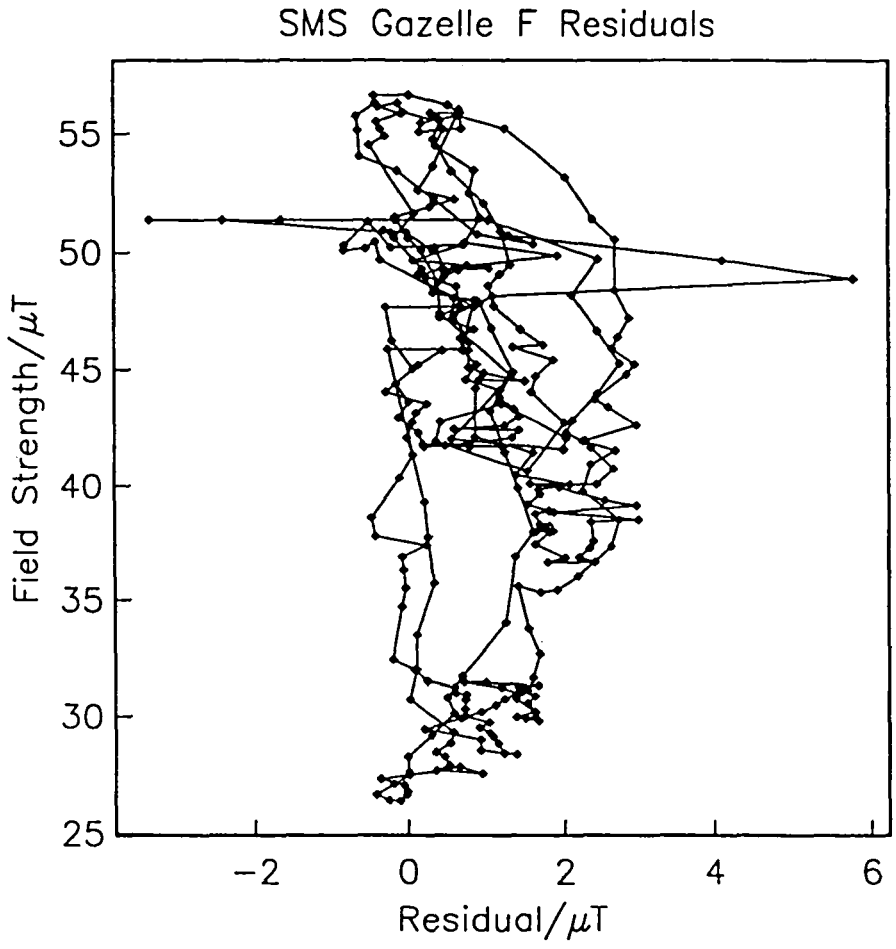

Figure 11: Residuals between data reduced to epoch 1882.5 and model predictions for total field (F) data from the *Gazelle*, plotted versus local field strength. Dots indicate individual residuals, consecutive residuals are joined by straight lines. The residuals argue against induced magnetisation, and suggest either permanent magnetisation or incorrect calibration.

5.1 Case studies: *SMS Gazelle* and the *Vanadis*

Here we give two examples of possible problems in 19th century data, caused by the influence of ship's magnetisation. The first is that of the ship *SMS Gazelle* which circumnavigated the globe in 1874–76. The *Gazelle* was a German *Man-O-War* whose mission was the observation of the transit of Venus on Kerguelen Island in 1874. Although the reported values of D and I appear satisfactory, we found *Gazelle* F data to be somewhat biased; Figure (11) shows the differences between total field data measured on board and predicted values from a field model based on contemporary data. The residuals are almost all positive, though they are uncorrelated with the local (calculated) field strength, which argues against induced magnetisation which would have caused the residuals to be roughly proportional to the local field strength. The correlation between consecutive values rather argues for semi-permanent magnetisation or incorrect calibration.

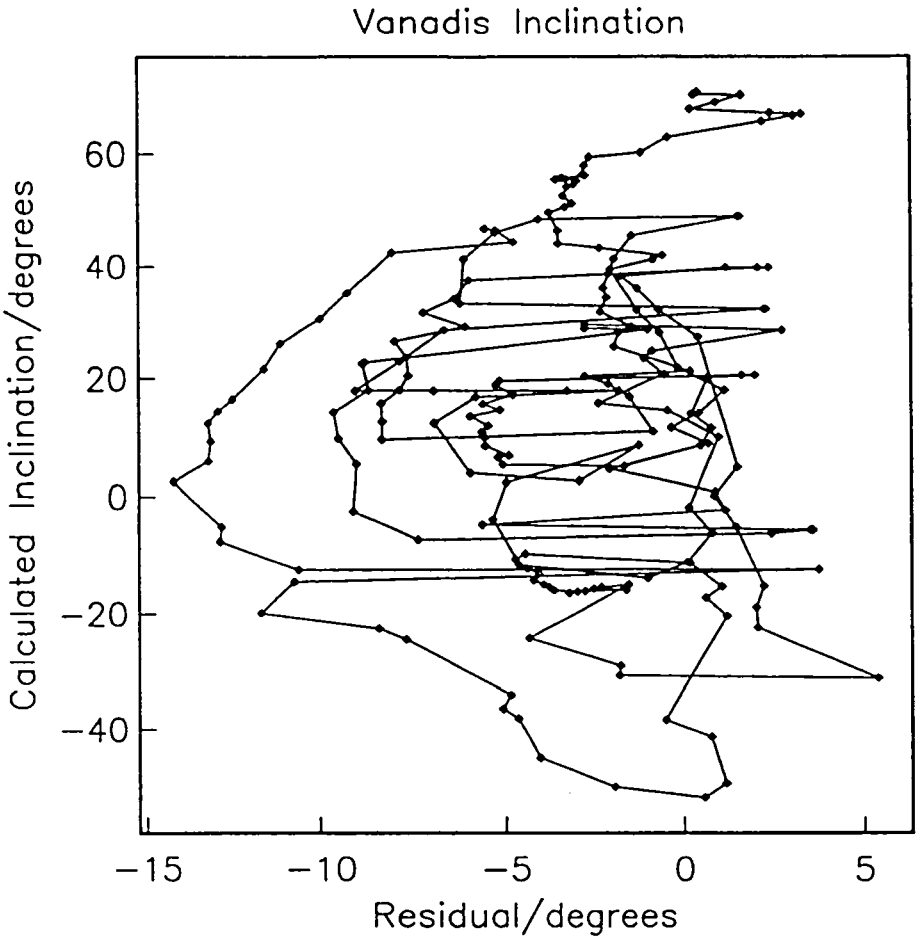

Figure 12: Residuals between *Vanadis* inclination observations and those predicted by a field model, plotted against local field strength. Dots indicate individual residuals, consecutive residuals are joined by straight lines. Note the preponderance of negative values.

A second example we give is that of the Swedish frigate *Vanadis*. These data were located by the late Dr. Folke Eleman (unpublished manuscript, 1987); the data had never been published and only manuscripts remain. The ship performed a circumnavigation during 1883–85, but the data are almost completely undocumented in the literature (although see *Nature*, volume 29, page 185 (1883)). All three components of field were measured on board, observations aimed at intensity determination being made in the form of oscillation and vibration experiments using Fox's circle. Unfortunately, the measurements appear to have been improperly reduced after the voyage. For example, Figure (12) shows the inclination residuals which are calculated with respect to a model of the field at that epoch. Note that the residuals are very large (much bigger than the errors the crustal field can produce, which are typically of the order of half a degree), and predominantly negative. Again, it would appear that improper corrections for the effect of the ship have been made (if any were made at all). Figure (13) shows the route taken by the ship.

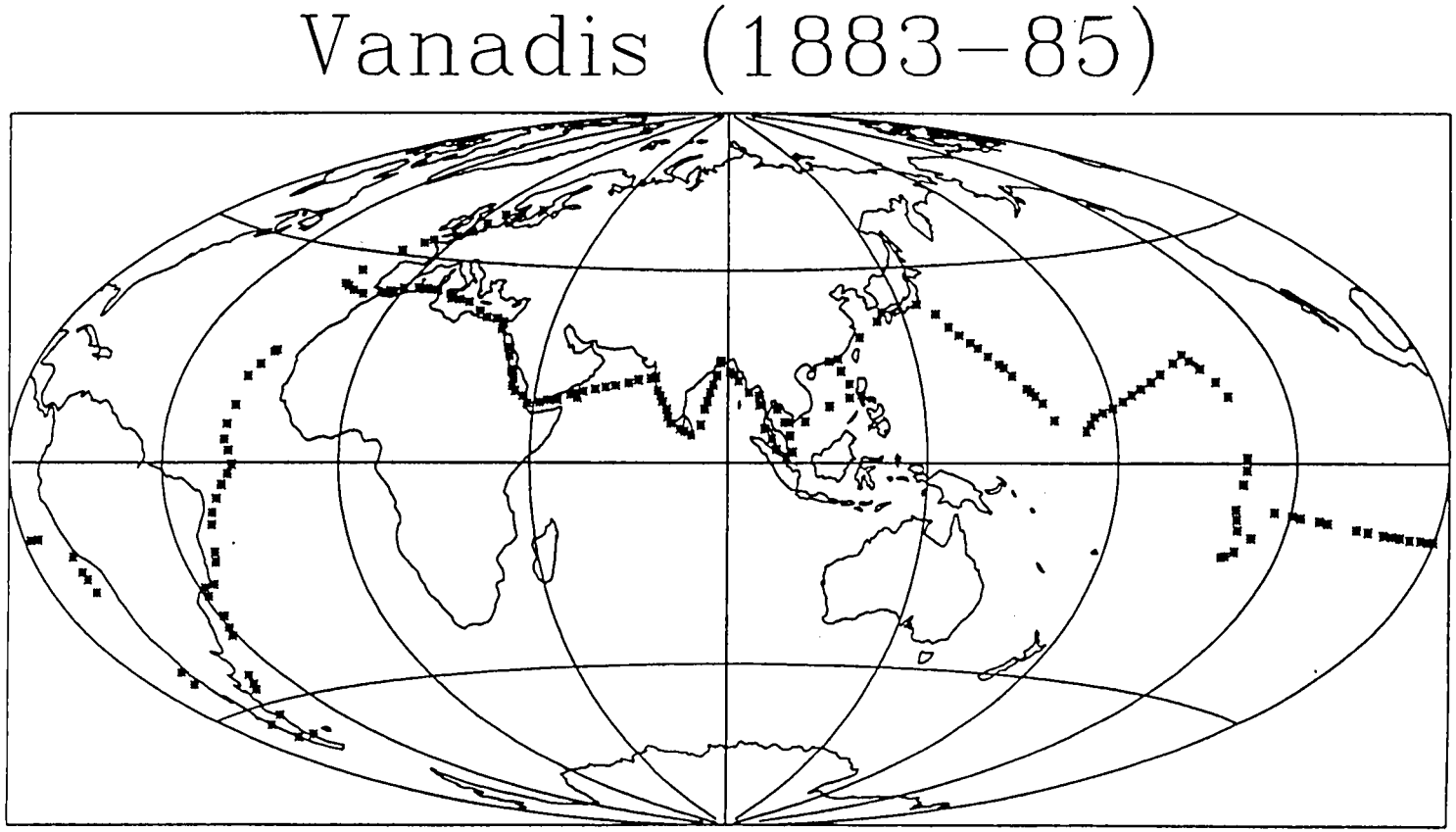

Figure 13: Route taken by the *Vanadis* in 1883–85.

1500 – 1599	251	data
1600 – 1699	3 135	data
1700 – 1799	9 571	data
1800 – 1899	42 956	survey data
1800 – 1899	2 538	observatory annual means
	58 451	total data

Table 1: Resumé of numbers of data in the pre-20th century database

6 Availability & Access

From beginning of 1992 the database described herein will be lodged at the World Data Centres. It will also be available by anonymous file transfer from two sites. Firstly, for those with Internet access, use anonymous ftp to `geophysics.harvard.edu`, specifying the username as `anonymous` and your e-mail address (*yourname@youraddress*) as the password. Data will be found in the directory `pub/geomag/data` (see the file README). For sites with access to the UK's JANET, the files can be transferred using *Network Independent File Transfer Protocol*, often called *Blue Book* protocol. The files reside in the same directory as above, and the user should connect using the name `guest` and password as above. The OSI FTAM protocol may also be used with username anon.

7 Appeal for data

Table (1) gives a summary of the numbers of data available for the different periods. We hope that the compilation is as complete as possible, although it is always possible that some source of data was overlooked, or more importantly, that someone has access to data which is not commonly available, for example, because it was never published. I have attempted to publish in the Appendix the references to all data which has been compiled. I therefore urge anyone who believes that they may have access to data which is not included to contact me.

Acknowledgements

It is clear that this document represents a summary of the work of several people, especially David Gubbins, David Barraclough, Jeremy Bloxham and Ken Hutcheson; I am grateful to all of them for access to the data they collected and for help in the preparation of this report. We also thank S. R. C. Malin, L. Newitt, V. N. Vadkovsky, K. Bretterbauer, D. J. Kerridge and F. Eleman for their help.

Much of the author's work was performed whilst he was the recipient of a UK NERC studentship at the University of Cambridge and a visitor to the British Geological Survey, Edinburgh who he thanks for their hospitality. This work has subsequently been supported by the Royal Society of London.

References

References to sources of data are given in the Appendix.

Admiralty, 1863. *Admiralty Manual for the Deviations of the Compass.* (Eds. F. J. Evans & Archibald Smith.) London: Admiralty.

Barraclough, D. R., 1978. Spherical harmonic analysis of the geomagnetic field. *Geomagn. Bull. Inst. Geol. Sci.*, **8**.

Barraclough, D. R., 1982. Historical observations of the geomagnetic field. *Phil. Trans. R. Soc. Lond. A*, **306**, 71–78.

Barraclough, D. R., 1985. Halley's Atlantic magnetic surveys. In *Historical events and people in geosciences*, (Ed. W. Schröder), New York: Peter Lang.

Bemmelen, W. van, 1899. *Die Abweichung der Magnetnadel: Beobachtungen, Säcular-Variation, Wert- und Isogonensysteme bis zur Mitte des XVIIIten Jahrhunderts*, supplement to *Obsns. Roy. Mag. Met. Observatory, Batavia*, **21** 1–109.

Bloxham, J., 1985. *Geomagnetic Secular Variation.* Unpublished Ph.D. thesis, University of Cambridge.

Bloxham, J., 1986. Models of the magnetic field at the core-mantle boundary for 1715, 1777 and 1842. *J. Geophys. Res.*, **91**, 13954–13966.

Bloxham, J., Gubbins, D. & Jackson, A., 1989. Geomagnetic secular variation, *Phil. Trans. R. Soc. London*, **329**, 415–502.

Chapman, S. & Bartels, J., 1940. *Geomagnetism*, vol. II, London: Oxford University Press. 2 vols, 1049 p.

Crichton Mitchell, A., 1932. Chapters in the history of terrestrial magnetism I, *Terr. Magn. Atmos. Electr.*, **37**, 105–146.

Crichton Mitchell, A., 1937. Chapters in the history of terrestrial magnetism II, *Terr. Magn. Atmos. Electr.*, **42**, 241–280.

Crichton Mitchell, A., 1939. Chapters in the history of terrestrial magnetism III, *Terr. Magn. Atmos. Electr.*, **44**, 77–80.

Gauss, C. F., 1833. *Göttingen Comment*, **8**, 3–44.

Good, G. A., 1985. Geomagnetics and scientific institutions in 19th century America, *EOS Trans. Amer. Geophys. Un.*, **66**, 521–526.

Good, G. A., 1988. The study of geomagnetism in the late 19th century, *EOS Trans. Amer. Geophys. Un.*, **69**, 218–232.

Hendricks, S. J. & Cain, J. C., 1963. World magnetic survey data. *NASA Goddard Space Flight Centre, technical report, August 1963.*

Hutcheson, K. A., 1990. *Geomagnetic field modelling.* Unpublished Ph.D. thesis, University of Cambridge.

Hutcheson, K. A. & Gubbins, D., 1990. Earth's magnetic field in the seventeenth century, *J. Geophys. Res.*, **95**, 10769-10781.

Jackson, A., 1989. *The Earth's magnetic field at the core-mantle boundary.* Unpublished Ph.D. thesis, University of Cambridge.

John II's commission, 1509. *Regimento do astrolabe e do quadrante*, Lisbon.

London Quarterly Review, 1865. *Review — The Mariner's Compass.* October issue, 1–22.

Malin, S. R. C., 1982. Sesquicentenary of Gauss's first measurement of the absolute value of magnetic intensity, *Phil. Trans. R. Soc.*, **A306**, 5–8.

Malin, S. R. C., 1987. Historical introduction to geomagnetism. In *Geomagnetism, Volume I*, (Ed. J. A. Jacobs). London: Academic Press. pp. 1–49.

Malin, S. R. C. & Bullard, E. C., 1981. The direction of the earth's magnetic field at London, 1570–1975. *Phil. Trans. R. Soc.*, **A299**, 357–423.

Malin, S. R. C. & Gubbins, D., 1983. The need for archival magnetic measurements. *J. Hist. Astron.*, **14**, 70–75.

McConnell, A. 1980. *Geomagnetic instruments before 1900; an illustrated account of their construction and use.* London: Harriet Wynter.

Merrill, R. T. & McElhinny, M. W., 1983. *The erth's magnetic field: Its history, origin and planetary perspective*, London: Academic Press.

Mountaine, W. & Dodson, J., 1757. A letter to the Right Honourable the Earl of Macclesfield, President of the Council and Fellow of the Royal Society, concerning the variation of the magnetic needle; with a set of tables annexed, which exhibit the results of upwards of fifty thousand observations, in six periodic reviews, from the year 1700 to the year 1756, both inclusive; and are adapted to every 5 degrees of latitude and longitude in the more frequented oceans. *Phil. Trans. R. Soc. Lond.*, **50**, 329-350.

Multhauf, R. P. & Good, G., 1987. A brief history of geomagnetism and a catalogue of the collections of the National Museum of American History, *Smithsonion Studies Hist. Technol.*, **48**, Washington: Smithsonian Institution Press, 87 p.

Needham, J., 1962. *Science and civilisation in China* Vol.4 Pt.1, Cambridge: Cambridge University Press.

Poisson, S. D., 1824. Deux mémoires sur la théorie du magnétisme. *Mem. Acad. Sci. Paris*, **5**, 247–338 & 488–533.

Raulin, V., 1867. Sur les variations seculaires du magnetisme terrestre, *Act. Soc. Linn. Bordeaux*, **26**, 1–92.

Sabine, E., 1843. Contributions to Terrestrial Magnetism. — No. V. *Phil. Trans. R. Soc. Lond.*, **133**, 145–231.

Sabine, E., 1846. Contributions to Terrestrial Magnetism. — No. VIII. Containing a magnetic survey of the southern hemisphere between the meridians of 0° and 125° east and parallels of −20° and −70°. *Phil. Trans. R. Soc. Lond.*, **136**, 337–432.

Sabine, E., 1868. Contributions to Terrestrial Magnetism. — No. XI. *Phil. Trans. R. Soc. Lond.*, **158**, 371–416.

Sabine, E., 1872. Contributions to Terrestrial Magnetism. — No. XIII. *Phil. Trans. R. Soc. Lond.*, **162**, 353–433.

Sabine, E., 1875. Contributions to Terrestrial Magnetism. — No. XIV. *Phil. Trans. R. Soc. Lond.*, **165**, 161–203.

Sabine, E., 1877. Contributions to Terrestrial Magnetism. — No. XV. *Phil. Trans. R. Soc. Lond.*, **167**, 461–508.

Smith, P. J. & Needham, J., 1967. Magnetic declination in mediaeval China, *Nature*, **214**, 1213–1214.

Veinberg, B. P., 1929–1933. *Catalogue of Magnetic Determinations in USSR and in Adjacent Countries from 1556 to 1926*, 3 vols. Leningrad: Central Geophysical Observatory

Veinberg, B. P. & Shibaev, V. P., 1969. *Catalogue. The results of magnetic determinations at equidistant points and epochs, 1500–1940*, (Ed. A.N. Pushkov). Moscow: IZMIRAN. (Translation 0031, Canadian Department of the Secretary of State, Translation Bureau, Ottawa).

Appendix: References to sources of data

Admiralty, 1901. *List of magnetic observations made by the officers of H.M. ships and Indian Marine Survey during the years 1890–1900.* London: Admiralty.

Anonymous, 1890. Déterminations magnétiques effectuées en 1889 dans diverses localités du Chili par les Astronomes de l'observatoire National de Santiago. (Extrait de la Noticias hidrograficas No. 12, Santiago, 1890) *Annales Hydrographiques*, **12**, 247.

Anonymous, 1895. Resultats des observations de déclinaison magnétique faites en 1893 et en 1894 sur la côte de Norvège, entre Christiania et Skolver. (Efterretninger for Sjofarende, No. 3/139, Christiania, mars 1895) *Annales Hydrographiques*, **17**, 95.

"Arethuse", 1888. Arethuse 1887–1888. Resultats des mesures magnétiques effectuées. *Annales Hydrographiques*, **10**, 600–625.

Aubry, 1888. Note sur les observations magnétiques faites à bord de la Minerve (1886–1888) par M. Aubry, Lieutenant de Vaisseau. *Annales Hydrographiques*, **10**, 290–303.

Barraclough, D. R., 1985. Halley's Atlantic magnetic surveys, in *Historical events and people in geosciences*, (Ed. W. Schröder), New York: Peter Lang.

Bauer, L. A., 1908. The earliest values of the magnetic declination, *Terr. Mag. Atmos. Electr.*, **13**, 97–104.

Beattie, J. C., 1909. *Report of a Magnetic Survey of South Africa.* Cambridge: University Press (for the Royal Society).

Becquerel, A. C., 1840. *Traite experimental de l'electricite et du magnetisme*, Paris: Fermin Didot Freres.

Bemmelen, W. van, 1893. *De Isogonen in de XVIde en XVIIde Eeuw*, Utrecht: J. van Druten.

Bemmelen, W. van, 1899. *Die Abweichung der Magnetnadel: Beobachtungen, Säcular-Variation, Wert- und Isogonensysteme bis zur Mitte des XVIIIten Jahrhunderts*, supplement to *Magn. Met. Obs. Batavia*, **21**.

Bernardières, M., 1884. *Résumé des déterminations magnétiques effectuées en 1882–1883 par la mission chargée de l'observation du passage de Venus au Chili, et de la mesure de différences de longitude sur la côte occidentale de l'Amérique du sud.* Extrait des annales hydrographiques, 1er semestre. Paris: Imprimerie Nationale.

Bessels, E., 1876. *Scientific Results of the U.S. Arctic Expedition.* Vol. 1, Physical Observations. Washington.

Borchgrevink, C. E., 1902. *Magnetic and Meteorological Observations made by the 'Southern Cross' Antarctic Expedition, 1898–1900.* London: Harrison & Sons (for the Royal Society).

Brewster, D., 1837. *A Treatise on Magnetism.* Edinburgh: Adam and Black.

Cannellier, 1890. Observations magnétiques faites dans différents mouillages de la Méditerranée Orientale, par M. Le Cannellier, Lieutenant de Vaisseau à bord du Cuirasse d'escadre Amiral-Baudin. *Annales*

Hydrographiques, **12**,240–245.

Carlheim-Gyllenskold, V., 1896. Sur la forme analytique de l'attraction magnetique de la terre exprimee en fonction du temps, *Astron. Iakttag. Unders. Anstalda Stockholms Obs.*, **5**, No. (3), 29.

Cassini, J. D., 1791. De la déclinaision et des variations de l'aguille aimantée, *J. Phys.*, 52–55.

Chief Astronomer, 1910. Report of the Chief Astronomer for the year ending March 31 1909, *Department of the Interior Sessional paper No. 25a*, Ottawa.

Cirera, P. Ricardo, 1893. *El Magnetismo Terrestre en Filipinas.* Observatorio Meteorologico de Manila, Manila.

Cook, J., King, J. & Bayly, W., 1782. *The original astronomical observations made in the course of a voyage to the northern Pacific ocean*, London: Commissioners of the Longitude.

Cornwall, Capt., 1722. Observations of the variation on board the Royal African Pacquet, in 1721, *Phil. Trans. R. Soc.*, **32**, 55–56.

Courmes, 1892. Observations magnétiques faites pendant la campagne du croiseur Le Dubordieu (1889–1891), par M.L. Courmes, Lieutenant de Vaisseau. *Annales Hydrographiques*, **14**, 302–349.

Creak, E. W., 1879. On the results of the magnetical observations made by the officers of the Arctic Expedition 1875–76. *Proc. Roy. Soc. Lond.* **29**, 29–42.

Cunningham, J., 1704. Observations of the weather, made in a voyage to China, *Phil. Trans. R. Soc.*, **24**, 1639–1647.

Dalrymple, A., 1775. *A collection of voyages, chiefly in the south Atlantick Ocean*, 5 pts, London.

Dalrymple, A., 1778. Journal of a voyage to the East Indies, in the ship Greville, Captain Burnet Abercrombie, in the year 1775, *Phil. Trans. R. Soc.*, **68**, 389–418.

Dampier, W., 1729. *A voyage to New Holland*, London. Reprinted in *Dampier's Voyages* (Ed. J. Masefield), London: Grant Richards (1906).

Douglas, R., 1776. The variation of the compass; containing (a) 1719 observations to, in, and from, the east Indies, Guinea, West Indies, and Mediterranean, with the latitudes ad longitudes at the time of observation. The longitude for the most part reckoned from the Meridian of London; if otherwise, it is taken notice of in the margin, *Phil. Trans. R. Soc.*, **66**, 18–72.

Drygalski, E. V., 1897. *Grönland-Expedition der Gesellschaft für Erdkunde zu Berlin (1891–93)*, Band 2. Berlin: W.H. Kuhl.

Favereau, 1886. Déterminations Magnétiques faites dans l'océan Indien en 1884–1885, par M. Favereau, Lieutenant de Vaisseau. *Annales Hydrographiques*, **8**, 445–449.

Feuillee, L., 1714-1735. *Journal des observations physiques, mathematiques et botaniques faites par ordre du Roi sur les côtes Orientales de l'Amerique Meridionale & aux Indes Occidentales*, 2 vols, Paris: Pierre Giffart (1714) & Jean Mariette (1735).

"Franz Loschober", 1891. Déterminations magnétiques faites en 1889–1890, et ramenés au commencement de 1890, sur les côtes de la mer Adriatique, par le capitaine de corvette Franz Loschober, Directeur de l'observatoire impérial et royal de Pola. (Hydrographische Nachricht, No. 28, Pola, 1891.) *Annales Hydrographiques*, **13**, 266–267.

Freeden, W. V., 1869. *Die Wissenschaftlichen Ergebnisse der Ersten Deutschen Nordfahrt 1868. Geographie und Erforschung der Polar Regionen Nr. 27* (Aus Petermann's Geogr. Mittheilungen 1869, Heft 6). Gotha: Justus Perthes.

Fritsche, H., 1893. *Ueber die Bestimmung der geographischen Länge und Breite und der drei Elemente des Erdmagnetismus durch beobachtung zu lande sowie erdmagnetische und geographische Messsung an mehr als tausend verschiedenen Orten in Asien und Europa, ausgefuhrt in den Jahren 1867–1891.* St Petersburg.

Greely, A. W., 1888. International Polar Expedition. *Report on the Proceedings of the U.S. Expedition to Lady Franklin Bay, Grinnel Land.* Vol. II. Washington: Govt. Printing Office.

Halley, E., 1683. A theory of the variation of the magnetical compass, *Philos. Trans. R. Soc. London*, **13**, 208–221.

Halley, E., 1692. An account of the cause of the change of the variation of the magnetic needle, with an hypothesis of the structure of the internal parts of the Earth, *Philos. Trans. R. Soc. London*, **16**, 563–578.

Halley, E., 1732. Observations of latitude and variation, taken on board the Hartford, in her passage from Java Head to St Helena, *Phil. Trans. R. Soc.*, **37**, 331–338.

Hansteen, C., 1819. *Untersuchungen über den Magnetismus der Erde*, Christiana: Lehmann & Gröndahl.

Harris, J., 1733. An account of some magnetical observations made in the months of May, June and July 1731 in the Atlantick or Western Ocean, *Phil. Trans. R. Soc.*, **38**, 75–79.

Hazard, D. L., 1917. United States Magnetic Tables and Magnetic Charts for 1915. *U.S. Coast & Geodetic Survey Special Publication No. 44.*

Hedges, C., 1704. *A Collection of Voyages and Travels, Some Now Printed From Original Manuscripts*, vol.1. London: Awnsham and J. Churchill, The Black Swan.

Herbert, W. H. & McKnight, J. H., 1924. Magnetic Results in Western Canada. *Topographical Survey of Canada, Bulletin 52.* Ottawa.

Houette & Morache, 1896. Mission magnétique en Islande et en Scandinavie, de l'Aviso-transport la Manche, par M. Houette, Capitaine de Frégate, Commandant, et M. Morache, Lieutenanant de Vaisseau à bord de ce bâtiment. *Annales Hydrographiques*, **18**, 49–68.

Hoxton, W., 1742. The variation of the magnetic needle, as observed in three voyages from London to Maryland, *Phil. Trans. R. Soc.*, **41**, 171–175.

Hutchins, T., 1775. Experiments on the dipping needle made by desire of the Royal Society, *Phil. Trans. R. Soc.*, **65**, 129–138.

Hydrographischen Amt des Reich-Marine-Amts, 1888-90. *Die Forschungsreise SMS Gazelle in den Jahren 1874–1876 unter Kommando des Kapitans zur See Freiherrn von Schleinitz.* II. Theil: Physik und Chemie. Berlin.

Keeling, B. F. E., 1907. Magnetic Observations in Egypt 1895–1905, with a summary of previous magnetic work in Northern Africa. *Ministry of Finance, Egypt. Survey Department paper, No. 6.* Cairo: National Printing Dept.

Knott, Cargill G. & Tanakadate, Aikitsu, 1888. A Magnetic Survey of all of Japan by Order of the President of the Imperial University. *The Journal of the College of Science, Imperial University, Japan.* Vol. II., part III. Japan: Tokyo.

Koldewey, K., 1874. *Die Zweite Deutsche Nordpolarfahrt 1869–70.* Band 2. Leipzig: F.A. Brockhaus.

Lancelin, 1894. Observations de déclinaison magnétique dans la Méditerranée orientale (Fevrier- Mai 1894) par M. G. Lancelin, Enseigne de Vaisseau à bord du Croiseur le Cosmao. *Annales Hydrographiques*, **16**, 141–143.

Leconte de Roujou, 1892. Déterminations magnétiques en extrême-Orient par M. Leconte de Roujou, Lieutenant de Vaisseau à bord de la Tromphante. *Annales Hydrographiques*, **14**, 112–155.

Lephay, 1889. Extrait des Observations magnétiques faites dans le Levant en 1885–1886 par M. J. Lephay, Lieutenant de Vaisseau à bord de La Venus. *Annales Hydrographiques*, **11**, 49.

Leroux, Ernest, Ed., 1894. *Voyage de 'La Manche' à l'Île Jan Mayen et au Spitzberg.* Paris.

Lundquist, K. Z., 1957. Magnetic observations in Svalbard 1596–1953. *Norsk Polarinstitutt, Det Kongelige Departement for Industri og Håndverk, Skrifter Nr. 110.* Oslo: Fabritius & Sønners.

Lyons, H. G., 1901. Magnetic Observations in Egypt, 1893–1901. *Proc. R. Soc.*, **71**, 1–25.

Malin, S. R. C. & Bullard, E.C., 1981. The direction of the earth's magnetic field at London, 1570–1975, *Phil. Trans. R. Soc.*, **A299**, 357–423.

Middleton, C., 1731. Observations on the weather, in a voyage to Hudson's Bay, *Phil. Trans. R. Soc.*, **37**, 76–78.

Middleton, C., 1733. Observations of the variations of the needle and weather, amde in a voyage to Hudson's Bay, *Phil. Trans. R. Soc.*, **38**, 127–133.

Middleton, C., 1736. Observations made of the latitude, variation of the magnetic needle, and weather, *Phil. Trans. R. Soc.*, **39**, 270–279.

Mion, 1893. Déterminations magnétiques à la côte Ouest de Madagascar, et aux Comores, par M. Mion, Ingenieur hydrographe de la Marine. 1888–1890. *Annales Hydrographiques*, **15**, 205–207.

Mizon, 1889. Observations magnétiques recueillies à la côte Occidentale d'Afrique par M.L. Mizon, Lieutenant de Vaisseau. *Annales Hydrographiques*, **11**, 36–47.

Moidrey, J. de, 1904. Note sur quelques anciennes déclinaisons, *J. Geophys. Res.*, **9**, 18–24.

Mottez, 1893. Déterminations magnétiques faites sur la côte ouest d'Amérique pendant une campagne dans l'océan Pacifique à bord du croiseur Le Dubordieu (1892–1893) par M. Luis Mottez, Lieutenant de Vaisseau. *Annales Hydrographiques*, **15**, 408–431.

Mountaine, W., 1776. A letter from Mr William Mountayne, FRS to the Rt Hon James Earl of Morton, PRS, *Phil. Trans. R. Soc.*, **56**, 216–223.

Musschenbroek, P. van, 1729. *Physicae experimentales et geometricae de magnete, tuborum capillarium vitreorumque speculorum attractione, magnitudine terrae, cohaerenta corporum firmorum. Dissertationes ut et epheremides meteorologie ultrajectinae*, Samuelem Luchtmans, Leiden.

Nares, G. S., 1882. *Report on the Scientific Results of the Voyage of HMS Challenger during the years 1873–1876, under the command of Captain George S. Nares RN FRS and Captain Frank Tourle Thomson RN. Prepared under the superintendence of the late Sir C. Wyville Thomson and of John Murray.* Vol. II: Narrative. 50 vol. London.

Norwood, R., 1659. *The Seaman's Practice*, London.

Perry, S. J., 1878. Magnetic observations taken during the transit of Venus expedition to and from Kerguelen island. *Proc. Roy. Soc. Lond.*, **27**, 1–11.

Pickersgill, R., 1778. Track of His Majesty's armed brig Lion from England to Davis's Streights and Labrador, with observations for determining the longitude by sun and moon and error of common reckoning; also the variation of the compass and dip of the needle, as observed during the said voyage in 1776, *Phil. Trans. R. Soc.*, **68**, 1057–1063

Pond, 1888. Océan Pacifique Nord. Californie. Observations de déclinaison magnétique, d'inclinaison et d'intensité, faites par le Lieutenant Charles F. Pond, du steamer hydrographe des États-Unis, Commander F.A. Cooke, en 1887–1888. *Annales Hydrographiques*, **10**, 626.

Pond, 1889. Déterminations magnétiques faites sur les côtes ouest de la basse Californie par le Lieutenant Charles F. Pond, de la marine des États-Unis, à bord du navire hydrographe Ranger. (Extrait de la Notice to Mariners No. 47 de Washington 1889.) *Annales Hydrographiques*, **11**, 233.

Pond, 1890. Océan Pacifique Nord. Basse Californie (côte ouest). Déterminations magnétiques faites dans la baie Ballenas et sur l'Île Ascuncion, par le Lieutenant Charles F. Pond, à bord du navire hydrographe Ranger. (Notice to Mariners No. 50 Washington 1890.) *Annales Hydrographiques*, **13**, 86.

Preston, 1891. Océan Atlantique. Déterminations magnétiques faites par M.E.D. Preston, Assistant du Coast & Geodetic Survey, pendant un voyage du navire Pensacola dans l'océan Atlantique, 1890–1891.

(U.S.C. & G.S., Bull. no. 22, Washington Fevrier 1891) *Annales Hydrographiques*, **13**, 268.

Purchas, S., 1625. *His Pilgrimes*, London.

Purchas, S., 1905. *Hackuytus Posthumus (or) Purchas His Pilgrimes: Containing a History of World in Sea Voyages and Lande Travells by Englishmen and Others.* Glasgow: J. Maclehose.

Raulin, V., 1867. Quelques vues generales sur les variations seculaires du magnetisme terrestre, *Actes Soc. Linneene Bordeaux*, **26**, 1–92.

Rayet, M. G., 1876. Recherches sur les observations magnétiques faites à l'observatoire de Paris de 1667 à 1872, *Mem Ann. Obs. Paris,., 13.*

Rogers, W., 1721. The variation of the magnetical compass, observed by Capt. Rogers, *Phil. Trans. R. Soc.*, **31**, 173–176.

Ryckevorsel, Dr Van, 1880. *Verslag aan Zijne Excellentie den Minister van Kolonien over eene Magnetische Opneming van den Indischen Archipel, in de jaren 1874–1877 gedaan. (Report to his excellency the minister for the colonies on a Magnetic Survey of the Indian Archipelago, made in the years 1874–1877.)* Amsterdam: Johannes Muller for the Royal Academy of Sciences, Amsterdam.

Ryckevorsel, Dr. Van & Engelenburg, C. E., 1890. *Magnetic Survey of the Eastern Part of Brazil.* Amsterdam: Johannes Muller for the Royal Academy of Sciences, Amsterdam.

Ryder, C., 1895. *Meddelelser om Grønland, Den Ostgrønlandske Expedition 1891–92.* Kjøbenhavn.

Sabine, E., 1868. Contributions to Terrestrial Magnetism. — No. XI. *Phil. Trans. R. Soc. Lond.*, **158**, 371–416.

Sabine, E., 1870. Contributions to Terrestrial Magnetism. — No. XII. The magnetic survey of the British Islands, reduced to the epoch 1842.5. *Phil. Trans. R. Soc. Lond.*, **160**, 265–275.

Sabine, E., 1872. Contributions to Terrestrial Magnetism. — No. XIII. *Phil. Trans. R. Soc. Lond.*, **162**, 353–433.

Sabine, E., 1875. Contributions to Terrestrial Magnetism. — No. XIV. *Phil. Trans. R. Soc. Lond.*, **165**, 161–203.

Sabine, E., 1877. Contributions to Terrestrial Magnetism. — No. XV. *Phil. Trans. R. Soc. Lond.*, **167**, 461–508.

Sanderson, W, 1720. Observations on the variation of the needle made in the Baltic, Anno 1720, *Phil. Trans. R. Soc.*, **31**, 120.

Schott, C. A., 1890. *The magnetic observations made on Bering's first voyage to the coasts of Kamchatka and Eastern Asia in the years 1725 to 1730*, U.S. Coast Geodetic Survey, Bulletin No. 20.

Schott, C. A., 1896. *Secular variation of the Earth's magnetic force in the United States and in some adjacent foreign countries*, U.S. Coast Geod. Surv., Part II, Appendix 1, pp. 167–320.

Schwerer, 1892. Étude sur le magnétisme terrestre a Terre-Neuve, par M.A. Schwerer, Lieutenant de Vaisseau. *Annales Hydrographiques*, **14**, 88–111.

Schwerer, 1896. Observations à la mer de M. Schwerer, Lieutenant de Vaisseau à bord du Dubordieu. *Annales Hydrographiques*, **18**, 177–187.

Scott-Hansen, 1901. Determination of Magnetic Declination by Compass. In: *The Norwegian North Polar Expedition 1893-1896. Scientific Results. Vol II, No. 6. (Geelmuyden. Astronomical Observations, Part D.)*, (Ed. Fridtjof Nansen). Longmans, Green & Co. for the Fridtjof Nansen Fund for the Advancement of Science.

Shadwell, C., 1877. A Contribution to Terrestrial Magnetism; being the Record of observations of the magnetic Inclination or Dip, made during the voyage of H.M.S. "Iron Duke" to China and Japan etc., 1871–1875. *Phil. Trans. R. Soc. Lond.*, **167**, 138–143.

Steen, A. S., 1901. In: *The Norwegian North Polar Expedition 1893–1896. Scientific Results. Vol II, No. 7. Terrestrial Magnetism, General Results.* (Ed. Fridtjof Nansen). Longmans, Green & Co. for the Fridtjof Nansen Fund for the Advancement of Science.

Stevin, S., 1599. *De Havenvinding*, Leyden: Plantiin.

Tanakadate, A., 1904. A Magnetic Survey of Japan reduced to the epoch 1895 and the sea level carried out by order of the Earthquake Investigation Committee. *The Journal of the College of Science, Imperial University, Japan.* Vol XIV. Japan: Tokyo.

Tillo, A. von, 1881. Ueber die geographische Vertheilung und säculäre Aenderung der Declination und Inclination im europäischen Russland. *Repertorium Für Meteorologie*, **8**, No. 2. 1–82. St Petersburg.

Tillo, A. von, 1885. Ueber die geographische Vertheilung und säculäre Aenderung der erdmagnetischen Kraft im europäischen Russland. *Repertorium Für Meteorologie*, **9**, No. 5. 1–78. St Petersburg.

U.S. Bureau of Navigation, 1886. *The Variation of the Compass, as determined in various parts of the World (chiefly at Sea), by Officers of the United States Navy, while Navigators of Ships, between the Years 1881 and 1885.* (Naval Professional Papers: No. 19.) Washington: Government Printing Office.

U.S. Hydrographic Office, 1894. *Contributions To Terrestrial Magnetism, The Variation of the Compass. From observations made in the United States Naval Service during the period from 1891 to 1894.* (Pub. No. 109.) Washington: Government Printing Office.

Veinberg, B. P., 1929–1933. *Catalogue of Magnetic Determinations in USSR and in Adjacent Countries from 1556 to 1926*, 3 vols. Leningrad: Central Geophysical Observatory

Veinberg, B. P., 1933. *Catalogue of magnetic determinations in the polar regions.* (Sections I & II.) Moscow: The Central Administration of the Hydro-Meteorological service of the USSR.

Wales, W., 1788. *Astronomical observations made in the voyages which were undertaken by order of his Present Majesty for making discoveries in the Southern Hemisphere and successively performed*

by Commodore Byron, Captain Wallis, Captain Carteret and Captain Cook in the Dolphin, Tamer, Swallow and Endaevour, London: Commissioners of the Longitude.

Wales, W. & Bayly, W., 1777. *The original observations made in the course of a voyage towards the South Pole and around the world*, London: Board of Longitude.

Weyprecht, C., 1878. Die Magnetische Beobachtungen der Østereichisch-Ungarischen Arctischen Expedition 1872–1874. *Denkschriften der Kaiserlichen Academie der Wissenschaften. Mathematische-naturwissenschaftliche Classe. Wien.* **35**, 69–292.

Wijkander, A., 1876. Observations Magnétiques faites pendant l'expédition Arctique Suédoise en 1872–1873. *Kongl. Svenska Vetenskaps-Akademiens Handligar*, **13**, No. 15, Stockholm.

Wijkander, A., 1883. Observations Magnétiques, faites pendant l'expédition de la Vega 1878–1880. *Vega Expeditions Vetenskapliga Iakttagelser*, Bd II, Stockholm.

Wilhjelm, J., 1971. Ground-based geomagnetic measurements in Greenland with an account of a survey in 1965 and a general summary of observations performed since 1587. *Danish Met. Inst. Geophys.*, Paper R–15.

Wille, C. & Mohn, H., 1882. *Den Norske Nordhavs-Expedition 1876–1878. 2. Magnetiske Observationer (C. Wille)* Vol. V, Christiania.

Measurements of Declination at the Helsinki Magnetic-Meteorological Observatory 1844-1853

Heikki Nevanlinna, Anneli Ketola and Tuulikki Kangas

Geomagnetism Division
Finnish Meteorological Institute
P.O.Box 503
SF-00101 Helsinki
Finland

Abstract

A project was started with the goal to treat all the old unpublished magnetic data into computer readable form in February 1991 at the Finnish Meteorological Institute (*FMI*), the successor of the Helsinki magnetic-meteorological observatory. Altogether there are available about 2.5 million visual observations of D, H and Z made during the time interval 1844-1905. The first 10 years (1844-1853) period of declination data now converted to electronic form, include observations made at every tenth minute. The total number of observations is 489 152. In this paper we present some examples of declination observations in forms of tables and graphs showing hourly, daily, monthly and annual means.

Secular variation of the declination in 1844-1853 have been extremely linear showing a steady eastward increase of 8.0'/year that is more than two times larger than the present annual rate of secular change in Finland. The standard deviation of the daily and monthly residuals, after removing the linear secular variation trend for the whole time period, is about 1' demonstrating high stability and reliability of the observations. For this reason the data may suit for e.g. deriving 3-hour activity index K and daily Ak numbers giving new information for extending the existing long series of activity characters backwards in time.

1 INTRODUCTION

Helsinki magnetic observatory was founded in 1838 and it started regular magnetic observations on July 1st, 1844. Observations were eye readings aided with a telescope (Fig. 1) as was the common practice before the advent of photographically recording variometers. The observation interval was 10 minutes up to 1857 and after that one hour. Observed were D, H and Z by using variometers constructed in Göttingen according to Gauss' instructions. In 1905 magnetic recordings were stopped as useless due to disturbances caused by nearby tramway traffic started in 1901.

On the observatory area there were a wooden building for variometers and meteorological instruments and a small hut for absolute measurements. The observatory site was near to the centre of present day Helsinki City where today is the main building of the Finnish Meteorological Institute. Geographical coordinates of the observatory were ϕ = 60° 10.3' N, λ = 24° 59.0' E. The geomagnetic latitude (Φ) was 58.4° in 1844 as calculated from the dipole coefficients given by *Barraclough* (1974). (Note that in the time-dependent geomagnetic coordinate system Helsinki observatory was about 1° north

of the Nurmijärvi observatory site locating 40 *km* to the north from Helsinki.)

Early magnetic results from 1844 to 1848 have been published by the first director of the observatory, J.J. Nervander (1805-1848), in 1850 (*Nervander*, 1850). Unfortunately no later results have ever been treated for publication. However, they are still available in the original observation notebooks and not much of the data have been lost. After a thorough examination of the old recordings, they revealed to have been made very carefully and the variometers seem to have recorded magnetic field changes reliably giving useful series of magnetic data (more than two million observation values) for studies on magnetic activity and secular variations from a time span covering about 60 years since 1844.

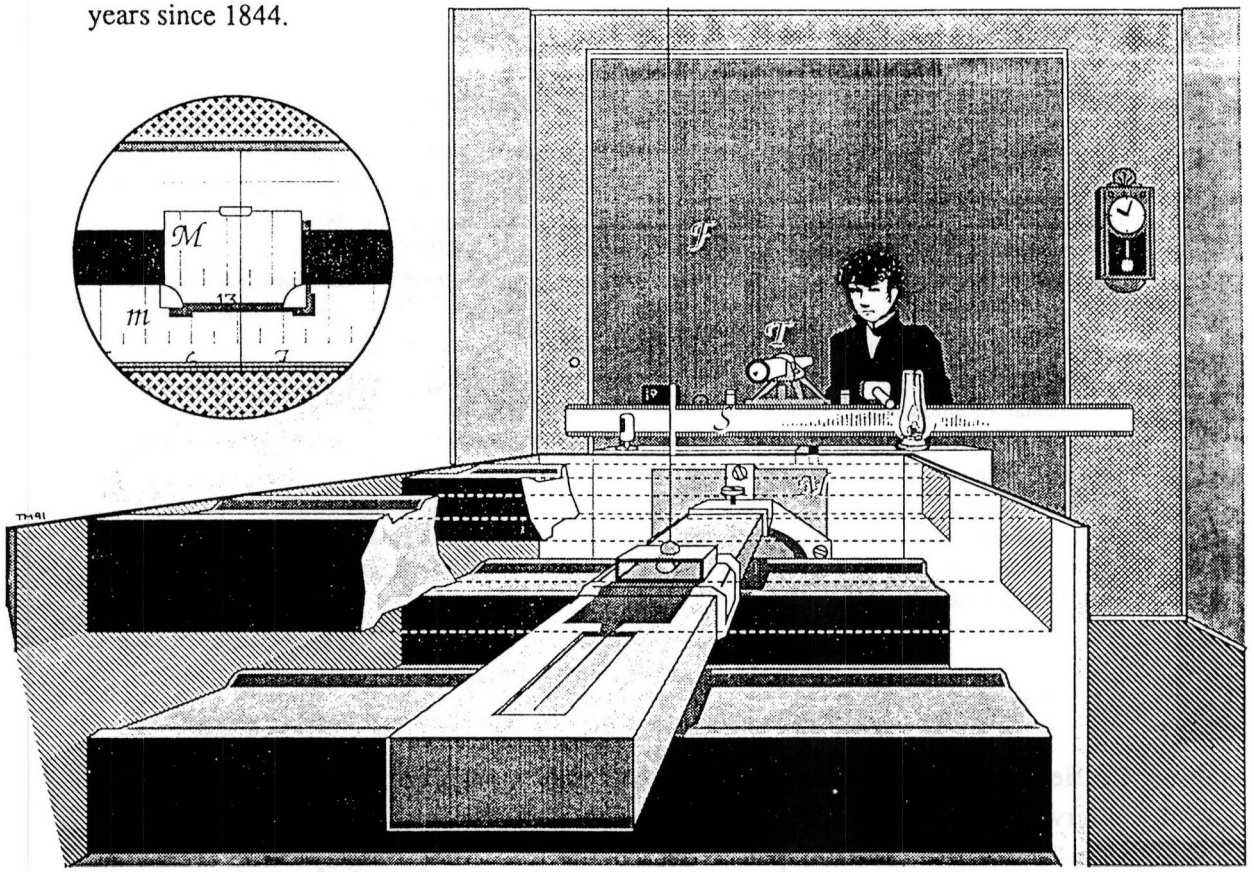

Fig. 1. Semi-artistic view of the classical declination variometer developed by Gauss. It consists of a horizontal magnet suspended by a silk fibre (*F*). The magnet forms an angle *D* (declination) with the true North direction. The suspended magnet will follow variations of *D* and so will a mirror, *M*, attached to the magnet. Changes in the magnet direction are obtained by observing the reflection of the illuminated (by an oil-lamp) scale *S* in mirror *M* through the telescope *T*. There is a second mirror, *m*, fixed on the shelter near the magnet. As viewed from the telescope (shown on the left upper corner) there will be seen two reflected scale values, the base-line value (d_o) from the fixed mirror *m*, and a changing one (*d*) from the magnet mirror *M*. The magnet was put between copper bars perpendicular to it as shown in the picture. Induced eddy currents in copper bars damped short period vibrations of the magnet. The whole system, including the suspension fibre, was covered by a wooden church-shaped shelter (not shown here) shielding the magnet for air currents.
(Illustration by *Teemu Mäkinen*).

The purpose of this paper is to give preliminary results of declination observations put on diskettes. There are available in digital form about 490 000 D values from the period 1844-1853. The objective is to continue this work and publish all the historical data in yearbooks starting from D observations because they are most reliable of the three magnetic components observed.

2 *The eye-telescope declination variometer*

The basic principle of the D-variometer of the magnet type has been the same since introduced by Gauss. Fig. 1 illustrates the working principle of a simple D-variometer from the Gaussian time, used in Helsinki observatory. It consists of a horizontal magnet suspended by a fibre (F) with negligible torsion, so that the magnet will always orientate itself towards the magnetic meridian forming an angle D with the true North direction. The suspended magnet will follow variations of D and so will a mirror, M, attached to the magnet. Changes in the magnet direction are obtained by observing the reflection of the illuminated scale S in mirror M through the telescope T. There is a second mirror, m, fixed on the shelter near the magnet. As viewed from the telescope, there will be seen two reflected scale values, the so-called base-line value (d_0) from the fixed mirror m, and a changing one (d) from the magnet mirror M.

In a first approximation a change in declination, ΔD, is calculated from the variometer readings d and d_0 as follows

$$\Delta D = D - D_0 = \varepsilon(d - d_0) \tag{1}$$

where ε is the optical scale value defined by:

$$\varepsilon = 1\ rad/2R = 3438'/2R, \tag{1.1}$$

where R is the distance (in mm) between the scale S and the mirror M. If the absolute value of D_0 is not known as was the case in the Helsinki observatory, the variometer values (ΔD) give information about variations of the declination relative to an unknown absolute level.

ε was assumed to be constant during the whole time period studied here as it depends only on the distance between the magnet mirror and the scale. The value of ε given by *Nervander* (1850) seems to be reliable because the diurnal variations at Helsinki and Nurmijärvi observatories show very similar behavior being the same within 1' under corresponding solar activity conditions (Fig. 2). The baseline values d_0, read for each observation, have been very stable changing almost linearly only 1' during the time period analyzed.

In the Helsinki observatory the D-variometer (called unifilar magnetometer) consisted of a 60 cm long copper bar where the magnet with dimensions 30.0 x 3.0 x 0.7 cm was embedded. The weight of the system was 1.3 kg and it was suspended by a 2.7 m long silk fibre (Fig.1). Changes in the direction of the magnet were observed by a telescope at the distance (R) of 5.15 m, thus from Eq. (1.1) ε = 0.334'/mm

In a more detailed theory of unifilar magnetometer (e.g. *Laursen & Olsen*, 1971), the difference $d - d_o$ in Eq. 1, should by multiplied by the factor

(1.2) $$1 + (k/M + C)/H,$$

where k is the torsion constant of the fibre, M the magnetic moment and C the magnetic field caused by other magnets (mainly from H- and Z-variometers nearby). If the factor (1.2) cannot be neglected, the variometer values will also be temperature dependent as k and M vary with temperature. The upper limit of C (< 50 nT) can be rather reliably calculated from the known properties of the magnets and distances between the variometer piers. The error in ε due to C is < 0.003', thus negligible small. The effect of the torsion of the fibre may be made small enough by increasing the magnetic moment M. Although we have no information about the torsion properties of the silk thread for determining the effect of the ratio k/M, there are good reasons to assume it has been insignificant because Nervander was known as an ingenious experimentalist and constructor of magnetometers invented by himself.

3 *Results*

The observed 10-minute declination values (d) together with time (Göttingen mean time which is one hour ahead of Universal Time) and base-line values (d_o) were put on diskettes. Totally there are in electronic form 489 152 observations of declination (out of 499 724 possible) covering the time span of 3471 days from 1st of July 1844 to 31st of December 1853. Entirely missing are two months data (August and September 1852) when the observational routines were interrupted due to reparations in the observatory building. Observations are also missing from the night hours (1-4 h local time) in August 1853 because of the disastrous cholera epidemic, killed about 2 500 people in a few months, forcing to decrease the number of observers to less than half of the normal amount. In addition to these data gaps 1024 other observations were discarded as clearly erroneous or impossible to interpret from the original handwritings. (In the figures below there is one year temporary gap (1847) because the treatment of that data is not yet finished).

The hourly, daily and monthly means of ΔD will be published as monthly tables in the series *Geophysical Publications of the Finnish Meteorological Institute* in spring 1992 . An example of the monthly summary is given in Table *A*.

Although all declination observations were relative, an estimate of the absolute declination level of each month will be given. This was achieved by fixing the monthly mean value of ΔD from July 1844 to be equal to the declination (= D_p = -9.2°) calculated from a time and space (ϕ,λ) dependent polynomial (*Nevanlinna*, 1979) that has been determined by using all available absolute measurements of the declination data (260 data points) from different parts of Finland and from different epochs. The probable error in D_p is ±0.5°. Later "absolute" values (D_a) were calculated simply as

(2) $$D_a = D_p + (\Delta D - \Delta D_{July\ 1844})$$

where ΔD - $\Delta D_{July\ 1844}$ represents the true secular change including external contributions. Fig. 3 shows monthly means of D calculated from Eq. (2.1). One can see that there have been very stable linear increase of declination by 8.0'/year that is about twice as high as the annual secular change has been in South Finland in recent years. When calculated from the polynomial model, derived independently from the Helsinki data, the corresponding annual rate was 7.2' supporting the reality of the secular change deduced from the present data. The secular acceleration, as calculated from a quadratic fit of the monthly mean values, is $<< 0.01'/(year)^2$ emphasizing the extrem linearity of the data.

By removing the linear secular change trend, the residual daily and monthly means show very small scatter, standard deviation (*STD*) is < 1.5', except during 1845-46 when a new brick house for absolute measurements was erected quite close to the observatory variometer building. The about 0.1° swing in D during 1845-46 may be a signature of the disturbances caused by the construction work.

In each month 5 most disturbed and quietest days were selected by using the daily *STD* of the 144 individual observation as the criterion of quietness. Table *A* shows an example of the monthly table depicting daily averages of the declination together with some other statistical parameters.

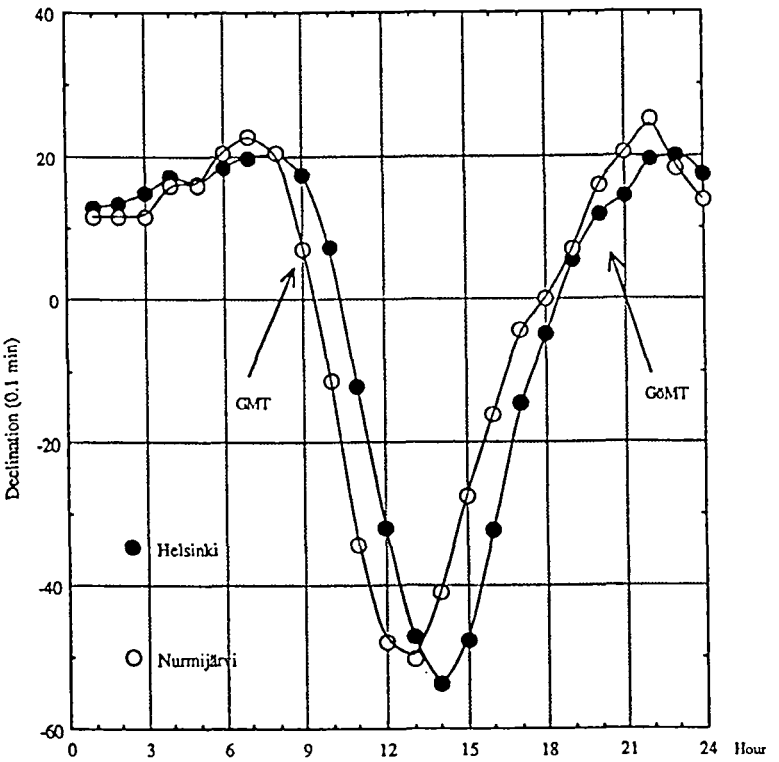

Fig. 2. This diagram depicts one-year average diurnal variation of D recorded in 1844-45 compared with corresponding values from Nurmijärvi in 1986 when the sunspot cycle was in the same phase near its minimum roughly 13 solar cycles later. The figure demonstrates the similarity in shape of the daily variation curve at the two observatories as is excepted because the observatories are so close to each other. The one hour (exactly $1h\ 0m\ 4s$) difference in the location of D minimum is the difference between the Universal Time used at Nurmijärvi and the Göttingen Mean Time used in Helsinki.

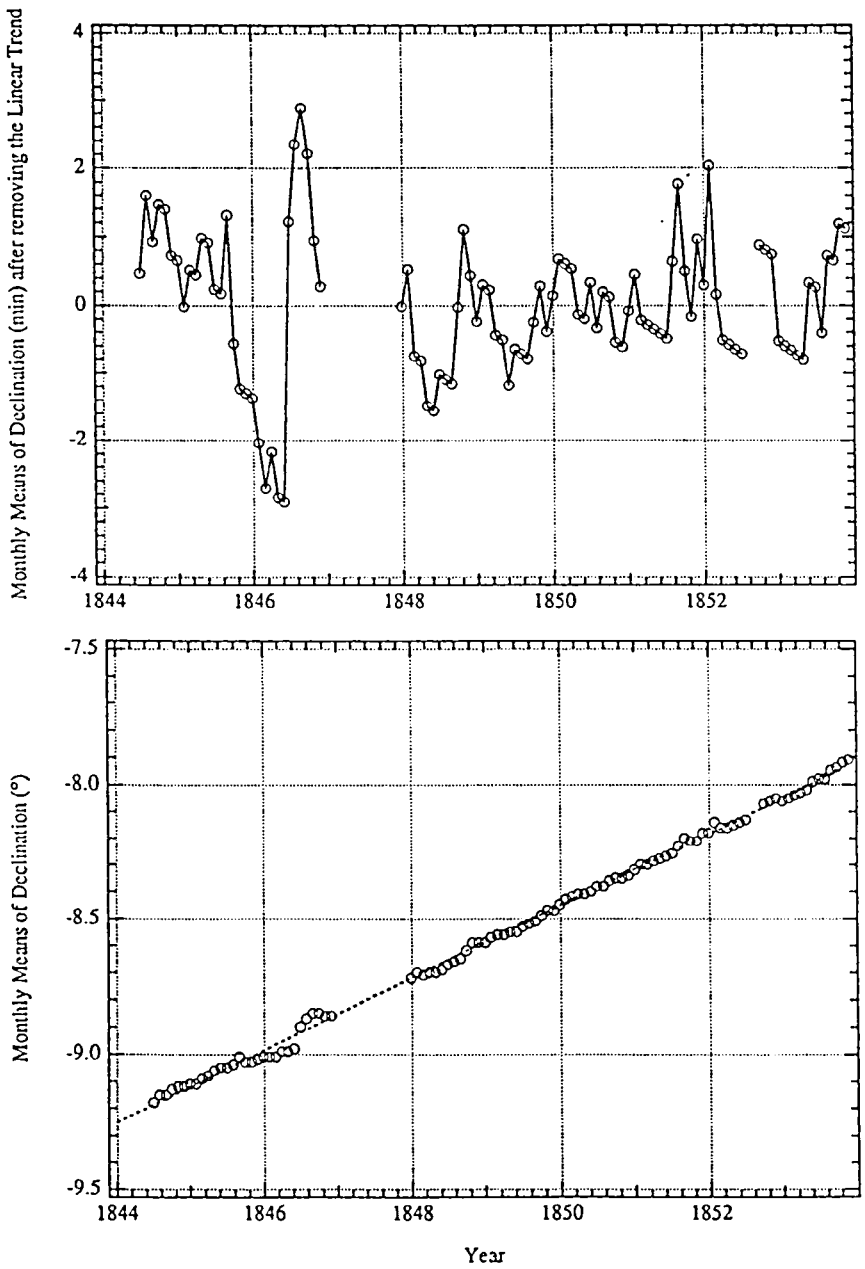

Fig. 3. *Lower part*: Monthly means (all-days) of declination. A linear fit (dashed line) gives the annual secular change rate 8.02'±0.04'. When only five quietest days were selected, using daily standard deviation as the criterion of quietness, no significant difference was found in the annual secular change rate.

Upper part.: Monthly means residuals after subtracting the linear fit. The standard deviation of the residuals is 1'. The jumps in 1845-46 are probably caused by disturbances from construction works of a brick house erected close to the observatory. The sharp peaks in 1851-52 are due to disturbances of many recurrent big magnetic storms 3-4 years after the sunspot maximum (1848).

STD of the daily 144 observations for each day 1844-1853 is shown in Fig. 4. One can clearly see the typical regular annual variation: *STD* in winter is about 50 % smaller than in summer.

Fig. 5 depicts an example of the 27*d* recurrence tendency of magnetic disturbances through the year 1845. The curve in it was determined by a superposed epoch analysis in which the day $i = 0$ was a disturbed day in each month. *STD* of the most disturbed days was normalized to 100. The figure shows the average normalized *STD* of the days from $i = -5$ to $i = 35$. At the zero day the mean *STD* has been 75 % of that of the most disturbed day, and at $i = 26$-28 there is peak in *STD* demonstrating the recurrent characteristic of magnetic disturbances connected to the solar rotation period.

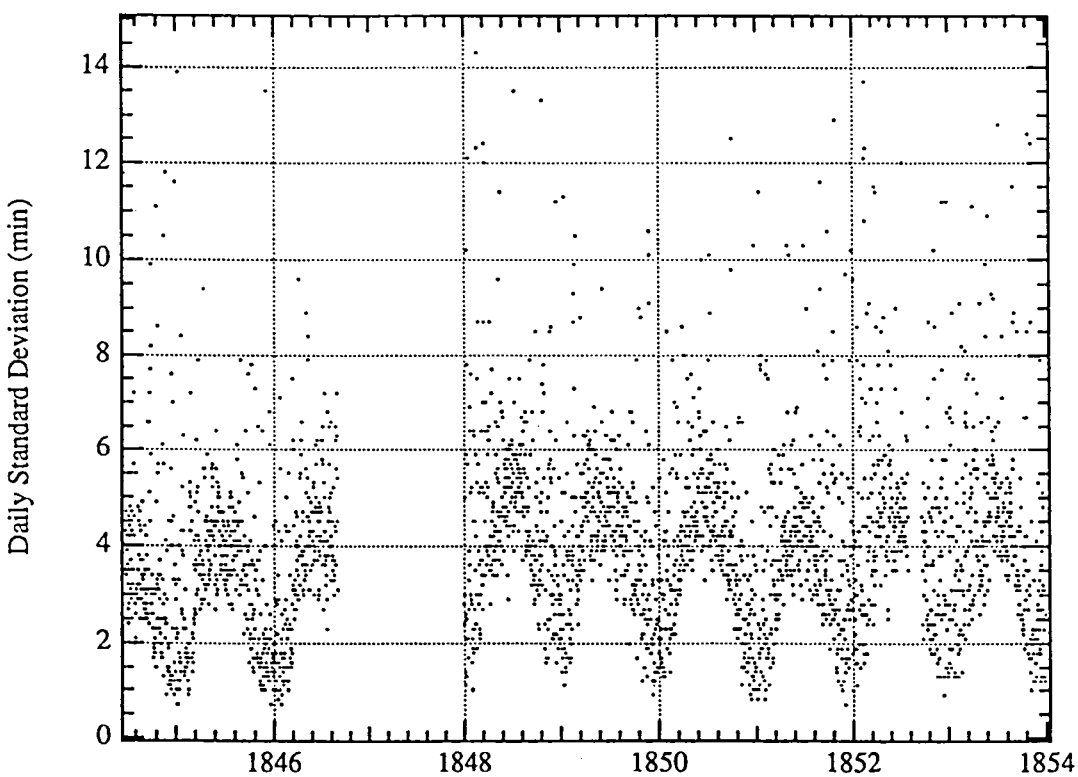

Fig. 4. Standard deviation (minutes of arc) of 144 daily observations of declination.

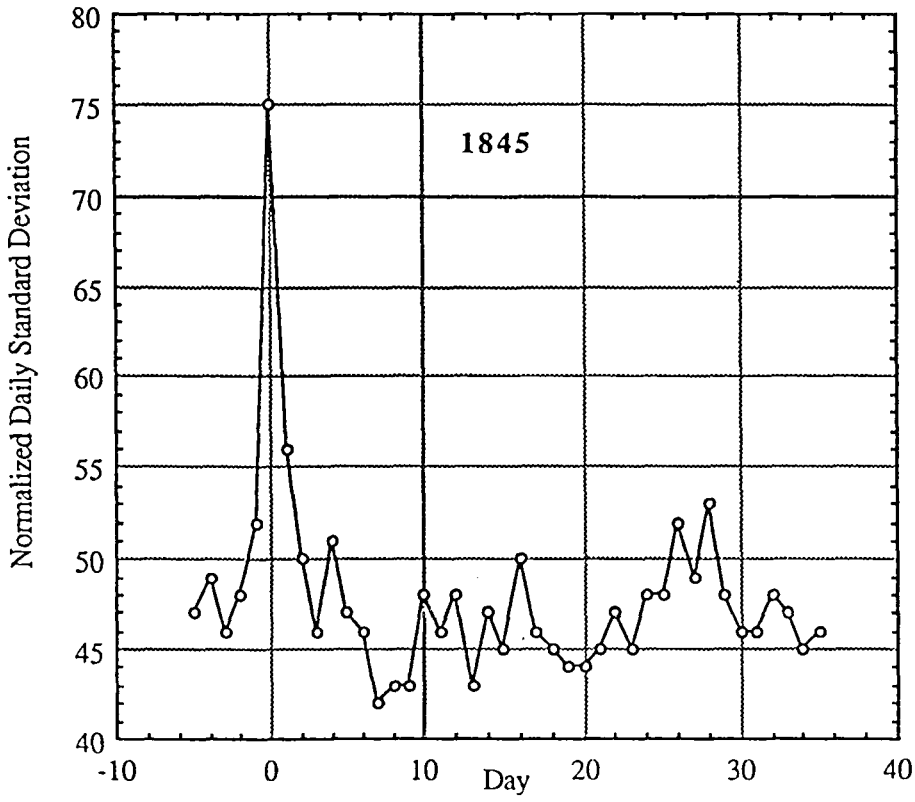

Fig. 5. Superposed epoch analysis of the 27*d* recurrence tendency of magnetic disturbances in 1845. The ordinate is mean daily standard deviation of the 144 declination observations of each day. There is a local maximum at the day 26-28 about one solar rotation after the disturbed zero day.

4 CONCLUSIONS

Preliminary results from the 10 minute declination observations of Helsinki magnetic-meteorological observatory (1844-1853) have been demonstrated here. The data are of good quality, reliable and reveal all typical regular and nonregular features of the time varying geomagnetic field, e.g. diurnal, daily, 27 *d* storm recurrence, annual variation due to external sources, and the internal secular variation. The level of magnetic activity is measured by the daily standard deviation and by differences between successive daily means and their monthly averages. However, they are not the best available indices for many reasons (*Mayaud*, 1980) It is, therefore planned to calculate the 3 hour *K*-indices and daily *Ak* numbers derived from them as they better reflect the magnetic activity than statistical parameters and are easily calculated from computer readable data. Recently there have been developed many algorithms suitable for determining *K*-indices directly from digital magnetic data (e.g. *Sucksdorff et al.*, 1991).

Table A. An example of monthly tables of daily averages and other statistical parameters of declination observations to be published in the series *Geophysical Publications of the Finnish Meteorological Institute* in spring 1992

H E L S I N K I D E C L I N A T I O N 1 8 5 2

YEAR	MONTH	DAY	D	N	STD	RANGE	DIFF.	R
1852	Dec	1	1.34	141	3.3	24.8	2.1	48
1852	Dec	2	1.33	144	4.7	34.2	-0.5	50
1852	Dec	3	1.34	143	2.6	17.2	1.1	49
1852	Dec	4	1.36	144	3.9	21.2	1.1	43
1852	Dec	5	1.36	144	2.6	12.7	0.1	58
1852	Dec	6	1.33	144	5.2	33.4	-1.9	42
1852	Dec	7	1.35	144	2.5	12.0	1.2	43
1852	Dec	8	1.35	144	3.8	21.0	-0.4	29
1852	Dec	9	1.35	142	5.4	37.6	-0.1	40
1852	Dec	10 d3	1.35	144	7.7	47.0	0.5	35
1852	Dec	11	1.37	144	4.3	23.3	0.9	33
1852	Dec	12 d1	1.27	143	11.2	63.7	-5.6	27
1852	Dec	13	1.37	142	5.8	44.6	5.5	28
1852	Dec	14	1.37	143	3.0	18.8	0.4	26
1852	Dec	15 q3	1.35	143	1.3	6.9	-1.1	21
1852	Dec	16 q1	1.34	141	0.9	4.5	-0.8	28
1852	Dec	17	1.36	144	2.6	11.3	0.9	30
1852	Dec	18	1.37	144	4.5	31.3	0.6	25
1852	Dec	19	1.34	143	2.8	15.1	-1.3	19
1852	Dec	20	1.36	143	2.9	15.8	1.2	28
1852	Dec	21 q5	1.34	142	1.5	8.3	-1.4	26
1852	Dec	22	1.36	144	4.5	23.1	1.2	15
1852	Dec	23 d5	1.37	141	5.8	31.9	0.7	18
1852	Dec	24	1.37	143	4.8	24.2	0.0	69
1852	Dec	25	1.37	143	5.0	30.0	-0.3	72
1852	Dec	26	1.35	143	2.3	19.8	-1.1	78
1852	Dec	27	1.34	144	1.5	7.3	-0.4	82
1852	Dec	28 d4	1.30	143	6.8	33.4	-2.2	76
1852	Dec	29 d2	1.44	143	11.2	52.2	8.2	111
1852	Dec	30 q4	1.36	143	1.4	7.0	-4.9	92
1852	Dec	31 q2	1.36	143	1.3	6.3	-0.1	65

Means			D	STD1	STD	RANGE	DIFF.	R
1852	Dec	All	1.35	1.5	4.1	23.9	0.1	45.4
1852	Dec	Quiet	1.35	0.5	1.3	6.6	-1.7	46.4
1852	Dec	Dist.	1.35	3.4	8.5	45.6	0.3	53.4

```
D     = Daily mean of relative declination (degrees)
N     = Number of observations (max N = 144)
STD   = Standard deviation of momentary values of D (minutes)
STD1  = Standard deviation of daily means (minutes)
DIFF.= Difference of successive daily means
R     = Daily sunspotnumber
Daily Range = max D - min D (minutes)
d1...5      = five most disturbed days
q1...5      = five most quiet days

Approximate absolute monthly mean of D (all days) is  -8.15 (west)
and calculated from a polynomial model                 -8.03

Maximum momentary value of D is     -7.48  (Dec 29)
Minimum momentary value of D is     -8.89  (Dec 12)
```

REFERENCES

Barraclough, D.R., 1974. Spherical harmonic analyses of the geomagnetic field for eight epochs between 1600 and 1910. *Geophys. JR astron. Soc.*, 36, 497-513.

Laursen, V. and Olsen, J., 1971. Classical methods of geomagnetic observations. In. Encyclopedia of Physics (S. Flügge, ed.) p. 277-322, Springer Verlag.

Mayaud, P.N., 1980. Derivation, meaning and use of geomagnetic indic es. *Geophys. Monogr.*, 22, 154p., AGU, Washington, DC.

Nervander, J.J., 1850. Observations a L'observatoire Magnetique et Meteorologique de Helsingfors 1844-1848, Tome I-IV.

Nevanlinna, H., 1979 The geomagnetic field and its secular variation in Finland and nearby countries. *J. Geophys.*, 46, 201-216.

Sucksdorff, C., Pirjola, R. and Häkkinen, L., 1991. Computer production of K-indices based on linear elimination. *Geophys. Trans.* 1991, 36, 333-345.

SURVEY DATA FOR GEOMAGNETIC FIELD MODELLING

D. R. Barraclough, S. Macmillan
Geomagnetism Group, British Geological Survey, Edinburgh, UK

1. Introduction

The survey data to be discussed here are based on observations made relatively recently at points on land. A special subset of land survey data consists of those made at specially designated sites known as repeat stations. This class of data will be discussed in another part of this document (Barton, 1991b), so only the briefest of references will be made to repeat stations here.

This discussion of "ordinary" land survey data will begin with a description of the spatial and temporal distributions of available survey data based on observations made since 1900. (The reason for this rather arbitrary choice of cut-off date is that this was the value used in the production of the computer file of magnetic survey data (land, sea, air, satellite, rocket) that is the primary source of data for geomagnetic main-field modelling and for much of this paper.) This is followed by a description of the various types of error to which these survey data are, or may be, subject and a discussion of the likely effects of such errors on field models produced from the data. Finally, there is a short section on the availability of geomagnetic survey data, which also describes how the data files are maintained.

2. Spatial distribution of geomagnetic survey data

For convenience of data storage and manipulation we at BGS have split the very large file of global post-1900 geomagnetic survey data, an earlier version of which has been described by Fabiano & Cain (1971), into (at present) 18 smaller and more manageable files each containing data based on observations made during a five-year interval centred on epoch T_0, where T_0 is chosen to be a multiple of 5. Each file contains data for times (t) in the range $(T_0 - 2.5) \leq t < (T_0 + 2.5)$. The earliest and latest time windows are slightly non-standard, the earliest being 7.5 years long (containing data with epochs in the range $1900.0 \leq t < 1907.5$) and the latest currently rather shorter than 5 years (containing data for 1987.5 onwards).

Each data record in the files has an associated data-type code, a value of 1 indicating land survey data and 9 signifying repeat station data. The positions of all land survey data for each of the 18 time windows are plotted on the maps shown in Figures 1 to 18, inclusive. Similar plots of repeat station positions are given in Barton (1991b).

Figure 1 shows dense data coverage over the USA (though many of these should probably be coded as repeat station data) and Mexico, in south-eastern Europe, in India and in Indonesia. Note also the data in the Arctic and Antarctic, representing the beginnings of modern polar exploration and research. The global data coverage is quite good.

Some explanation is needed for the "land survey" positions in Figure 6 that lie in the Atlantic and Pacific Oceans. These are positions of observations made on the last cruise of the *Carnegie* (the Carnegie Institution of Washington's specially built non-magnetic ship) in 1928 and 1929. Most of them have been coded as land survey observations in error and will be

re-coded as marine data in the near future (almost certainly before this report is published).

Comparison with the plots of repeat station positions shows that, in the early years of this century, most land magnetic observations aimed at a detailed, once and for all coverage of the territory concerned rather than the establishment and systematic reoccupation of a network of repeat stations. That this was deliberate policy is illustrated by the following quotation from Bemmelen (1909).

> In a list inserted at the end of the present work (table I) a short description of each station is given. The writer did not enter into full details in composing the same, as it seems of little value to him, whether observations may be made on the very same spot by another later on. For, if the magnetic field at that station is so disturbed as to render it expedient to be at the same place as the former surveyor, the secular variation, which necessitates a repeated observation, will be abnormal. And if the field is undisturbed there is no call for an observation in exactly the same spot.

These arguments would by no means be accepted today, but the trend noted above continues until after the second World War.

Figure 12, for the interval 1957.5-62.5, includes the International Geophysical Year and the associated World Magnetic Survey programme (Zmuda, 1971). It shows a good coverage of all the major land masses except for southern Asia. The enhanced activity in the polar regions (particularly in Antarctica) is noteworthy. Many of the Arctic data are based on observations made on floating ice islands - it is not immediately obvious whether these should be classified as land or marine data.

A jump of ten years, to the interval 1967.5-72.5 (Figure 14), shows much reduced activity in ordinary land magnetic surveying, and this trend has continued up to the present (some of the 1982.5-87.5 land survey data shown in Figure 17 should probably be coded as repeat stations).

Readers with a knowledge of their national magnetic surveying activities (past and present) are asked to study carefully Figures 1 to 18, inclusive, (and the equivalent Figures in Barton, 1991b) and to report any errors or omissions to one of the World Data Centres mentioned in Section 5.

3. Temporal distribution of geomagnetic survey data

Figure 19 shows the distribution of land survey data with time from 1900 to the present. Each block represents the number of observations made in the 12 months centred on the beginning of the indicated year. The enormous spike (61452 observations) represents mainly data for the USSR reduced to epoch 1940.5 and used for producing magnetic charts of the USSR for that epoch. There may well be some duplication here, because it is suspected that many of the (unreduced) observations are also in the files under their date of observation, derived from the comprehensive collection of Veinberg (Veinberg, 1929, 1932; Veinberg & Rogachev 1933). The next largest block (11122 observations) consists mainly of observations of declination reduced to epoch 1944.5 and used by Bock (1948) in producing his series of declination charts for Europe. Many of the 8647 observations centred on 1985.0 were collected in connection with the production of a mathematical model of the declination for

Europe for this epoch. The increased data sampling centred at about 1915 represents the Carnegie Institution's global surveying efforts.

4. Errors in geomagnetic survey data

The following errors will be considered: errors produced in the process of transcribing the data into computer files, including the presence in the files of duplicate data; uncertainties in the positions of the data points; and sources of what, from the point of view of modelling the main geomagnetic field and its secular variation, constitutes noise.

4.1 Errors of transcription

Gross errors of transcription, such as transposing latitude and longitude, entering colatitude for latitude or *vice versa*, or getting the sign wrong for one of the values entered, are usually detectable without too much difficulty. A standard screening technique (see, for example, Langel *et al.*, 1988) for such errors is to compare the observed values with values computed from a global geomagnetic field model such as the International Geomagnetic Reference Field (IGRF) (Barraclough, 1987) and to examine closely any residuals (observed value minus computed value) that are large in absolute magnitude. Large is usually taken to be about 1000 nT, the elements declination (D) and inclination (I) being first converted from angular measure to nanoteslas. (Here, and in this rest of the paper, reference to the IGRF is to be taken to mean the set of definitive (DGRF) and preliminary (PGRF) models that constitute the fourth generation of the IGRF.) Gross transcription errors and the corrections needed are usually immediately obvious, though reference to the original source is sometimes necessary and always desirable. More subtle transcription errors are only detectable by comparing every single observed value with the corresponding value in the original source. This has never, to our knowledge, been attempted and it must therefore be presumed that some, at least, of these smaller errors exist in the dataset.

4.2 Self-consistency

Each record of survey data contains values of the elements observed and also values of those other elements that can be computed from them. It is easy to check that these computed values are correct but, as far as we are aware, this has never been done systematically for the whole dataset. Most modellers use only values of the observed elements, so this particular quality control deficiency is probably not of great practical importance.

4.3 Duplication

It is surprisingly easy for the same information to get into the dataset more than once. Such duplication, if left uncorrected would invalidate any carefully considered scheme for the relative weighting of data in the modelling process. The group at the Goddard Space Flight Center has done a great deal to detect and delete duplicate data and it can be assumed that there remain very few such records remain in the survey data files.

4.4 Data uncertainties

We turn now to a consideration of the uncertainties in the values that are now assumed to be correct in the sense that they accurately reflect the values in the original sources. Typical values from the surveying activities in the UK (described in more detail in the UK section of Barton, 1991a), which apply equally to repeat station and ordinary land survey sites, will be used as examples.

4.4.1 Positional uncertainties

There will be an uncertainty in the positional coordinates assigned to a survey site. For the UK sites, the position, in National Grid coordinates, in metres, is read off from a 1:50000 map of the area surrounding the site, and the accuracies of the coordinates derived in this way are estimated to be rather less than ± 100 m. That these are reasonably accurate estimates was verified by using a GPS receiver at a selection of sites during the 1990 field season. A typical modern land survey observation should thus certainly have an uncertainty in its position of better than ± 0.1′ in latitude and longitude (i.e. approximately 0.001°, which is the precision of the colatitude and longitude values in the survey data files). Data from earlier this century might possibly have greater positional uncertainties, but these should not exceed about ± 1 km or about ± 0.01°. Even these larger uncertainties are relatively unimportant for main-field modelling purposes.

4.4.2 Uncertainties in the magnetic elements

The observed values of the magnetic elements will also have uncertainties associated with them. In the UK surveys D and I are measured with a fluxgate mounted on a non-magnetic theodolite acting as a null detector and the total intensity (F) is measured using a proton magnetometer. The field observations are estimated to be accurate to about ± 0.1′ for D and I and ± 1 nT for F. These field observations are then corrected as far as possible for the effects of external electric currents (daily variations and magnetic disturbance) by using data from the three UK magnetic observatories, giving values reduced to a quiet field level near the time of observation. Estimates of the uncertainties in these reduced values are ± 1.0′ for D, ± 0.5′ for I and ± 5 nT for F.

Other modern survey results quote values broadly in agreement with these estimates, as can be seen in Table 1 (H is the horizontal intensity and Z is the vertical component).

Table 1. Typical uncertainties quoted for modern land survey data

Type	$D(')$	$I(')$	H(nT)	Z(nT)	F(nT)
Field	0.2	0.1	2	2	3
Reduced	1.5	0.8	6	6	5

For earlier epochs, the uncertainties in D are probably about the same as these. The use of

dip needles or earth inductors for measuring I implies larger uncertainties, probably of ± 0.5′ to ± 1′ for the field observations and 3 to 4 times these estimates for the reduced values. Before the use of proton magnetometers became widespread in about 1960, the uncertainties in the force elements (usually H and Z) were several tens of nanoteslas for the field observations and about twice this for the reduced observations.

4.5 Sources of noise

From the point of view of main-field modelling there are two main sources of noise likely to be present in land survey data: the effects of electric current systems in the ionosphere and magnetosphere; and the effects of differently magnetised crustal rocks.

4.5.1 External noise sources

As mentioned in Section 4.4.2, all well-executed magnetic surveys involve the correction of the resulting field observations for daily variations and magnetic disturbance by using data from neighbouring magnetic observatories or from a specially deployed temporary variometer station.

In the absence of further information it has usually to be assumed that all land survey data in the files have been corrected in this way, although this is almost certainly not the case. This could mean that there are external effects still present in the data ranging from a few tens of nanoteslas for observations in mid-latitudes during reasonable quiet times when the main uncorrected effect is the daily variation to several hundred nanoteslas for observations at auroral latitudes during disturbed times. It is usually assumed that survey observations will not have been made during very disturbed times. This could be checked by using magnetic disturbance indices, such as the *aa* index. Unless the time of day has been included in the data record a fairly coarse check involving the degree of disturbance for the day of the observation would have to be used. This sort of selection of quiet values, though commonly used for aeromagnetic, marine and satellite surveys, has rarely, if ever, been used with land survey data.

4.5.2 Crustal noise sources

Unless the sites of land survey observations have been very carefully chosen, they will all be more or less contaminated (from the point of view of main-field modelling) with short-wavelength signal from crustal sources. In other words they will be more or less anomalous.

The screening procedure described during the discussion of transcription errors in Section 4.1 can be used to flag large anomalies (greater than about 1000 nT) and these can then be omitted from subsequent analyses. Smaller anomalies can be screened out, if the areal density of land survey data is high enough, by taking areal means and applying a Chauvenet-type criterion for data rejection (see, for example, Barraclough, *et al.*, 1975). Here, the mean and standard deviation of the mean are derived for all data within the area concerned. Each individual contributing data point is then compared with the mean value. If it differs from the mean by more than a selected number of standard deviations (we currently use a factor of 2.36), the data point is rejected, the mean and standard deviation are recomputed and the procedure is repeated until no further points are rejected. The procedure will not work when

the area considered contains only a few (less than 10 or so) points.

The screening procedure also produces statistics for the residuals of observed values from a global field model such as the IGRF. Modern data, for example those centred on 1965 whose distribution of residuals is shown in Figure 20, have distributions that peak sharply about a residual of zero and are reasonably symmetrical. A certain amount of skewness is sometimes present as in the case of the data centred on 1980 (Figure 21). Earlier data (approximately, pre-1940) show a greater scatter of residuals, and greater skewness, for example the data centred on 1925 (Figure 22) and those in the earliest time window (Figure 23). In these cases, what we are seeing is mainly caused by defects in the field models used. The series of IGRF models were used for comparison purposes back to 1940, but before that epoch the series of models produced by Vestine *et al.* (1947) (which extend only to spherical harmonic degree and order 6) were used. These models could certainly be improved on and, indeed, such a project is under active consideration.

The statistics for the 18 time windows are summarised in Figure 24 which shows the mean and root-mean-square (rms) residual as functions of time. A typical global value for the rms crustal noise is about 200 nT. The post-1940 data have rms values of about this size. The larger rms (and mean) values for the pre-1940 data are, as just mentioned, probably largely due to model deficiencies.

Figure 25 summarises the statistics of the residuals for the entire post-1900 land survey dataset. The overall mean and rms residuals for the 270749 observations are 20 nT and 295 nT, respectively.

5. Availability and maintenance of land survey data files

The following brief remarks concerning the availability of land survey data and how the dataset is maintained apply equally to the other forms of data used for main-field modelling.

Versions of the post-1900 main-field data files are currently held by World Data Center for Solid Earth Geophysics in Boulder, Colorado; by the Geodynamics Branch at Goddard Space Flight Center; and by World Data Centre C1 for Geomagnetism in Edinburgh.

These versions are similar to one another but are certainly not identical. It is not sensible, with a dataset that is still in the process of being added to and amended, to expect that different versions will ever be identical in their entirety, but we can aim for an improvement over the present situation. The three organisations are making some progress in this direction. Particularly for past data, earlier than about 1970 or 1975, we should be able to move towards a set of data which we all agree is as accurate as we can reasonably get it. More recent data can then be treated as more volatile and subject to additions and amendments.

Our collection procedures are rather haphazard in that, for the most part, we take what comes or is brought to our attention. We are in fairly regular contact with most of the organisations that operate magnetic observatories and, since many of these also carry out magnetic surveys (particularly, nowadays, repeat station surveys), we get many land survey data from them at the same time as they send us their observatory data. This field of data collection and liaising

with the other holders of similar data to ensure that each is at least aware of what data the others hold, is one where quite a lot of work needs to be done.

6. Conclusions

This review of geomagnetic land survey data has attempted to give some idea of what data are available for the time interval from 1900 onwards and how they are distributed spatially and temporally. It has highlighted actual and potential sources of error and assessed their likely magnitude and has briefly discussed the availability and maintenance of the survey data files.

References

Barton, C. E., 1991a. National repeat station network descriptions (IAGA magnetic repeat station reporting scheme), *Bureau Min. Res., Geol. & Geophys. Record* No. 1991/72.

Barton, C. E., 1991b. Magnetic repeat station data, this issue.

Barraclough, D. R., 1987. International Geomagnetic Reference Field: the fourth generation, *Phys. Earth Planet. Inter.*, 48, 279-292.

Barraclough, D. R., Harwood, J. M., Leaton, B. R. & Malin, S. R. C., 1975. A model of the geomagnetic field at epoch 1975, *Geophys. J. Roy. Astr. Soc.*, 43, 645-659.

Bemmelen, W. van, 1909. Magnetic survey of the Dutch East-Indies made in the years 1903-1907, *Obsns. Roy. Magn. Met. Obsy. Batavia*, **30**, Appendix I, 69pp.

Bock, R., 1948. *Atlas of Magnetic Declination of Europe for Epoch 1944.5*. Washington: U.S. Army Map Service.

Fabiano, E. & Cain, S. J., 1971. Coverage by land, sea, and airplane surveys, 1900-1967, in Zmuda (1971), pp.94-98.

Langel R. A., Barraclough, D. R., Kerridge, D. J., Golovkov, V. P., Sabaka, T. J., & Estes, R. H., 1988. Definitive IGRF models for 1945, 1950, 1955, and 1960, *J. Geomagn. Geoelectr.*, **40**, 645-702.

Veinberg B. P., 1929. *Catalogue of Magnetic Determinations in U.S.S.R. and in Adjacent Countries from 1556 to 1926*, Leningrad: Central Geophysical Observatory.

Veinberg B. P., 1932. *Catalogue of Magnetic Determinations in U.S.S.R. and in Adjacent Countries from 1556 to 1926, Part II*, Leningrad: Central Geophysical Observatory.

Veinberg B. P. & Rogachev, I. M., 1933. *Catalogue of Magnetic Determinations in U.S.S.R. and in Adjacent Countries, Part III Determinations made from 19126 to 1930*, Leningrad: Central Geophysical Observatory.

Vestine, E. H., Lange, I., Laporte, L. & Scott, W. E., 1947. The geomagnetic field, its description and analysis, *Publ. Carnegie Inst. Washington*, No. 578.

Zmuda, A. J. (Editor), 1971. World Magnetic Survey 1957-1969, *Bull. Int. Assoc. Geomagn. Aeron.*, No. 28.

Acknowledgements

We thank Ricky Reader for help in producing the figures. This paper is published with the approval of the Director of the British Geological Survey (NERC).

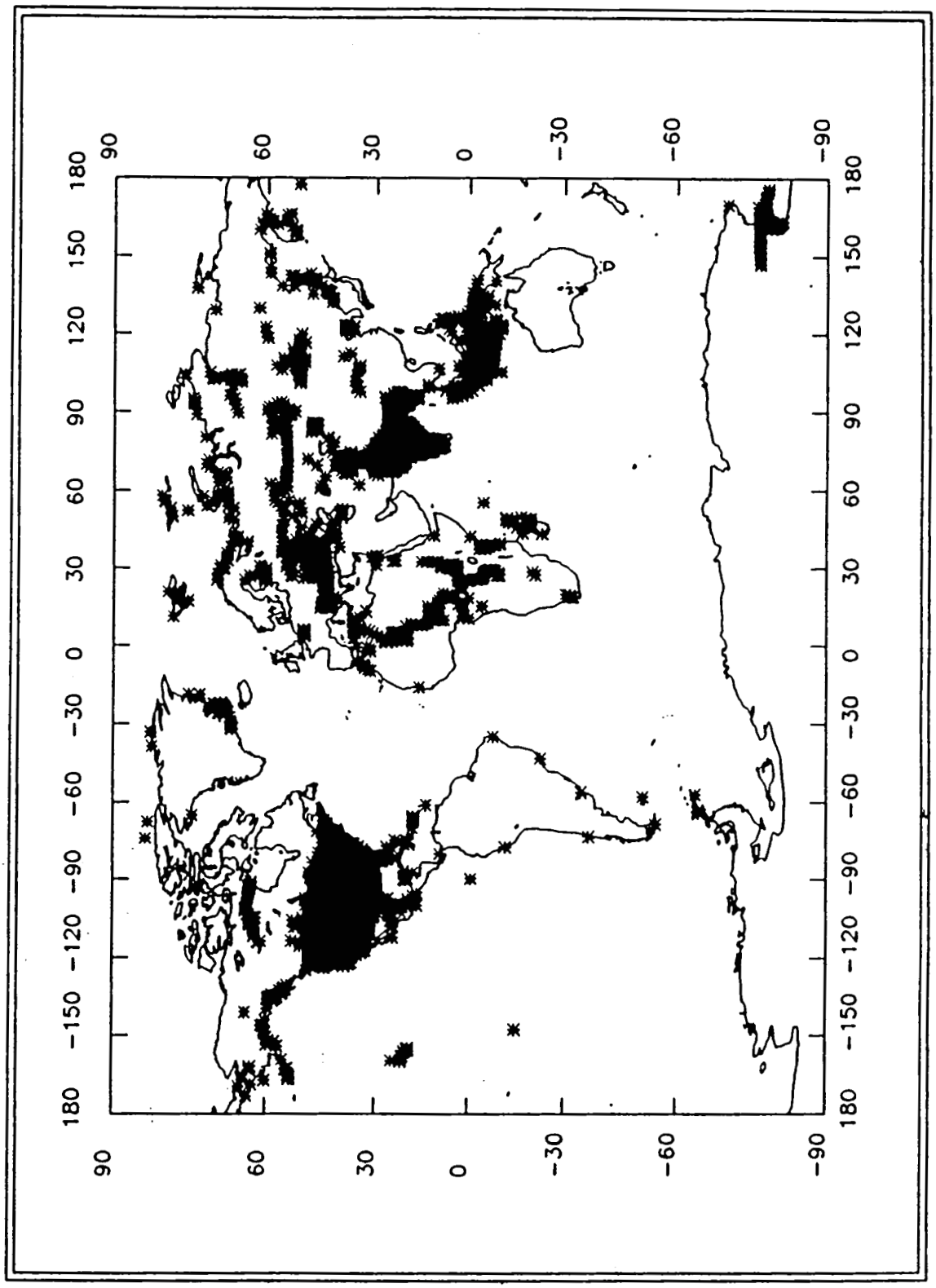

Figure 1. Positions of land survey data based on observations made between 1900.0 and 1907.5.

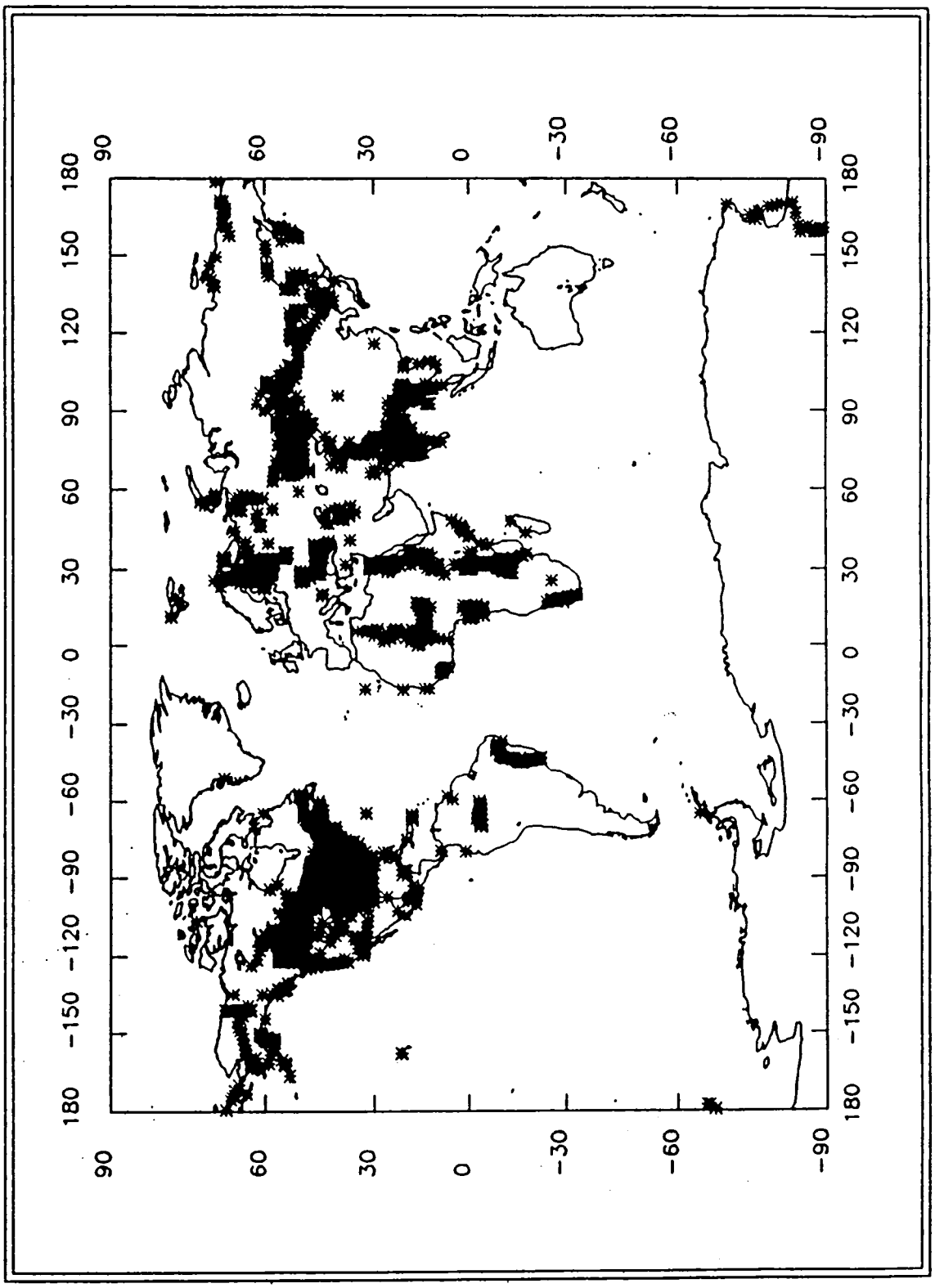

Figure 2. Positions of land survey data based on observations made between 1907.5 and 1912.5.

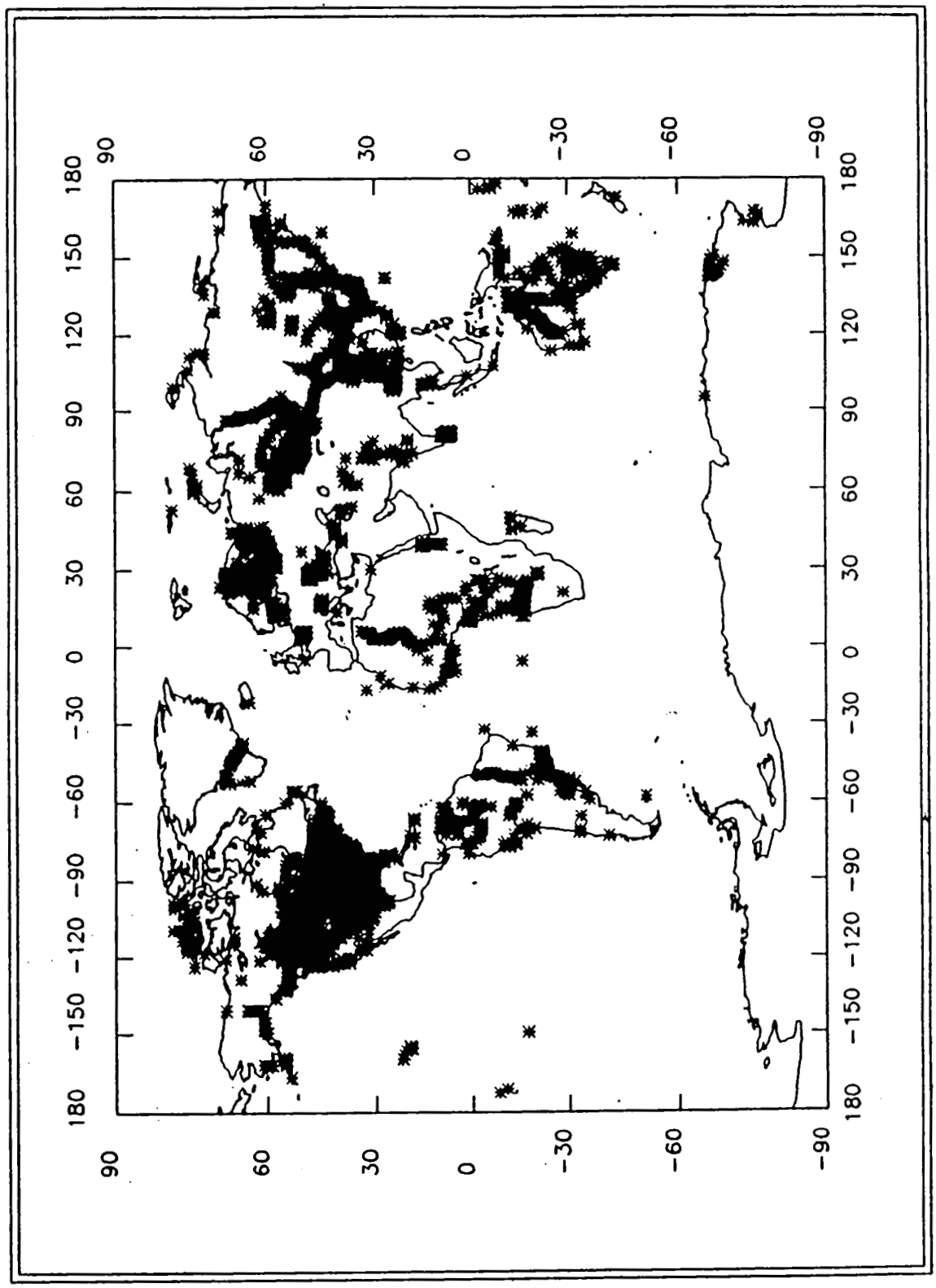

Figure 3. Positions of land survey data based on observations made between 1912.5 and 1917.5.

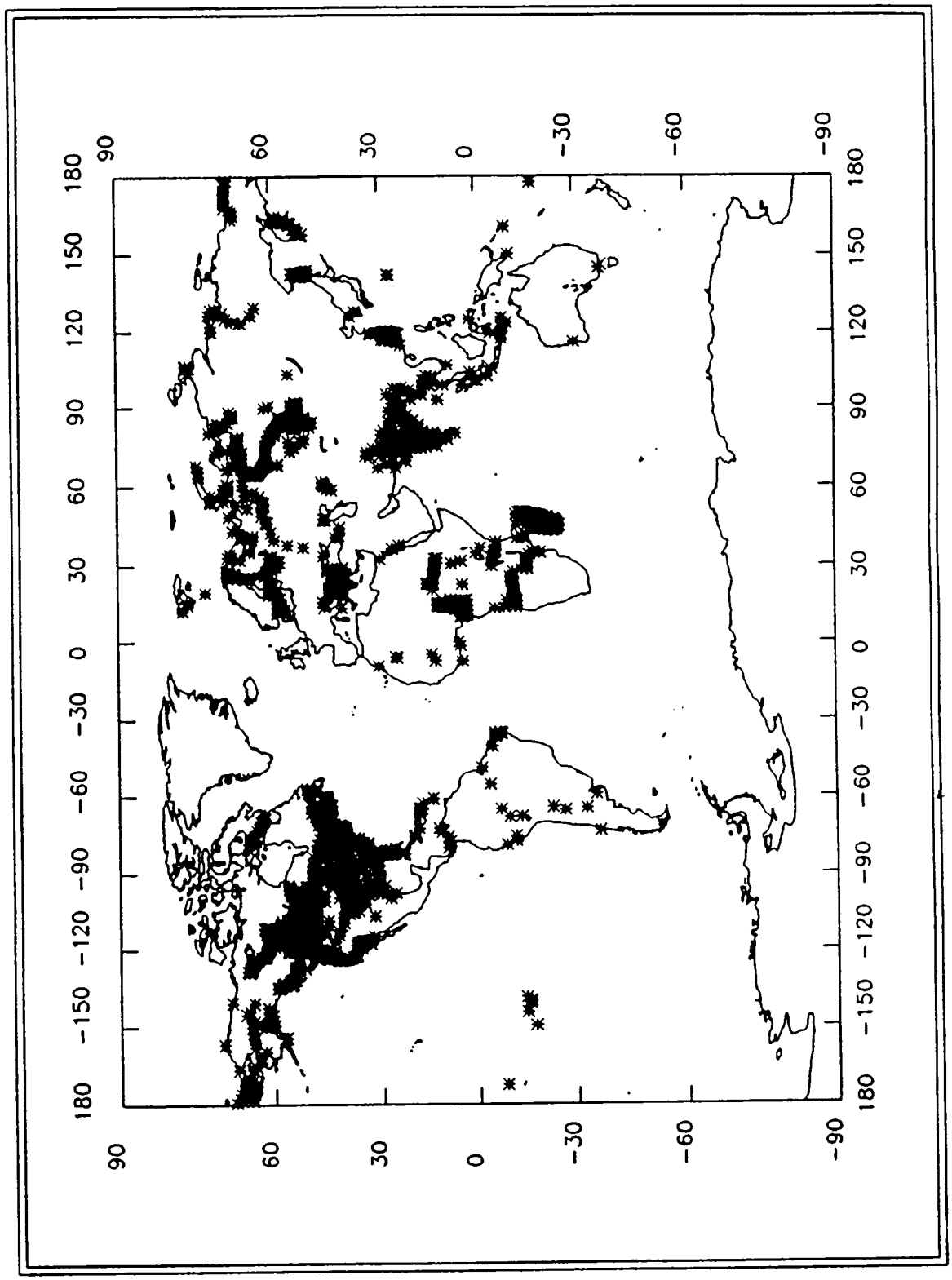

Figure 4. Positions of land survey data based on observations made between 1917.5 and 1922.5.

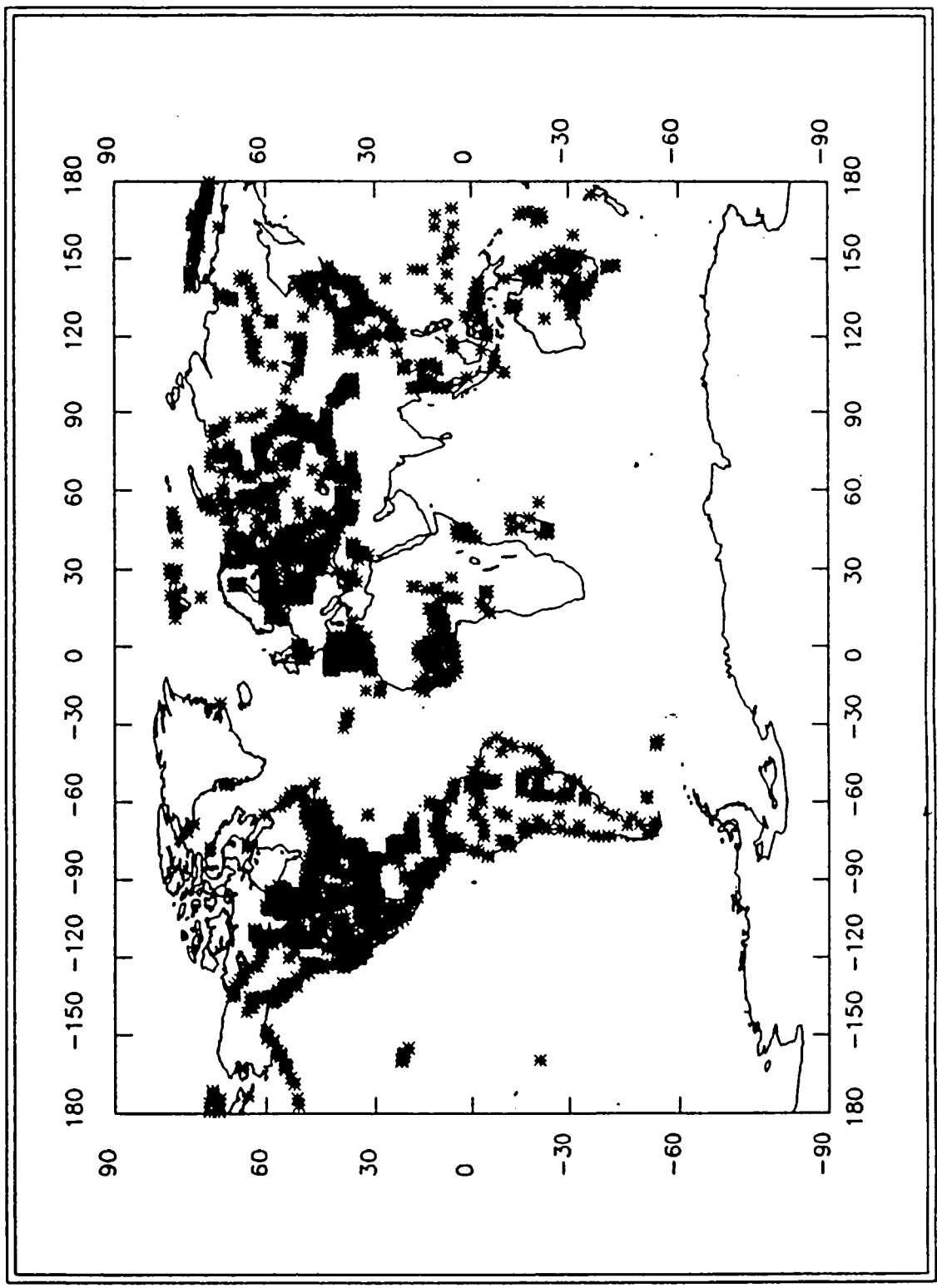

Figure 5. Positions of land survey data based on observations made between 1922.5 and 1927.5.

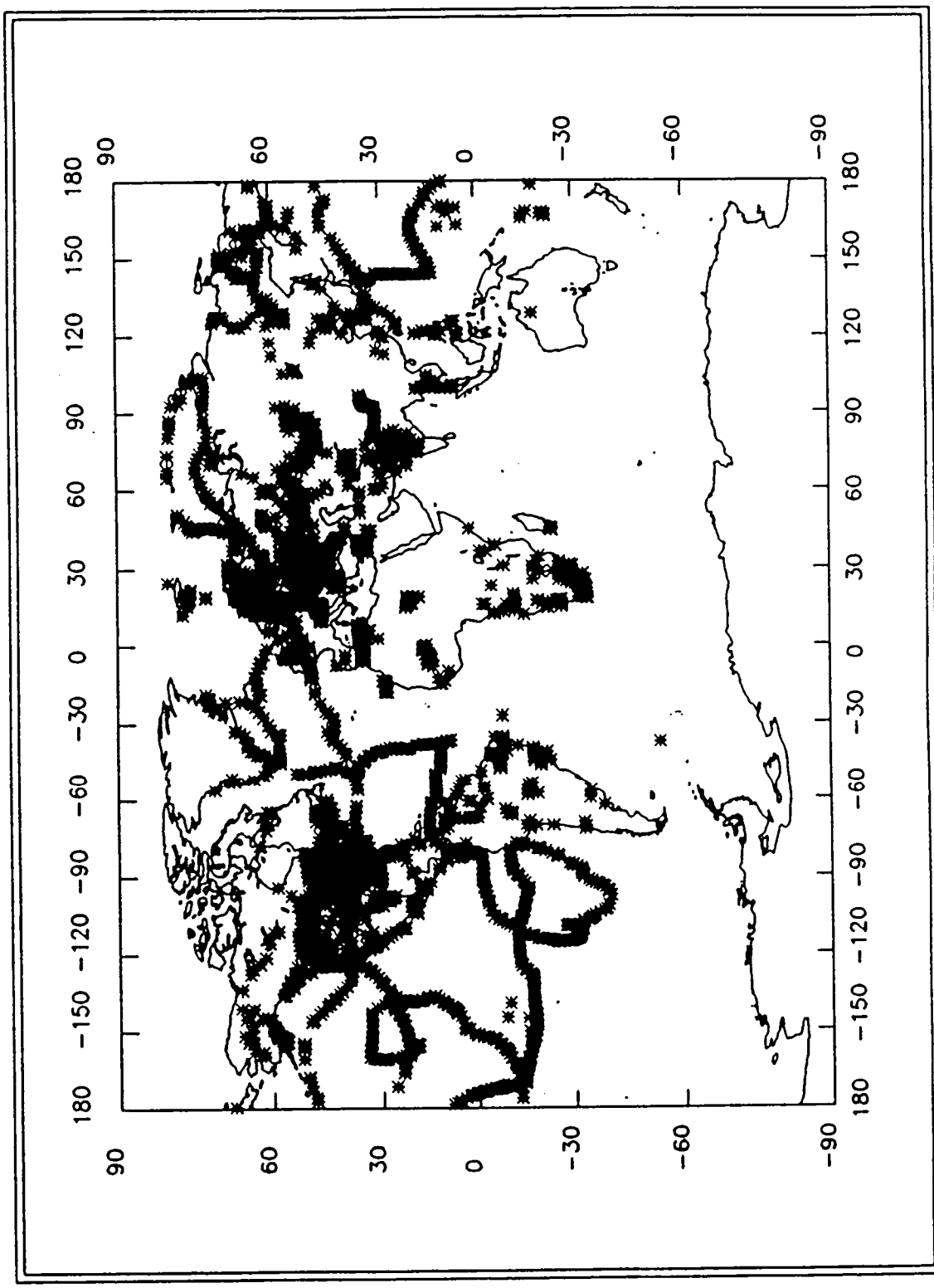

Figure 6. Positions of land survey data based on observations made between 1927.5 and 1932.5.

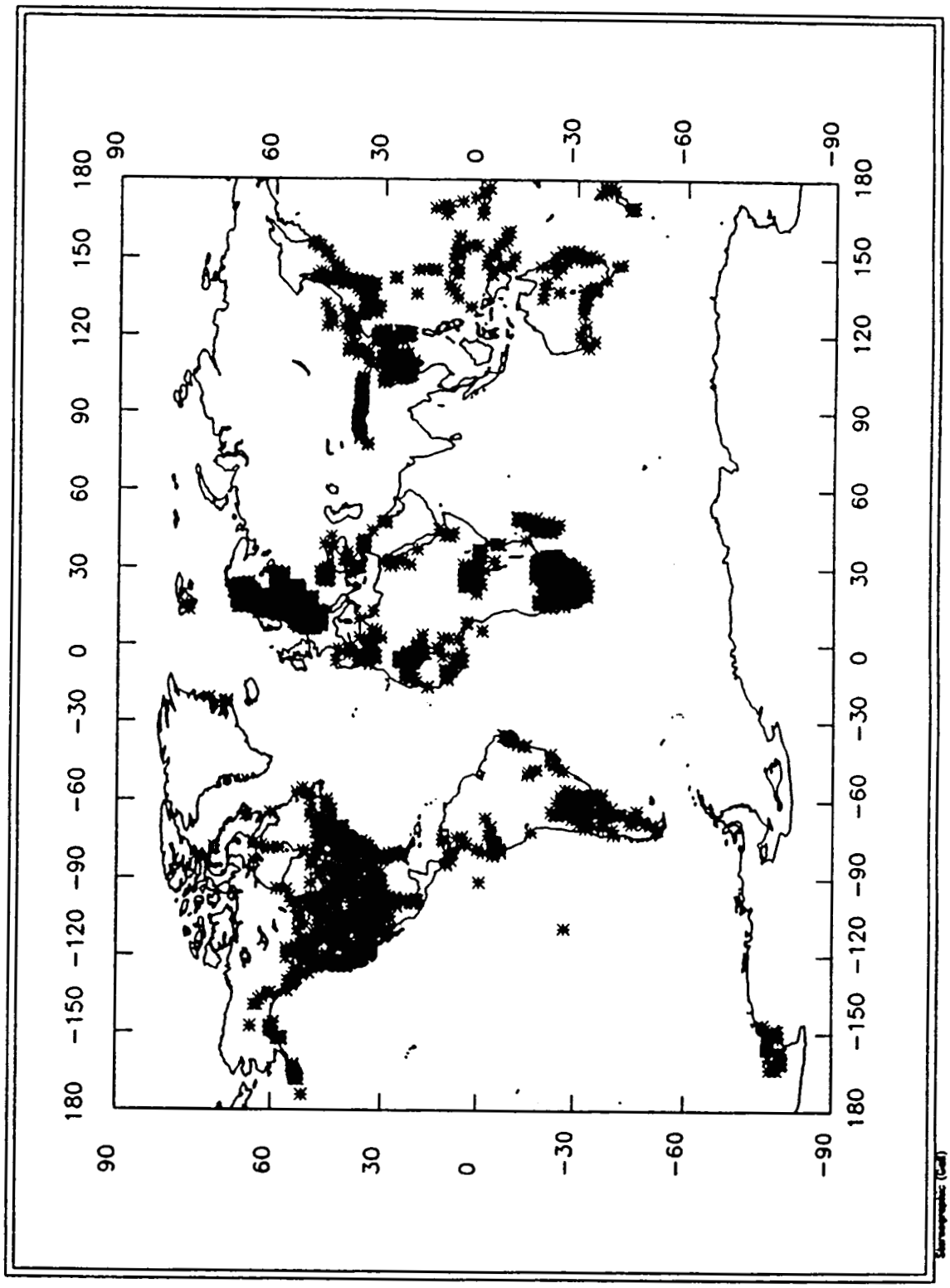

Figure 7. Positions of land survey data based on observations made between 1932.5 and 1937.5.

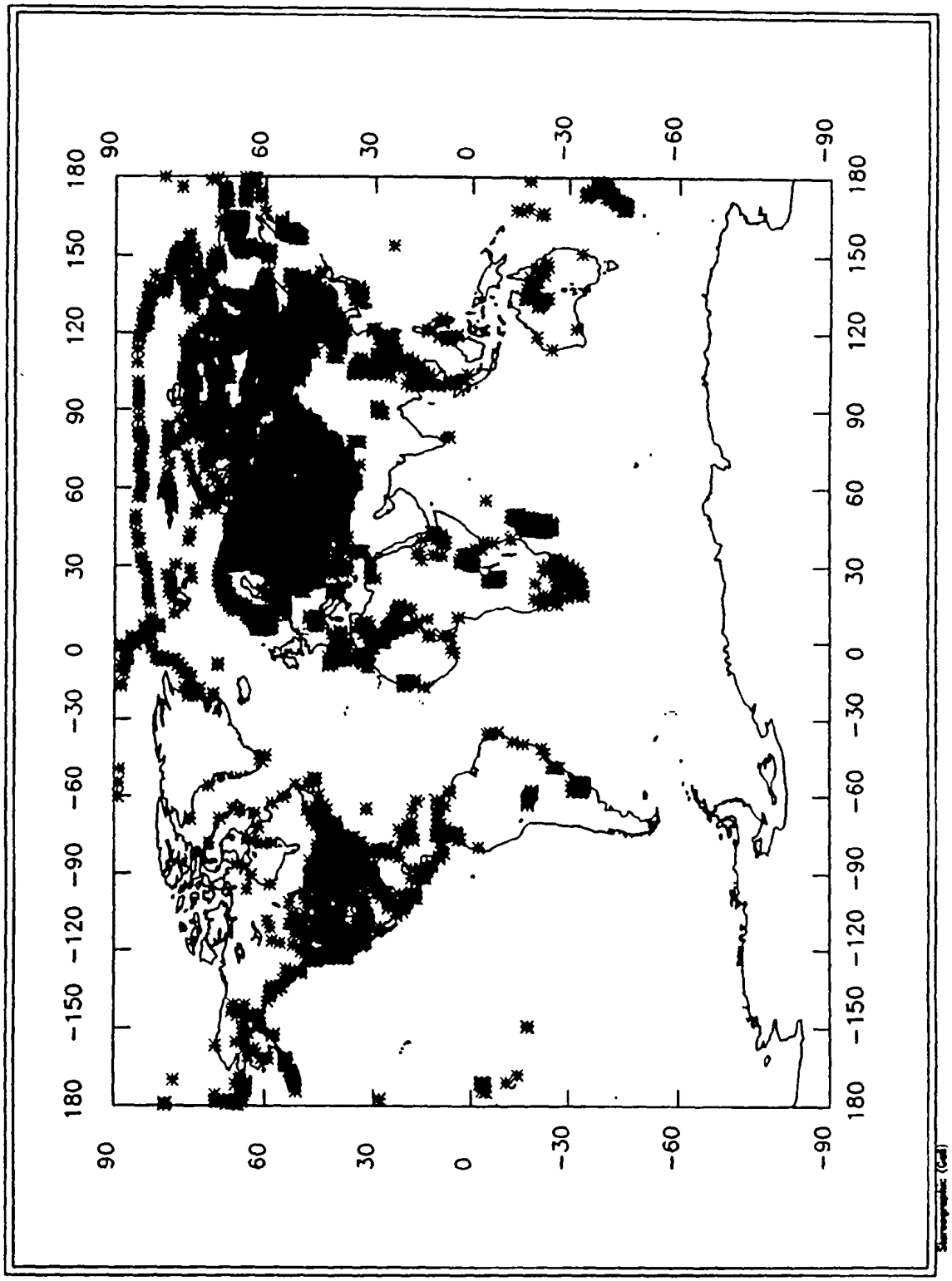

Figure 8. Positions of land survey data based on observations made between 1937.5 and 1942.5.

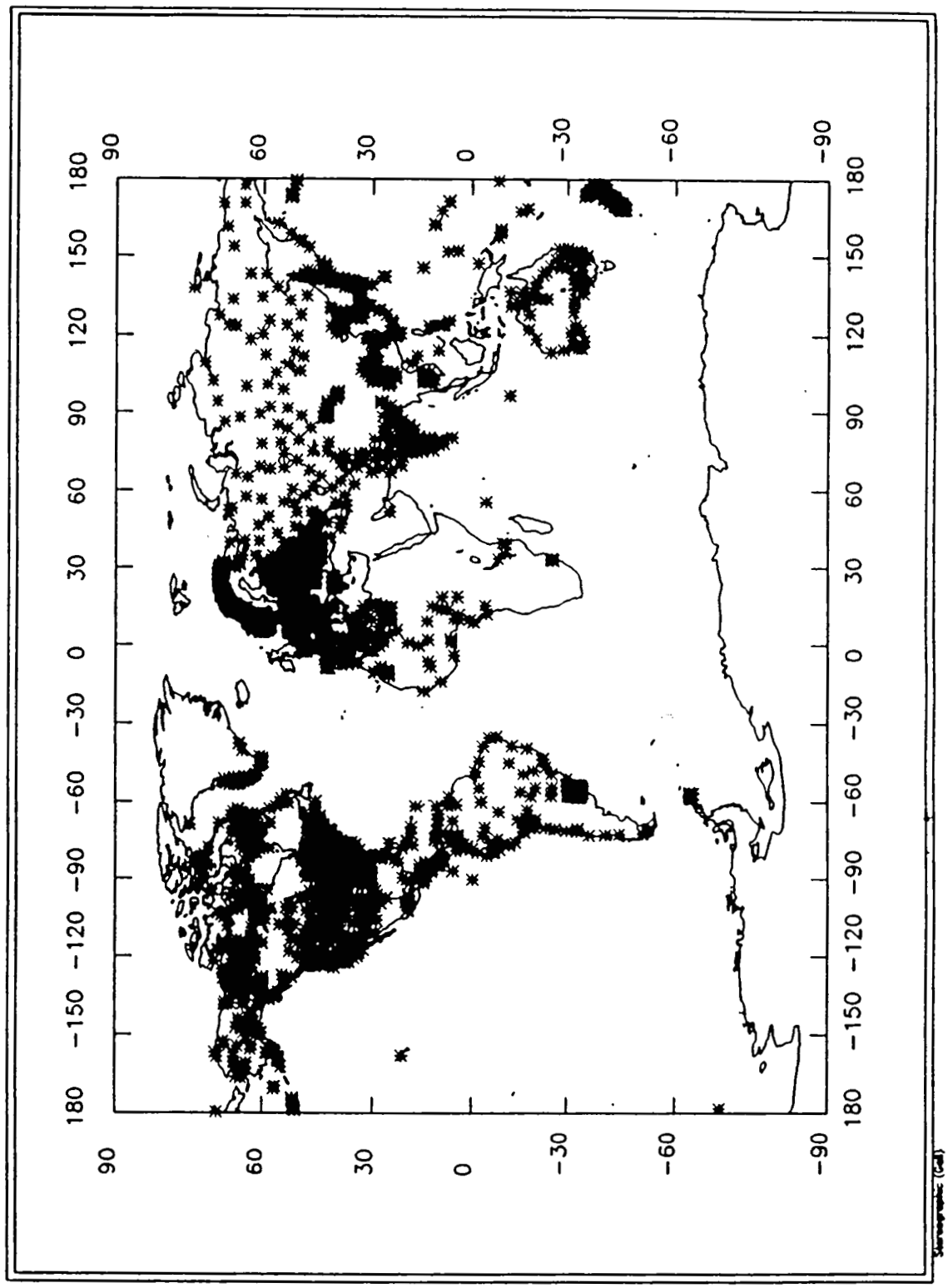

Figure 9. Positions of land survey data based on observations made between 1942.5 and 1947.5.

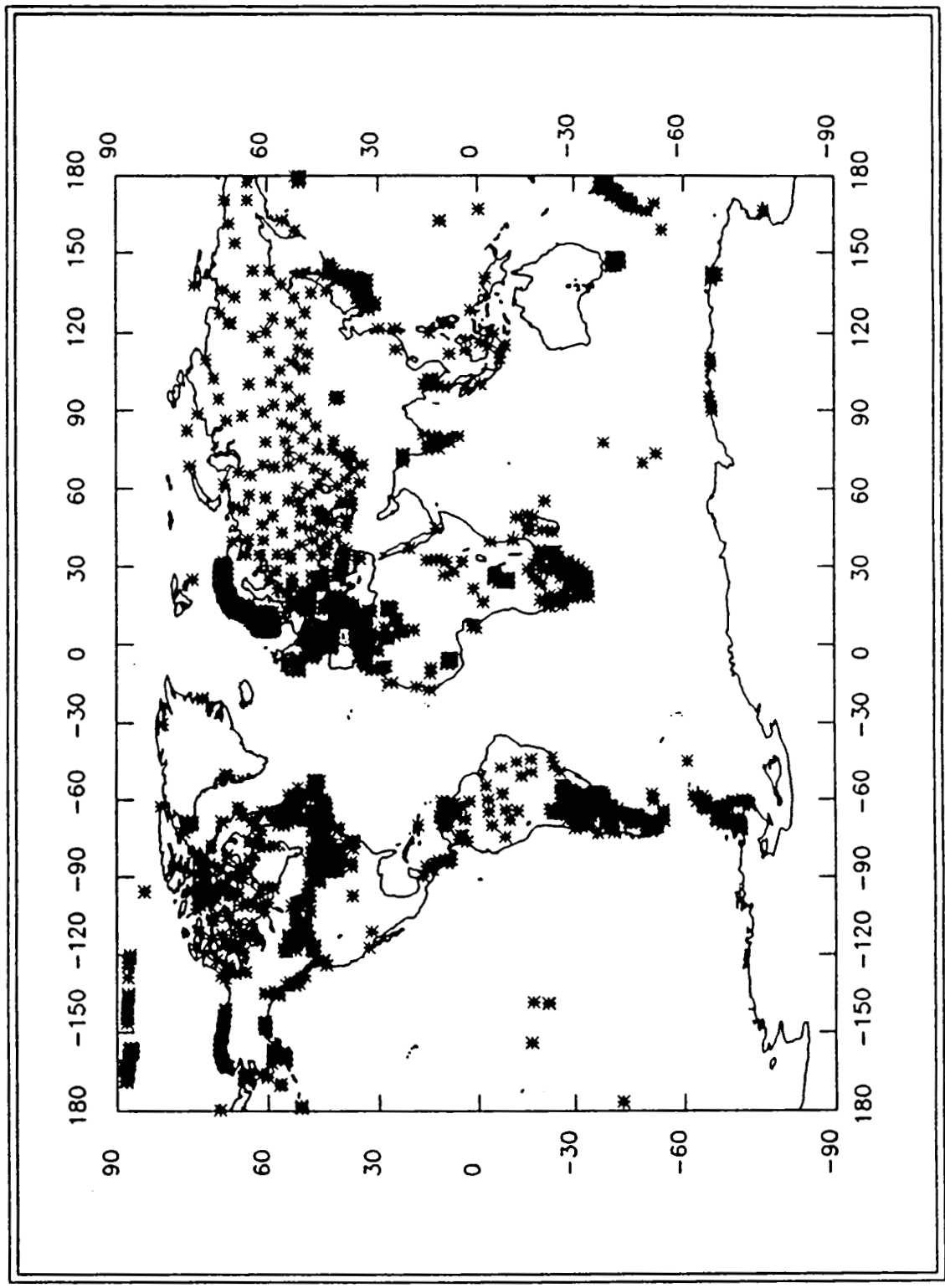

Figure 10. Positions of land survey data based on observations made between 1947.5 and 1952.5.

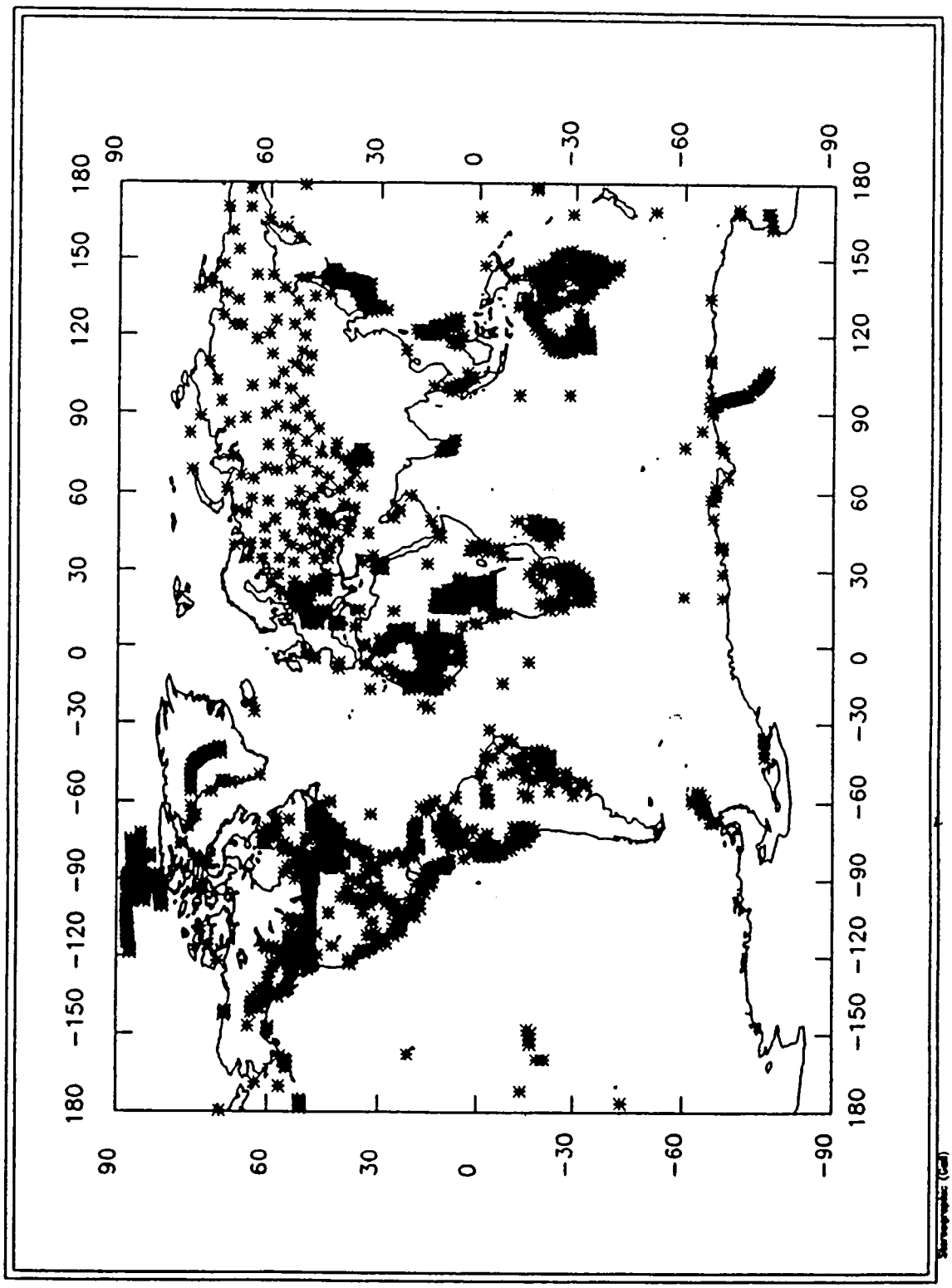

Figure 11. Positions of land survey data based on observations made between 1952.5 and 1957.5.

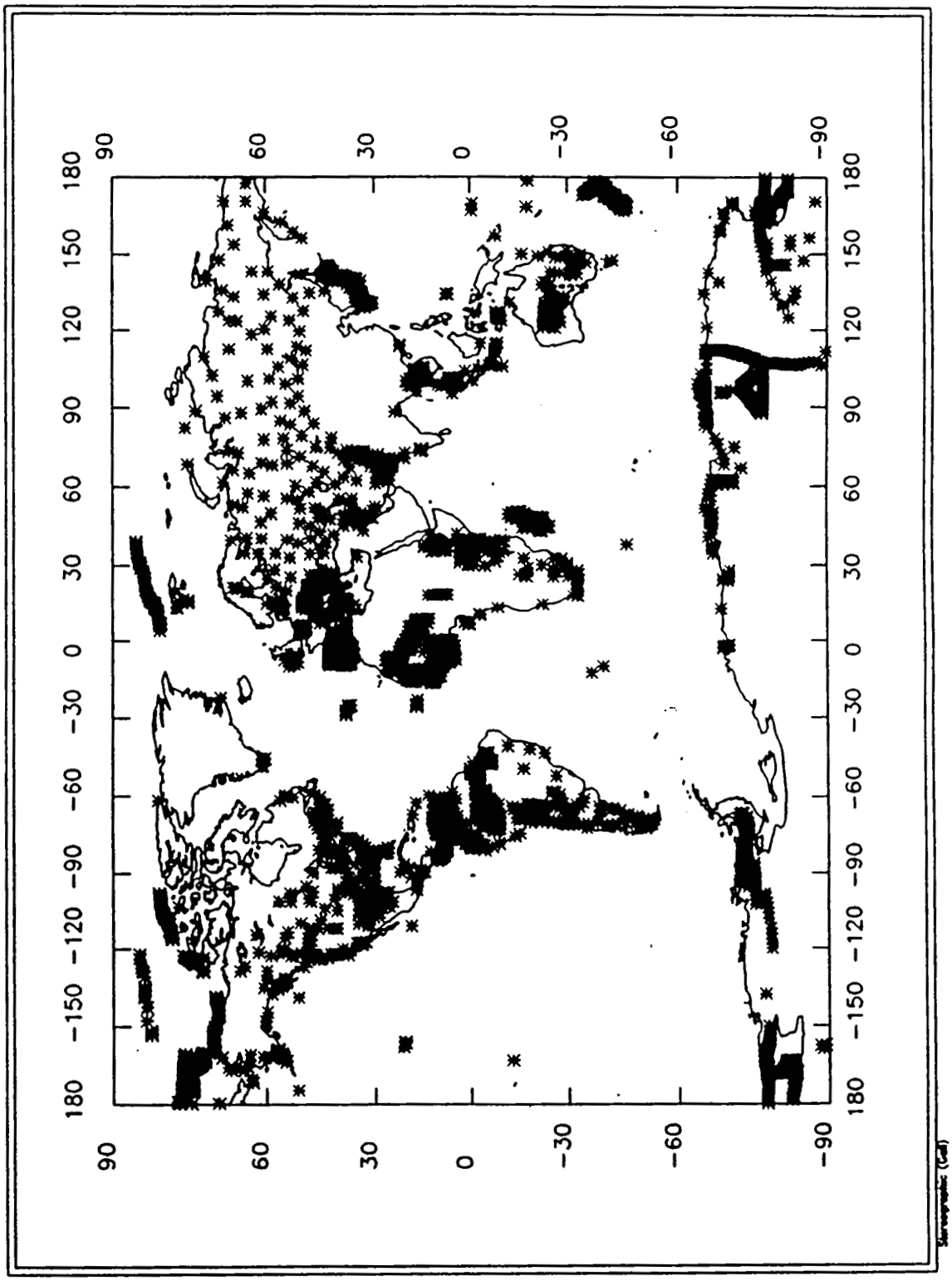

Figure 12. Positions of land survey data based on observations made between 1957.5 and 1962.5.

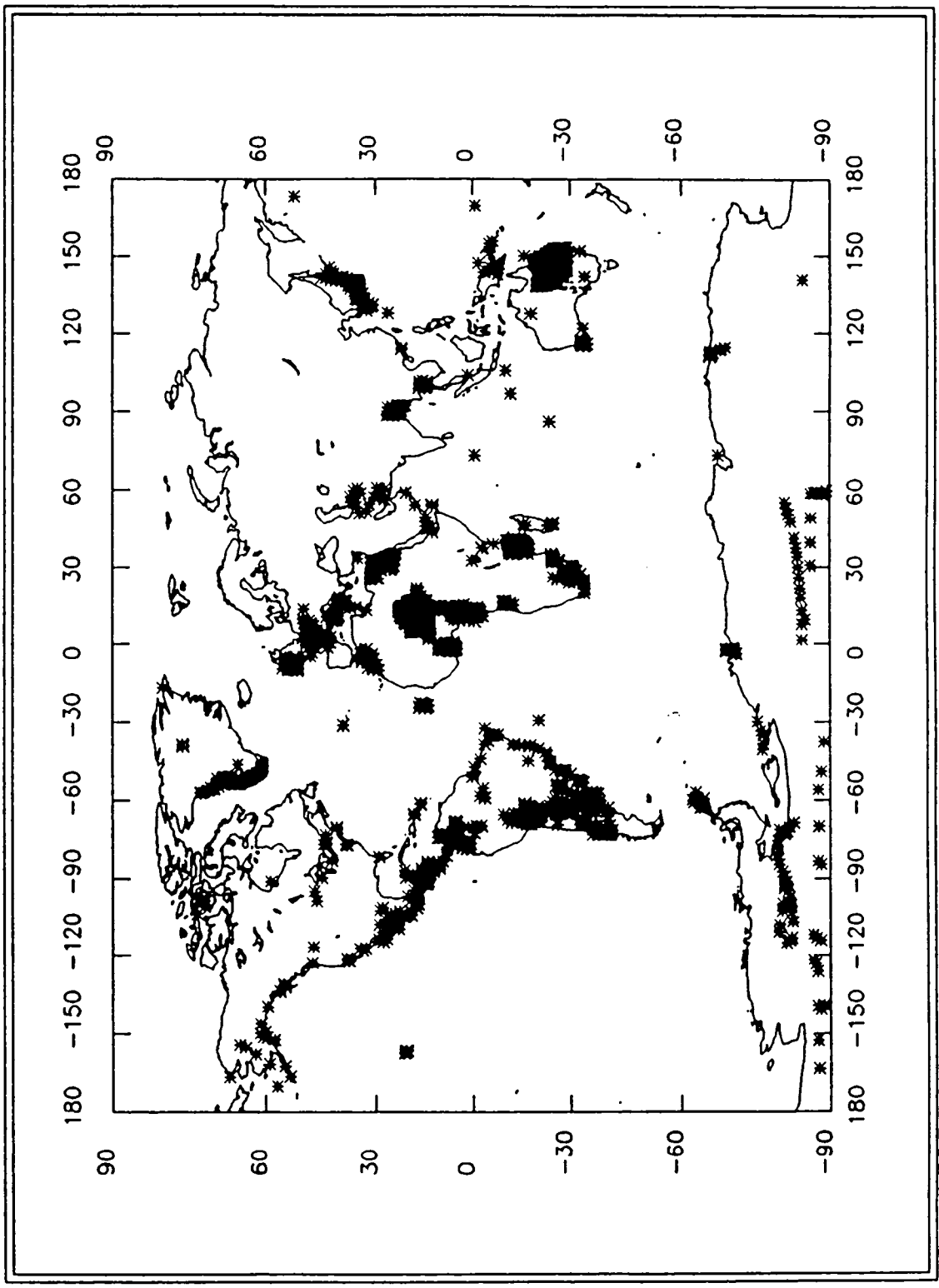

Figure 13. Positions of land survey data based on observations made between 1962.5 and 1967.5.

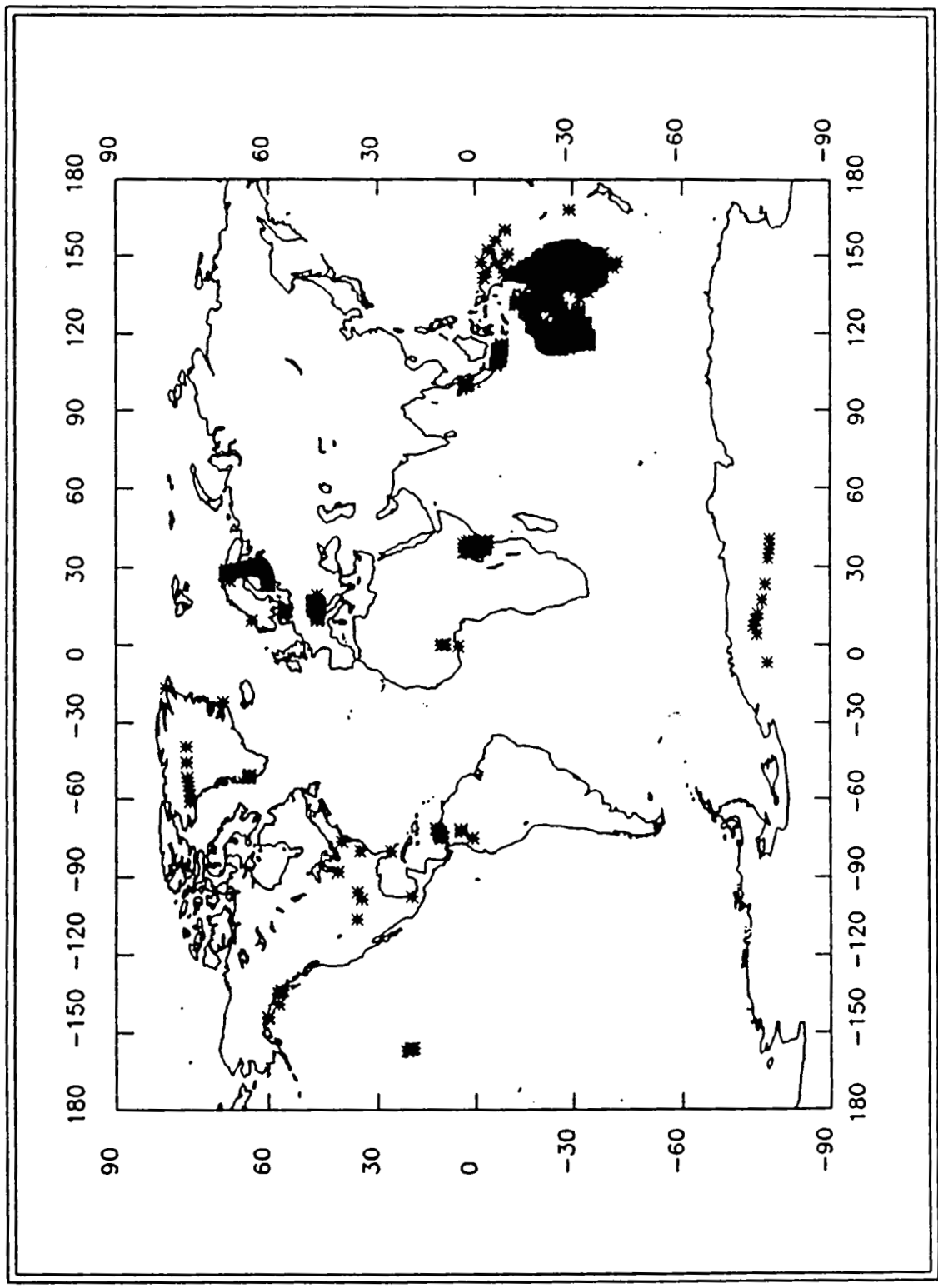

Figure 14. Positions of land survey data based on observations made between 1967.5 and 1972.5.

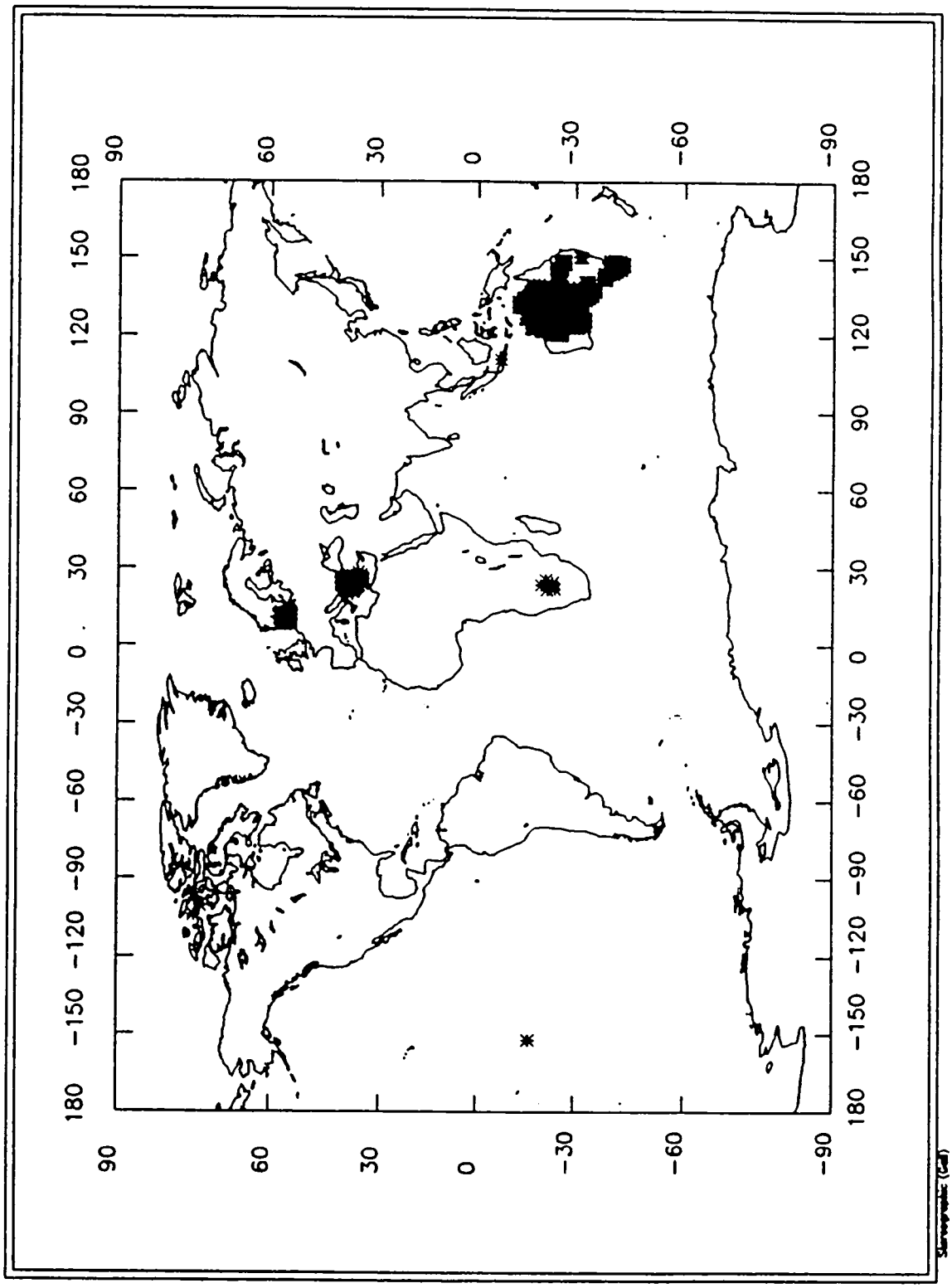

Figure 15. Positions of land survey data based on observations made between 1972.5 and 1977.5.

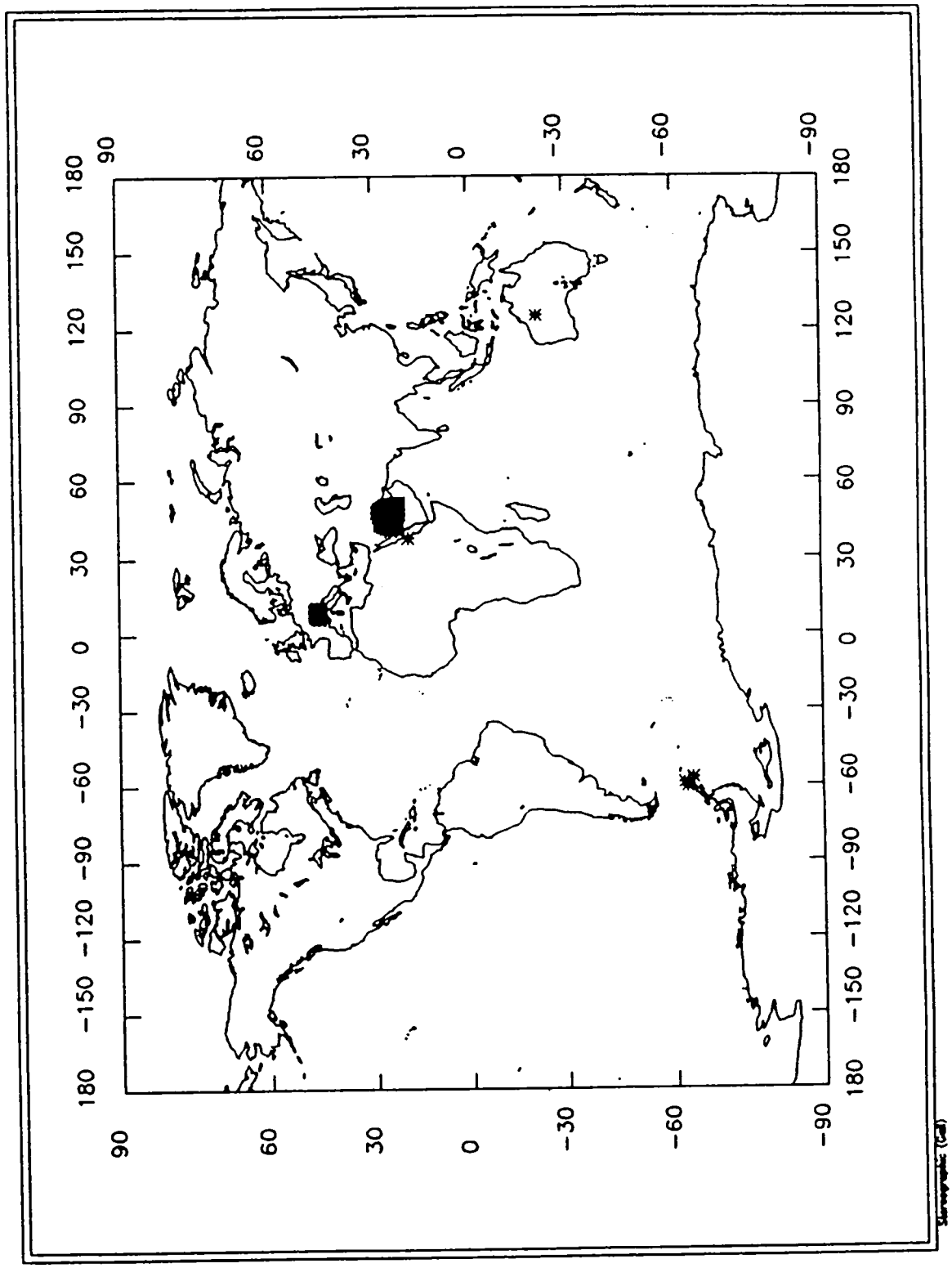

Figure 16. Positions of land survey data based on observations made between 1977.5 and 1982.5.

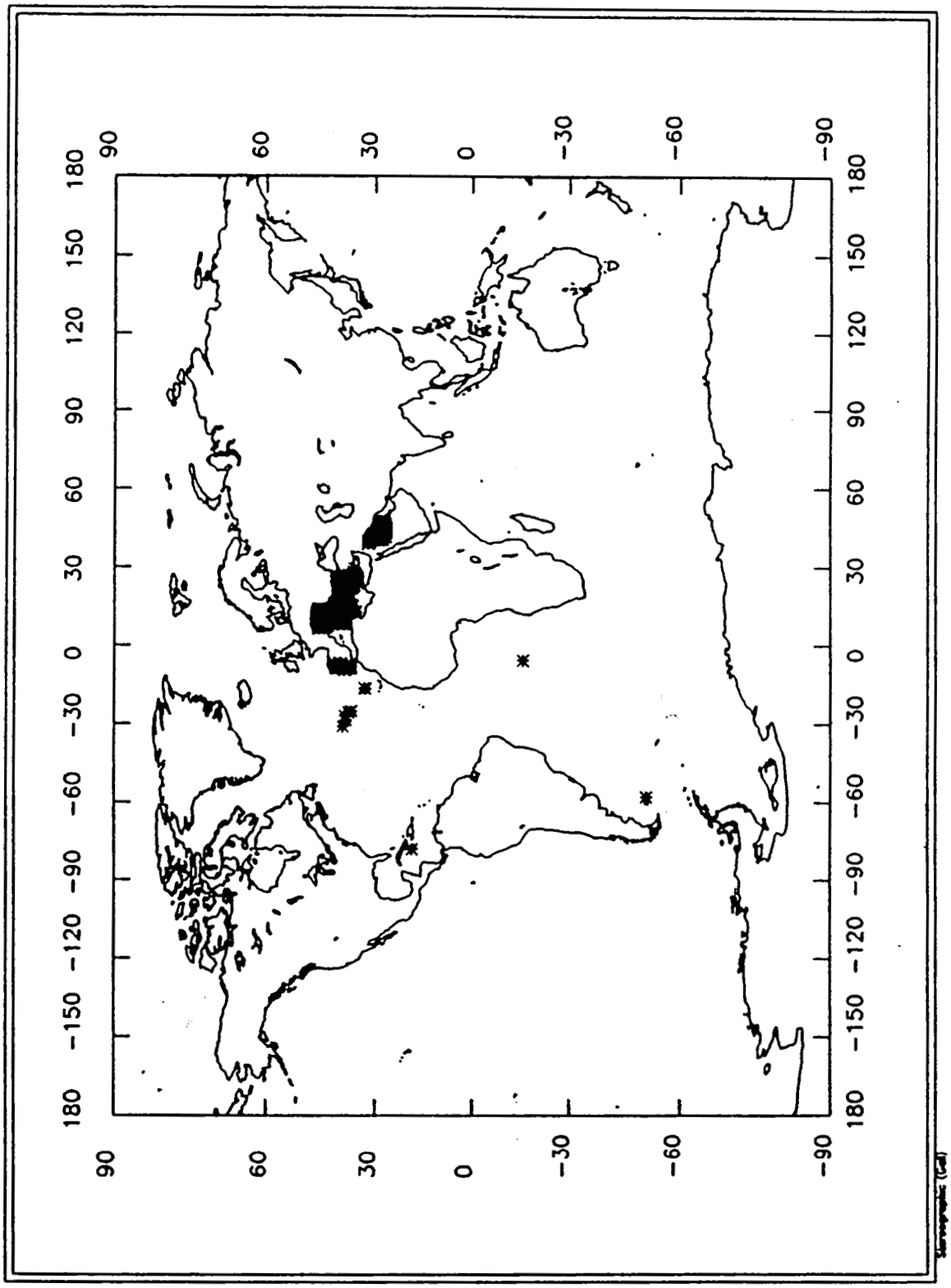

Figure 17. Positions of land survey data based on observations made between 1982.5 and 1987.5.

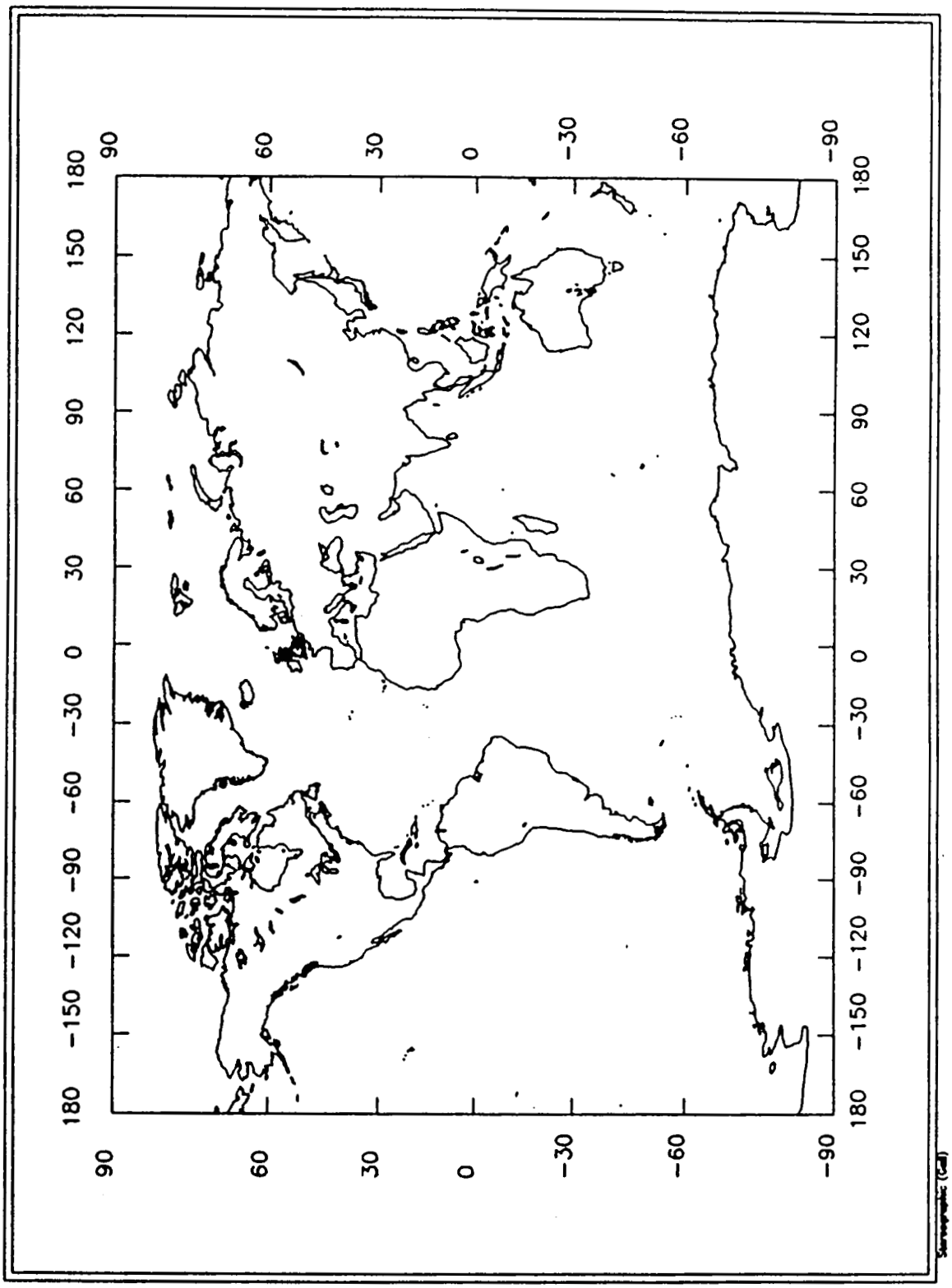

Figure 18. Positions of land survey data based on observations made from 1987.5 onwards.

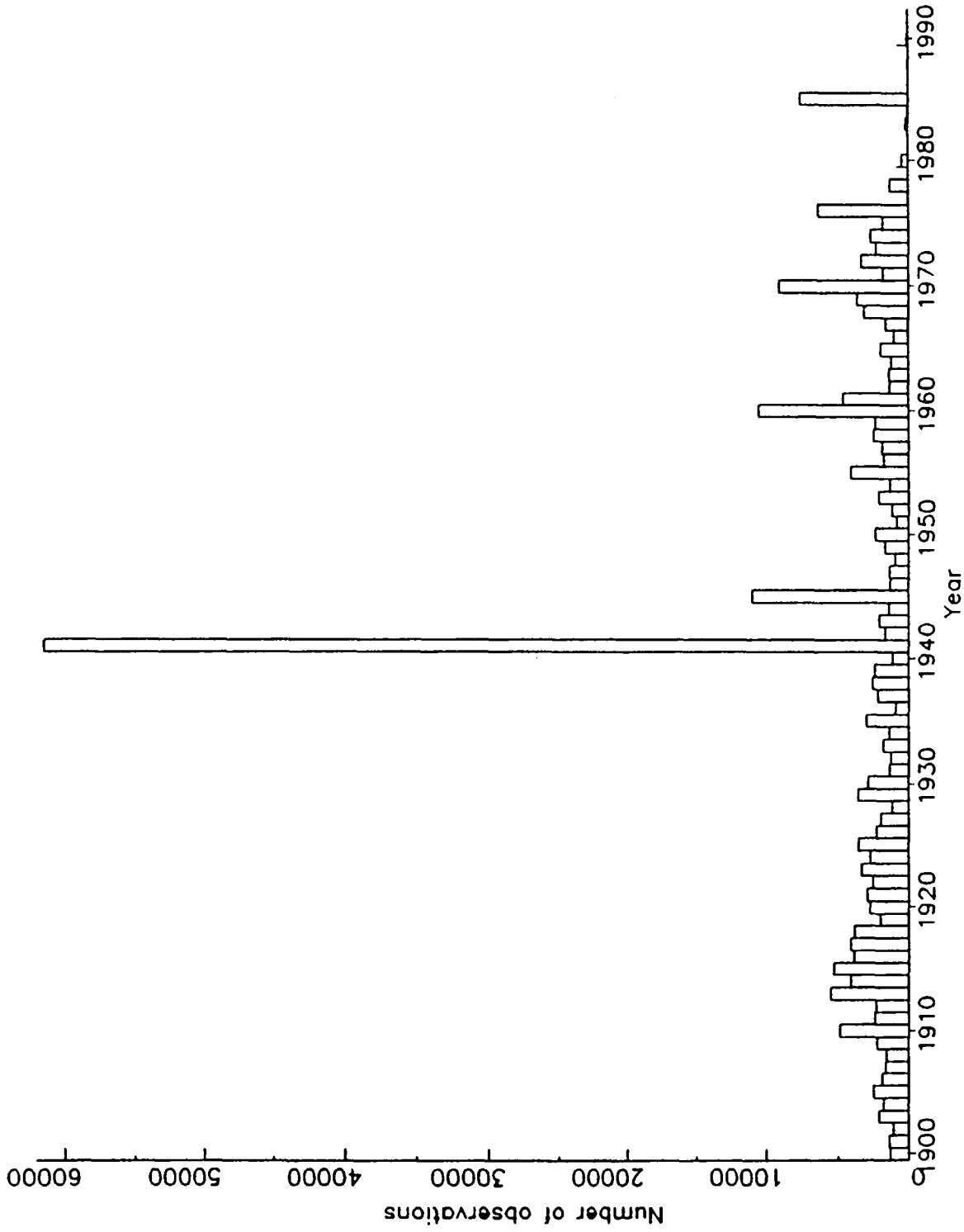

Figure 19. Distribution of land survey data with time. Each block represents the number of observations made in the 12 months centred on the beginning of the indicated year.

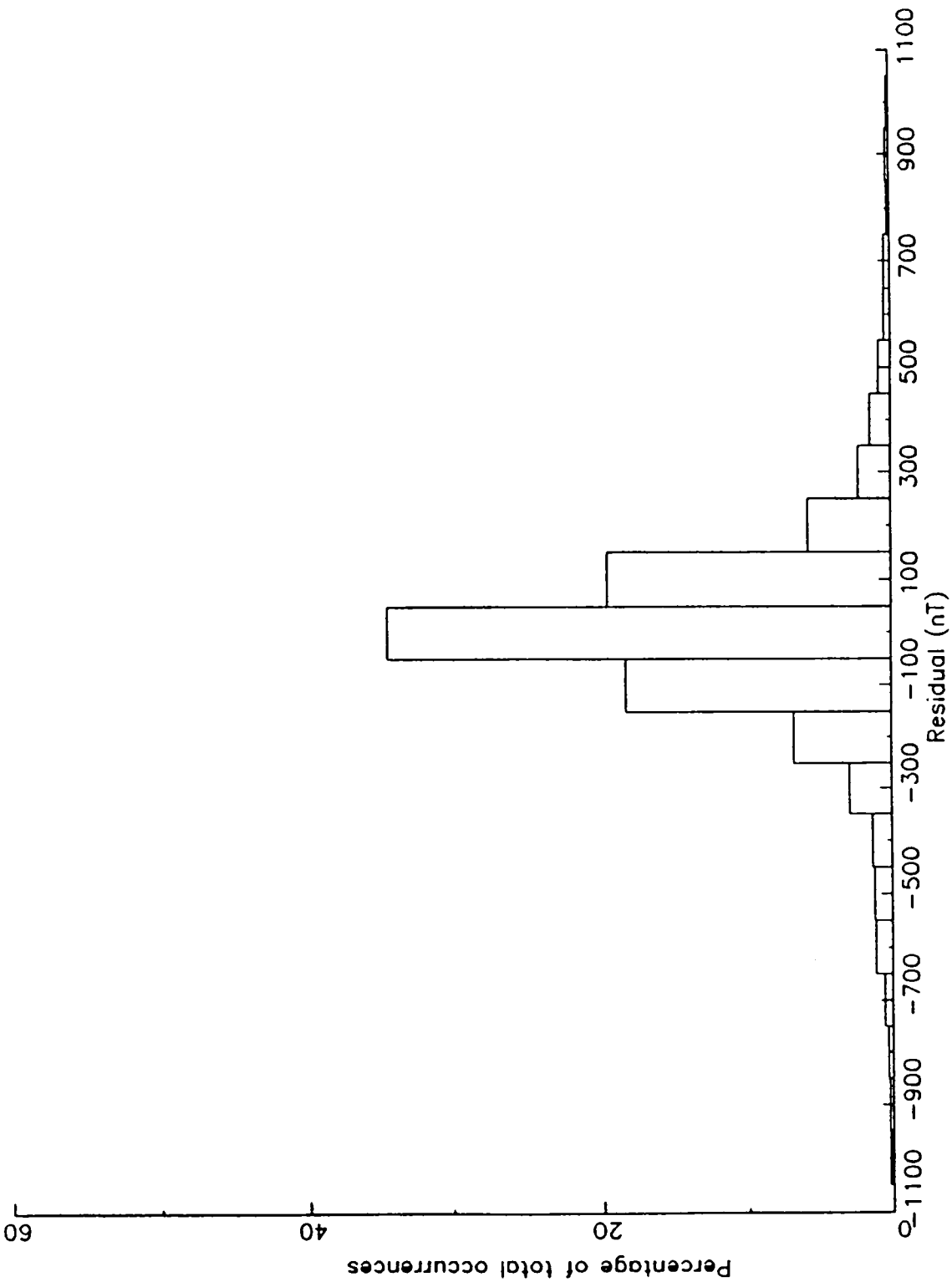

Figure 20. Distribution of the residuals between observed values and those computed from the IGRF for data based on observations made between 1962.5 and 1967.5.

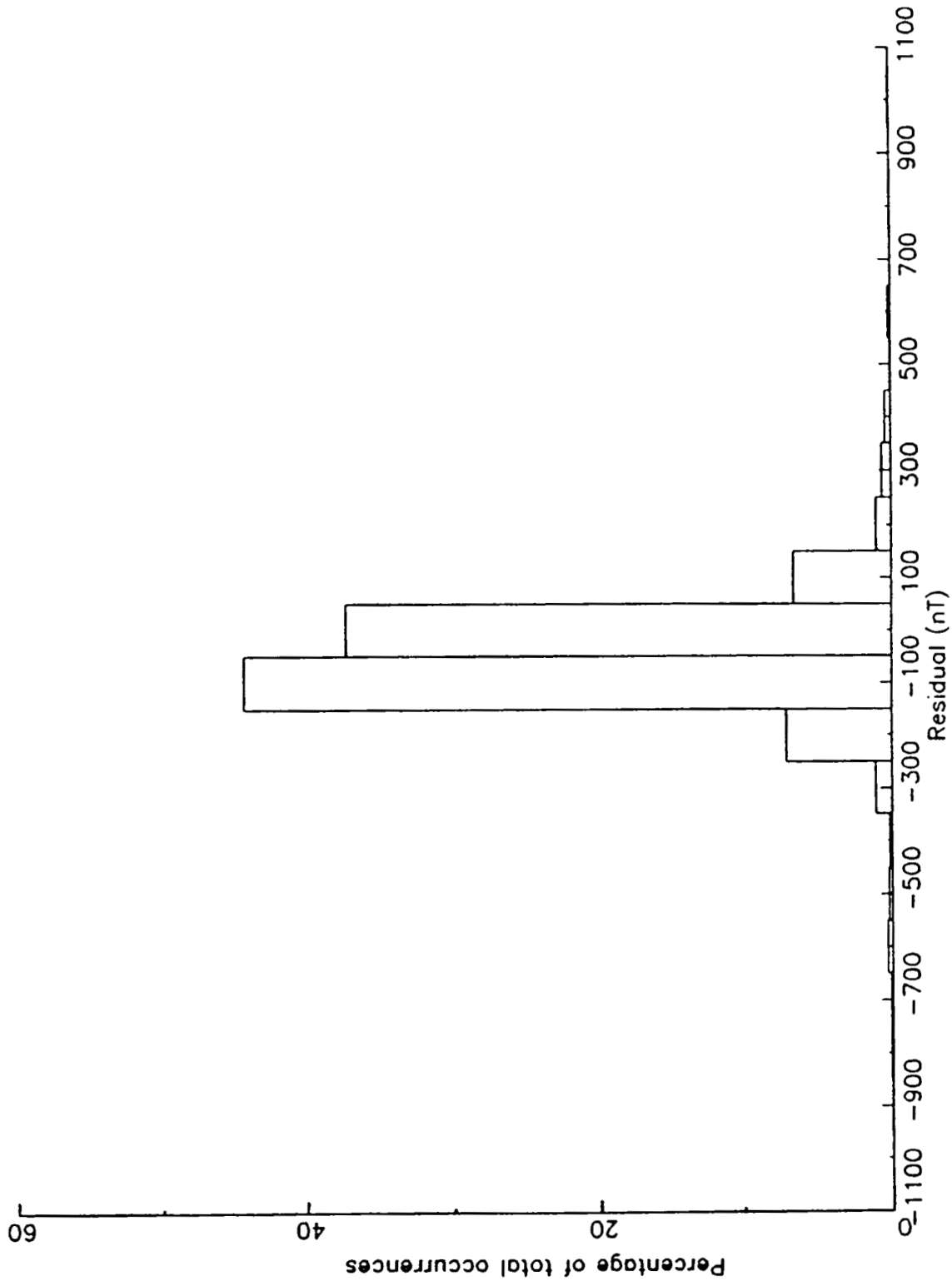

Figure 21. Distribution of the residuals between observed values and those computed from the IGRF for data based on observations made between 1977.5 and 1982.5.

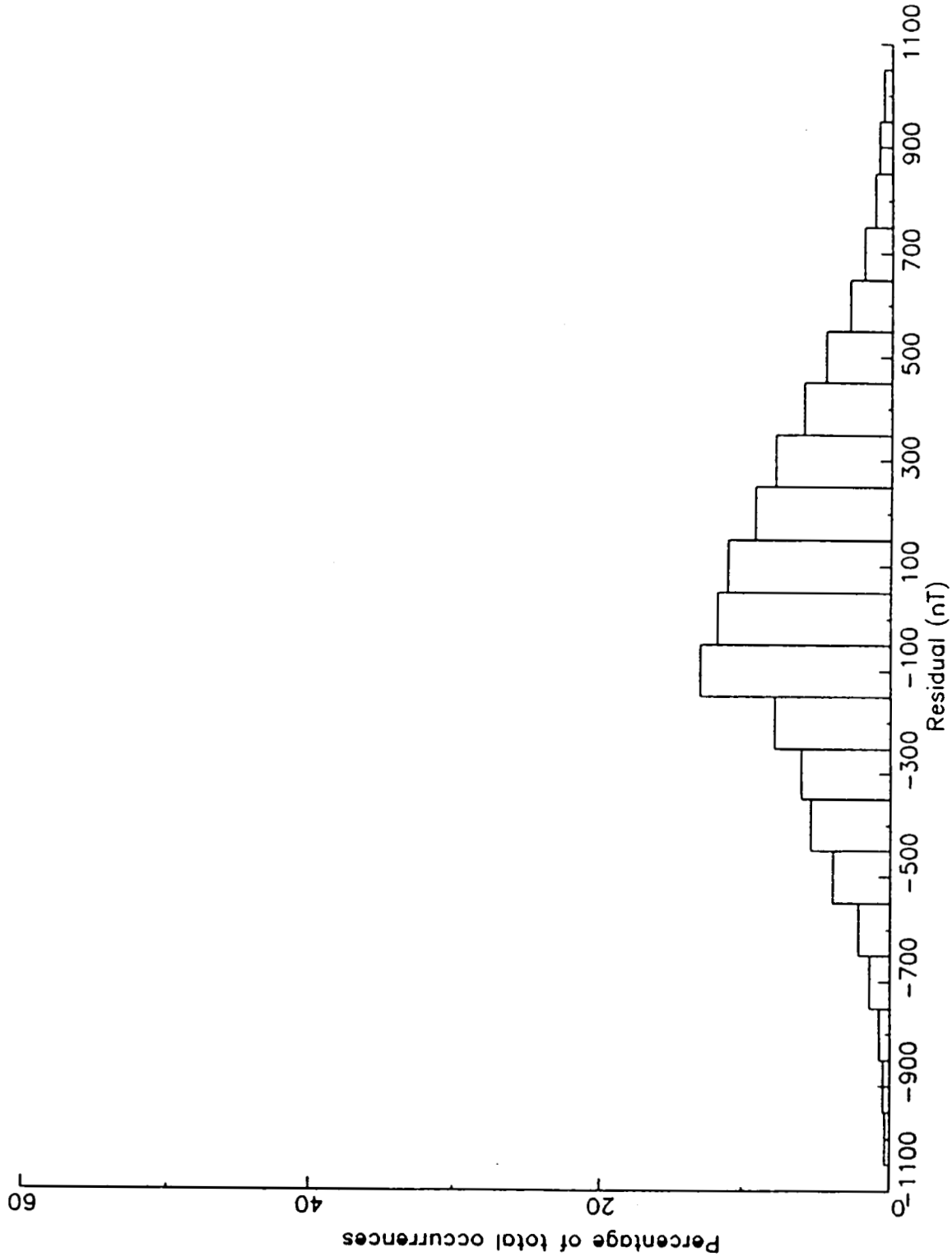

Figure 22. Distribution of the residuals between observed values and those computed from the field models of Vestine *et al.* (1947) for data based on observations made between 1922.5 and 1927.5.

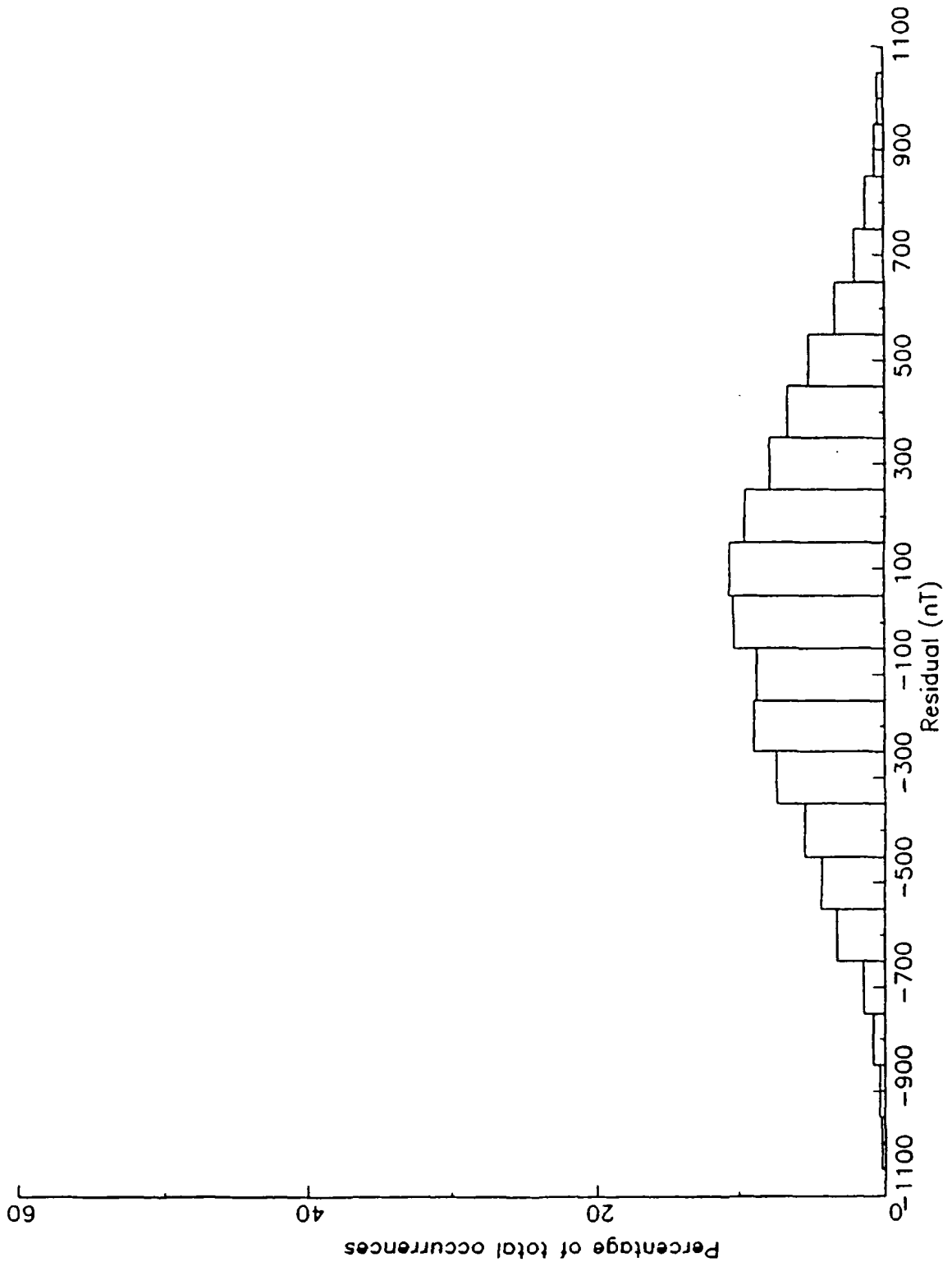

Figure 23. Distribution of the residuals between observed values and those computed from the field models of Vestine *et al.* (1947) for data based on observations made between 1900.0 and 1907.5.

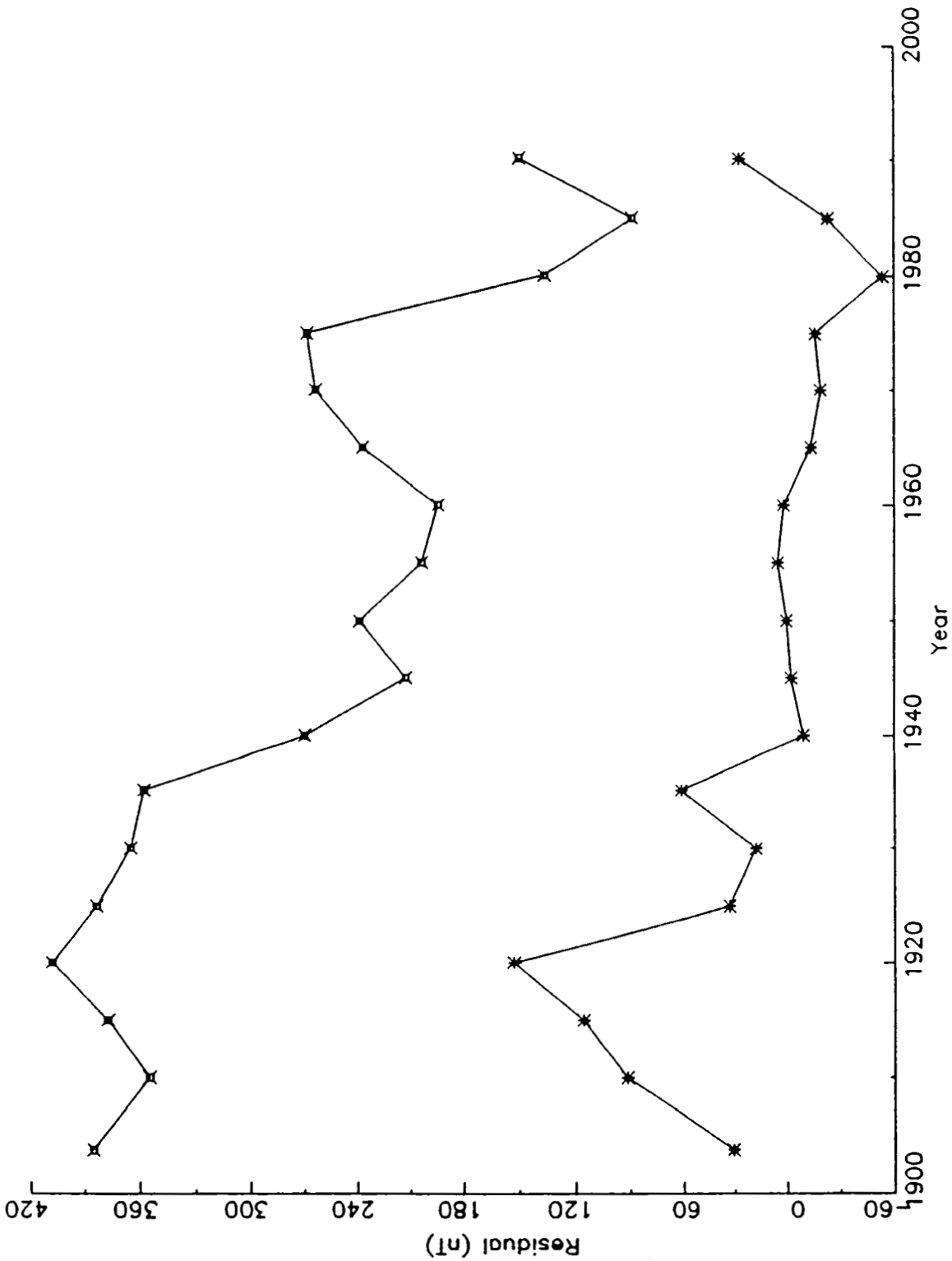

Figure 24. Mean and root mean square residuals between observed and computed values for each of the 18 time windows.

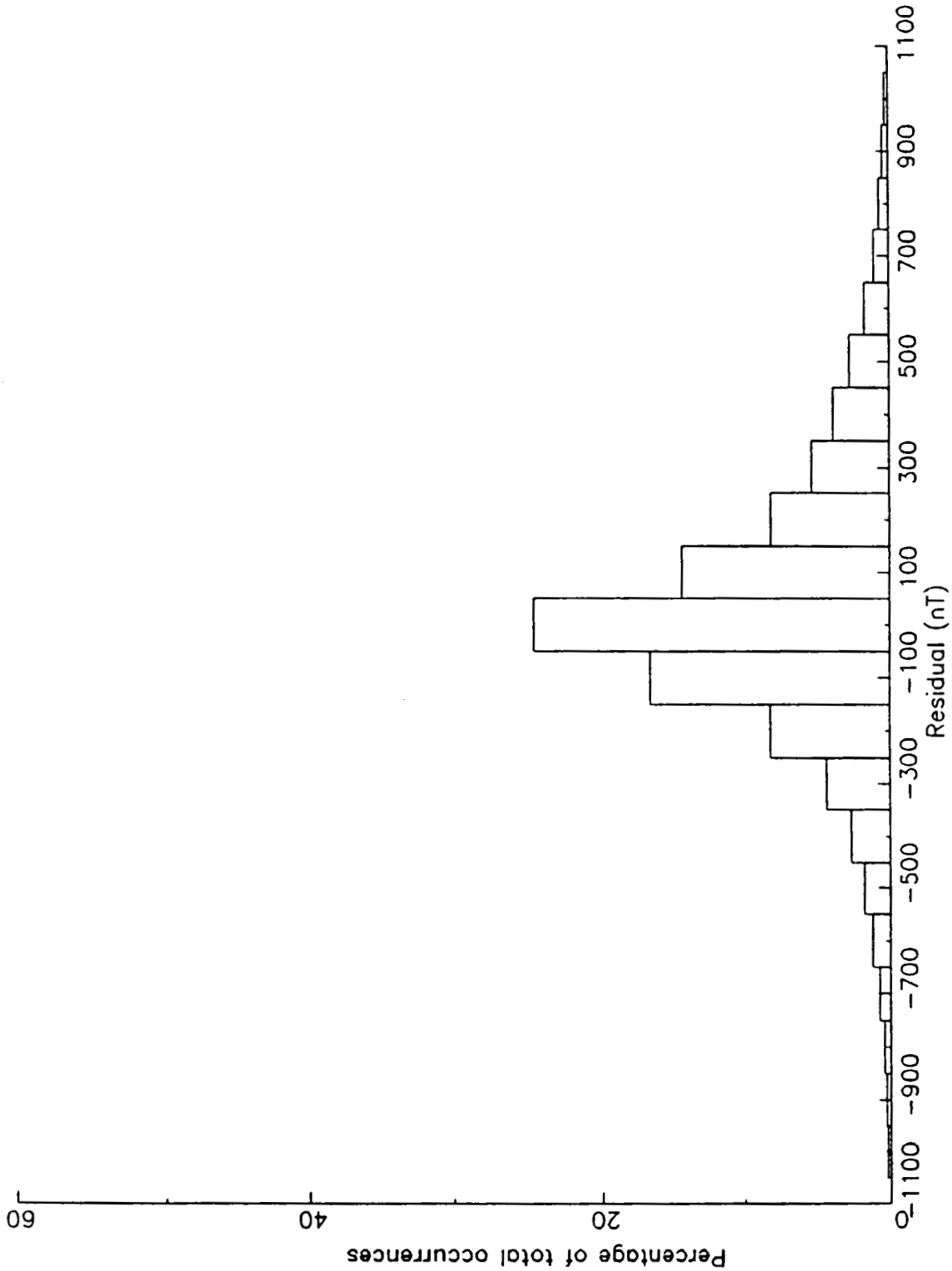

Figure 25. Distribution of the residuals between observed values and those computed from the field models of Vestine *et al.* (1947) or from the IGRF for the entire dataset (based on observations made from 1900.0 onwards).

SATELLITE DATA FOR

GEOMAGNETIC FIELD MODELING

R. A. Langel
Geodynamics Branch, Code 921
Goddard Space Flight Center
Greenbelt Md. 20771, USA

R. T. Baldwin
Hughes STX Corp.
Lanham Md. 20706, USA

ABSTRACT

Satellite measurements of the geomagnetic field began with the launch of Sputnik 3 in May of 1958 and have continued sporadically since. Spacecraft making significant contributions to main field geomagnetism will be reviewed and the characteristics of their data discussed, including coverage, accuracy, resolution and data availability. Of particular interest are Vanguard 3; Cosmos 49; OGO's -2, -4, and -6; Magsat; DE-2; and POGS. Spacecraft make measurements on a moving platform above the ionosphere as opposed to measurements from fixed observatories and surveys, both below the ionosphere. Possible future missions, such as Aristoteles and GOS are reviewed.

1.0 INTRODUCTION

The geomagnetic field at the surface of the earth is due to sources within the Earth's core and crust and sources external to these, within the ionosphere and magnetosphere. These fields have historically been measured at or near the Earth's surface by observatories, repeat stations, land, marine, and aeromagnetic surveys. Such measurements lack uniform global coverage, a shortcoming resolved by satellite data. The resulting data have been used to derive the most accurate descriptions of the main field and, for the first time, have permitted global mapping of crustal fields of wavelength greater than 400 km.

With data only below the ionosphere, it is not possible to map the locations and characteristics of ionospheric and field aligned currents. To a large degree, satellites have succeeded in carrying out such a mapping.

In this article we are concerned only with the volume within an altitude of about 2000 km, because it is measurements from this region which are pertinent to the study of the solid Earth.

The quality of satellite data is contingent upon the nature of the instrumentation, the accuracy of its position and time determination, the attention paid to spacecraft magnetic cleanliness and to the ability to acquire continuous data. For use in main field modeling it is also important to be able to select data for periods of magnetic quiet.

Acquisition of magnetic field data by satellite commenced beginning with Sputnik 3 in May of 1958. The latest such are being acquired with the US Navy's Polar Orbiting Geomagnetic Survey (POGS). We will begin by reviewing aspects of magnetic field measurement either peculiar to, or crucial to, the satellite platform. Then the various error sources will be discussed and the error estimates for relevant missions summarized. A summary of characteristics of the various satellite missions is given and potential future missions are noted.

2.0 FEATURES PARTICULAR TO SATELLITE DATA

2.1 Effects of Orbit Parameters: Geographic and Local time Coverage.

Before specifically discussing magnetic field measurements it is useful to understand something about the nature of satellite orbits. Referring to Figure 1, an Earth orbiting satellite traverses an elliptical path with the center of mass of the Earth located at one focus of the ellipse. As the satellite traverses this path, its altitude above the Earth's surface varies due to the orbital ellipticity (or eccentricity); the closest and farthest points from the Earth are called perigee and apogee, respectively. At near-earth altitudes, at 200 to 2000 km, the time for one full orbit, the orbital period, varies from about 90 to 200 minutes. The plane of the satellite path is called the orbital plane. Its angle, with respect to the Earth's equatorial plane, is the inclination, i, and the intersection of the orbital plane and the

equatorial plane, at the point where the satellite is going north, is the ascending node. To a first approximation, the orbit geometry remains fixed in inertial space, while the earth rotates beneath. The projection of the satellite position onto the surface of the Earth is called the ground track, or subsatellite track, and this path over a period of time is a measure of the amount of coverage or amount of the globe from which data may be acquired.

Figure 1 illustrates that data are only acquired at latitudes up to the value of the inclination. The latitude coverage is 100% at $i = 90^{o}$. The dependence of coverage on inclination is illustrated in Figure 2, which shows ground tracks from the Magsat satellite with an inclination of 97.15^{o}, and Figure 3, from the OSTA-1 mission with an inclination of 38^{o}. Magsat gave near global coverage, whereas OSTA-1 only acquired data below 38^{o} latitude. (An inclination greater than 90^{o} means that the rotational component of the satellite direction is opposite the Earth's direction of rotation, called a retrograde orbit; orbits which are not retrograde are called prograde.)

Two other aspects of data coverage are important besides the latitude range of the satellite. These are data spacing in longitude and in local time. Data spacing in longitude depends upon the way the subsatellite tracks move in longitude. For example, it is possible to choose the orbital parameters so that the tracks repeat after a fixed number of orbits, leaving large gaps in longitude coverage, or so that the tracks never repeat. Data spacing in longitude is a complicated function of satellite altitude, orbit ellipticity, and inclination.

Figure 4 shows the longitude change between ascending nodes for a circular orbit at inclination 90° as a function of satellite altitude. For example, at an altitude of about 380 km the longitude of successive equator crossings changes by 23°. As long as an integral multiple of this change does not equal an integral multiple of 360°, the tracks will not exactly repeat from day to day and the coverage in longitude will become denser as time goes on.

Another factor in spacecraft surveys is that due to the fact that the Earth is aspherical, or nonsymmetric, the plane of a satellite orbit precesses very slowly in inertial space. The rate of this precession depends on the orbital geometry, i.e. apogee, perigee, inclination, ellipticity. Since the Earth's rotation brings each longitude under the orbit plane, the data are globally well distributed. However, all observations at one latitude may have nearly the same local time for an extended period of time. In fact, the orbital parameters may be chosen so that the orbital plane remains fixed in its relation to the sun and hence fixed in local time. Such an orbit is called sun-synchronous. The Magsat spacecraft was in sun-synchronous orbit in the dawn-dusk meridian plane of the Earth. Figure 5 shows the daily change in local time of the ascending node of the orbital plane as a function of inclination and of altitude. For prograde orbits the local time is decreasing with time; the rate of decrease becomes smaller as the satellite altitude increases and as the inclination increases. The local time of a satellite in a 90° inclination orbit changes between 3 and 5 minutes a day.

To illustrate some facets of satellite orbits it is convenient to plot the location of perigee in local time-latitude coordinates as a function of time. Figures 6 and 7 show such a plot for the OGO-2 and Magsat spacecraft. Given the location of perigee at a particular date and knowledge of the satellite inclination, which can be inferred from the poleward extent of the points on figures such as 6 and 7, one can draw a line through the perigee location and tangent to the circle at 90^{o} - i; the satellite track will lie on such a line. From Figure 6 one can see that the perigee of OGO-2 varied through all local times in about 3 months whereas, from Figure 7, Magsat only acquired data near dawn and dusk local times.

2.1 Data Recovery. Of major importance to achieving optimal coverage is the capability to store and transmit data. In the absence of onboard data storage, data acquisition can only occur at those times when the satellite transmits data directly to a ground receiving station, called "real time" data acquisition. The total time available for data acquisition at near-earth altitudes, as a satellite passes by a ground receiving station, is generally from 3 to 15 minutes. Relying on real time data acquisition severely limits the actual coverage capability. Usually a storage device, e.g. a tape recorder, is flown onboard the spacecraft. Data is then recorded and, at a convenient time, is played back at accelerated speed to a receiving station.

2.2 Satellite Data Peculiarities. Sources ofthe near-Earth magnetic field include currents in the ionosphere between 100-130 km. At the Earth's surface, ionospheric fields reveal themselves through daily variations in magnetograms at permanent observatories. However, from surface measurements alone it is only possible to determine that such fields originate external to the Earth; their location in the ionosphere is inferred from other measurements, e.g. satellite or rocket, or from theoretical considerations. Similarly, satellite data alone can only determine that such fields are internal to the volume in which the data are acquired but cannot distinguish sources in the ionosphere from sources within the Earth. However, surface and satellite data together can, in principle, determine which portion of the field originates in the Earth, which in the ionosphere, and which external to the ionosphere. For main field modeling purposes, fields of ionospheric origin constitute noise so the ability to separate them from fields of origin within the Earth is important.

Fields from the crust are also a noise source when attempting to model the main field. These are difficult to distinguish from the main field when data are acquired at only fixed locations on the Earth's surface. The global mapping capability of satellite measurements makes it possible to at least make a good start at distinguishing such fields on a spectral basis (see, e.g., Langel and Estes, 1982).

When acquiring data from a fixed location at the Earth's surface, it is relatively easy to distinguish the long term secular variation from the shorter term variations due to ionospheric and magnetospheric sources. Satellite data do not acquire time series at a fixed location. Since the satellite does not continually acquire data at a fixed location, temporal changes must be modeled globally or must be inferred from simultaneous observatory data.

A related problem with satellite data is that it, alone, cannot distinguish between temporal variations and variations due to the satellite motion through a spatially changing field.

As with any observation, accurate time and position information is essential for quality data. For vector data, attitude determination is also a primary concern. Although these considerations are present also for surface data, they are particularly acute for a satellite which does not occupy a fixed stable location and cannot be routinely serviced. These will be discussed further in the section on data errors.

3.0 ERROR SOURCES

The error sources in satellite data are of three sorts. First are the usual, traditional, errors that affect any magnetic field measurement whether in space or on Earth. These include: instrument error, contaminating fields, and digitization error or resolution. The second sort are those errors that are satellite peculiar but which are

present for every satellite mission. These include errors due to imprecise knowledge of time and position, imprecise knowledge of the magnetometer attitude or pointing (and the stability of that knowledge). Finally, there are those errors which are experiment peculiar.

3.1 Instrument Error. Scalar instruments are usually absolute instruments in that their basic accuracy depends only upon knowing the value of some atomic constant. These include the Proton Precession magnetometer and the various Alkali Vapor (Helium, Rubidium, Cesium) magnetometers. In practice the accuracy achieved is about 1 to 2 nT, although in principle it ought to be possible to do better than this.

Vector magnetometers, on the other hand, have, to date, been relative instruments, subject to drift as electronic components age, as the ambient temperature changes and causes expansion and/or contraction of parts or variation in value of resistors or capacitors. Mechanical alignments of the axes are particularly susceptible to mechanical and thermal change. The most common type of vector magnetometer is the three-axis fluxgate. Such an instrument may drift anywhere from zero to several hundred nT per year. However, these instruments can be calibrated by use of a co-located absolute scalar instrument. By intercomparison between the scalar and vector magnetometers, the error due to drift can be reduced to nearly the accuracy of the scalar measurement, if the vector and scalar instruments are experiencing the same field to within about 0.1 nT (Lancaster et al., 1980; Langel et al., 1981). Alternately, it is sufficient to know the magnitude and direction of any difference in field between the vector and scalar

instruments to within this tolerance by knowledge of the gradient of the contaminating fields.

3.2 Digitization Error or Resolution. Digitization of a frequency in general has an ambiguity of ± one count either of the signal being digitized or of a reference frequency. This is the resolution of the signal. Similarly, there is a finite resolution when digitizing an analogue voltage. In principle, the resolution limit is imposed by the quality of the analogue to digital converter. These have steadily improved over the years so that today a magnetometer signal in the Earth's field can easily be resolved to a tenth of a nT. On the other hand, some measurements are limited by the number of bits available to store the signal onboard the spacecraft or to telemeter the digitized measurement to the ground.

3.3 Position and Time Error. Position (ephemerides) and time error can also be factors in magnetic field measurements. In practice, a time error translates into a position error. For example, the velocity of the satellite is about 7.5 km/second, so a time error of one second is equivalent to a position error of 7.5 km, along track. If the time is known to a millisecond or better, the equivalent orbit error is 7.5 m along track, which should be negligible.

Estimating the field error due to position error is done by computing the field difference between the actual position and the estimated position. By far the largest differences are due to the gradients in the main geomagnetic field. Table 1 summarizes the global maxima of the various field gradients and Tables 2 and 3 show the

equivalent magnetic field error for various time accuracies and for a position error of 100 meters. Table 4 summarizes the probable position errors for several satellites.

3.4 Contaminating Fields. Any field at the magnetometer which originates in the spacecraft or instrument is a source of inaccuracy. Such fields are usually minimized by placing the magnetometers on a boom of sufficient length to reduce the spacecraft fields to less than 1 nT. The necessary length of such a boom depends upon the strength and geometry of the spacecraft fields.

An alternative technique is to configure the measurement in such a way that the spacecraft field can be determined. From Magsat, we know that if the spacecraft field is constant and not too large (< 50 nT, say), it can be determined as part of the field modeling process. For ARISTOTELES large spacecraft fields which change with time are anticipated. This problem is approached by planning to sufficiently characterize the contaminating fields such that they can be modeled on the basis of ground measurements and on-orbit data such as torquer bar currents.

3.5 Attitude Error. Instrument error is not the only source of inaccuracy. For vector measurements, the major source of inaccuracy is the ability to measure the attitude, or pointing direction, of the instrument. The Earth's field is about 60,000 nT in the polar region. This means that an attitude error of 5 arc seconds will result in a 1.5 nT error in a direction normal to the Earth's field (See Figure 8). For high accuracy missions the spacecraft attitude is typically

determined by star sensors (or "cameras"). These have accuracies in the range of 5 - 10 arc seconds. Early star sensors were themselves highly magnetic and had to be located away from the magnetometers, at the spacecraft end of the isolating boom. In this case an optical system, called an "attitude transfer system" is used to measure the angular transformation between the star sensors and the vector magnetometer. Also useful are high precision sun-sensors, which can be made non-magnetic and located near the vector magnetometer. Techniques are now being developed to manufacture star sensors with extremely low magnetic fields. If successful, such sensors could be located at the end of the boom eliminating the need for the attitude transfer system.

Besides the accuracy of measurement of the star sensors, sun sensor, and attitude transfer system, the accuracy to which the relative positions of these instruments, and of their position relative to the magnetometer, is known also contributes to the overall attitude accuracy.

Experience from Magsat suggests that, given negligible or small but stable variation (less than 2nT in an orbit) of the spacecraft fields at the magnetometer location, and given stable attitude determination system position (variation less than 2 arc seconds in a day) relative to the magnetometer, both the stable spacecraft field and any change in relative location between the star camera and magnetometer can be solved for as part of our solution for the Earth's main field. The notation used is

{g,h} are parameters in a spherical harmonic analysis

(r, θ, ϕ) are the usual spherical coordinates

$\{\epsilon\}$ are transformation angles from magnetometer to spacecraft coordinates

$\{\beta\}$ are transformation angles from spacecraft to geocentric coordinates

B_S is the vector spacecraft field, in spacecraft coordinates.

If, then, it is assumed that $\{\beta\}$ are known but that $\{\epsilon\}$ and B_S are different than expected, but do not vary appreciably during the analysis, then the measurements can be modeled by B_C, where:

$$B_C = F\ (r, \theta, \phi, \{g,h\}, \{\epsilon\}, \{\beta\}) + B_S, \qquad (1)$$

and where the solution parameters include {g,h}, {e}, and B_S. The accuracy of such a solution is about 5-8 arc seconds.

This procedure was followed for the Magsat mission. In particular corrections were made to the pitch, roll, yaw attitude determinations (Langel et al., 1981). These corrections are shown in Figure 9 which shows that the roll angle (filled in circles) was essentially constant for the first 80 days after which it changed linearly; the yaw angle (x symbols) varies linearly at first until about day 100 when it becomes nearly constant; and the pitch angle (open circles) remains essentially constant.

For Magsat the spacecraft field found by this method was negligible. On the other hand the DMSP spacecraft field was so large and variable that the method failed (Ridgway et al., 1989).

3.6 Error budget summary by satellite. Table 5 summarizes our estimates of the accuracies achieved by the various satellites contributing, or possibly contributing in the future, to modeling the main magnetic field. The position errors attributed to Vanguard 3 and to Cosmos 49 are estimated maximum errors. In both cases the usual position error is likely smaller, much smaller in the case of Vanguard 3. In both of these cases the error is probably less than 50 nT in most circumstances. Note that the spacecraft field for Cosmos 49 was compensated by onboard magnets. The success of such a technique requires that neither the compensated nor the compensating field change with time, i.e. both magnetizations are "hard". This is generally true of the compansating field but cannot, in general, be guaranteed for the spacecraft field being compensated, which means the practice carries some risk.

Vanguard 3 had two instrument particular error sources. The spacecraft was spinning which introduces a shift into the field measured by the proton precession magnetometer. The maximum shift was 6.7 nT; on average, the shift was about 2 nT. The other source was the result of signal noise. The Larmor frequency from the proton precession instrument was transmitted directly to ground, recorded, and then digitized. The resulting signal had a noise level which introduced an error of up to 4 nT.

The accuracy figure for the Magsat vector magnetometer, 3.0 nT, is the rss (root sum square) after calibration using the scalar magnetometer.

DE-1 is included in the table although this data has not yet been tested in main field modeling. We are currently in the process of collecting data from locations near perigee which will be processed and used in modeling attempts.

Two sets of statistics are compiled in the Table. The first are the mean and σ about that mean of the data from each satellite to a field model derived from that data alone. The σ from such models gives a good idea of the scatter, or internal consistency, in that data set. Note that the numbers for POGS are very preliminary since the universal time of that data has not yet been established with adequate accuracy.

The second set of statistics are the mean and σ about that mean from the relevant IGRF. In most cases this was a DGRF. Note that the higher means and σ`s for these models may, in some cases, reflect the truncation level of the model, which is degree 10 for the IGRF.

4.0 MAGNETIC SATELLITE HISTORY

4.1 General Summary. Spacecraft which have made significant contributions to our understanding of the near-earth geomagnetic field are listed in Table 6 (see also Potemra, 1987). The very first satellite magnetic field measurement was accomplished by a fluxgate magnetometer onboard Sputnik 3. The instrument was mounted in a gimballed fashion so

that it could be reoriented in flight. One axis was maintained along the ambient field by reorienting the instrument until the fields measured by the other axes were zero. The axis parallel to the field gave the field magnitude; the position of the gimbal gave the orientation of the spacecraft relative to the field; i.e. the magnetometer was used to measure the spacecraft attitude; a common practice on many spacecraft. Spacecraft fields were high on Sputnik 3 and the coverage was limited to the Soviet Union.

The US Navy satellite 1963-38C was magnetically stabilized to within about 6^{o} of the ambient magnetic field by a large permanent magnet. Its fluxgate magnetometers gave useful data only on the field transverse to the permanent magnet. These data provided the first evidence for the presence of transverse magnetic fields due to field-aligned currents in the auroral belt (see, e.g., Potemra, 1982 for a review). The Navy Triad satellite, operative from late 1972 to early 1984, carried a triaxial fluxgate which obtained higher quality data than 1963-38C and thoroughly mapped the characteristics of the fields due to the field-aligned currents.

Measurement of the magnetic field alone is not sufficient for a thorough study of ionosphere-magnetosphere coupling. The latest generation of satellites have been designed to carry out a complement of measurements, often including not only magnetic field measurements but also measurements of particle precipitation, auroral imaging and electric fields. Missions of this nature include, DE-2 (Hoffman, et al., 1981; Farthing et al., 1981), ICB-1300 (Serafimov et al., 1982; Stanev et al., 1983; and Arshinkov et al., 1986), AUREOL-3 (Khmyrov et

al., 1982 Berthelier et al., 1982), HILAT (Fremouw et al., 1983), DMSP F-7 (Rich et al., 1985), and Polar Bear (Bythrow et al., 1987). ICB-1300, or "Intercosmos-Bulgaria 1300", was a joint U.S.S.R.-Bulgarian satellite; AUREOL-3 was a joint U.S.S.R.-French satellite flown as part of a larger joint project called ARCAD-3. Hilat and Polar Bear were flown by the Johns Hopkins Applied Physics Laboratory, in the U.S., as follow-on missions to TRIAD. The DMSP F-7 spacecraft was primarily intended to provide optical image information for weather monitoring. The imager also was useful for mapping auroral activity and plasma experiments were included by the Air Force Geophysical Lab, including a magnetometer. Unfortunately this magnetometer was located within the spacecraft proper where the ambient fields were several thousand nT in magnitude and variable.

Other than mapping field-aligned currents, uses of the data from all of these satellites was minimal for several reasons. Except for DMSP F-7, none had really adequate attitude determination; none carried an absolute magnetometer to calibrate the fluxgate; and except for DE-2, had no onboard data storage forextended coverage. ICB-1300 and AUREOL-3 had limited onboard data storage so that extended periods of data could be obtained, but the coverage was not 100%.

Although the DE-2 spacecraft was intended to measure primarily fields from field-aligned and auroral currents, the scalar magnitude of the field has been used in studies of the Earth's main field.

As can be seen from Table 6, until Magsat other surveys suitable for main field or crustal field studies were performed with either proton-precession or alkali-vapor magnetometers which measured only the field magnitude. Lack of onboard recording devices limited the coverage of Vanguard 3 and of 1964-83C, whereas the Cosmos, POGO, Magsat and DE-2 satellites all carried tape recorders and achieved full orbit coverage. Spacecraft fields were well above the noise level for Sputnik 3, 1963-38C, Cosmos 49, 1964-83C, S3-2, ICB-1300, AUREOL-3, and DMSP F-7. An additional error source in the Cosmos 49 data arose because the time assigned to the data was uncertain to $\pm$0.5 second.

The first survey to combine near polar inclination, onboard data storage, and high measurement accuracy was conducted by the OGO 2, 4 and 6 (POGO) satellites which operated between 1965 and 1971. Magsat, launched in October of 1979, was the first, and to date only, satellite to survey the vector components of the field with high accuracy.

Not included in Table 6 are satellites which observed the effects of field-aligned currents deep in the magnetosphere or which had substantially eliptical orbits, i.e. satellites which are not considered near-Earth, such as ISIS 2 (McDiarmid et al., 1978a,b), S3-3 (Rich et al., 1981; Catell et al., 1979), ISEE (Kelly et al., 1986; Frank et al., 1981) and OGO-5 (Sugiura, 1975). Also not included were some near-Earth satellites whose measurements cannot really be considered to be surveys, such as AZUR (Theile and Praetorius, 1973) and AE-C (Bythrow et al., 1980).

4.2 Satellites for Main Field Modeling. Those satellites which have contributed to the GSFC data base for are summarized in Table 7. The following paragraphs briefly describe some characteristics of each.

4.2.1 Vanguard 3. Vanguard 3 made absolute measurements of the magnetic field with a proton precession magnetometer from September 18 to December 11, 1959. Perigee and apogee were 510 km and 3750 km respectively. Data were acquired in real time only, i.e. when the satellite was in sight of a Minitrack station (Figure 10). These stations were located at Ft. Myers, Florida, Woomera, Australia, Quito, Equador, Lima, Peru, Antofagasta, Chile, Santiago, Chile, Antigua, British West Indies, Chula Vista, California, Blossom Point, Maryland, and Johannesburg, Union of South Africa. A description of the experiment and a catalog of data are given in Cain et al. (1962). The observations were obtained during all magnetic local times as shown in Figure 11.

4.2.2 Cosmos 49. The following description is taken from "The Survey with Cosmos-49" by Benkova (1971). "The satellite was launched into an orbit with inclination 49°, perigee 260 km, and apogee 490 km. The orbit precessed westward at a rate of 4.5° per day." "The measurements were made each 32.76 seconds during the interval October 24 to November 6 in 1964, a magnetically quiet period." The satellite had onboard memory so the coverage was global, equatorial of 49°. "Two proton precession magnetometers were orthogonally mounted in the satellite...the time of the measurement is uncertain to $\pm$0.5 second. The magnetometers are mounted 3.3 meters from the center of the satellite,

whose magnetic effects are compensated to an accuracy of 2 nT by an array of permanent magnets producing a homogeneous compensating field at the sensor locations.....In addition to the uncertainty of ±0.5 second earlier discussed, errors in satellite position existed that could reach 3 km in the direction of the flight path and 1 km in altitude as well as in the direction of the normal to the satellite orbit. Random errors due to unfavorable orientation of one of the magnetometer sensors were rejected." "The usable scalar intensity values totaled 18,000 and were published in catalogue form." Figures 12 and 13 show the global and local time distribution of data for COSMOS 49.

4.2.3 POGO. The POGO satellites carried rubidium vapor magnetometers into a near polar orbit and collected scalar data over a 6 year time span.

OGO-2 (10/65-9/67), with apogee and perigee at 413 and 1510 km respectively, collected mostly dawn and dusk scalar observations as a result of battery problems which necessitated dayside operations. The global distribution of data is reviewed in Figures 14 (a,b,c,d, & e) and the local time data distribution is shown in Figure 15. A description of the OGO-2 data and its processing may be found in Langel (1967).

OGO-4 observed the magnetic field from 7/67 to 1/69. A global data coverage map (Figure 16) and a local time histogram (Figure 17) summarize the spatial and temporal distribution. OGO-4 acquired data at all local times in about 5 months.

The OGO-6 (6/69-7/71) data are globally distributed as shown in Figures 18 (a,b,c,& d) and have local time distribution as shown in Figure 19. The local time coverage was completed in approximately 5 months.

4.2.4 Magsat. Magsat was launched in November of 1979 into a 97° inclination orbit with apogee at 550 km and perigee at 325 km. It successfully made scalar (Cesium) and vector (fluxgate) measurements over its lifetime. Data used in main field modeling as described by Langel and Baldwin (1991) are shown in Figure 20. Local time variations (Figure 21) are indicative of a sun-synchronous orbit. A general description of data characteristics, calibrations, and corrections may be found in Langel et al., 1981.

4.2.5 DE-2. Data from the DE-2 satellite (Sept. 1981- Jan. 1983) has been useful in determining the field during 1982. The DE-2 orbit was polar with apogee and perigee of 309 km and 1012 km. Although vector data were acquired with DE-2, the attitude accuracy (about 1-2°) was not adequate for spherical harmonic modeling. Scalar magnitude data from the DE-2 satellite were derived from the fluxgate components for use in main field modeling. Ridgway (1988) and Langel et al. (1988) give details of the mission and data. The data furnished to us after processing for quiet intervals are distributed geographically as shown in Figure 22 and are mainly from dawn and dusk local times (Figure 23).

4.2.6 DE-1. The DE-1 satellite launched in September 1981 carried a triaxial fluxgate magnetometer at the end of a 6 meter boom. This instrument had a resolution of 1.5 nT and a range of ± 62000 nT. DE-1

was in a near polar orbit with a perigee of 600 km and an apogee of 24800 km (since 1981 the orbit has decayed). Data from near perigee will be evaluated as to its usefulness for main field analysis. This is a spinning satellite which results in additional uncertainties in attitude determination in inertial space due to uncertainties in determining the phase of the spacecraft roll angle.

4.2.7 POGS. POGS (Polar Orbiting Geopyhisical Satellite) was launched from Vandenberg Air Force base in April of 1990 into a circular polar orbit of approximately 800 km. The US Naval Oceanographic Office (NOO) sponsored this DMSP type platform deployed from an Atlas E rocket. The satellite was equipped with a vector fluxgate magnetometer mounted on an eight foot earth-pointing boom. The instrument has a range of ±65535 nT with a resolution of 2 nT. There was no absolute instrument onboard the spacecraft to correct for instrument drift, and the available altitude information was insufficient for useful attitude corrections. The instrument drift rate was proposed to be no greater than 50 nT/yr (Acuna, personel communication) and the attitude accuracy is to within 0.5° to 1.0°. Because of deployment problems, the satellite was injected into orbit upside down causing problems with the solar panels and telemetry antenna. This resulted in downlink problems at the two ground stations. Although this problem has currently been resolved by reconfiguring the ground station tracking software, the data used in this study suffers from large gaps. At present, the main problem with POGS satellite data concerns the magnetometer clock. The clock accuracy relative to GMT is in error by as much as 5.5 seconds. An attempt to correct this problem is discussed in Langel et al. (1991).

5.0 Missions Under Consideration

Although the future of some seems bleak, there are several missions being considered for future measurement of the geomagnetic field. These include the NASA EOS (Polar Platform) experiment, Geomagnetic Observing System (GOS); two ESA/NASA missions: Advanced Particles and Fields Observatory (APAFO) on the ESA Polar Platform and ARISTOTELES; the Department of Defence (DOD) follow on missions to DMSP and POGS; and the possibility that NOAA would include magnetic field measurements on their meterological satellites.

5.1 EOS/GOS. This is projected for the second, or EOS-B, Polar Platform. Included would be a scalar Helium and vector fluxgate magnetometer mounted at the end of a long, perhaps 25 m, boom. Non-magnetic star sensors would also be included at the end of the boom. A second fluxgate would be mounted inboard on the boom to aid in modeling the spacecraft field. The overall investigation would also include a plasma wave experiment consisting of two sets each of a triaxial search coil and triaxial electric field antennas. Figure 24 shows a sketch of the configuration of GOS on the platform.

The status of GOS is in extreme doubt. Reconsideration of EOS investigations and of the number and nature of the platforms is presently under way in the light of realistic fiscal constraints.

5.2 APAFO. APAFO is one of two space science investigations selected by ESA for their Polar Platform in response to their Announcement of Opportunity. The proposed instrumentation is as follows:

MEASUREMENT	RANGE/FOV	ACCURACY	SAMPLING RATE
Scalar Magnetic Field	20-70,000 nT	2.0 nT	2/sec
Vector Magnetic Field	$\pm$64,000 nT	4.0 nT	8-128/sec
Ion Velocity (E-Field)	0 - 40 eV	0.1^{o}	4-64/sec
	40^{o}x40^{o} FOV	0.1 mV/m	
Electron Analysis	5 eV - 600 keV	.001-.01 cm^{2}-sr	4-32/sec
	220^{o}x36^{o} FOV	1 - 7.5^{o}	

Figure 25 is an artists conception of the ESA Polar Platform including APAFO.

While APAFO has been selected by ESA it is currently not supported by NASA's Earth Science and Applications Division. The NASA Space Physics Division has APAFO under consideration.

5.3 ARISTOTELES. ARISTOTELES is an acronym for Applications and Research Involving Space Technologies Observing the Earth's Field from Low Earth Orbiting Satellite. Figure 26 shows an artists conception of the proposed spacecraft. Its mission is to measure the gravity and magnetic fields of the Earth. The project is joint between NASA and ESA with NASA furnishing the scalar and vector magnetometers, a Global Positioning System (GPS) receiver and tracking, and the launch vehicle.

ESA would furnish the spacecraft, the gravity gradiometer and the mission operations.

There are essentially three phases to the mission profile.

One: The checkout phase at an altitude of about 400 km. During this period the spacecraft will be checked out and any calibration procedures executed for the gravity and magnetic measurements.

Two: The Low Altitude phase at an altitude of about 200 km for a duration of about 6-8 months. During this period high spatial resolution measurements (about 100 km) will be obtained for both the magnetic and gravity fields.

Three: The High Altitude phase at an altitude of about 500 km for the remainder of the mission lifetime, anticipated at about three years. The primary measurements during this phase will be of the geomagnetic secular variation.

ARISTOTELES is not an approved program of either ESA or NASA. It is under consideration by both for launch in or after 1997. In the NASA framework it would come under the Earth Probe program.

5.4 DMSP/POGS. The missions under consideration would be follow on to previous DMSP and POGS missions, upgraded for main field studies. Two DMSP series are involved in these missions and both the Air Force and the Navy are involved. Plans in each agency are very similar, but apparently not exact. The present discussion is based on information received from F. Rich (personal communication) of the Air Force.

The current DMSP series is known as BLOCK 5. Subseries 5D-2 consists of spacecraft F-8 through F-14. This subseries will continue to carry the body mounted fluxgate magnetometer which did not prove useful for main field studies. Subseries 5D-3 consists of spacecraft S-15 through S-20. Current plans are that S-15 will be POGS-II. Figure 27 is an artists conception of POGS-II. Its magnetometer will be the same as for sub-series 5D-2 except that it will be mounted at the end of a 5 m boom. Launch is projected for the 1990 to 2000 time frame. At present, the status of magnetometers for spacecraft S-16 through S-20 is unclear, though the presumption is that if S-15 is indeed approved then similar magnetometers will be included on these also.

The next DMSP series is known as BLOCK 6. For this series an improved magnetometer design is planned. The first launch is projected at about the year 2005. Like POGS and DMSP the DOD requirements call only for a fluxgate magnetometer. NASA participation will be sought to provide an upgrade to the experiment to Magsat quality. This would include further upgrade of the vector fluxgate magnetometer, addition of a scalar magnetometer, and addition of an attitude transfer system.

Final approval is still pending on all of these missions.

5.5 NOAA satellites. These are under discussion with no available plans.

5.6 Projected Ideal Launch Schedule. Table 8 shows the currently published projected launch dates for the missions discussed above.

REFERENCES

Arshinkov, I.S., A.Z. Bochev, N.S. Abadjiev, E.G. Zaharieva, K.I. Arshinkova, V.H. Velev, and Y.B. Mandil, Magnetic field measurements in the ionosphere-magnetosphere region, Adv. Space Res., 6, No. 9, 111-114, 1986.

Benkova, N.P. & S.S. Doliginov, The survey with Cosmos-49, in World Magnetic Survey, IAGA Bulletin #28, ed. A.J. Zmuda, 1971.

Berthelier, J.J., A. Berthelier, Yu.I. Galperin, V.A. Gladyshev, G. Gogly, M. Godefroy, C. Guerin, and J.F. Karczewski, DC magnetic field observations on board the AUREOL-3 satellite: the TRAC experiment, Ann. Geophys., 38, 635-642, 1982.

Bythrow, P.F., R.A. Heelis, W.B. Hanson and R.A. Power, Simultaneous observations of field-aligned currents and plasma drift velocities by Atmospheric Explorer C, Jour. Geophys. Res., 85, 151, 1980.

Bythrow, P.F., T.A. Potemra, L.J. Zanetti, F.F. Mobley, L. Scheer, and W.E. Radford, The Polar Bear magnetic field experiment, Johns Hopkins APL Technical Digest, 8, 318-323, 1987.

Cain, J., I.R. Shapiro, J.D. Stolarik, and J.P. Heppner, Measurements of the geomagnetic field by the Vanguard III satellite, NASA TM D-1418, 1962.

Cattell, C.A., R.L. Lysack, R.B. Torbert and F.S. Mozer, Observations of differences between regions of current flowing into and out of the ionosphere, Geophys. Res. Lett., 6, 621, 1979.

Farthing, W.H., M. Sugiura, B.G. Ledley, and L.J. Cahill, Jr., Magnetic field observations on DE-A and -B, Space Science Instrumentation, 5, 551-560, 1981.

Frank, L.A., R.L. McPherron, R.J. DeCoster, B.G. Burek, K.L. Anderson, and C.T. Russell, Field-aligned currents in the earth's magnetotail, Jour. Geophys. Res., 86, 687, 1981.

Fremouw, E.J., C.L. Rino, J.F. Vickrey, D.A. Hardy, R.E. Huffman, F.J. Rich, C.-I. Meng, K.A. Potocki, T.A. Potemra, W.B. Hanson, R.A. Heelis, and L.A. Wittwer, The HILAT Program, EOS, Trans. AGU, 64, 163-170, 1983.

Hoffman, R.A., G.D. Hogan, and R.C. Maehl, Dynamics Explorer spacecraft and ground operations systems, Space Science Instrumentation, 5, 349-367, 1981.

Kelly, T.J., C.T. Russell, R.J. Walker, G.K. Parks, and J.T. Gosling, ISEE-1 and -2 observations of Birkeland currents in the Earth's inner magnetosphere, Jour. Geophys. Res., 91, 6945, 1986.

Khmyrov, B.E., S.S. Kavelin, A.M. Popel, I.N. Lyssenko, I.M. Polluksov, V.S. Varyvdin, K.V. Rodin, and V.V. Ovsyanikov, The AUREOL-3 satellite, Ann. Geophys., 38, 547-556, 1982.

Lancaster, E.R., T. Jennings, M. Morrissey, and R. Langel, Magsat vector magnetometer calibration using Magsat geomagnetic field measurements, NASA TM 82046, November 1980.

Langel, R.A., Processing of the total field magnetometer data from the OGO-2 satellite, GSFC report X-612-67-272, 1967.

Langel, R.A. and R.H. Estes, A Geomagnetic Field Spectrum, Geophys. Res. Letters, 9, 250-253, 1982.

Langel, R.A. and R.T. Baldwin, Geodynamics branch data base for main magnetic field analysis, NASA TM 104542, April, 1991.

Langel, R.A., J. Berbert, T. Jennings, and R. Horner, Magsat data processing: A report for investigators, NASA TM 82160, November, 1981.

Langel, R.A., J.R. Ridgway, M. Sugiura and K. Maezawa, The geomagnetic field at 1982 from DE-2 and other magnetic field data, submitted to J. Geomagn. Geoelectr., 1988.

Langel, R.A., T.J. Sabaka, and R.T. Baldwin, An initial analysis of the data from the Polar Orbiting Geophysical (POGS) Satellite, NASA TM 104551, November 1991.

McDiarmid, I.B., J.R. Burrows, and M.D. Wilson, Comparison of magnetic field perturbations at high latitudes with charged particle and IMF measurements, Jour. Geophys. Res., 83, 681, 1978a.

McDiarmid, I.B., J.R. Burrows, and M.D. Wilson, Magnetic field perturbations in the dayside cleft and their relationship to the IMF, Jour. Geophys. Res., 83, 5753, 1978b.

Potemra, T.A., Birkeland currents: present understanding and some remaining questions, in High-Latitude Space Plasma Physics, ed. B. Hultqvist and T. Hagfors, Nobel Symp. 54, 335, 1982.

Potemra, T.A., Birkeland currents, recent contributions from satellite magnetic field measurements, Physica Scripta, T18, 152-157, 1987.

Rich, F.J., C.A. Cattell, M.C. Kelley, and W.J. Burke, Simultaneous observations of auroral zone electrodynamics by two satellites: Evidence for height variations in the topside ionosphere, Jour. Geophys. Res., 86, 8929, 1981.

Rich, F.J., D.A. Hardy, and M.S. Gussenhoven, Enhanced ionosphere-magnetosphere data from the DMSP satellites, Eos Trans. AGU, 66, 513, 1985.

Ridgway, J.R., Reduction of DE-2 satellite magnetic field data for modeling the main field of the Earth, Technical Report, #SAR-NAS5-28200-4-88-1., 1988.

Ridgway, J.R., T.J. Sabaka, D. Chinn, and R.A. Langel, Processing of DMSP magnetic data and its use in geomagnetic field modeling, NASA TM 100750, November, 1989.

Serafimov, K.B., I.S. Arshinkov, A.Z. Bochev, M.H. Petrunova, G.A. Stanov and S.K. Chapkanov, A measuring equipment for electric and magnetic fields in the range of the ionosphere-magnetosphere plasma mounted aboard the "Intercosmos-Bulgaria 1300" satellite, Acta. Astr., 9, 397-399, 1982.

Stanev, G., M. Petrunova, D. Teodosiev, I. Kutiev, K. Serafimov, S. Chapkunov, V. Chmyrev, N. Isaev, P. Puschaev, I. Pimenov, and S. Bilichanko, An instrument for DC electric field and AC electric and magnetic field measurements aboard 'Intercosmos-Bulgaria-1300' satellite, Adv. Space Res., 2, No. 7, 43-47, 1983.

Sugiura, M., Identifications of the polar cap boundary and the auroral belt in the high-altitude magnetosphere: A model for field aligned currents, Jour. Geophys. Res., 80, 2057, 1975.

Theile, B. and H.M. Praetorius, Field aligned currents between 400 and 3000 km in auroral and polar latitudes, Planet. Space Sci., 21, 179, 1973.

Table 1: Gradient of Magnetic Field: Equivalent Measurement Error for 1 km of Orbit Error.

COMPONENT	MAXIMUM GRADIENT (nT/km)		
	Vertical	Along Track	Cross Track
Br	-28.0	-13.3	6.8
$B\theta$	18.0	-6.5	23.4
$B\phi$	8.4	-2.0	23.3
B	-28.0	-6.1	5.7

Table 2: Field Error Due to Timing Error

Assuming a Satellite Velocity of 7 km/sec and a polar orbit.

	POSITION ERROR	EQUIVALENT FIELD ERROR (nT)			
TIME ERROR (sec)	ALONG TRACK (km)	B_r	$B\theta$	$B\phi$	B
0.001	0.007	0.09	0.05	0.014	0.04
0.01	0.07	0.93	0.46	0.14	0.43
0.1	0.7	9.31	4.55	1.4	4.27
1.0	7.0	93.1	45.2	14.0	42.7

Table 3: TRANSLATION OF POSITION ERROR TO EQUIVALENT FIELD ERROR

	EQUIVALENT MAXIMUM FIELD ERROR (nT)			
POSITION ERROR	B_r	$B\theta$	$B\phi$	B
100 m Vertical	2.8	1.8	0.8	2.8
100 m Along Track	1.3	0.7	0.2	0.6
100 m Cross Track	0.6	2.3	2.3	0.5

Table 4: Estimated Position Error for Various Satellites

		TYPICAL POSITION ERROR (m)		
SATELLITE	TRACKING SYSTEM	VERTICAL	ALONG TRACK	CROSS TRACK
POGO [1965-1971]	Range and Range Rate	250	1000	1000
Magsat [1980]	Doppler	30 - 60	60 - 200	20 - 60
ARISTOTELES [1997 ?]	GPS Nominal	0.1-0.2	0.1-0.2	0.1-0.2
	Best	0.01	0.01	0.01

Table 5.

ERROR BUDGET SUMMARY BY SATELLITE

SATELLITE	VANGUARD 3	COSMOS 49	POGO -2	POGO -4	POGO -6	MAGSAT SCALAR	MAGSAT VECTOR	DE-2	DE-1 (PERIGEE)	POGS
INSTRUMENT (nT)	<1	2.0	0.9	0.9	0.9	1.5	3.0 (CALIBRATED)	?	?	?
DIGITIZATION RESOLUTION (nT)	NEGLIGIBLE	?	0.44	0.44	0.6	0.6	0.5	1.5	1.5	2.0
INSTRUMENT PARTICULAR (nT)	SPIN FREQ SHIFT 6.7 nT [2 nT AVG.] SIGNAL NOISE: 4 nT									
TIME: MS	100	500	30-70	30-70	10	1	1	5(?)	5(?)	≥2.5
: nT	4.3	21.4	1.3-3	1.3-3	0.43	0.04	0.04	0.21	0.21	1.1
SPACECRAFT FIELD	<1.0	2 (COMPENSATED)	<1.0	<1.0	<1.0	<1.0	<1.0	<1.0	<1.0	<5.0
POSITION:										
VERTICAL: KM	4(?)	1	0.25	0.25	0.25	0.06	0.06	0.12	0.12	0.06
: nT	112(?)	28	7	7	7	1.7	0.8	3.4	3.4	1.7
HORIZ : KM	9(?)	3	1	1	1	0.2	0.2	0.6	0.6	0.2
: nT	207(?)	69	6	6	6	5.6	1.4	16.8	16.8	5.6
ATTITUDE: ASEC							20			
: nT							4.8			
STATISTICS FROM MODEL FIT TO THE DATA										
MEAN	1.2	?	0.3	0.1	-0.6	0.5-1.0	1.0-2.0	-3.5		-0.05
σ	12.0	22.0	5.2	6.8	6.3	7.0	6-8.2	23.0		60.0
STATISTICS FROM IGRF MODEL										
MEAN	-1.1	-7.8	1.4	-1.1	-4.6	-5.1	-7.8	-8.0		
σ	12.1	69.3	14.0	18.2	17.6	15.6	12.0	31.7		

Table 6.

SPACECRAFT OBTAINING NEAR-EARTH MAGNETIC FIELD MEASUREMENTS

SATELLITE	INCLINATION	ALTITUDE RANGE (km)	DATES	INSTRUMENTS	APPROXIMATE ACCURACY (nT)	COVERAGE
Sputnik 3	65°	226-1881	5/58-6/58	Fluxgates	100	USSR
Vanguard 3	33°	510-3750	9/59-12/59	Proton	10	near ground station
1963-38C	Polar	1100	9/63-1/74	Fluxgate	unknown	near ground station
Cosmos 26	49°	270-403	3/64	Proton	unknown	whole orbit
Cosmos 49	50°	261-488	10/64-11/64	Proton	22	whole orbit
1964-83C	90°	1040-1089	12/64-6/65	Rubidium	22	near ground station
OGO-2	87°	413-1510	10/65-9/67	Rubidium	6	whole orbit
OGO-4	86°	412-908	7/67-1/69	Rubidium	6	whole orbit
OGO-6	82	397-1098	6/69-7/71	Rubidium	6	whole orbit
Cosmos 321	72°	270-403	1/70-3/70	Cesium	unknown	whole orbit
Triad	Polar	750-832	9/72-1/84	Fluxgate	about 200	near ground station
S3-2	97°	230-900	10/72-5/1/78	Fluxgate	>300	whole orbit
Magsat	97°	325-550	11/79-5/80	Fluxgate and Cesium	6 3	whole orbit
DE-2	89.97	309-1012	8/81-2/83	Fluxgate	about 100 per axis 28 for scalar	whole orbit
DE-1	89.91	570 - 3.6 RE	8/81-3/91	Fluxgate	----------	whole orbit
ICB-1300	81°	825-906	10/81-8/7/83	Fluxgate	>75	part orbit
AUREOL-3	82.5°	408-2012	9/81-?	Fluxgate	>150	part orbit
Hilat	82°	800	6/83-7/18/89	Fluxgate	about 200	near ground station
DMSP F-7	Polar	835	11/83-1/88	Fluxgate	>1000	whole orbit
Polar Bear	Polar	1000	11/86-present	Fluxgate	about 200	near ground station
POGS	Polar	800	7/90-present	Fluxgate	TBD	whole orbit (?)

TABLE 7: GSFC SATELLITE DATA BASE FOR MAIN FIELD MODELING

Satellite	Inclination	Altitude Range (km)	Dates	Local Time Coverage	Number of Data Points
Vanguard 3	33°	510-3750	9/59-12/59	Most	3,872
Cosmos 49	50°	261-488	10/64-11/64	All	17,429 scalar
POGO					
OGO-2	87°	413-1510	10/65-9/67	Concentrated at dawn & dusk	12,773
OGO-4	86°	412-908	7/67-1/69	All in about 5 months	18,431
OGO-6	82°	397-1098	6/69-7/71	All in about 5 months	16,196
Magsat	97°	325-550	11/79-5/80	Dawn and Dusk	48679 vector (below 50° lat) 25016 scalar
DE-2	90°	309-1012	8/81-2/83	Concentrated at dawn & dusk	5100 scalar
POGS	89.9°	639-769	6/90---	All	

Table 8: PROJECTED LAUNCH SCHEDULE

ARISTOTELES	MID 1997
APAFO	LATE 1999
GOS	MID 2001
DMSP/POGS	
S-15	1995-2000
BLOCK 6	~ 2005

ACKNOWLEDGEMENTS

We would like to thank T. Sabaka, J. Slavin, and P. Taylor for critical reading of the manuscript and R. Orem for help with the Figures and logistics. This work was supported by NASA RTOP 579-31-02 for which we are grateful.

FIGURES

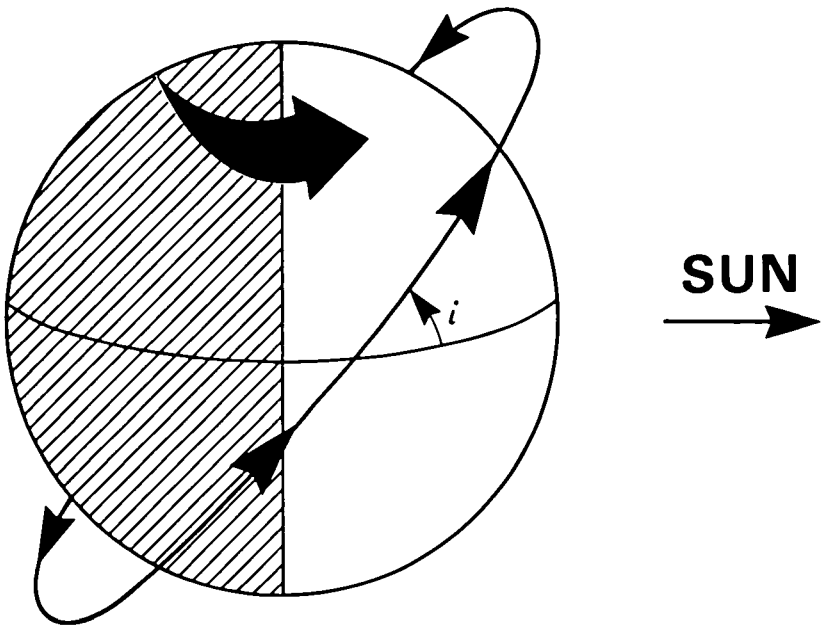

figure 1

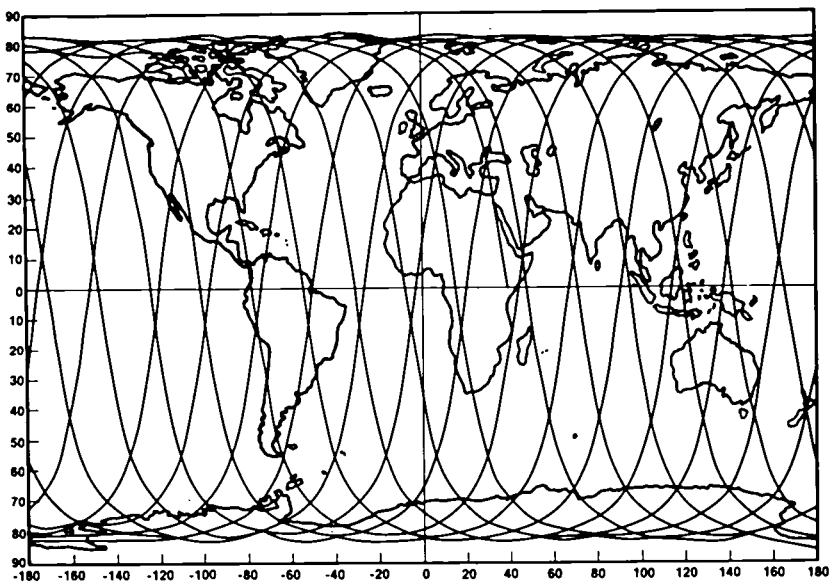

figure 2

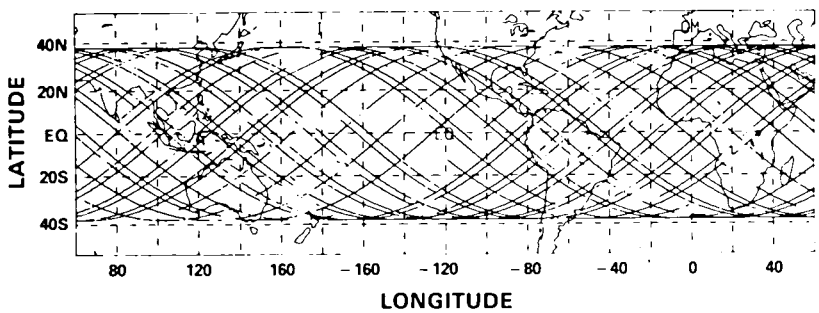

figure 3

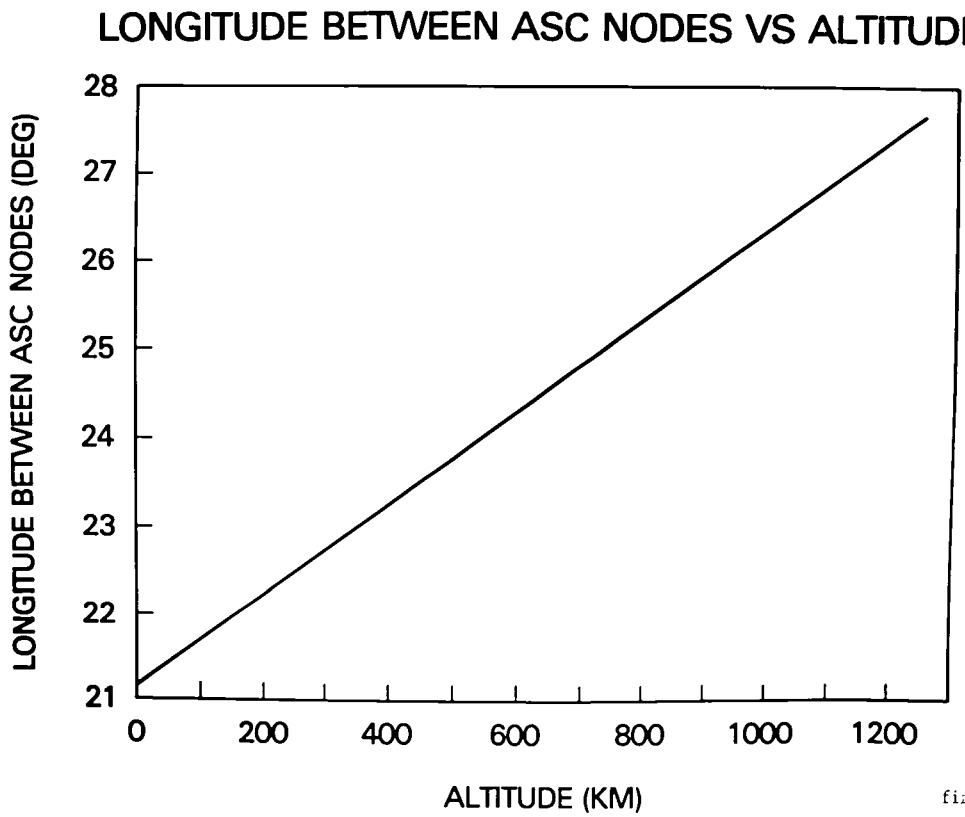

figure 4

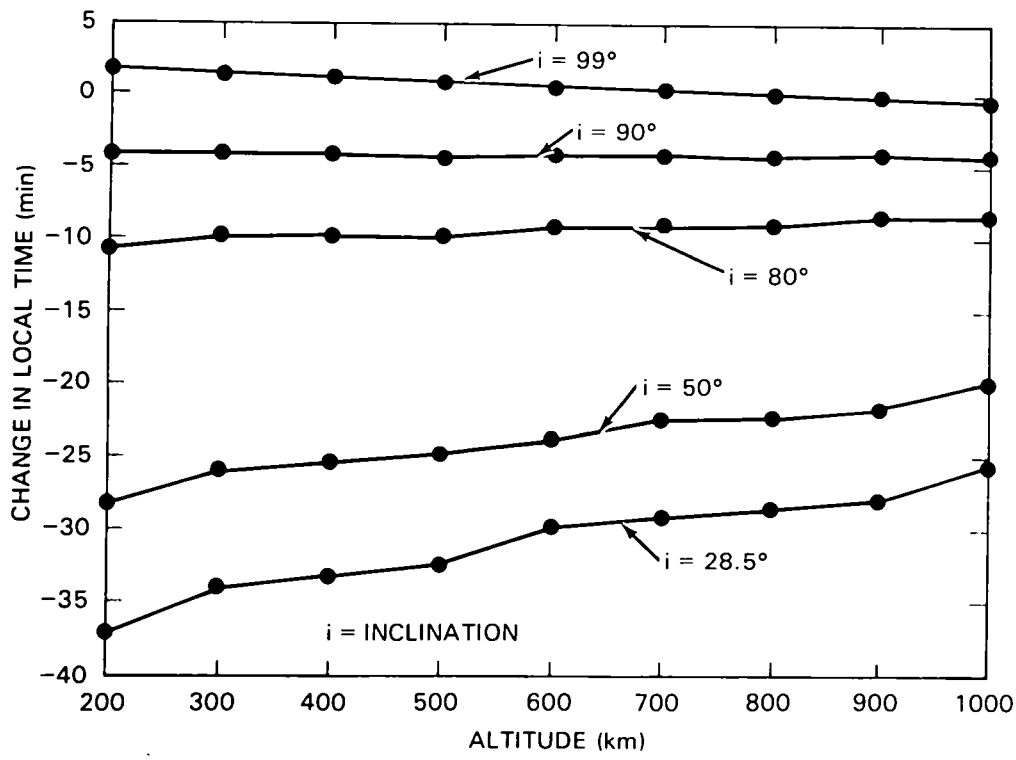

figure 5

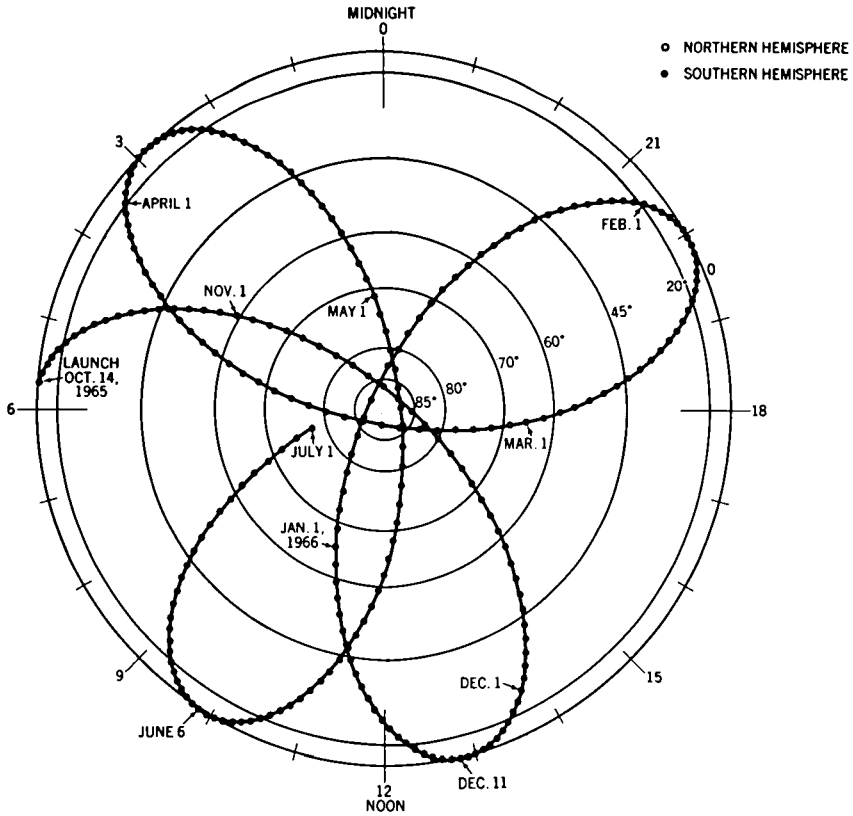

PERIGEE MOTION OF POGO -1 ORBIT
OCT. 14, 1965 - JULY 1, 1966

figure 6

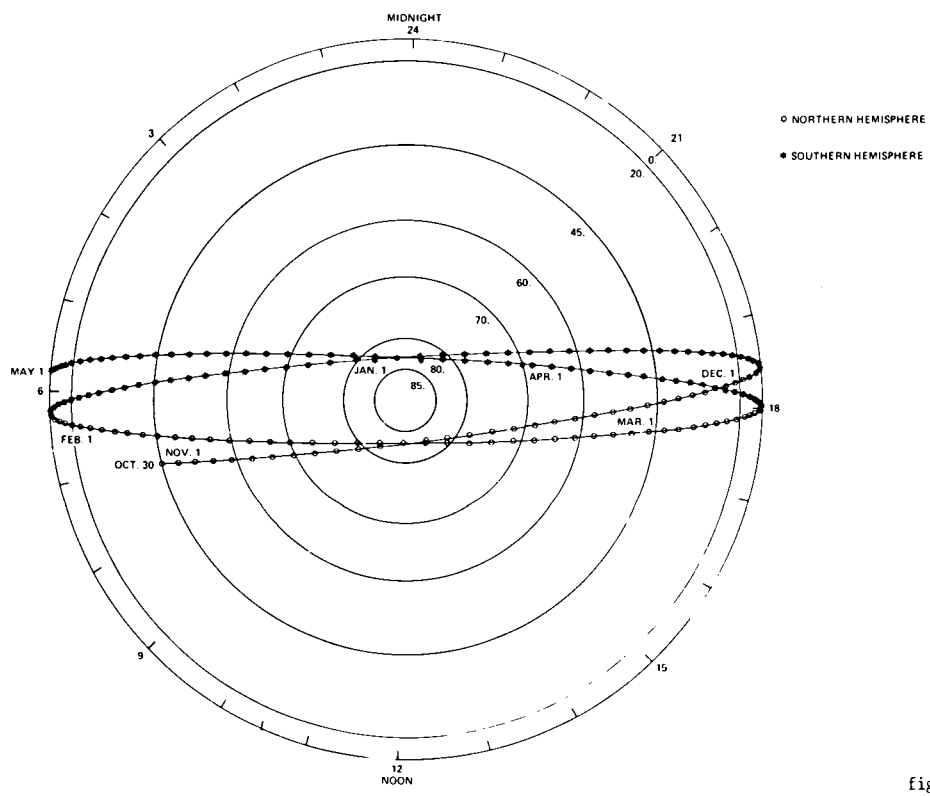

figure 7

ATTITUDE ERROR

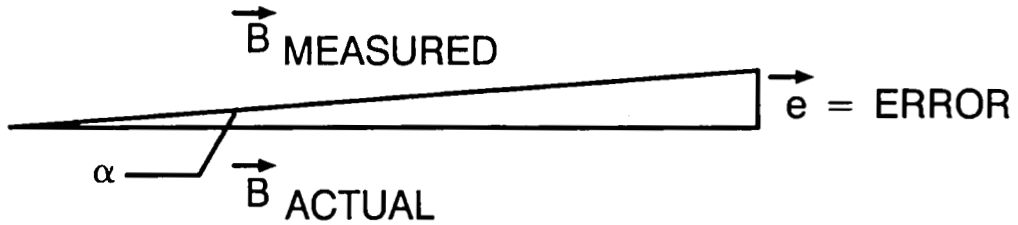

$$\frac{|\vec{e}| = |B| \sin\alpha}{\cos\alpha/2} \approx |B| \sin\alpha \quad \text{FOR SMALL } \alpha$$

FOR $|B| = 50.000$

α	$\lvert\vec{e}\rvert$ (nt)
1°	872
0.5°	436
1 MINUTE	14.5
0.5 MINUTE	7.3
1 SECOND	0.242

figure 8

CHANGES IN ATTITUDE ALIGNMENT, DATA ADJUSTMENTS, FOR THE PITCH, ROLL, AND YAW AXIS. FINE ATTITUDE DATA ONLY

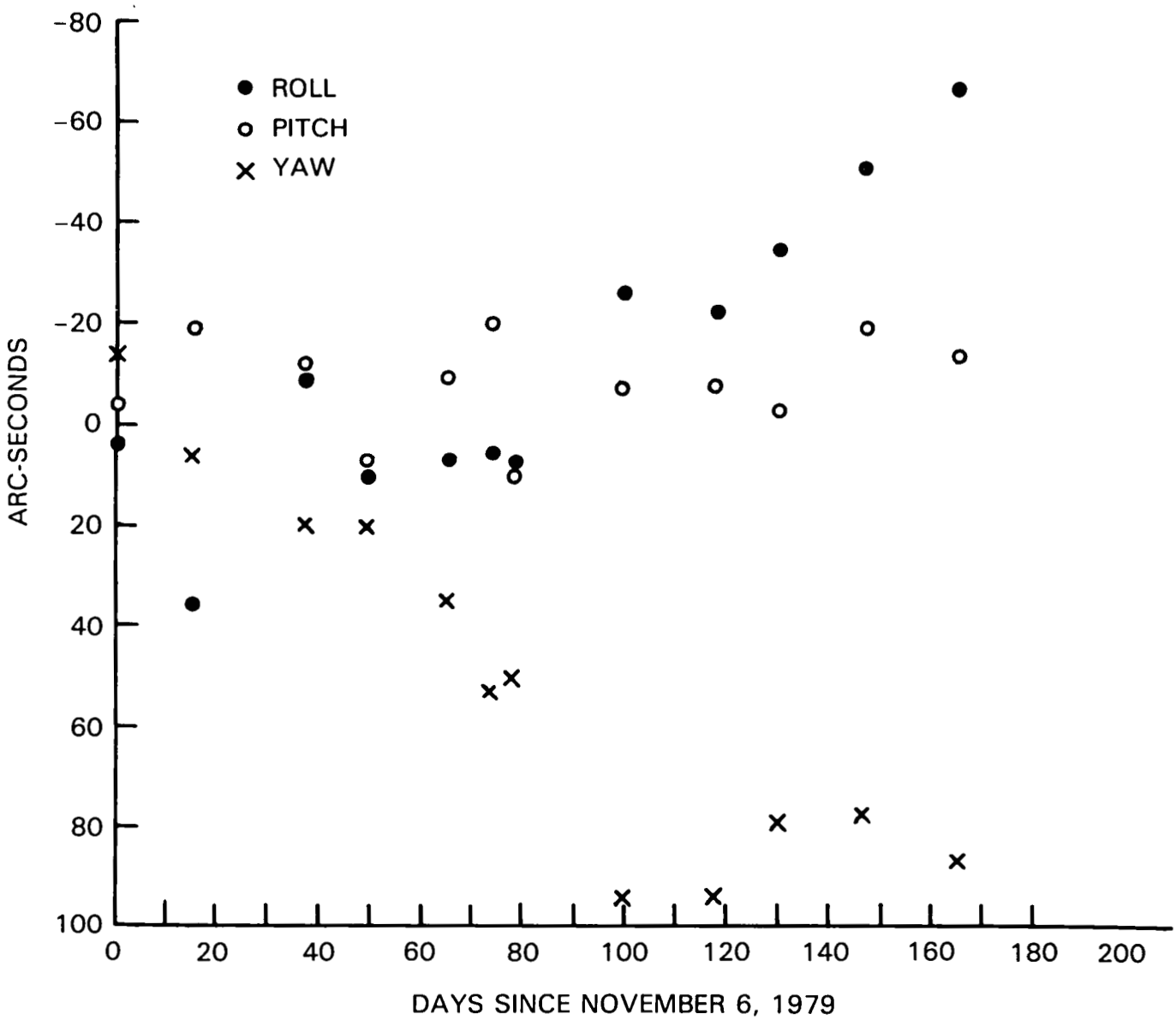

figure 9

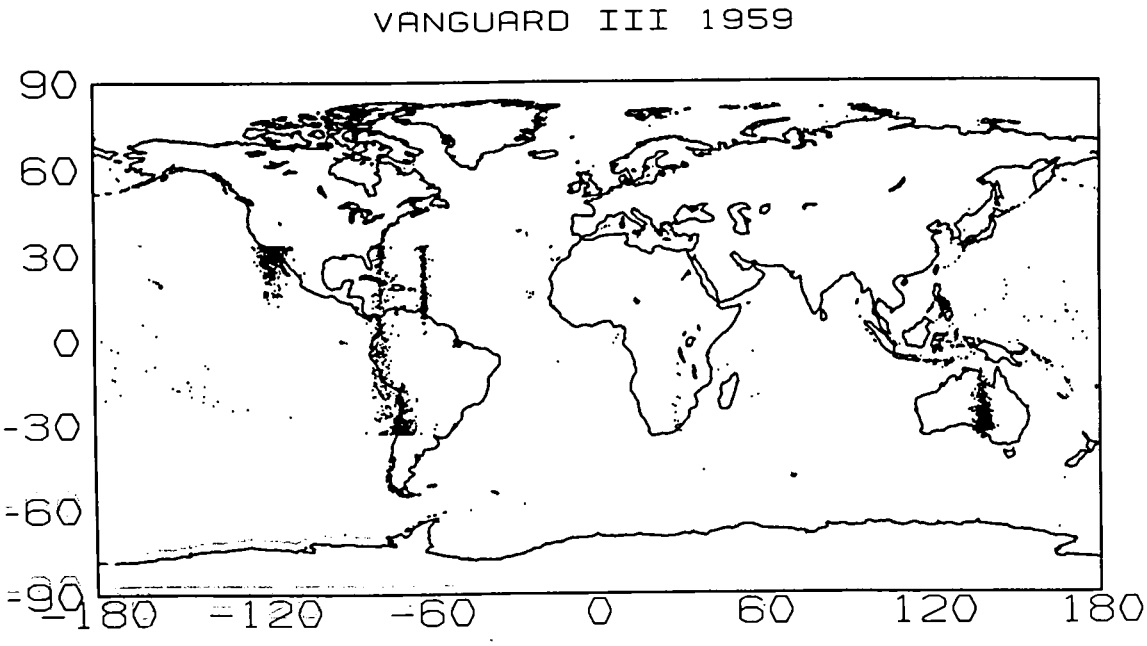

figure 10

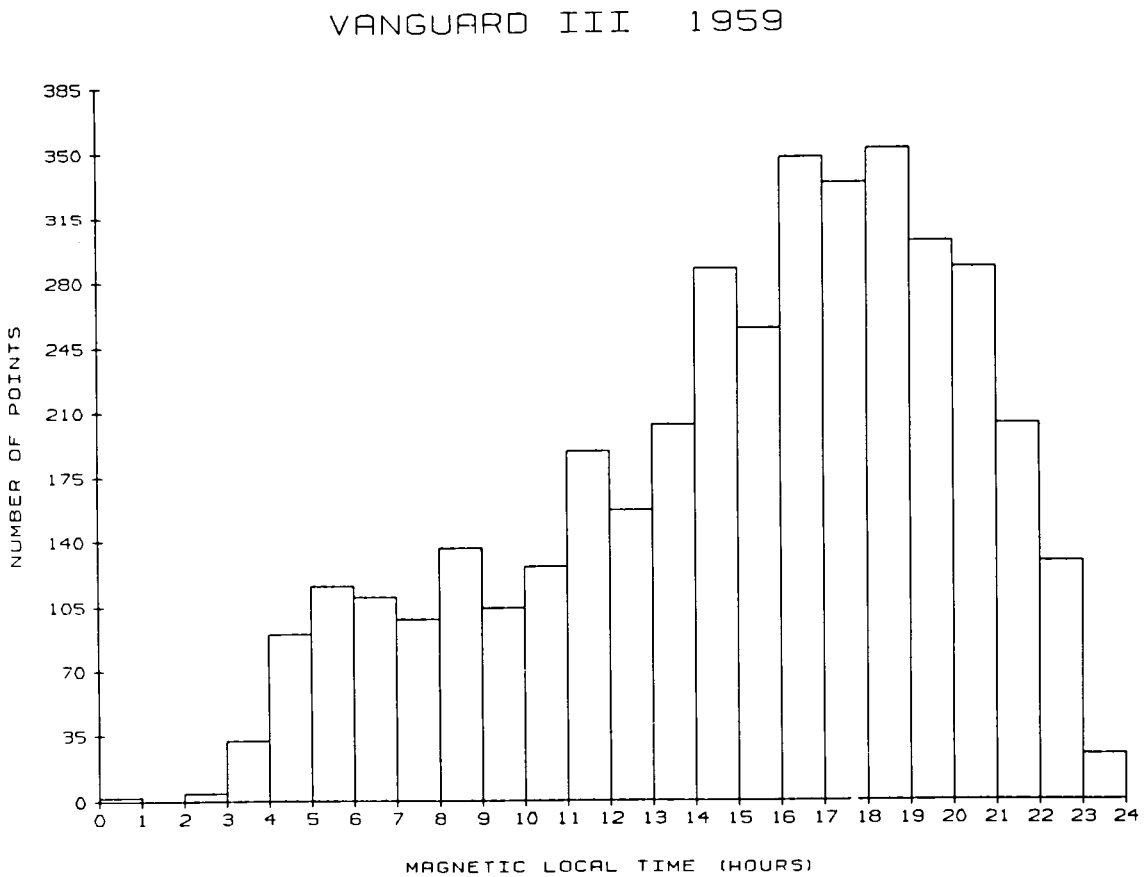

figure 11

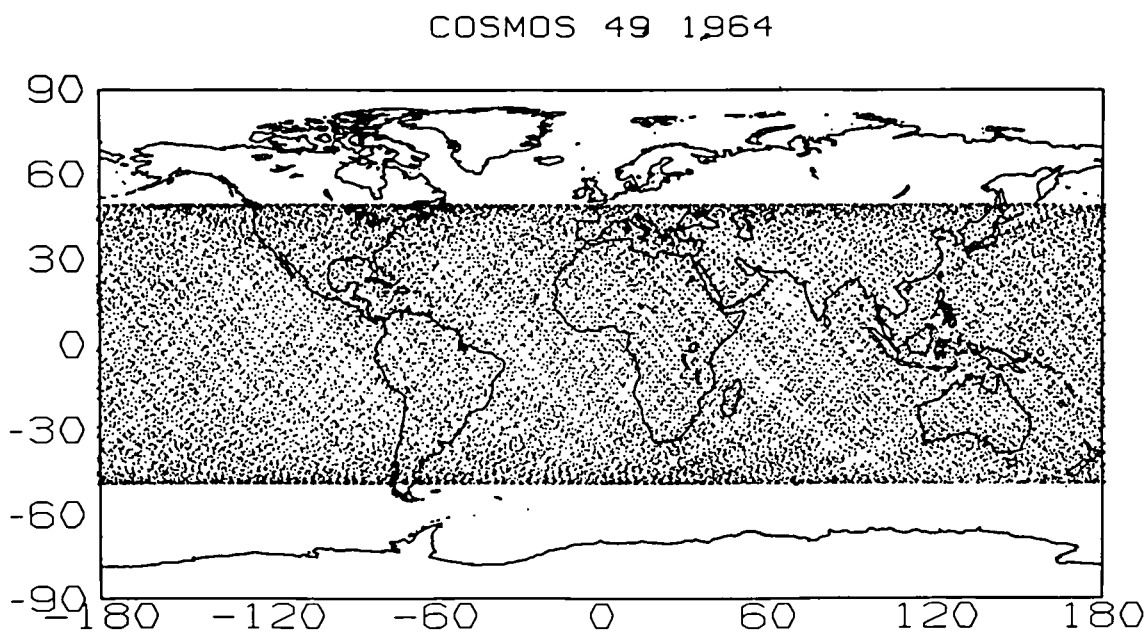

figure 12

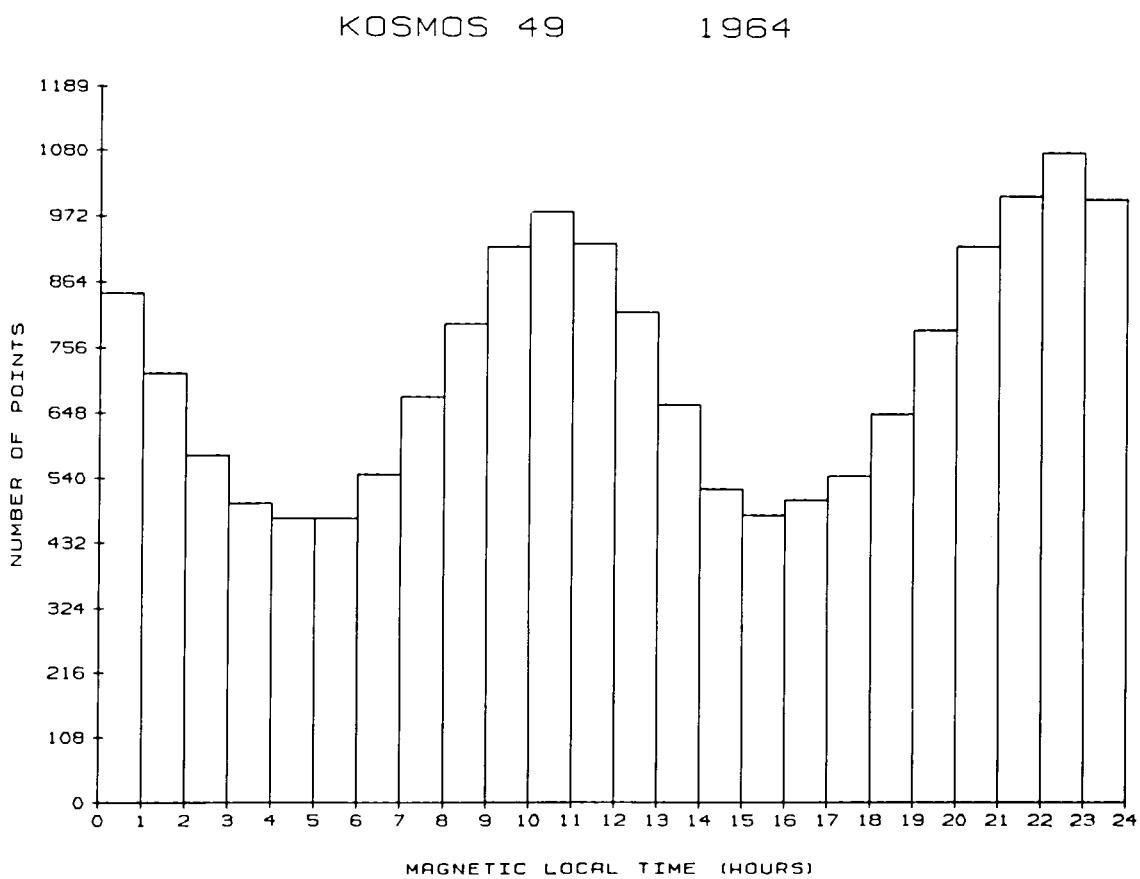

figure 13

OGO – 2
7/65 – 12/65

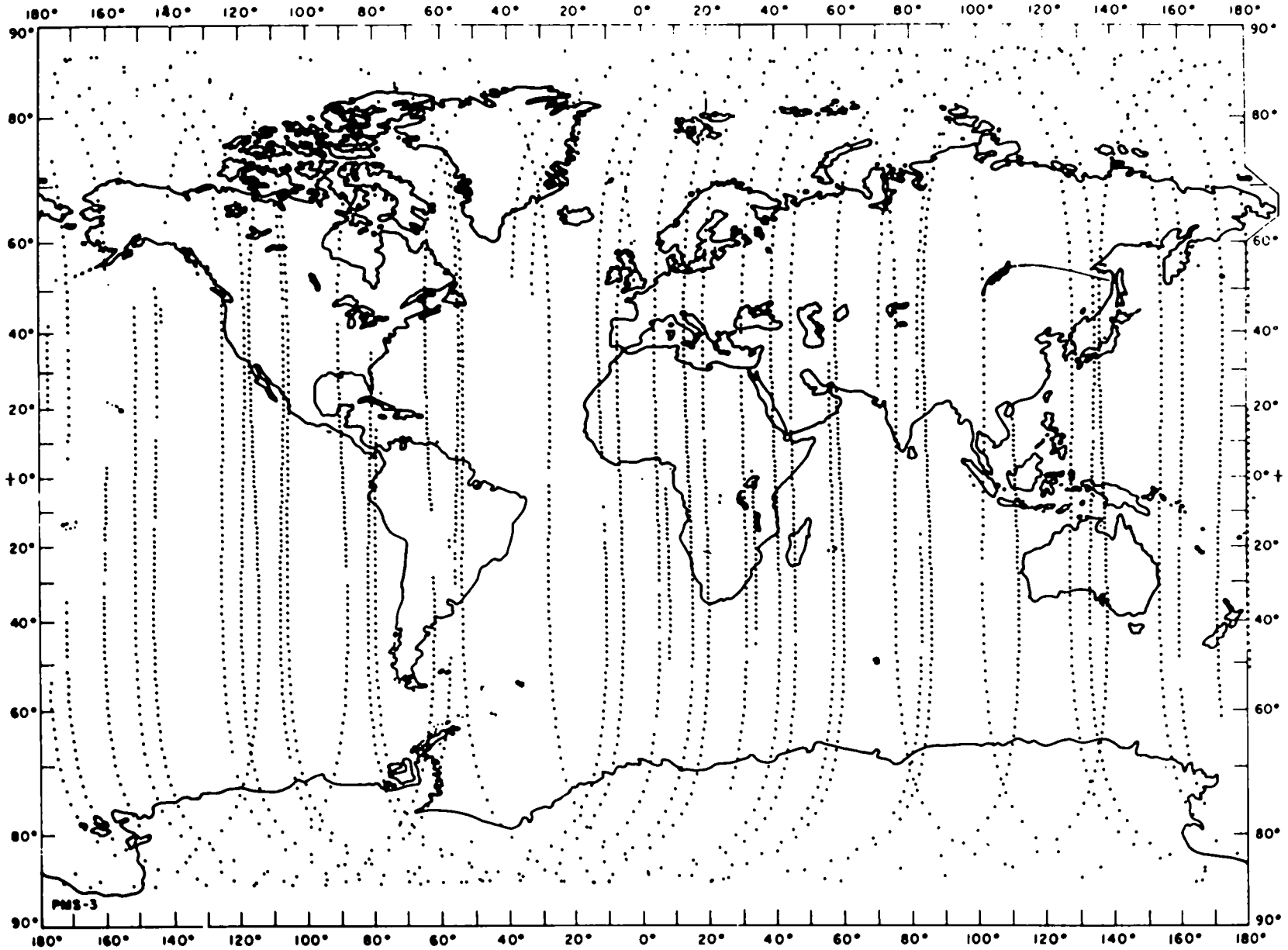

figure 14a

OGO - 2

1/66 - 6/66

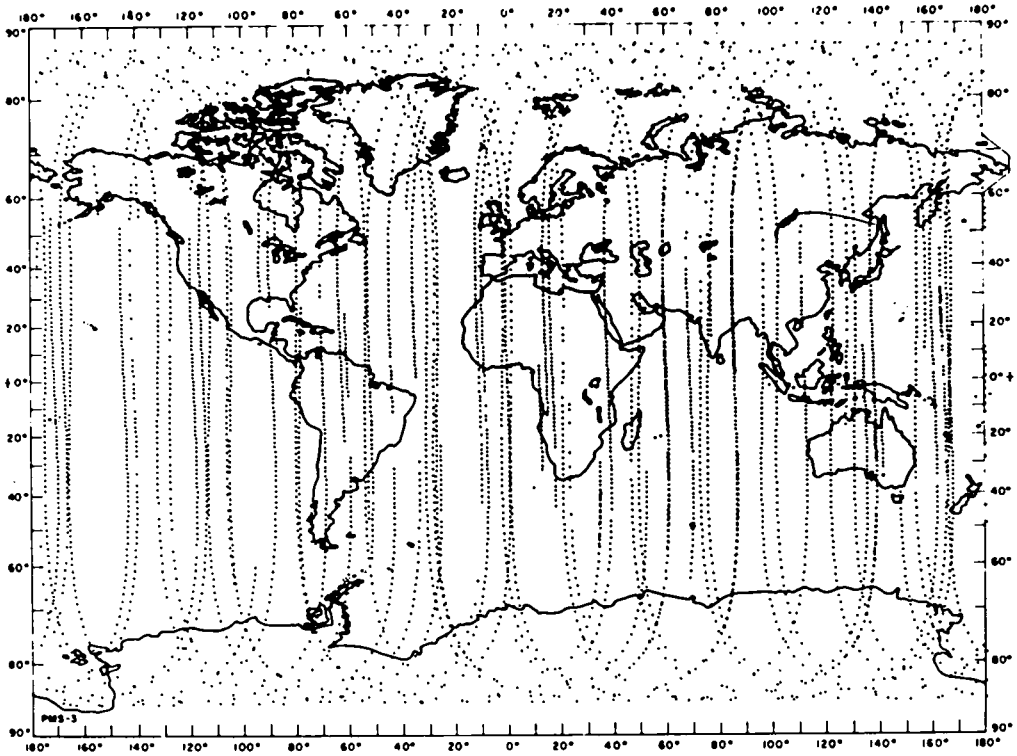

figure 14b

7/66 - 12/66

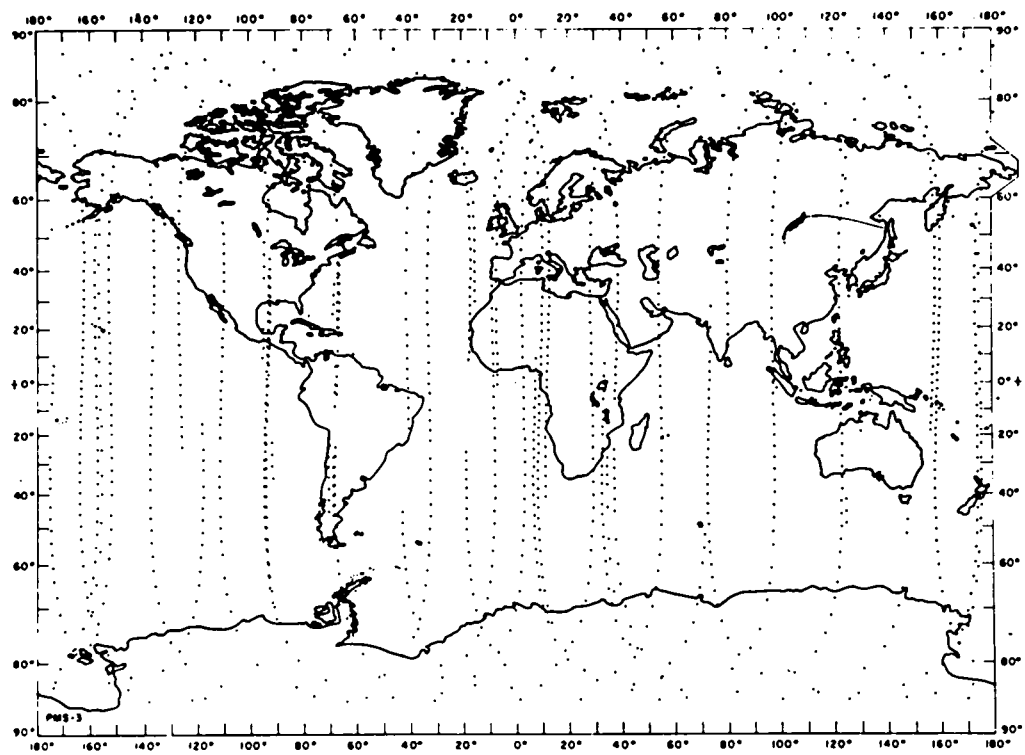

figure 14c

OGO - 2

1/67 - 6/67

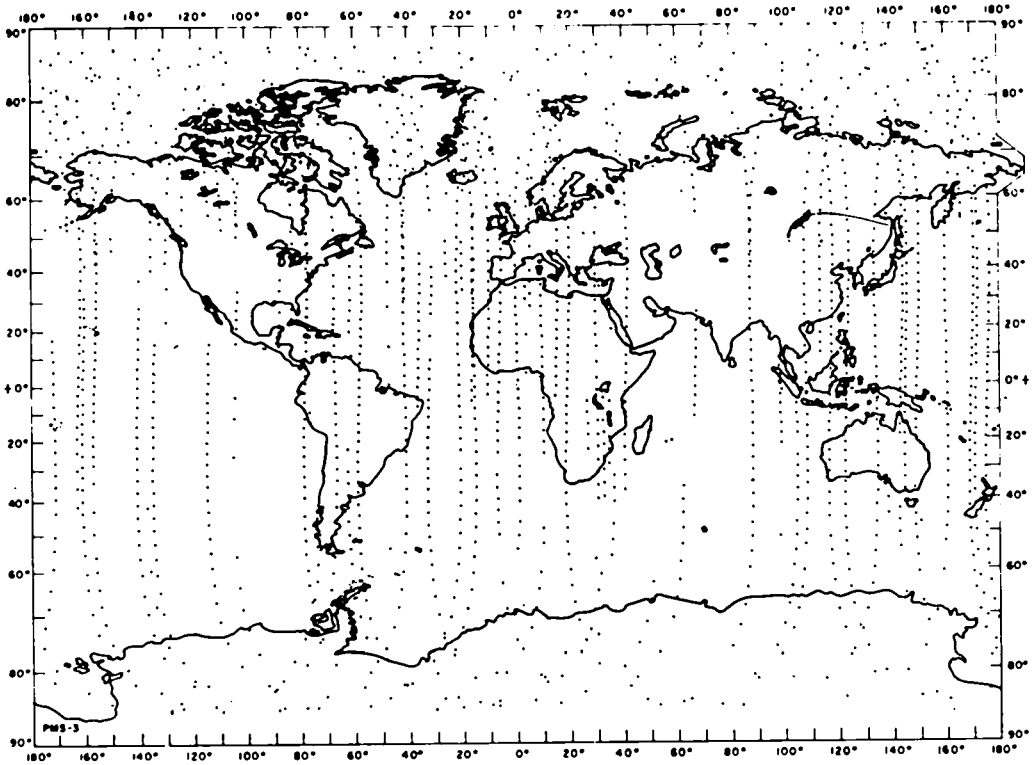

figure 14d

7/67 - 12/67

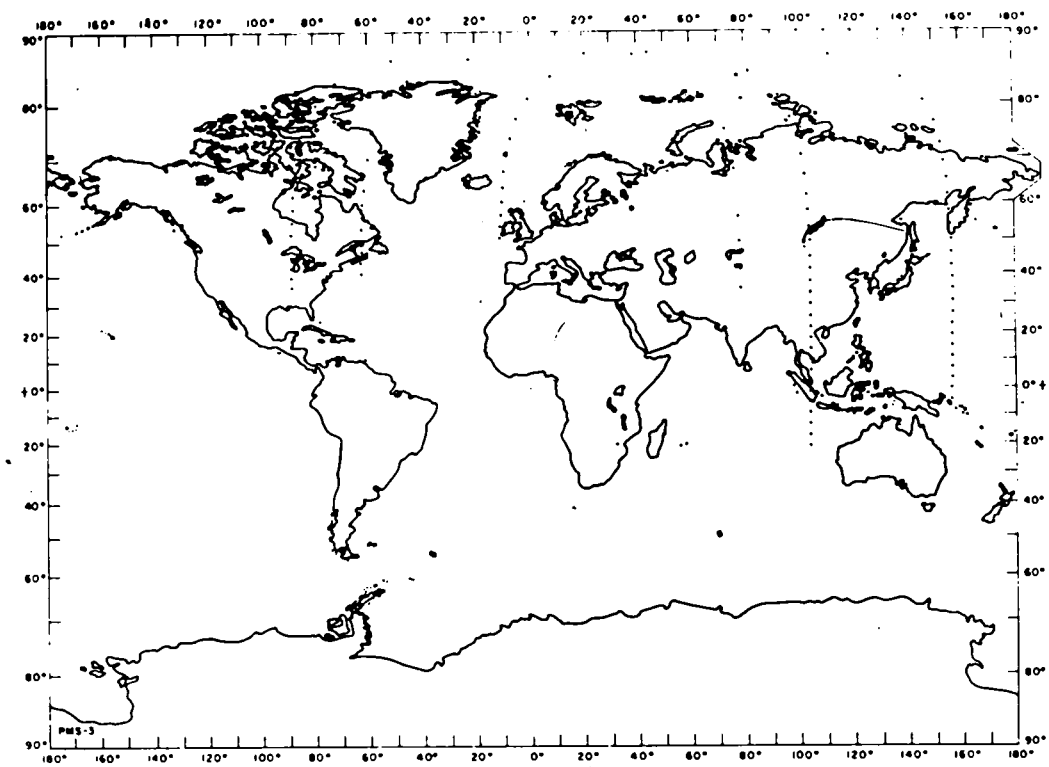

figure 14e

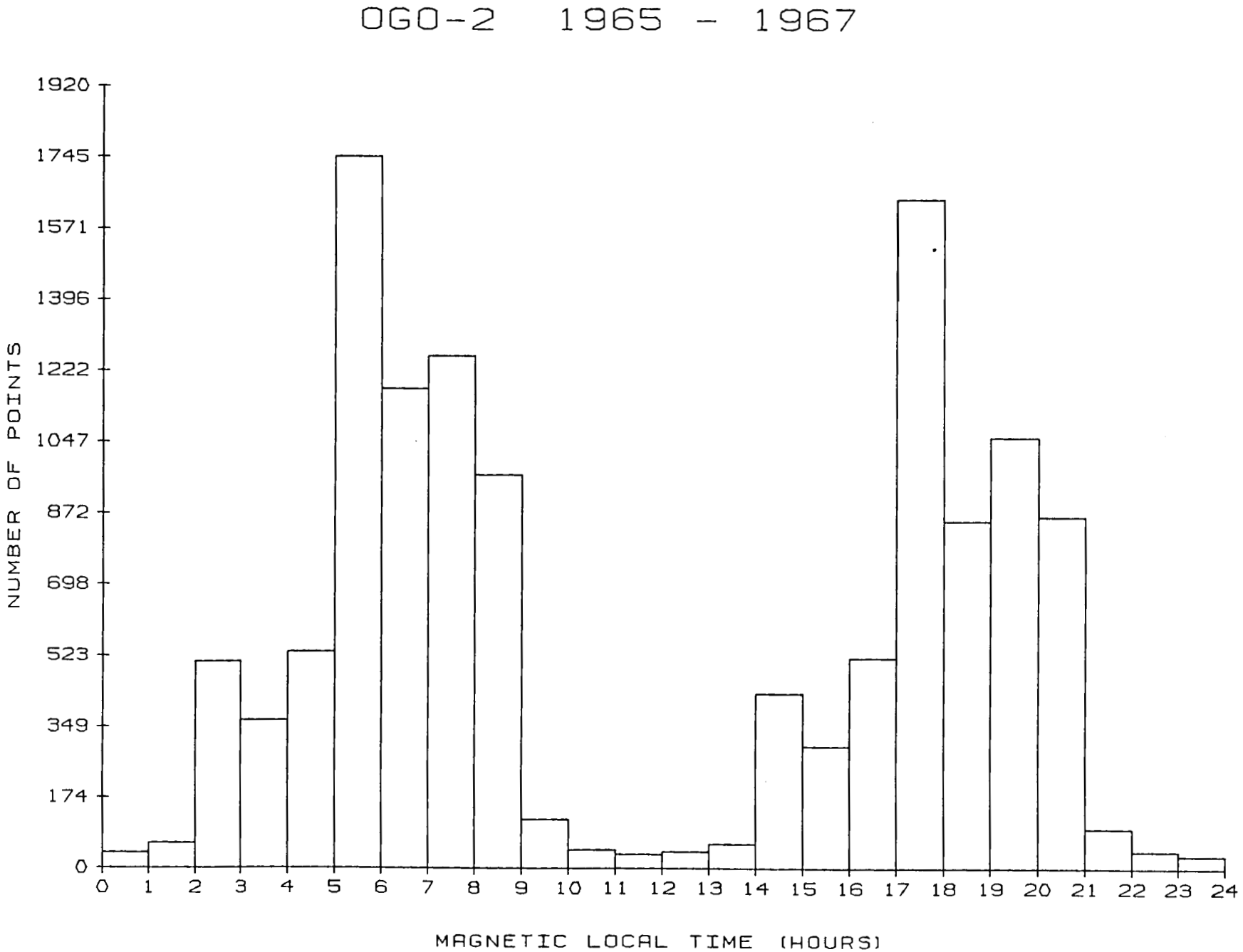
OGO-2 1965 - 1967
NUMBER OF POINTS
1920
1745
1571
1396
1222
1047
872
698
523
349
174
0
0 1 2 3 4 5 6 7 8 9 10 11 12 13 14 15 16 17 18 19 20 21 22 23 24
MAGNETIC LOCAL TIME (HOURS)

figure 15

OGO-4
7/67 - 12/67

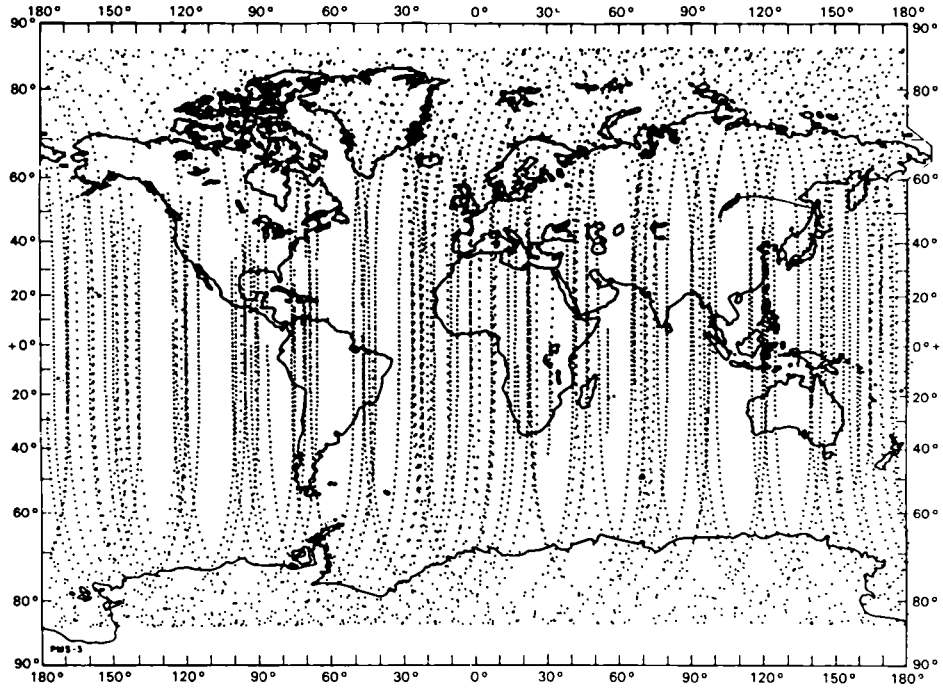

figure 16

OGO-4 1967 - 1969

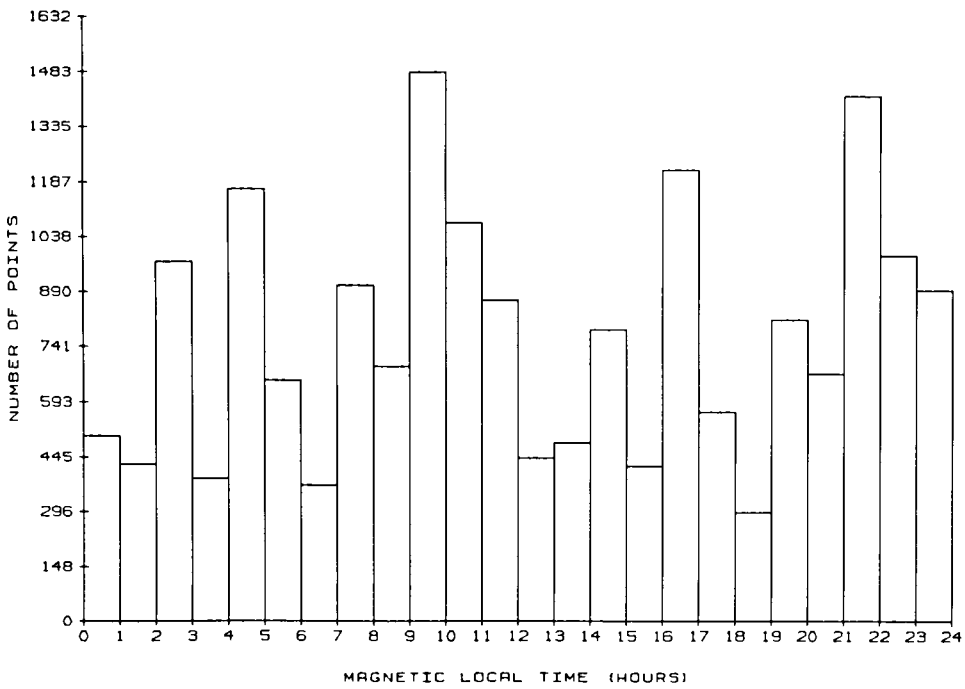

figure 17

OGO - 6

1/69 - 6/69

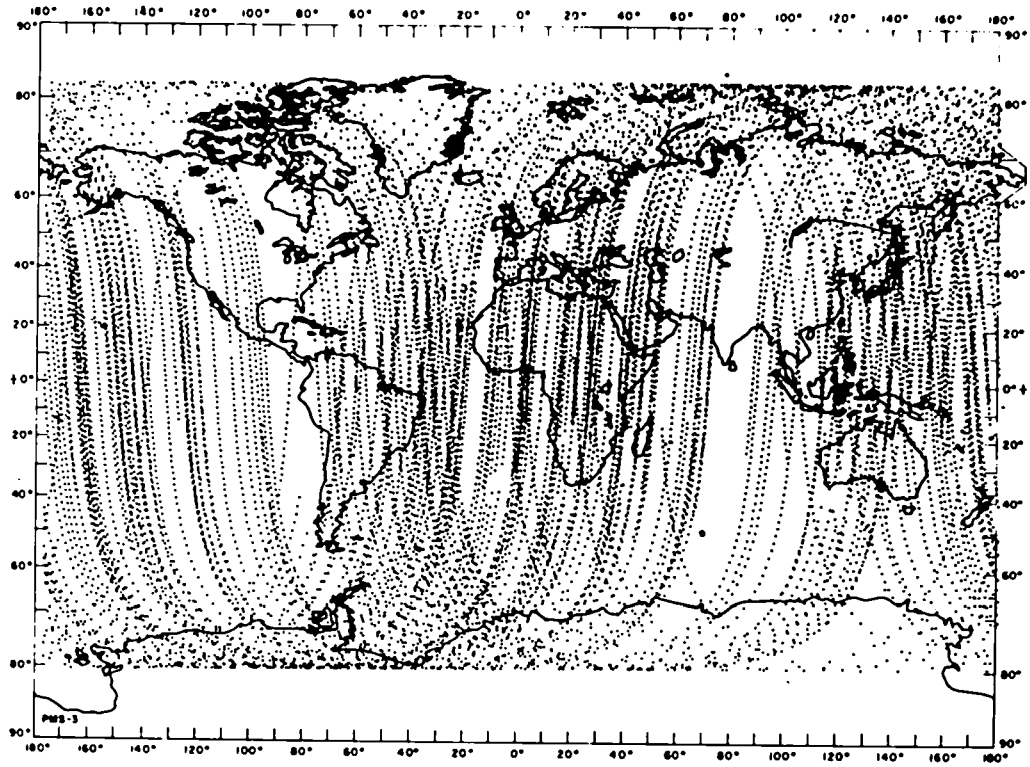

figure 18a

7/69 - 12/69

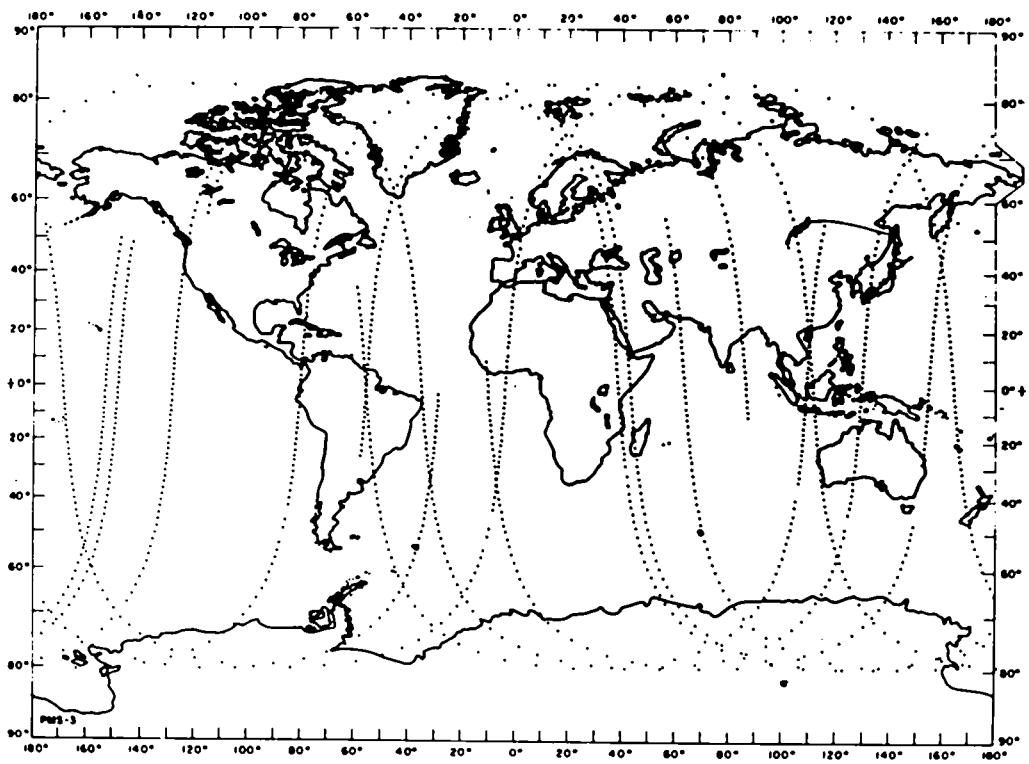

figure 18b

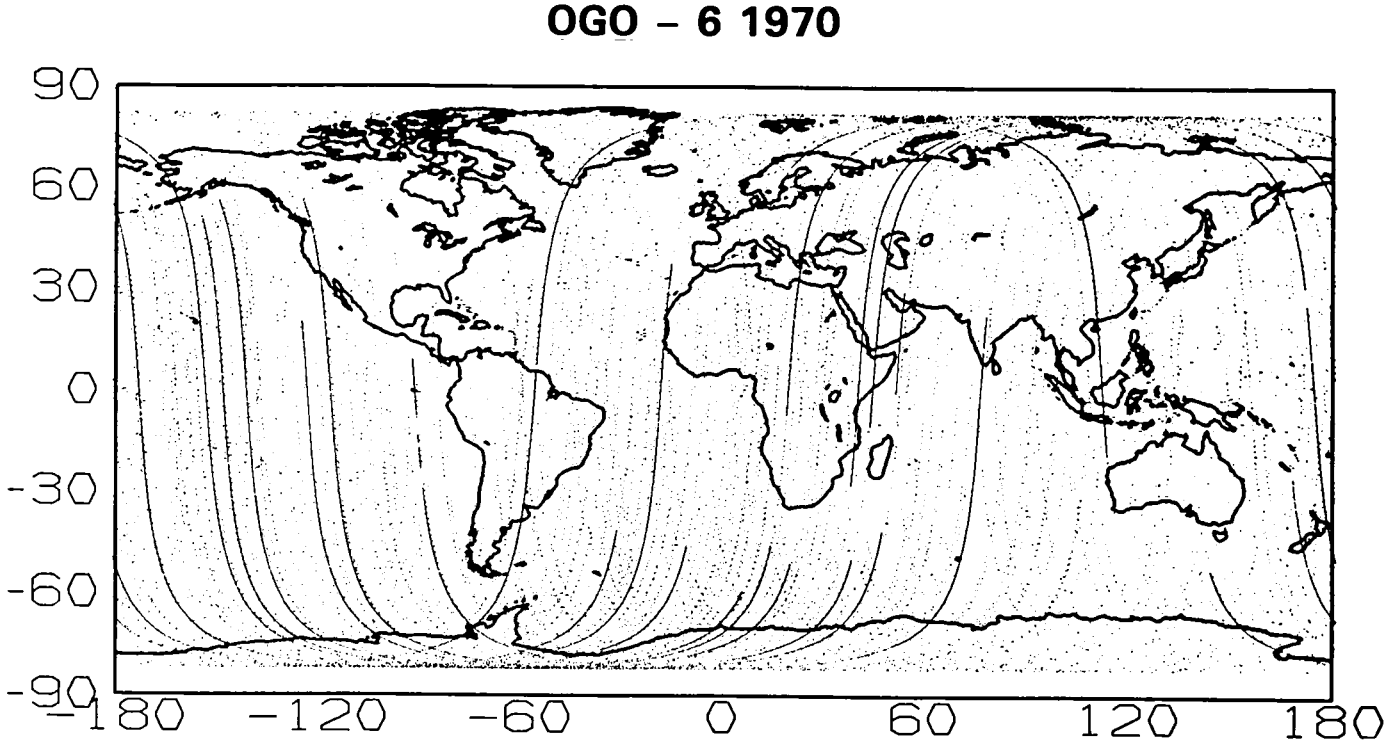

figure 18c

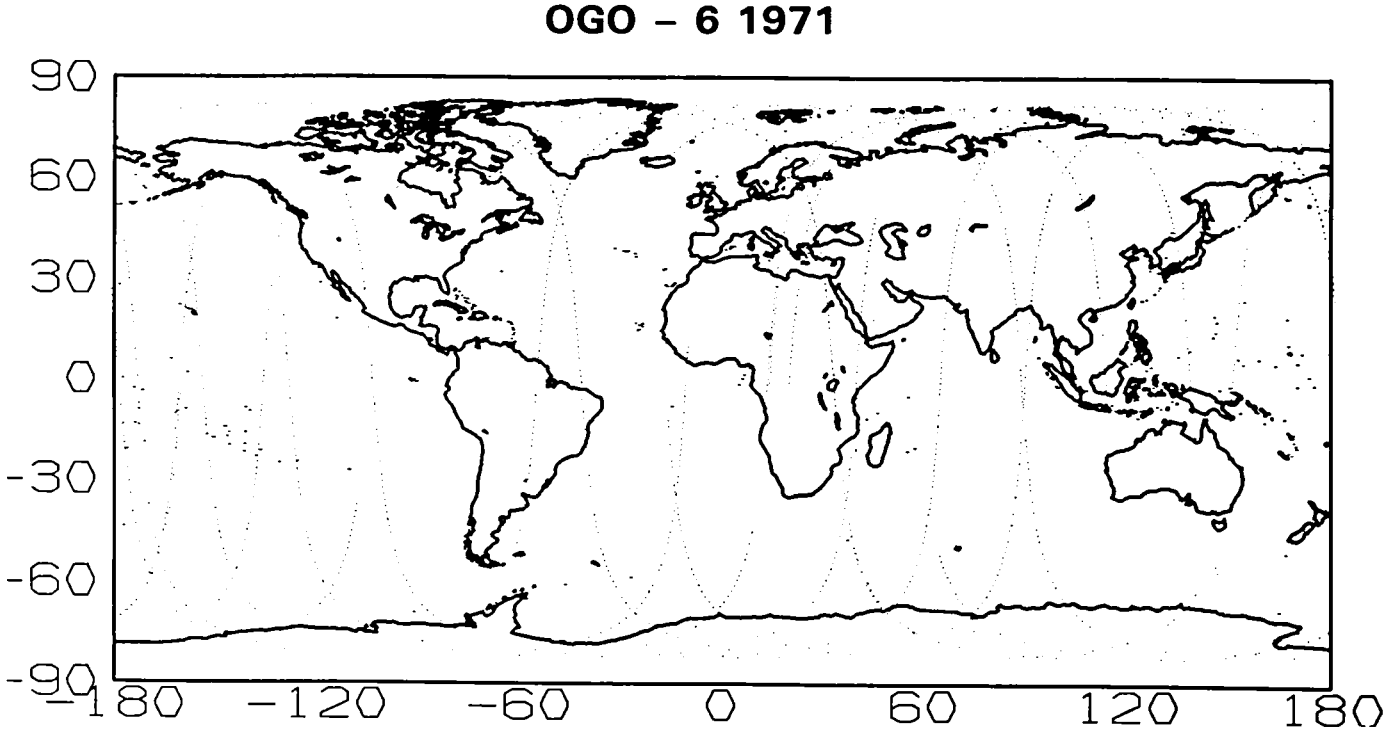

figure 18d

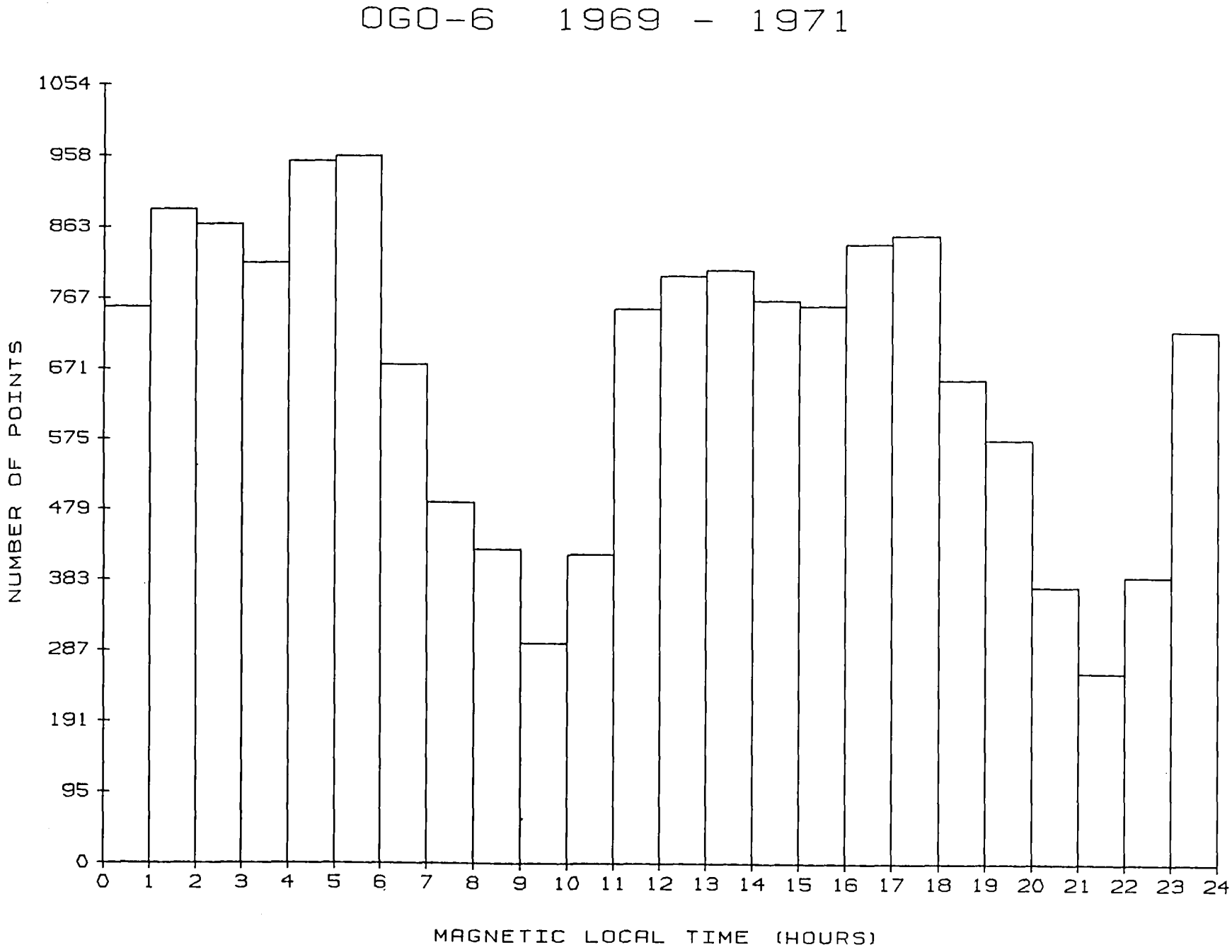
OGO-6 1969 - 1971
NUMBER OF POINTS
1054
958
863
767
671
575
479
383
287
191
95
0
0 1 2 3 4 5 6 7 8 9 10 11 12 13 14 15 16 17 18 19 20 21 22 23 24
MAGNETIC LOCAL TIME (HOURS)

figure 19

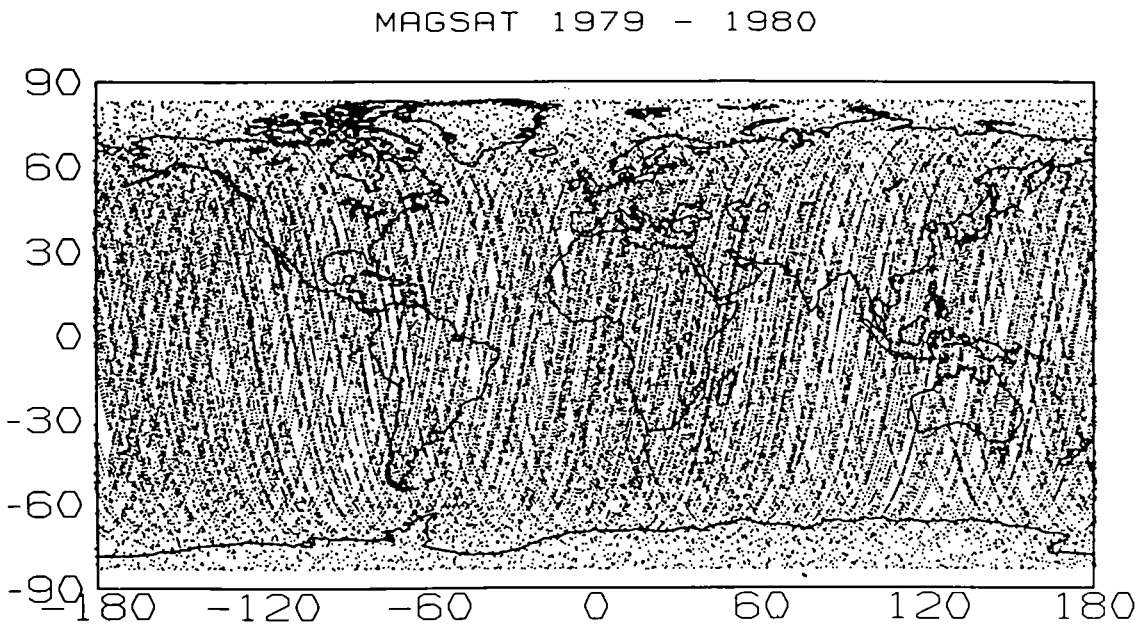

figure 20

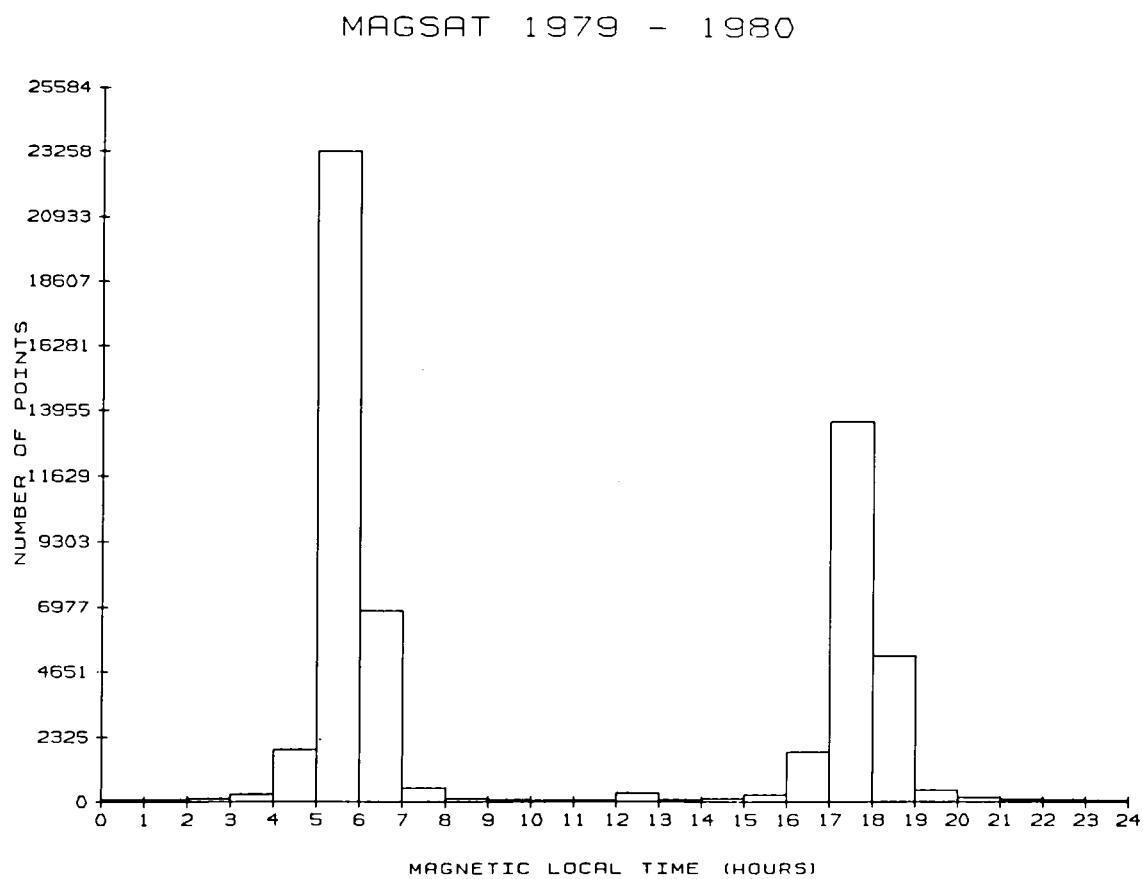

figure 21

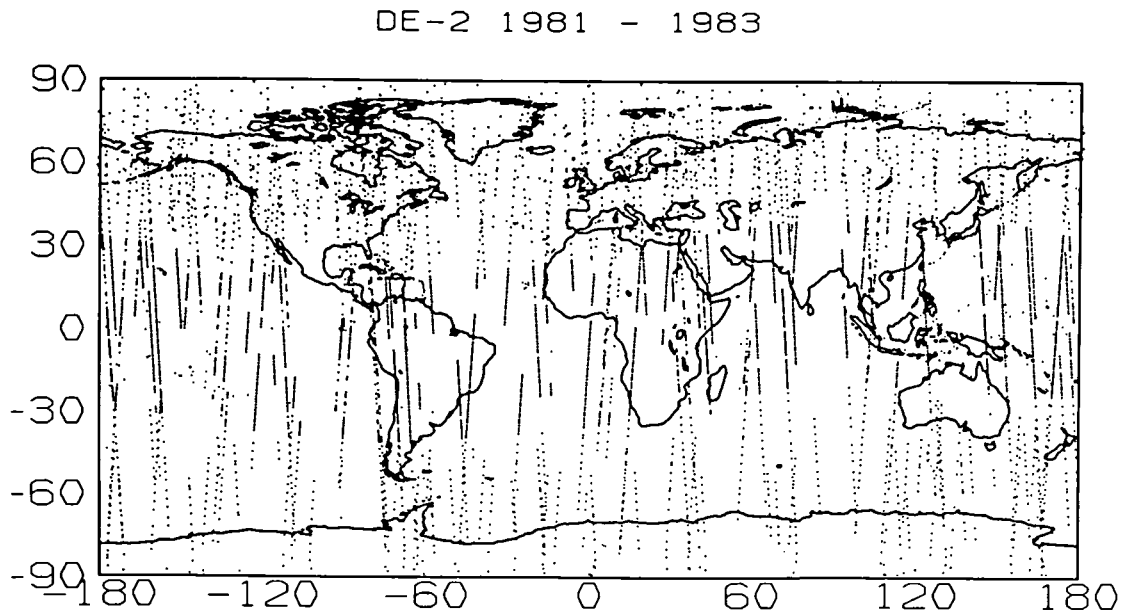

figure 22

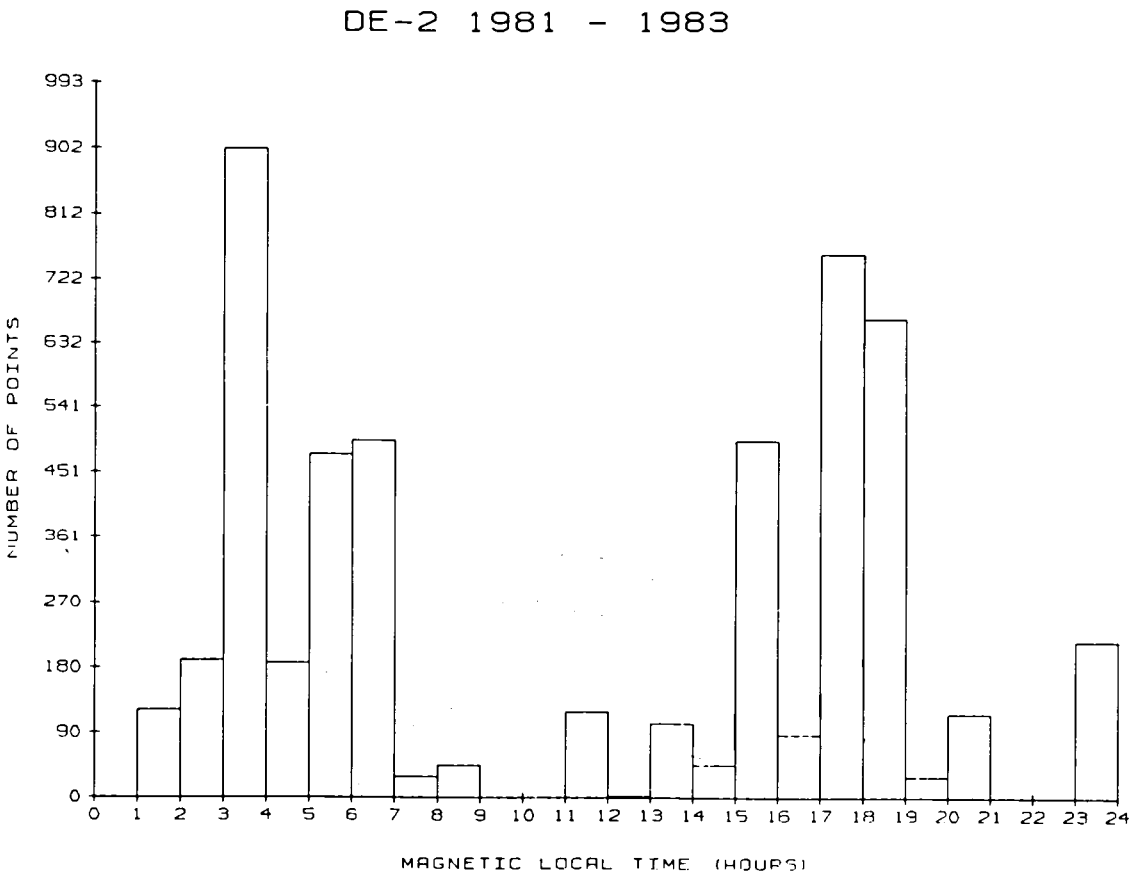

figure 23

GEOMAGNETIC OBSERVING SYSTEM (GOS)

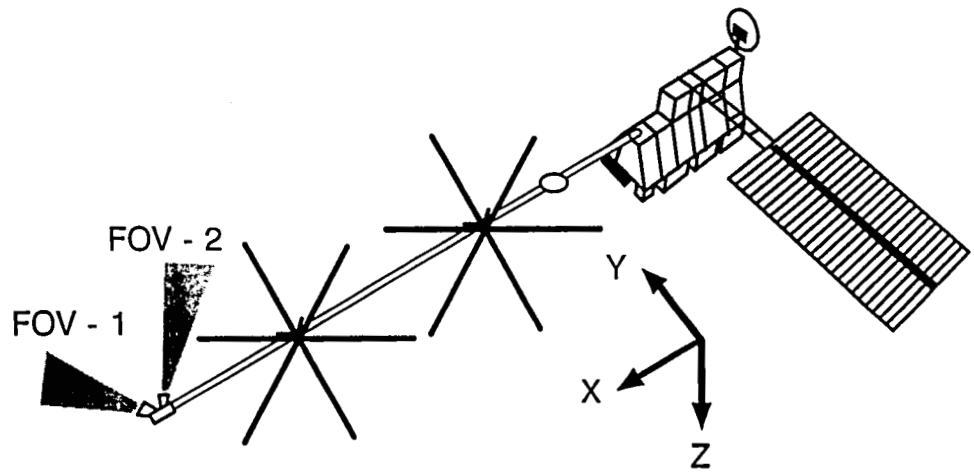

figure 24

APAFO

ADVANCED PARTICLES AND FIELDS OBSERVATORY

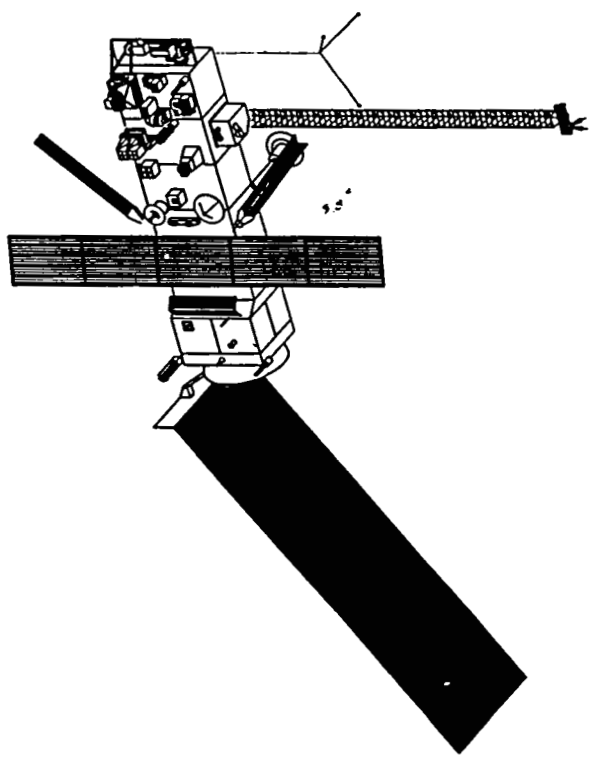

figure 25

ARISTOTELES

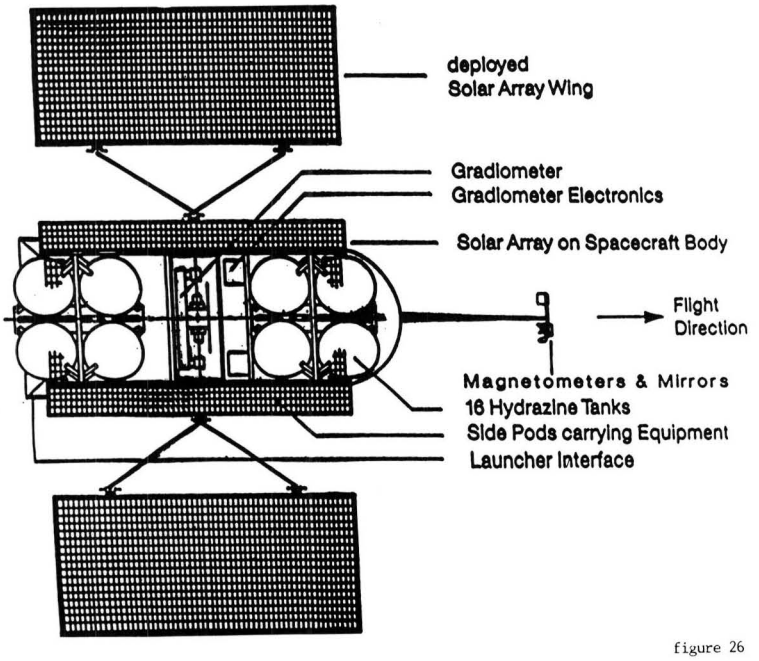

figure 26

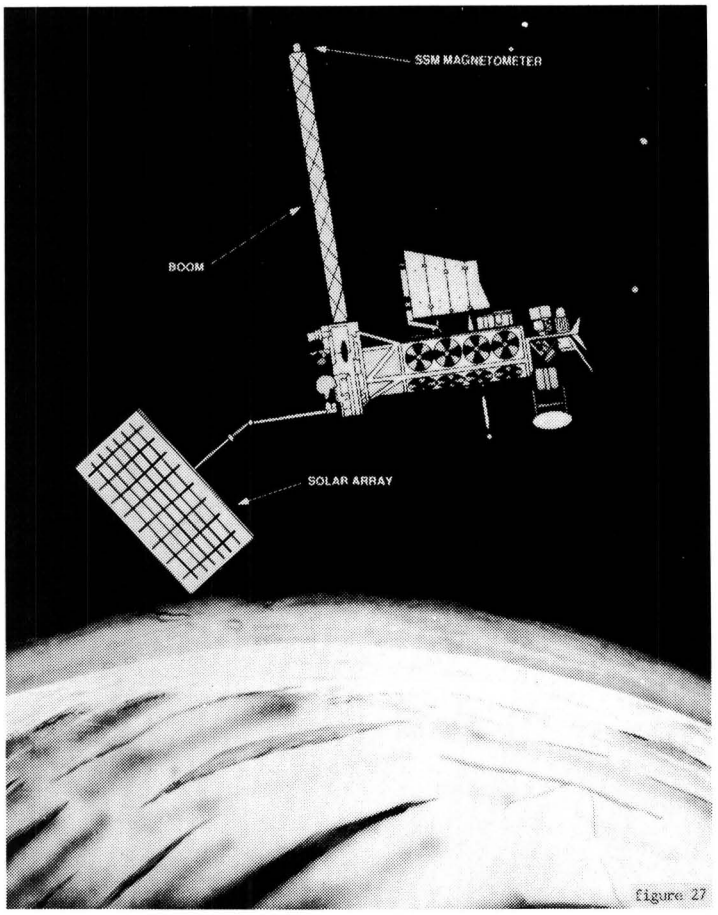

figure 27

Marine Magnetic Data Holdings of World Data Center A for Marine Geology and Geophysics

George F. Sharman
Dan Metzger

Marine Geology and Geophysics Division
National Geophysical Data Center
Boulder, CO 80303

The World Data Center-A for Marine Geology and Geophysics is co-located with the Marine Geology & Geophysics Division of NOAA's National Geophysical Data Center, Boulder, CO. Fifteen million digital marine magnetic trackline measurements are managed within the GEOphysical DAta System (GEODAS). The bulk of these data were collected with proton precession magnetometers under Transit Satellite navigational control. Along-track sampling averages about 1 sample per kilometer, while spatial density, a function of ship's track and survey pattern, range from 4 to 0.02 data points / sq.km. In the near future, the entire geophysical data set will be available on CD-ROM.

Introduction

The Marine Geology and Geophysics Division (World Data Center-A for MGG), of the National Geophysical Data Center, handles a broad spectrum of marine geophysical data, including measurements of bathymetry, magnetics, gravity, seismic reflection sub-bottom profiles, and side-scan images acquired by ships throughout the world's oceans. Digital data encompass the first three, while the latter two are in analog form, recorded on 35 mm microfilm. The marine geophysical digital trackline data are contained in the GEOphysical DAta System (GEODAS) data base which includes 11.6 million nautical miles of cruise trackline coverage contributed by more than 70 organizations worldwide. The inventory includes data from 3206 cruises with 33 million digital records and indexing to 5.3 million track miles of analog data on microfilm.

Data Management Philosophies

At NGDC, two fundamental philosophies drive the practices of data management, archiving, and distribution. The first is that the data should be self-documenting, that is the initial information a user extracts should be a complete description of content, formats, and access methodology. The second is that the data should be intimately linked with abundant metadata: data describing the primary data in terms of who collected it, how it was processed, necessary supporting information that went into that processing, intermediate stages through which the data has been taken, *etc.* These metadata not only provide some degree of quality assurance to the data, but make them accessible to purposes not necessarily envisioned at the time of the original collection and processing. This linking of both documentation and metadata to the data set is designed to ensure the integrity of the data and to facilitate access to the data by users of the future.

At present the distribution and exchange format of the data is the MGD77 data exchange format for magnetic tape. This format is fully described in a separate document available from NGDC, Hittleman, *et al.*, (1977) "The Marine Geophysical Data Exchange Format - MGD77," Key to Geophysical Records Documentation No. 10., Revised 1989. The self-documenting aspect of this format is contained in the first physical record of the magnetic tape (and of each data file), referred to as "header records." Those records are structured, ASCII listings of metadata, including a description of the FORTRAN format of the following data records, as well as information on the source institution, geographical location of the data, instrumentation, interpolation schemes, reference fields used, methods of deriving residual field, 10° geographical area identifiers, and a 560-character field for additional, free-form, documentation. This documentation (*i.e.* metadata) is linked, by means of this initial, "header," record to the data to which it applies. This linkage assures that these details of collection and processing will always be available to users of the data.

Data Management

Data management at NGDC begins with receipt, from institutions and agencies, of incoming data on 9-track magnetic tape, by direct file transfer using various networks, on floppy diskettes, or on special, agreed-upon, transfer media. Contributors are responsible for providing adequate metadata, a standard for which is the "header information" of the MGD77 format. Data provided in other formats are accepted when accompanied by sufficient metadata and documentation of format.

Upon arrival, the data are copied for archival security, scanned to confirm the format, and transferred to a high-end PC. On the PC, a quality control program is run to reformat the data into complete MGD77 format and to check for obvious problems in the data set. Such checks include data values outside expected ranges and improbable navigational patterns (see Table 1). In addition to these checks, plots of the navigation are reviewed. Questionable data are further reviewed by staff personnel and, if deemed necessary, contributors are consulted. The operational philosophy regarding quality assurance of data is: the prime responsibility for quality of data rests with the collector or custodian of the raw data. Most often it is the collector, alone, who has the only reliable information by which adjustments can be made. NGDC, in it's quality assurance function, can only act as a filter, to screen out erroneous data. It has neither the resources, nor the requisite information to edit and correct data submitted from outside sources.

Table 1. Expected ranges for Geophysical Data Parameters:

-90°	≤	Latitude	≤	+90°
-180°	≤	Longitude	≤	+180°
0 seconds	<	Two-Way Travel Time	<	15 seconds
0 meters	≤	Corrected Depth	≤	11,000 meters
22,000 nannoTeslas	≤	Total Magnetic Field	≤	72,000 nannoTeslas
977,000 mgals	≤	Gravity	≤	985,000 mgals
		Ship's Speed	<	20 knots
0	<	Incremental time		

Two additional checks are done at this point in the assimilation process. First, the header record is reviewed for possible data entry errors. Second, randomly selected data values are compared against published values as a check for possible errors such as misplaced decimal points, incorrect units, erroneous conversions, or positioning.

Following these quality assurance checks, the data are inventoried, using software developed in-house, to create an abstract (inventory) of the MGD77 data which becomes the basis for providing information to the user about data location. This inventory file includes just enough data to define the trackline of the original cruise, usually about 2% of the total, along with various quantitative information about the data, as well as the MGD77 Header. The inventory trackline is displayed on a computer screen, where it is once again reviewed for obvious errors such as ship travel across a land mass, gaps in the cruise track, or unusual navigational deviations. This completes the quality assurance process.

The final assimilation steps are data management and archival functions. All assimilated cruises are added to a master inventory, available to NGDC and its clients. The master data file for each cruise is archived both on- and off-site for security. The inventory file, used as part of the data request system, is also duplicated and stored in two locations. As a final point of quality validation, the results of the quality control checks are offered to the contributor of the data along with a copy of the assimilated data set.

The GEODAS system software has been cloned for the management of aeromagnetic data in a companion, NGDC data management system, known as ARODAS. While the bulk of the aeromagnetic data are over land, this extremely large database contains approximately a million flightline kilometers of data over water. The indexing functions of GEODAS will include ARODAS in the CD-ROM version of GEODAS to permit identifying marine aeromagnetic data.

Along similar lines, GEODAS will provide the indexing function for the approximately 6 Gigabytes of multibeam, bathymetry the MGG division is in the process of assimilating into a new, multibeam bathymetry database. This indexing function will supply the necessary information for access and retrieval of data from this new database.

Data Characteristics

The character of the digital marine magnetic data available from NGDC is largely shaped by the storage and exchange format, MGD77. All magnetic field values are stored with a resolution of one tenth of a nannotesla (gamma). Five fields and a flag are available for magnetic data. The five fields are: one each for two, different, leading and trailing, sensors of total magnetic intensity; one field for residual magnetic intensity (total field with reference field removed); a field specifying magnetic diurnal correction; and a final field specifying depth or altitude of lead magnetic sensor. The flag specifies which sensor was used to calculate residual field. Metadata contained in the header and specific to marine magnetics are: the digitizing rate, the sampling rate, the sensor tow distance and depth, horizontal sensor separation for dual sensor systems, and the reference field and method used to determine residual magnetic intensity.

The quantity of current data holdings within the GEODAS system is summarized in Table 2. Navigation refers to total ship's track, independent of the functioning status of various data collection systems. The various categories of geophysical data reflect the

extent of actual data collected and available from within GEODAS. Note that magnetic data are the second most abundant; collection of these data became an automatic operation with onboard digital computers and proton precession magnetometers. Magnetic data are more easily logged and processed than bathymetric data.

Table 2. Current NGDC Digital Marine Geophysical Data Holdings

Data Type	Quantity of Trackline data		
	naut.mi.	km.	records
Navigation	11,598,690	21,480,774	33,213,960
Bathymetry	10,968,980	19,314,551	22,103,421
Magnetics	7,998,936	14,814,029	15,372,215
Gravity	5,200,607	9,631,524	9,708,165
Seismics*	45,053	83,438	241,549
Sidescan & other*	19,749	36,575	145,971

* Navigational control for corresponding analog records on microfilm

The time-history of marine magnetic data collection and entry into GEODAS, in terms of cumulative surveys (cruises) and in terms of cumulative records (individual data) is shown in Figure 2. Given the significant points in the history of marine geophysical data collection, these curves can be used to estimate the quantity and quality of data. For example the sharp rise in data collection in the mid-1960's corresponds to the introduction of the proton-precession magnetometer and it's commercial availability.

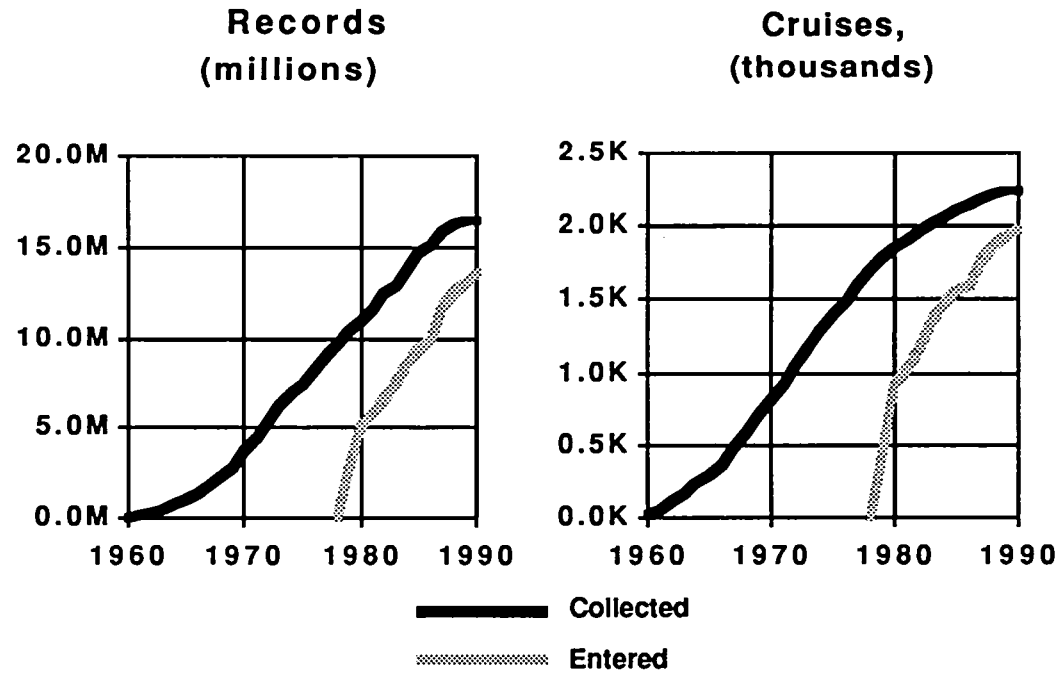

Figure 1 Cumulative time-histories of magnetic data collection (dark) and entry (light) into GEODAS

Independent of the pattern of collection, but important in terms of quality assessment, three intervals of time demarcate varying levels of navigational quality. Between 1965 and 1970, the introduction of Transit Satellite navigation marks the increase in positional accuracy from celestial to satellite navigation. The next major improvement in global navigation, Global Positioning Systems, was coming on line in a 1990 time frame. The three periods are then: pre-1968, with predominantly celestial navigation; 1968-1990, with predominantly Transit (doppler) satellite navigation; and post-1990, with predominantly GPS (hyperbolic) satellite navigation. The inference to be drawn is that the bulk of the 16 million marine magnetic data in GEODAS (about 14 million) were collected under Transit Satellite navigational control.

Several other inferences can be drawn from the two graphs. The roll-over of the cruise collection curve suggests that collection effort for marine magnetics has passed it's peak. In fact, the peak in collection rate, *i.e.* the steepest part of the curve, corresponds to the early 1970's and the burst of research effort in plate tectonics, for which the mapping of marine, magnetic, anomaly patterns was crucial to understanding the formation and evolution of the large, oceanic, lithospheric plates. This period of intense interest was characterized by a demand-driven collection peak, enabled by the introduction and commercial availability of the proton-precession magnetometer and brought to a close by mapping sufficient to the problem and changing research priorities. The relatively ragged character of the curve of data entered into GEODAS, compared to that of data collected, reflects the "bunching" effects of data processing and transfer. GEODAS was intitiated in 1977, hence the initial, steep curve represents a certain amount of catching up, while the later irregularities represent the clustering of data due to proprietary holds placed on the data, gathering of data onto magnetic tape, and periodic transfer of data from collecting institutions. The leveling off of the data collection curve in later years may also be, in part, a sampling problem, since the collection of data cannot be confirmed until it is entered into the system; a constraint of these plots is that the two curves must intersect at the present.

The spatial distribution of digital magnetic track line data is shown in Figures 2, a through e. These plots were chosen for time intervals of roughly equal data collection, the ten-year period of 1960-69 in Figure. 2a, and subsequent five-year intervals in Figure 2b (1970-74), Figure 2c (1975-79), Figure 2d (1980-84), and and the final period, 1985 to present in Figure 2e. Trends in spatial patterns of magnetic data collection are evident from this series of plots. The 1960's and early 70's produced broad, regional surveys, such as the SEAMAP data between Hawaii and Alaska and the PIONEER survey off the west coast of the United States, and traverse tracklines across broad reaches of ocean. The late 1970's and early 1980's show smaller survey patterns with transit to and from those surveys. The most recent plot shows both the lower collection rate and the persistence of smaller, regional surveys.

Mean spatial sampling interval, along track, is 1.1 ±0.6 kilometers, derived from a sample of 19 random, 5° squares of latitude and longitude. These numbers reflect the sampling and digitizing intervals and nominal ship's speeds. The *density* of coverage understandably has a much wider variation, depending on the nature of the ship tracks and survey patterns. Mean values are 1.0 ± 1.2 magnetic data per square kilometer, based on a sample of 15, random 5° squares. More importantly, the values for individual 5° squares range from dense 4.6 data / km^2 along the Reykjanes Ridge in the North Atlantic, to a sparse 0.03 data / km^2 in the Southcentral Pacific.

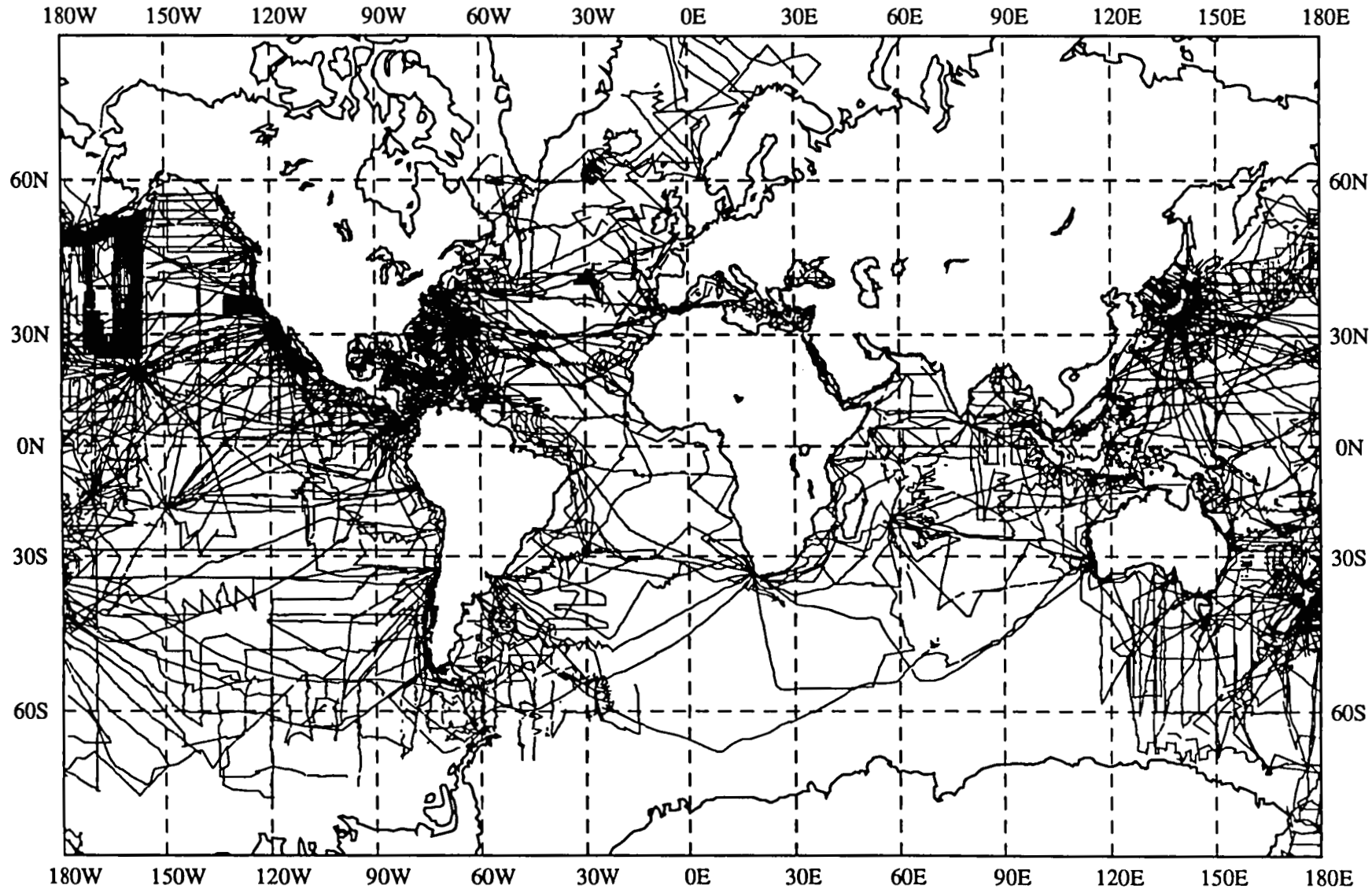

2a. Marine Magnetic Data, 1960-1969

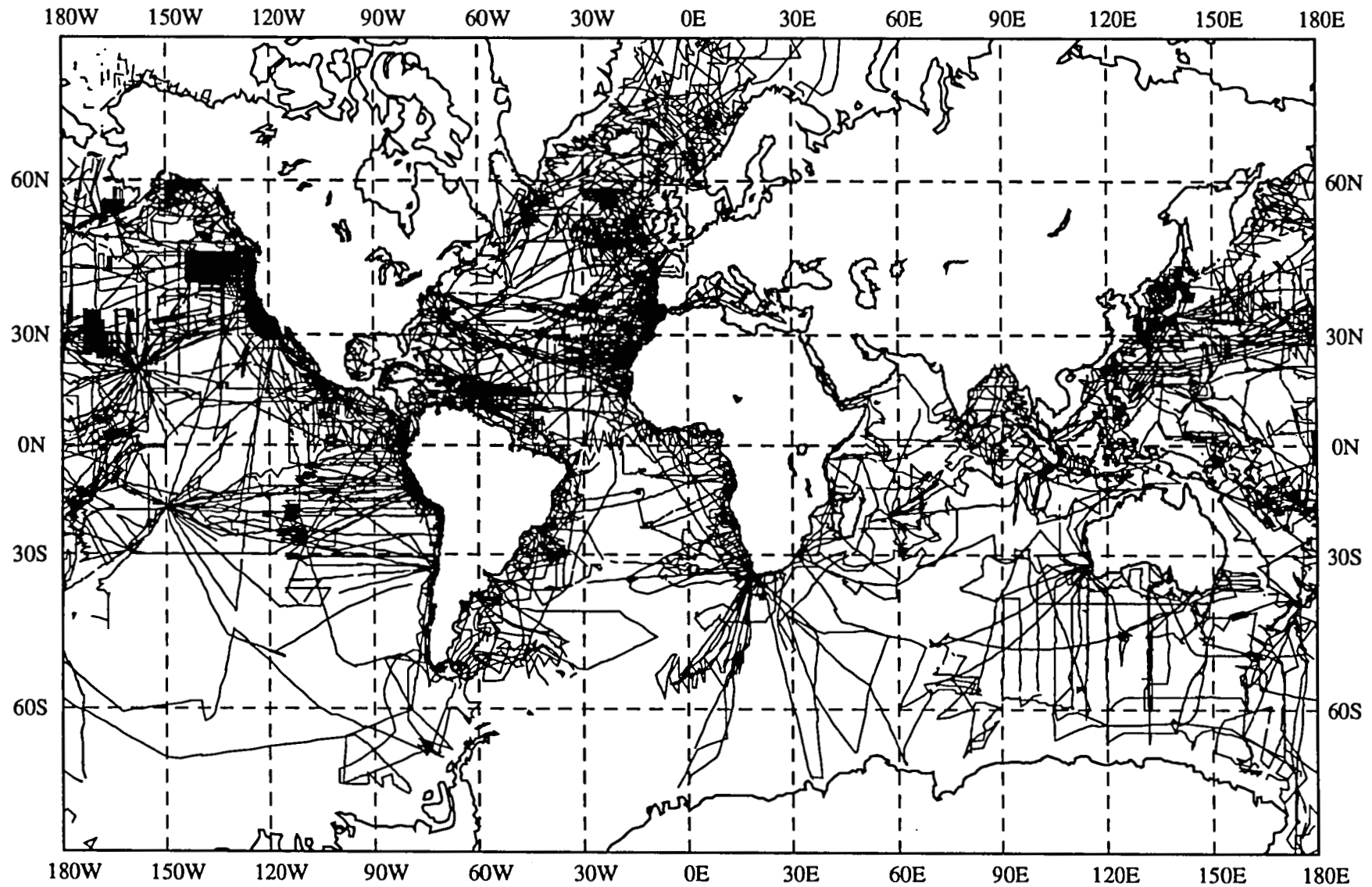

2b. Marine Magnetics Data, 1970-1974

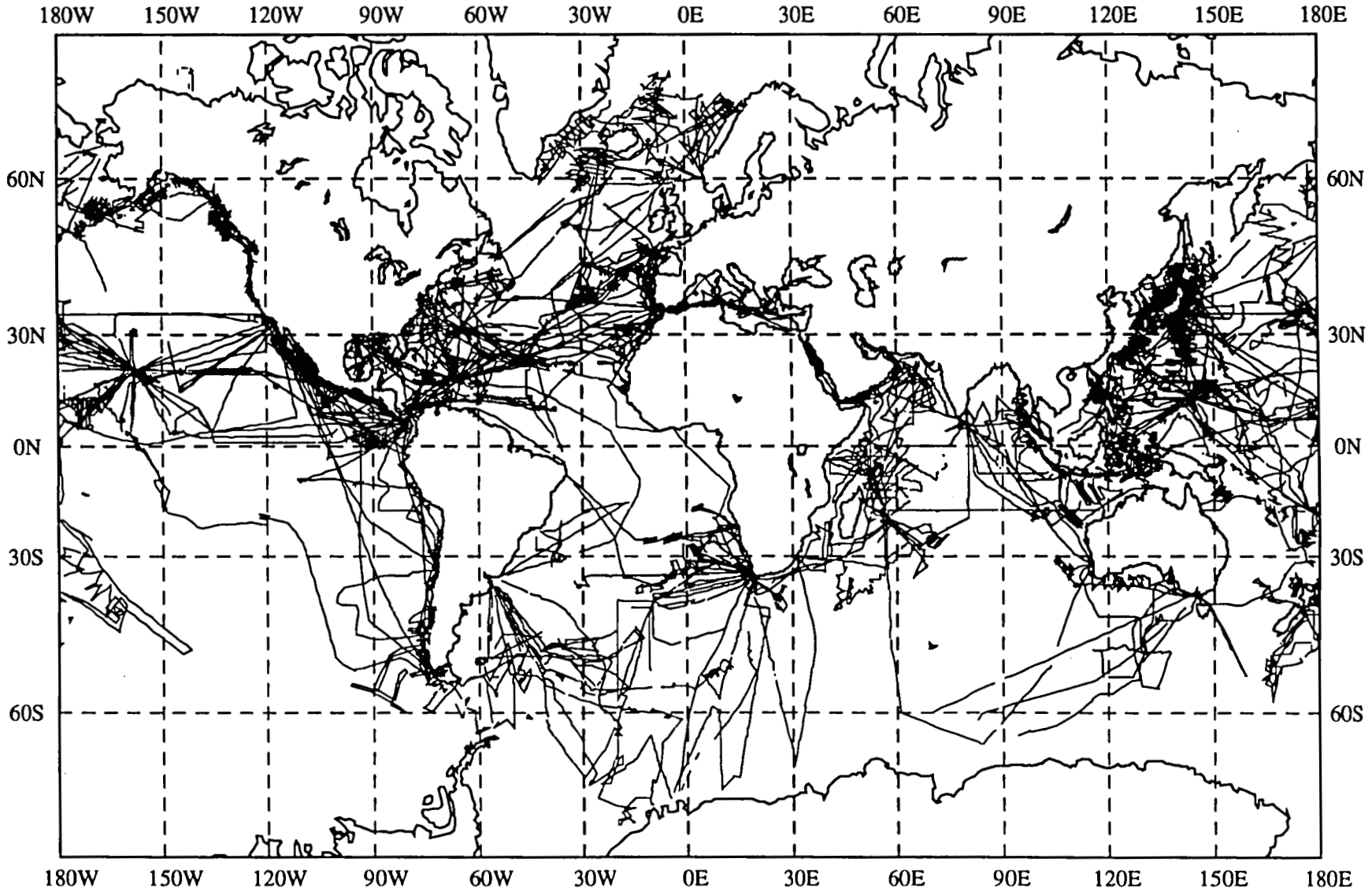

2c. Marine Magnetics Data, 1975-1979

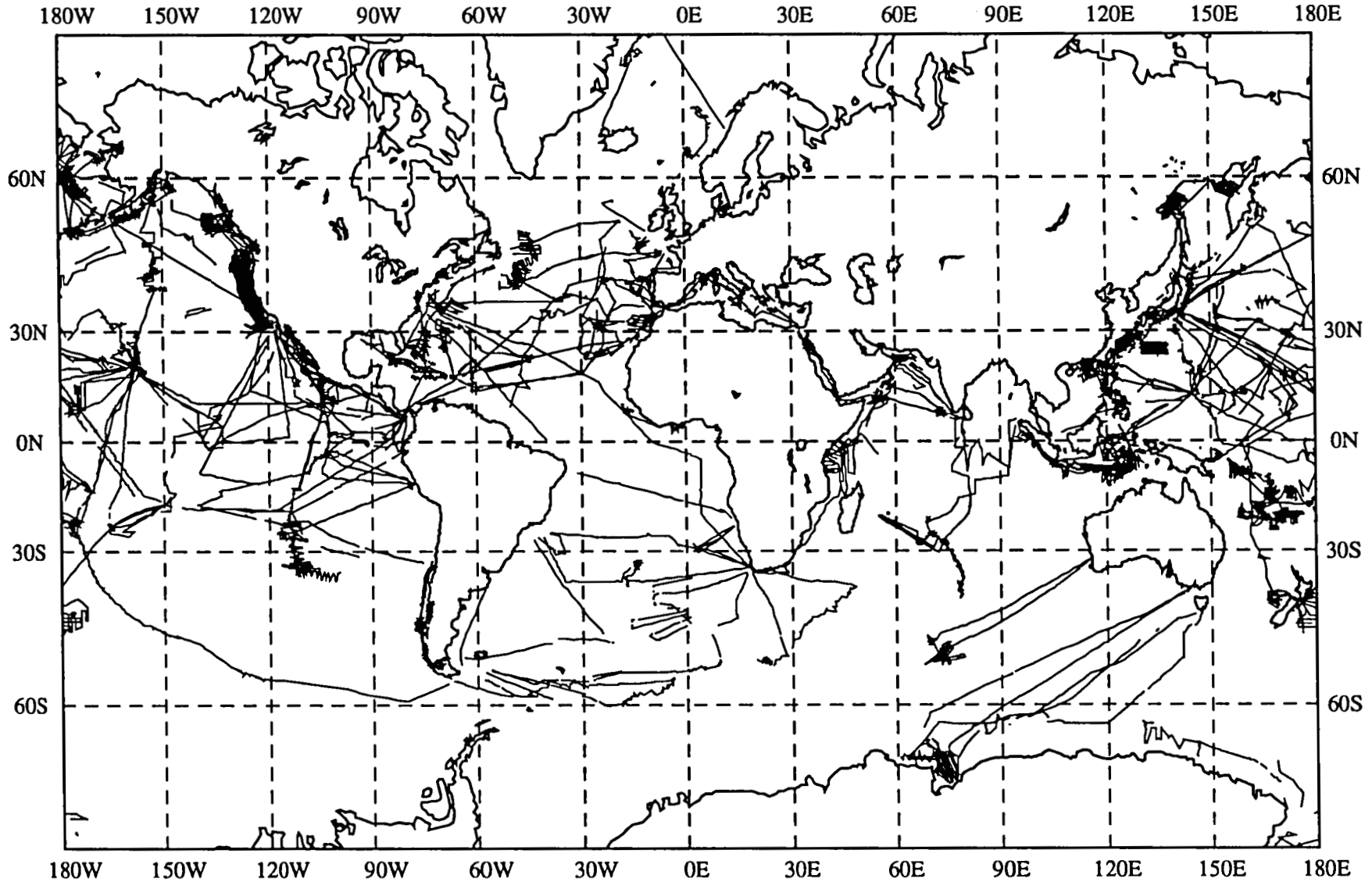

2d. Marine Magnetics Data, 1980-1984

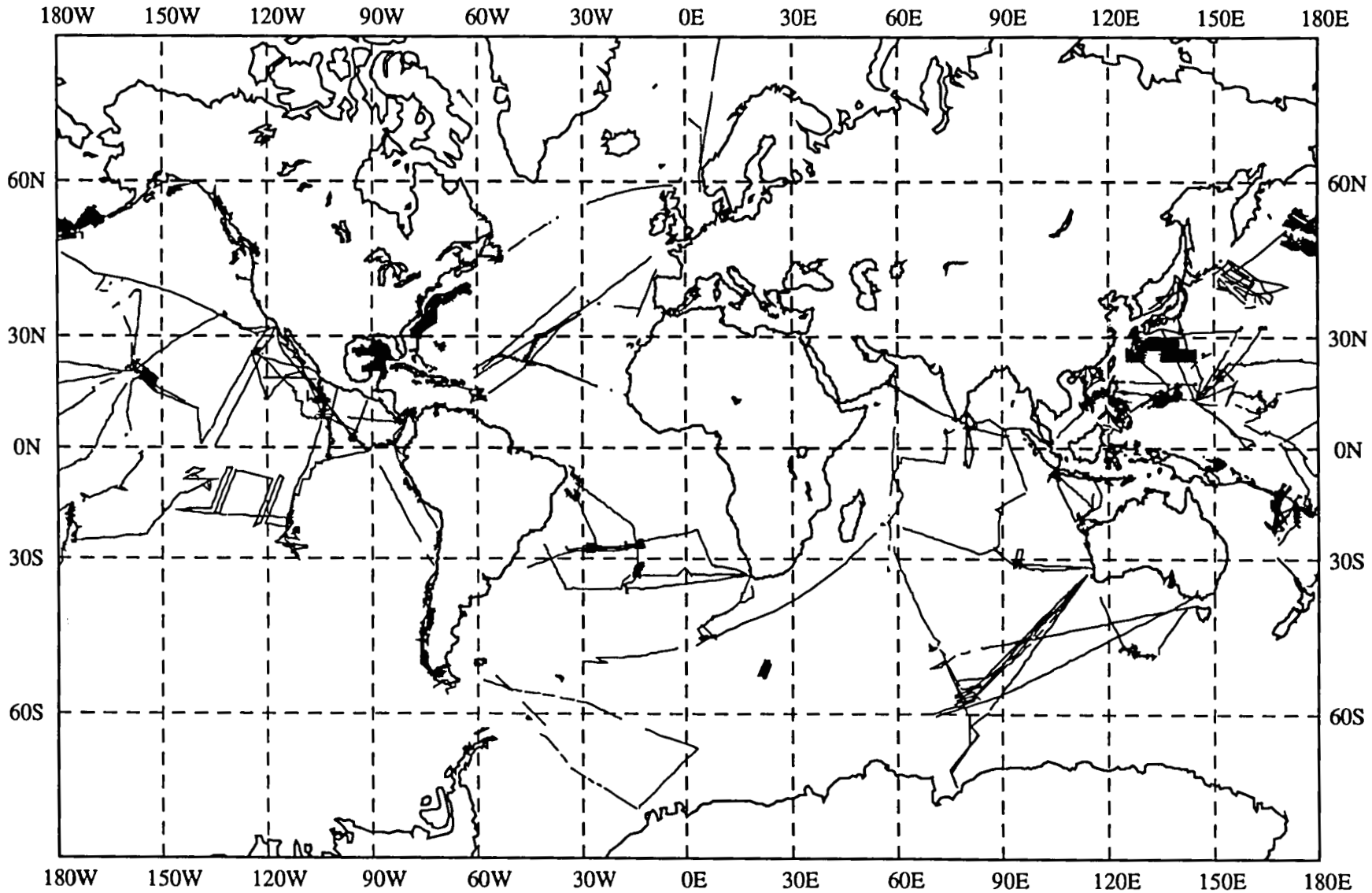

2e. Marine Magnetics Data, 1985-present

Users of NGDC Marine Geophysical Data

The marine geophysical data from NGDC is available to the general public, either by purchase or on an exchange basis with contributing institutions. An analysis of users of the GEODAS system during the last fiscal year shows that 57% of underway, marine, geophysical data acquired from NGDC was on just such an exchange basis; the balance of data were purchased. Of the total data supplied, 50% was to domestic users, another 22% was to other branches of the U.S. Government, and the balance of 28% was to international users of the data. The breakdown of these various users of the data is shown in figure 3. Since these data are supplied in the MGD77 format, there is no separation of data types contained within the format and, thus, no indication of the specific applications to which the data were put.

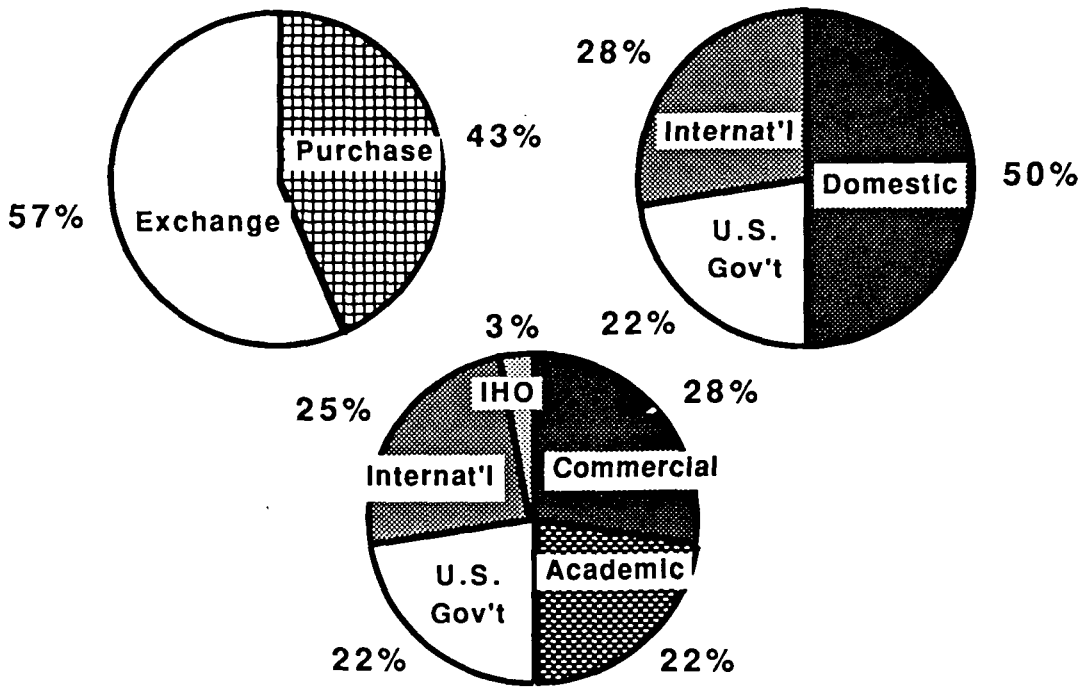

Figure 3. Various partitions of total FY91 data users of NGDC MGG GEODAS data

Near-Future Developments for GEODAS

GEODAS developments in the immediate future center around placing the entire database on two CD-ROM's and making it available with access software for IBM compatible PC's. This will permit direct access by users to the entire data set at a cost which will be less than that of only several cruises retrieved and supplied on magnetic tape under the present system. The data on disk will be compressed by simple removal of unused fields for each data file but the access software will make this compression

transparent to the user. That access software will also permit browsing and searching of the data by source, time, or geographic area, and will permit retrieval and decompression of the data onto disk in standard MGD77 format. While initial design of access software was for MS-DOS machines (IBM-compatibles) to accommodate the largest population of users, continued development of software for similar access by Macintosh, Sun UNIX, and other users is underway.

Reference

Hittleman, A.L., R.C. Groman, R.T. Haworth, T.L. Holcombe, G. McHendrie, and S.M. Smith, "The Marine Geophysical Data Exchange Format - 'MGD77' (Bathymetry, Magnetics, and Gravity)," Key to Geophysical Records Documentation No. 10 , February, 1989 (Revised), National Geophysical Data Center, Boulder, Colorado.

REDUCTION OF MARINE MAGNETIC DATA FOR MODELING THE MAIN FIELD OF THE EARTH

R. T. BALDWIN
J. R. RIDGWAY

ST SYSTEMS CORPORATION (STX)

W. M. DAVIS

NATIONAL GEOPHYSICAL DATA CENTER

APRIL 1990

LIST OF ILLUSTRATIONS

LIST OF ILLUSTRATIONS (Continued)

LIST OF TABLES

INTRODUCTION

The marine magnetic data set archived at the National Geophysical Data Center (NGDC) consists of shipborne surveys conducted by various institutes worldwide. This data set spans four decades (1953, 1958, 1960–1987), and contains almost 13 million total intensity observations. These observations are often less than 1 km apart. They typically measure seafloor spreading anomalies with amplitudes of several hundred nanotesla (nT) which, since they originate in the crust, interfere with main field modeling. The sources for these short wavelength features are confined within the magnetic crust (i.e., sources above the Curie isotherm). The main field, on the other hand, is of much longer wavelengths and originates within the earth's core. It is desirable to extract the long wavelength information from the marine data set for use in modeling the main field. This can be accomplished by averaging the data along track. In addition, those data which are measured during periods of magnetic disturbance can be identified and eliminated. Thus it should be possible to create a data set which has worldwide data distribution, spans several decades, is not contaminated with short wavelengths of the crustal field or with magnetic storm noise, and which is limited enough in size to be manageable for main field modeling.

Marine Data Set

The raw data used in the preparation of the marine magnetic data set for main field modeling was extracted from the data holdings of NGDC's Marine Geophysics and Geology Division using a data base-management system known as GEODAS. (For a detailed description of this software system see Hittleman and Metzger 1983, and Hittleman et al., 1977). In brief, GEODAS was employed to retrieve all the total intensity magnetic field observations which reside in digital form in NGDC's central tape depository in Asheville, NC, for each of the years 1953, 1958, and 1960–1987. The format of the marine data follows that which is discussed by Talwani et al., 1972. In addition to recovering the desired data sets, the software produced listings of the cruise identifiers, MGG numbers (Marine Geology and Geophysics; an NGDC assigned cruise number), the contributing institutions, the length of the ship tracks, and the number of selected records. Table 1 summarizes some of this information for all years for each contributing institution.

Additional listings which briefly describe the navigational systems employed, the magnetic instrumentation, the sampling interval, the project scientist, and ancillary information are also generated for each cruise. This information is too voluminous to present for each of the 1850 cruises processed but is available upon request at NGDC. The vast majority of the data collected were measured with a proton precession magnetometer and were located by using dead-reckoning between the more precise fixes provided by satellite navigation systems

(e.g., SATNAV) or LORAN radio-beacons. Typically, magnetic measurement positions were determined by linearly interpolating between these navigation determinations. The magnetic field sampling rates varied from continuous recording on strip charts to 15 minutes in many digital systems. Most of these data were digitized or resampled to 15 minutes. At normal cruise speeds, these sample rates translate into measurement separations of about 1/4 of a kilometer.

In the course of the data selection, a small number of erroneous data were encountered. These included cruises where the total field measurements were replaced with residual field values and where the times of the observed data were not defined. Since the total field measurements were not reproducible with any surety and the dates of the measurements were not sufficient to define the state of the external magnetic field (i.e., Kp or Dst index) these data were excluded. In addition, about eight cruises in the 1982 selection proved to be unanalyzable for reasons which have yet to be determined. These data will be processed when the problem is resolved.

Marine Data Processing

Isolation of a viable data set for main field modeling from the total marine data set is accomplished by along track filtering. The filtering is achieved by taking an unweighted average of the data along the shiptrack. The first step is to remove the field computed from an International Geomagnetic Reference Field (IGRF) or Definitive Geomagnetic Reference Field (DGRF) [see e.g., Langel, 1987; Barraclough, 1988] from the observed total intensity measured along each shiptrack. Table 2 lists the field models used for each of the time intervals. The models were linearly interpolated between the times of their epoch. Each track is then segmented into 220 km segments in which every other point is sampled. Point samples must meet spatial and amplitude constraints so that the computer averages are not influenced by spurious or redundant data. Residuals from the appropriate IGRF or DGRF are calculated within each segment. These are flagged and rejected if they are greater than 500 nT or less than -500 nT. Data point locations must be at least 40 m apart, or they are rejected, and 45 acceptable observations are required for each segment before an average value is calculated. After selection based on the above criterion, the data are processed by computing the mean and standard deviation of the residual scalar anomalies for each 220 km segment. These values are assigned the average of the latitude and longitude coordinates from the data points within the segment.

To ensure data coverage only during periods of magnetic quiet, the average of the global Kp index is calculated for each segment. If this value exceeds 2+, then the mean total intensity for the segment is rejected. External field effects are also accounted for by calculating an average Dst value for each segment. Dst is a hourly

measure of the degree to which the magnetic field is influenced by external sources and is a parameter which is sometimes utilized in deriving main field models; it is not associated with any rejection criterion. A value of -10 nT was used for years before 1957 and after 1985 where digital Dst values are not available. When possible, these values will be replaced by the true Dst.

The effect of daily magnetic variations (i.e., Sq currents) on the marine data set was not dealt with in the filtering process. These fluctuations will be briefly discussed later in this report.

The weight assigned to an average marine data value is the inverse of the standard error of the mean for that segment. (Within each segment, the accuracy of each measured point is assumed to be the standard deviation for the segment. Since all measurements contribute to the average value, the weight of the average value is taken as the inverse of the standard error of the mean.) This is computed by dividing the standard deviation by the square root of the number of measurements in each segment.

The marine data set for main field modeling was processed with computer programs developed and utilized at Goddard Space Flight Center (GSFC) and the NGDC at Boulder, CO. This processing has been fully documented in four volumes entitled "Marine Magnetic Data: 1950–1969, 1970–1974, 1975–1979, and 1980–1987" located at GSFC, Code 622. These manuscripts contain a description of source code, listing of surveys conducted by institute, world distribution maps, comments on shiptracks, and profiles of each shiptrack.

An overview of the averaging process for a single shiptrack can be found in Table 3 and Figure 1. Cruise CRCS01SB has been assigned an MGG identification number of 15060039 by NGDC. This cruise was conducted in 1963 in the Pacific Ocean by Scripps Institute of Oceanography. The magnetic field profile from the cruise (Figure 1) shows the large amplitude high frequency signature associated with sea-floor spreading anomalies. The averaged points from the filtering process are depicted as asterisks. The averaging noticeably smooths out the short wavelength crustal anomalies while retaining long wavelength variation which may contain main field information.

A point at 2100 km down track has been selected in the profile to show the mean (μ), standard error (σ_e), and Kp. Points near the end of the profile have been discarded because they exceed the Kp limit. The mean (μ_1) and standard deviation (σ_1) for the entire shiptrack is shown at the end of the profile. Table 3 describes the statistics computed for the entire profile, segment by segment.

World Data Distribution and Statistics

The distribution of averaged marine data over the world is represented, by year in Figures 2–31. These maps show a sparsity of data in the 1950's, early 1960's, and the mid 1980's, and they show an abundance of observations in the late 1960's and 1970's. Overall, the data distribution is good as seen in Figure 32 where all the averaged data locations have been plotted.

A tabulation of various statistics by year is found in Table 4. This includes for each the number of averaged points, the mean deviation of the entire years data from the IGRF or DGRF, the standard deviation relative to the mean, the mean of the standard errors, and the standard deviation of the standard errors. A histogram of the number of averaged points per year, shown in Figure 33, indicates the years of sparse and abundant data mentioned above. For each year, the mean deviation from the DGRF and IGRF and its standard deviation were calculated from the averaged residuals computed along each shiptrack. Histograms of these quantities are shown in Figures 34 and 35. Similarly, a mean and standard deviation was computed for each year from the standard errors compiled from each segment; histograms are shown in Figures 36 and 37. These histograms (Figures 34–37) reveal the degree from which the marine data deviates from the IGRF or DGRF models and the extent of weighting necessary for improved main field modeling. Note that the mean deviation is generally negative indicating an overestimate of the main field and that the standard error decreases with time, reflecting improvement in the accuracy of marine measurements.

Finally, the extent to which the marine data set was affected by daily magnetic variations can be measured by estimating the amount of Sq currents produced based on the sun spot number at each local time. When the marine data set was compiled, there were no routines operational which could make such a correction. However, the number of averaged observations per local time interval is shown in Figure 38 for each year. This reveals an estimate of the number of observations adversely affected by periods of high Sq currents and shows that the distribution of data with respect to time is approximately equal. Figure 39 shows the worldwide data distribution at noon local time for 1953, 1958, 1960–1987. The largest discrepancy (though small) will be during the peak Sq periods (i.e., 0900–1500 local time). The distribution of data at other local times is comparable to Figure 39. An account of the total number of local time observations for each year and for the entire data set is shown in Table 4. Sq currents influence the magnetic field on the average by about 70 nT. An accurate Sq current model is needed before the marine data set can be corrected.

Errors

There are certain points of concern which arise from an analysis of marine magnetic profiles. Occasionally, the average of the observations within a segment result in a spurious value. This may be a result of instrument malfunction or drift for a particular section. These stray values are of concern because they may fall within the ± 500 nT error bounds. In addition, the signal observed along shiptrack may sometimes repeat itself indicating that the ship may be backtracking or is in close proximity to sections of the same track. This results in average points being calculated less than 220 km apart which violates spatial constraints. Areas with dense data coverage bias solutions which are derived from main field modeling. In order to ensure the adequacy of the marine magnetic data, it was necessary to deal with the above inconsistencies on a case by case basis. Points found to be lacking were deleted from the data set.

Conclusion

The along track filtering process described above has proved to be an effective means of condensing large numbers of shipborne magnetic data into a manageable and meaningful data set for main field modeling. Its simplicity and ability to adequately handle varying spatial and sampling constraints has outweighed considerations of more sophisticated approaches. This filtering technique also provides the benefits of smoothing out short wavelength crustal anomalies, discarding data recorded during magnetically noisy periods, and assigning reasonable error estimates to be used in the least squares modeling. A useful data set now exists which spans 1953–1987.

REFERENCES

Barraclough, D. R., "International Geomagnetic Reference Field Revision 1987," EOS Transactions, Am. Geophys. Union, p. 577, April 26, 1988.

Hittleman, A. M., and Metzger, D. R., 1983, Marine Geophysics: Database Management and Supportive Graphics, Computers and Geoscience, Vol 9, No. 1, pp. 27–33.

Hittleman, A. M., Groman, R. C., Haworth, R. T., Holcombe, T. L. McHendrie G., and Smith, S. M., 1977, The Marine Geophysical Data Exchange Format - "MGD77:" KGRD 10, NOAA, EDIS, Boulder, Colorado, 18p.

Langel, R. A., The Main Field, in Geomagnetism, Vol. 1, J. Jacobs (Editor), Academic Press, 1987.

Talwani, M., Grim P., Halcombe, T., Luyendyk B., Meyers, H. and Smith, S., 1972, Formats for Marine Geophysical Data Exchange: National Academy of Sciences, Washington, D.C., 19p.

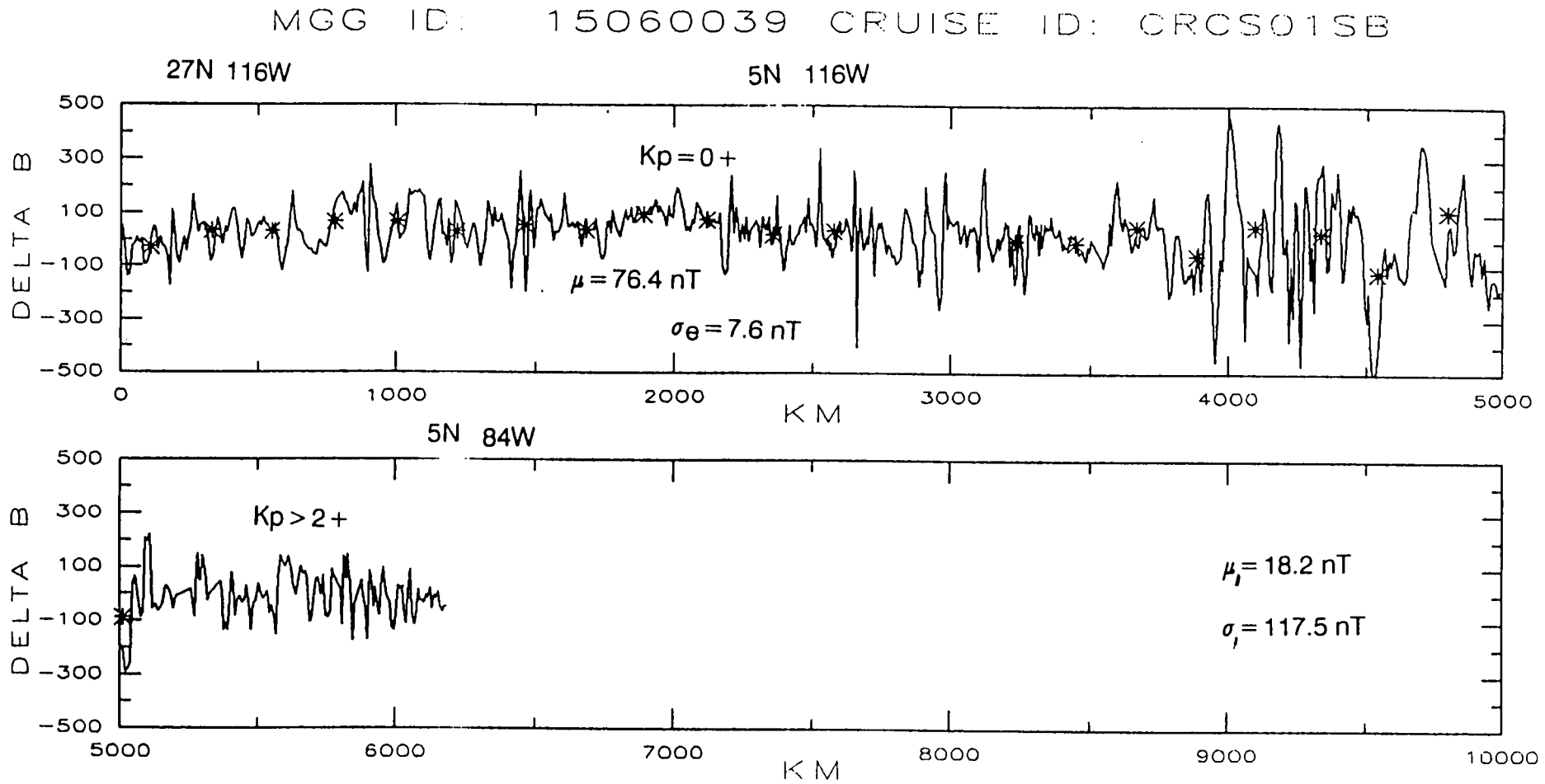

FIGURE 1. PROFILE OF CRUISE CRCS01SB CONDUCTED BY SCRIPPS INSTITUTE OF OCEANOGRAPHY IN 1963

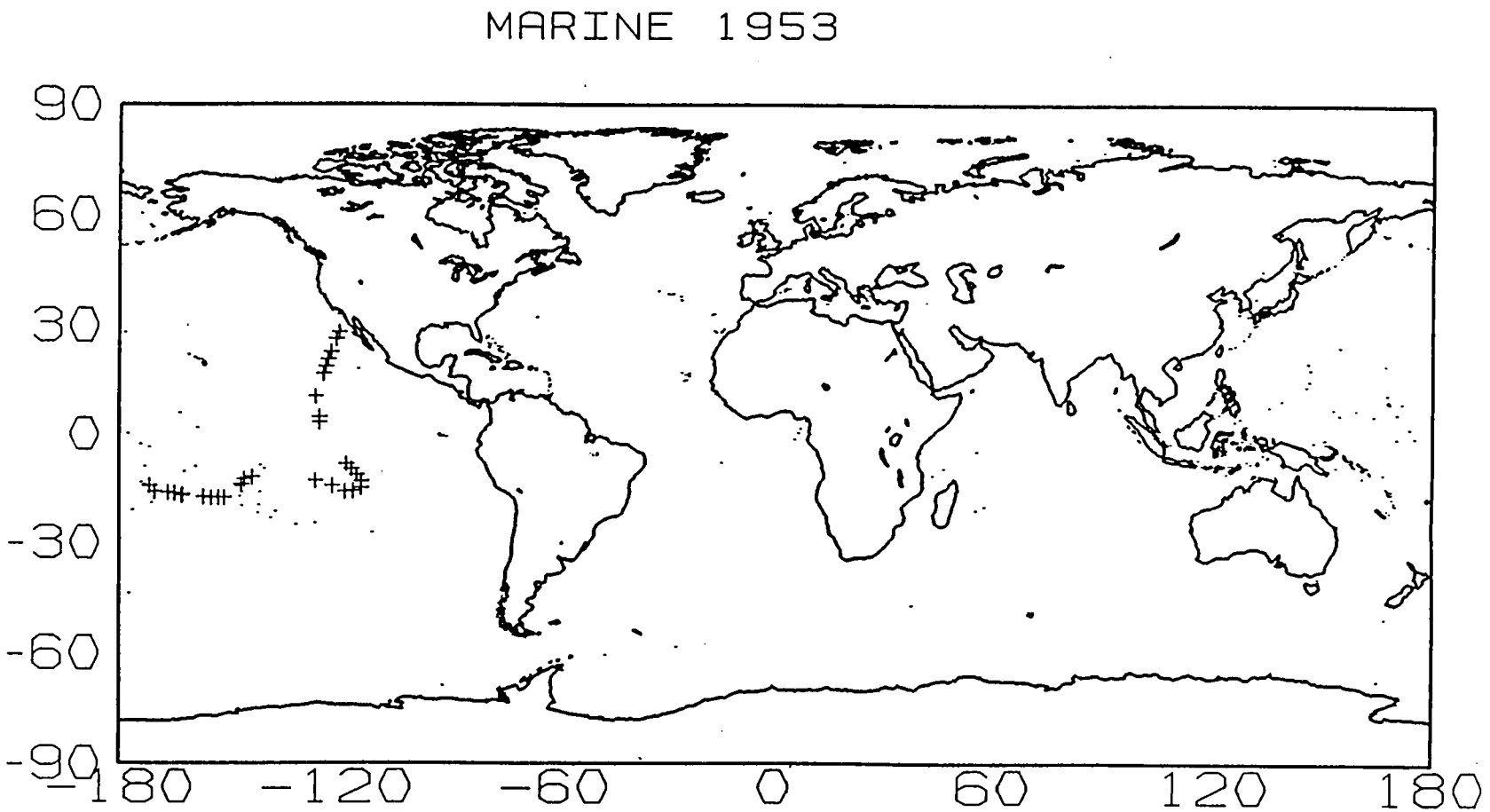

FIGURE 2. WORLD DATA DISTRIBUTION FOR 1953

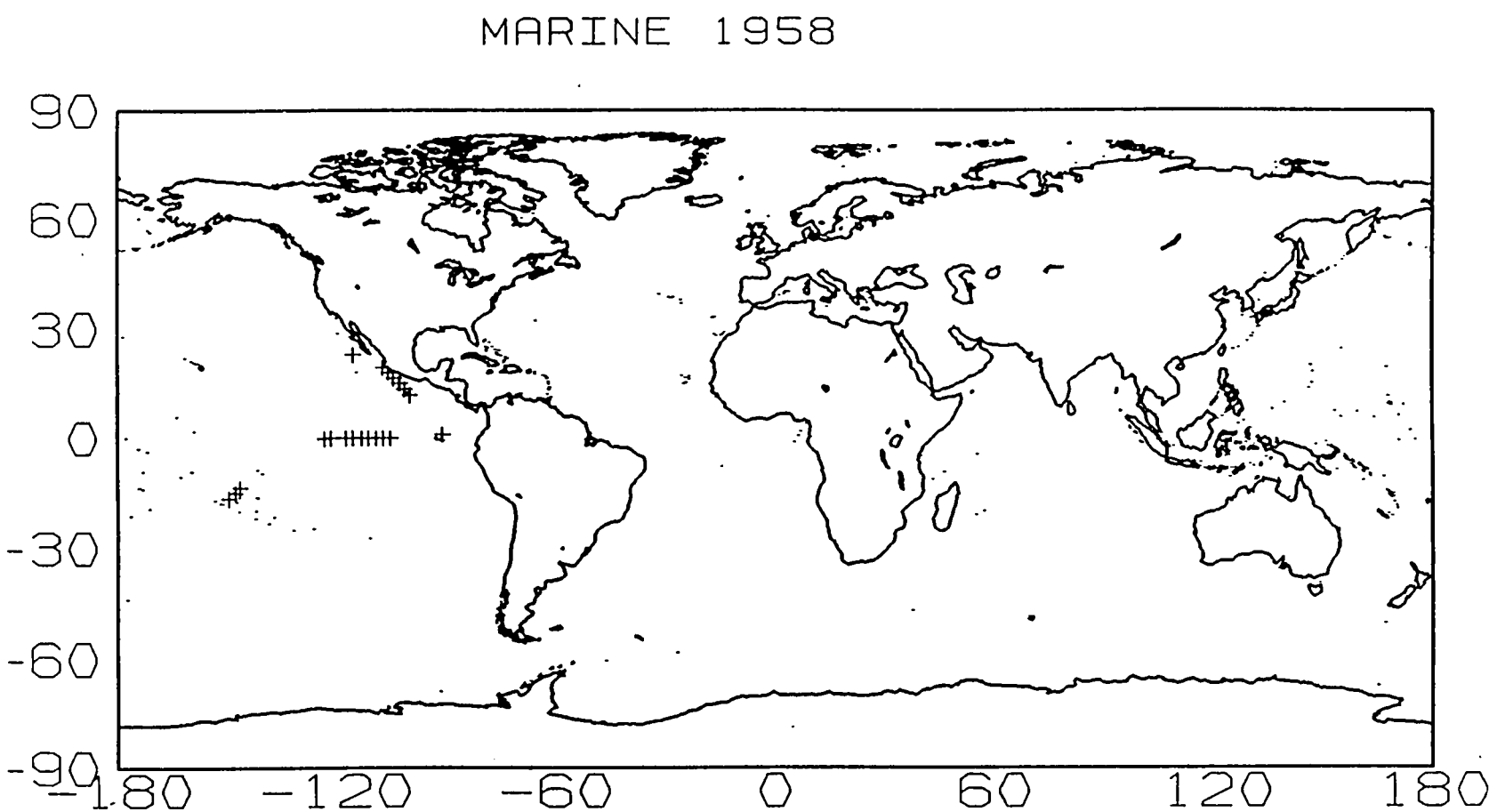

FIGURE 3. WORLD DATA DISTRIBUTION FOR 1958

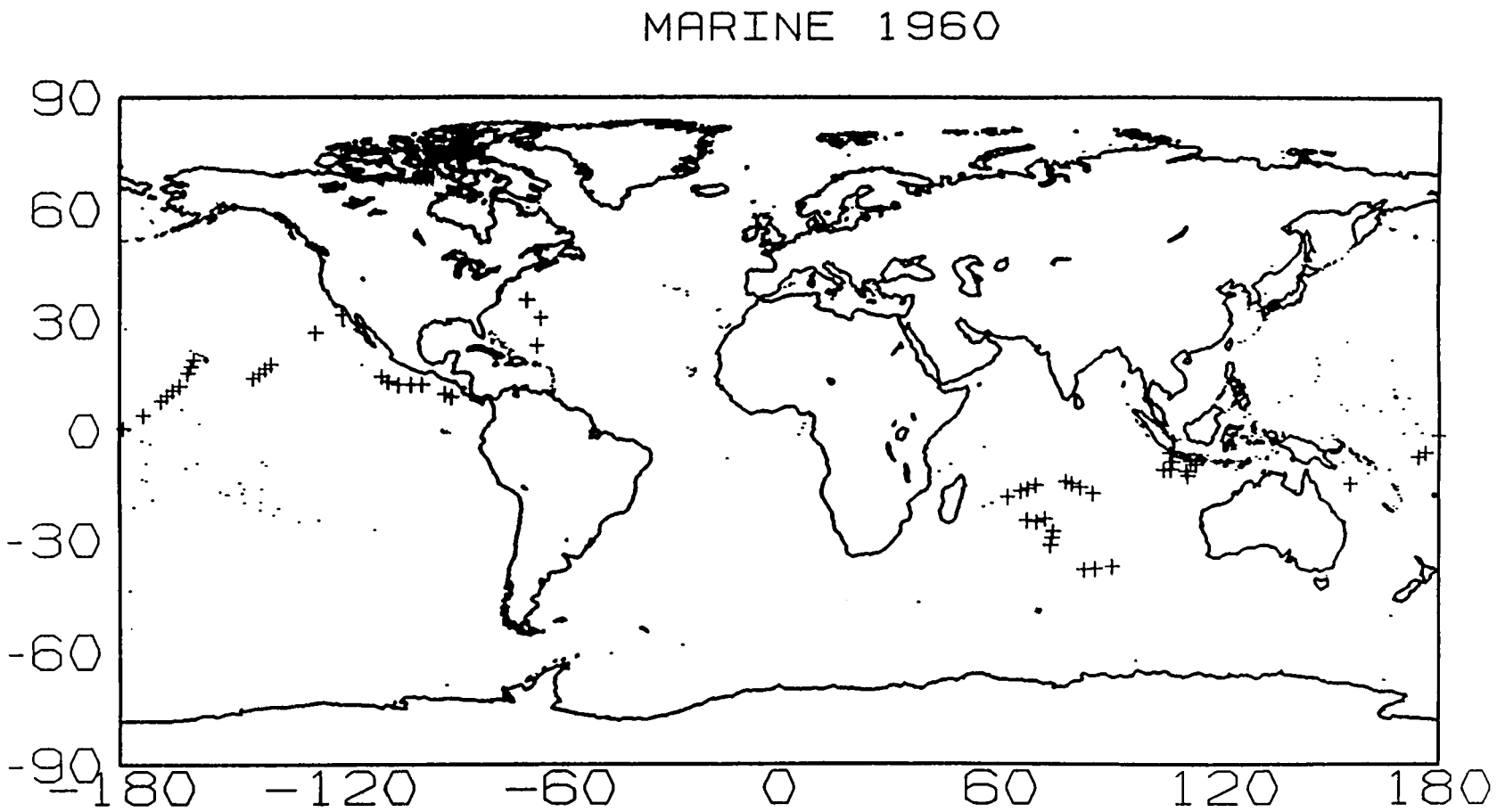

FIGURE 4. WORLD DATA DISTRIBUTION FOR 1960

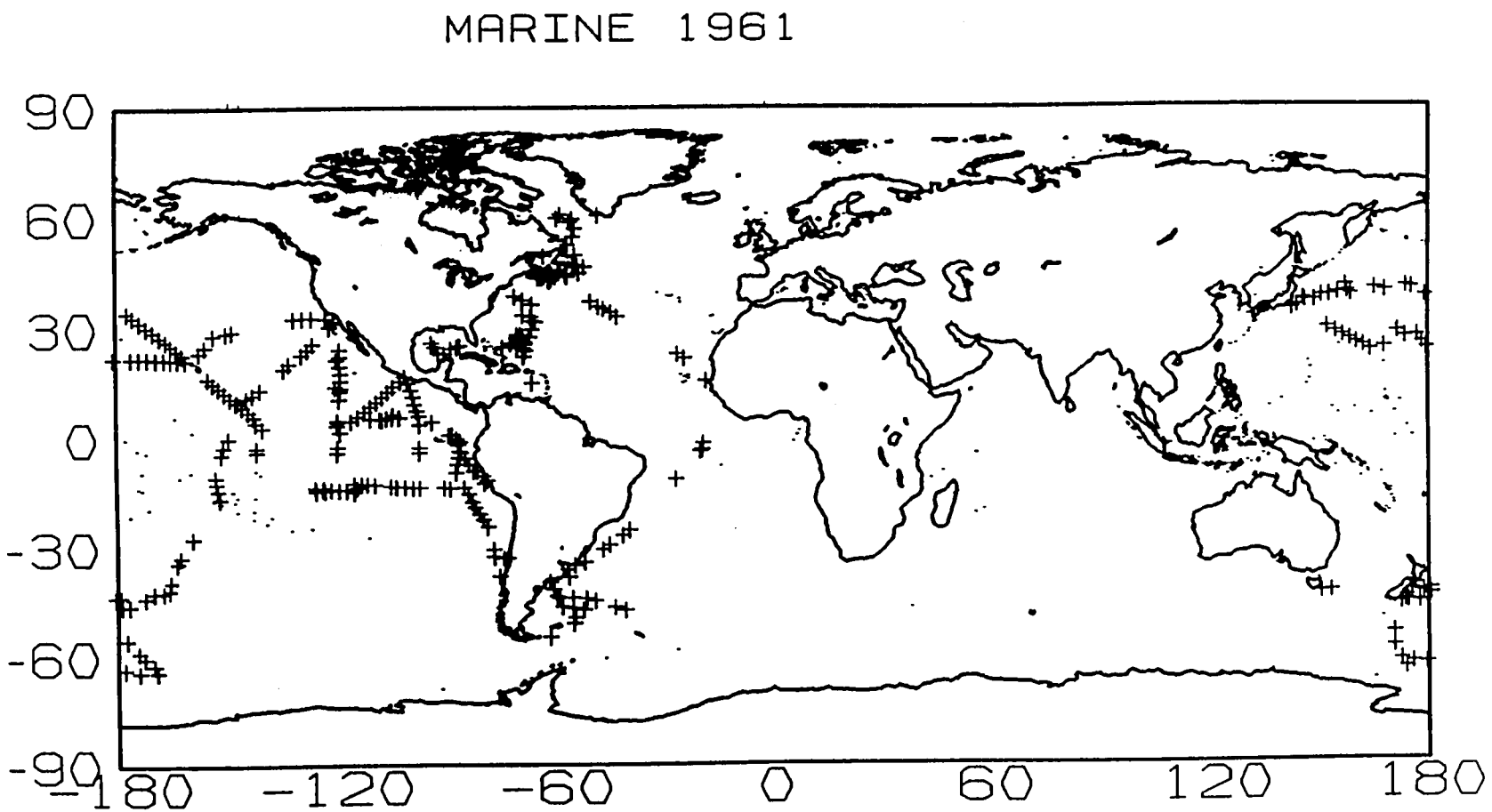

FIGURE 5. WORLD DATA DISTRIBUTION FOR 1961

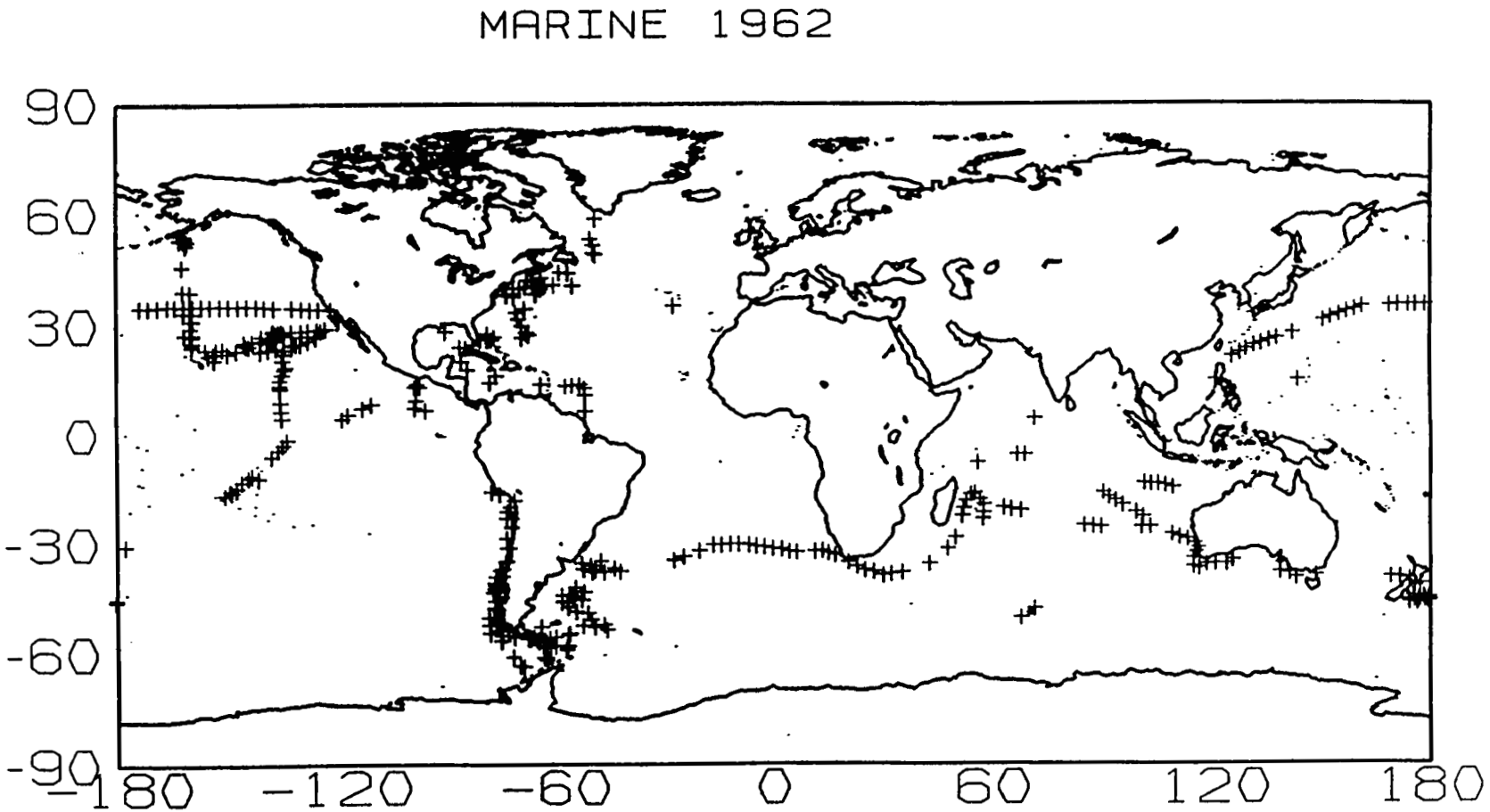

FIGURE 6. WORLD DATA DISTRIBUTION FOR 1962

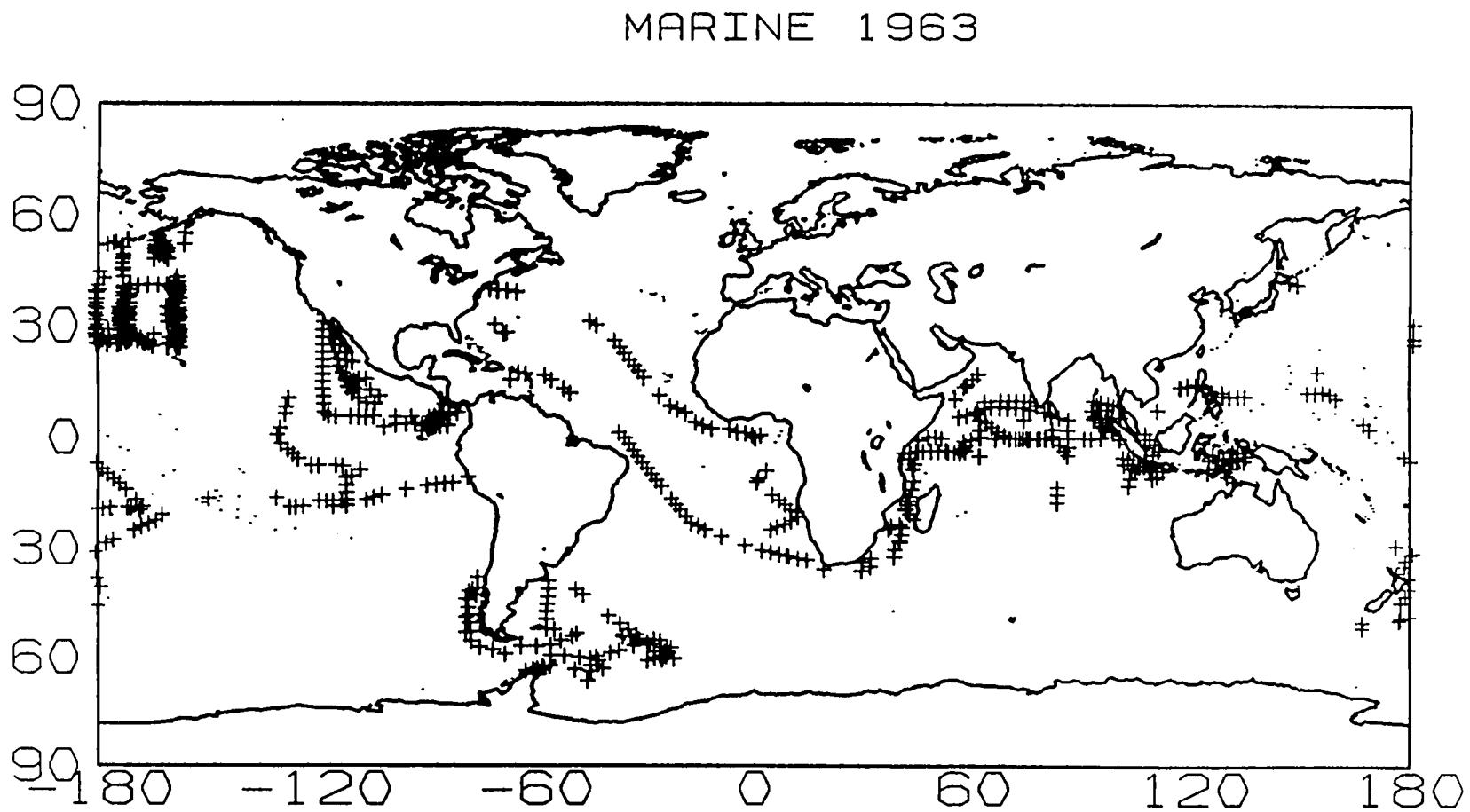

FIGURE 7. WORLD DATA DISTRIBUTION FOR 1963

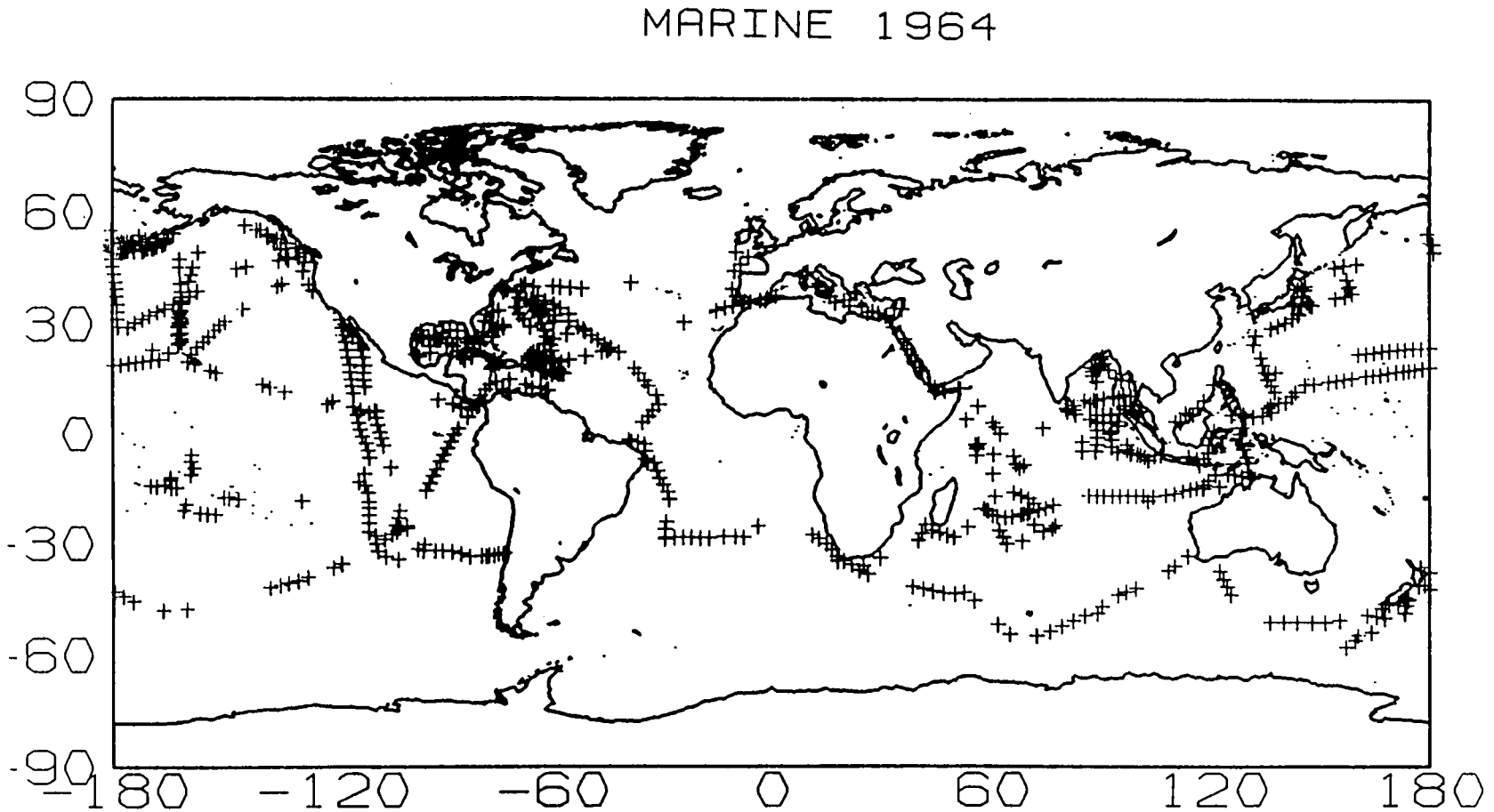

FIGURE 8. WORLD DATA DISTRIBUTION FOR 1964

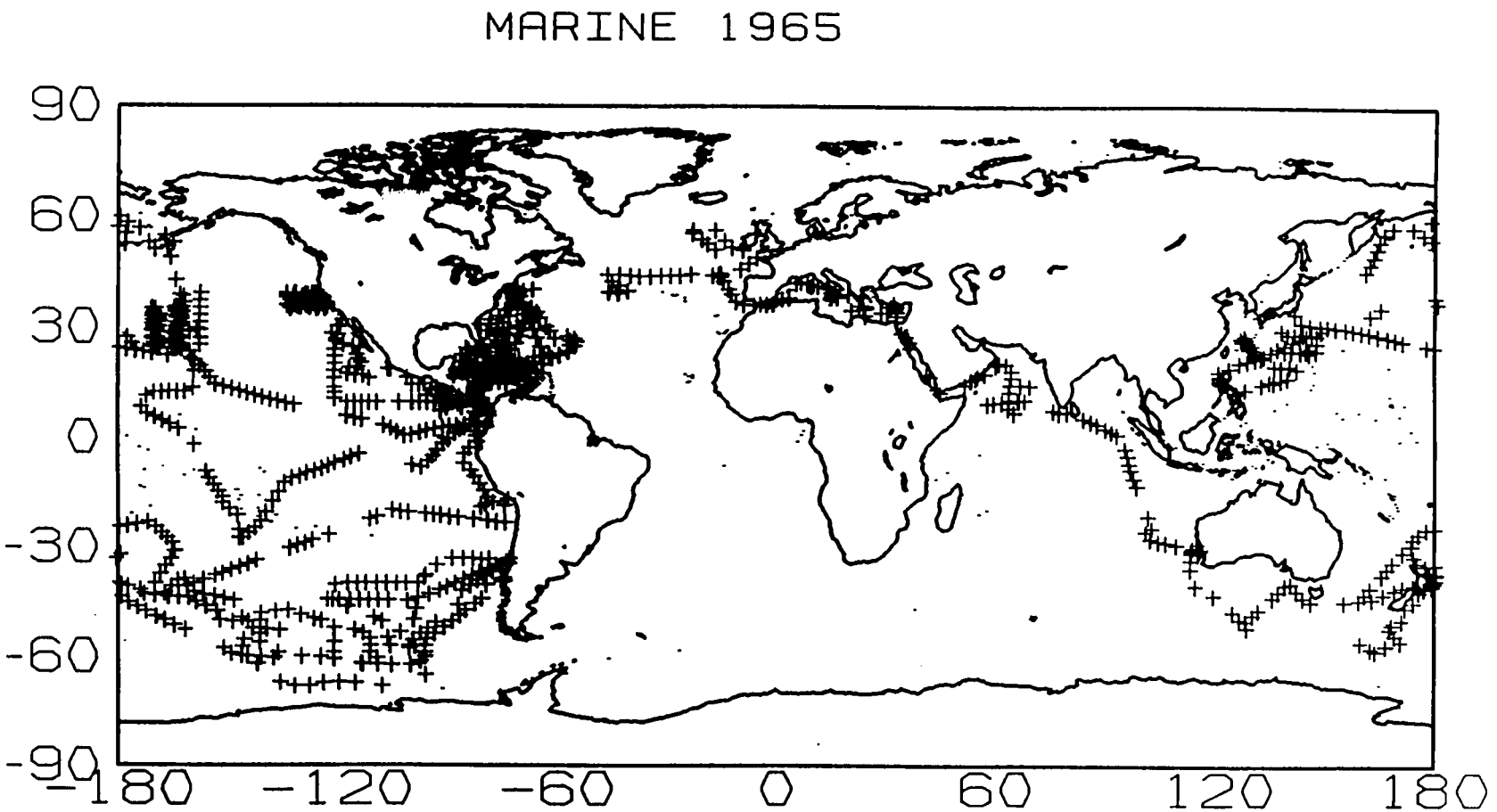

FIGURE 9. WORLD DATA DISTRIBUTION FOR 1965

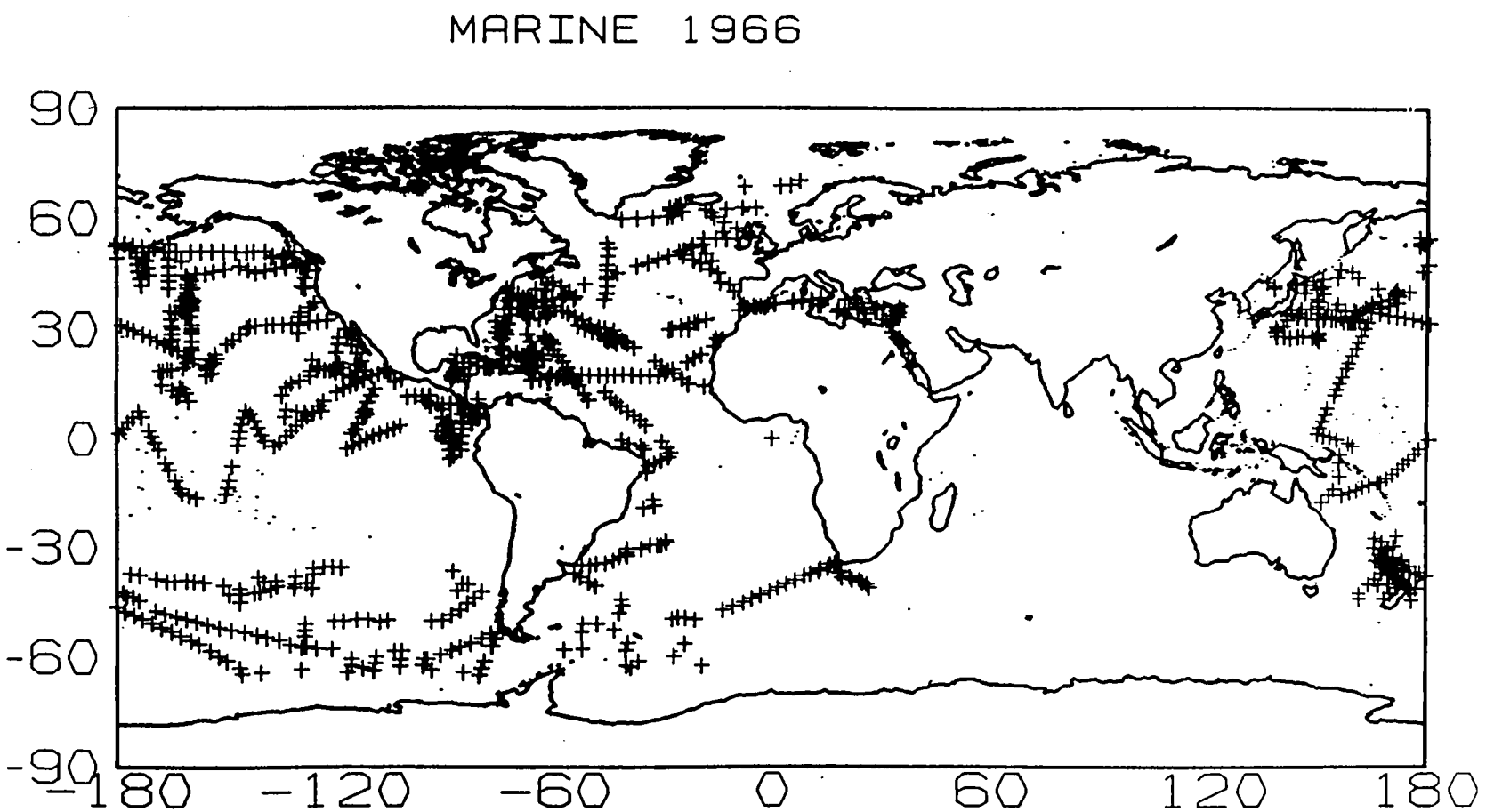

FIGURE 10. WORLD DATA DISTRIBUTION FOR 1966

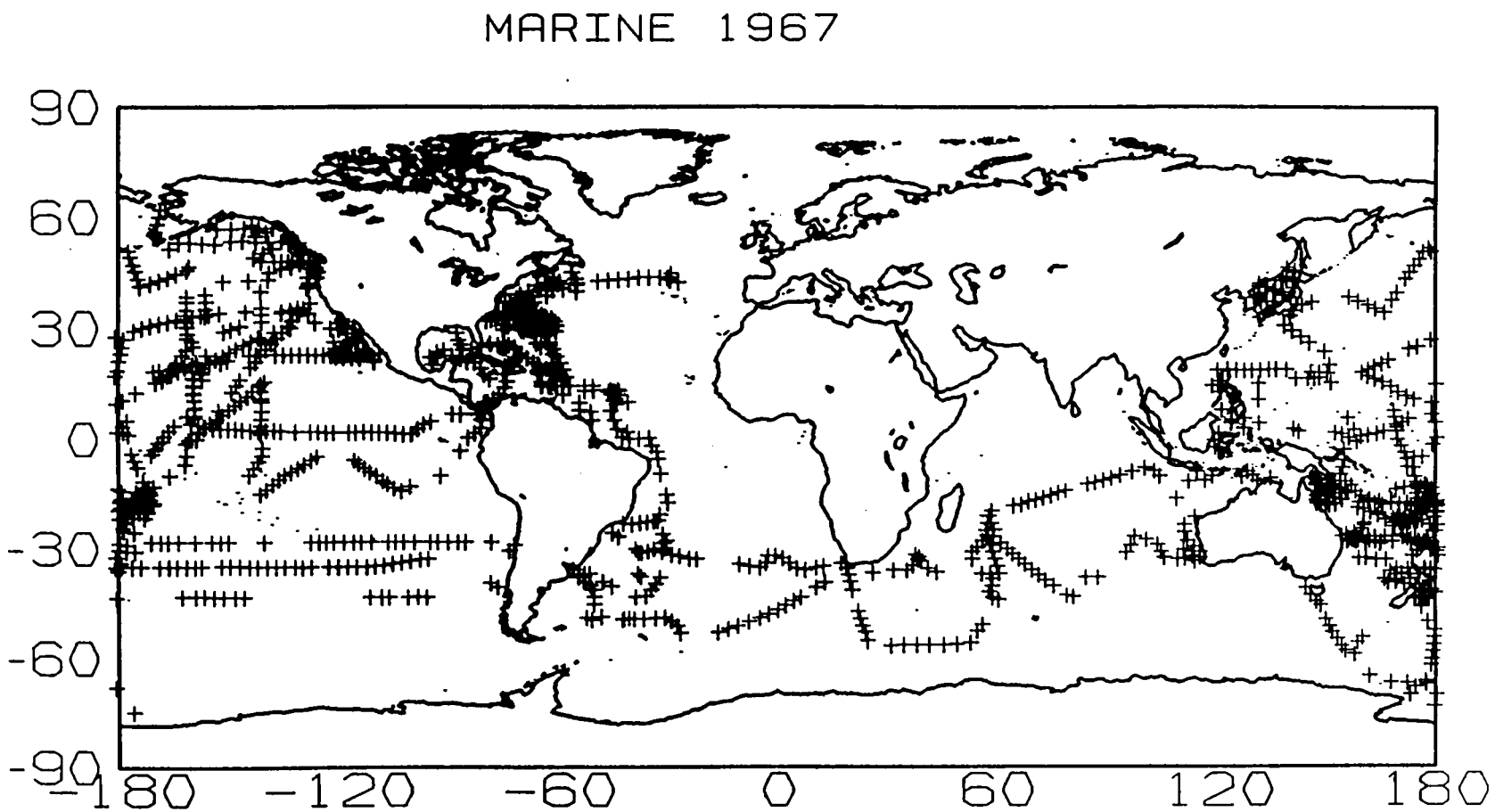

FIGURE 11. WORLD DATA DISTRIBUTION FOR 1967

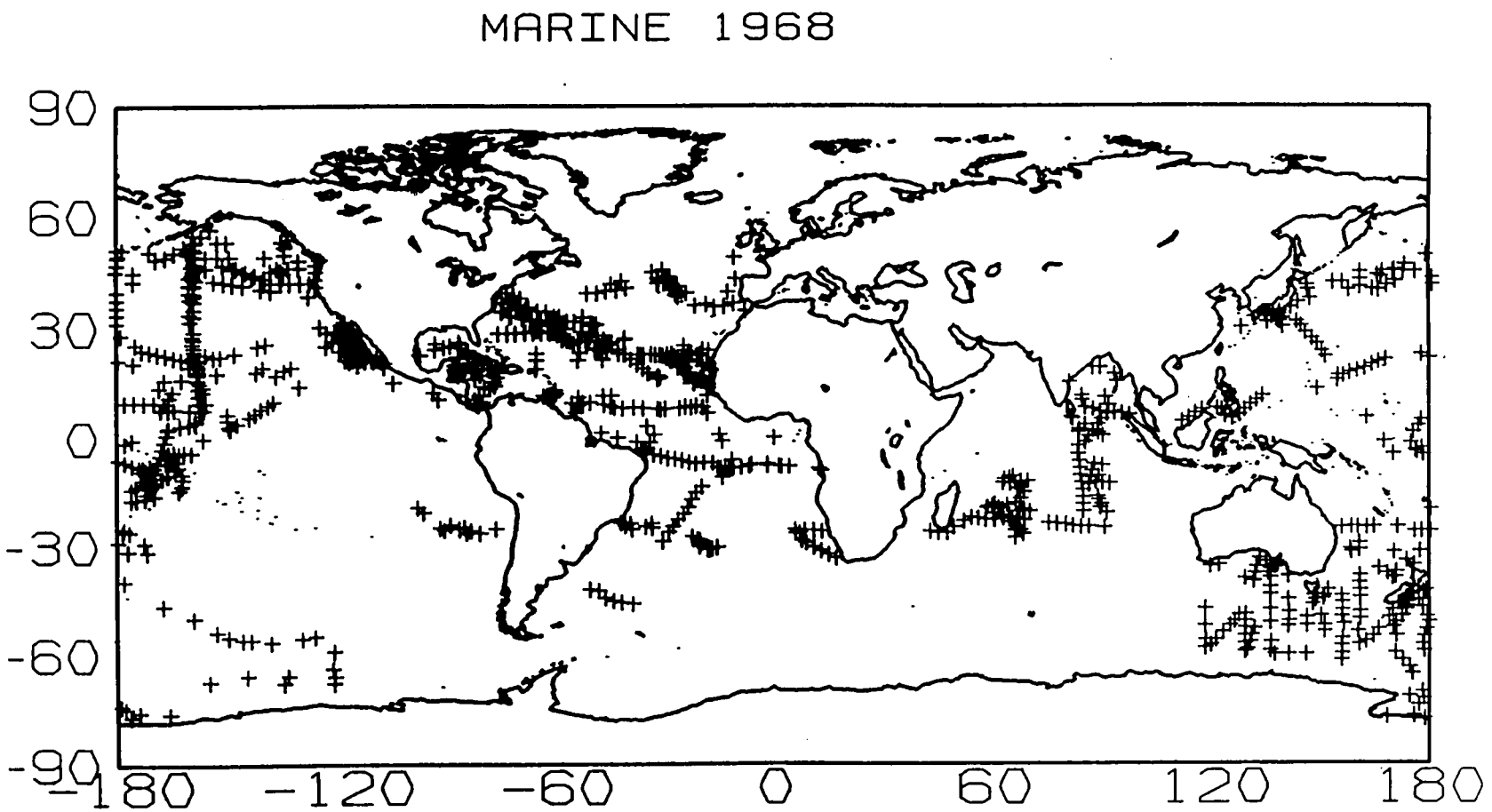

FIGURE 12. WORLD DATA DISTRIBUTION FOR 1968

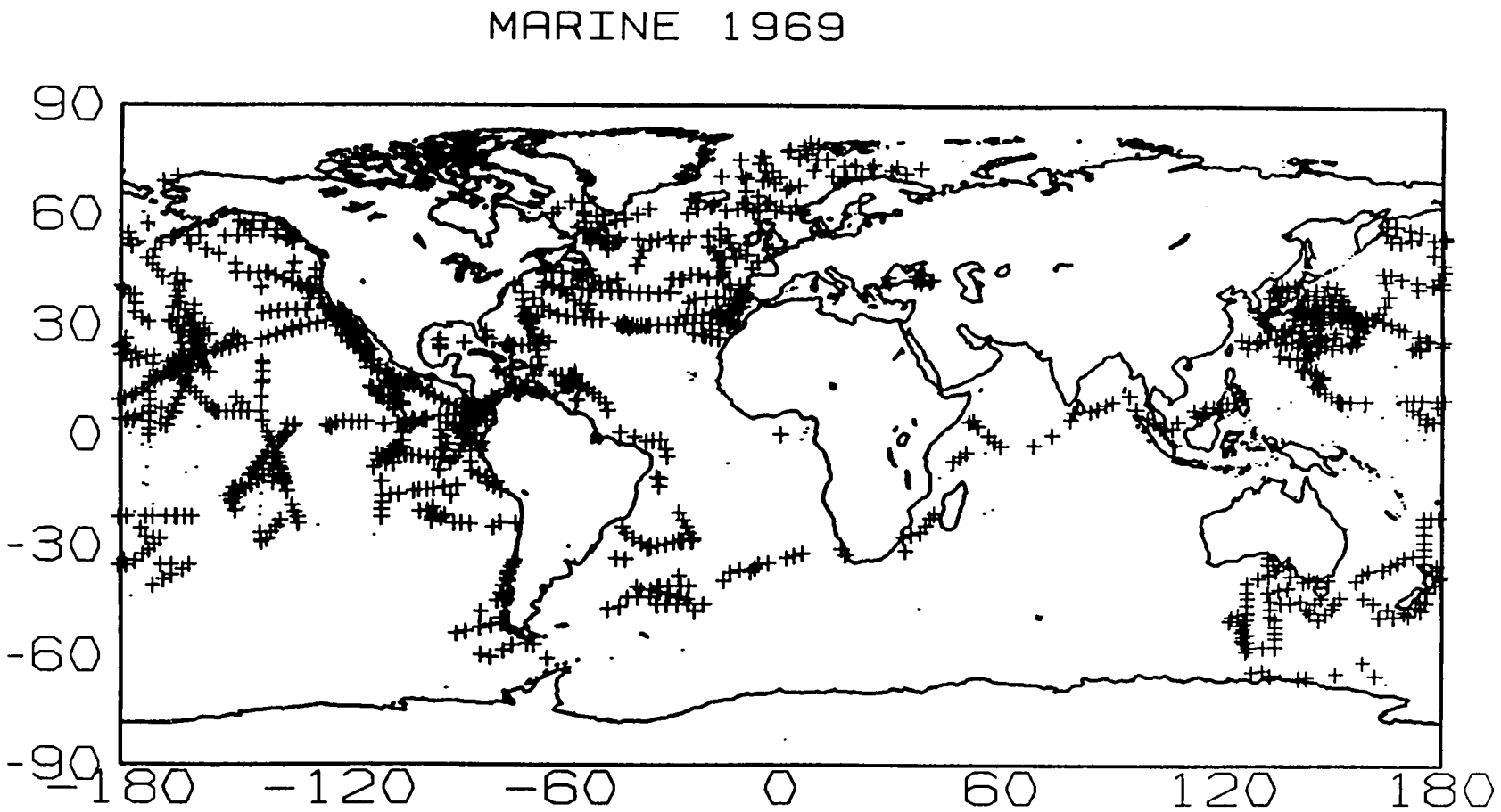

FIGURE 13. WORLD DATA DISTRIBUTION FOR 1969

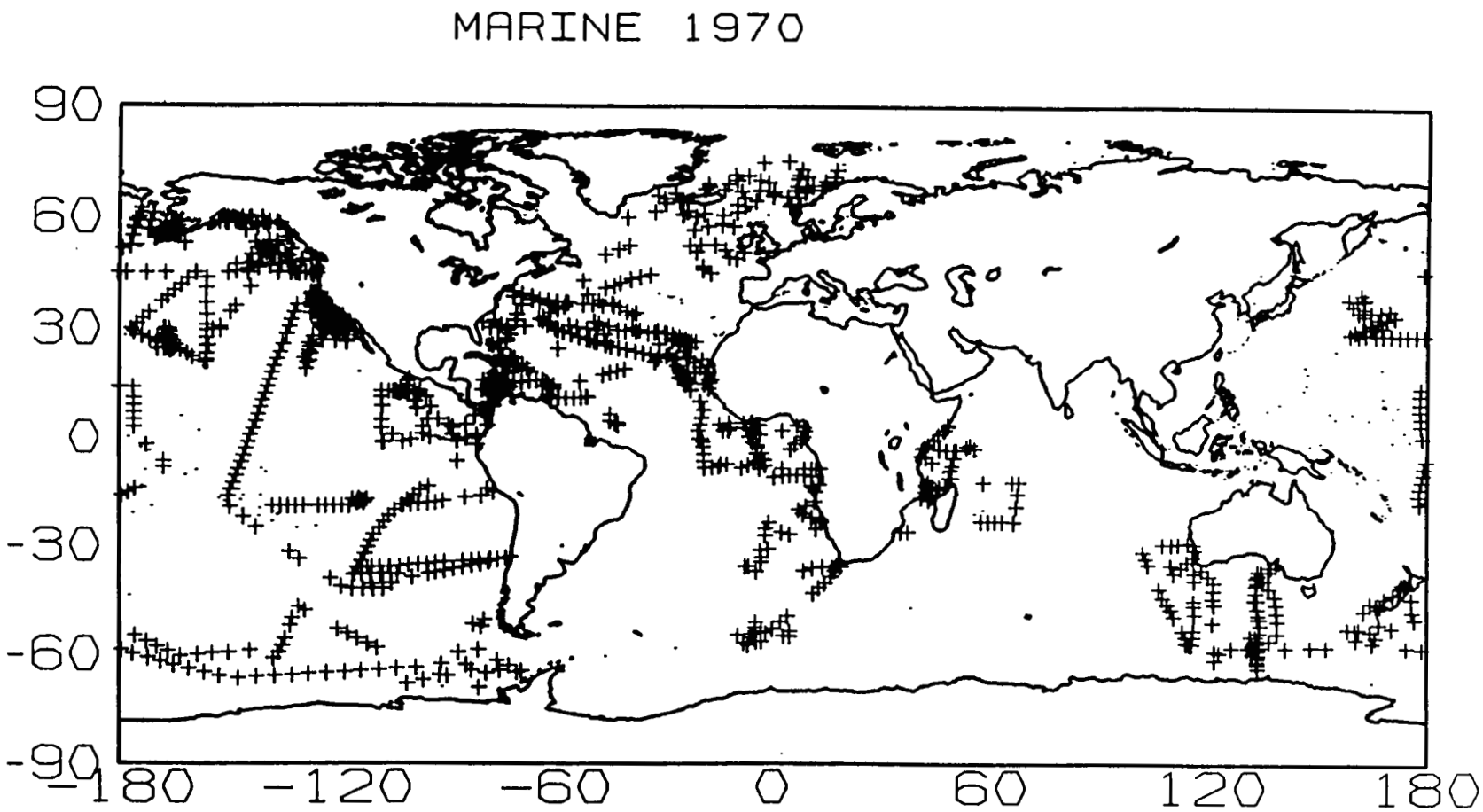

FIGURE 14. WORLD DATA DISTRIBUTION FOR 1970

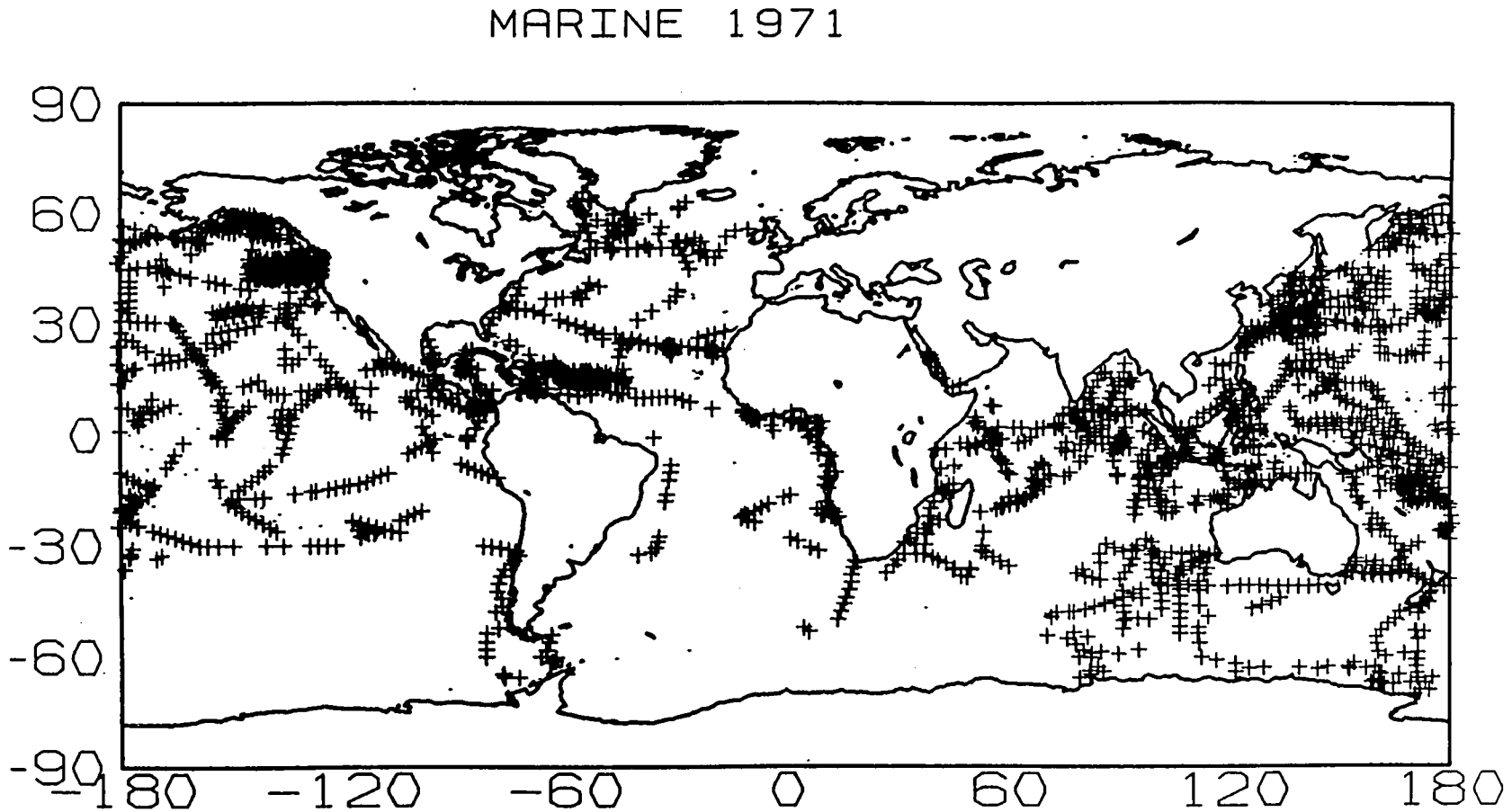

FIGURE 15. WORLD DATA DISTRIBUTION FOR 1971

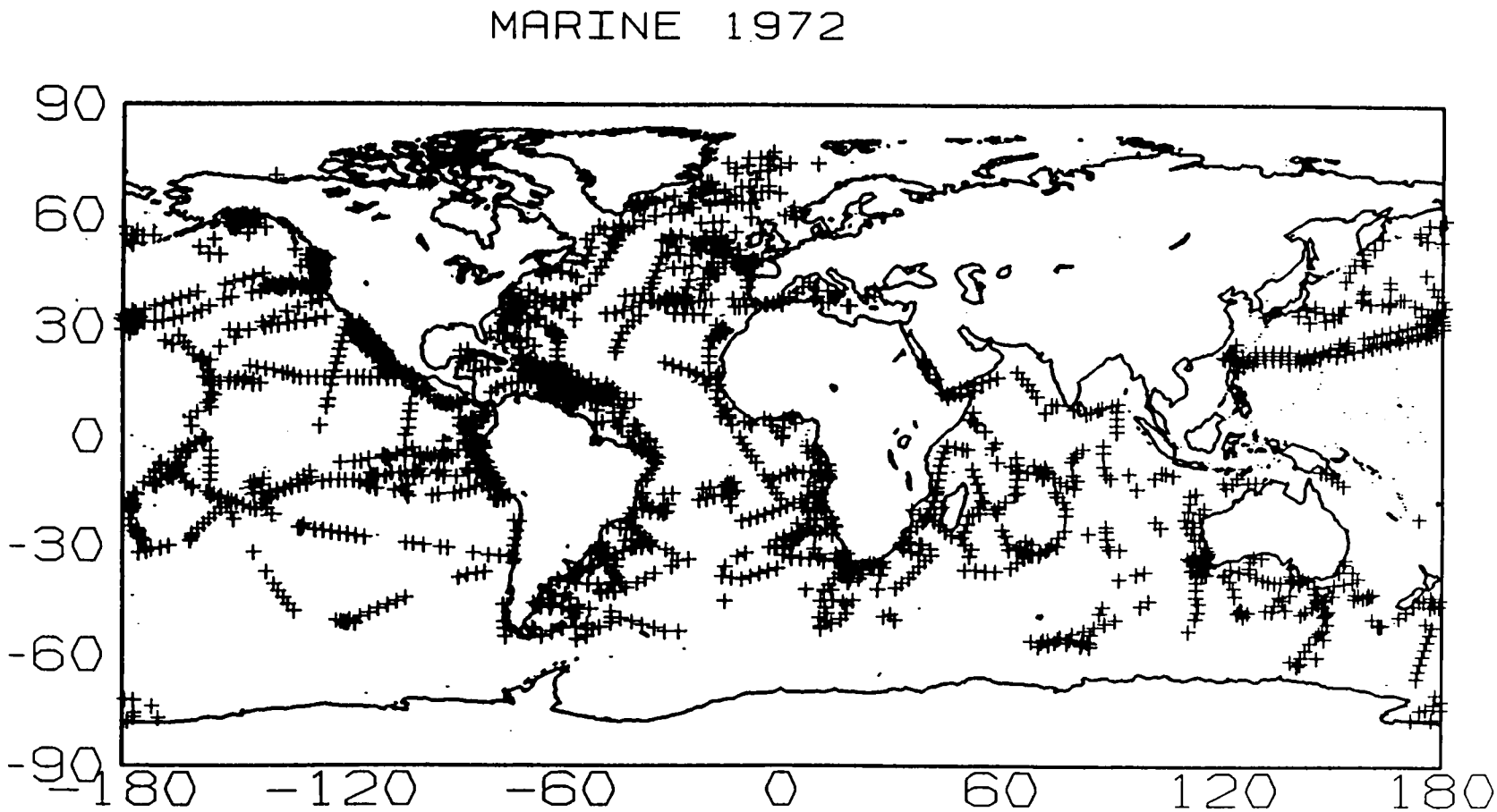

FIGURE 16. WORLD DATA DISTRIBUTION FOR 1972

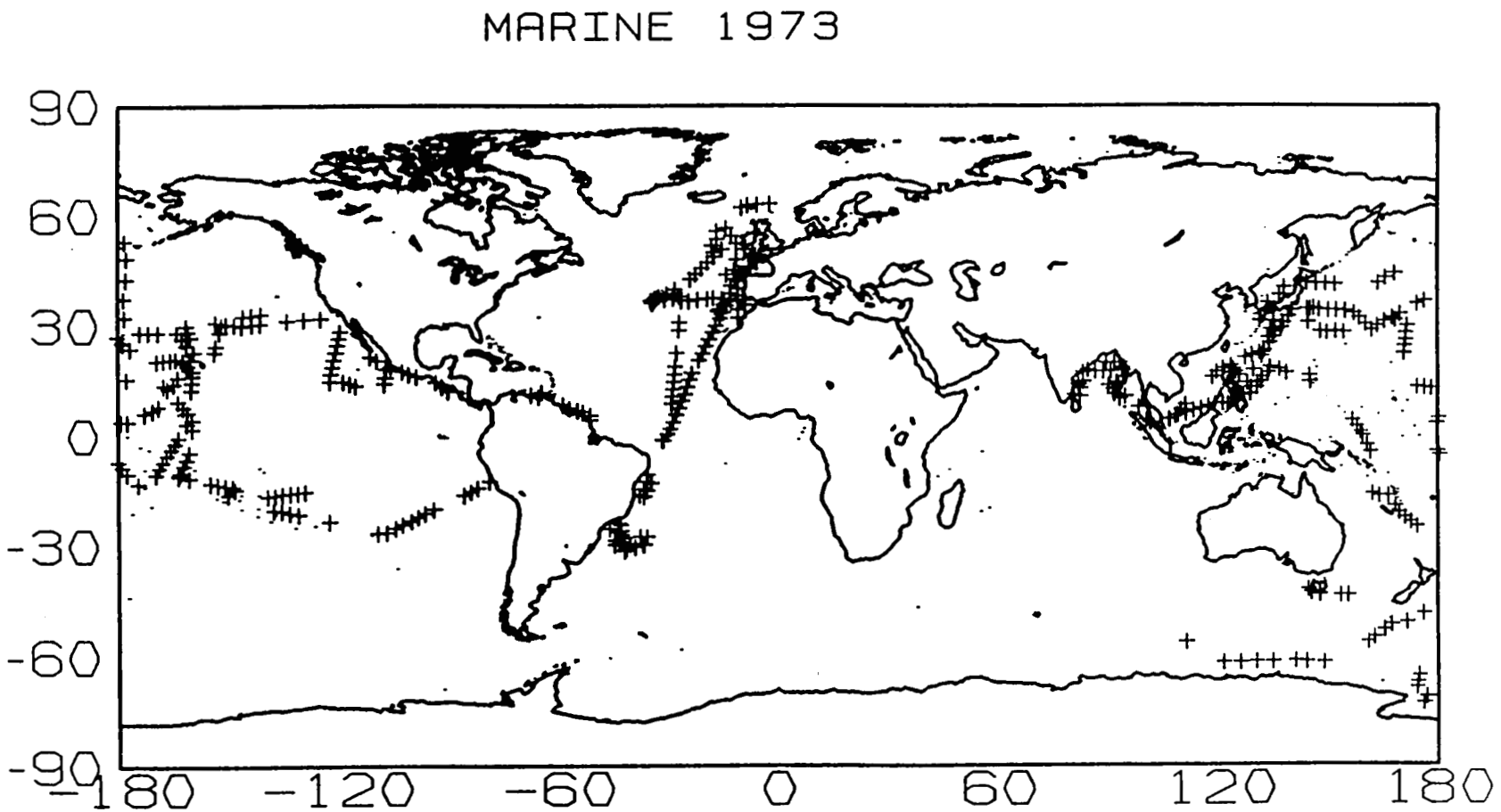

FIGURE 17. WORLD DATA DISTRIBUTION FOR 1973

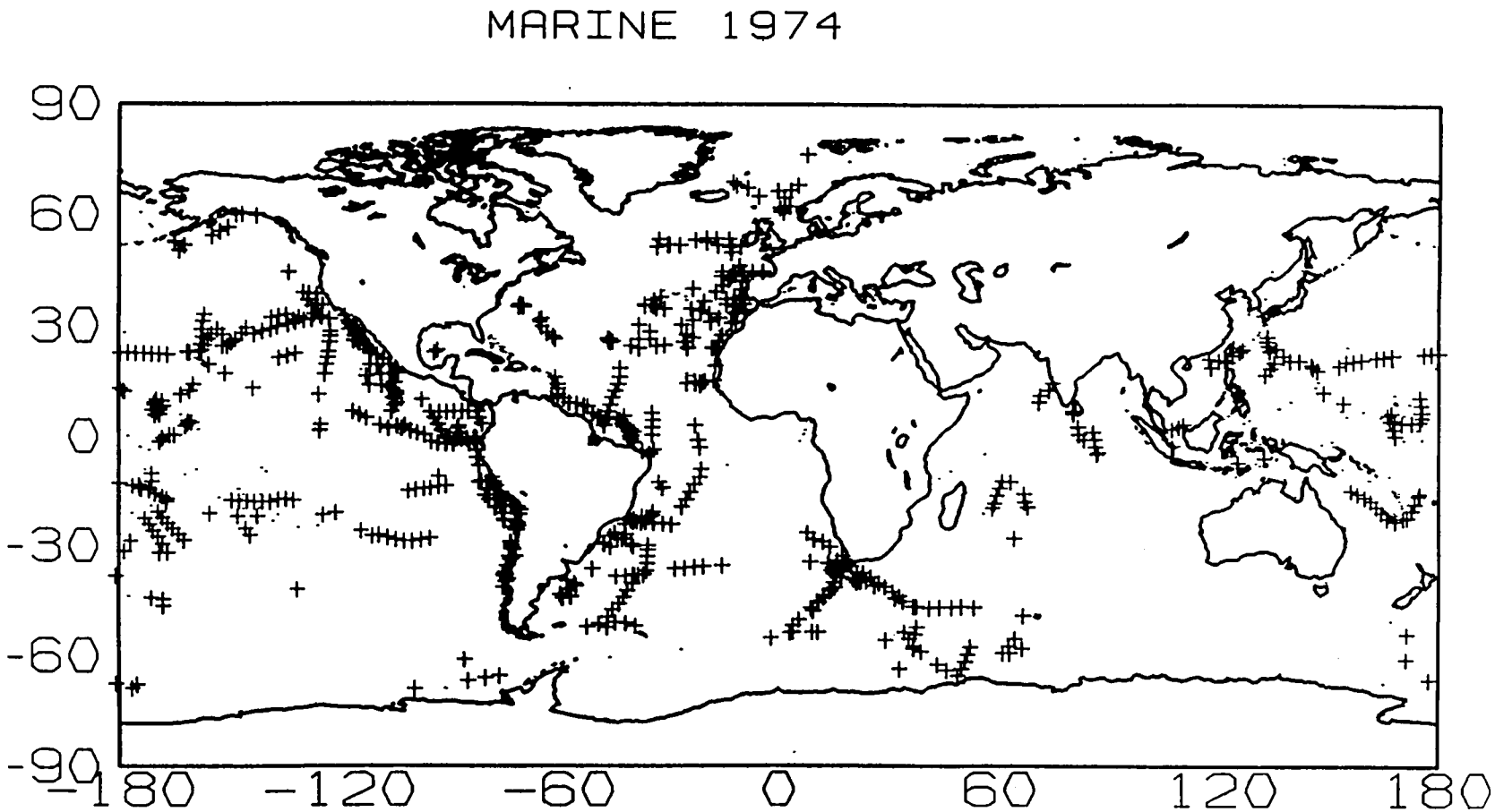

FIGURE 18. WORLD DATA DISTRIBUTION FOR 1974

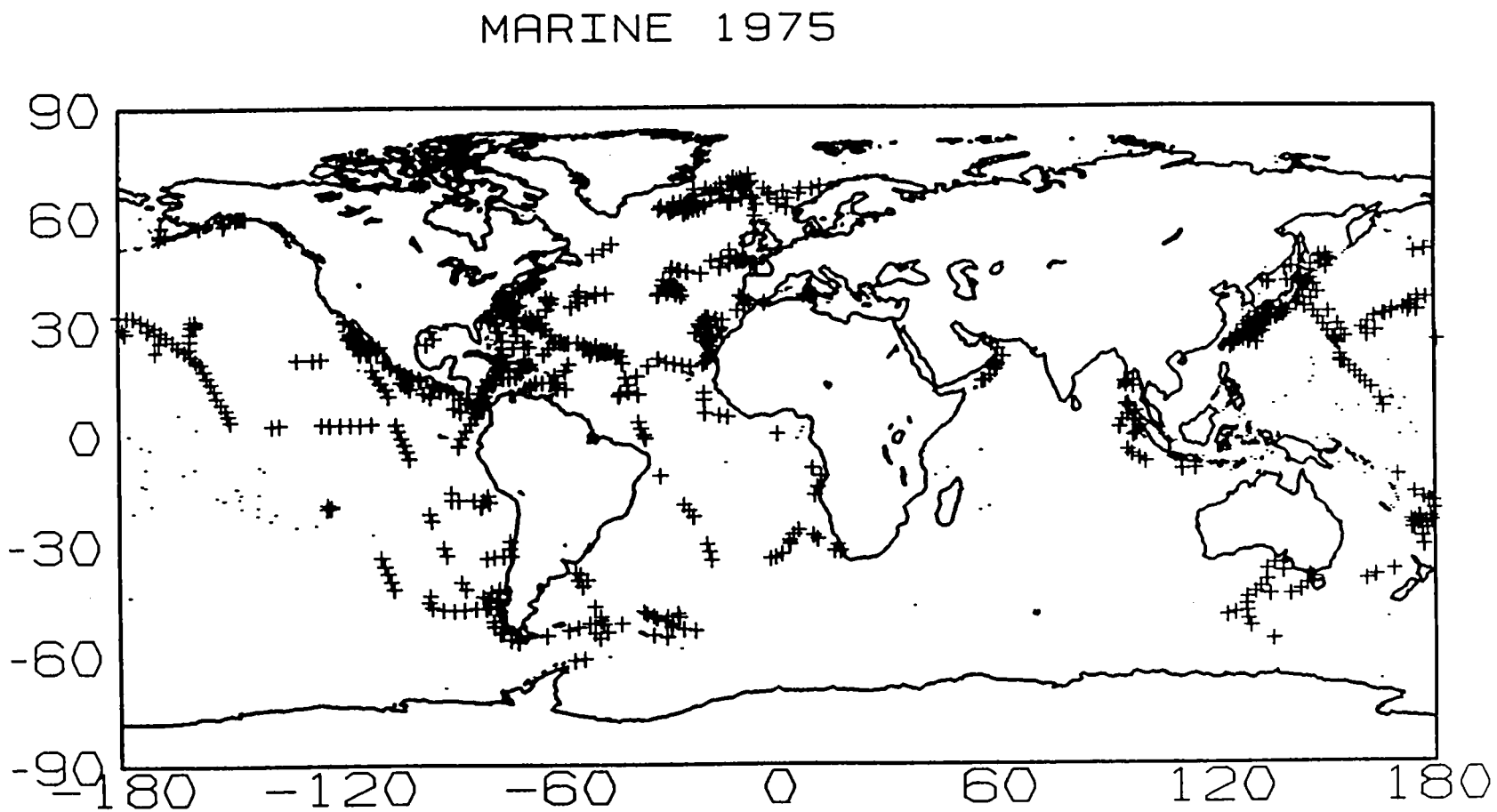

FIGURE 19. WORLD DATA DISTRIBUTION FOR 1975

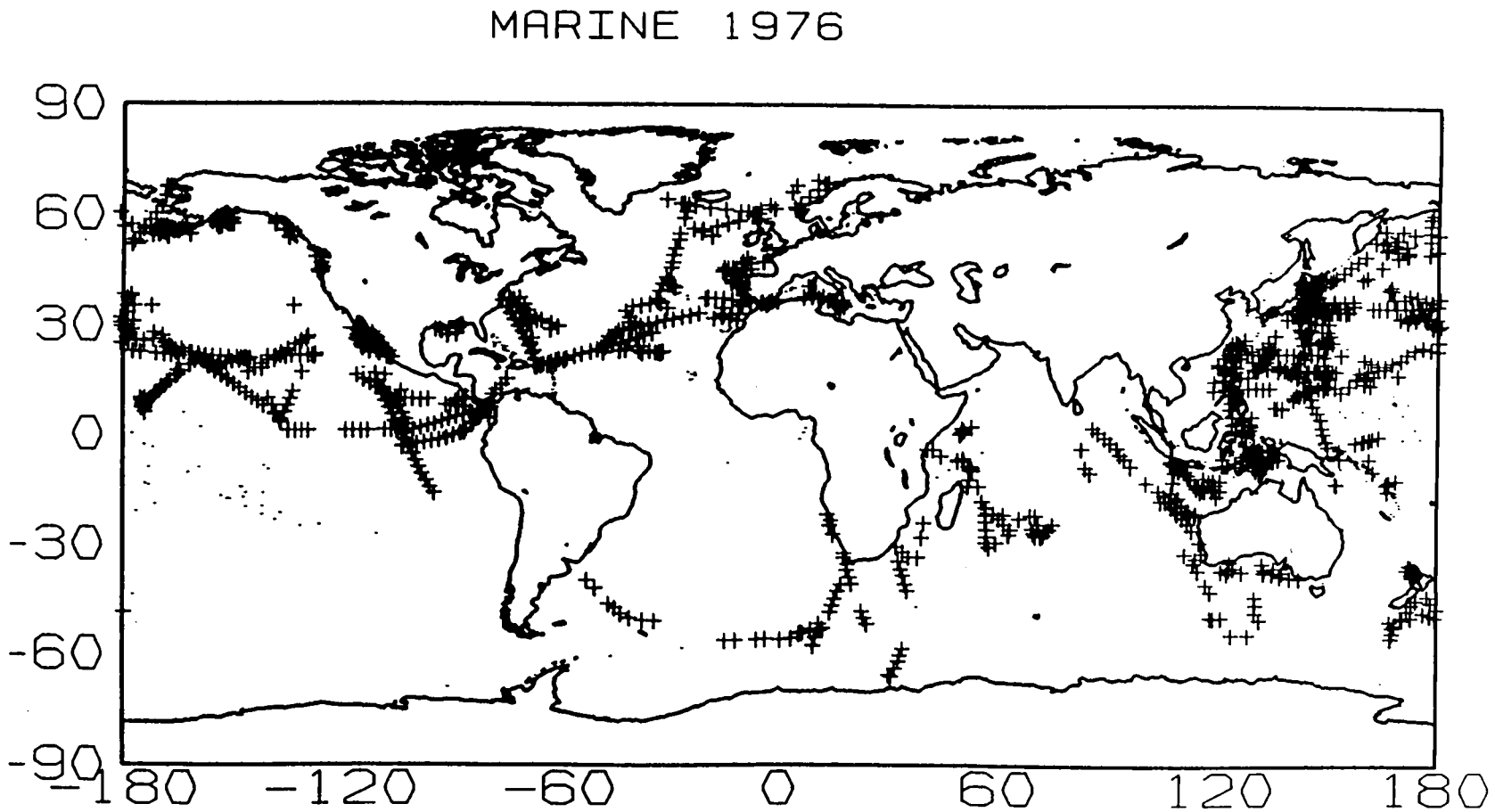

FIGURE 20. WORLD DATA DISTRIBUTION FOR 1976

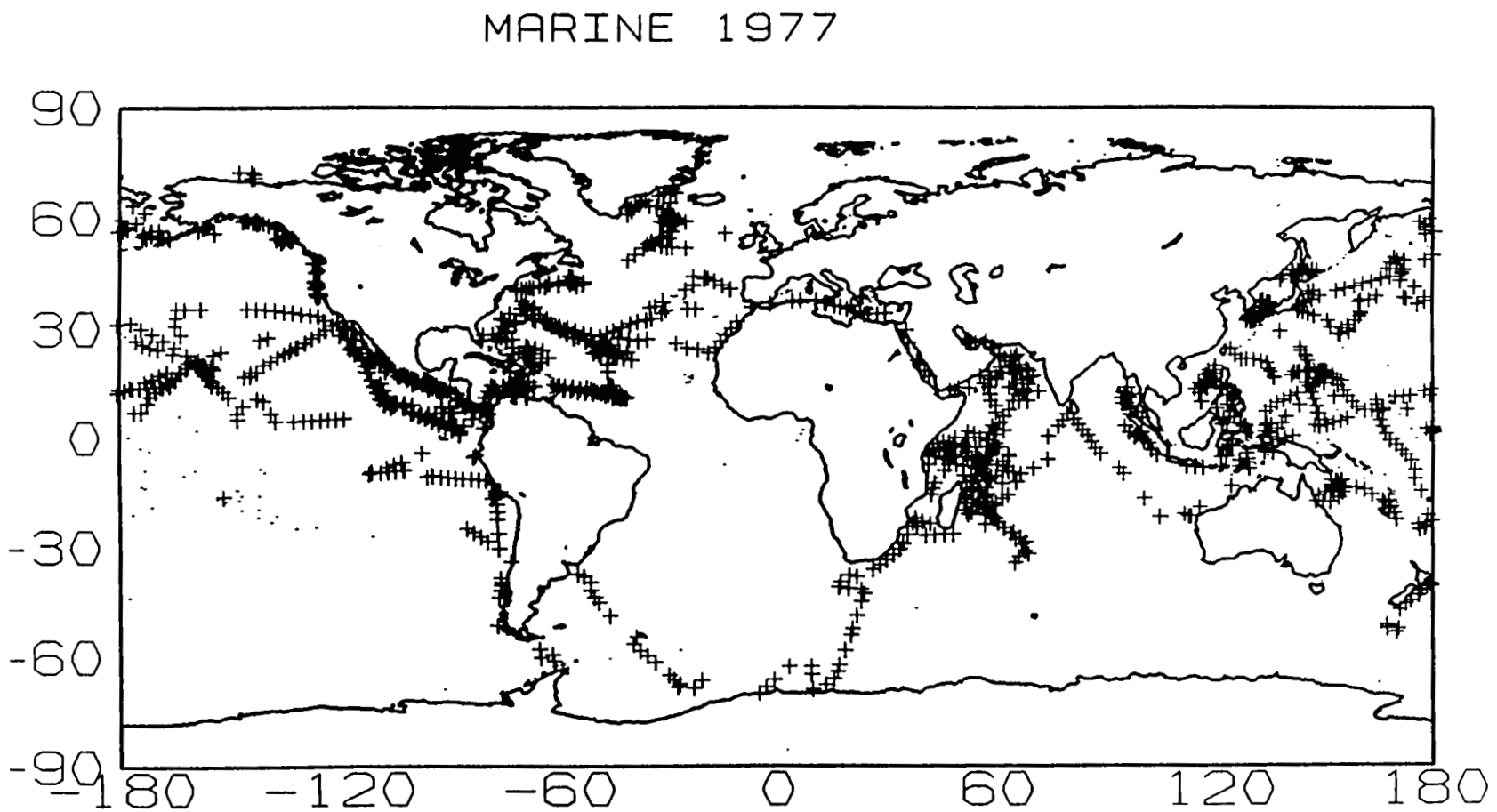

FIGURE 21. WORLD DATA DISTRIBUTION FOR 1977

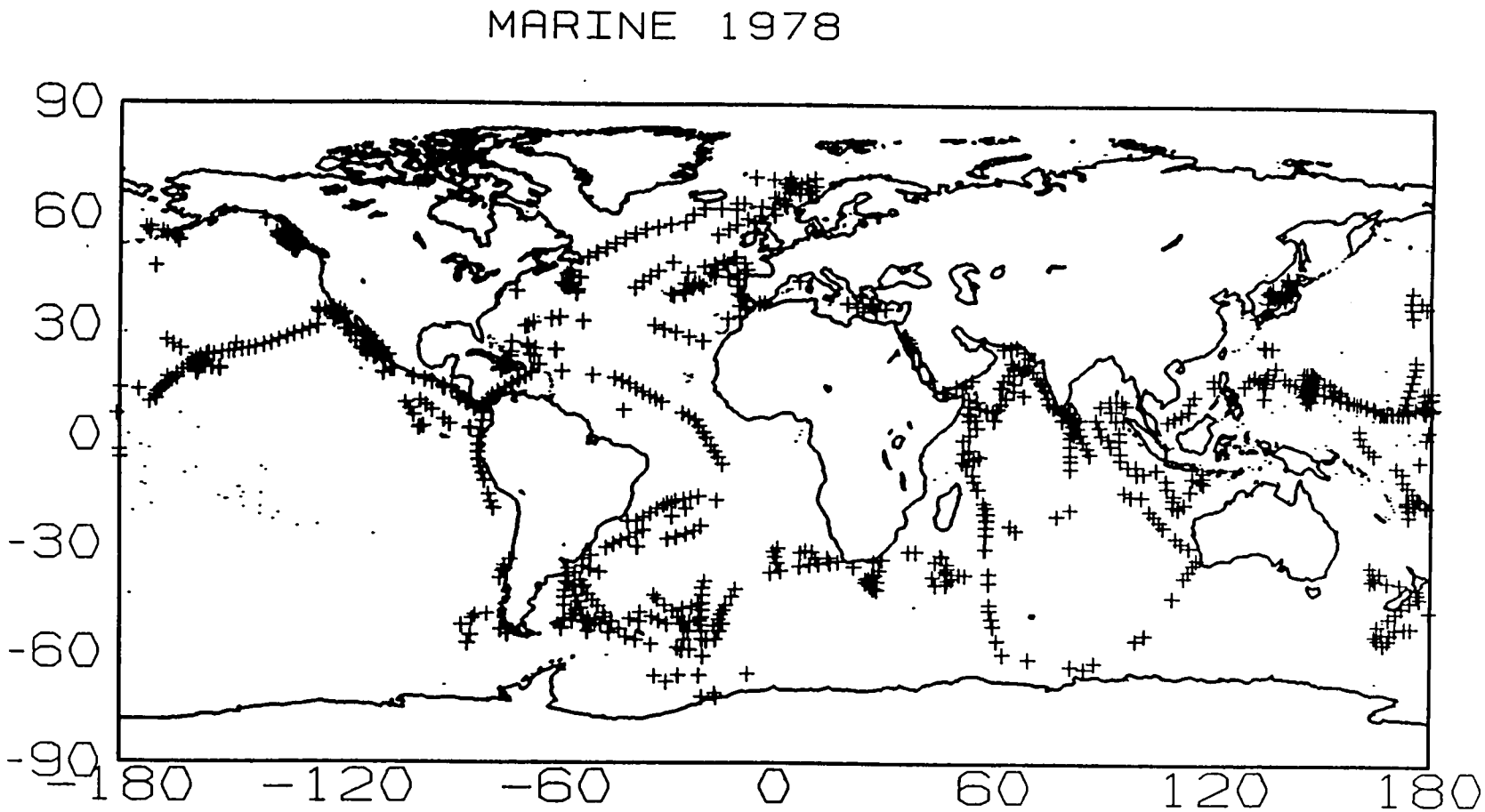

FIGURE 22. WORLD DATA DISTRIBUTION FOR 1978

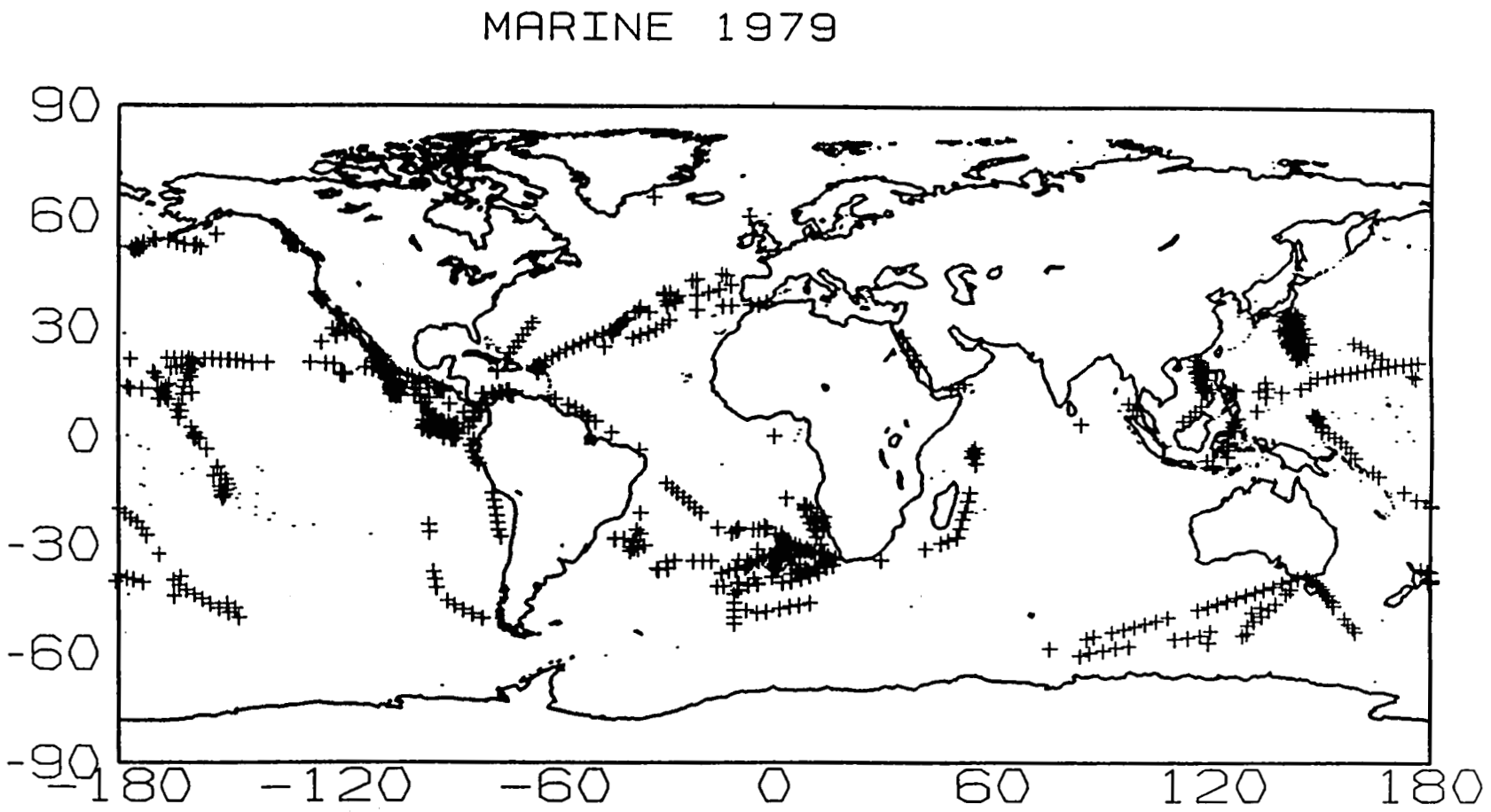

FIGURE 23. WORLD DATA DISTRIBUTION FOR 1979

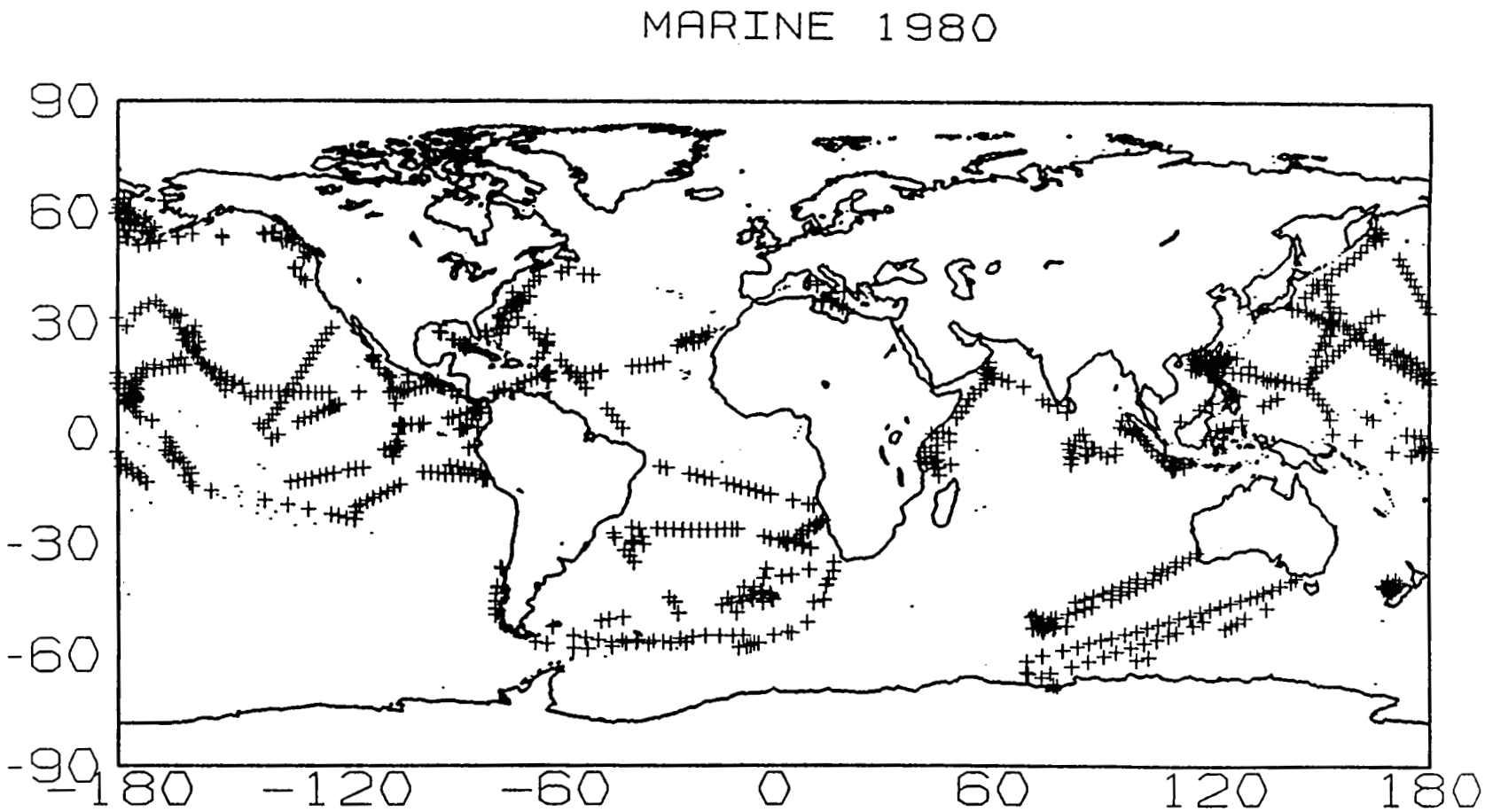

FIGURE 24. WORLD DATA DISTRIBUTION FOR 1980

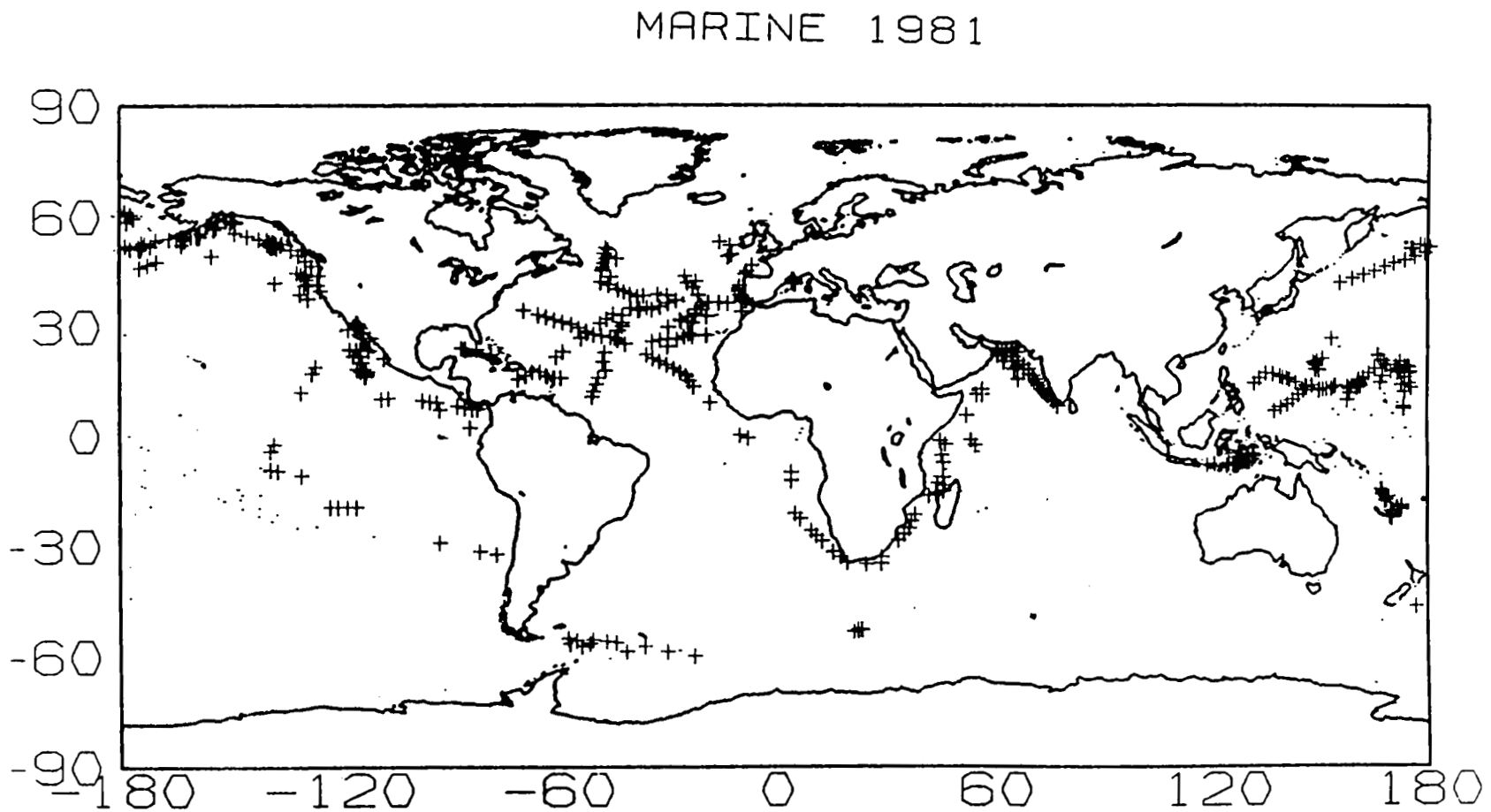

FIGURE 25. WORLD DATA DISTRIBUTION FOR 1981

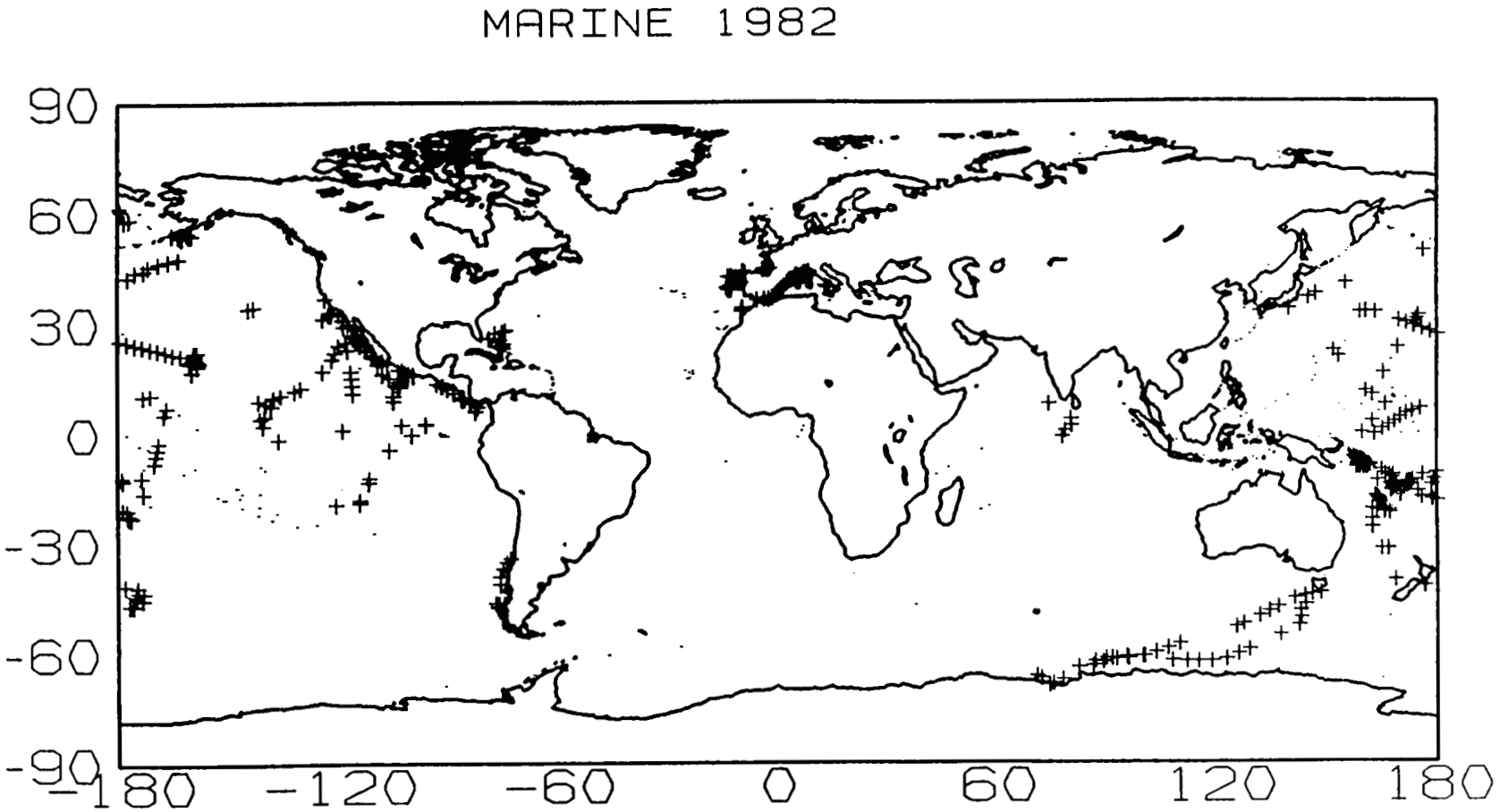

FIGURE 26. WORLD DATA DISTRIBUTION FOR 1982

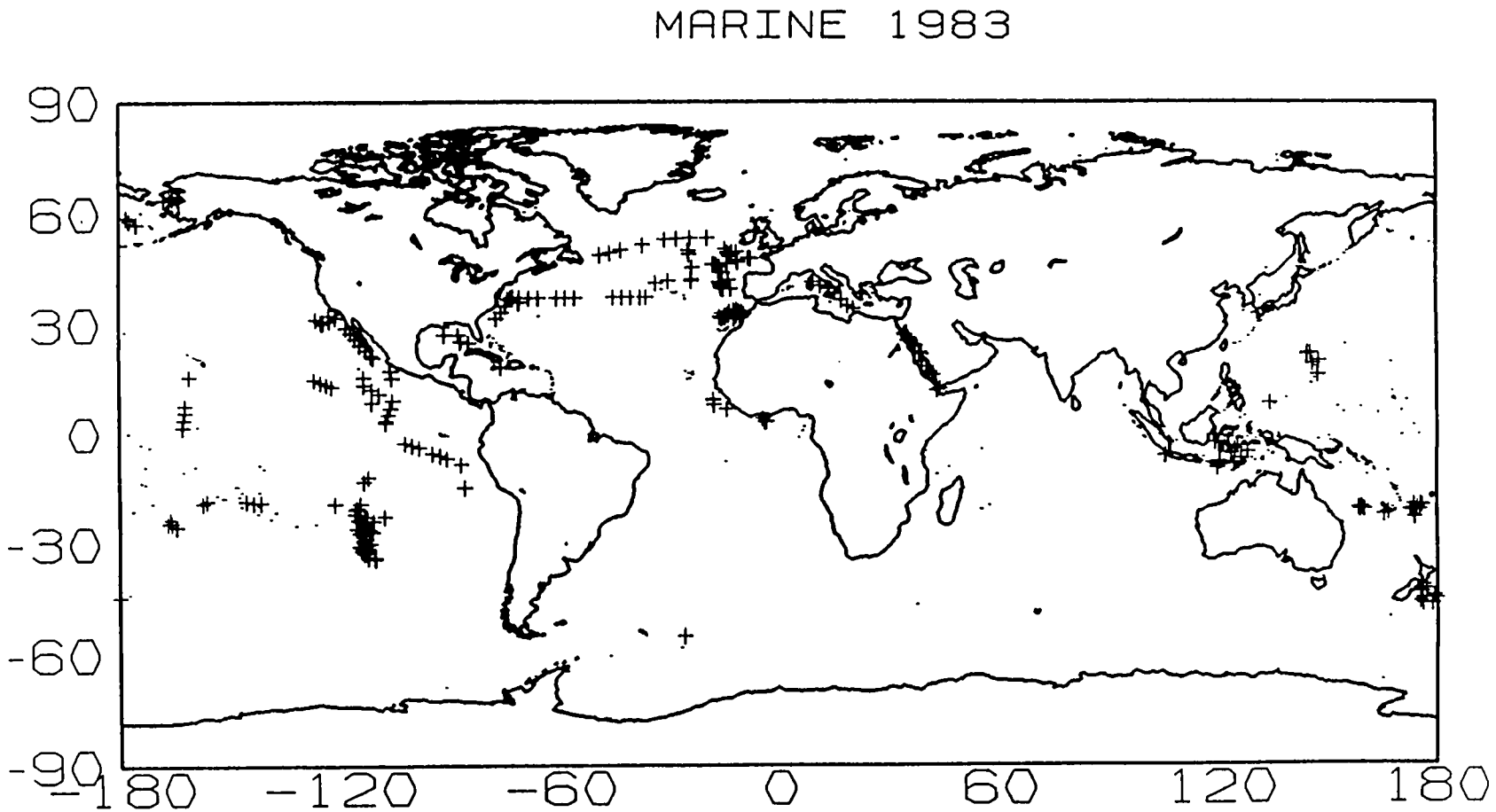

FIGURE 27. WORLD DATA DISTRIBUTION FOR 1983

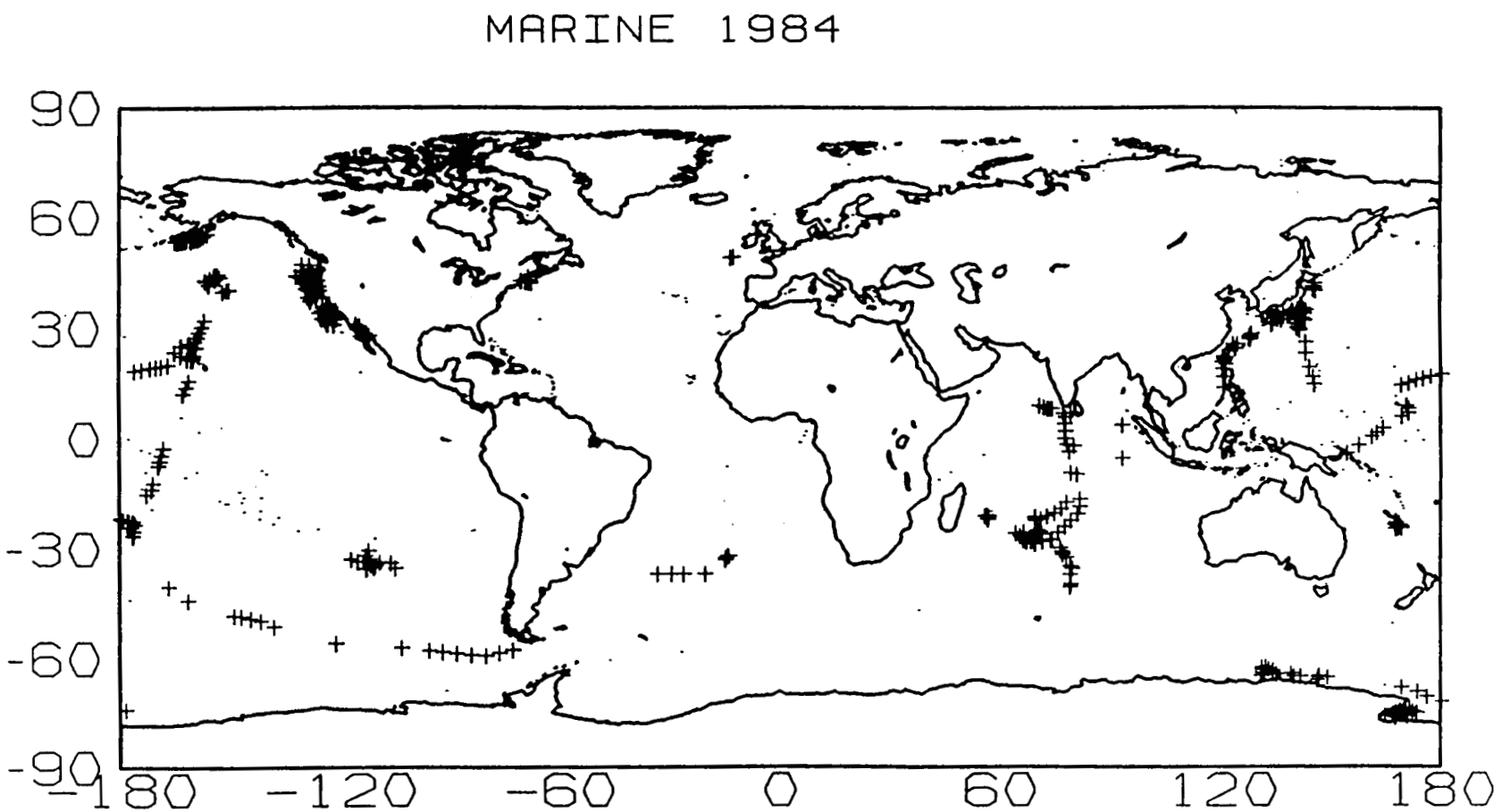

FIGURE 28. WORLD DATA DISTRIBUTION FOR 1984

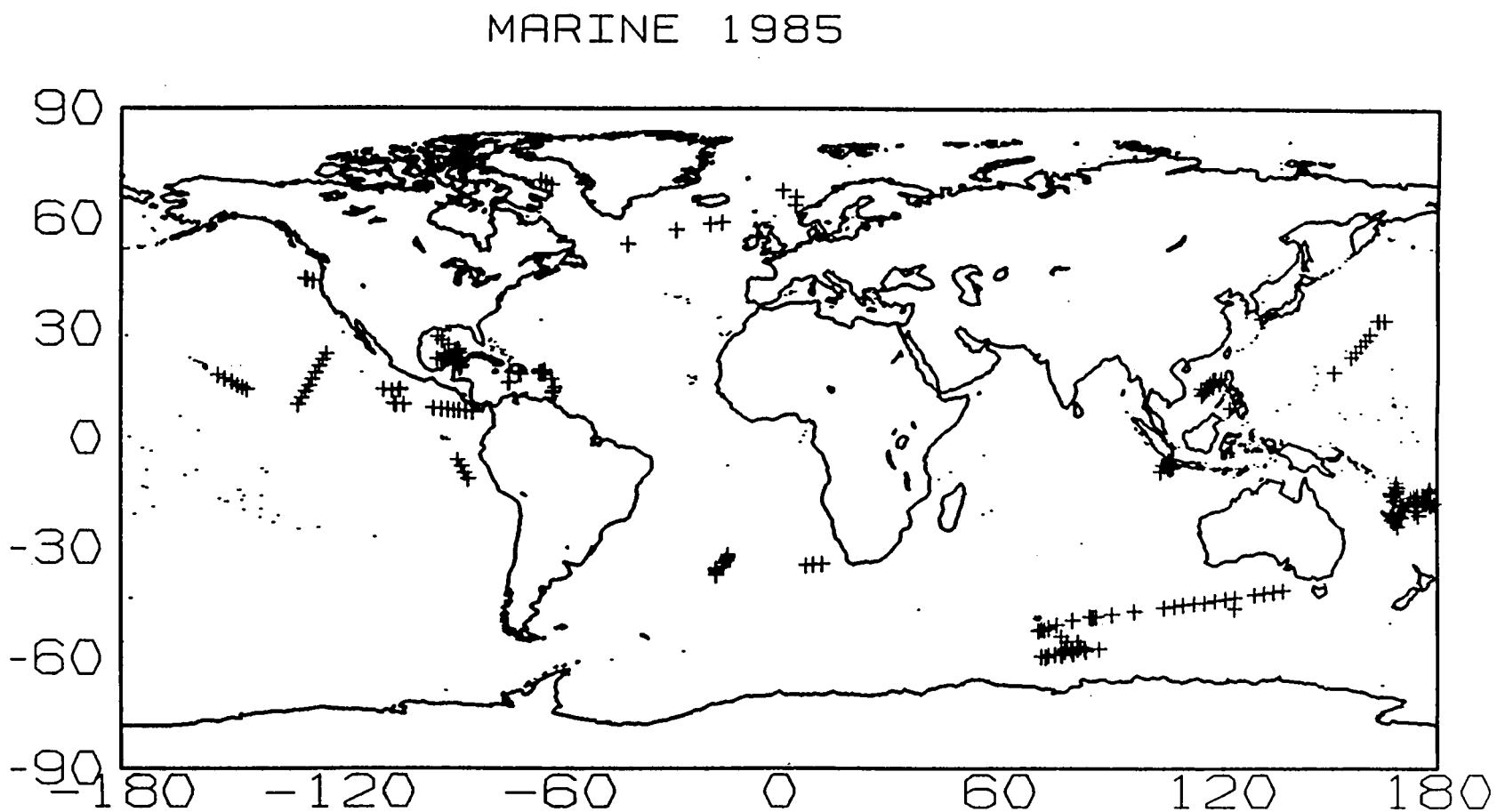

FIGURE 29. WORLD DATA DISTRIBUTION FOR 1985

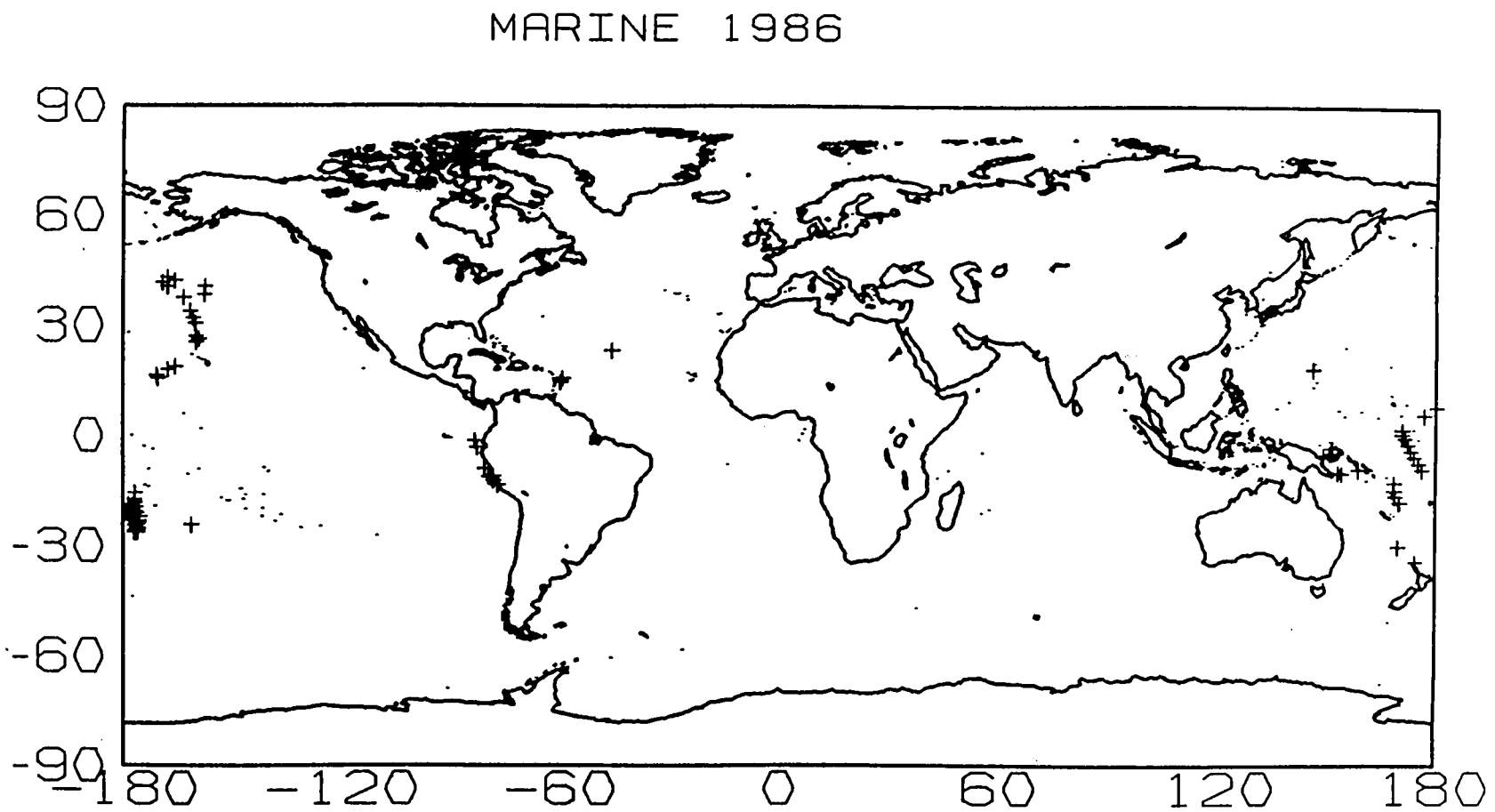

FIGURE 30. WORLD DATA DISTRIBUTION FOR 1986

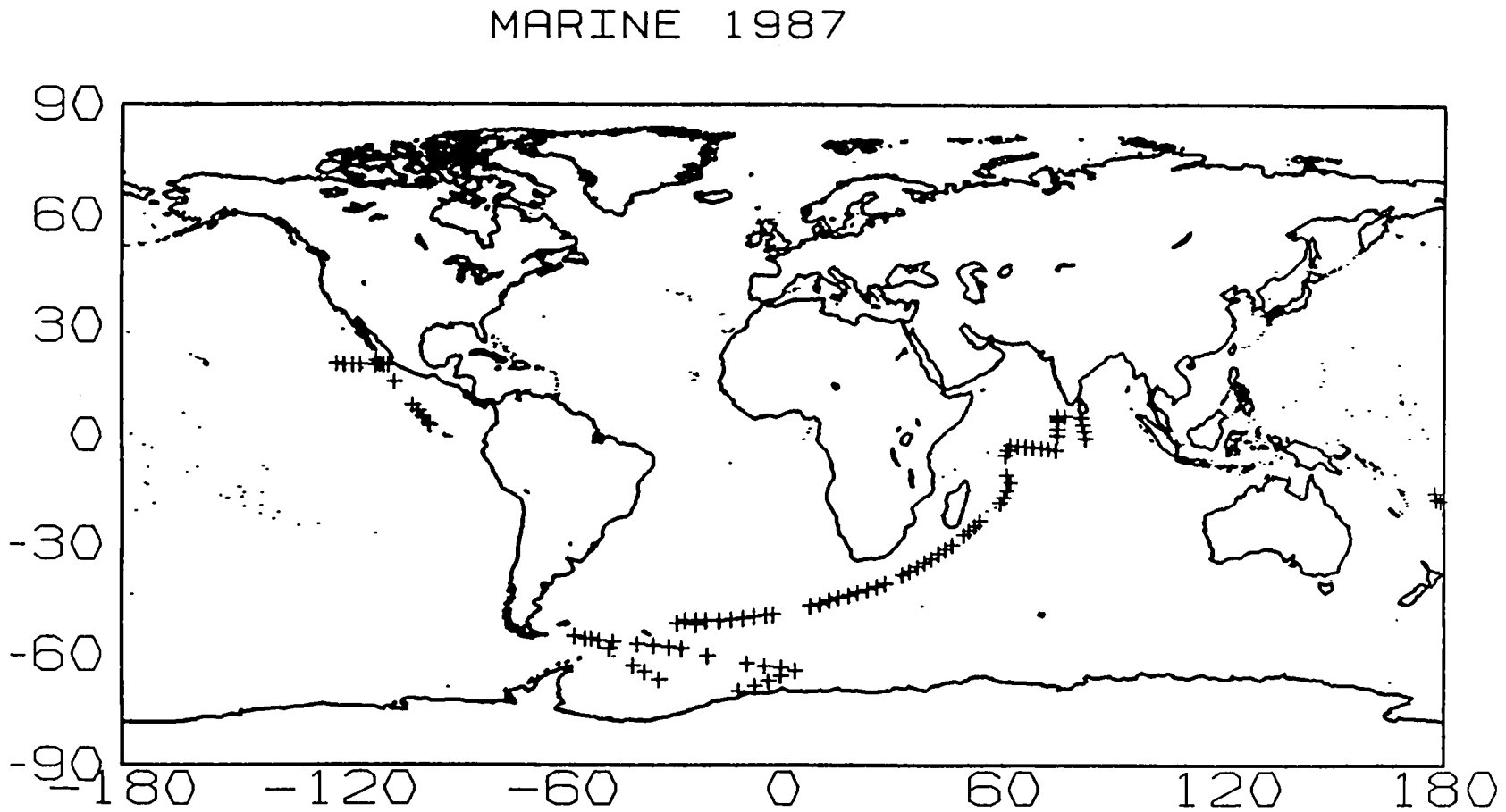

FIGURE 31. WORLD DATA DISTRIBUTION FOR 1987

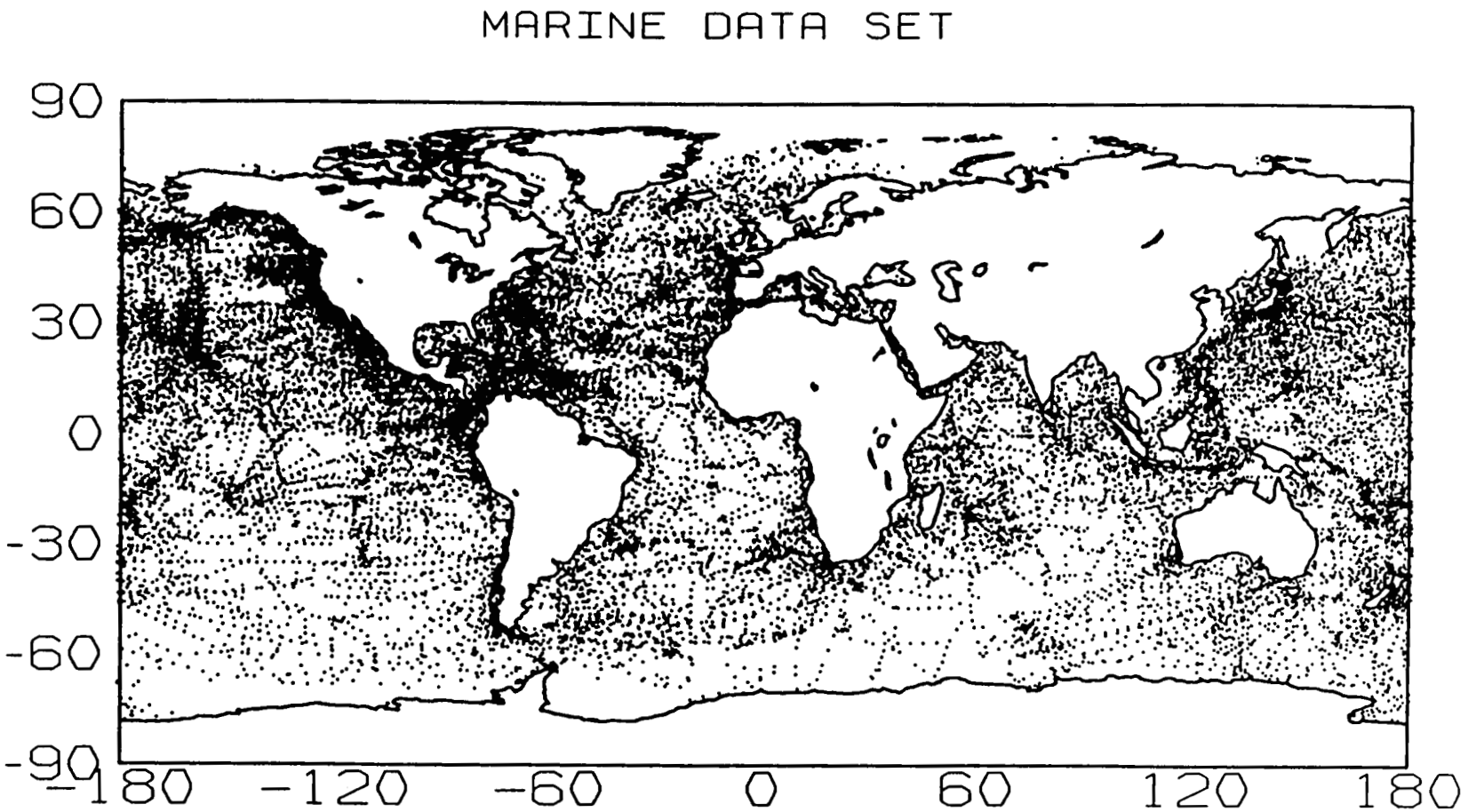

FIGURE 32. WORLD DATA DISTRIBUTION FOR ALL AVERAGED VALUES

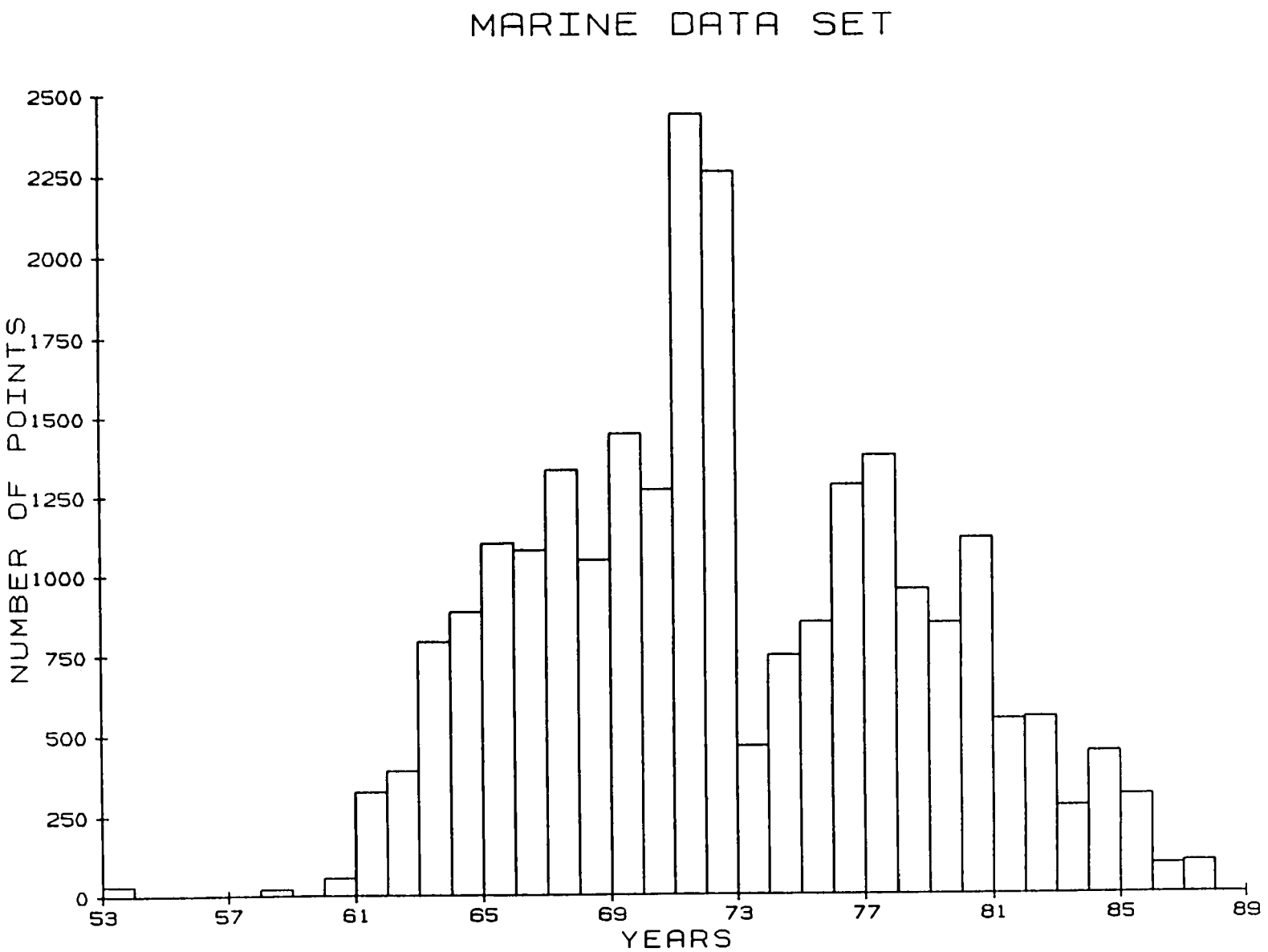

FIGURE 33. HISTOGRAM OF THE NUMBER OF AVERAGE VALUES PER YEAR IN THE MARINE DATA SET

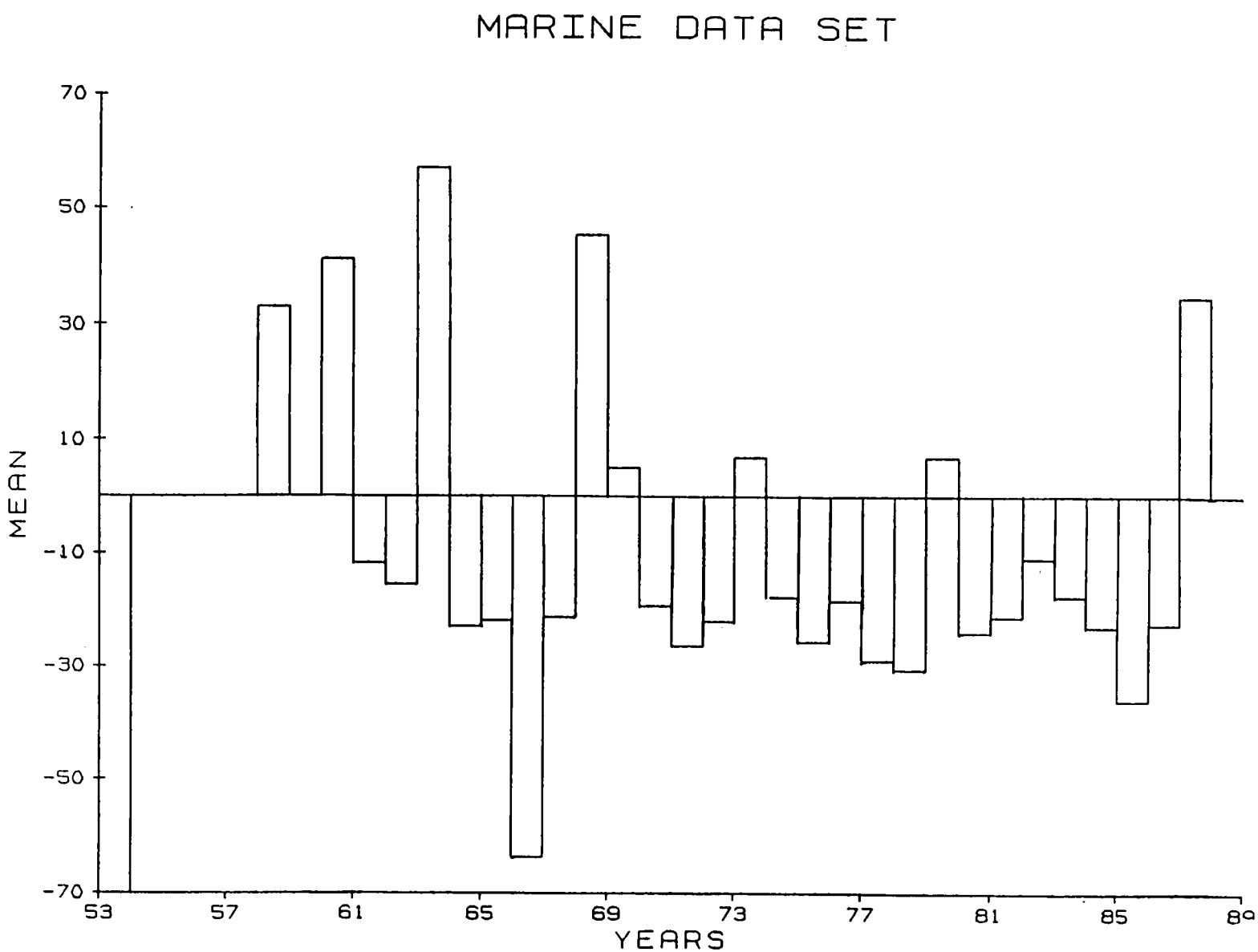

FIGURE 34. HISTOGRAM OF THE MEAN DEVIATION FROM THE IGRF OR DGRF PER YEAR FOR THE MARINE DATA

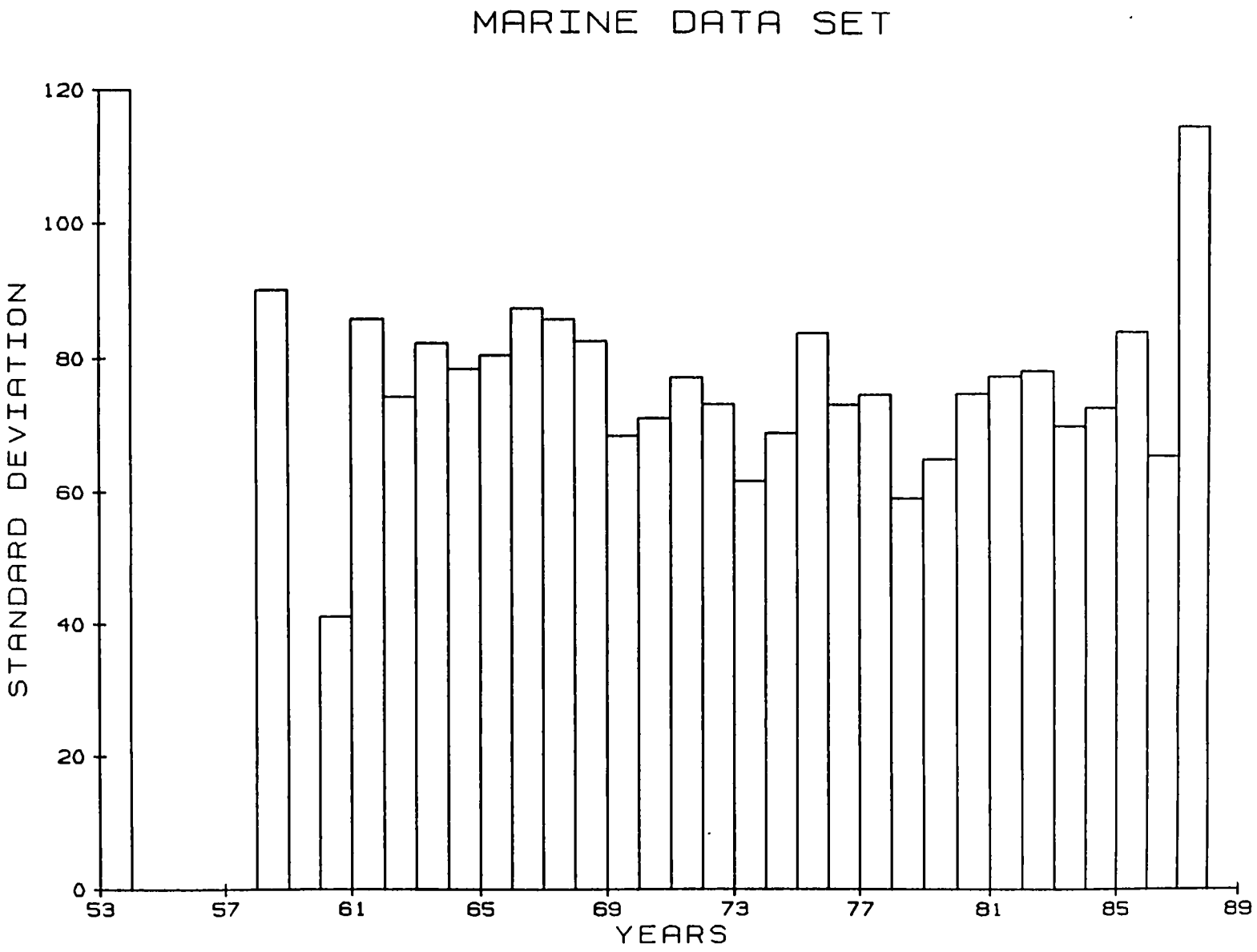

FIGURE 35. HISTOGRAM SHOWING THE STANDARD DEVIATION RELATIVE TO THE MEAN PER YEAR

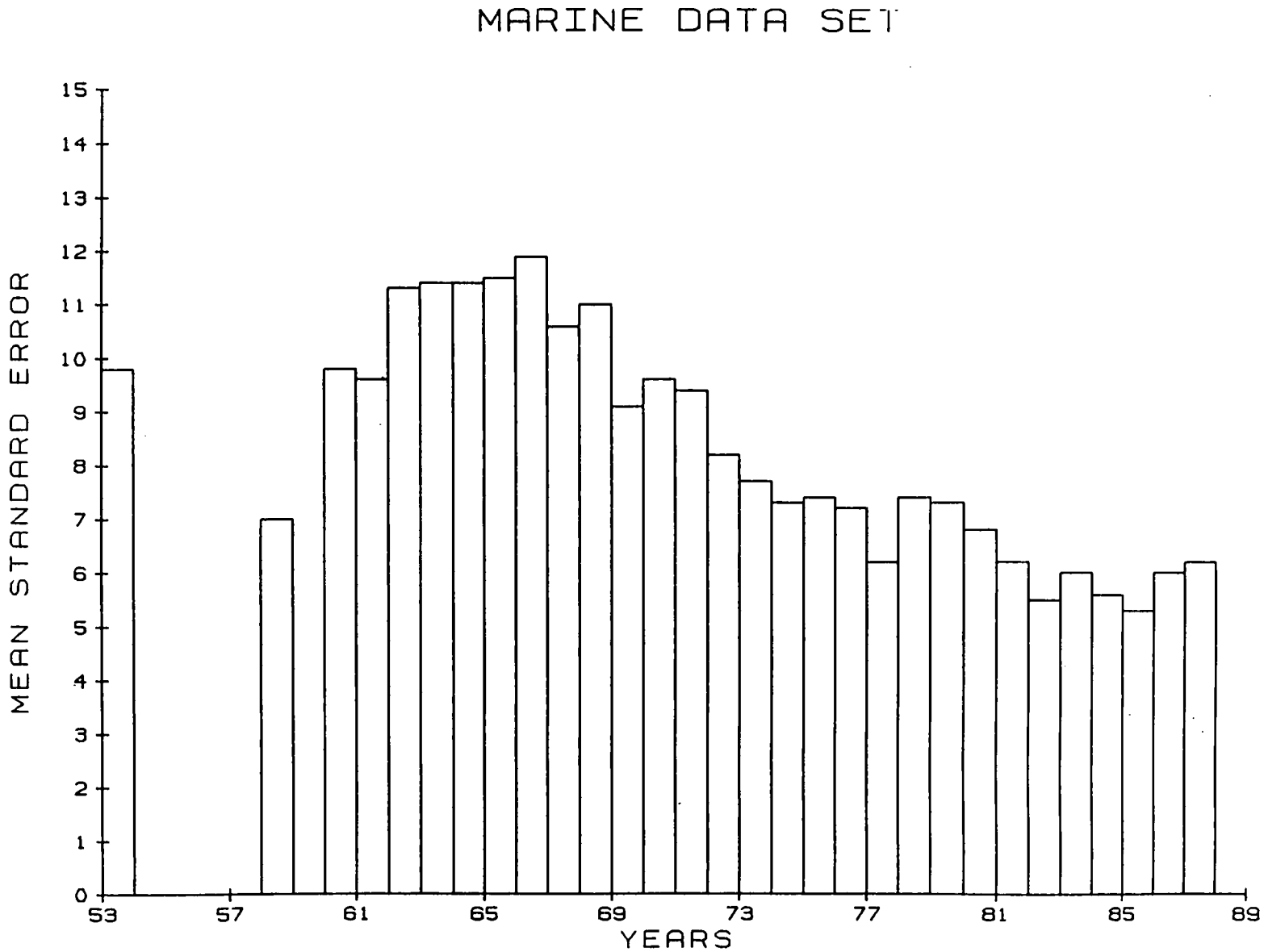

FIGURE 36. HISTOGRAM OF THE MEAN OF THE STANDARD ERROR COMPUTED FOR EACH YEAR

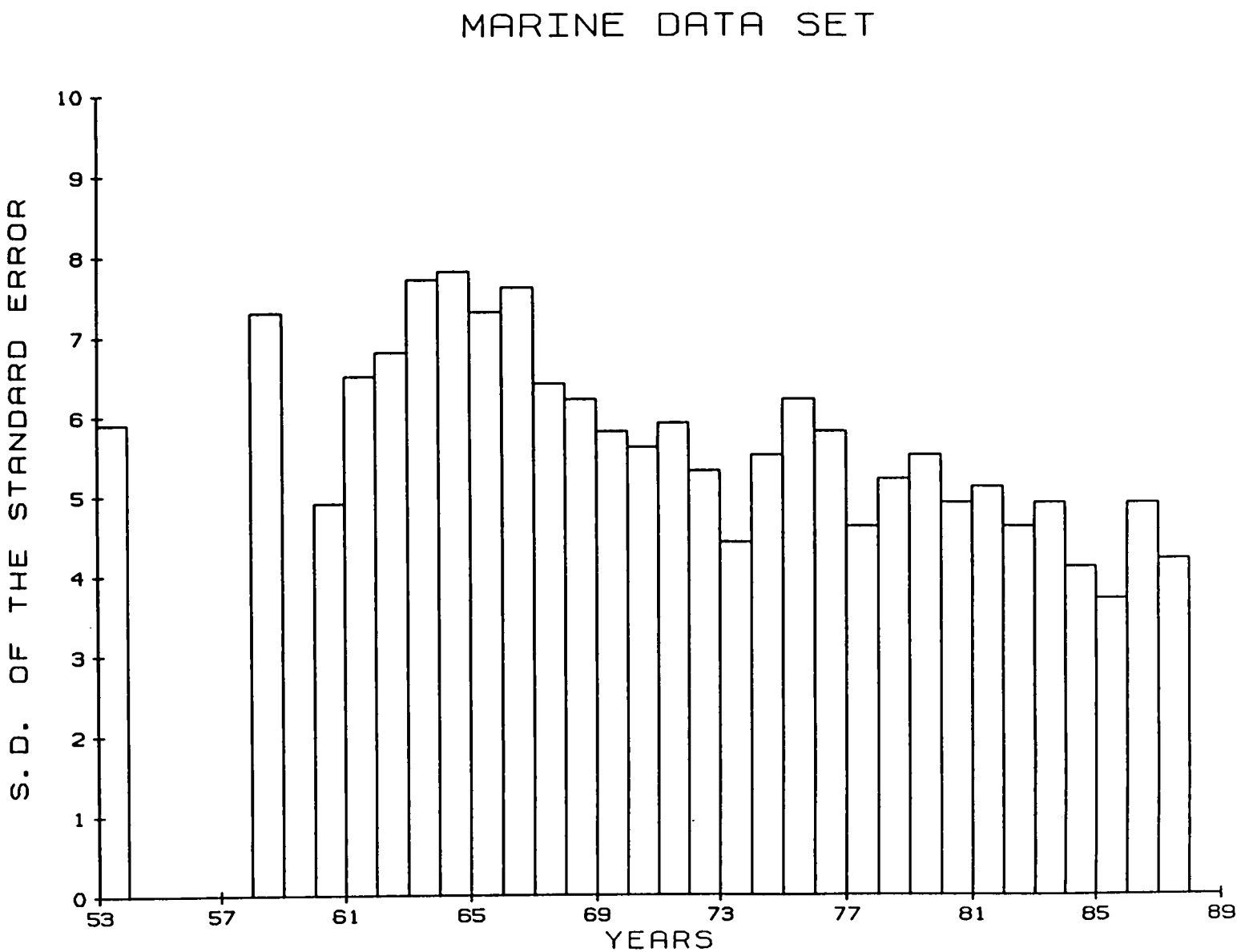

FIGURE 37. HISTOGRAM OF THE STANDARD DEVIATION OF THE STANDARD ERROR FOR EACH YEAR

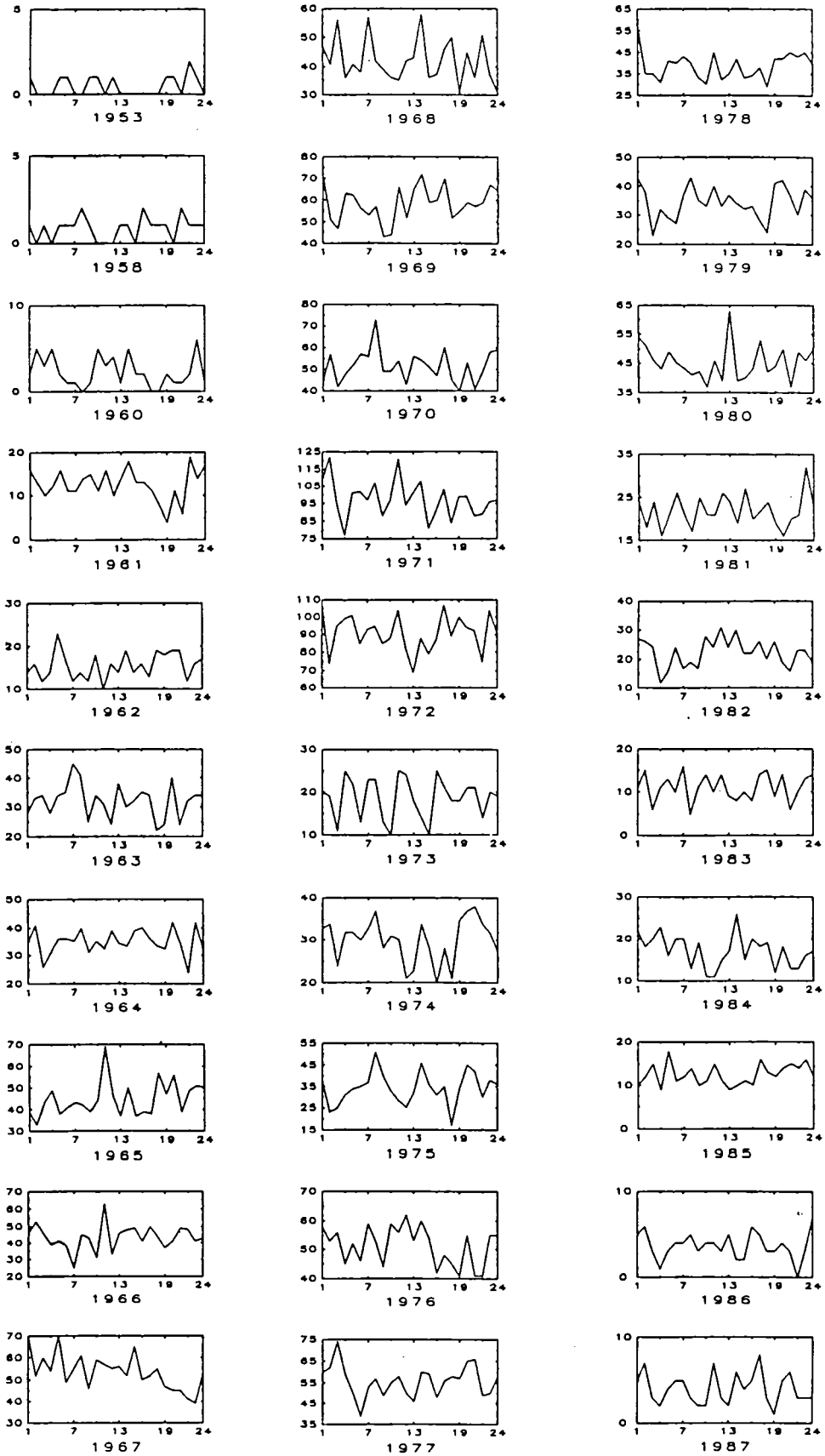

FIGURE 38. NUMBER OF AVERAGED VALUES OBSERVED PER LOCAL TIME FOR EACH YEAR

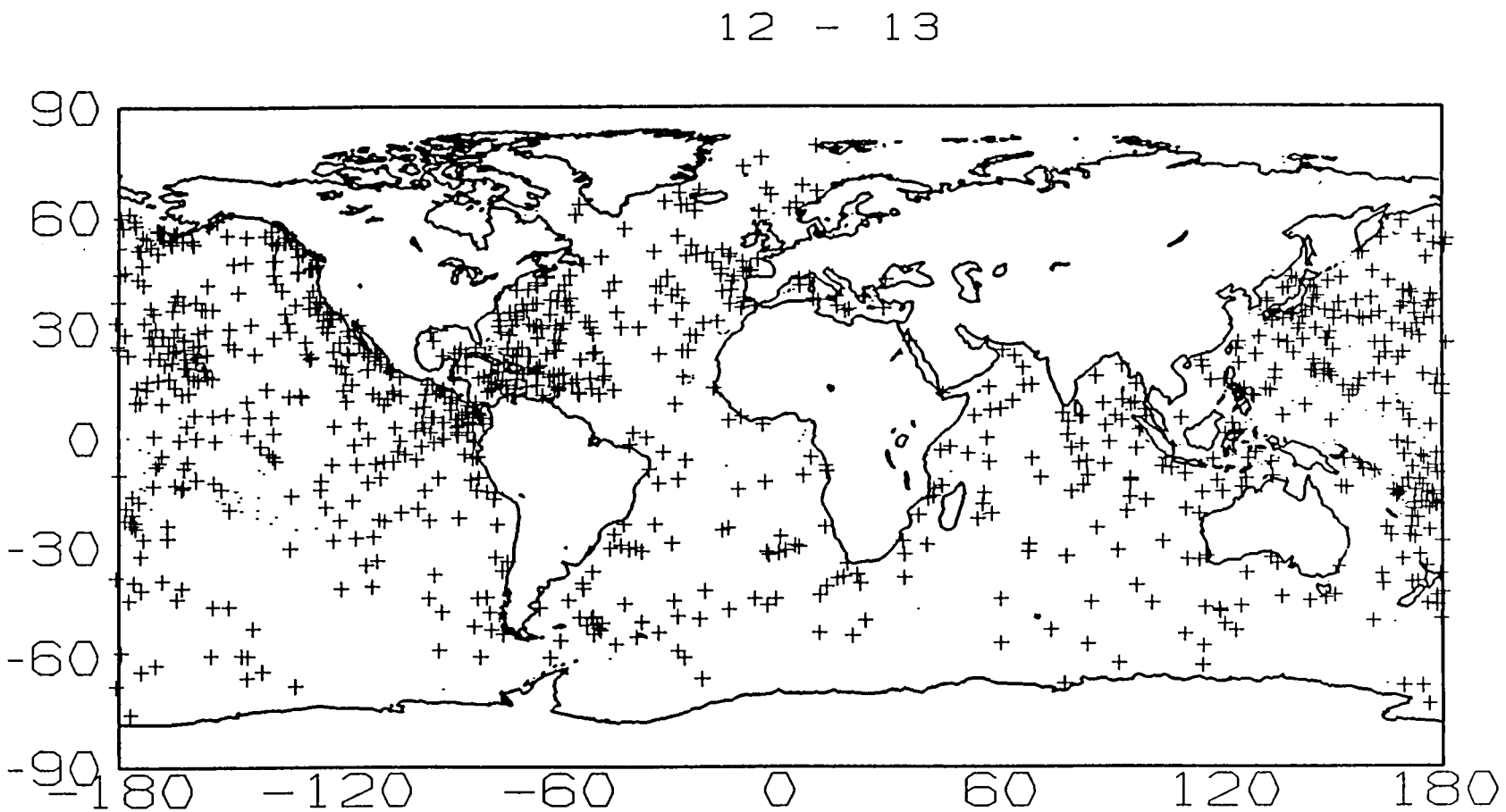

FIGURE 39. THE WORLD WIDE DATA DISTRIBUTION AT LOCAL NOON (12TH–13TH HOUR) FOR ALL YEARS

TABLE 1. INSTITUTIONS WHICH HAVE CONTRIBUTED TO THE MARINE DATA SET AT NGDC

Marine Magnetics Data Summary

Institution	Cruises	Nautical Miles of Shiptrack	Digital Records
Australian Bureau of Mineral Resources	5	44580.0	272922
Canadian Geological Survey	6	28783.0	162503
Institut Francais de Recherche pour l'Exploitation de la Mer (IFREMER)	23	268528.0	1363508
Deutsches Hydrographisches Institut	1	1669.0	10853
Hawaii Institute of Geophysics	93	320862.0	1104720
Japan Oceanographic Data Center	111	484578.0	403220
Lamont-Doherty Geological Observatory	471	1901733.0	2869940
Royal New Zealand Navy	40	56160.0	209950
NOAA National Ocean Service	78	557494.0	529654
Oregon State University, Department of Geology (CONMAR)	46	126523.0	195344
Institut Francais de Recherche Scientific pur le Development en Cooperation Laboratoire de Geophysique (ORSTOM)	14	37835.0	51035
Scripps Institution of Oceanography	430	1392836.0	2118505
Republic of South Africa, National Hydrographic Office	16	44950.0	54407
Ocean Drilling Program, Texas A&M University	10	15009.0	52604
University of Rhode Island, Graduate School of Oceanography	2	7164.0	9594
United Kingdom, Marine Information and Advisory Service (MIAS)	34	87145.0	308496
University of Texas, Institute for Geophysics	19	41710.0	75470
United States Geological Survey	105	160384.0	1007146
U. S. Navy, Naval Ocean Research and Development Activity and the Naval Research Lab	109	372439.0	1508146
Woods Hole Oceanographic Institute	102	362782.0	594546
Totals	1815	6313164.0	12902563

TABLE 2. THE GEOMAGNETIC FIELD MODELS USED AND THE TIME INTERVALS WHERE THE SECULAR VARIATION TERMS WERE APPLICABLE FOR EACH YEAR OF THE MARINE DATA SET

Model	Time
DGRF 1950	1950 - 1955
DGRF 1955	1955 - 1960
DGRF 1960	1960 - 1965
DGRF 1965	1965 - 1970
DGRF 1970	1970 - 1975
DGRF 1975	1975 - 1980
DGRF 1980	1980 - 1985
IGRF 1985	1985 -

TABLE 3. SUMMARY OF PROCESSING STATISTICS CALCULATED FOR CRUISE CRCS01SB

MGG Cruise Id= 15060039 Processing complete.
3313 Measurements in cruise

DATA SUMMARY: CRUISE MEAN= 18.2 STANDARD DEVIATION=117.47 BAD PTS= 0 TOTAL POINTS= 3313

SECTION	START(KM)	END(KM)	PTS	AV. DIST	MEAN TF	MEAN DF	SIGMA	KP MEAN	GAP	COMMENTS
1- 105	0.	221.9	104	111.0	46333.8	-28.1	7.21	1.0		GOOD POINT
2- 206	224.1	444.3	101	333.6	45301.6	33.7	5.75	2.3		GOOD POINT
3- 306	446.5	667.2	100	556.4	44231.9	31.0	5.98	0.9		GOOD POINT
4- 412	669.4	891.3	106	783.1	43173.5	68.0	8.46	0.3		GOOD POINT
5- 503	893.6	1114.7							22.8	INTERIOR GAP
5- 503									22.8	GAP .LT. 20 KM. PROCESS
5- 503	893.6	1114.7	91	1007.6	41984.9	67.9	11.17	0.5		GOOD POINT
6- 617	1116.5	1337.3	114	1222.4	41025.3	32.0	6.95	1.3		GOOD POINT
7- 734	1339.4	1560.9	117	1463.3	39946.2	56.0	9.98	0.8		GOOD POINT
8- 867	1562.7	1784.0	133	1684.7	38974.8	39.4	4.46	1.1		GOOD POINT
9- 990	1786.2	2006.2	123	1893.8	38161.8	96.0	2.98	1.4		GOOD POINT
10-1105	2008.2	2229.2	115	2118.6	37578.8	76.4	7.64	0.4		GOOD POINT
11-1251	2231.2	2451.5	146	2356.4	37098.5	20.4	4.24	0.5		GOOD POINT
12-1412	2452.9	2673.4	161	2577.2	37145.6	34.8	9.04	1.7		GOOD POINT
13-1554	2674.6	2895.6						2.6		KP TOO HIGH
14-1699	2896.6	3117.9						2.7		KP TOO HIGH
15-1886	3119.6	3340.7	187	3231.5	34178.6	-1.6	6.01	2.0		GOOD POINT
16-2036	3342.0	3562.1	150	3446.4	34530.2	-10.6	3.61	1.5		GOOD POINT
17-2164	3563.6	3784.8	128	3668.3	34841.4	48.7	6.46	1.8		GOOD POINT
18-2277	3786.6	4007.1	113	3885.7	34872.1	-57.0	17.25	1.2		GOOD POINT
19-2383	4009.3	4230.2	106	4097.6	34681.0	52.9	22.39	0.9		GOOD POINT
20-2507	4232.1	4452.7	124	4331.1	34927.0	28.9	16.62	0.8		GOOD POINT
21-2617	4454.7	4675.4	110	4538.5	34487.1	-119.1	18.63	1.0		GOOD POINT
22-2699	4677.5	4898.2							42.6	INTERIOR GAP
22-2699									42.6	GAP .LT. 20 KM. PROCESS
22-2699	4677.5	4898.2	82	4793.7	34890.5	111.2	17.16	1.5		GOOD POINT
23-2798	4900.4	5122.4	99	5010.8	34837.3	-87.2	14.29	1.3		GOOD POINT
24-2882	5124.7	5361.8							37.3	MORE THAN ONE GAP
25-2998	5362.3	5583.9						4.3		KP TOO HIGH
26-3100	5586.2	5806.3						4.2		KP TOO HIGH
27-3222	5807.7	6027.7						3.3		KP TOO HIGH
28-3222										
28-3222								3.0		KP TOO HIGH. NEXT CRUISE

TABLE 4. STATISTICS COMPUTED BY YEAR OF THE NUMBER OF AVERAGED POINTS, THE MEAN DEVIATION, THE STANDARD DEVIATION RELATIVE TO THE MEAN, THE MEAN OF THE STANDARD ERRORS, AND THE STANDARD DEVIATION OF THE STANDARD ERRORS

Year	Number of points	Mean	S.D. of the mean	Mean of the standard error	S.D. of the standard error
1953	11	-70.0	120.0	9.8	5.9
1958	20	32.9	90.1	7.0	7.3
1960	55	41.1	41.1	9.8	4.9
1961	314	-11.8	85.9	9.6	6.5
1962	388	-15.5	74.3	11.3	6.8
1963	789	57.2	82.3	11.4	7.7
1964	856	-22.8	78.4	11.4	7.8
1965	1098	-21.8	80.5	11.5	7.3
1966	1068	-63.6	87.5	11.9	7.6
1967	1323	-21.2	85.9	10.6	6.4
1968	1045	45.4	82.6	11.0	6.2
1969	1442	5.1	68.4	9.1	5.8
1970	1265	-19.3	71.1	9.6	5.6
1971	2422	-26.5	77.2	9.4	5.9
1972	2244	-22.1	73.2	8.2	5.3
1973	461	7.0	61.7	7.7	4.4
1974	746	-17.7	68.9	7.3	5.5
1975	849	-25.6	83.9	7.4	6.2
1976	1277	-18.4	73.2	7.2	5.8
1977	1375	-29.0	74.7	6.2	4.6
1978	952	-30.6	59.0	7.4	5.2
1979	846	6.9	65.0	7.3	5.5
1980	1110	-24.0	74.8	6.8	4.9
1981	544	-21.2	77.4	6.2	5.1
1982	550	-10.9	78.1	5.5	4.6
1983	275	-17.6	69.9	6.0	4.9
1984	442	-23.0	72.7	5.6	4.1
1985	307	-36.1	84.1	5.3	3.7
1986	90	-22.5	65.6	6.0	4.9
1987	99	34.9	114.8	6.2	4.2

TABLE 5. NUMBER OF AVERAGED OBSERVATIONS AT LOCAL TIME FOR EACH YEAR AND THE TOTAL NUMBER OF LOCAL TIME OBSERVATIONS

YEAR	LOCAL TIME																							
	1	2	3	4	5	6	7	8	9	10	11	12	13	14	15	16	17	18	19	20	21	22	23	24
1953	1	0	1	0	1	1	0	0	1	1	0	1	0	0	0	0	0	0	1	1	0	2	1	0
1958	1	0	2	0	1	1	1	2	1	0	0	0	1	1	0	2	1	1	1	0	2	1	1	1
1960	2	5	3	5	2	1	1	0	1	5	3	4	1	5	2	2	0	0	2	1	1	2	6	1
1961	16	13	11	12	16	11	11	14	19	11	16	11	14	18	16	13	11	9	4	11	7	19	14	17
1962	14	16	14	14	23	20	12	14	12	18	10	17	14	19	17	16	13	21	18	19	22	12	16	17
1963	28	33	37	28	34	36	45	41	26	34	31	26	38	30	36	35	34	26	24	40	27	32	34	34
1964	35	41	28	31	36	37	35	40	37	35	32	42	34	33	42	40	36	33	32	42	37	24	42	32
1965	39	33	48	49	38	43	43	42	42	44	69	49	37	50	40	39	38	60	47	56	42	49	51	50
1966	46	53	50	39	41	40	25	45	47	31	63	37	46	48	50	41	50	54	37	41	52	48	41	43
1967	70	52	65	54	70	56	55	61	49	59	57	65	56	52	69	50	52	58	47	45	48	41	39	53
1968	47	41	60	36	41	42	57	42	43	36	35	49	43	58	38	37	46	57	31	45	42	51	37	31
1969	71	51	49	63	62	57	53	57	55	44	66	59	65	72	61	60	70	62	55	59	61	59	67	64
1970	45	57	46	48	52	59	56	73	56	49	54	47	56	54	53	47	60	48	40	53	46	49	58	59
1971	109	122	101	77	101	114	97	107	107	97	121	109	101	108	86	91	103	93	99	99	98	89	96	97
1972	106	74	101	99	101	93	93	95	90	88	104	93	69	88	92	87	107	99	100	94	101	75	104	91
1973	20	19	15	25	22	14	23	23	17	10	25	25	18	14	11	25	21	18	18	21	24	14	20	19
1974	33	34	28	32	32	31	33	37	30	31	30	26	23	34	32	20	28	25	35	37	42	34	32	27
1975	38	23	27	31	34	39	37	51	42	33	28	30	32	46	41	31	35	22	34	45	46	30	38	36
1976	58	53	61	45	52	50	59	53	50	59	56	71	53	60	59	42	48	53	41	55	48	41	55	55
1977	60	62	80	59	50	44	53	57	54	55	58	56	46	60	62	48	56	65	57	65	71	49	50	58
1978	57	35	39	31	41	43	43	40	37	30	45	35	35	42	35	34	38	31	42	42	49	43	45	40
1979	43	38	26	32	29	31	37	43	40	33	40	34	37	34	34	33	28	27	41	42	39	30	39	36
1980	54	51	50	43	49	47	43	41	46	37	46	39	63	39	44	43	53	46	44	50	37	49	46	50
1981	24	18	26	16	21	29	21	17	26	21	21	30	24	19	32	20	22	25	19	16	21	21	32	23
1982	27	26	30	12	16	26	17	19	18	28	24	33	24	30	24	22	26	21	26	19	17	23	23	19
1983	11	15	6	11	13	11	16	5	14	14	10	16	9	8	11	8	14	15	9	14	8	10	13	14
1984	22	18	22	23	16	21	20	13	20	11	11	16	17	26	18	20	18	21	12	18	13	13	16	17
1985	10	12	16	9	18	12	12	14	10	11	15	12	9	10	11	10	16	14	12	14	18	14	16	12
1986	5	6	3	1	3	4	4	5	4	4	4	3	5	2	2	6	5	3	3	4	4	0	3	7
1987	5	7	3	2	4	5	5	3	2	2	7	4	2	6	4	5	8	4	1	5	6	3	3	3
TOTALS	1097	1008	1046	927	1019	1018	1007	1054	996	931	1081	1039	972	1066	1022	927	1037	1011	932	1053	1029	927	1038	1006

SECULAR VARIATION ACROSS THE OCEANS: A RETROSPECTIVE STUDY FROM 35 YEARS OF SHIPBOARD TOTAL FIELD MEASUREMENTS IN THE NE ATLANTIC

C. A. Williams[1], J. Verhoef[2], and R. Macnab[2]

[1]Bullard Laboratories, University of Cambridge, Cambridge, UK
[2]Atlantic Geoscience Centre, Geological Survey of Canada, Dartmouth, Canada

ABSTRACT

This is a pilot study to determine whether secular variation information can be retrieved from underway shipboard total field measurements with sufficient accuracy to complement geomagnetic data from land-based observatories. Applying various new techniques described in this report, we extracted values of the total field at 42,677 crossovers or ship track intersection points contained in data sets collected between 28°N and 50°N in the NE Atlantic, and extending temporally from 1955 to 1990. We used an edited subset of these total field values to derive the secular variation at 30,140 different locations in the study area, and compared the results with the DGRF secular variation over the study area, calculated at 5 year intervals. The derived and DGRF values agree well showing that indeed marine data can be a source for secular variations. However the analysis demonstrated that due to inherent noise in the marine data, only minor improvement on the DGRF values for the secular variation can be achieved.

Key words: *Secular variation, NE Atlantic, total field magnetic measurements, crossover*

INTRODUCTION

The study of the time variations of the geomagnetic field is of great importance to the understanding of the behaviour of the earth's core. The usual approach is to monitor the geomagnetic field at observatories and to apply a spherical harmonic analysis to these data in order to obtain main field models for different epochs (e.g. Barraclough, 1976). The best known example is the International Geomagnetic Reference Field (IAGA, 1988). Several studies have used more localized observatory data to obtain regional models for the geomagnetic fields (e.g. Haines [1985] used a spherical cap model to obtain the geomagnetic field over Canada).

Unfortunately, magnetic observatories are irregularly distributed: all are situated on continents or islands, so the distribution of data is biased towards land areas. More recently, satellite data have been providing coverage across the oceans, but these measurements cannot yet enhance our knowledge of the secular variation over periods of several decades. Moreover, these measurements have inherent problems in correlating with the crustal field at satellite altitudes (Bloxham & Jackson 1989).

Meanwhile there is a potential wealth of geomagnetic information available from numerous research ships whose track coverage over the years continues to accumulate. Marine data sets now reach back 30 - 35 years and this is becoming a useful time period in terms of secular variation. Therefore, it is appropriate to carry out a retrospective study of all available magnetic data in a specified region. The primary objective of this study was to determine whether secular variation information could be retrieved from underway shipborne total field measurements with sufficient accuracy to complement land-based observations in oceanic areas. We also wanted to see whether these data could provide better information on rates of secular variation across the oceans than currently provided by the DGRF. (By DGRF we imply the definitive fields for epochs 1955 to 1980 [IAGA Division I Working Group I, 1988] and the DGRF 1985 and IGRF 1990 adopted by IAGA Working Group 8 of Division V during IUGG Vienna 1991). Although similar studies have been performed before (e.g. Williams, 1967; Whitmarsh & Jones, 1969; Hall, 1979 and Verhoef & Scholten, 1983), the analyzed data sets were much smaller and the timespans shorter.

A significant problem with shipboard data is that measurements are made while the ship is moving, unlike observatory data which are collected at a fixed position. It is therefore necessary to separate the time variations of the magnetic field from the varying 'background' level. One solution is to use only pairs of observations that are situated at track crossover points, and which in theory should differ only by their time-varying components.

MATHEMATICAL FORMULATION OF THE PROBLEM

For the purposes of this study, a crossover point is defined as the location of the intersection between two straight segments of ships' tracks; each segment is bracketed by a pair of data points whose separation, by our definition, can be no more than 3 km. Associated with each crossover point is a pair of crossover observations located at the intersection, and derived by interpolation between the data points at the end of each track segment.

At latitude λ and longitude ϕ, an observation at sea level of the total intensity of the magnetic field at time t consists of three components:

$$F(\lambda,\phi,t) = C(\lambda,\phi,t) + g(\lambda,\phi) + e \qquad (1)$$

where: $C(\lambda,\phi,t)$ is the time dependent component which is believed to originate in the core and which varies smoothly with the spatial coordinates λ and ϕ; $g(\lambda,\phi)$ is the short wavelength 'geological' component originating in the crust with amplitude variations of several hundreds of nanotesla, and which can be considered independent of time over the interval spanned by our data base; e represents 'external' magnetic field variations and other non-coherent noise.

The secular variation is defined as the yearly variation of the function $C(\lambda,\phi,t)$. To determine it, we use the difference between two observations F_1 and F_2 at times t_1 and t_2, taken at locations that are a distance $d\lambda$ and $d\phi$ apart. If $d\lambda$ and $d\phi$ are small enough, we can eliminate the position-dependent 'geological' component $g(\lambda,\phi)$. In this study, we used observations at the intersection points of ship tracks and, therefore, took $d\lambda$ and $d\phi$ to be zero, within navigation inaccuracies. We have no information on the unknown component e in equation (1), so initially we assume that its effect is small and that it can be ignored at the crossover point. Thus we define the difference between a given pair of crossover observations as:

$$dF = F(\lambda,\phi,t_2) - F(\lambda,\phi,t_1) = C(\lambda,\phi,t_2) - C(\lambda,\phi,t_1) \qquad (2)$$

Next we assume that the time-dependent core component can be described by:

$$C(\lambda,\phi,t) = C_0(\lambda,\phi) + a(\lambda,\phi).t + b(\lambda,\phi).t^2 + h.o. \qquad (3)$$

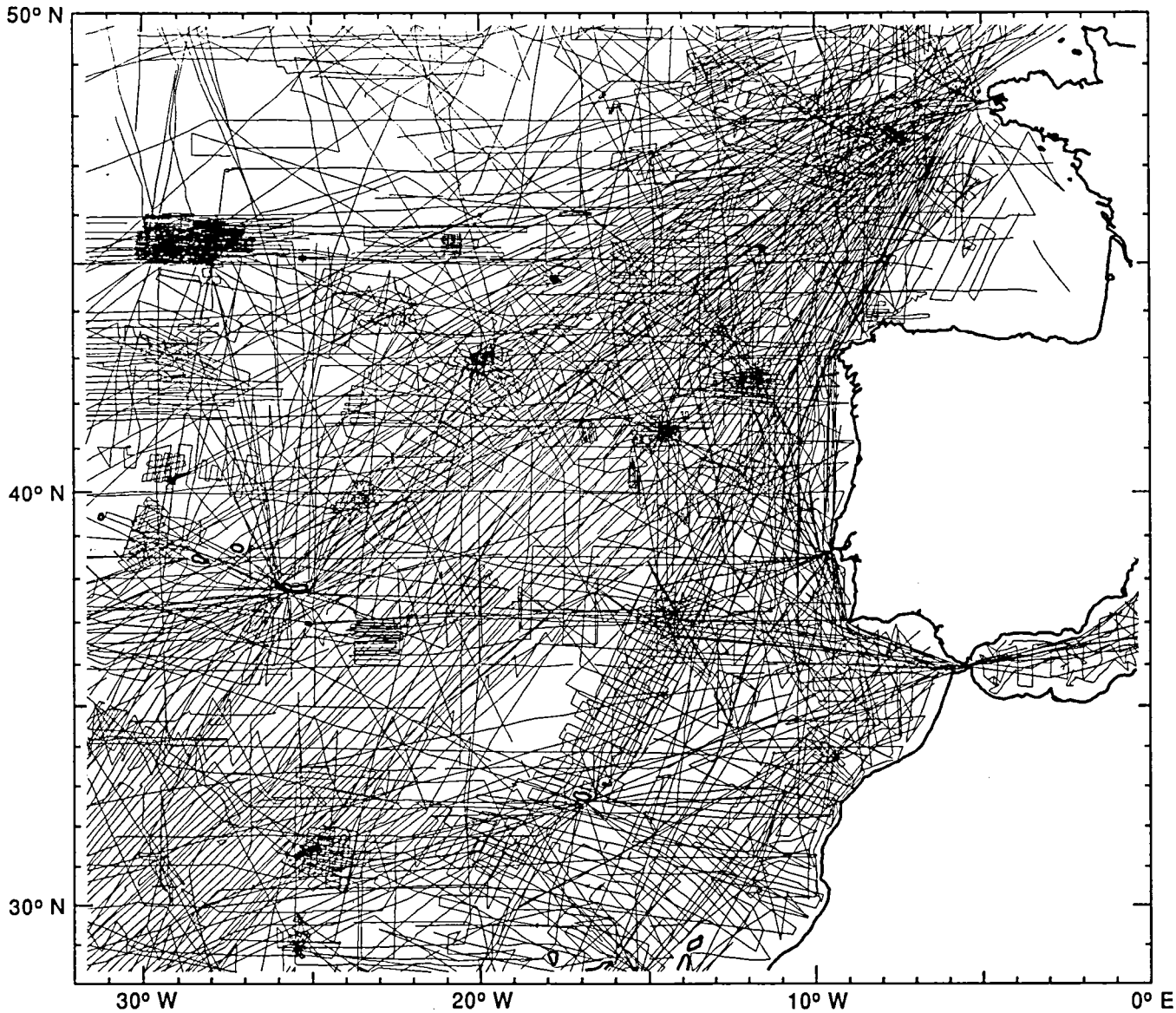

Fig. 1. Distribution of marine magnetic observations along ships' tracks during the period 1955.0 - 1989.9

where $C_0(\lambda,\phi)$, $a(\lambda,\phi)$ and $b(\lambda,\phi)$ are unknown functions of the position, and h.o. indicates that we may need higher order powers of the time t to accurately describe the time variation of the geomagnetic field. We took our time-origin to be in the middle of our data set, at 1970, i.e. t denotes the time in years with respect to 1970. Now equation (2) can be simplified to:

$$dF = a(\lambda,\phi).\ (t_2 - t_1) + b(\lambda,\phi).\ (t_2^2 - t_1^2) \qquad (4)$$

This equation contains the unknown functions $a(\lambda,\phi)$ and $b(\lambda,\phi)$. For any crossover point we know dF and $(t_2 - t_1)$; if we have two or more crossovers at a given location, we can solve equation (4) for the unknown functions a and b.

In practice, two or more crossovers rarely occupy the same point, but for those located near to each other, we can assume that the functions a and b are constant. Therefore we group crossovers according to their locations into a series of appropriately-sized bins covering the entire study area. For each bin, we use all cross overs inside that bin to obtain a least squares solution of equation (4) for the functions a and b. We used a standard error analysis also to obtain the standard deviations of the best fitting functions. The secular variation and its error bounds over the study area can then be calculated by inserting the values of a and b, and their standard deviations for each bin into the derivative of equation (3):

$$sv(t) = a(\lambda,\phi) + 2b(\lambda,\phi).t \qquad (5)$$

THE DATA BASE

For this investigation we used part of the large marine magnetic data base compiled at the Atlantic Geoscience Centre of the Geological Survey of Canada (Verhoef & Macnab, 1987; Macnab et al, 1990) containing data collected between 1956 and 1990. Such a data base is ideally suited to relatively short-term retrospective studies such as this. We have concentrated upon the region with the greatest density of ship tracks in an area of the Northeast Atlantic bounded by 28°N and 50°N, and 0° and 32°W. The data here show a good temporal and spatial track distribution (Figure 1), with just minor gaps in the NW corner and near 35°N, 19°W.

There are of course problems in using shipboard total magnetic field measurements: most are uncorrected for external field effects e.g. diurnal variation and magnetic storms, and also for surface effects such as the ship's orientation (Bullard & Mason, 1961). In addition there are navigation errors, especially in the data collected prior to the introduction of satellite navigation. The latter could be an important consideration in zones of high magnetic gradient, e.g. across lineated marine magnetic anomalies and magnetised topographic features (seamounts, etc.). We are very aware of these limitations upon our data and have gone to considerable efforts to

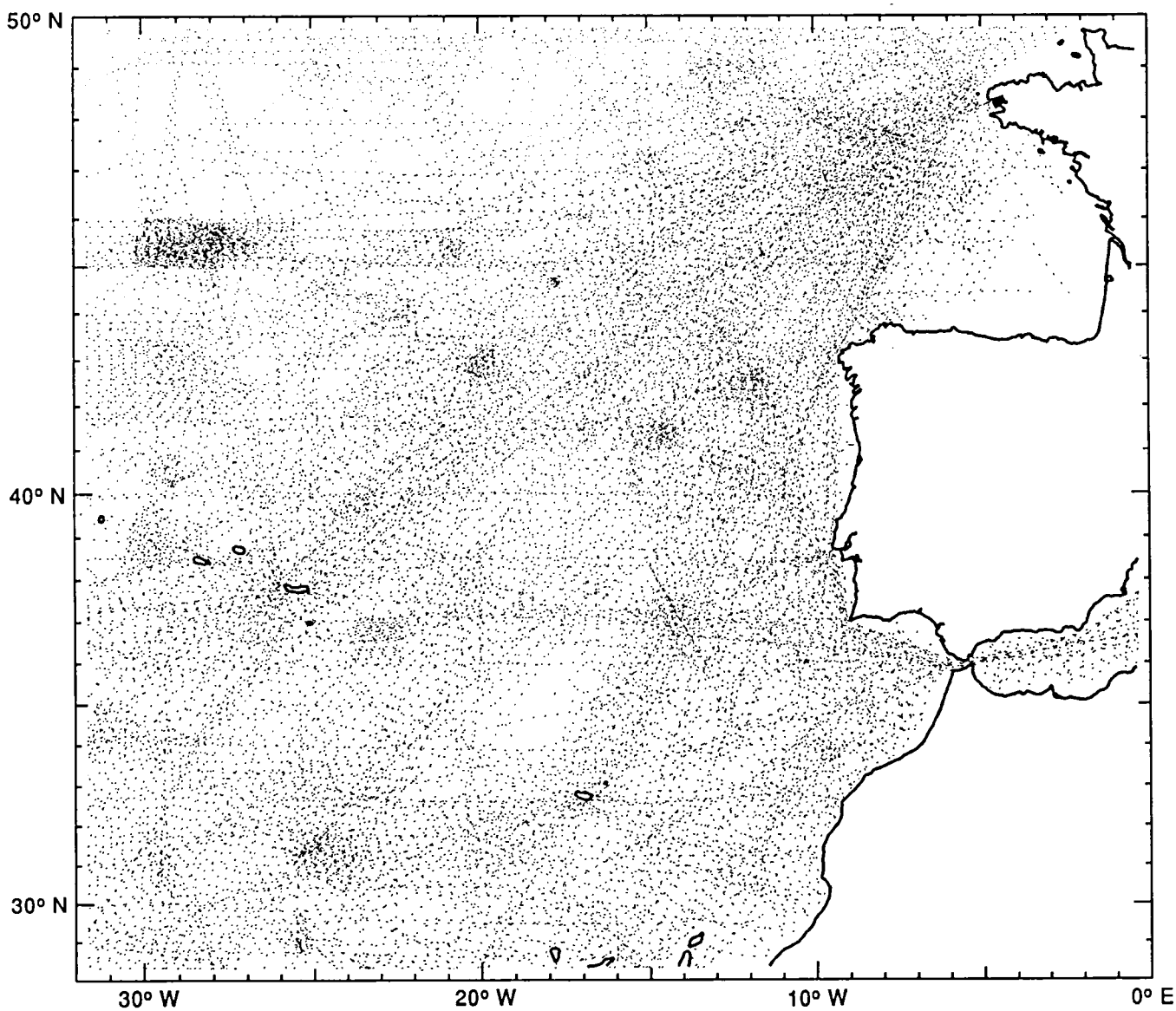

Fig. 2. Locations of track intersections (crossover points) in Figure 1.

minimise their effects upon our results.

PROCESSING CROSSOVER POINTS AND OBSERVATIONS

We used a procedure for extracting crossovers that had been applied in previous studies (Verhoef & Macnab, 1987; Verhoef et al, 1991). Time, position (lat & long) and total field value were retrieved for every observation in the data base and loaded into a table of track segments. The segments were then sorted by ascending longitude, and compared against each other to detect intersecting pairs. Where intersections occurred, times and total field values were interpolated at crossover points and stored in a second table; this table also contained crossover locations and local gradients calculated by using pairs of total field values on either side of the crossover observations.

We extracted 42,677 crossover points with the distribution shown in Figure 2. For a variety of reasons not all were equally reliable, so we reduced their number by various controlled processes of elimination based on the following criteria:

(1) Secular variation in the study area was not expected to exceed ± 80nT per year (see Figure 3). 464 crossovers were eliminated because they differed by more than this amount.

(2) We had found previously that crossovers spanning an interval of 12 months or less were unreliable on account of noise levels that were too dominant relative to the short time interval. 7,460 crossovers were eliminated for this reason.

(3) It is difficult to locate accurately the crossover point between two tracks that intersect at an angle of less than 10°. 2,232 crossovers were eliminated for this reason.

(4) A small navigation error in a region of high magnetic gradient can produce a spurious indication of secular variation. After examining a contour map of the local gradients in the study area (Figure 4) we chose 50nT/km as the gradient cut off value, and eliminated 2,548 crossovers for this reason.

(5) At a later stage, bins with fewer than 10 points were discarded. This eliminated 35 points.

Taken altogether, these eliminations reduced the number of usable crossovers from 42,677 to 30,140. Figure 5 shows yearly totals of crossover observations; note that each crossover point is counted twice in this histogram as there are two observations per intersection.

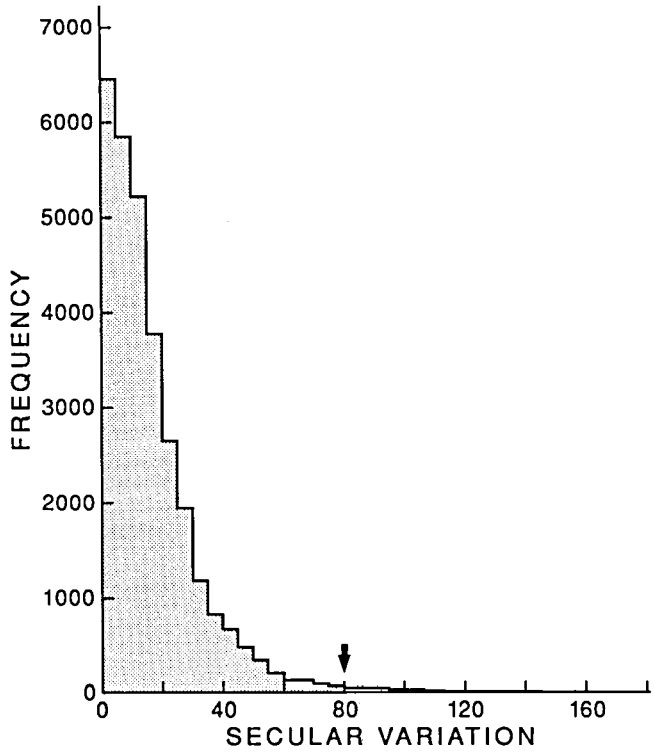

Fig. 3. Frequency distribution of the observed secular variations obtained at the crossover points shown in Fig. 1. 80 nT was used as a cutoff value for eliminating crossovers that indicated unrealistically high secular variations.

We grouped the usable crossovers into 2° x 2° bins covering the entire study area. We chose this bin size because it was the smallest we could use without setting too many bins to zero through lack of data; it was also considered to be reasonable for the deep source long wavelength information we were expecting to find. Bins containing fewer than ten crossovers were not used in subsequent manipulations.

Before fitting second order curves to the observations to solve for functions **a** and **b** in Equation (4), we tested the technique on a series of DGRF values calculated at three locations for each year between 1955 and 1990 (Figure 6). These values served as 'observations' through which we attempted to achieve the best fitting second order curve, using equation (4). In Figure 6, the curve representing the DGRF reference field is seen to contain some angular changes, resulting from the way the reference fields are defined: main field values every 5 years, with linear interpolation for the years in between. The degree of angularity varies across the study region, and our examples in Figure 6 have been specially chosen to demonstrate that a second order

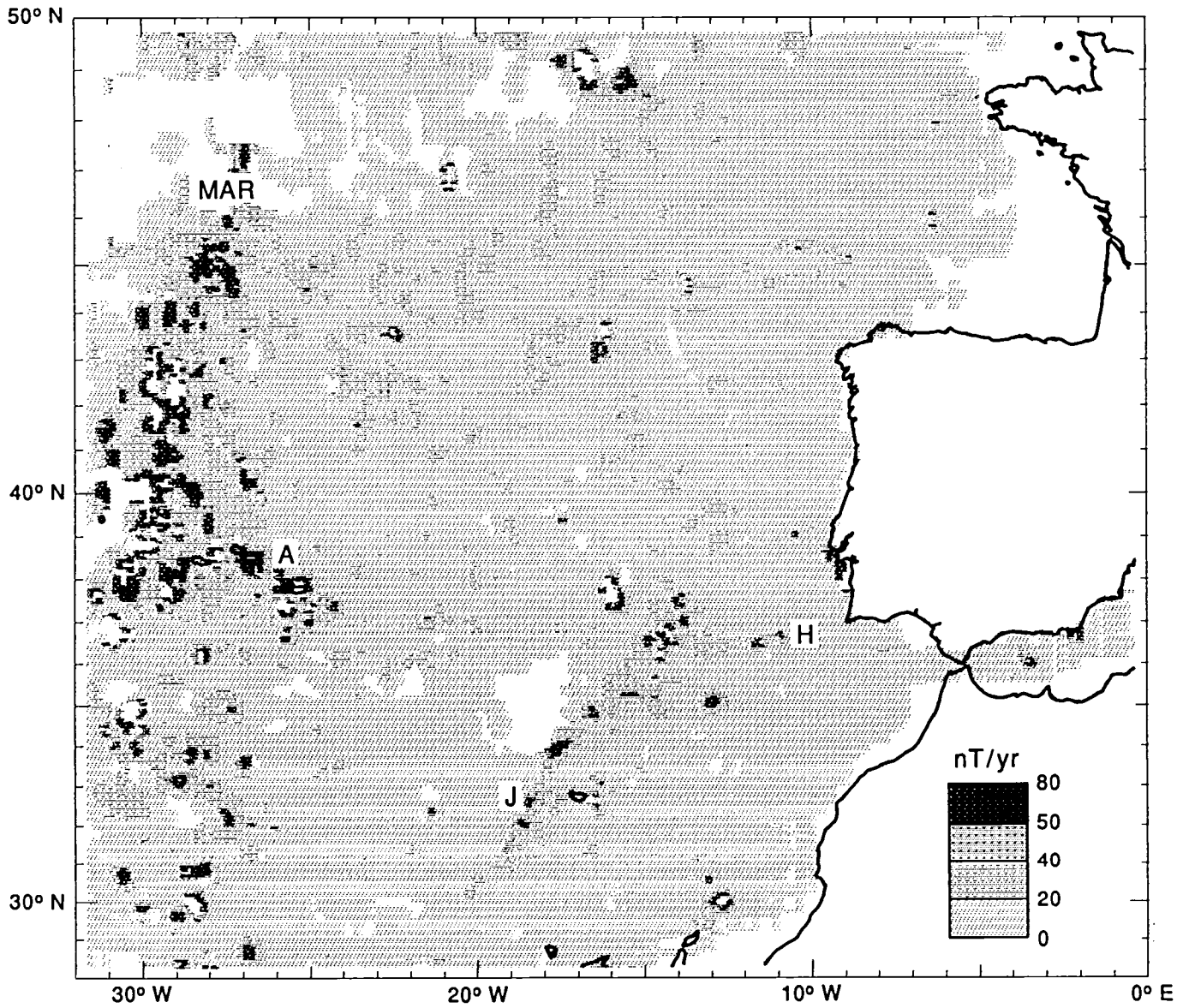

Fig. 4. Average local gradients at crossover points, in nT/km. The regions of highest gradient overlie the Mid-Atlantic Ridge (MAR) and the Azores Ridge (A), where shallow depth of source to the more highly magnetized fresh basalts cause higher amplitudes and gradients. Other regions of high gradient correlate with elevated seafloor topography such as the Horseshoe Seamounts (H), and the J-Anomaly Ridge (J).

polynomial can be fitted adequately through all types of curve. Third order polynomials are also shown in Figure 6, and at some locations the fit is significantly improved. However in view of the noise in our observations, we expected no significant improvement from a third order fit and concentrated on the second order curves. Further on, we will show some comparisons between 2nd and 3rd order fits through our observations.

By fitting second order curves to each group of binned observations, we solved for functions **a** and **b** in Equation (4) at a series of points corresponding to the centre of each bin. The variation of these functions over the study area was found to be much more irregular than expected from a field originating deep within the earth. Therefore we smoothed these functions by filtering them over 4° x 4°, in order to obtain functions for comparison with DGRF fields.

With the resulting values for functions **a** and **b**, we evaluated Equation (5) to determine the observed secular variation at the center of each bin and for all epochs between 1955 and 1990. We then calculated the differences between observed and corresponding DGRF

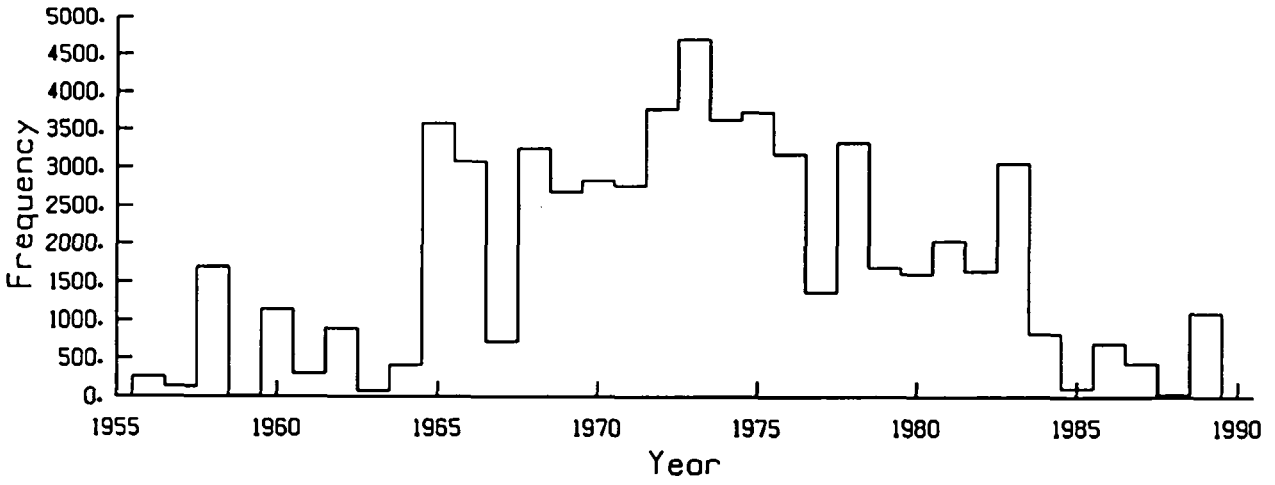

Fig. 5. Frequency of crossover observations per year (note that there are two observations per crossover point).

variations by subtracting the former from the latter.

ANALYSIS OF RESULTS

It was not practical to plot comparisons between derived and DGRF secular variations for each bin and for all epochs, as this would have involved the production and analysis of 1050 separate graphs. To illustrate a typical comparison, we show in Figure 7 the results that correspond to the bin centred at 34°N, 30°W: there is reasonable agreement between observed and DGRF variations, as evidenced by the close match between the second order curve and the DGRF curve.

In Figure 8 we compare rates of secular variation for the same bin by displaying the second order curve fitted to the observed values, bracketed by its one sigma error bounds. The results can be compared directly with the DGRF values and show that there is a reasonable agreement. Discontinuities in the 5-year DGRF secular variations are also evident in this figure, particularly prior to 1975: true secular variation more likely resembles the continuous curve of the observed variation.

Also shown in Figure 8 is the secular variation as obtained from fitting a third order curve through the observations. Since this secular variation curve lies within the one sigma error bounds of the second order curve, no significant improvement is expected from the fitting of a third order curve, and this was not pursued any further.

Combining the results for all bins, Figure 9 displays and compares derived and DGRF variations over the 5-year epochs between 1960.0 and 1989.9 (the epoch 1955-60 was omitted since it contained only 2093 data points, also, we did not expect the results to be of sufficient accuracy due to poor navigation). As shown in the first column, the best data coverage occurs between 1965 and 1980. The second column shows the distinct differences in the DGRF secular variation prior to 1975, in contrast to more gradual changes between later epochs. The third column illustrates the generally close agreement between the observed and DGRF variations. The fourth column, the difference with the DGRF, indicates maximum errors in 1960-65: this could be due to typically large positioning errors of the pre-satellite navigation era, as errors are in the 0 - 5 nT range during subsequent epochs by which time navigation systems were much improved.

With the passage of time, the contours of observed variation in the third column change from predominantly positive to predominantly negative. This conforms with the passage of a cell of negative flux moving in a northwesterly direction from the coast of NW Africa, and mapped from satellite and observatory data between 1948 and 1980 by Bloxham & Jackson (1986).

A TOTAL PERFORMANCE ANALYSIS

For reasons already mentioned, it was impractical to compare the derived and DGRF variations for each bin as was done in Figures 7 and 8. However it was clear that an overall comparison was necessary to evaluate the feasibility of extracting secular variation information from marine total field observations.

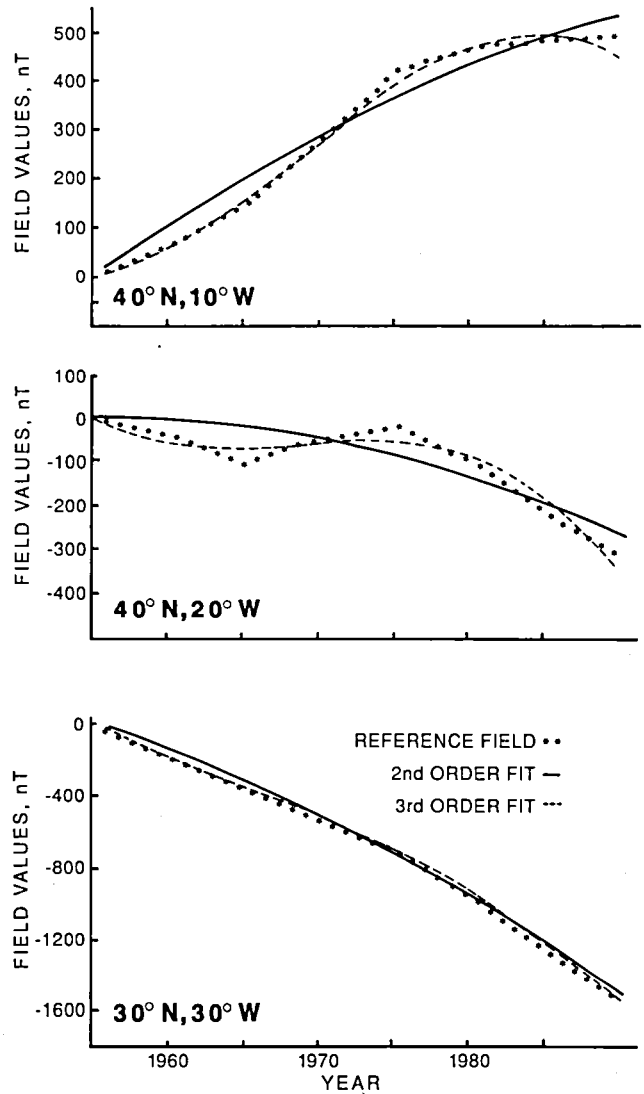

Fig. 6. Second and third order polynomial fits to the DGRF secular variation throughout the 35 year period of our study, at three different locations in the Northeast Atlantic. The different trends of the curves indicate that the rate of secular variation is not constant throughout the region.

We based this evaluation on an analysis of the errors represented by the function **e** in Equation (2). We began by correcting our observations at the intersection points for the main field values as obtained from our observed and DGRF fields. Since the 'geological' component at a crossover point cancels out, subtracting these corrected observations gives the uncorrelated error function **e** (see equation 1). We obtain for each crossover point two values for this function, one when using our observed main field and the other one after using the DGRF field. The average for all these errors is expected to be close to zero. We calculated and compared the root mean square of these errors at every crossover point. We repeated this process several times in succession, each time using a diminished data set where older crossover observations were progressively eliminated for a series of cut-off years beginning in 1955: new functions **a** and **b** were derived as previously described, and used to re-calculate reference fields and anomalies. In each cycle, DGRF anomalies were simply recalculated from observations dating after the cut-off year.

Figure 10 compares two pairs of root mean square errors for derived and DGRF reference fields, as functions of cut-off year. The upper pair was derived from an analysis of all data points; the lower pair from a reduced data set in which statistical outliers beyond 2 x sigma were eliminated. Figure 10 also shows the number of crossovers as a function of cut-off year, to indicate how many points were used in each calculation. Between 1955 and 1963, use of the DGRF secular variation resulted in rms errors that were lower by 5 to 10nT; between 1963 and 1974, the derived secular variation yielded lower errors, by about 5 nT. When the number of datapoints began to decrease substantially after 1976, the DGRF secular variation once again produced the smaller error. This confirms that marine total field observations can be used to derive reliable secular variation information, but that many data points are necessary to produce a statistical improvement over the DGRF secular variation.

CONCLUSIONS

(1) With the methods described in this study, it is feasible to extract secular variation information from underway marine total field measurements.

(2) The accuracy of the observed secular variation information is comparable to the DGRF variation in this particular study area, providing it is based upon a statistically substantial data base that can compensate for the inherent noise in the data. In other regions where the DGRF secular variation is not so well controlled, it may be feasible to use marine geomagnetic measurements to offset inadequacies in the theoretical model.

(3) Between 1960 and 1990, rates of secular variation in the study area have varied between -50 and +30 nT per year. This confirms the results of previous studies (Williams 1967, Verhoef & Scholten 1983), as well as rates calculated from the DGRF.

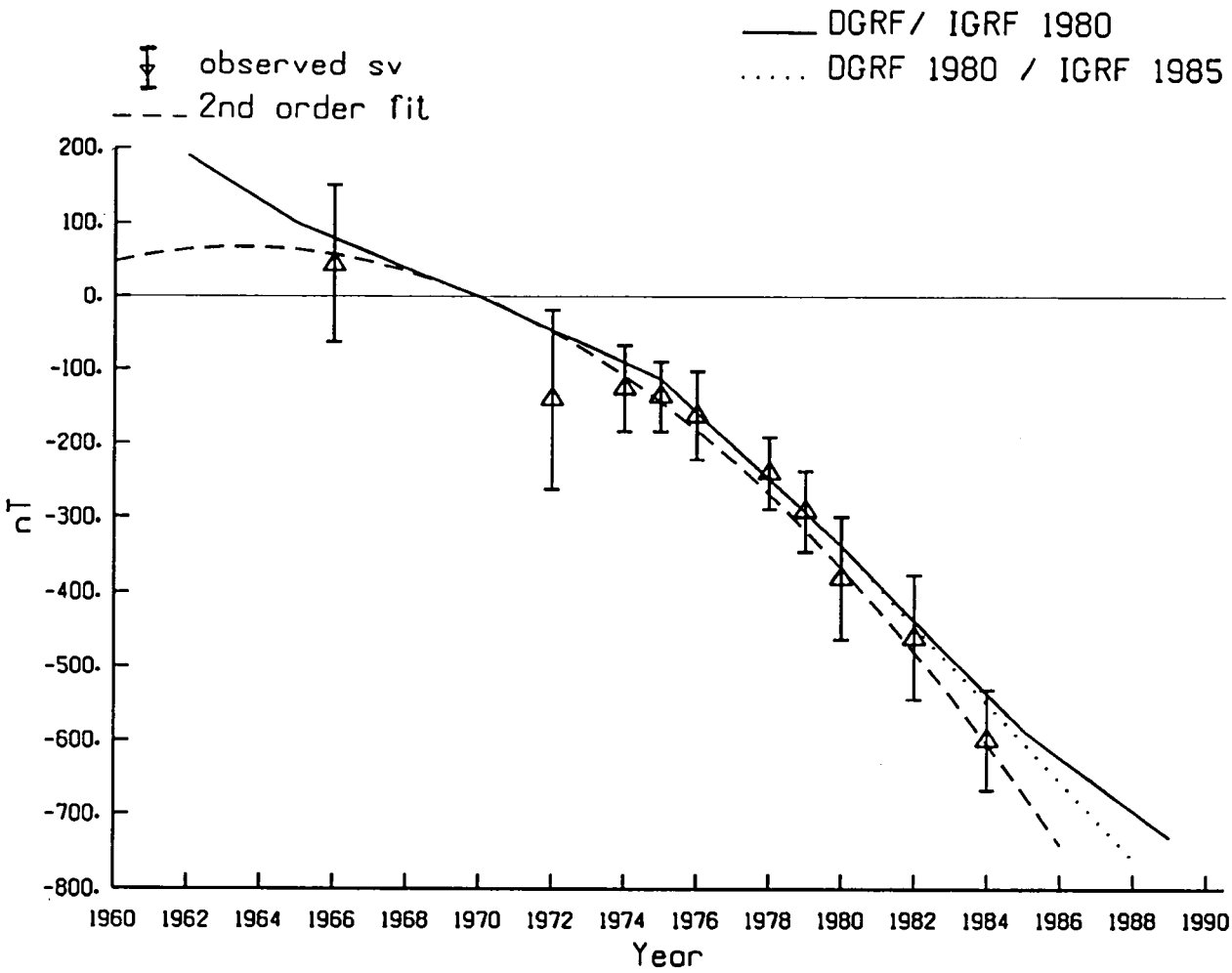

Fig. 7. A comparison between observed and DGRF secular variations for the 2° square centred at 34°N, 30°W. The second order fit is a good approximation to the observed secular variation values, so is the DGRF curve.

(4) The ability to extract secular variation information over fine time intervals suggests possibilities for studies involving phenomena with short time constants, such as the effect of sunspot cycles on secular variation.

(5) Secular variation in the study region has changed gradually from predominantly positive in 1957.5, to predominantly negative by 1987.5. This confirms the findings of Bloxham & Jackson (1989), who mapped the motion of a cell of negative core flux moving in a northwesterly direction across the NE Atlantic. By 1987.5 this negative cell had encroached upon half the study region.

(6) The effect of reduced data points during the late 1980's illustrates how important it is that ships continue to stream their magnetometers, even in areas that are apparently well covered by earlier magnetic measurements.

ACKNOWLEDGMENTS

We acknowledge all organizations who provided us with the data for our data base, either directly, or indirectly via the National Geophysical Data Center in Boulder, Colorado. CW is indebted to the Royal Society, who through their Maurice Hill Fund, made possible a study visit to the Atlantic Geoscience Centre. Art Cosgrove of the Technographics Section of the Bedford Institute of Oceanography arranged the production of final figures. In the UK this work was supported by the Natural Environment Research Council Grant No GR3/7704. This is Contribution No 2278 of the Department of Earth Sciences of the University of Cambridge.

BIBLIOGRAPHY

Bloxham, J. & Jackson, A., 1989 Simultaneous stochastic inversion for geomagnetic main field and secular variation. J. Geophys. Res. 94, 15,753-15,769.

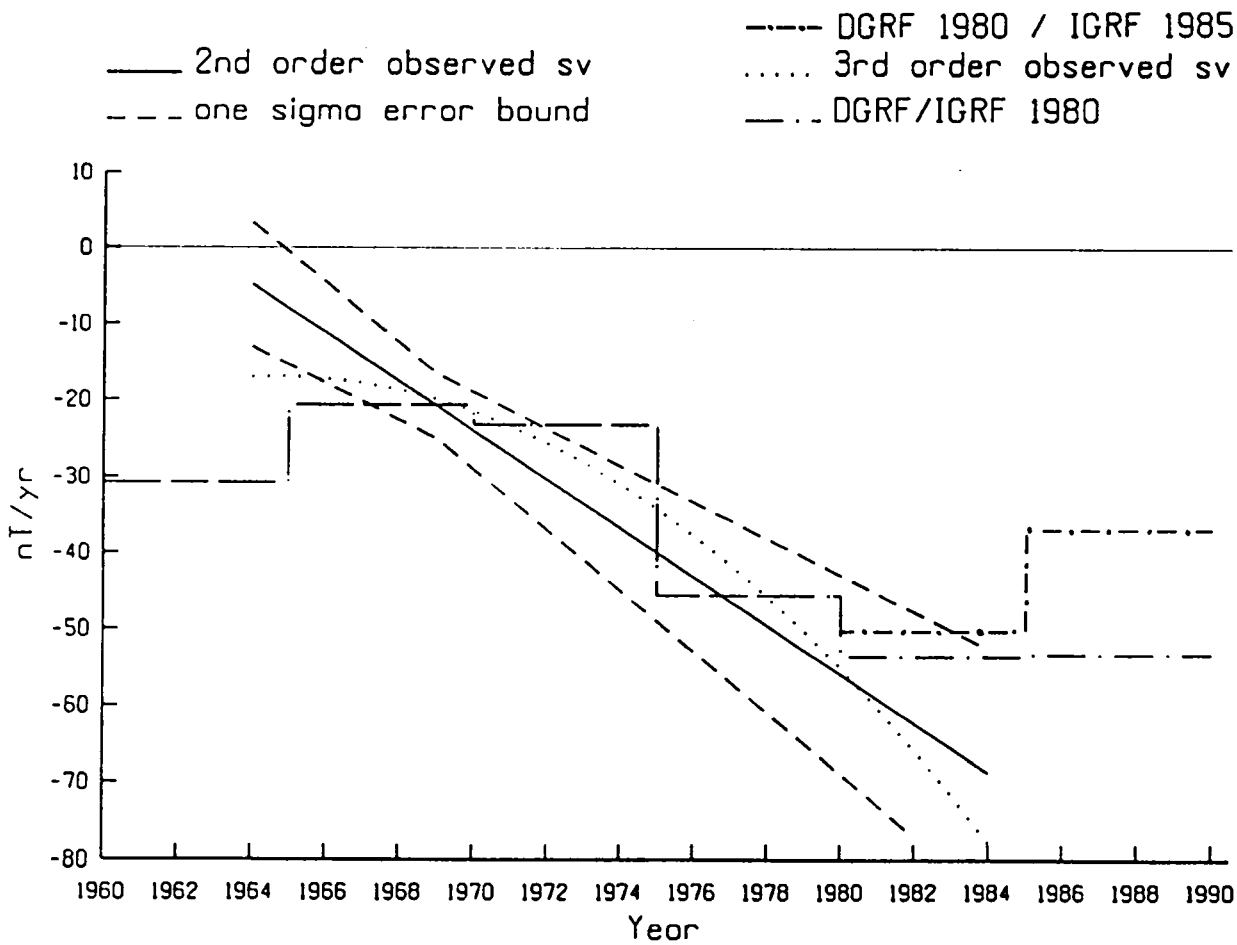

Fig. 8. Rates of observed secular variation compared to DGRF/IGRF 1980 and DGRF 1980/IGRF 1985 secular variations, for the 2° degree square centred at 34°N, 30°W. The dotted lines on either side of the second order curve are error limits based on one standard deviation of the second order polynomial when the reference year is 1970.0. The DGRF values lie within the bounds of the error limits, confirming that our results are comparable to the DGRF values but do not significantly improve the DGRF results. Also shown is the secular variation as obtained from the fit of a third order curve through our observations.

Barraclough, D.R., 1976 Spherical harmonic analysis of the geomagnetic secular variation - a review of methods. Phys. Earth Planet. Int. 12, 365-382, 1976.

Bullard, E.C. & Mason, R.G., 1961 The magnetic field astern of a ship. Deep Sea Res. 8,20-27.

Earth Physics Branch 1986 Integration of Atlantic Geoscience Centre Marine Gravity Data into the National Gravity Data Base. Geol. Surv. Can., Open file 1232 p.54.

Haines G.V., Spherical cap harmonic analysis. J. Geophys. Res. 90, 2583-2591, 1985.

Hall S.A. 1979 Geomagnetic secular variation and secular acceleration in the Red Sea Area. Geophys. J. R. Astr. Soc. 58, 583-592, 1979.

IAGA Division I Working Group I, 1988 IGRF revision 1987, Eos Trans. AGU, 69, 557.

Macnab, R., Verhoef, J. and Srivastava, S.P. 1990 A compilation of magnetic data from the Arctic and North Atlantic Oceans. in Current Research Part D, Geological Survey of Canada Paper 90-1D, p. 1-9.

Verhoef, J. & Scholten, R.D., 1983 Cross-over analysis of marine magnetic anomalies. Mar. Geophys. Res. 5, 421-435.

Verhoef, J., Collette, B.J., Danobeita, J.J., Roeser, H.A. & Roest, W.R. 1991 Magnetic anomalies off West-Africa (20-38 N). Mar. Geophys. Res. 13,81-103.

Verhoef, J. & Macnab, R., 1987 Magnetic data over the continental margin of eastern Canada: Preparation of a data base and construction of a 1:5 million magnetic anomaly map. Geological Survey of Canada Open File 1504

Whitmarsh, R.B. & Jones, M.T. 1969 Daily variation and secular variation of the geomagnetic field from shipboard observations in the Gulf of Aden. Geophys. J.R.Astr. Soc. 43, 555-572.

Williams, C.A ., 1967 Rates of secular variation in the N.E. Atlantic. Nature 5109,1468-1469.

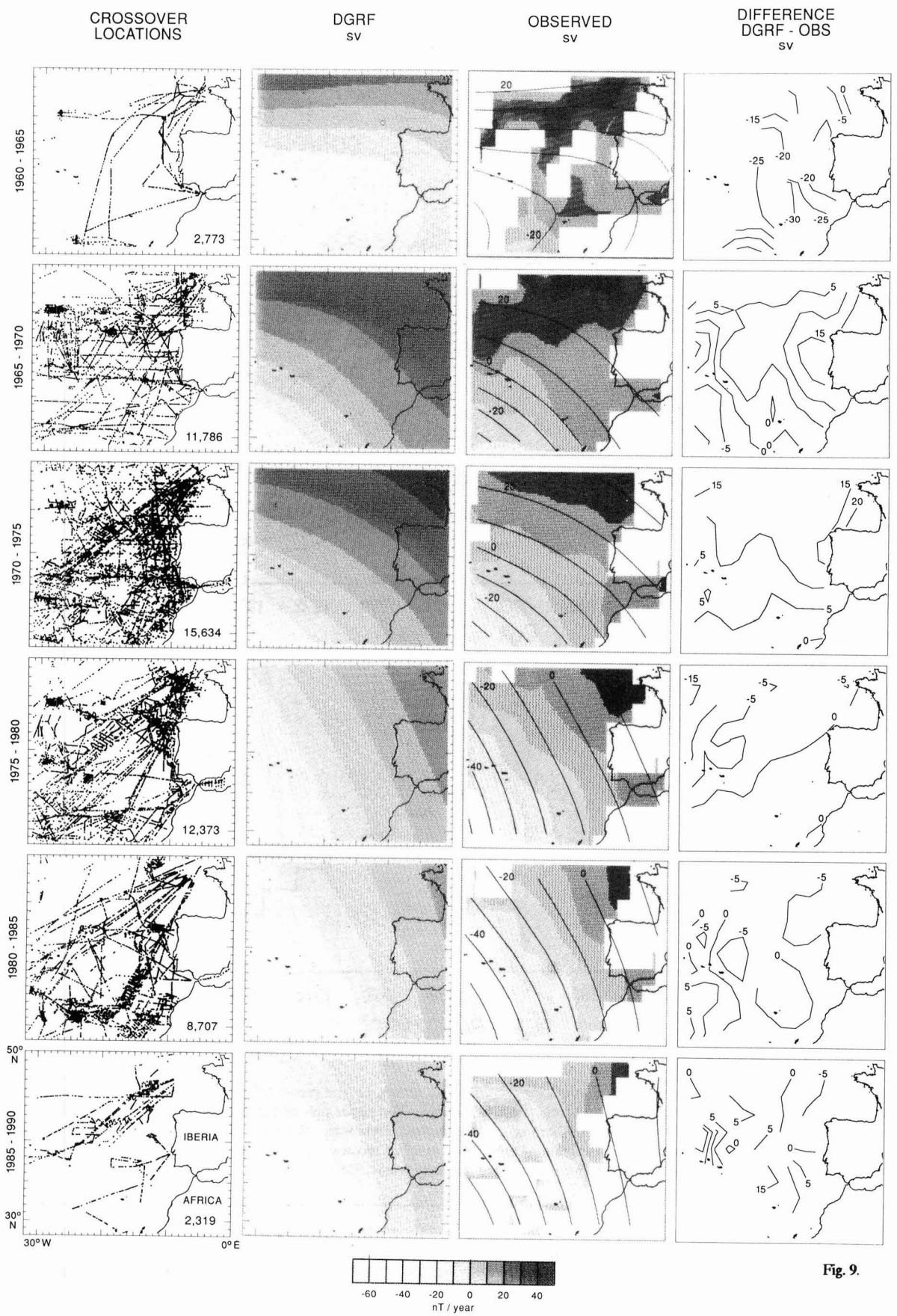
CROSSOVER LOCATIONS
DGRF sv
OBSERVED sv
DIFFERENCE DGRF - OBS sv
1960 - 1965
2,773
1965 - 1970
11,786
1970 - 1975
15,634
1975 - 1980
12,373
1980 - 1985
8,707
1985 - 1990
IBERIA
AFRICA
2,319
50° N
30° N
30° W
0° E
-60 -40 -20 0 20 40
nT / year

Fig. 9.

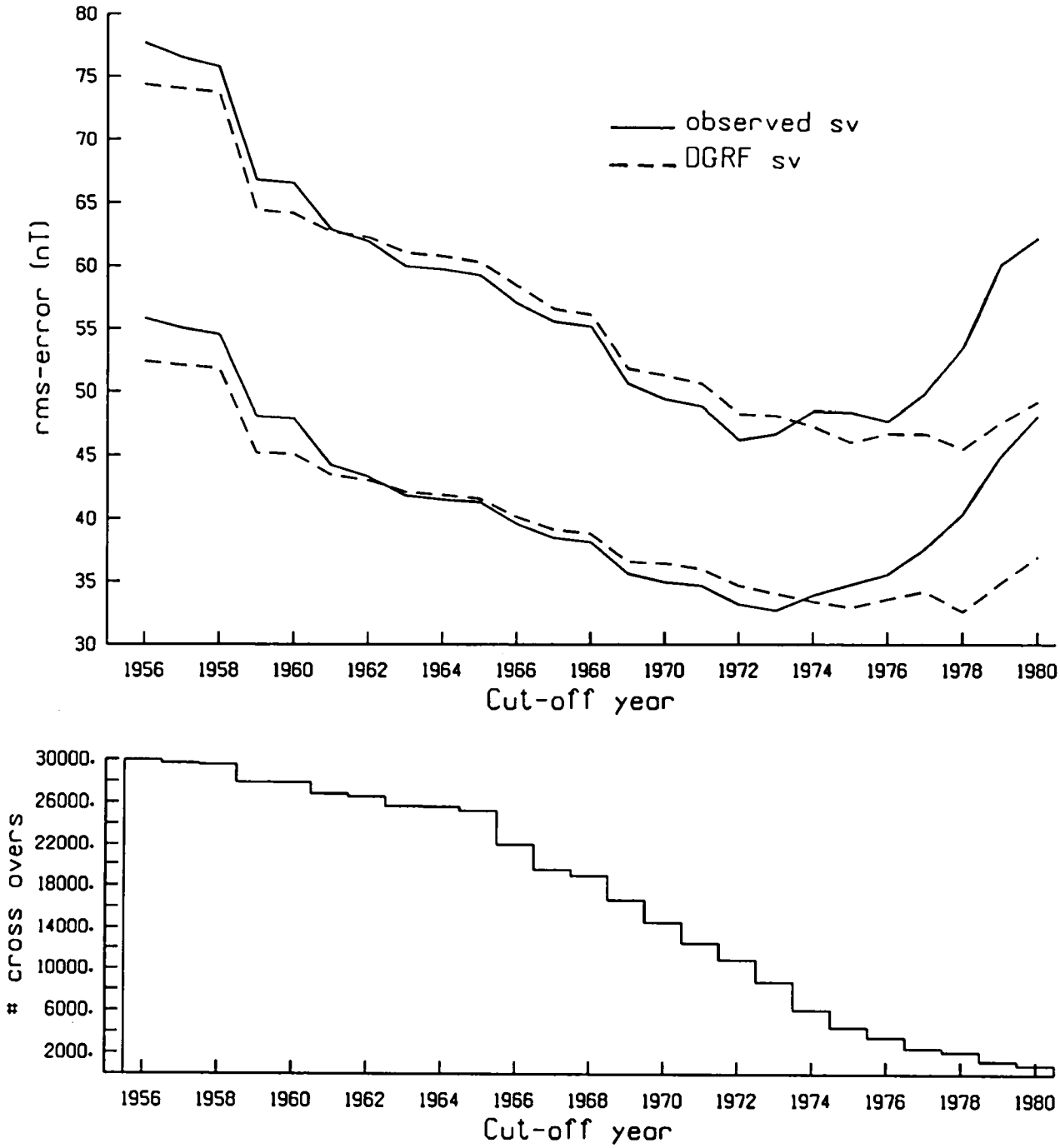

Fig. 10. Comparison of the root mean square errors of all data for the crossover errors, i.e. the errors left over after correcting the observations for the main field as obtained from our second order curve and from the DGRF field. The upper pair of curves shows rms errors for the total data set; the lower pair shows errors after elimination of statistical outliers beyond 2 standard deviations. Between 1962 and 1974, the observed data have a marginally smaller error than the DGRF. Beneath is a histogram of the total number of crossover points used in calculating the rms errors; data from previous years were progressively eliminated as rms errors were calculated annually from 1955 to 1980.

Fig. 9. Comparison of observed and DGRF secular variations, by five-year epoch. From left to right, the columns illustrate: 1) number and distribution of crossover points; 2) DGRF secular variation; 3) observed secular variation averaged to the mid-epoch (shaded) and overlain by the DGRF secular variation contours for comparison; 4) contours of the difference between observed and DGRF secular variations. The scale at the bottom defines values of the shading in the second and third columns.

PROJECT MAGNET HIGH-LEVEL VECTOR SURVEY DATA REDUCTION

Rachel J. Coleman
U.S. Naval Oceanographic Office
Geopotential Division
Stennis Space Center, MS 39522-5001

ABSTRACT

Since 1951, the U.S. Navy, under its Project MAGNET program, has been continuously collecting vector aeromagnetic survey data to support the U.S. Defense Mapping Agency's world magnetic modeling and charting program. During this forty-year period, a variety of survey platforms and instrumentation configurations have been used. The current Project MAGNET survey platform is a Navy Orion RP-3D aircraft which has been specially modified and specially equipped with a redundant suite of navigational positioning, attitude, and magnetic sensors. A review of the survey data collection procedures and calibration and editing techniques applied to the data generated by this suite of instrumentation will be presented. Among the topics covered will be the phenomenological magnetic compensation model and the determination of its parameters from the low-level calibration maneuvers flown over geomagnetic observatories.

Historical Introduction

Project MAGNET is a U.S. Navy vector aeromagnetic survey program which has been ongoing for forty years. The high-level survey coverage during this period is presented in figure 1. Early test flights began in 1951. Full operational capability was established in 1953. Since that time five separate aircraft have been employed as the survey platform. Each succeeding aircraft represented a significant improvement in range, speed, or altitude. One aircraft, an NC-121 Super Constellation, crashed in Antarctica in 1960. The flight capabilities and deployment dates of these aircraft are summarized in table 1.

During the period 1953 through 1989, each aircraft has been dedicated to global aeromagnetic surveys primarily over ocean areas. However, during the period 1990 through 1991, the current Project MAGNET aircraft, an Orion RP-3D (figure 2.), which is a specially modified P-3C aircraft, has undergone an extensive reconfiguration as a multipurpose airborne survey platform. Its mission now includes gravity surveying, ocean acoustics monitoring, and ocean temperature monitoring, in addition to traditional aeromagnetic surveying. Besides the economy introduced by multipurpose platforms, this reconfiguration reflects the reduced need for high-level vector aeromagnetic surveys due to the successful launch of the Polar Orbiting Geomagnetic Survey (POGS) satellite on April 11, 1990 and the proposed Defense Meteorological Satellite Program/Polar Orbiting Geomagnetic Survey (DMSP/POGS) satellite follow-ons to POGS. The

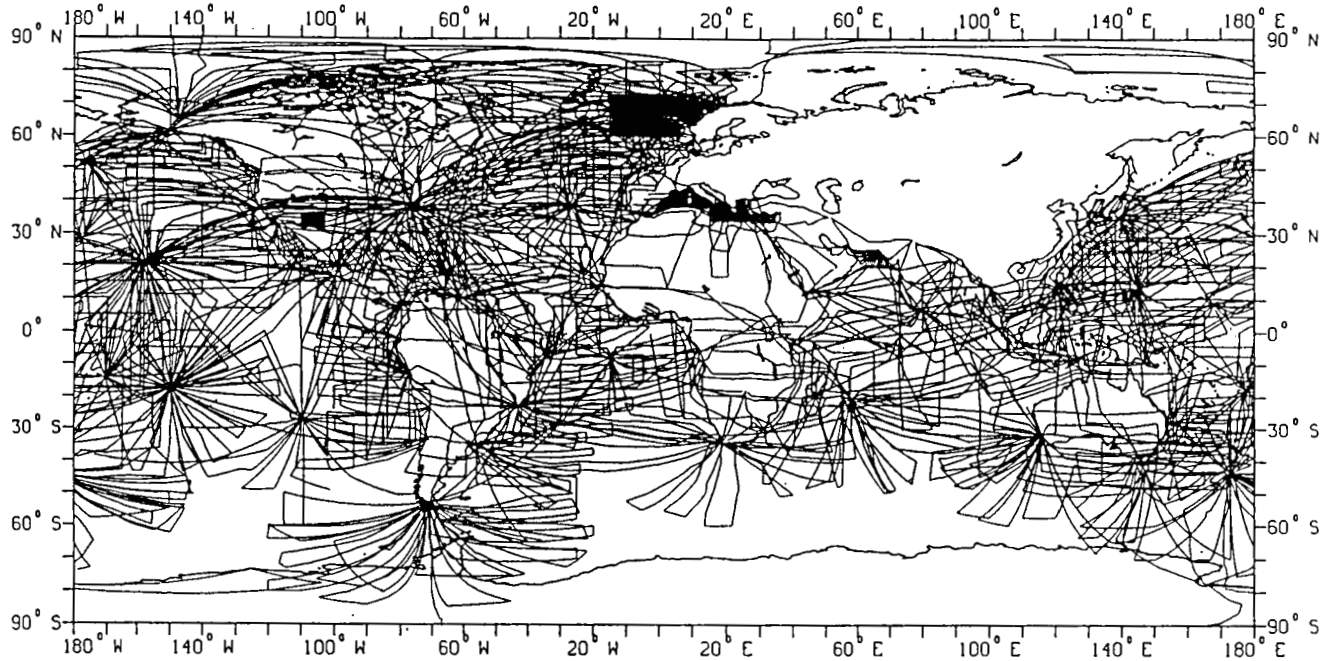

Figure 1. Project MAGNET Data Distribution (1950 - 1990).

Table 1. Project MAGNET Aircraft History.

- 1953 - P-2V Neptune
  Range: 2200 nm
  Survey Altitude: 9,000 - 13,000 ft
  Speed: N/A

- 1955 - NC-54 Skymaster
  Range: Greater than 2350 nm
  Survey Altitude: 9,000 - 13,000 ft
  Speed: 175 kts

- 1958/1962 - NC-121 Super Constellation
  Range: Greater than 4000 nm
  Survey Altitude: 25,000 ft
  Speed: 210 kts

- 1970/Present - RP-3D Orion (modified P-3C)
  Range: 5,000 nm high-level
  2,800 nm low-level
  Survey Altitudes: 25,000 ft high-level
  500 ft low-level
  Speed: 340 kts high-level
  240 kts low-level
  Wing Span: 99 ft 8 in
  Length: 107 ft 10 in

Figure 2. Current Project MAGNET Aircraft.

DMSP/POGS effort, initially, will collect scalar data, just as POGS itself is doing now. During the period 1995 to about 2005, full vector capability from a vector magnetometer calibrated with an absolute scalar magnetometer will be available with an attitude accuracy of ±1 arcminute.

The DMSP effort itself began in 1967 and is expected to continue through the first quarter of the next century and beyond into the indefinite future. The reconfigured Project MAGNET aircraft will, therefore, in the future be mainly restricted to high-level surveying within ±20° of the geomagnetic equator. This survey effort will supply sufficient vector magnetic data to supplement the scalar magnetic satellite data in order to avoid the Backus effect problem in world magnetic modeling. These surveys must be repeated periodically due to the generally slow, but sometimes sudden and erratic, secular changes in the Earth's main magnetic field. The reconfigured aircraft will also perform special local and regional low-level aeromagnetic surveys.

The primary purpose of the high-level Project MAGNET aeromagnetic surveys is to supply data in support of the World Magnetic Modeling (WMM) program, which in turn supports civilian and military global navigation needs. Most Global Positioning System (GPS) receivers made in the United States incorporate the WMM either as a piece of hardware in the form of a computer chip, or as a piece of software. The model also is used to control drift rates in inertial navigation systems. Other applications of the WMM include its use as a boundary

condition at the Earth's core-mantle boundary for the magnetohydrodynamic fluid flow problem and as an aid for geophysical prospecting and resource evaluation.

Survey Systems

During the period 1953 through 1970, the survey aircraft did not fly much higher than 15,000 feet and, since most surveys were conducted in remote ocean areas, navigation was limited to periodic celestial fixes, some Loran and dead reckoning. By today's standards, therefore, navigation during this period was rather poor, with accuracies no better than about five nautical miles (±5 nm). The data acquisition system consisted primarily of strip chart recorders and navigation logs. Consequently, the majority of this data was hand digitized. All vector magnetic data collected during this early period is now summarized in the U.S. Naval Oceanographic Office (NAVOCEANO) Special Publication #66 (SP-66) and is also digitized on magnetic tape at five minute intervals. Table 2 summarizes the capabilities of the early magnetic survey system. This data set has been sent to the National Geophysical Data Center (NGDC) in Boulder, Colorado.

During the last twenty years, since 1970 and the introduction of the Orion aircraft, the high-level vector aeromagnetic surveys are considered to be those conducted above 15,000 feet, usually between 20,000 feet and 25,000 feet. Navigational accuracy during this period was generally within ±1 nm, although some flights since the

Table 2. Project MAGNET Survey System 1953-1970.

MAGNETOMETERS

Vector Airborne Magnetometer (VAM-2A)
- Type - Self-Orienting Fluxgate
- Measures - D, I, F
- Accurcy - +/- 15 nT (for F)

Optically Pumped Metastable Helium Magnetometer
- Type - Towed
- Measures - F
- Accuracy - +/- 4 nT

NAVIGATION

- Type - Dead Reckoning
  - Celestial Fixes
  - LORAN (where available)
  - Radar
- Accuracy - +/- 5 nm (at best)

ALTITUDE

- Type - Aneroid Barometic Altimeter (Standard Pressure Used)
- Accuracy - +/- 30 m

TIME

- Type - 24 hr Chronometer
- Accuracy - 0.8 sec/24 hrs

RECORDING

Magnetics
Punched Paper Tape, Strip Chart Recorders, and Magnetic Tape (late 1960's)
Navigation
Paper Charts, Navigation Log

introduction of GPS receivers in 1987 have positioning accuracies on the order of 30 to 100 meters whenever there was a good GPS window.

The fluxgate vector magnetometer and the electrically suspended gyro (ESG) are shock mounted on a rigid aluminum beam in a magnetically clean area at the rear of the aircraft. The ESG has been the primary inertial navigation and attitude determination instrument during most of the past twenty years. It has been augmented, first with two ASN-84 inertial systems and later by two Litton inertial systems which were located on shock mounts toward the middle of the aircraft. The two Litton inertial systems are referred to as INS-1 and INS-2. These inertial systems were not mounted on the rigid beam with the magnetometer or the ESG. Therefore, due to the flexure of the fuselage of the aircraft, attitude as specified by these instruments did not as accurately represent the orientation of the magnetometer in space as did the ESG. Nevertheless, they provided a sufficiently accurate redundant attitude capability to be used in data reduction in the event of ESG failure.

The scalar magnetometer used during the past twenty years has been the ASQ-81 optically pumped metastable helium magnetometer. Its purpose is to calibrate the vector magnetic data collected from the fluxgate magnetometer, which has a tendency to drift. The ASQ-81 magnetometer is located in the stinger at the rear of the aircraft, which can be seen in figure 2. Table 3 summarizes the Project MAGNET survey capabilities for the period 1971-1990.

Table 3. Project MAGNET Geomagnetic Airborne Survey System (GASS) 1971-1990.

MAGNETOMETERS

Fluxgate Vector Magnetometer
Measures: X, Y, Z Acc\Res: +/- 40 nT \ +/- 5 nT

Optically Pumped Metastable Helium Magnetometer
Measures: F Acc\Res: +/- 1 nT \ +/- .01 nT

INERTIAL NAVIGATION SYSTEMS

Electrically Suspended Gyro (ESG)

Measures:		Accuracy:
	position	0.1 nm/hr
	roll/pitch	3 arc min
	heading	3 arc min

Two ASN-84's (1971-1982)

Measures:		Accuracy:
	position	2 nm/hr
	roll/pitch	+/- 12 arc min
	heading	+/- 6 arc min

Two Litton 72's (1982-1990)

Measures:		Accuracy:
	position	2 nm/hr
	roll/pitch	+/- 10 arc min
	heading	+/- 6 arc min

ALTITUDE

Type: Barometric Altimeter Accuracy: +/- 30 m

TIME

Type: Cesium Standard Accuracy: 1 millisec

DATA COMPUTERS/LOGGERS

Two 16K Computers
Two Tape Drives

Since mid-1990, the Project MAGNET aircraft has been undergoing extensive maintenance and reconfiguration which will be completed in late 1991 or early 1992. The old fluxgate magnetometer will be replaced with a NAROD, ring-core fluxgate vector magnetometer, while the ASG-81 scalar magnetometer will be retained. The ESG and the two Litton inertial systems will be replaced with one ring-laser gyro (RLG) inertial system which will be shock mounted on a rigid beam along with the ring-core fluxgate vector magnetometer in the magnetically clean area in the rear of the aircraft. A spare RLG will be carried aboard the aircraft for use in case of failure of the other RLG. The RLG will be used primarily for attitude, while GPS, which is now becoming globally available, will be the primary navigational system.

Due to the inclusion of aerogravimetric surveying capability on the aircraft, more accurate and redundant altitude instrumentation has been included. These instruments and their accuracies along with other details of the Replacement Geophysical Airborne Survey System (RGASS) are given in table 4. Early testing of this system should begin in February 1992. The first survey, a gravity survey of Greenland, should begin in late May 1992.

Survey Planning

Typically, a Project MAGNET survey is planned six to eight months in advance of the actual survey. This lead time is required in order to arrange for logistic support (e.g., fuel for the aircraft) and flight clearances through the U.S. State Department for the

Table 4. Project MAGNET Replacement Geophysical Airborne Survey System (Geomagnetic Equipment) 1991.

MAGNETOMETERS

Ring-Core Fluxgate Vector Magnetometer
Measures: X,Y,Z Acc\Res: +/- 40 nT \ +/- 6 nT

Optically Pumped Metastable Helium Magnetometer
Measures: F Acc\Res: +/- 1 nT \ +/- .01 nT

NAVIGATION SYSTEMS

Ring-Laser Gyro Inertial System (RLG)

Measures:		Accuracy:	
	position		0.8 nm/hr cep*
	roll/pitch		0.05 deg
	heading		0.10 deg

Global Positioning Satellite System (GPS)

Measures:		Accuracy:	
	position		15 mcep

ALTITUDE

GPS Altimeter	Accuracy:	20-25 m
Radar Altimeter	Accuracy:	+/-(5ft +0.5% alt)
Precision Baro Altimeter	Accuracy:	1 ft

Time

GPS	Accuracy:	0.2 millisec

SURVEY CONTROL/DATA ACQUISITION SYSTEMS

Four 386 Microcomputers
2 - Sensor Control
1 - Survey Control
1 - Survey Analysis
Two 9 - Track Tape Drives @ 6250 BPI each
Two 330 Mbyte Hard Drives

* 10 hr flight or less

cep - circular error probability
mcep - meter circular error probability
msep - meter spherical error probability

countries that will be visited. A full survey lasts approximately two and a half months during which twenty to twenty-five, ten to twelve hour flights are scheduled. This group of flights is referred to as a "project" and is assigned a project designation such as C32-452. The "C32" is an accounting designation which changes once a decade or so. The "452" indicates the project was conducted in FY84 using the fifth Project MAGNET aircraft during the second quarter of the fiscal year. Each flight of a project is also tagged with an identifying number. For example, flight 4061 indicates that this flight took off from an airport in area 4 of a world divided into seven areas. This would be the sixty-first flight to have taken off in this area during the existence of the Project MAGNET program. Flights in the 9000 series are low-level flights below 15,000 feet and are usually constrained to a small geographical area. These identifiers always accompany the Project MAGNET data which is routinely sent to NGDC World Data Center A. There is generally a six to twelve month delay between the completion of a survey deployment and the final distribution of the processed data to NGDC.

Calibration

A typical project begins with a low-level (approximately 1,000 feet) calibration flight, called an airswing, over a geomagnetic observatory as indicated in figure 3. Usually the observatory in Fredericksburg, Virginia, which is nearest to the Patuxent River Naval Air Station where the Project MAGNET aircraft is based, is

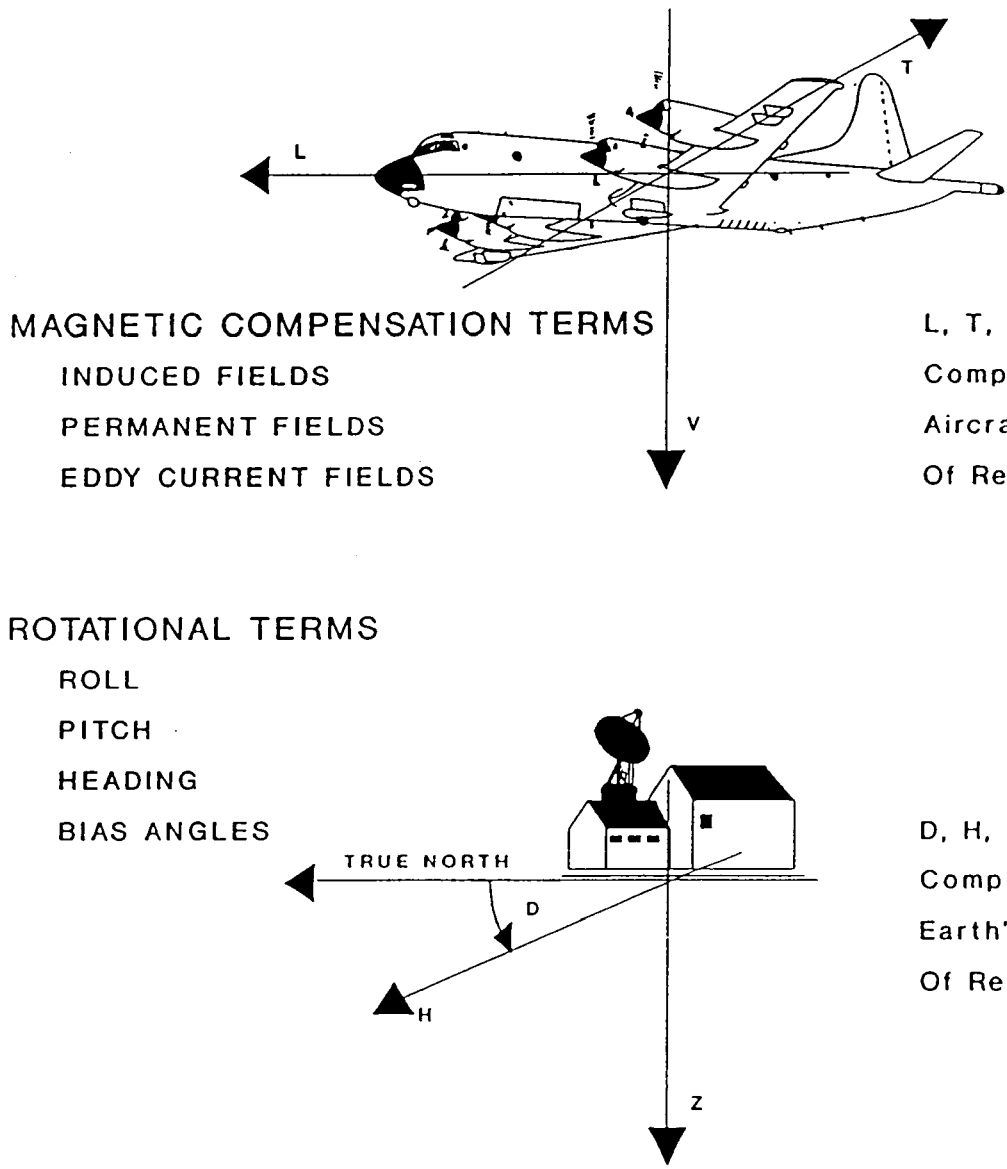

Figure 3. Concept of Compensation and Rotation Terms via Aircraft Maneuvers over a Geomagnetic Observatory.

used for airswing purposes at the beginning and at the end of a project. Other airswings are flown during the course of a project, as observatory proximities permit. Usually, three to four airswings are performed during each project. It is particularly important to fly airswings in both the North and South geomagnetic hemispheres if surveying covers both hemispheres. A calibration flight consists of, performing over the observatory, a roll maneuver in each of the four cardinal directions, North, South, East, West, a pitch maneuver in all four cardinal directions, and a yaw maneuver in all four cardinal directions. Additionally, straight and level passes over the observatory in all four cardinal and intercardinal directions are performed. The straight and level passes are sometimes flown at a somewhat higher altitude than the maneuvers. The yaw, pitch, and roll maneuvers are automatically controlled at ±5° fluctuations about the mean aircraft orientation. An example of an airswing track pattern over Fredericksburg is given in figure 4, while figure 5 illustrates the aircraft attitude for one pitch maneuver in the South direction. The purpose of these maneuvers is to provide data to compute the coefficients of a phenomenological magnetic compensation model which characterizes the contaminating magnetic fields associated with the permanently magnetized portion of the aircraft, the magnetic fields induced in the aircraft's metal parts by the Earth's main (core generated) field, and the magnetic fields generated by eddy-currents that are driven by the changes in the Earth's main and crustal field as the aircraft travels through them.

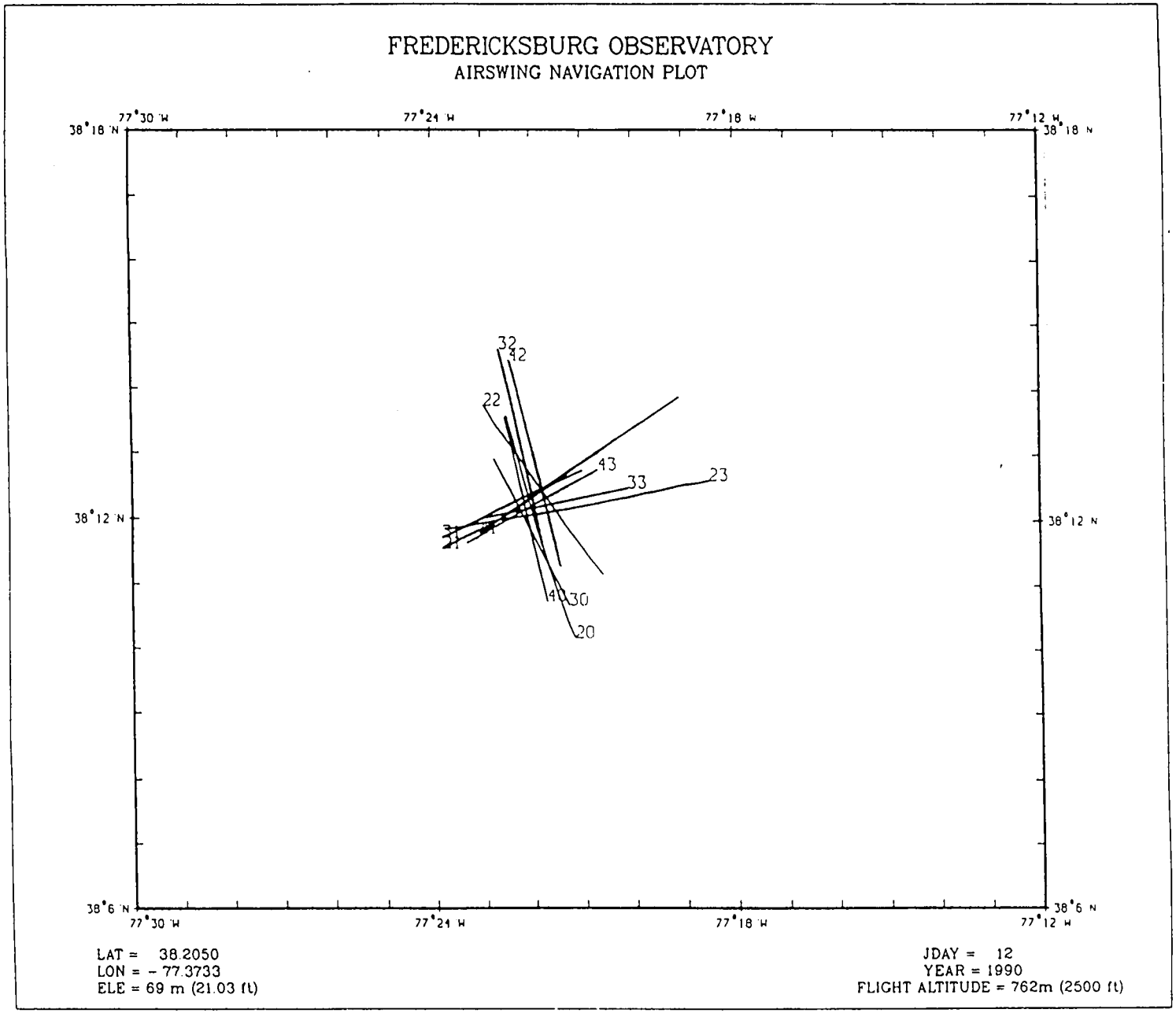

Figure 4. Airswing Navigation Plot.

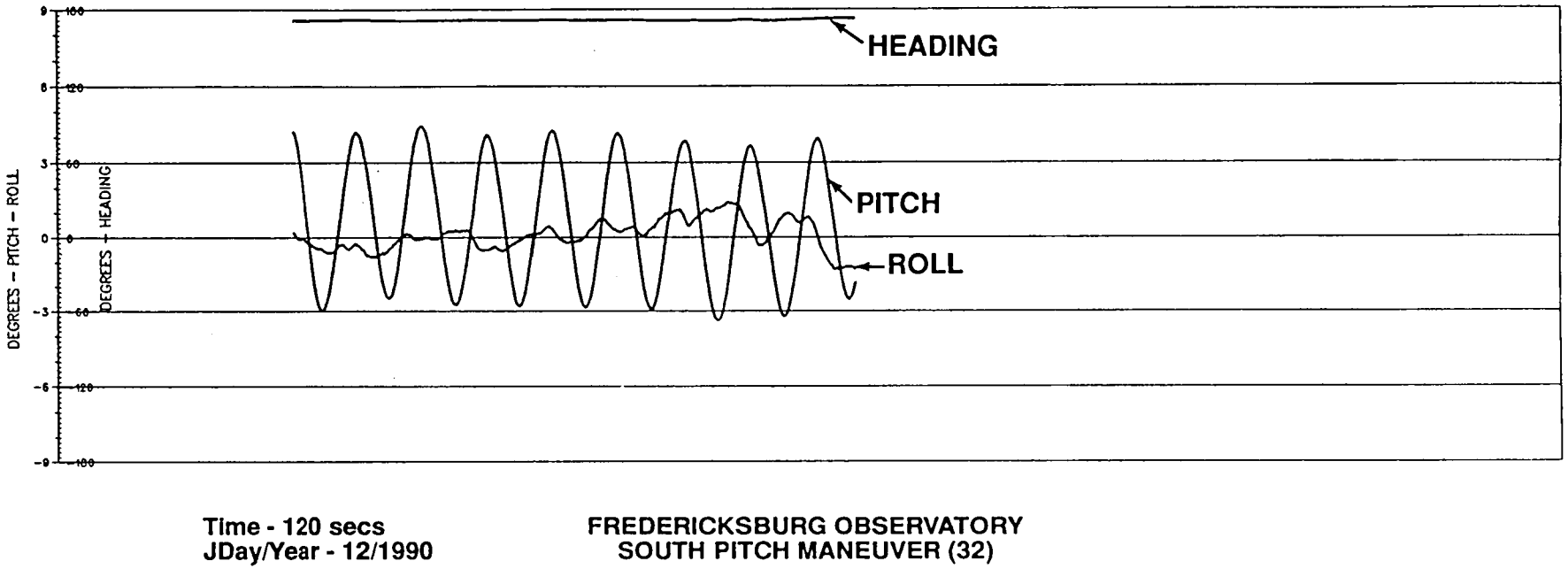

Figure 5. Aircraft Attitude Plots - South Pitch Maneuver.

Of course, there is also a certain amount of feedback and coupling among these fields which also interfere with the magnetic field as seen in the absence of the aircraft. The aircraft is primarily made of aluminum. However, many other metals such as copper and iron may be found in and around the aircraft. The airswing data flow is illustrated in figure 6.

The compensation model used by the Project MAGNET aircraft program is a modified version of that developed by Leliak (1961). In aircraft coordinates, the mathematical expression for the corrected (compensated) magnetic field observation is:

$$B_C = \underset{\text{OBSERVED FIELD}}{B_{MA}} - \underset{\text{PERMANENT FIELD}}{B_P} - \underset{\text{INDUCED FIELD}}{\vec{\delta} \times B_{MA}} - \underset{\text{EDDY-CURRENT FIELD}}{\vec{\xi} \times \frac{dB_{MA}}{dt}} \qquad (1)$$

where the unknown compensation coefficients are more explicitly given in the following form:

$$B_P = \begin{pmatrix} B_{PL} \\ B_{PT} \\ B_{PV} \end{pmatrix}$$

PERM COEFFICIENTS

$$\vec{\delta} = \begin{pmatrix} \delta_{LL} & \delta_{LT} & \delta_{LV} \\ \delta_{TL} & \delta_{TT} & \delta_{TV} \\ \delta_{VL} & \delta_{VT} & \delta_{VV} \end{pmatrix}$$

INDUCED COEFFICIENTS

$$\vec{\xi} = \begin{pmatrix} \xi_{LL} & \xi_{LT} & \xi_{LV} \\ \xi_{TL} & \xi_{TT} & \xi_{TV} \\ \xi_{VL} & \xi_{VT} & \xi_{VV} \end{pmatrix}$$

EDDY-CURRENT COEFFICIENTS

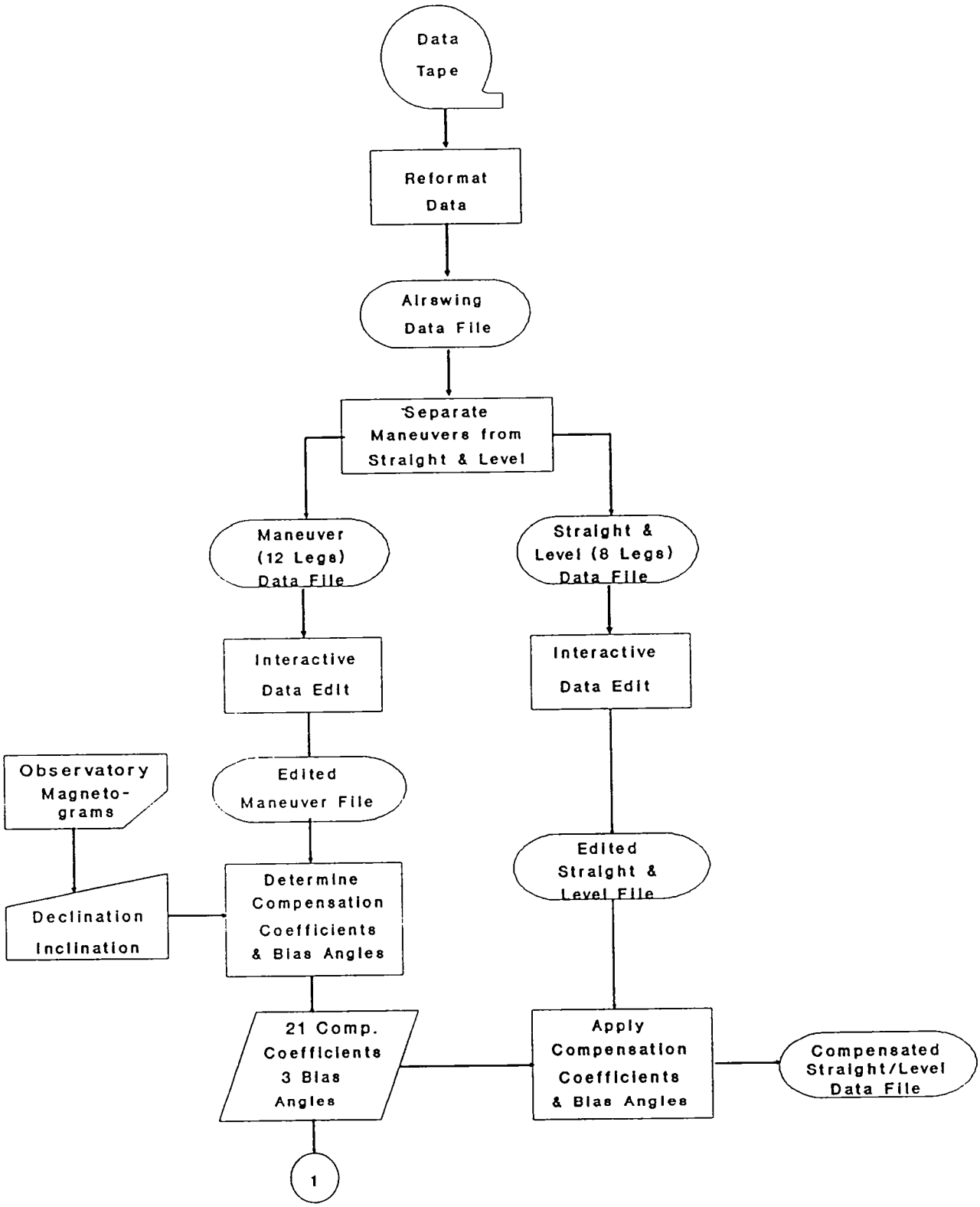

Figure 6. Airswing Data Flow.

The subscripts L, T, and V refer to the longitudinal, transverse, and vertical axes of the aircraft's coordinate system.

B_C is the Earth's magnetic field as seen in aircraft coordinates after correcting for the presence of the aircraft. B_{MA} is the magnetic field as seen by the aircraft's vector magnetometer after rotation from magnetometer coordinates to aircraft coordinates. Generally, the magnetometer is installed in the aircraft so that its coordinate axes are parallel to the aircraft coordinate axes. However, in practice, this is never done exactly. Consequently, a general three dimensional rotation through three small bias angles is required to put the observed magnetic field into aircraft coordinates. Each bias angle is on the order of just a few tenths of a degree. The bias angles tend to change when the magnetometer is removed for maintenance, sometimes during a flight due to vibration from turbulence and also sometimes due to the sudden impact of landing. Similar comments pertain to the inertial navigation/attitude systems, which have their own sets of three bias angles. The ESG is the inertial system of preference for data reduction due to its proximity to the vector magnetometer. In practice, as part of the compensation model, we solve for the relative difference bias angles between the magnetometer and the inertial system, since there is no absolute definition of the aircraft coordinate system. Consequently, there is a certain indeterminacy in these bias angles which forces us to solve for the

difference angles rather than the biases themselves. An equivalent alternative view is to simply say that the magnetometer angles are zero, in which case the aircraft coordinates coincide with the magnetometer system coordinates, which just leaves the inertial system bias angles to be solved for as part of the compensation model. We use this view.

B_P in equation (1) is the permanent field due to the aircraft's metal parts. It has three constant but unknown coefficients. $\bar{\delta}$ is a 3x3 matrix of constant coefficients characterizing the induced field. These coefficients are also unknowns of the compensation model. Finally, $\bar{\xi}$ is another 3x3 matrix of unknown constant coefficients which characterizes the effect of the fields generated by the eddy-currents on the metal surfaces of the aircraft. The compensation model, therefore, consists of 21 coefficients plus 3 bias angles. Various other sources of magnetic fields associated, for instance, with electrical systems in the aircraft and the running of the four engines, not all of which are necessarily running simultaneously as the pilot may switch from one set of engines to another, may also have some influence on the compensation coefficients.

The corrected magnetic field, B_C, is also equal to the magnetic field of the observatory after it is upward continued to the aircraft altitude and rotated from geodetic into aircraft coordinates. During the airswing, a leg of which lasts only a few minutes, the observatory

field is essentially constant. Upward continuation is accomplished by assuming that the direction of the Earth's field is the same at ground level as it is at aircraft altitude (1,000 feet). Consequently, the observatory magnetic declination (D) and inclination (I) are combined with the total intensity (TI) of the aircraft's scalar magnetometer (i.e., the ASQ-81) to obtain the complete upward continued magnetic field vector, B_O, which is then rotated into aircraft coordinates yielding B_{OA}. This rotation from geodetic to aircraft coordinates is accomplished using the roll, pitch, and heading information from the ESG. Therefore, we have:

$$B_C = B_{OA}$$

Consequently, the 21 compensation coefficients can be solved for by a least-squares process which minimizes the total intensity differences:

$$\chi^2 = \sum_i (|B_C| - |B_{OA}|)^2$$

with respect to these coefficients. The sum is over the measurements taken over all the maneuvers. This is a nonlinear algebra problem even though the compensation model is linear in the compensation coefficients. Therefore, the problem is solved iteratively, initially assuming that the three inertial bias angles are zero and using the initial guess that $B_P = 0$, $\vec{\delta} = 0$, and $\vec{\xi} = 0$ (i.e., $B_C = B_{OA}$).

Given an initial least squares estimate of the compensation coefficients, we then solve a second least-squares problem for the inertial system bias angles. The upward continued components of the observatory field are given by the following relations:

$$B_X = B\cos I_O \cos D_O$$

$$B_Y = B\cos I_O \sin D_O$$

$$B_Z = B\sin I_O$$

where B is the ASQ-81 total intensity and I_O and D_O are the observatory inclination and declination respectively. Rotating into aircraft coordinates yields:

$$\begin{pmatrix} B_{XOA} \\ B_{YOA} \\ B_{ZOA} \end{pmatrix} = \begin{pmatrix} \cos H\cos P & \sin H\cos P & -\sin P \\ \cos H\sin R - \sin H\cos R & \sin H\sin P\sin R + \cos H\cos R & \cos P\sin R \\ \cos H\sin P\cos R + \sin H\sin R & \sin H\sin P\cos R - \sin R\cos H & \cos P\cos R \end{pmatrix} \begin{pmatrix} B_X \\ B_Y \\ B_Z \end{pmatrix}$$

where the roll (R), pitch (P), and heading (H) are the observed inertial system values plus bias angle corrections:

$$R = R_I + \delta R$$

$$P = P_I + \delta P$$

$$H = H_I + \delta H$$

Using the estimated compensation coefficients from the previous least-squares problem to obtain B_C, we now minimize the quantity

$$\chi^2 = \sum_i \{(B_{XC} - B_{XOA})^2 + (B_{YC} - B_{YOA})^2 + (B_{ZC} - B_{ZOA})^2\}$$

with respect to R, P, and H, or equivalently, δR, δP, and δH. Here again, the summation is taken over the data collected from all of the aircraft maneuvers flown over the observatory. The straight and levels are reserved as a check on the final solution for the compensation coefficients after these two least-squares problems are repeated for several iterations until convergence is achieved. Both least-square problems are unweighted.

Once the coefficients and bias angles (compensation model) are determined, they are then applied to the straight and level passes over the observatory as well as the maneuvers. The corrected aircraft field observations after rotation into geodetic coordinates are examined to see that for each magnetic component for each pass of each maneuver yields the same value. The vector total intensity is also compared to the total intensity from the ASQ-81. The total intensity RMS error is usually in the neighborhood of 35 nT. These comparisons for an airswing over the College, Alaska Geomagnetic Observatory are given in figure 7.

As was mentioned earlier, the compensation model is a phenomenological model and as such is not complete. The model can break down as the survey moves away from the location of the airswing or be poorly determined due to a lack of robustness in maneuver frequency and amplitude. In particular, the compensation coefficients have been taken to be constants. A more detailed compensation model should include frequency dependence and geomagnetic latitude dependence. Project MAGNET has, over many

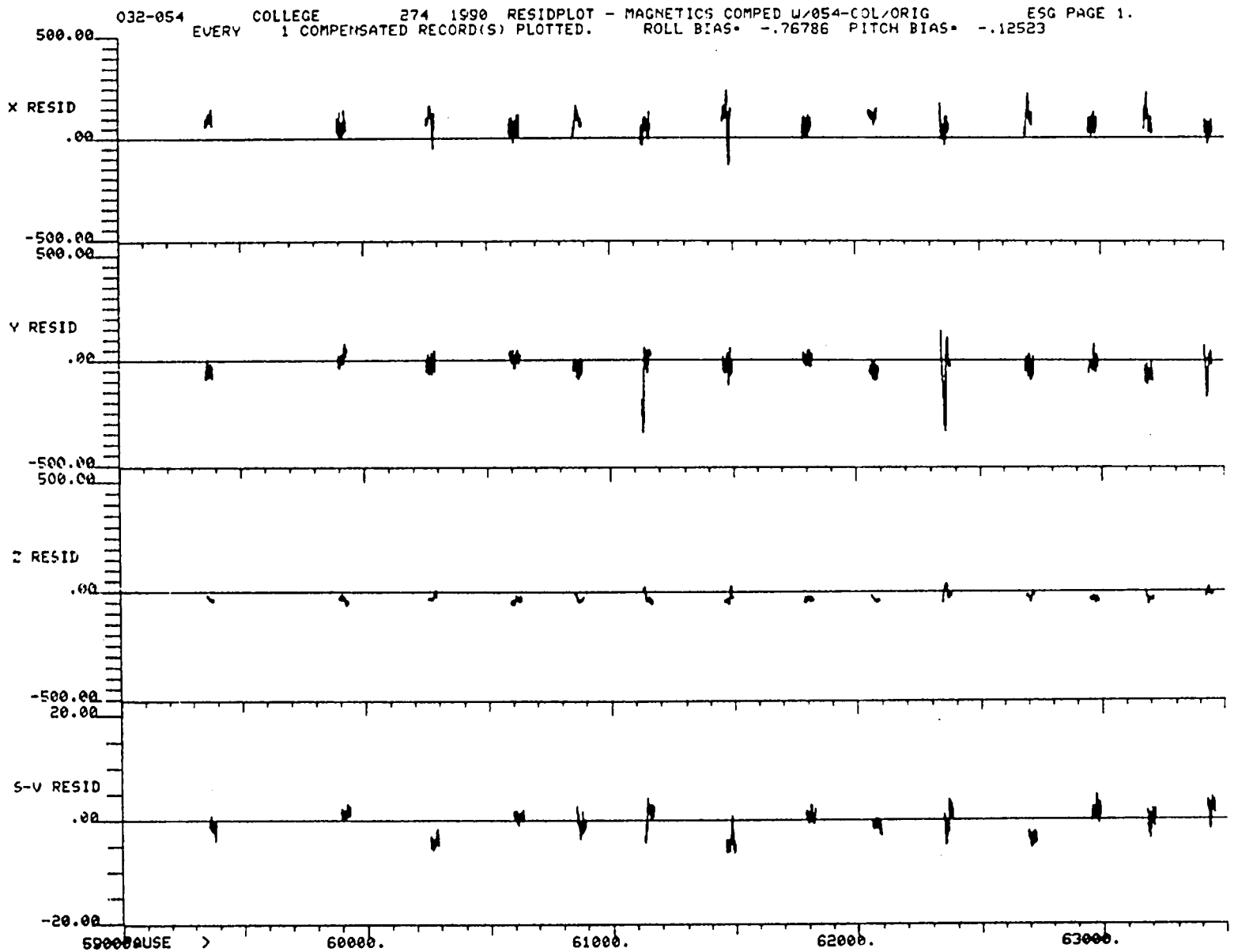

Figure 7. College, Alaska Geomagnetic Observatory Residual Plots.

years, performed numerous repeat airswings at observatories all over the world. The coefficients averaged from these repeat airswings form a data base which can be used to examine how the coefficients change with latitude. Plots of some of these averaged coefficients as a function of geographic latitude are given in figures 8, 9, and 10. At low latitudes equatorial electrojet effects have significant influence on the ξ_{TV} coefficients while δ_{TL} appears to have some periodic latitude dependence which is symmetric about the geomagnetic equator. The coefficient δ_{VL} also has a strong latitude dependence which appears to be asymmetric about the geomagnetic equator. Further detailed studies of the coefficient dependencies on frequency and latitude are required in order to improve the general applicability of the compensation model. In lieu of such improvements, it has been customary that several airswings be conducted during the course of a Project MAGNET deployment and then to use that set of compensation coefficients which were derived from the observatory closest to the area where a particular survey flight occurred.

The data flow for a typical survey flight is given in figure 11. An example of the processed data for Flight Number 5048 of Project C32-352 for day 155 of 1983 which went from Perth, Australia to Hobart, Tasmania via an indirect route is given in figures 12a, 12b, and 12c. Figure 12a shows aircraft altitude and magnetic inclination and declination for the flight. Figure 12b shows the ASQ-81 total intensity, the total intensity derived from the fluxgate

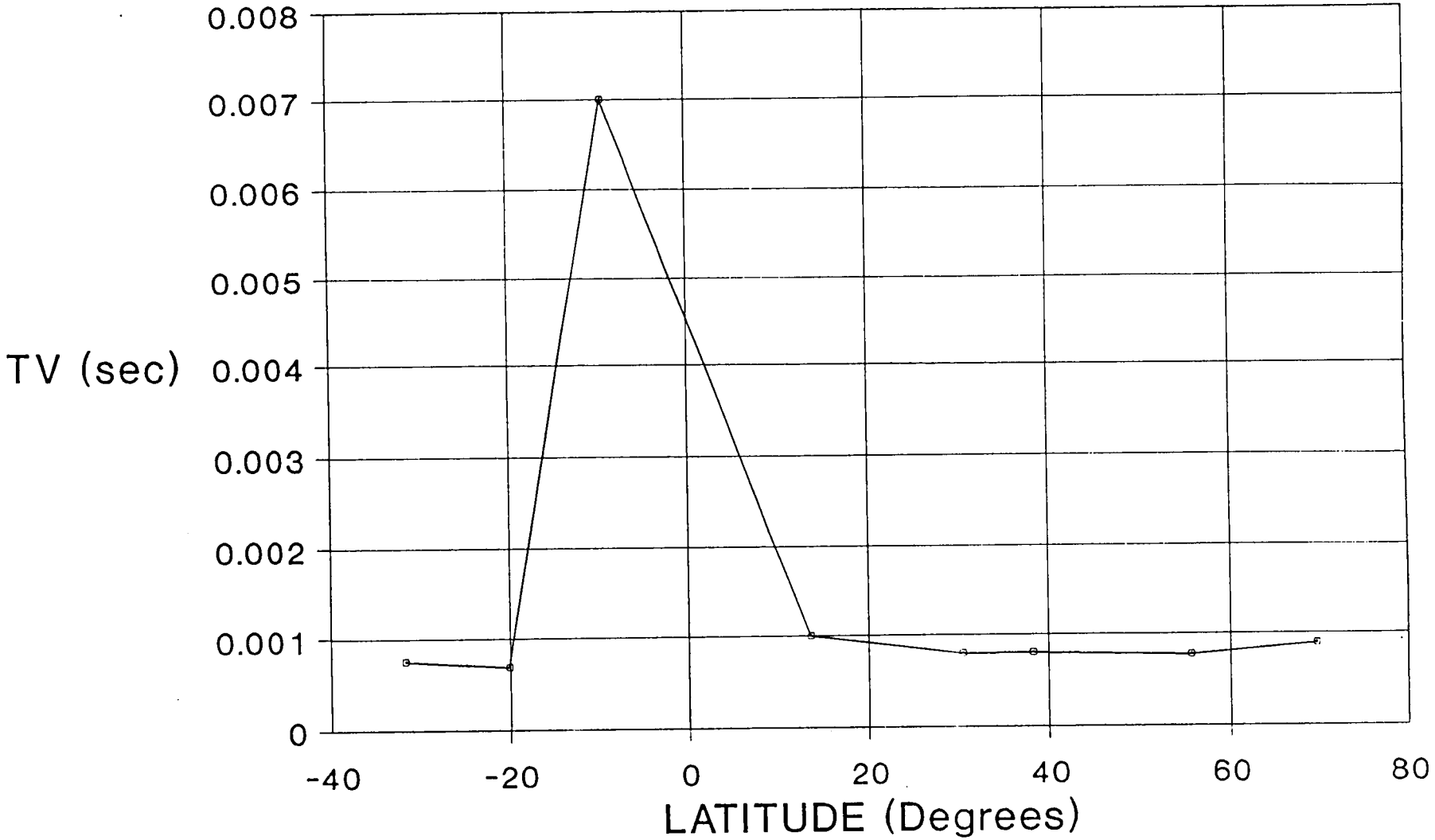

Figure 8. Eddy-Current (TV) Mean Latitude Dependence.

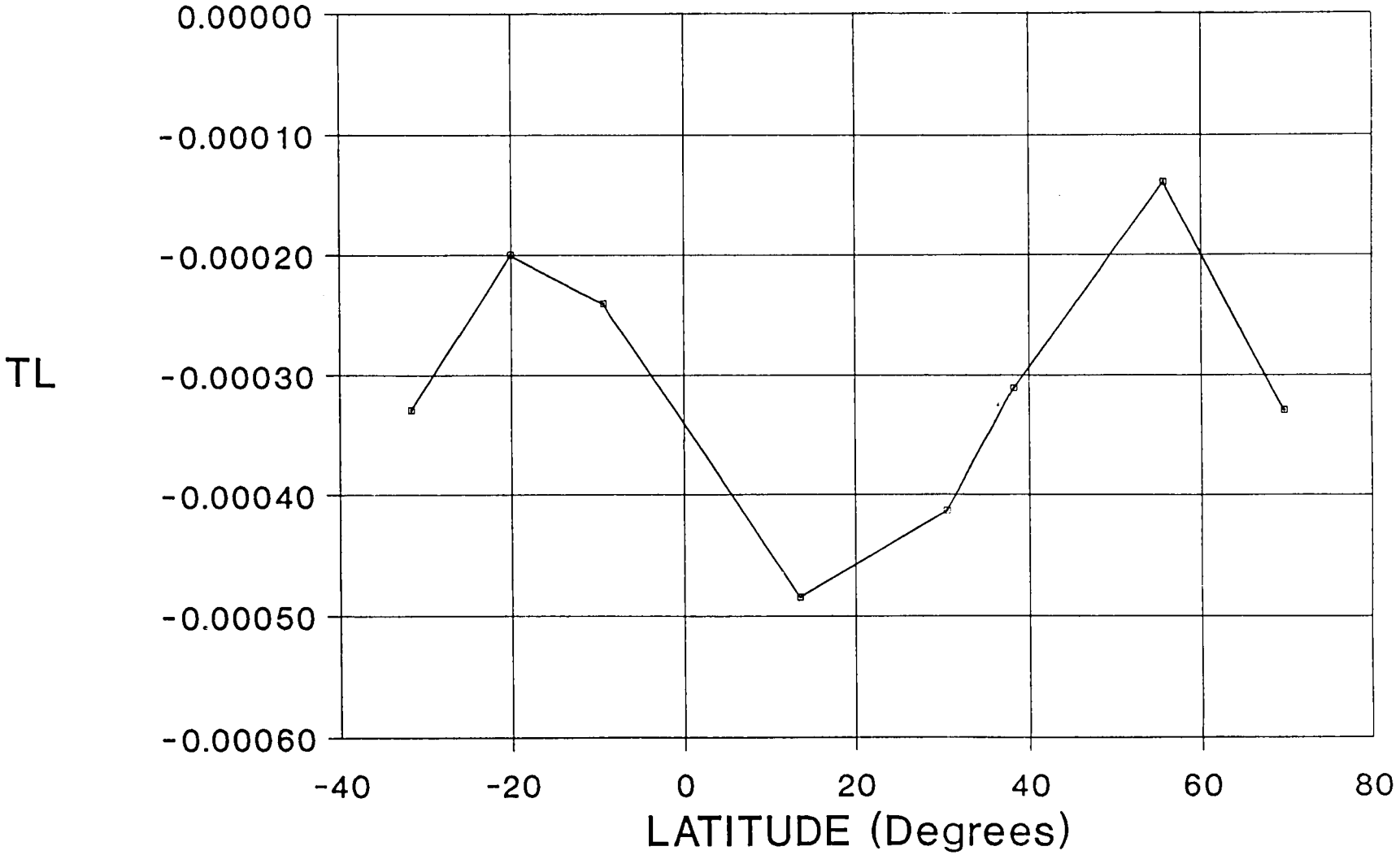

Figure 9. Induced (TL) Mean Latitude Dependence.

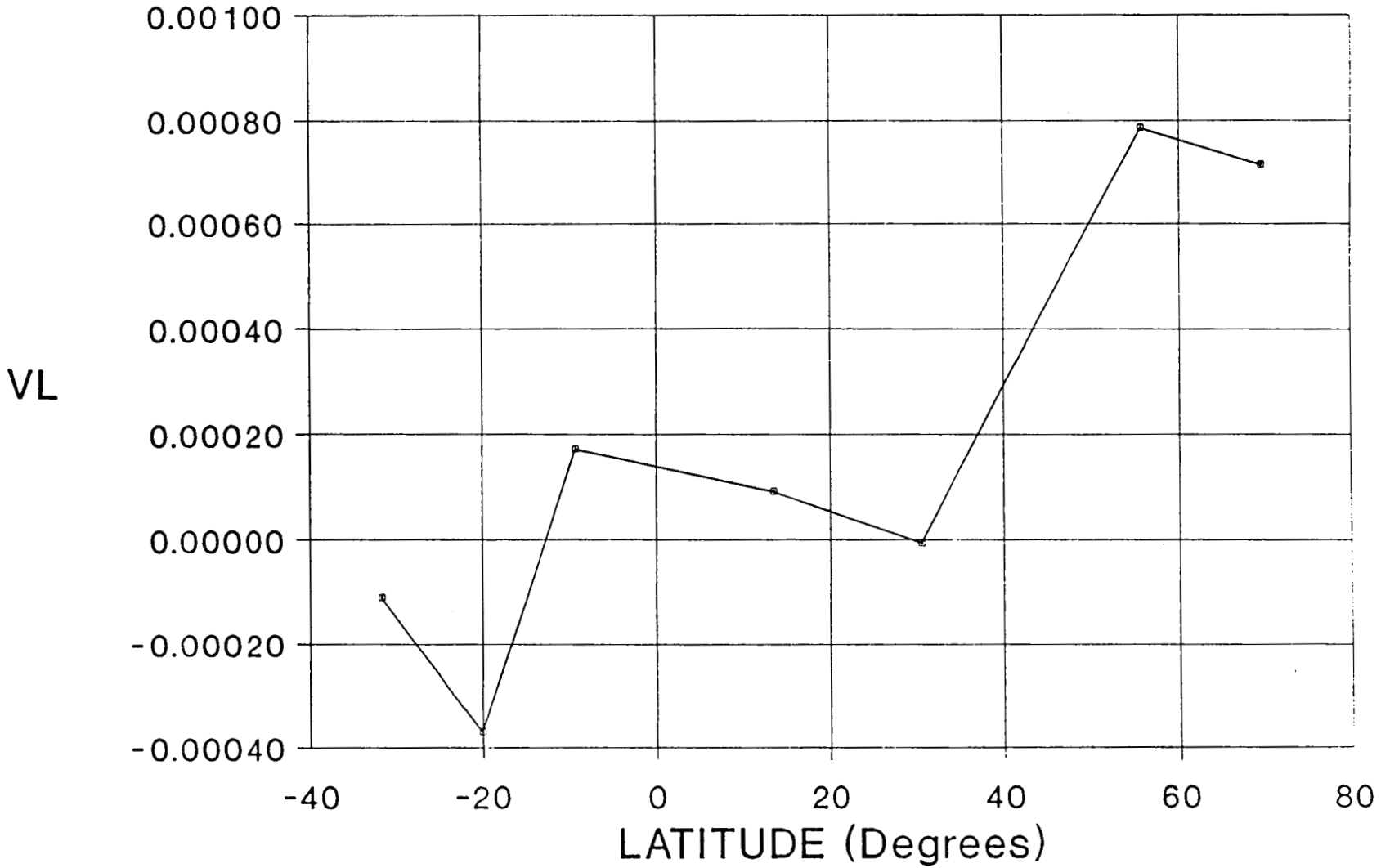

Figure 10. Induced (VL) Mean Latitude Dependence.

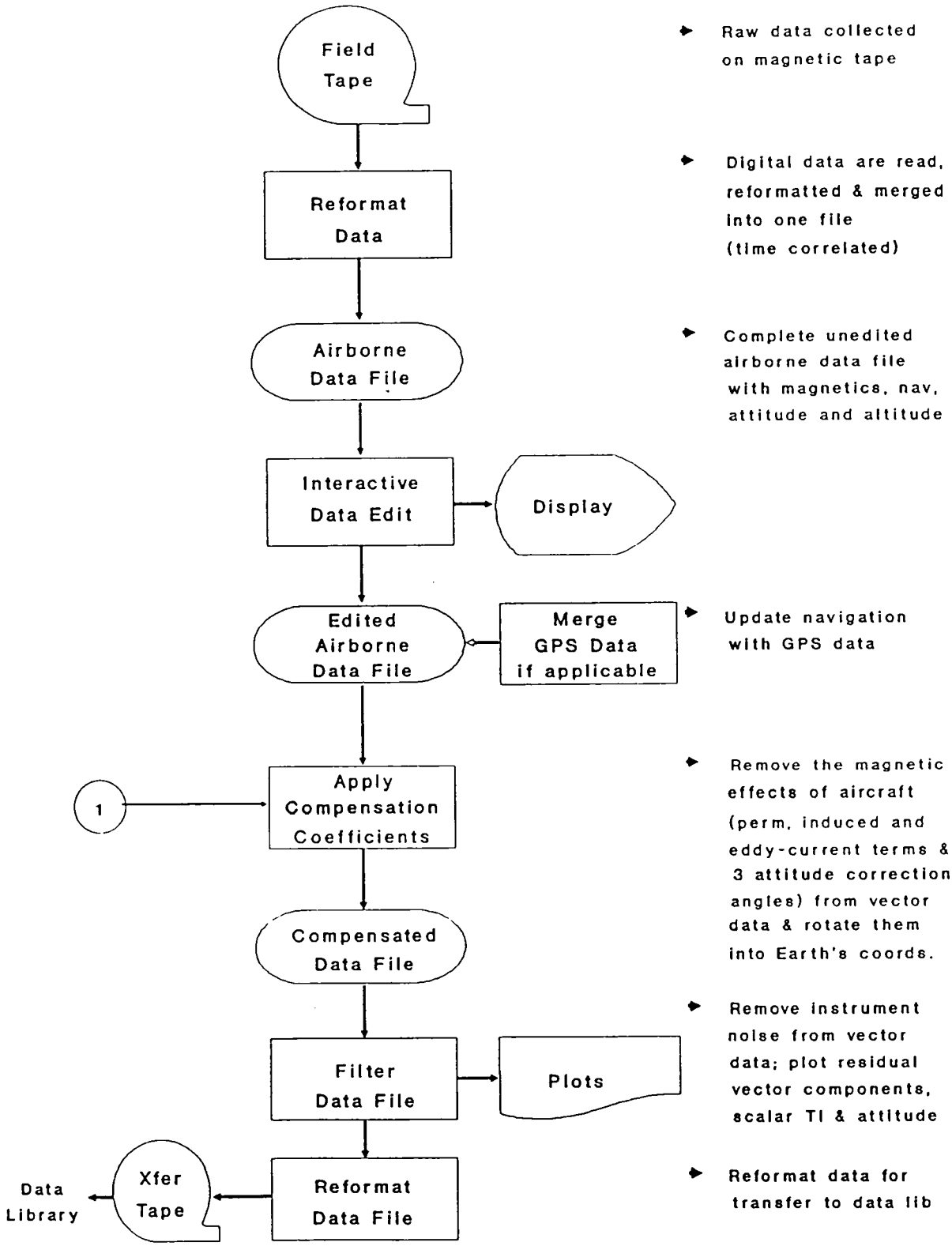

Figure 11. Project MAGNET Data Flow.

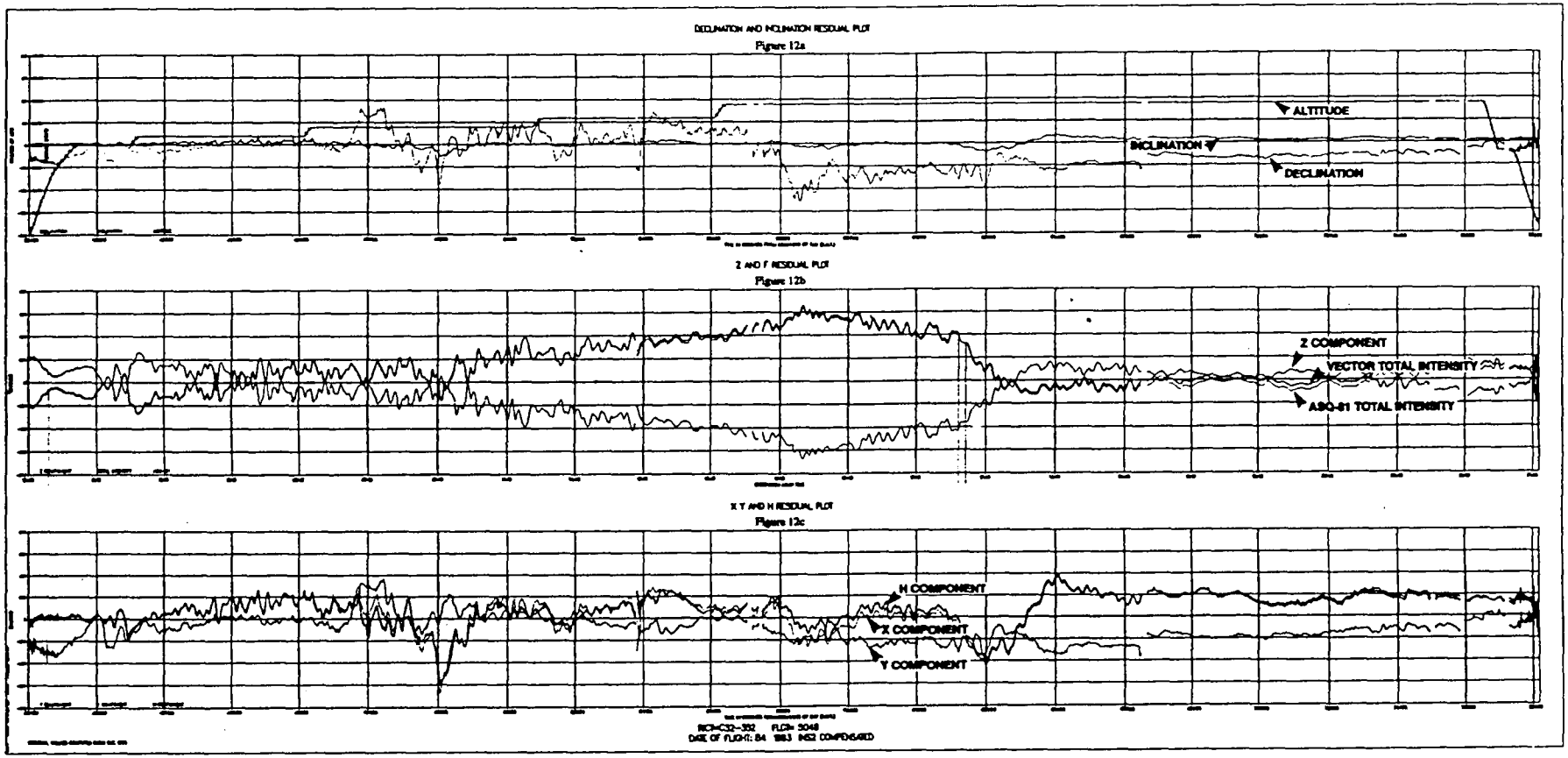
DECLINATION AND INCLINATION RESIDUAL PLOT
Figure 12a
ALTITUDE
INCLINATION
DECLINATION
Z AND F RESIDUAL PLOT
Figure 12b
Z COMPONENT
VECTOR TOTAL INTENSITY
ASQ-81 TOTAL INTENSITY
X Y AND H RESIDUAL PLOT
Figure 12c
H COMPONENT
X COMPONENT
Y COMPONENT

magnetometer, and the vertical magnetic component. Figure 12c shows the east magnetic component, the north magnetic component, and the horizontal intensity. Figure 12b is of particular interest since the total intensity from the vector and scalar instruments can be compared. They should be identical. However, about two-thirds of the way into this flight a significant deviation occurs, the beginning of which corresponds to a heading change. This difference is on the order of 50 nT, which is still considered good even though, in this case, the Litton INS-2 inertial system was used for attitude and navigation rather than the ESG.

Prior to the days when GPS was widely available (i.e., most of the last forty years) other navigation errors such as Schulering were present in the data and were never removed. Figure 13 illustrates the magnitude of this problem when the Litton INS-2 was used. GPS navigation eliminates this problem.

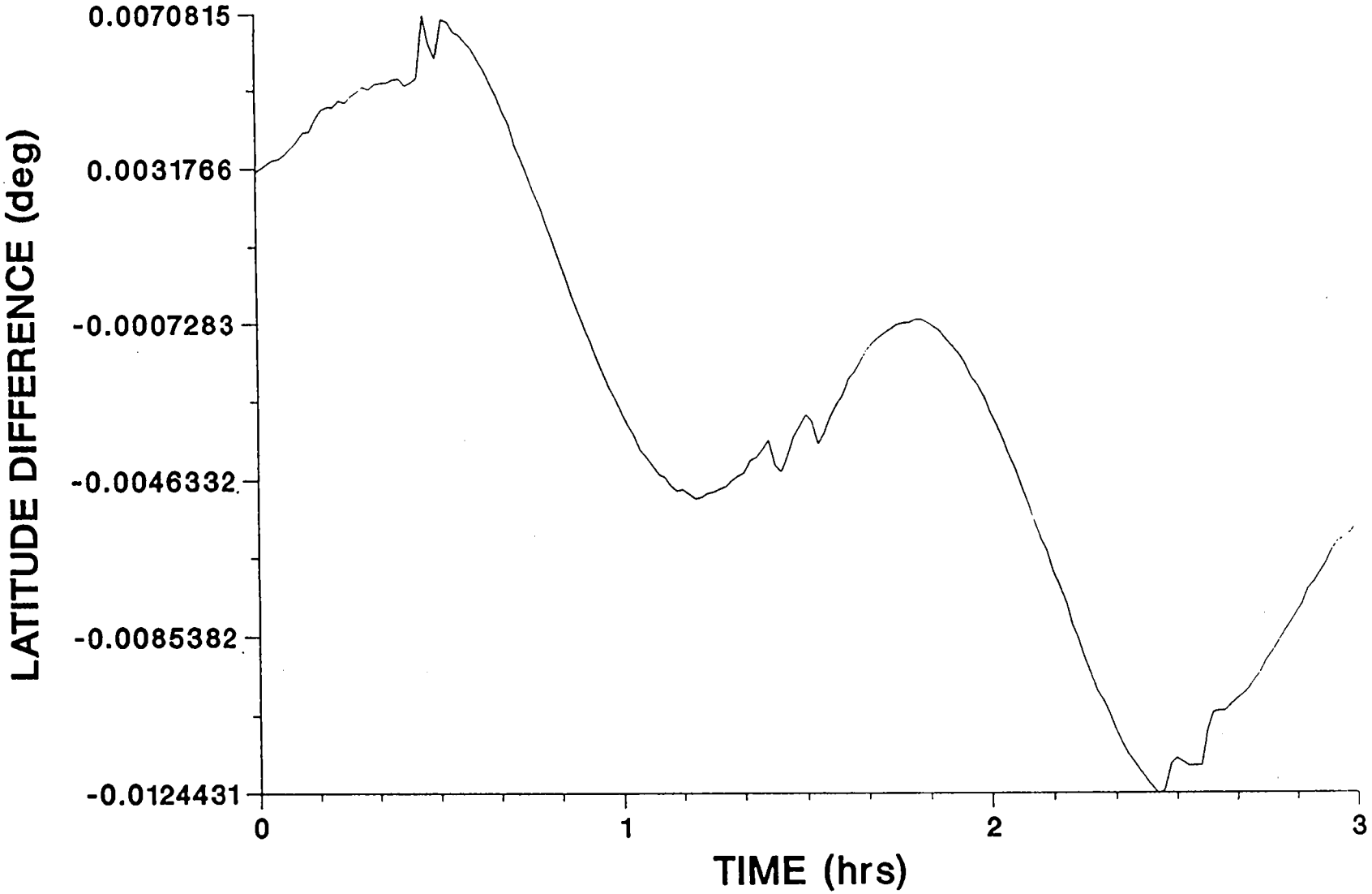

Figure 13. Inertial Schuler Error (GPS - INS2).

REFERENCES

Leliak, Paul, "Identification of Magnetic Field Sources of Magnetic Airborne Detector Equipped Aircraft", IRE Transactions on Aerospace and Navigational Electronics (September 1961), pp. 95-105.

CANADA

DEPARTMENT OF ENERGY, MINES AND RESOURCES

GEOLOGICAL SURVEY OF CANADA

Survey Parameters and Availability of Low-Level Aeromagnetic Data for Geomagnetic Field Modelling

by

Peter Hood

Mineral Resources Division

Ottawa

1991

249

Abstract

Since aeromagnetic surveying started immediately after World War II a considerable area of the earth's surface both onshore and offshore (in excess of 25 million sq. km) has been magnetically surveyed. For about the first 15 years or so fluxgate magnetometers were employed in aeromagnetic surveys but the introduction of proton free-precession magnetometers resulted in absolute readings being recorded. Proton precession magnetometers have now been replaced to a large extent by the more sensitive optical absorption magnetometers. Some care has to be taken to calibrate aeromagnetic survey systems and this is best done using a calibration range tied to a magnetic observatory so that accuracies of 10 nT or better are achieved for the total field values recorded.

Survey navigation has always posed a problem for aeromagnetic surveys especially offshore. Over land, vertically pointing 35 mm cameras were initially used to recover the aircraft track using a combination of aerial photos and topographic maps. Over featureless areas it was necessary to utilize existing electronic positioning systems such as Loran C or set up special navigation systems. The advent of the satellite-based Global Positioning System (GPS) has to a large extent solved the navigational problem because there is now almost continuous worldwide coverage to 10 m accuracy in the differential mode. The resultant aeromagnetic data is normally compiled into contour maps in which the diurnal variation and aircraft heading effects are removed. The resultant digital data are normally made publicly available both in gridded and profile form along with the published contour maps.

Most aeromagnetic coverage has been obtained in the developed western countries but elsewhere a considerable amount of surveying has been carried out and as an example some 80% of Africa has been surveyed mostly as a result of aid programs. The data is usually held by the national geological survey or equivalent organization but in a number of cases the data e.g. for the Magnetic Anomaly Map of North America, is also held by the World Data Centres.

1. Introduction

The purpose of low-level aeromagnetic surveys is to map the small variations of the earth's magnetic field essentially in a horizontal plane above the surface that are produced by the differing magnetizations of the underlying igneous rocks, i.e. the crustal field. The magnetic field produced by the igneous rocks of the earth's crust is about 2000 nanoteslas in amplitude. This is superimposed on the main earth's field which derives from the earth's core. In addition, there is a small time-varying field due to polarized charges that emanate from the sun and impinge on the earth's atmosphere. Over the course of a day, this diurnal variation usually amounts to less than 100 nanoteslas in amplitude except in the so-called auroral zones which extend in a circle around the geomagnetic poles and are 750 km or so wide.

It should be appreciated that for geomagnetic modelling purposes, the short wavelength variations due to near-surface geology can be as short as one kilometre depending on the distance between the survey aircraft and igneous basement, and will essentially be a form of noise to be removed from the data by filtering or some other suitable technique such as upward continuation.

2. Aeromagnetic Survey Practice

Aeromagnetic surveying activity commenced shortly after the end of World War II and the aircraft utilized were mostly the military transport and reconnaissance aircraft of that period, particularly the Douglas DC-3 aircraft (Balsley, 1952). This type of aircraft was utilized for more than a decade with the magnetometer being trailed in a towed bird so that the magnetic effects of the ferrous portions of the aircraft, such as the engines, were minimized. However towed birds are greatly affected by the air turbulence at low altitudes because of their small mass. In Canada, trailing a towed bird in icy conditions often led to dangerous flying conditions and the consequent loss of the magnetometer. To improve this situation inboard installations were then developed in which the

Figure 1. Aerocommander aircraft equipped for aeromagnetic and VLF electromagnetic surveys.

magnetometer was installed in a boom which extended from the tail of the aircraft to remove the magnetometer as far from the magnetic field-producing components of the aircraft e.g. the engines as possible (see Fig. 1). It was found that these magnetic components would produce a noticeable signal hash on the chart record that was more pronounced with aircraft manoeuvres. It was realized that these magnetic effects could be minimized by suitable compensation techniques that nullified to a large extent the magnetic fields produced by the survey aircraft itself. As skill in these compensation techniques improved, it became feasible starting about 1960 to use light twin-engined aircraft (Fig. 1) in which the magnetometer-engine distance was much shorter. Their use resulted in acceptable quality data being produced at lower line mileage costs.

2.1 Aeromagnetic Survey Instrumentation

Aeromagnetic survey systems have advanced considerably in recent years and state-of-the-art systems usually incorporate a microcomputer that is built into the data-acquisition system to control the various functions such as sampling interval, the conversion of the magnetometer output frequency to total field values etc. The other essential components of an aeromagnetic survey system are the magnetometer with the necessary compensation system, and the navigation system plus altimeter. A brief description of each of the typical aeromagnetic survey system components is given in the following narrative.

2.1.1 Types of Magnetometers

Three varieties of airborne magnetometers have mostly been utilized in aeromagnetic surveying (Hood and Ward, 1969; Hood and Lefebvre, 1991), namely

(1) Fluxgate

(2) Proton precession-free and spin-precession

(3) Optical absorption

All measure the total field value of the earth's magnetic field whose background value varies from about 23,500 (in Brazil) to about 67,700 nanoteslas (offshore from Antarctica) at the earth's surface.

2.1.1.1 Fluxgate Magnetometers

These were the first practical airborne geophysical instruments utilized and were developed immediately after the end of World War II from the airborne magnetometers used in antisubmarine warfare (Fromm, 1952; Jensen, 1961).

The sensitive element of a saturable-core or fluxgate magnetometer consists of a short length of high-permeability ferromagnetic material having a narrow hysteresis loop which acts as a core for one or more windings connected to AC exciting and indicating circuits. The field component along the axis of the fluxgate element is measured and so it is necessary to keep the axis accurately aligned in the direction of the earth's magnetic field to measure the total field. This is accomplished by the use of a three-axis moveable platform in which two additional orthogonal fluxgate elements are mounted. The platform is kept oriented so that the orthogonal elements have zero output.

For the device to work most of the ambient field is bucked out by the use of an additional winding through which is passed on accurately controlled DC current. Thus the fluxgate magnetometer is a vector variometer in which the variations of the earth's magnetic field from a fixed datum are measured. The output of a fluxgate magnetometer may be recorded as a continuous trace i.e. without steps, on an analog record. When first introduced fluxgate magnetometers were considered to have a sensitivity of one nanotesla but with improved compensation the latter models could achieve sensitivities approaching 0.1 nanotesla. Fluxgate magnetometers were utilized for some 15 years or so and starting in the late 50's were progressively replaced by proton precession

magnetometers. Fluxgate sensors are however still utilized in active compensation systems.

2.1.1.2 Proton Free-Precession Magnetometers

The proton free-precession magnetometer as been the most commonly utilized airborne magnetometer during the past 35 years and was developed during the middle 1950's (Packard and Varian, 1954). The sensor is much simpler in design than the mechanically complicated fluxgate magnetometer consisting essentially of a bottle of hydrogen-rich liquid, such as water or kerosene, around which is wound a coil of copper wire. The principle of operation depends upon the fact that hydrogen(but not the oxygen) protons have a magnetic moment due to their spin. First an external field is applied to the bottle of hydrogen protons by passing a DC current through the coil for a short period of time, typically one half-second or so. Then the field is switched off allowing only the earth's magnetic field to act. The effect is somewhat like kicking a child's spinning top, and the spinning hydrogen protons begin to wobble i.e. precess. The frequency of precession (f) is directly proportional to the ambient earth's field (T) and is related to it by the following formula $T=Kf$ where $K=2\pi/$gyromagnetic ratio of the proton = 23.4874 (Driscoll and Bender, 1958). Consequently the proton precession magnetometer is an absolute scalar instrument.

The hydrogen protons which are precessing in unison will induce an audio signal into the surrounding copper coil. This audio signal decays exponentially to zero within several seconds. The audio signal is amplified and in so-called direct-reading instruments multiplied in frequency to increase the sensitivity of the reading before being counted for a set period of time to yield the earth's magnetic field value directly in gammas (Hood, 1970). The sensitivity of direct-reading proton free-precession magnetometers ranges from 0.1 to 1.0 nanotesla; the sampling rate is usually 1 second, and their range is typically 20,000 to 100,000 nanoteslas to permit their use worldwide.

Perhaps the most serious drawback of proton free-precession magnetometers is that the output is not continuous because of the necessity to polarize the sensor each time before measuring the frequency of precession. This puts a limitation on the rate at which measurements can be recorded and also the instrument sensitivity. For instance for the popular Geometrics G803 proton magnetometer, sensitivities of 0.5 nanotesla for a 0.8 second sampling, 1 nanotesla for a 0.5 second rate and 2 nanoteslas for a 0.33 second sampling rate are achievable.

2.1.1.3 Spin-Precession or Overhauser Magnetometers

Spin-precession magnetometers are somewhat similar to the proton free-precession type in that the sensor consists of a coil system enclosing a liquid sample containing hydrogen protons. However a parametric salt is dissolved in the liquid sample which has the special property that the spin energy of the orbital electrons can be transferred to the protons to keep them precessing by the use of high-frequency fields. This is called the Overhauser (1953) effect after the discoverer. The resultant audio frequency is measured utilizing similar techniques as for the proton free-precession magnetometer since the constant of proportionality (23.4874) is the same between the measured field and the output frequency. Because the output is continuous, the sensitivity can be made to exceed 0.1 nanotesla, so they are well suited to medium sensitivity surveys. Overhauser magnetometers have not however been much utilized in aeromagnetic surveying except by French organizations.

2.1.1.4 Optical Absorption Magnetometers

Optical absorption magnetometers were developed during the 1960's (Bloom, 1960; Giret, 1965; Hood, 1970; Jensen, 1965) and have an order of magnitude better sensitivity than the proton precession magnetometer that is around 0.01 nanotesla. They were not greatly utilized in aeromagnetic surveying

up to the late 1980's for a number of reasons although that situation has changed. The first reason is that their use has been restricted by worldwide patents (in Canada up to September 10, 1987 when the important Dehmelt (1968) patent expired) so that only a few contractors were licensed to provide surveys using such magnetometers. The second reason is that for regional aeromagnetic surveys, the sensitivity of the proton precession magnetometer is adequate for the purpose. However the use of optical absorption magnetometers has increased considerably by their being utilized in aeromagnetic gradiometer systems consisting of two optical absorption magnetometers vertically separated by a short (2 metre or so) distance. Such short-baseline aeromagnetic gradiometers require the higher sensitivity that optical absorption magnetometers possess. Optical absorption magnetometers can also sample the magnetic field at a much higher rate than proton precession magnetometers at high sensitivity - up to 10 times per second which is useful for mineral exploration surveys at 100 m or so elevation.

An optical absorption magnetometer sensor consists of a glass cell containing an alkali vapour that is irradiated by radio frequency light corresponding to a specific line in the alkali vapour spectrum. The effect of the irradiation is to pump alkali vapour electrons to higher energy orbits from which they will fall spontaneously to a lower energy state. When they absorb light energy the glass cell becomes opaque to the incident light and when the electrons fall back to the lower energy state they actually emit light and the cell is transparent. Thus the light passing through the cell flickers at the Larmor precession frequency of the electron which depends on the ambient field. Initially rubidium metal vapour was utilized in the cells but this was subsequently replaced by cesium because of the improved operating characteristics of the resultant magnetometer. For cesium the Larmor frequency is 3.498 hertz per nanotesla. Thus the resultant output frequency is much higher than that produced by the proton precession magnetometer for the same magnetic field and falls in the range 80-250 KHz depending upon location on the earth's surface.

Cesium magnetometers have a number of drawbacks. The first of these is that there are actually eight spin states for Cesium 133 that gives rise to eight closely spaced Larmor frequencies of varying amplitudes producing a composite output frequency. The relative amplitudes of the eight Larmor frequencies change as the angle of the optical axis of the magnetometer changes with respect to the ambient field. This orientation error ranges up to about 8 nanoteslas for a single cell instrument. The orientation error is reduced considerably (to less than 1 nT) by the use of split beam instruments in which the circular polarization of the light passing through one half of the cell is made to be in the opposite sense to that passing through the other half of the cell. After passing through the cesium cell, the split beams are focussed on a photoelectric cell producing an averaged frequency and giving a flatter response for the combined effect of the eight Larmor frequencies mentioned earlier.

The second drawback is that the instrument has an active zone of orientation of about 65° in which it will operate, and polar dead zones of 30° and 210° from magnetic north in which the magnetometer will not work. For optimum operation, the cesium magnetometer is set at an angle of 45° from the total field vector.

To avoid the heading error and dead zone problems the Canadian NRC National Aeronautical Establishment developed a two-axis orienting instrument based on the minimization of a small audio frequency signal superimposed on the ambient field. The technique was utilized in the military ASQ-501 and ASQ-502 magnetometers built by Canadian Aviation Electronics Ltd. and adopted by the Geological Survey of Canada in magnetometers built for its Beechcraft B-80 Queenair survey aircraft. Such two-axis orienting magnetometers have a minimal orientation error and there are no dead zone problems.

A second technique for minimizing the orientation error is by the use of a so-called strap down magnetometer which employs a non-oriented split-beam cesium magnetometer. The orientation errors are minimized by incorporating the necessary corrections into the algorithm of the active magnetic compensation system used in the magnetometer installation. In such microprocessor-based compensators, aircraft manoeuvres are sensed using a triaxial fluxgate sensor.

Helium magnetometers neither have an orientation error nor do they have polar dead zones although there are 30° equatorial dead zones. Furthermore the higher Larmor frequency ratio (28.02468 Hz/nT) of the He magnetometer as compared to the lower (3.498 Hz/nT) of the cesium vapour magnetometer, provides significantly higher resolution at a higher field sampling rate. However helium magnetometers have been utilized far less than cesium magnetometers for aeromagnetic survey work up to the present time in part because of their commercial availability although Geometrics is now marketing a helium magnetometer, the G833 whose sensor was developed by the Ministry of Geology and Mineral Resources in China (Hood, 1991b).

For the reasons described earlier, optical absorption magnetometers have over the past four years gradually been replacing proton precession magnetometers for aeromagnetic surveys. The reasons include their higher sensitivity and sampling rate but especially the fact that the use of optical absorption magnetometers is now royalty free.

2.1.2 Compensation Systems

As stated earlier, inboard installations of airborne magnetometers were made possible by improvements in the magnetic compensation of aircraft. There are three different sources of interference produced by the aircraft itself. The first is the permanent magnetism of the various components made of steel, such as the engines, whose direction remains fixed with respect to the aircraft. The second

source is the induced field due to the magnetic susceptibility of these same ferrous components and the earth's field. Its polarity and magnitude depend upon the orientation of the aircraft with respect to the earth's magnetic field. The third source of interference is that caused by the magnetic effect of eddy currents generated in the skin and other conducting parts of the aircraft by their motion in the earth's magnetic field.

In earlier passive compensation systems, the permanent magnetism was eliminated by the use of a set of three-orthogonal compensating coils mounted together near the magnetometer head and on the roll axis of the aircraft and through which the appropriate DC currents were passed. The induced components were eliminated by the use of strategically placed permalloy strips, and the eddy currents were compensated for by the use of coils of wire mounted in close proximity to the sensor. It was necessary to carry out a set of aircraft manoeuvres consisting of rolls, pitches and yaws of the aircraft in low gradient areas in order to separate the effects of the three sources of interference. The excellence of magnetic compensation of a given survey aircraft is measured by its "figure of merit" (FOM) as originally defined by the US Navy. This index is obtained by summing, without regard to sign, the peak-to-peak amplitudes in nanoteslas of the 12 magnetic signatures recorded when the aircraft carries out ± 10° rolls, ± 5° pitches, ± 5° yaws on north, east, south, and west headings over periods of 4 to 5 seconds.

Active 9-term aircraft magnetic compensation systems have been commercially available for more than 20 years (see for instance Hood, 1970, 1986a, 1991b). The use of these active compensation systems improve the "figure of merit" of a given aircraft considerably, and drastically reduces the time required for aircraft compensation. They are in fact mandatory for high resolution aeromagnetic survey work.

2.1.3 Data Acquisition Systems

Data acquisition systems normally consist of both digital and analog recording systems. The digital acquisition system records the digital data on a suitable medium that has traditionally been magnetic tape on reels but data cassettes and discs are becoming more common. It is desirable that the digital recorder has a read-after-write capability so that the recorded data can also be displayed in analog form on a chart recorder (or scrolled on a CRT display) so the instrument operator can ensure that the data is being properly recorded throughout the survey flight. The parameters that are digitally recorded include the magnetic field readings, radar and barometric altitudes, time, fiducial numbers and navigational information. Information such as aircraft registration, date, line number, line segment number, direction, flight number, start time of line and any relevant scale factors or datum levels should be included in a header record which precedes the relevant data. Such pertinent information should also be included on the analog records and noted on the flight log to be maintained by the instrument operator.

2.1.4 Airborne Positioning Systems

Positioning systems used for aeromagnetic surveys can be divided into two main categories:

(1) those which are self-contained within the aircraft; these include tracking cameras, Doppler and inertial navigation systems.

(2) those which require external references normally fixed radio transmitters on the ground. The ground-based navigation systems which have been most utilized up to the present time have been Decca and Loran C navigation systems. For the aeromagnetic surveys of extensive bodies of water, the use of an electronic positioning system is mandatory.

The most widely-used method of recovering the aircraft track up to the present time has been by the use of vertically-mounted 35 mm cameras, either continuous strip or the more usual single frame variety, or by the use of video cameras. Doppler navigation systems have been quite commonly utilized in airborne geophysical survey systems not only to aid in the flying of straight parallel flight lines but also to assist the subsequent flight path recovery process. The cumulative errors on most Doppler systems are usually between 1 and 2% of distance traversed. Inertial navigation systems (INS) that employ accelerometers whose output is doubly integrated with respect to time have also been extensively utilized to assist in recovering the aircraft track but like Doppler systems, the errors are cumulative.

After a long gestation period, the US Air Force Global Positioning System (GPS) has now reached the stage where it will provide accurate positions during daylight hours in most parts of the world and so it can be utilized as the prime navigation technique along with Doppler or INS (and with video flight path camera backup) in aeromagnetic surveys i.e. it is now an operational reality. As of August 1, 1991, sixteen satellites were operational in orbit with additional GPS satellites being launched approximately every two months or so.

The present plan of the US Air Force is to have a total of 21 GPS satellites plus 3 spares that will be equally distributed in six orbital planes around the earth. The full constellation should be in place by 1993. A similar 24-satellite system in 3 orbital planes called Glonass is also planned by the USSR and may be fully deployed about the same time as GPS. Both Trimble Navigation Ltd. and Ashtech Inc. both of Sunnyvale, California are building combined GPS/Glonass receivers.

GPS can provide positional fixes with an accuracy of about 10 metres that is more than adequate for airborne geophysical surveying. Unfortunately the

most recent series of satellites launched, the so-called Block II GPS satellites have a built-in capability of degrading the accuracy to civilian users by a combination of dithering the satellite clock and data manipulation of the ephemeris. This degradation is euphemistically referred to as Selective Availability and reduces accuracy to civilian users to no better than about 100 metres. Full accuracy can be restored by employing a second fixed ground receiver to record the dithering to that it can be nullified by a subtraction (or differential) process.

The use of GPS has already had a number of beneficial effects to the practice of aeromagnetic surveying. Firstly surveys can be carried out in any part of the world to the same navigational accuracy whatever the terrain. Secondly, a much more even network of traverse and control lines can be flown because the pilot does not have to navigate visually by map reading. He can simply utilize the GPS left-right indicator mounted in the cockpit to guide him along the survey lines. Indeed pilots are flying without the benefit of topographic maps; they only need to input the latitudes and longitudes of the waypoints along the lines into the GPS receiver. Thirdly the flight path recovery process can be automated because the GPS positions are digitally recorded and a minimum of visual point picking is then required to verify the position of the flight lines. This has reduced the overall cost of aeromagnetic surveys especially for offshore surveys and for surveying areas of featureless terrain where no existing electronic navigation chain is in place. It should be mentioned that GPS is normally utilized in combination with INS or with Doppler so that if there are short periods of GPS dropouts or reductions in the number of satellites in view, the INS or Doppler will fill in for short periods and otherwise reduce any scatter in the GPS fixes. Most airborne geophysical contractors are now utilizing GPS in their survey operations and its use should improve considerably the overall quality of the resultant survey data and maps.

2.1.5 Ground Diurnal Stations

In order to monitor the daily (diurnal) variation of the earth's magnetic field, it is imperative that a ground station be continuously operated at the base of operations. Because the resultant data should be free of interference from vehicular traffic etc., the sensor itself has to be located in a magnetically quiet location. The resultant data is normally digitally recorded at a one-second interval during survey operations but an analog recording is required on a continuous basis so that the general state of the diurnal activity can be ascertained over the previous few hours by the flight crew prior to the start of flying. Clearly if a magnetic storm is in progress or if the activity is unusual, there is no point in flying. Control lines are also best flown on quiet days. The diurnal data is normally a deliverable in most aeromagnetic surveys to the client organization.

2.2 Aeromagnetic Survey Specifications

Airborne magnetometer surveys for mining exploration are usually carried out at a mean terrain clearance of 150 metres and a line spacing of 400 metres or less. In Canada, where over 10,000,000 line kilometres of aeromagnetic survey have been flown by government agencies since 1947, a line spacing of 800 metres and a survey altitude of 300 metres has been used to obtain regional aeromagnetic coverage. Aeromagnetic surveys flown for mineral exploration purposes are usually flown at a constant mean terrain clearance to obtain the greatest detail in the field variations whereas those flown for petroleum exploration purposes are usually flown at a constant barometric altitude to permit the greatest accuracy in determining the sedimentary thickness by forward or inverse depth determination methods. The choice of survey altitude and line spacing are interrelated because, in contouring an aeromagnetic map, features have to be followed across the flight lines. Lower flight elevations will produce more detailed profiles i.e. greater resolution of the anomalies, and it is therefore necessary to reduce the distance between the flight lines in order for the contour map to accurately map the field. For optimum results, the flight line spacing should be about twice the distance

of the aircraft above the magnetic basement. For adequate sampling along the flight line, the sample interval should not be more than one-quarter of the vertical distance from the survey aircraft to the magnetic basement i.e. 75 metres for aeromagnetic surveys flown at 300 metres over Precambrian Shield terrain.

The flight line direction should normally be oriented to cross the geological strike of the basement rocks approximately at right angles. However at low magnetic latitudes (inclination less than 20°) because the magnetic anomalies are mostly produced by susceptibility changes across east-west striking rock contacts (and not by susceptibility changes across N-S striking rock contacts), it is mandatory to orient the flight lines approximately in a north-south direction regardless of the geological strike.

Because the aeromagnetic surveys carried out in the two decades following World War II were mostly flown with one-nanotesla sensitivity magnetometers and the superimposed noise level was relatively high, the contour interval of the resultant maps was commonly 10 nanoteslas. Such surveys are now referred to as standard-sensitivity aeromagnetic surveys, whereas those that utilize more recently developed airborne magnetometers having a sensitivity of 0.1 nT or better with much improved compensation are designated high sensitivity (or high resolution) aeromagnetic surveys. Medium sensitivity surveys are those using magnetometers with sensitivities between 0.1 and 1 nT. Table 1 summarizes the principal specifications for aeromagnetic surveys.

Table 1

PRINCIPAL SPECIFICATIONS FOR AEROMAGNETIC SURVEYS

		Typical Specification
1.	Magnetometer type and sensitivity	Proton Precession/0.1 nT
2.	Compensation Figure of Merit of aircraft and noise level for magnetic recording	4 ± nT/0.25 nT
3.	Sampling interval for magnetic field	0.5 sec.
4.	Navigation	GPS + Video
5.	Digitally recorded parameters - total field, fourth difference of total field, time, altitude, navigation	
6.	Flying height - Mean Terrain Clearance or Barometric	300 m
7.	Flight and control line spacing	1 x 14 km
8.	Diurnal variation allowable	< 5 nT excursion between control lines
9.	Final maps - levelling adjustment, grid size, contour interval, scale	1 nT/km 125 m for 1:50,000 (0.1 inch at map scale); 5 nT CI
10.	Digital data format - line profile and gridded data	

The above information is normally contained in the project report written by the airborne geophysical contractor who carried out the survey. The important parameters can usually be ascertained from the printed maps published by government agencies.

3. Compilation of Aeromagnetic Survey Data

There are five end products available at the completion of an aeromagnetic survey operation: digital magnetic tapes, cassettes or discs containing the total field, terrain clearance, time, and position co-ordinates, video camera tapes, the aircraft operators log, analog monitoring records of the recorded digital data and the diurnal ground station data.

Figure 2 summarizes the various processes involved in compiling aeromagnetic data into contour map form. The compilation process proceeds in two parallel activities. The flight paths of the survey aircraft are first plotted and inspected to see that no gaps in the coverage exists. It is usual for a speed check to be made at this stage to identify along-track errors in the flight path recovery process. The speed check consists essentially of computing the average speed of the aircraft between the picked fiducial points along the profile. Since the average speed along a given flight line (for a fixed-wing aircraft) remains constant within a few percent, a wrongly positioned fiducial point will result in adjacent high and low calculated speeds with respect to the average.

The second parallel activity consists firstly of editing the total field data and removing spikes etc. This can be done automatically utilizing the fourth difference technique (see Fig. 3) because individual spikes are amplified by a factor of ten in the fourth difference, whereas the geological signal is removed (Hood et al., 1979).

The next step is the levelling process which utilizes the differences at the intersections of a set of control lines flown at right angles to the main series of traverse lines and the traverse lines themselves. In the levelling process, the errors in the differences are minimized. Because subjective decisions must be made in the process, it is usually best to adjust the levelling in a series of iterations by printing out or plotting the differences for guidance.

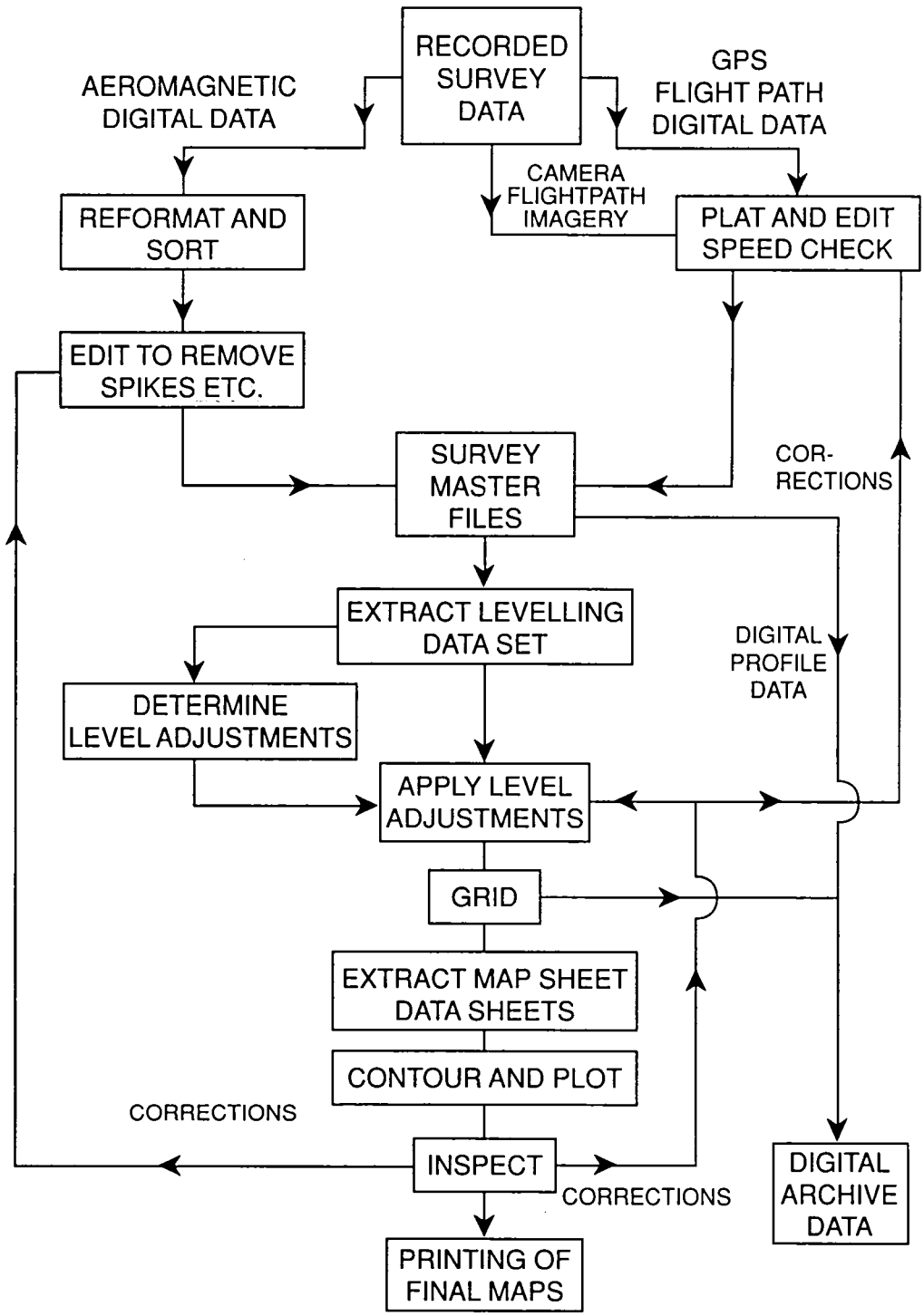

Figure 2 Flow chart for aeromagnetic data reduction

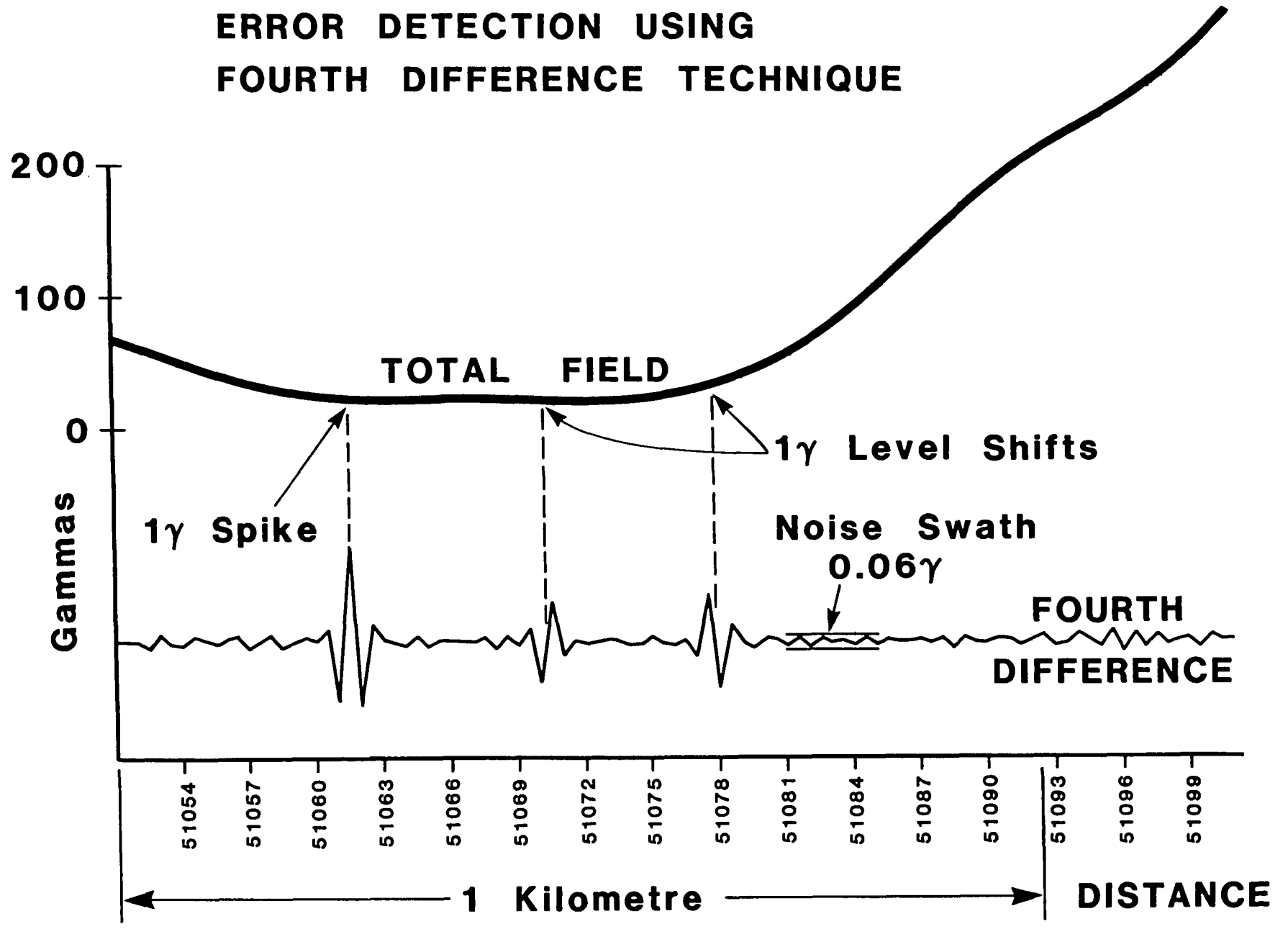

Figure 3 Error detection using the fourth difference technique

The data is then gridded using a suitable interpolation process such as the Akima technique (1960). A common grid size is 2.5 x 2.5 mm at the publication scale. In general, the gridding method involves fitting smooth, continuous interpolation functions along parallel lines normal to the flight line direction. Each function has values equal to the magnetic measurements on the flight lines at the points where the two sets of lines intersect. The interpolation function lines are spaced apart at an interval equal to the ultimately desired fine grid interval and the functions are evaluated along these lines at points separated by the same interval, thus producing the fine grid directly. By this method the contours when traced pass within 0.01 cm of their true flight line intercept position and all fine detail is preserved. The resultant contoured data is then inspected for noticeable aberrations since the compilation process itself is a rather stringent check on the quality of the data used in making the contour map.

The most common scale used by government agencies for the compilation of standard sensitivity aeromagnetic maps is 1:50,000 because it is the same scale used for the national geological map series and/or the national topographic map series. The resultant printed aeromagnetic maps normally have the flight line information shown in a different colour from the aeromagnetic contours so that users can assess how well a given anomaly has been defined. Thus for a 1 km flight line spacing, the flight lines appear at 2 cm intervals on 1:50,000 scale maps which is an appropriate presentation interval for airborne surveys. It is also usual to have the planimetry and drainage from the concomitant topographic maps appearing as a subdued background on the aeromagnetic maps so that the anomalies can be located with respect to geographic features to facilitate the ground follow-up of anomalies of interest.

It is also standard practice to produce aeromagnetic composite maps at a smaller scale of one-quarter to one-fifth that of the detailed contour maps. Thus to accompany 1:50,000 aeromagnetic maps, 1:250,000 maps are often prepared by

photographic reduction of the 1:50,000 maps. The flight lines are generally omitted from these composite maps because their resultant closer spacing usually distracts from the ready identification of regional geological trends. Upon the release of the published aeromagnetic maps, it is common practice for agencies to also make available both the gridded and line profile digital data.

4. Quality of Aeromagnetic Data

The overall quality of a particular aeromagnetic survey and the resultant data depends on the cumulative effects of a series of factors the most important of which may be summarized as follows:

(1) the accuracy and sensitivity of the magnetometer employed.

(2) the bias offset and noise level imposed on the data by the moving survey platform i.e. aircraft (see Fig. 3).

(3) the positioning accuracy of the navigation system employed.

(4) the overall suitability of the survey specifications utilized such as the flight line spacing/depth to magnetic basement ratio and direction with respect to the major geological strike (see Table 1).

(5) the suitability of the data reduction procedures employed in compiling the aeromagnetic data and the quality control procedures used in detecting and removing aberrations in the resultant data set (see Fig. 2).

4.1 Calibration and Compensation of Aeromagnetic Survey Instrumentation (Hood, 1991a)

In considering the influence of the survey aircraft itself on the magnetic field recorded by an inboard magnetometer, the interference can be divided into static and dynamic effects as follows:

(1) the static effect is due to the permanent and induced magnetic fields produced by the ferrous components of the aircraft, by eddy currents induced in the skin of the aircraft and by DC current loops in the electrical system which slightly change the base level of the magnetic readings. The amplitude of the static effect will depend on the heading of the aircraft with respect to magnetic north because the orientation of the induced magnetization of the various ferrous components will change as the earth's magnetic field vector changes with respect to the aircraft flight direction.

(2) the dynamic effects are produced by the various oscillatory movements that all aircraft experience as they fly and by electrical interference from within the aircraft. These dynamic effects show up as noise on the resultant recorded data.

Thus the total field value recorded at any instant by an inboard magnetometer will differ somewhat from the true value due to the magnetic field produced by the aeromagnetic survey aircraft itself. In any discussion of whether the measured total field values correspond to the actual total field values, there is also the question of the accuracy of the basic magnetometer circuitry utilized in measuring the frequency. Frequency measuring devices invariably require an accurate internal clock or timing device whatever the actual technique that is utilized. Consequently it follows that some form of calibration check is desirable in using airborne magnetometer system.

4.1.1 Noise on Aeromagnetic Survey Data

The different types of noise that are recorded in aeromagnetic survey operations may be divided into two main categories - continuous and discontinuous noise. Discontinuous noise occurs as isolated spikes or a series of closely-spaced spikes forming a wave train in the magnetic field data usually as a result of some action of the flight crew although there can be external causes. These external causes would include close lightning bursts, the presence of a DC train, street car (tram) or power line system in the survey area, and in the case of optical absorption magnetometers, the passing of the aircraft through a radar or TV repeater beam. The actions of the crew that would cause discontinuous noise include

(1) radio transmissions particularly HF,

(2) the switching of equipment drawing DC current, e.g. auto pilots,

(3) relocation of ferrous objects in the cabin of the aircraft such as tool boxes.

Continuous noise for inboard installations is produced both by the flexing of the aircraft during turbulence and by its overall manoeuvre pattern relating to the attitude of the aircraft as it flies. The flexing of the aircraft will produce a (high frequency) noise swath on the magnetic field signal while the overall manoeuvre pattern (rolls, pitches and yaws) will tend to modulate the magnetic field signal at a somewhat lower frequency. A lower frequency modulation can also be produced by bird swing if the magnetometer is towed such as in helicopter-borne vertical gradiometer systems. The period of oscillation depends on the length of the tow cable and is usually of the order of 10 seconds. In high sensitivity survey installations, the use of a flight path camera that has a DC motor can produce a small spike every time the shutter is activated. One of the

most effective ways of measuring the noise swath is by computing the fourth difference of the digital data (Hood et al., 1979). The noise at value ΔT_o

$$= \frac{\Delta T_{-2} - 4\Delta T_{-1} + 6\Delta T_0 - 4\Delta T_1 + \Delta T_2}{16}$$

where ΔT_{-2}, ΔT_{-1}, ΔT_1, and ΔT_2 are respectively the four recorded values located symmetrically with respect to the central value ΔT_o. Thus by calculating the fourth difference of the recorded data in flight using in turn five adjacent values, the noise level at the sampling frequency can be monitored by the instrument operator continuously using an analog chart recorder. Any spikes or changes in the datum level of the data will also be readily apparent to the operator, because these appear as a distinctive wave train on the fourth difference trace (see Fig. 3).

4.1.2 Acceptable FOM Levels

Under normal turbulence conditions, the noise level appears to be linearly dependent on the figure of merit (FOM) of the survey aircraft (see Section 2.1.2 for definition). In fact as a rough guide in average turbulence conditions over land areas, the empirical relationship appears to be

$$\textit{Noise Level} = \frac{FOM}{15} \quad (\textit{Hood}, 1986a)$$

which is slightly less than the average for the FOM manoeuvres as would be expected. But in very calm air, the noise level would be somewhat less.

Thus for the 1 nanotesla regional surveys of the 1970's in Canada, the FOM specified was 12 nanoteslas. With improved compensation the specified FOM has been reduced to 4 nanoteslas for a concomitant 0.25 nanotesla noise level.

4.1.3 Calibration of Aeromagnetic Survey Systems

General

The calibration of aeromagnetic survey systems should preferably be carried out immediately before and at the close of survey operations. In addition, if there are major repairs or changes to aircraft instrumentation during the course of a survey, then the calibration should be repeated to check that the units of the geophysical parameters recorded are accurate. If several aircraft are being utilized to survey adjacent areas then the calibration of each will avoid the possibility of level shifts in the measured geophysical parameter across the common boundary between the survey areas flown by the different aircraft.

Aeromagnetic Calibration Ranges

The first step in the calibration procedure is to compensate the survey aircraft as described earlier to obtain the lowest figure of merit possible. A check should then be made that the background noise of the data acquisition system itself has also been reduced to an acceptable level using the fourth difference technique.

The main purpose of the calibration check is however to establish that the measured total field values recorded by an aeromagnetic survey system correspond accurately to those actually existing at the magnetometer sensor. In Canada, for government aeromagnetic surveys utilizing proton precession or optical absorption magnetometers, an aeromagnetic calibration range has been set up in a low gradient area at a crossroads near Bourget, Ontario which is approximately 45 km east of Ottawa and easily recognizable from the air (Hood & Sawatzky, 1983) and a second calibration range is located in Meanook Alberta,

north of Edmonton. The values at the ground level at the respective calibration crossroads have been tied respectively to the Blackburn or Meanook Magnetic Observatories using calibrated proton precession magnetometers. The values at 150 m and 300 m elevation above the calibration crossroads have been measured by flying a survey aircraft at various heights across the crossroads to ascertain the vertical change which is about 12 nanoteslas in 300 m positively upwards. Thus the total field values at the two levels above the crossroads have been tied to within a few nanoteslas to the continuously recording magnetometer at the Blackburn or Meanook Magnetic Observatories. Because the diurnal variation at each of the calibration crossroads can be expected to follow closely the diurnal variation at the respective observatory, the value can be calculated at any instant of time by subtracting a constant difference value from the Blackburn or Meanook Observatory values.

Aeromagnetic survey aircraft are normally flown along the four cardinal headings across the calibration crossroads with their flight path cameras operating and the field values for each cardinal heading are ascertained at the point above the crossroads. The difference value is subtracted from the Observatory reading at the exact time that the survey aircraft crossed the calibration crossroads to get the true reading. The heading errors for the survey aircraft are also calculated as part of the same calibration procedure.

In general the calibration errors should not exceed 10 nT and the heading errors should be within 5 nT in an acceptable aeromagnetic survey system. For fluxgate magnetometers which measure the total field above an arbitrary datum, Helmholtz coils can be utilized to check the sensitivity of the aeromagnetic survey system in a similar way that ground systems are calibrated.

Some trimming of the compensation will be necessary when the dip and strength of the magnetic field in the survey area differs somewhat from that

where the survey area is normally based. For recently developed active compensation systems, a complete recompensation is easily carried out in a short survey flight.

4.1.4 Lag Tests

It is usually found that there is a difference in time between the instant that a flight path photo or image is registered and the magnetic value is recorded. This results from inertia in the camera motor, non-vertically of the camera, the fact that the magnetic reading is actually an average over a short period of time, etc. In order to ascertain this time difference, usually referred to as lag, it is necessary to fly over a sharp anomaly such as a bridge in both directions and plot the location of the peak of the anomaly with respect to its position on the ground from the imagery. The resultant displacement in the position of the peak of the anomaly will give twice the lag that is normally expressed in seconds. A typical value might be 0.5 seconds. Some care should be taken in the resultant compilation process that the lag is removed in the correct sense. If this is not done correctly, it will appear as so-called "herring boning" in the contouring across adjacent lines flown in the opposite direction.

5. Worldwide Aeromagnetic Survey Coverage

After the start of aeromagnetic surveying in 1946, the rate of coverage was initially slow because it took some years of surveys to demonstrate the efficacy of the technique in both petroleum and mineral exploration applications. The earliest airborne geophysical survey contractors were formed in the late 1940's initially to carry out work in North America. Since that time the numbers of such contractors have increased and presently there are some fifteen companies worldwide that carry out the vast majority of the survey work (Hood, 1986b). The principal clients of such contractors in order of importance are government agencies usually the geological surveys or the equivalent government

organization, petroleum and mining companies. Some government agencies of large countries have also equipped themselves to carry out aeromagnetic surveys.

Certain areas of the world have now been completely covered by low-level aeromagnetic surveys; by low-level we mean less than 1000 m terrain clearance with most regional surveys being flown at 300 m. The areas surveyed include most of the countries of Europe. Figure 4 shows the aeromagnetic coverage of North America and it can be seen that there has been almost complete coverage of the USA itself and about 75% coverage of Canada. The data was utilized in the compilation of the Magnetic Anomaly Map of North America published in 1987 by the Geological Society of America. The digital data set for the map (along with other aeromagnetic digital data) is available from the National Geophysical Data Center in Boulder, Colorado. However both the USGS and the Geological Survey of Canada have been carrying aeromagnetic surveys for many years so much of the original data is also available in digital form from those organizations.

Figure 5 shows the aeromagnetic survey coverage of Africa using information gathered from various sources including Reeves (1991). Much of the work has been carried out by or for the relevant government geological surveys. In particular, the Canadian International Development Agency, has funded aeromagnetic surveys in Botswana, Cameroon, Ivory Coast, Kenya, Lesotho, Mali, Niger, Rwanda, Upper Volta (Burkina Faso), Zambia and Zimbabwe (Morin et al., 1989). Most of these were carried out under the technical supervision of the Geological Survey of Canada. It can be seen that there has been approximately 80% aeromagnetic coverage of the African continent and that a number of the countries have essentially 100% coverage. About 90% of this data was not digitally recorded in the original survey but will be digitized as part of the African Magnetic Mapping Project (Reeves, 1991) that will produce a magnetic anomaly map of the continent.

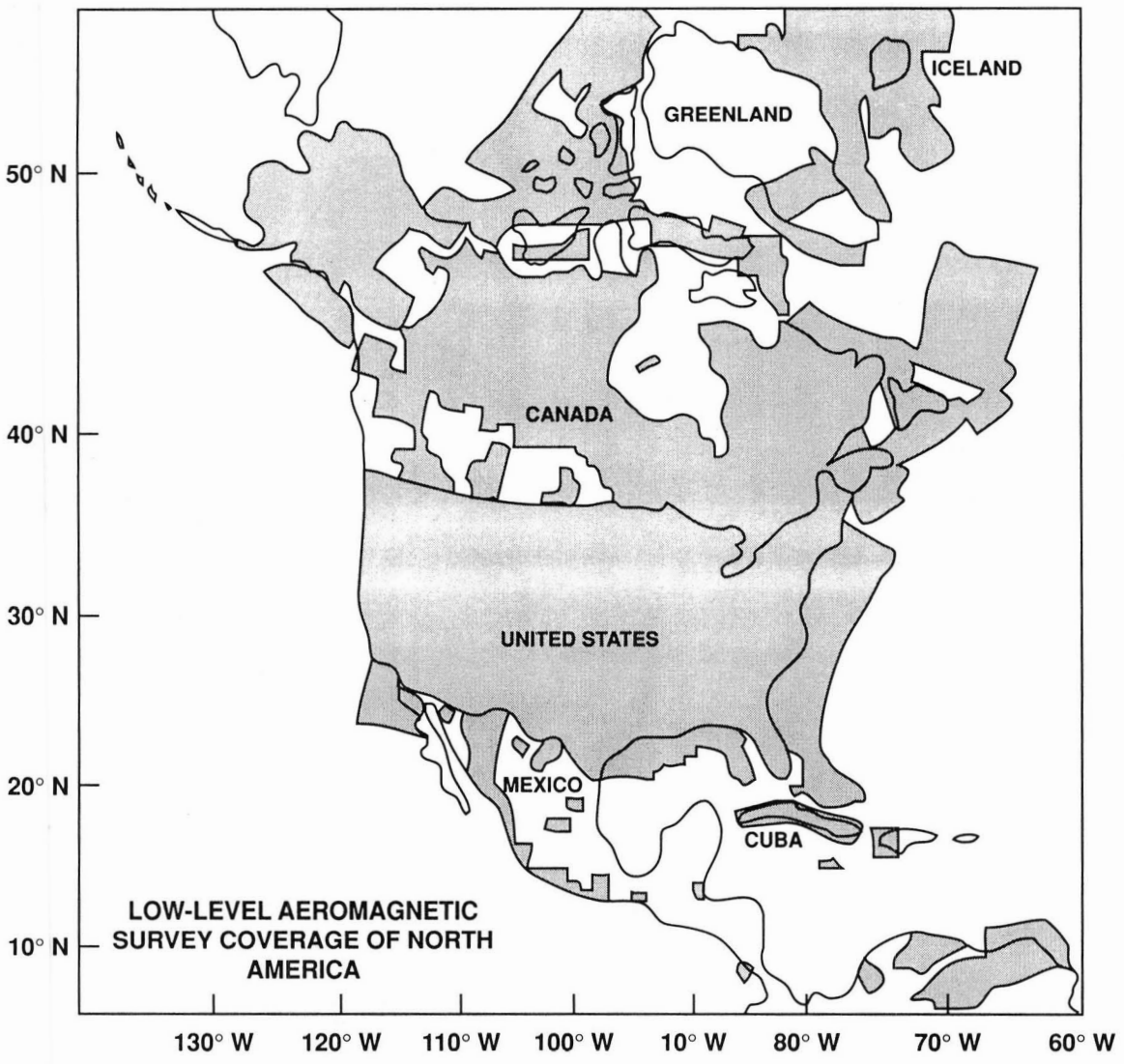

Figure 4 Aeromagnetic Coverage of North America

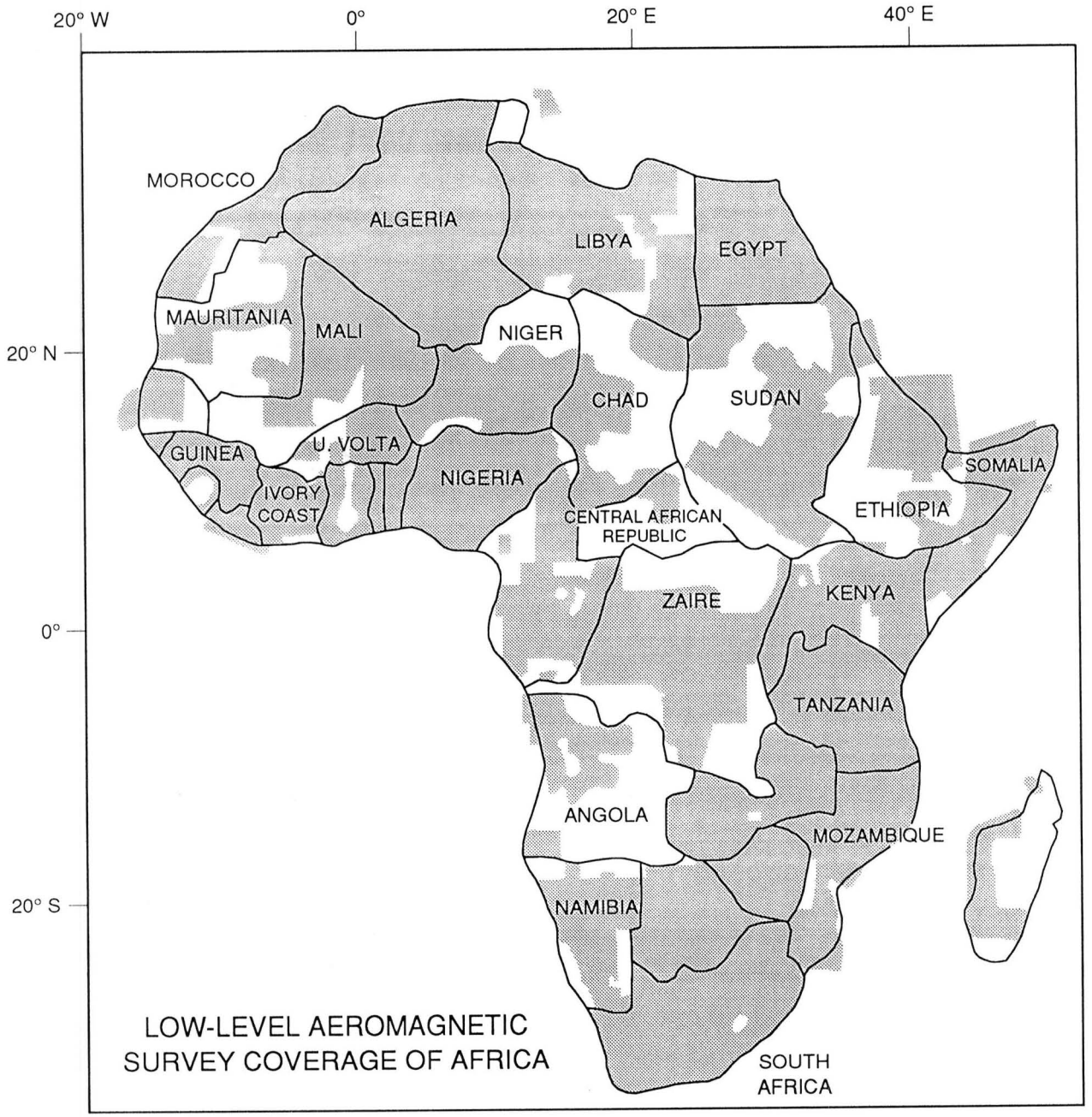

Figure 5 Aeromagnetic coverage of Africa

Figure 6 shows the known aeromagnetic coverage of South America where there appears to be about 50% coverage. Most aeromagnetic survey work appears to have been carried out in Brazil (Berbert, 1989).

Elsewhere in the world, the USSR has complete regional coverage at a 2 km line spacing or so (Makarova, 1974). The resultant 18 maps at a 1:2,500,000 scale were digitized by the US Naval Oceanographic Office and is available from the National Geophysical Data Center in Boulder, Colorado (Hittelman et al., 1991).

China has about 87% coverage that includes all of eastern China (Zou, 1989). Approximately 1:200,000 sq. km of the Yellow, East and South China Seas have also been covered by the Ministry of Geology and Mineral Resources.

A contracted aeromagnetic survey of the whole of Thailand was carried out during the period July 1984 to December 1989 by the Thailand Department of Mineral Resources (DMR). The data are available in both 1:50,000, 1:250,000 contour and 1:1,000,000 colour pixel map form as well as digital profile and gridded form on magnetic tape from DMR (DMR Technical Bulletin 4, 1989).

In Australia, aeromagnetic surveys covering about 80% of the Australian continent have been carried out since 1951 using a flight line spacing of 1.5 km and a terrain clearance of 150 m. About 75% of this data was obtained using fluxgate magnetometers and the remainder was obtained using proton precession magnetometers (Milligan and Tarlowski, 1991). The earlier data has been digitized for a magnetic anomaly map of Australia.

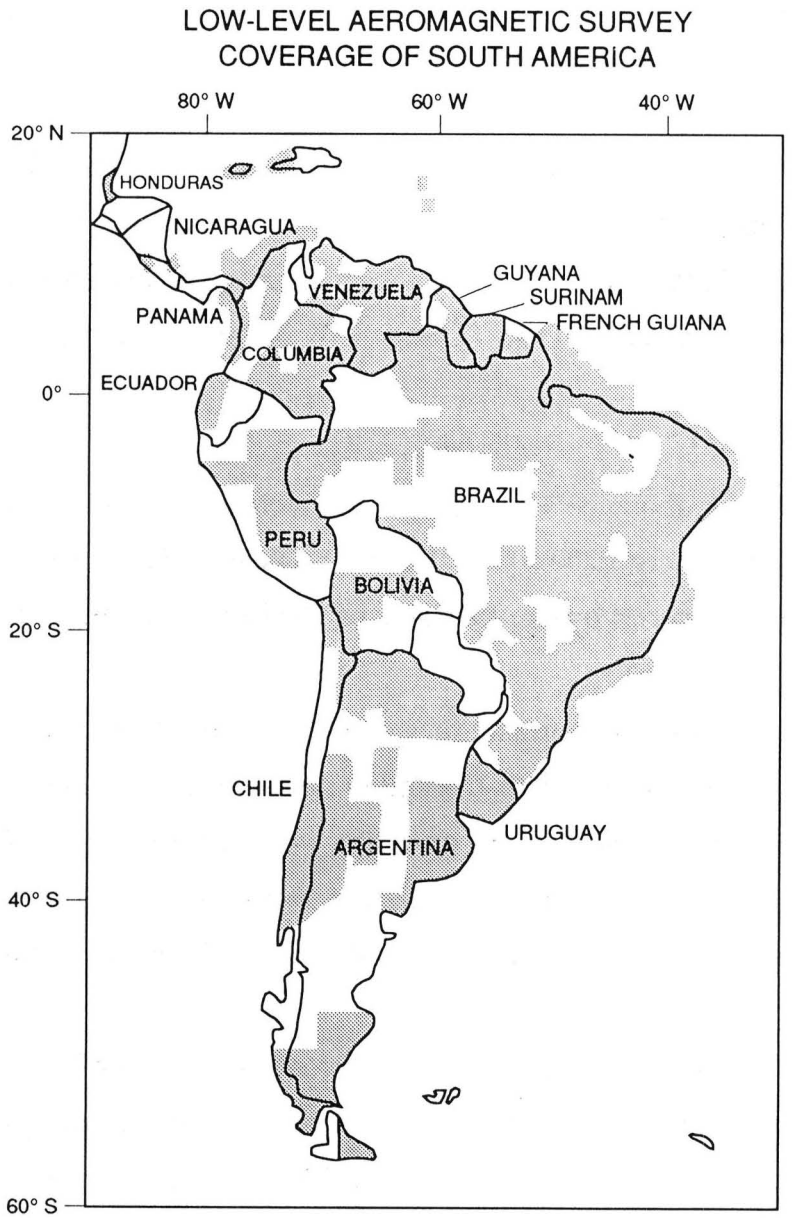

Figure 6 Aeromagnetic coverage of South America

Bibliography

Akima, H. (1970) A new method of interpolation and smooth curve fitting based on local procedures; J. Assoc. Computing Machinery, Vol. 17, No. 4, pp. 589-602.

Balsley, J.R. (1952) Aeromagnetic surveying, Advances in Geophysics; Academic Press Inc., New York, Vol. 1, pp. 313-349.

Berbert, C.O. (1989) Mineral exploration in Brazil: past and present; in Proceedings of Exploration 87 (G.D. Garland, Editor), Ontario Geological Survey, Special Volume 3, pp. 782-789.

Bloom, A. (1960) Optical pumping; Scientific American, Vol. 203, No. 4, pp. 72-80.

Committee for the Magnetic Anomaly Map of North America (1987) Magnetic anomaly map of North America; Geol. Soc. Amer., Boulder, Colo., 4 sheets, scale 1:5M.

Dehmelt, H.G. (1968) Optical absorption monitoring of oriented or aligned quantum systems; Canadian Patent 794,491, Patent Office, Ottawa, 82 pp.

Driscoll, R.L. & Bender, P.L. (1958) Proton gyromagnetic ratio; Physics Review Letters, Vol. 1, pp. 413-414.

Fromm, W.E. (1952) The Magnetic Airborne Detector; Advances in Electronics, Vol. 4, pp. 257-299.

Giret, R.I. (1965) Some results of aeromagnetic surveying with a digital cesium-vapour magnetometer; Geophysics, Vol. 30, pp. 883-890.

Hittelman, A., Buhmann, R. & Meyers, H. (1991) USSR magnetic anomaly data; in Magnetic Anomalies on Land & Sea, IAGA Working Group V-9 Newsletter, pp. 37-38.

Hood, P. (1970) Magnetic surveying instrumentation - a review of recent advances; in Mining and Groundwater Geophysics/1967, (L.W. Morley, Ed.), Geol. Surv. Can., Econ. Geol.. Rept. 26, pp. 3-31.

Hood, P. (1986a) Discussion on "Important design considerations for inboard magnetic gradiometers" by C.D. Hardwick, Geophysics, Vol. 49, pp. 2004-2018, Nov. 1984; Geophysics, Vol. 51, No. 1, pp. 192-193.

Hood, P. (1986b) Aerial prospecting; Mining Magazine, August, pp. 91-113.

Hood, P. (1991a) Calibration and compensation of aeromagnetic survey aircraft; Chapter 6 in Guide to aeromagnetic specifications and contracts, Aeromagnetic Standards Committee, Geol. Surv. Can., Open File 2349, pp. 48-52.

Hood, P. (1991b) Geophysics: The tools of the trade; N. Miner Mag., Vol. 6, No. 1, pp. 12-40.

Hood, P. and Lefebvre, D. (1991) Instrumentation; Chapter 4 in Guide to aeromagnetic specifications and contracts, Aeromagnetic Standards Committee, Geol. Surv. Can., Open File 2349, p. 28-41.

Hood, P.J., Holroyd, M.T. & McGrath, P.H. (1979) Magnetic methods applied to base metal exploration; in Geophysics and Geochemistry in the Search for Metallic Ores, Ed. P.J. Hood, Geol. Surv. Can., Econ. Geol. Rept. 31, pp. 77-104.

Hood, P. and Ward, S.H. (1969) Airborne geophysical methods; Adv. In Geophysics, Academic Press, New York, Vol. 13 pp. 1-112.

Hood, P. & Sawatzky, P. (1983) Bourget aeromagnetic calibration range; in Current Research, Part A, Geol. Surv. Can., Paper 83-1A, pp. 483-485.

Jensen H. (1961) The airborne magnetometer; Scientific American, Vol. 204, pp. 151-162.

Jensen, H. (1965) Instrument details and applications of a new airborne magnetometer; Geophysics, Vol. 30, pp. 875-882.

Makarova, Z.A. (Ed.) (1974) Map of the anomalous magnetic field of the territory of the USSR and adjacent water areas. USSR Ministry of Geology, St. Petersburg, 18 sheets, Scale 1:25M.

Milligan, P. & Tarlowski, C. (1991) The magnetic anomaly map of Australia; in IAGA Session GAM 5.18, National and International Magnetic Anomalies - Recent Results and Comparisons, 20th General Assembly IUGG, Vienna, Aug. 15.

Morin, M., Turkeli, A. & Lauzier, J.C. (1989) The Canadian International Development Agency (CIDA) and the mining sector; in Proceedings of Exploration 87 (G.D. Garland, Editor), Ontario Geological Survey, Special Volume 3, pp. 790-797.

Overhauser, A.W. (1953) Paramagnetic relaxation in metals; Physics Review, Vol. 89, pp. 689-700.

Packard, M. & Varian, R. (1954) Free nuclear induction in the earth's magnetic field, Physics, Review, Vol. 93, p. 941.

Reeves, C.V. (1991) The African Magnetic Mapping Project (AMMP); AGID News, No. 66, pp. 18-19.

Thailand Department of Mineral Resources (1989) Thailand nationwide airborne geophysical surveys, Thailand Department of Mineral Resources, Technical Bulletin No. 4, 12 p.

Zou, G. (1989) Integrated geophysical and geochemical exploration in China; in Proceedings of Exploration 87 (G.D. Garland, Editor), Ontario Geological Survey, Special Volume 3, pp. 771-781.

Magnetic Repeat Station Data

C.E. Barton, BMR Geology & Geophysics, PO Box 378, Canberra ACT 2601, Australia.

Abstract

The nature, purpose, availability and distribution of magnetic repeat station data are reviewed. Attention is paid to how repeat station data are obtained, sources of errors and limitations on accuracy. Repeat station results cannot achieve the accuracy of magnetic observatory estimates of the secular variation, but are, nevertheless, essential for improving the limited spatial coverage provided by observatories. The lack of appropriate standards and reporting procedures have meant that most global field modelers have made little, or no, use of repeat data. Partly to rectify this problem, IAGA Working Group V-4 has instigated a scheme for systematic reporting and classification of magnetic repeat station data. The scheme will help to ensure that proper use is made of the wealth of repeat data that is available, and will also promote better observational practices.

Introduction

From a practical point of view a knowledge of the secular variation of the Earth's magnetic field is important for up-dating magnetic survey data and forward-extrapolation of the field. Indeed, most regional and global models of the geomagnetic field (notably the International Geomagnetic Reference Field, IGRF) rely heavily on secular variation information.

The most accurate information we have about the secular variation is obtained from the global network of permanent magnetic observatories. The secular variation is usually derived from the difference between observatory annual means, the latter being calculated either for all days (the traditional approach) or for some particular selection thereof. Unfortunately the distribution of magnetic observatories is very irregular, with a large number of observatories in Europe and very few in many other parts of the world, particularly in the southern hemisphere and the oceans. The purpose of repeat station measurements is to determine the secular variation for land areas where observatory coverage is inadequate (Figure 1).

Repeat station data have been used widely for regional field modelling, but are rarely used for global field modelling, other than as ordinary vector survey data. The main reason for this is the large variation in quality of repeat data, and the inadequacy of international reporting procedures.

For detailed practical information about repeat station practices, the reader is referred to the new guide being prepared by Working Group V-4, Magnetic Surveys and Charts of the International Association of Geomagnetism and Aeronomy, IAGA (Newitt et al., due for completion in 1992).

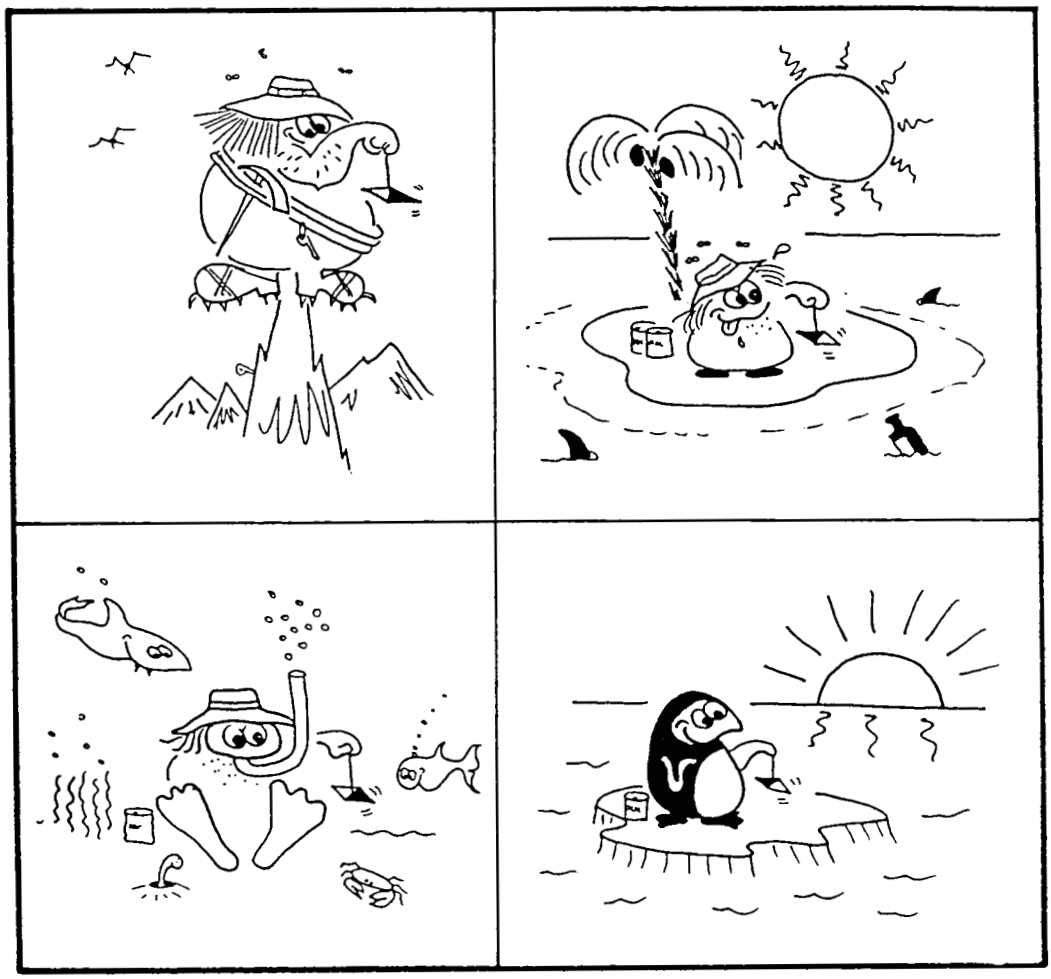

Figure 1. Repeat stations provide secular variation information where observatory coverage is inadequate.

Magnetic repeat stations and magnetic survey stations

A magnetic repeat station is a fixed point on the Earth surface marked either by a permanent non-magnetic marker at ground level (for example, a brass plaque set in concrete slab), or by a pier. The station is visited at regular intervals to make accurate absolute measurements of three or four components of the magnetic field.

In principle there is a fundamental difference between ordinary magnetic survey stations and repeat stations. The former are used for mapping the main (core) field plus crustal field. Because the crustal field contains short wavelength information, a high density of survey stations is necessary. Furthermore, the amplitude of field variations on a local scale is large compared to the secular variation, so there is no need either to locate magnetic survey stations accurately, or to make accurate corrections for external field effects. At repeat stations both these factors must be given careful attention. Vector measurements at ordinary

survey stations can take as little as half and hour (or only a few minutes if total field alone is measured), whereas repeat station observations usually span several days. Consequently it is only possible to occupy a limited number of repeat stations.

The distinction between ordinary magnetic survey data and repeat station data is often blurred, with the tag "repeat data" being used to describe any vector observations of the field made at a fixed point. This confusion affects some of the data held by the World Data Centers and has limited the usefulness of repeat data. IAGA has recently adopted a reporting scheme designed to overcome such problems (Appendix). If no correction is made for external field effects, and/or relocation of the station is not exact, "repeat" data can only be used to estimate the average secular change over a long interval of time. Under such circumstances there is no point in making frequent repeat observations.

Repeat station spacing requirements

Despite the many years of effort that have gone into observatory geomagnetism, it has never been possible to determine the surface station spacing required to sample the secular variation properly on a global scale. This is simply because no surface data set has ever had sufficient spatial resolution to over-sample the secular variation signal at the Earth's surface (although there is the expectation that long-duration low-altitude satellite missions will solve this problem in the future).

The International Union of Geodesy and Geophysics (IUGG) recommends that, for the purposes of main-field mapping, surface measurements of the magnetic elements should be made at a spacing of about 200 km (Vestine, 1961). A similar spacing is generally accepted as desirable for observing the secular variation. Given that main field sources lie in the core, more than 2800 km below the surface, a purely geometrical argument would suggest that a station spacing of 200 km should be more than adequate to sample the secular variation. However, in Europe, where the observatory spacing is typically of this order, many countries still operate repeat station surveys with considerably higher densities of stations. Results from such surveys do indeed indicate that they recover additional detailed information about the secular variation. This may well include a contribution from crustal sources, e.g. piezomagnetic effects in tectonically active regions, or seasonally-varying induction effects, particularly near the oceans.

Re-occupation interval

With the limited resources available to most survey agencies, it is usually necessary to strike a balance between the number of stations occupied, the frequency of occupation and the accuracy of data obtained from each station. With this in mind it is necessary to focus on the main purpose for making repeat station measurements. For example, for updating regional magnetic field charts every 5 years (say), repeat observations are needed only every five years (provided the observations are made near the 5-year epoch boundaries). Determination of the character of secular variation impulses (jerks) places the most stringent requirements on observations. In this context, even observatory data are barely adequate to decide whether

jerks are world-wide in character and of internal or external origin (Courtillot and Le Mouël, 1978). Repeat station occupation intervals suggested by Newitt et al. (in preparation) are:

5 years	for updating regional magnetic charts
2 years	for producing secular variation models
1 year	for detecting secular variation impulses (geomagnetic jerks)

The two-year re-occupation interval is recommended by IAGA.

Location of repeat stations

Repeat stations must be positioned where there is no change in the local magnetic environment between successive reoccupations. Localities with high magnetic gradients, or anomalous sub-surface electrical conductivity properties, should also be avoided. However, the former is not always possible, and the latter is usually unknown and therefore neglected. Induction-related problems (see below) can be ameliorated to some extent by conducting surveys under identical daily, seasonal and magnetic conditions.

External field corrections

Corrections must be applied to the absolute observations made at a repeat station to remove external effects and derive the main field plus static crustal field. (Herein the external field contribution is deemed to include fields produced by internal currents induced by transient external fields). The two approaches to this problem both require reference to records from permanent magnetic observatories.

By far the most convenient and elegant approach is to reference all observations made at the repeat station directly to one (or more) permanent magnetic observatories, and hence derive a pseudo annual mean value for the repeat station. It is assumed that transient (including diurnal) variations of the magnetic field are identical at both the repeat station and the chosen reference observatory during the interval of observations. Thus, the difference between the instantaneous value of an element, E(t), and its annual mean value, **E**, at the repeat station is the same as the difference between the corresponding values, $E_O(t)$ and $\mathbf{E_O}$, at the reference observatory:

$$E(t) - \mathbf{E} = E_O(t) - \mathbf{E_O}$$

hence

$$\mathbf{E} = \mathbf{E_O} + \{E(t) - E_O(t)\}$$

For this to be strictly true the secular variation must be the same at the two locations during the interval between the repeat station occupation and the epoch of the annual mean.

The first assumption is clearly crucial. Proximity of the nearest reference observatory (as reported on the IAGA record sheets - see Appendix 3) is not necessarily a good guide to the validity of this assumption. Depending on the nature and morphology of external field sources, it is possible to find stations as little as a few tens of kilometres apart at which the time-dependent field differences are unacceptably large. This is particularly common in polar latitudes where external field sources show the greatest variability. At the other extreme, Daniel Gilbert (personal communication) cites an example of a repeat station in the Indian

Ocean where very accurate results have been obtained by using reference observatories thousands of kilometres away. The marked difference between the latitude and longitude dependence of the daily variation is also an important factor to be considered when choosing a reference observatory. Some survey agencies (e.g. in South Africa and Britain) use more than one reference observatory and a weighted interpolation scheme that reflects their relative importance.

The second approach is to deploy a three (or four) component variometer on-site. Absolute measurements made at the repeat station are used to calibrate the variometer record. Results are processed in the same way as observatory data so as to derive the night-time value of the field (when disturbance levels are at a minimum, though rarely zero). Even when observations are made under fairly quiet conditions, the night-time value of the field will usually include a small external field contribution (typically up to a few nanotesla). A correction for this contribution has to be estimated from records from one or more observatories in the region. The correction can be applied either directly to get a final result for the internal field at the date of station occupation, or via the observatory record to get a pseudo annual mean value for the repeat station. In the latter case the secular variation assumption mentioned above is made.

Accuracy

Repeat station measurements are prone to several gross errors, such as mis-location of the repeat station, incorrect setting of instrument height above the station ground marker, introduction of magnetic contamination between station occupations, and inadequate procedures for correcting for external field effects. In the absence of such errors, some figures quoted for typical accuracies achieved during repeat station surveys are given in Table 1. The figures in the table do not take into account errors arising from weaknesses in the assumptions made when correcting for external field effects.

Table 1. Typical accuracies of repeat station results†

	D(')	*H(nT)*	*Z(nT)*	*F(nT)*	
Australia	1-2	4-10	5-10	5	McEwin (pers .comm.)
France	1	4	3.5	4	Bitterly and Gilbert, 1988
Italy	2	8	8	8	Molina et al., 1985
Germany	1	3-4	3-4		Mundt, 1980
Switzerland	1-2			10	Fischer et al., 1979
South Africa	2-4	12-24			Scheepers, 1969
U.K.	1.5	6	6	5	Barraclough (pers. comm.)

† After correcting for external field effects

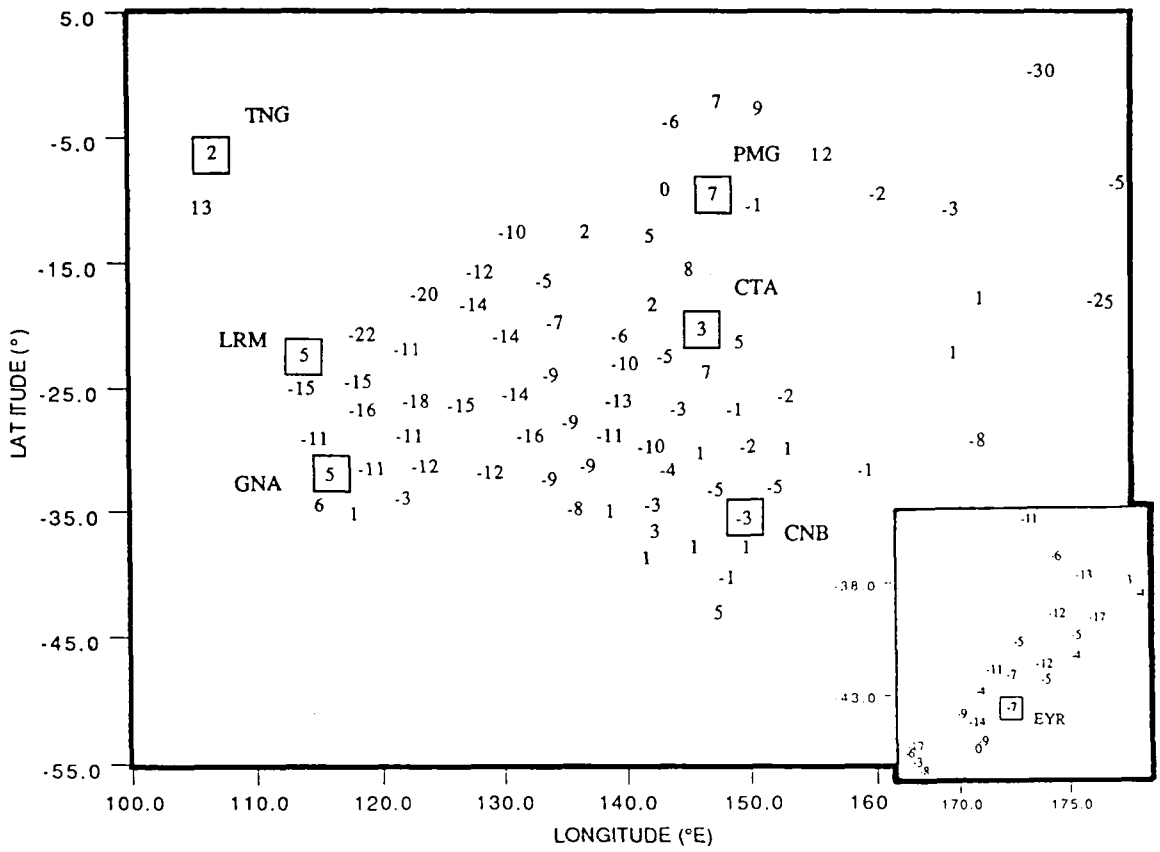

Figure 2. Differences in the annual change in Z for 1990.0 between repeat station estimates and IGRF90 (units of nT yr^{-1}). Boxed values are (observatory - IGRF90) differences. The region covers Australia, Papua New Guinea, Islands in the SW Pacific and New Zealand (inset, expanded to double scale). Observatory codes are: CNB = Canberra, CTA = Charters Towers, EYR = Eyrewell, GNA = Gnangara, LRM = Learmonth, PMG = Port Moresby, TNG = Tangerang. (Data provided by Andrew McEwin and Don McKnight).

An indication of the scatter in repeat station determinations of the secular variation is given by Figure 2. The posted numbers are differences between repeat stations determinations of the annual change in Z and the corresponding values given by IGRF90 (nT yr^{-1}). The area shown covers Australia, Papua New Guinea, some SW Pacific Islands and New Zealand (inset, enlarged by a factor two). This happens to be a good region to choose because the secular variation is quite small, and the data set is among the better ones available. Stations were occupied for a minimum of three days with on-site variometer control, and detailed corrections applied for external field effects. Values posted on the figure are estimates of the annual change of vertical field (Z) for 1990 in nT yr^{-1}; figures in boxes are for permanent magnetic observatories. The repeat station results are derived from a subjective fit to a time series of observations at each station, made at intervals of approximately 5 years. For many SW Pacific Island stations only two successive observations are available. There is overall consistency between the repeat and observatory data, and the repeat data are clearly providing additional information about the secular variation despite the scatter in the results. A noticeable anomaly occurs in the region of Learmonth (LRM) in Western Australia, where the observatory and surrounding repeat data are clearly at odds. Part of the reason for this is that the most recent repeat

observations in that region were made nearly 3 years prior to 1990, whereas the Learmonth value is for epoch 1990.0. However the discrepancy is still surprisingly large and suggests that there may be induction problems in the region. Over such a large region there are many stations where the distance to the nearest reference observatory is 1000 km or more; thus it is often difficult to get an accurate correction for the displacement of the night-time value of the field. This certainly contributes to the scatter in the observations.

The above discussion raises the question of whether good repeat data are adequate for modelling the secular variation over 2-year or 5-year time intervals? Figure 3 shows the present-day distribution over the Earth's surface of the secular variation in total field (F), given by IGRF1990 (IAGA Working Group V-8, in press). The histogram (Figure 3a) shows the percentage of the Earth's surface that experiences secular variation in class intervals of 5 nT/yr from -130 nT/yr to +75 nT/yr. The strong negative bias in the distribution reflects the decay of the Earth's dipole moment. It can be seen that over a significant part of the Earth's surface the annual changes in F are less than the uncertainties quoted in Table 1. This is shown more clearly in a cumulative distribution plot for the absolute value of the secular variation in F (Figure 3b). Some figures for the area of the Earth's surface over which the annual change in F lies within various bounds are listed in Table 2.

Table 2. Distribution of secular variation in F over the Earth's surface given by IGRF1990.

% Area of Earth (%)	*Bounds for SV in F (nT/yr)*
5	± 1
10	± 2.5
15	± 4.7
20	± 7
25	± 9
30	± 12

Suppose that the error in a repeat station result for F is ±5 nT (i.e. at the low end of the range quoted in Table 1), and we determine the secular variation by subtracting results from successive station occupations two years apart. The uncertainly in the secular variation obtained (±5 nT/yr) will therefore exceeds the actual secular variation over about 15% of the Earth's surface. If the repeat station errors were twice as large, then over almost one-third of the Earth's surface the secular variation would be less than the observational uncertainty. The problem is less serious if only the average secular variation is required from observations 5 years apart (or longer). Although these are only generalized figures, they do demonstrate that very careful measurements are required, with accurate corrections for external field effects, in order to obtain results that are useful for developing present-day and predictive secular variation models.

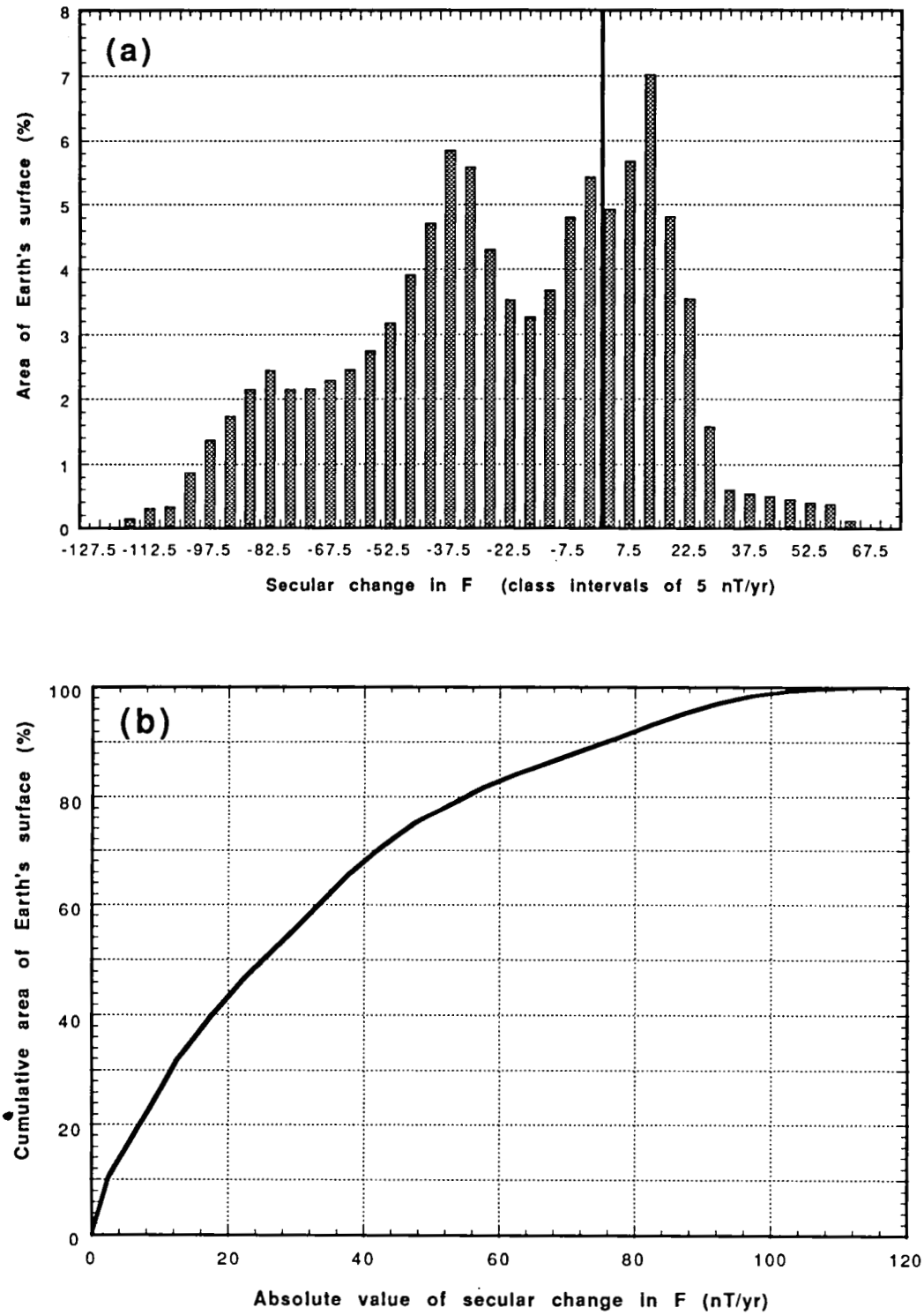

Figure 3. (a) Histogram showing the distribution over the Earth's surface of the secular change in F given by IGRF1990; (b) cumulative area plot of the same distribution.

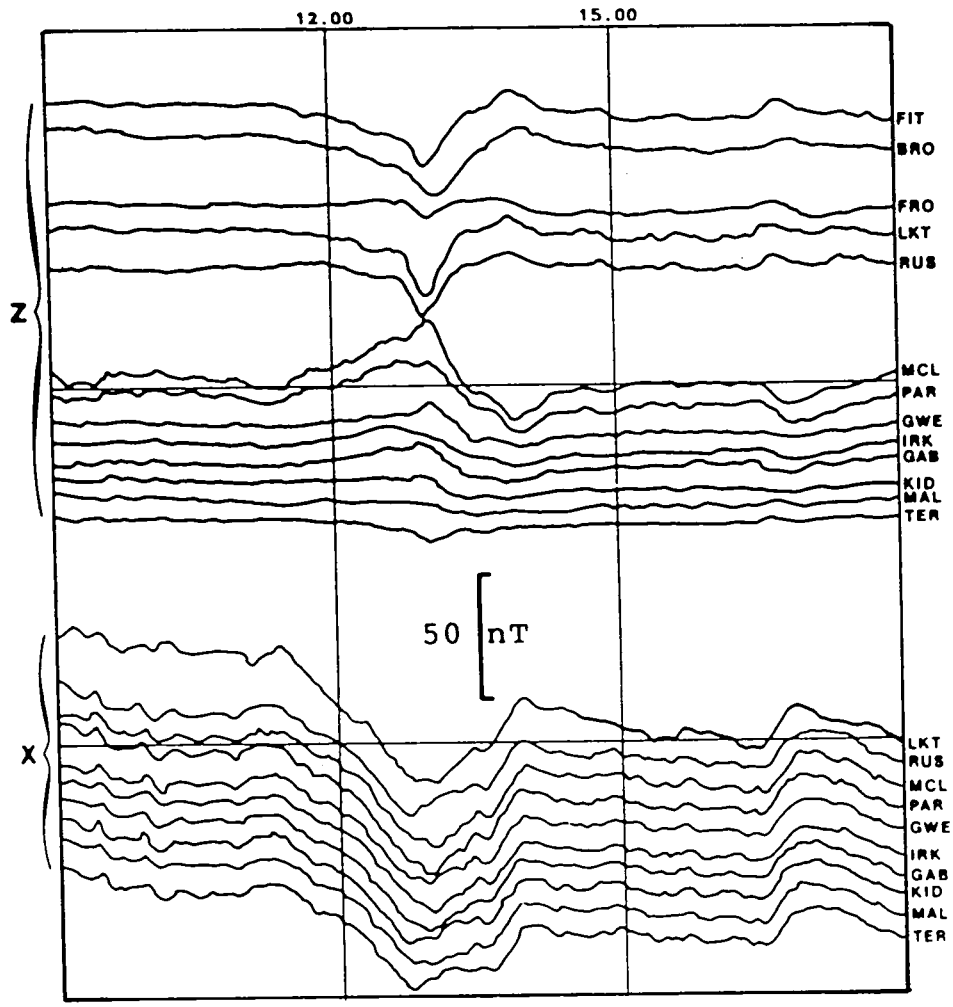

Figure 4. Stacked magnetograms for an event on 4th July 1985, obtained from an array of recording magnetometers in the Canning Basin, northwestern Australia (after Chamalaun and Cunneen, 1990).

Induction effects

Fields produced by internal electric currents induced by transient external sources are commonly treated as part of the external field and otherwise ignored. The problem with this simplification is that, whereas external sources are likely to provide a homogeneous signal over a large region (particularly for magnetospheric sources), the inductive response of the crust can be highly localized. This is illustrated by Figure 4, which shows X and Z magnetograms from an array of magnetometers deployed in the Canning Basin, northwestern Australia (Chamalaun and Cunneen, 1990). The spacing between stations varies between 100 km and 200 km. A sub-surface electrical conductor appears to run through the basin, causing a vertical field anomaly affecting the stations on one side of the conductor (FIT, BRO, FRO, LKT, RUS) in the opposite sense to those on the other side (MCL, PAR, etc.). Station FRO lies almost above the conductor and hence shows only a small Z-anomaly. Differences between signals from nearby stations thus differ by more than 50 nT. Although repeat station observations should not be made under such disturbed conditions, we can conclude that inductive problems may exert an important influence on the range over which reference observatories

can be used for reducing repeat data. The fact that most observatories lie within the range of oceanic induction effects does nothing to improve the situation. Furthermore, because external sources and ocean current systems are subject to seasonal variation, it cannot be assumed that induction effects will average out unless averages are taken over time intervals of several years. For example, Winch (personal communication) has identified a one cycle per year signal of amplitude 2 nT to 10 nT (peaking in March) in observatory annual mean values that he attributes to oceanic dynamo effects.

Early repeat station observations

Repeat station surveys were commenced during the latter part of the 19th century and early part of this century, largely through the efforts of the Carnegie Institution of Washington. External field corrections were generally ignored during these early surveys (Figure 5). The seriousness of this omission depends on the size of the secular variation signal and the time interval between successive station reoccupations. For example, suppose that observations were made during magnetically undisturbed conditions at mid-latitude, where the typical amplitude of the quiet daily variation is about 50 nT. Assuming that the error in the observations arising from external fields is, say, half this figure (25 nT) and that the observations are repeated every 10 years, then the secular variation would have to exceed 5 nT yr^{-1} in order to equal the error in the observations. The spatial distribution of secular variation today (Figure 3 and Table 2) indicates that this would be the case over about 85% of the Earth's surface. Thus uncorrected observations are still valuable for determining secular variation, provided that only an average is required over a sufficiently long interval of time. Bloxham, Gubbins and Jackson (1989) have been able to make good use of historical data for this same reason.

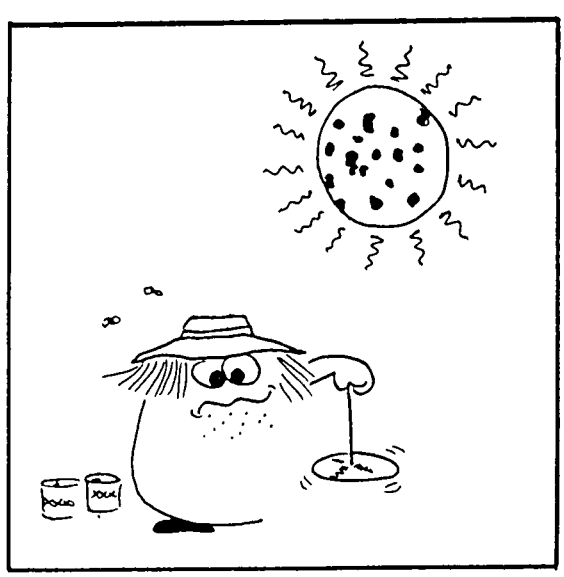

Figure 5. Influence of external field effects on repeat station observations.

World Data Center data holdings

The two principal World Data Centers holding data classified as repeat station data are WDC-A, Boulder, Colorado and WDC-C3, Edinburgh, Scotland. The holdings at these two centers are broadly similar, but by no means identical. The distribution through time of repeat data held by WDC-C3 is shown in Figure 6. Prior to World War-II, repeat station survey work was confined largely to the U.S.A. and Finland. Thereafter many other countries started to undertake repeat station surveys, the main regions of activity being in Europe, Central and South America, Japan, Australia, West Africa, and South Africa. The large peak in 1981 is caused by a large-scale survey in Europe carried out to produce a special declination model (Barraclough, personal communication) and a major new survey in China. Since 1960 the average level of repeat station activity has declined slowly. Some of the decline in recent years may be due to delays in reporting data to the World Data Centers. Figure 7 shows the geographical distribution of the repeat data held by WDC-C3 for five year intervals from 1900 onwards.

Only recent data are useful for present-day and predictive modelling of the secular variation. Data received by WDC-A since 1980, and classified as repeat data, are summarized in Table 3. Data that have been submitted according to the new IAGA specifications are listed in Table 4.

Table 3. Repeat station data held at WDC-A, Colorado submitted between 1980 and 1990.

Country	*Number of repeat stations*	*Date received by WDC-A*
Angola	1	Nov 1980
Botswana	5	Aug 1982
Brazil	~ 600	
Canada	~ 2000	Jan 1983
France	33	Jan 1987
Guatemala	290	May 1982
Japan	24	1980
New Zealand	10	Dec 1981
Peru	10	Jan 1983
Senegal	22	
South Africa	~ 60	Aug 1984
South Africa	13	
United States	60	
TOTAL	*3128*	

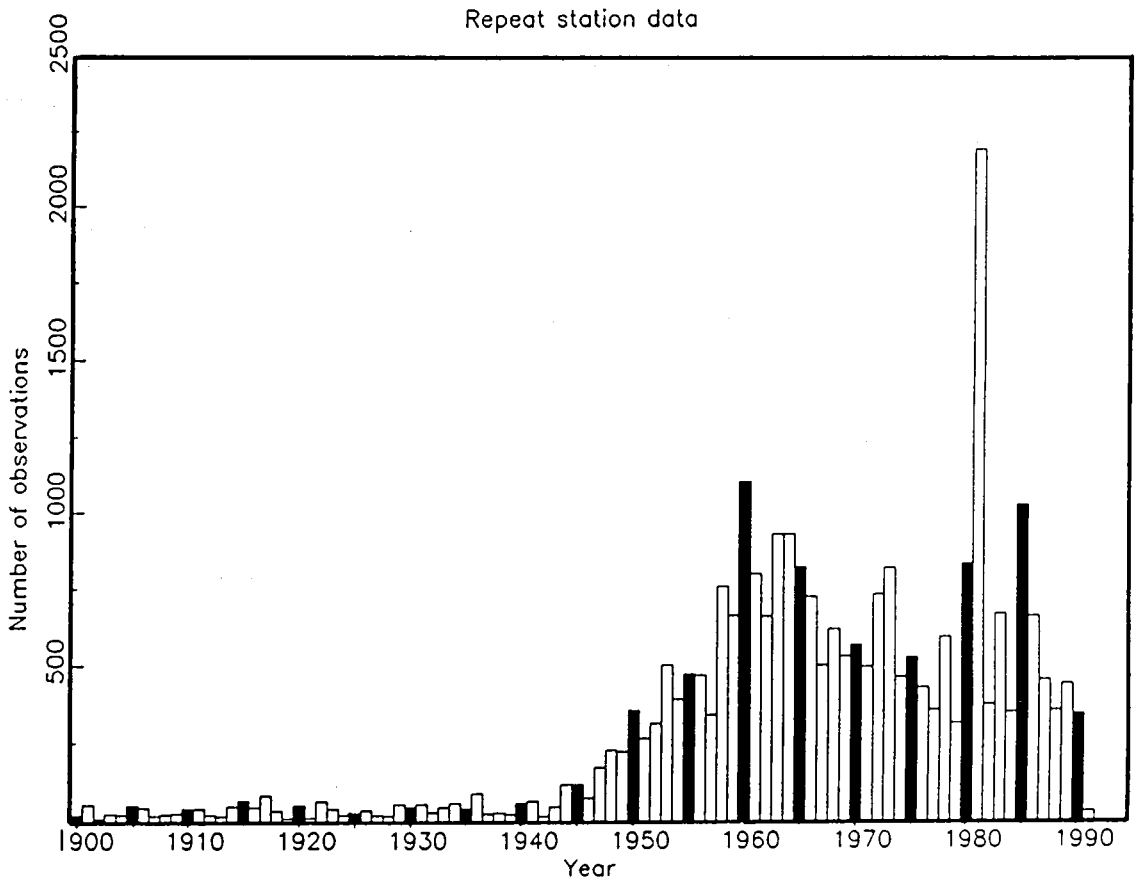

Figure 6. Distribution through time of repeat station data held by WDC-C3, Edinburgh, Scotland. Columns at 5-year intervals are shaded black. (Plot provided by D. Barraclough).

IAGA scheme for reporting and classifying repeat station data

A scheme for classifying and reporting magnetic repeat station data, developed by IAGA Working Group V-4, was formally adopted at the IAGA General Assembly in Exeter, July 1989. The scheme is designed to ensure regular reporting of repeat data in a standardized form. One of the principal aims is to improve quality control and provide sufficient information for the data to be used properly for global field modelling. It is hoped that the scheme will also encourage better observational procedures.

A description of the scheme is given in the Appendix. Each agency conducting repeat station surveys is asked to submit: (i) a regional magnetic repeat station network description giving general information about the network, observational methods and data reduction procedures, (ii) a record sheet for each occupation of a station, giving the main results, information about accuracy and an alpha-numeric classification code, and (iii) a computer file summarizing the results of a particular survey and/or a compilation of results from many surveys. Agencies are requested to lodge this information at WDC-A. IAGA Working Group V-4 maintains a catalog of the "Regional Magnetic Repeat Station Network

Descriptions" (IAGA Working Group V-4, 1991).

Countries that have lodged repeat station network descriptions under the IAGA scheme are listed in Table 4, together with the number of repeat stations operated and dates when data were sent to WDC-A.

Table 4. Countries participating in the new IAGA reporting scheme.

Country	*Number of repeat stations*	*Date received by WDC-A*
Albania	34	
Australia	68	1990+
+ Papua New Guinea	6	1990+
+ SW Pacific Is.	9	1990+
+ Antarctica	~50	
Brazil	105	
Britain	16	1990+
Canada	59	1990+
China	98	1990+
Finland	25	
France	38	1990+
+ Polynesia		
+ West Africa†	50	
+ Antarctica	1	1990+
Indonesia	59	
Italy	110	
Japan	105	
Mexico	50	
Moçambique	241 (single occupation)	
New Zealand	20	
+ SW Pacific Is.	5	
+ Sub-Antarctic Is.	3	
+ Antarctica	3	
South Africa	39	1990+
+ Namibia	19	1990+
+ Botswana	6	1990+
+ Zimbabwe	9	1990+
+ Antarctic Is.	2	1990+
Sweden	10	
U.S.A. incl. Pacific Is.	~110 current	
U.S.S.R.	130	1990+
TOTAL	**1480**	

† Burkino-Faso, Guinea, Ivory Coast, Mali, Niger, Senegal and Togo.

Repeat 1900.0–07.5

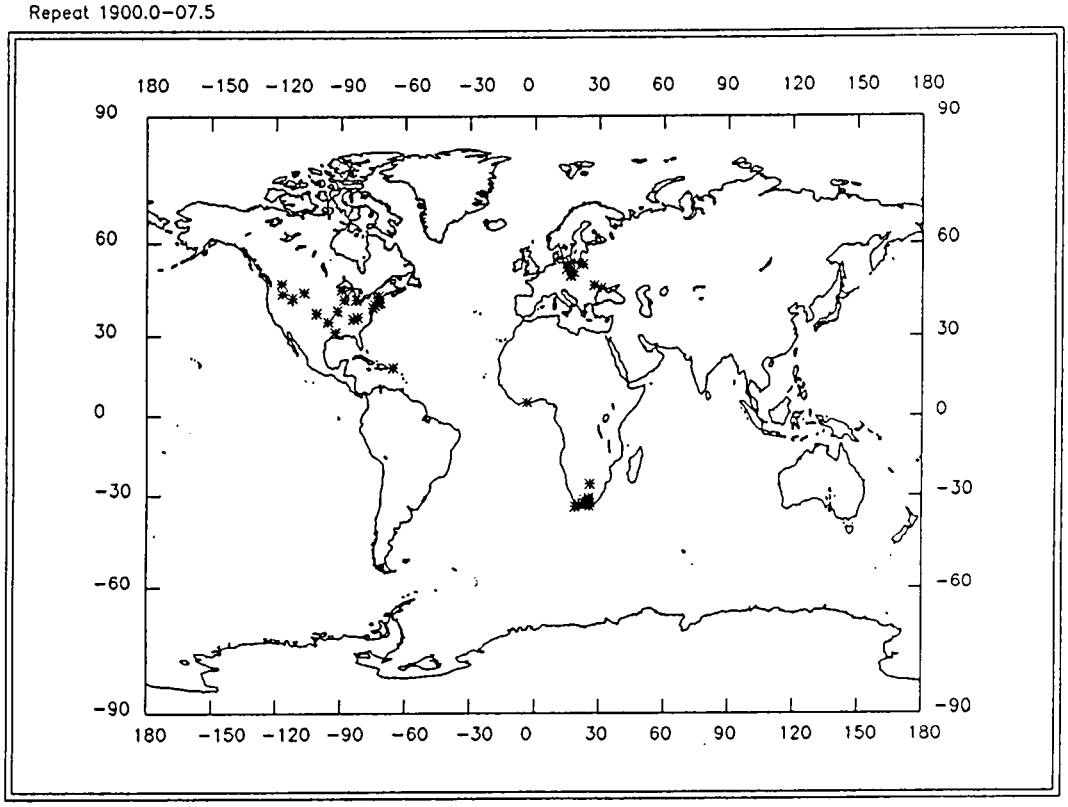

Repeat 1907.5–12.5

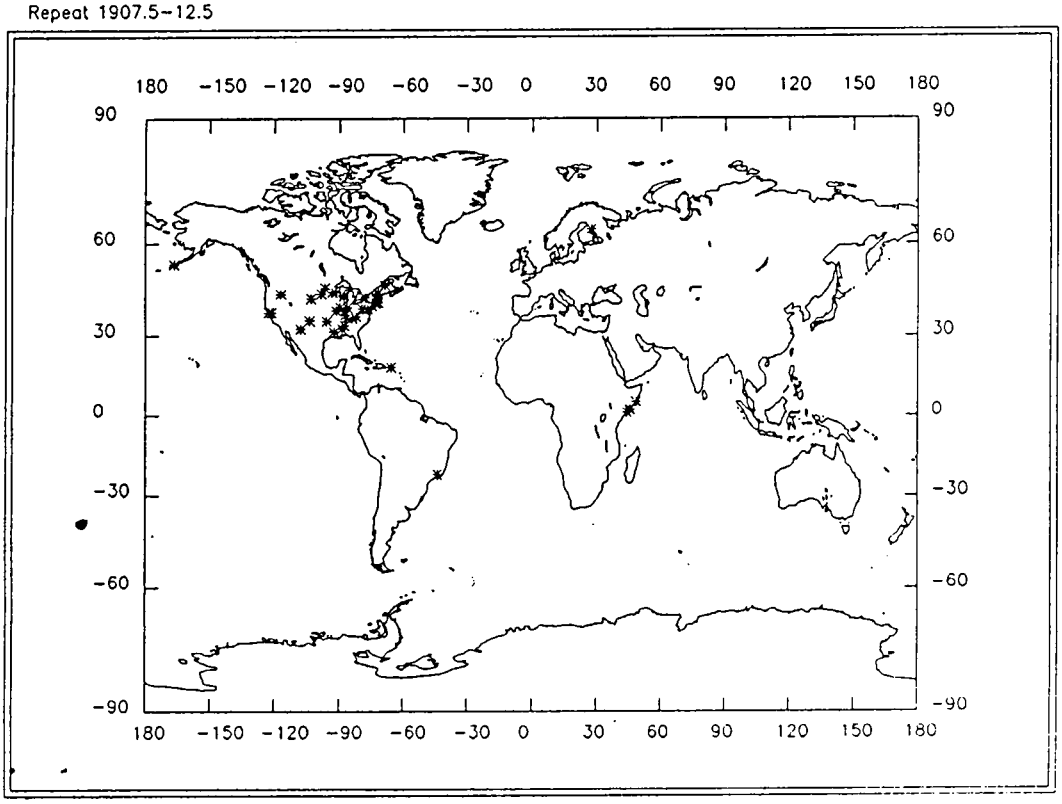

Figure 7(a)-(r). Geographical distribution of repeat station data held by WDC-C3, Edinburgh for 1900 onwards. Each plot covers a five year interval, except for (a) and (r). (Plots provided by D. Barraclough).

Repeat 1912.5−17.5

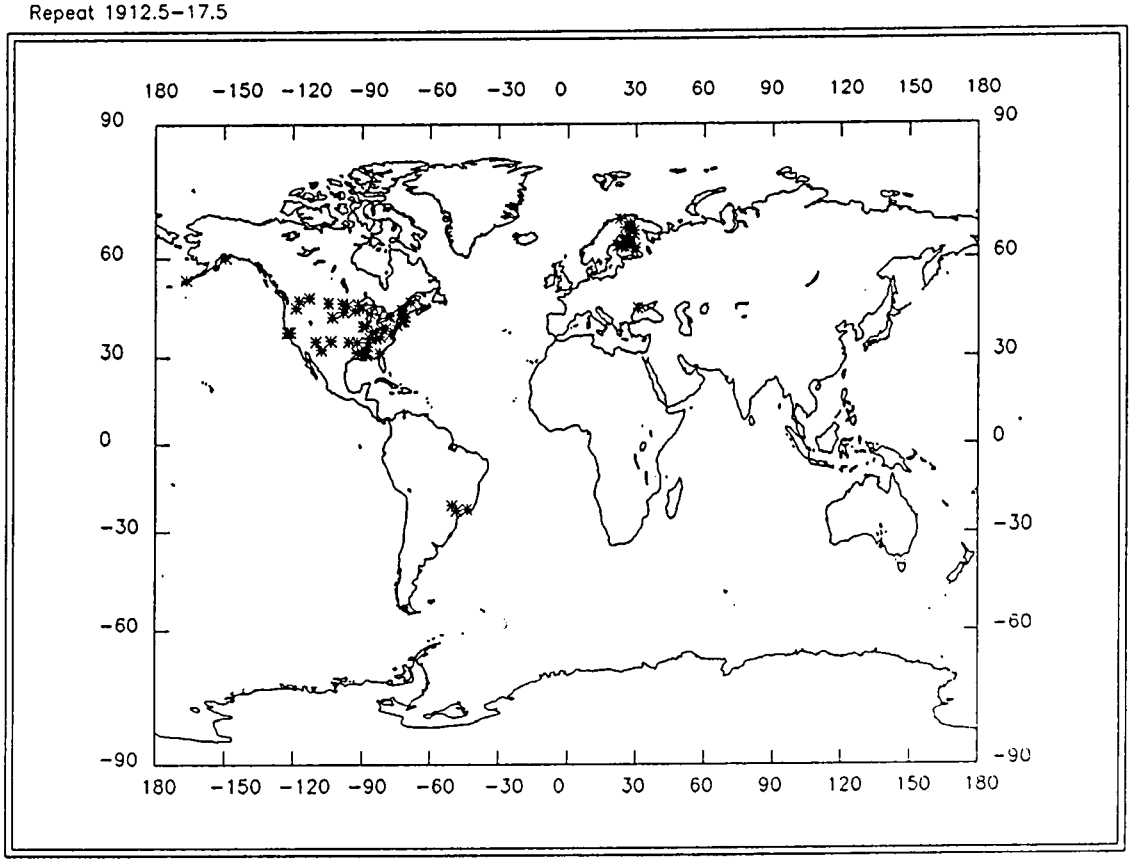

Repeat 1917.5−22.5

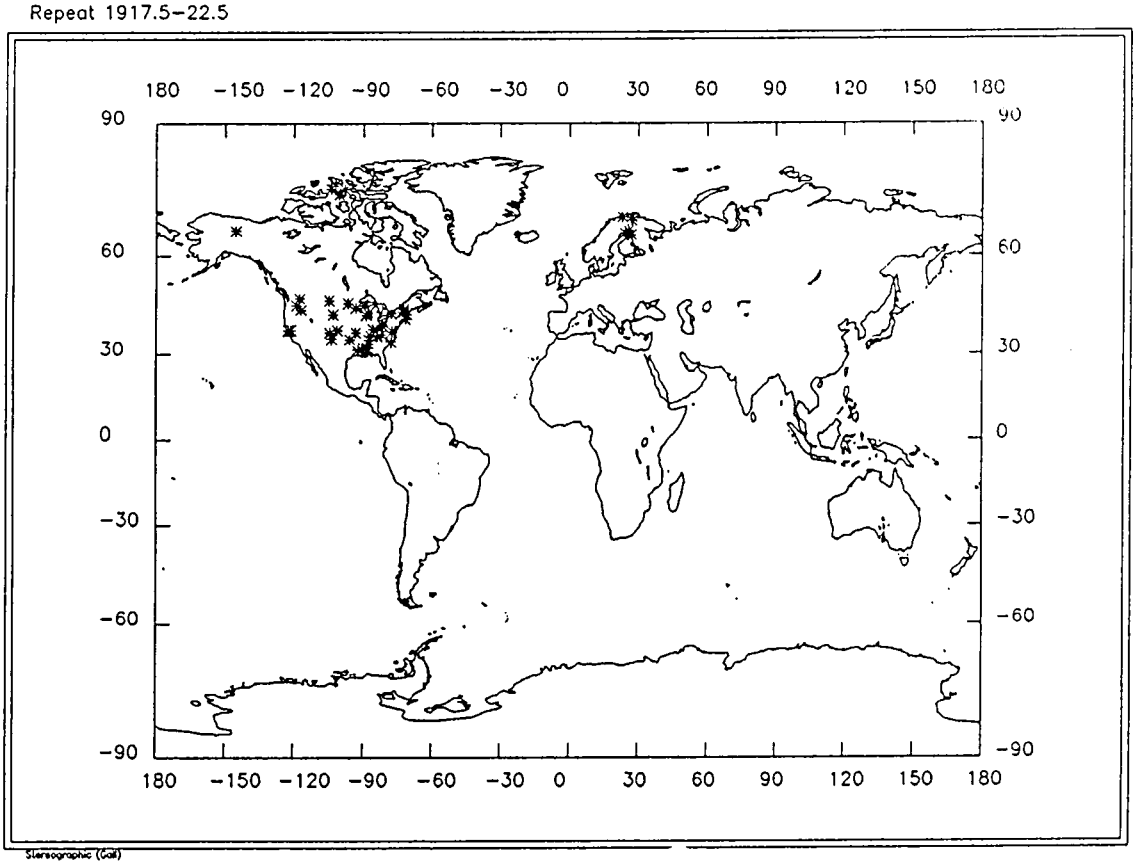

Figure 7 continued... (c) 1912.5 - 1917.5, and (d) 1917.5 - 1922.5

Repeat 1922.5-27.5

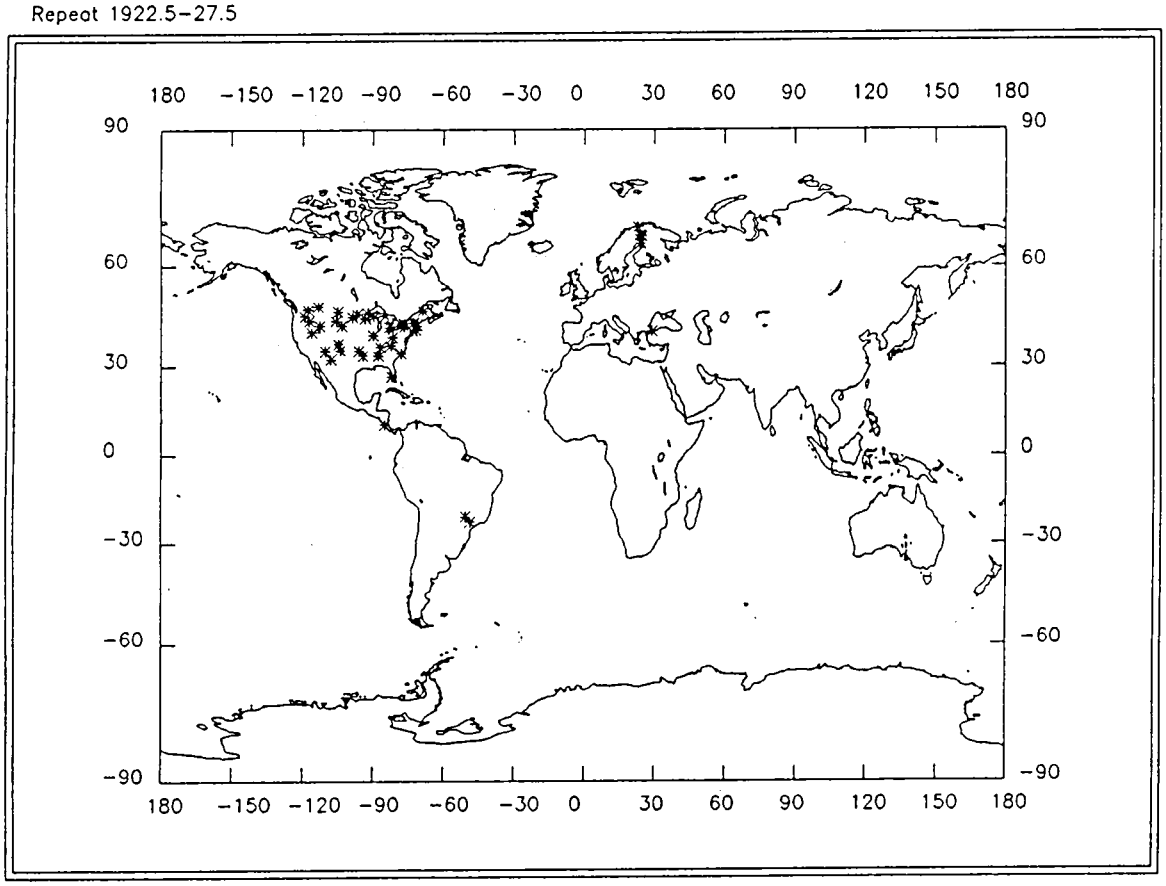

Repeat 1927.5-32.5

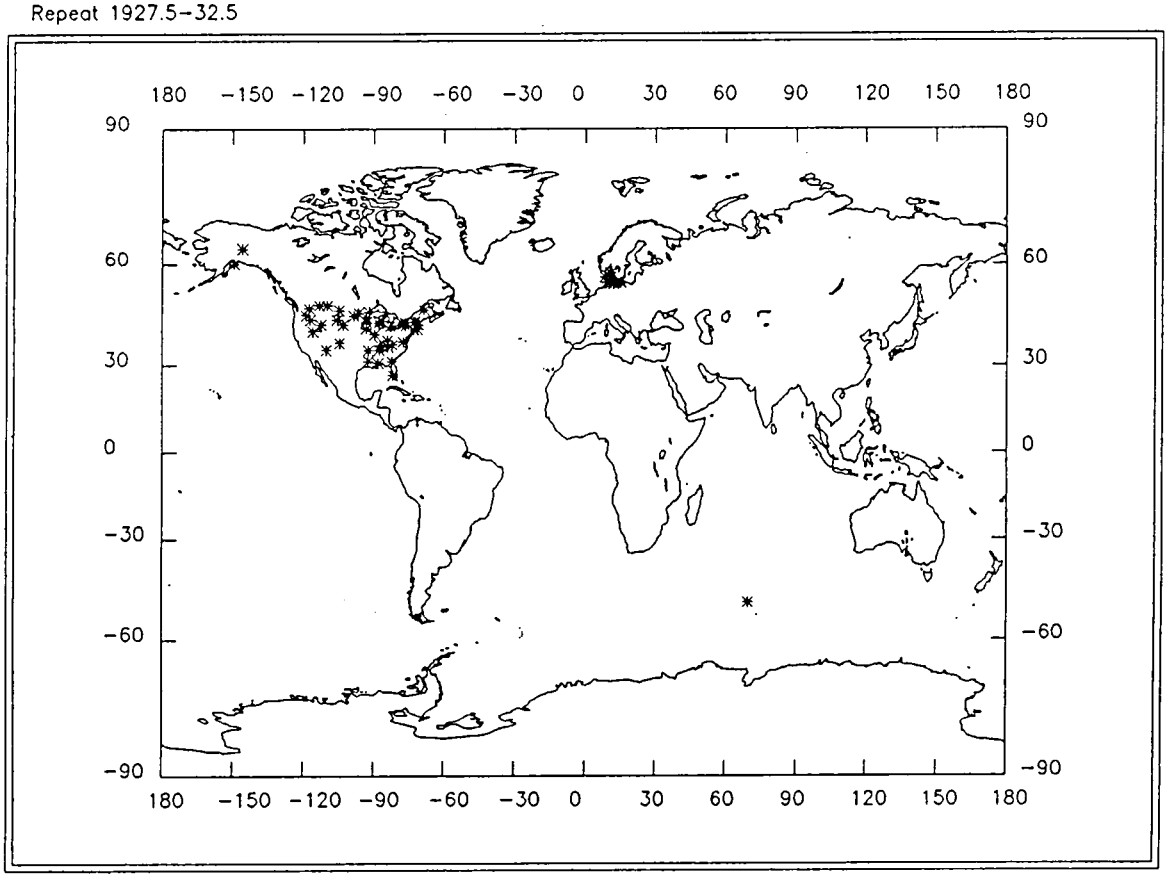

Figure 7 continued... **(e)** 1922.5 - 1927.5, and **(f)** 1927.5 - 1932.5.

Repeat 1932.5–37.5

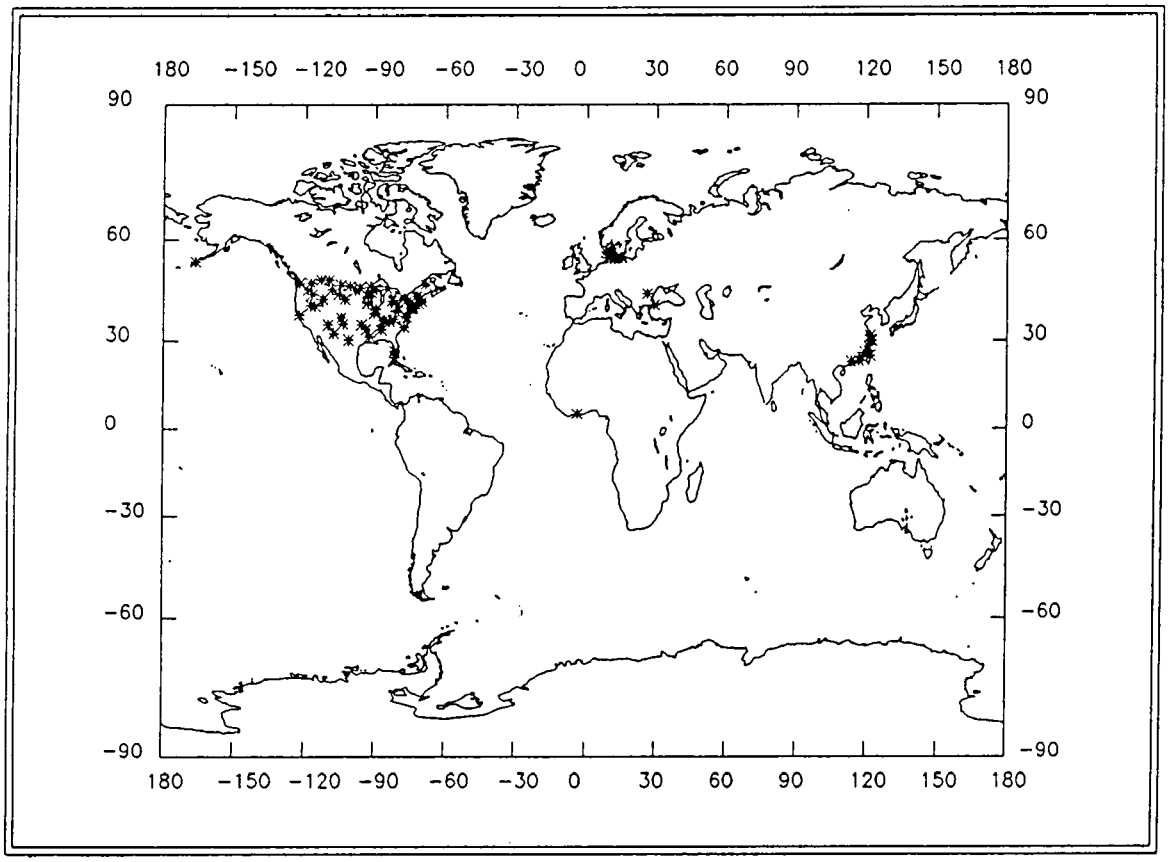

Repeat 1937.5–42.5

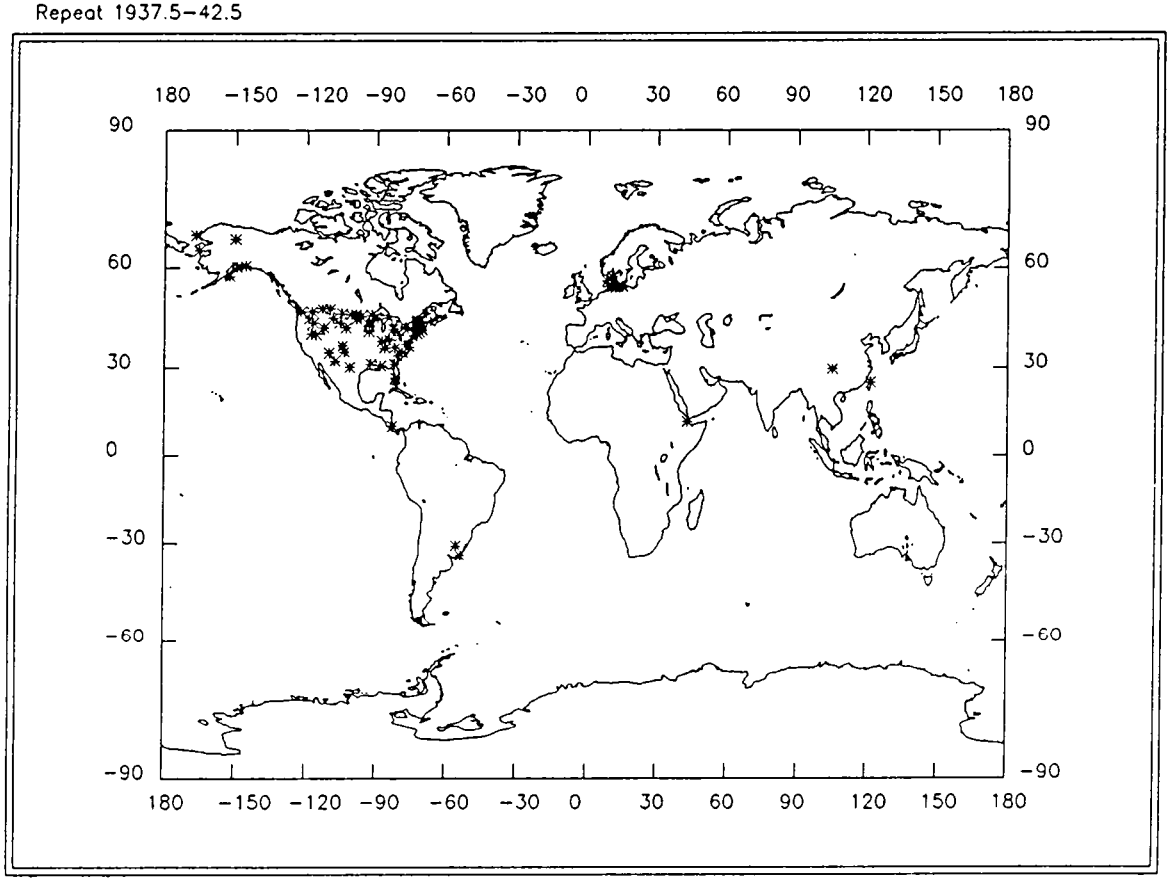

Figure 7 continued... (g) 1932.5 - 1937.5, and (h) 1937.5 - 1942.5

Repeat 1942.5–47.5

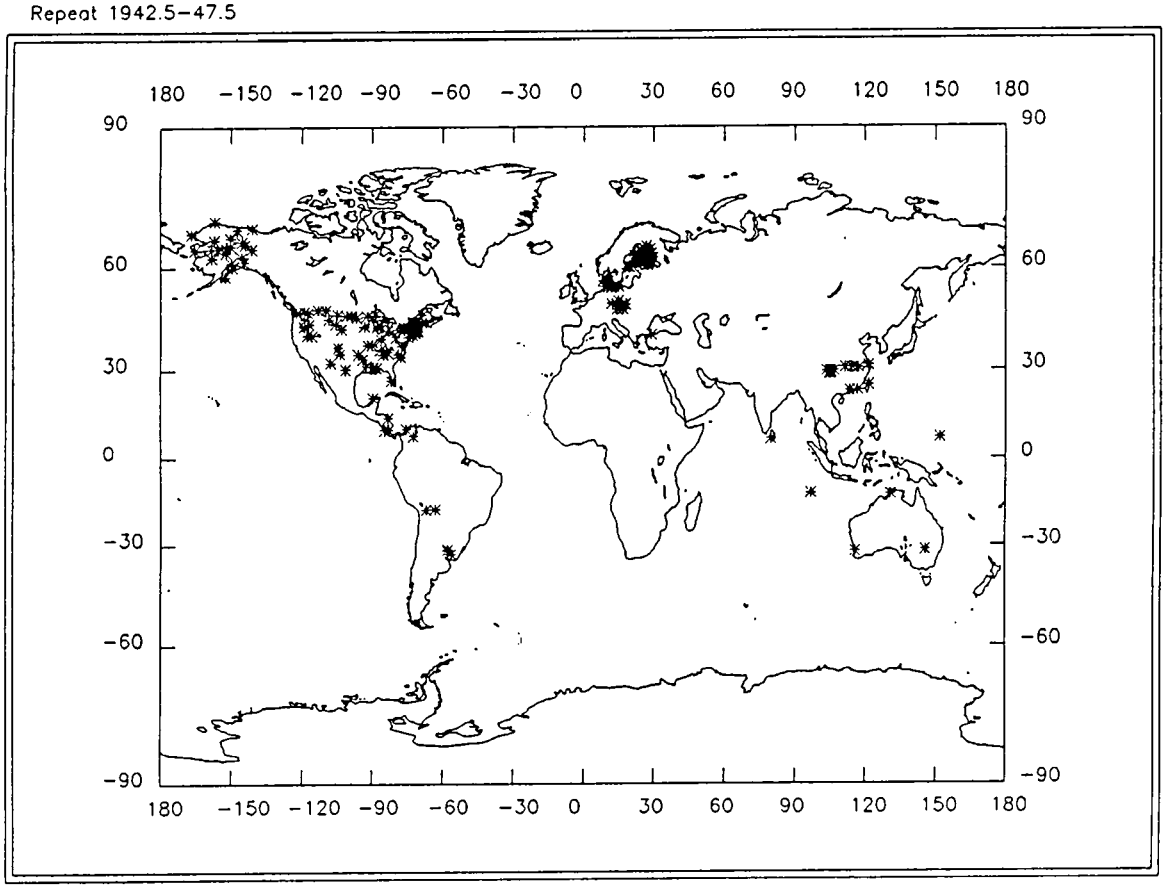

Repeat 1947.5–52.5

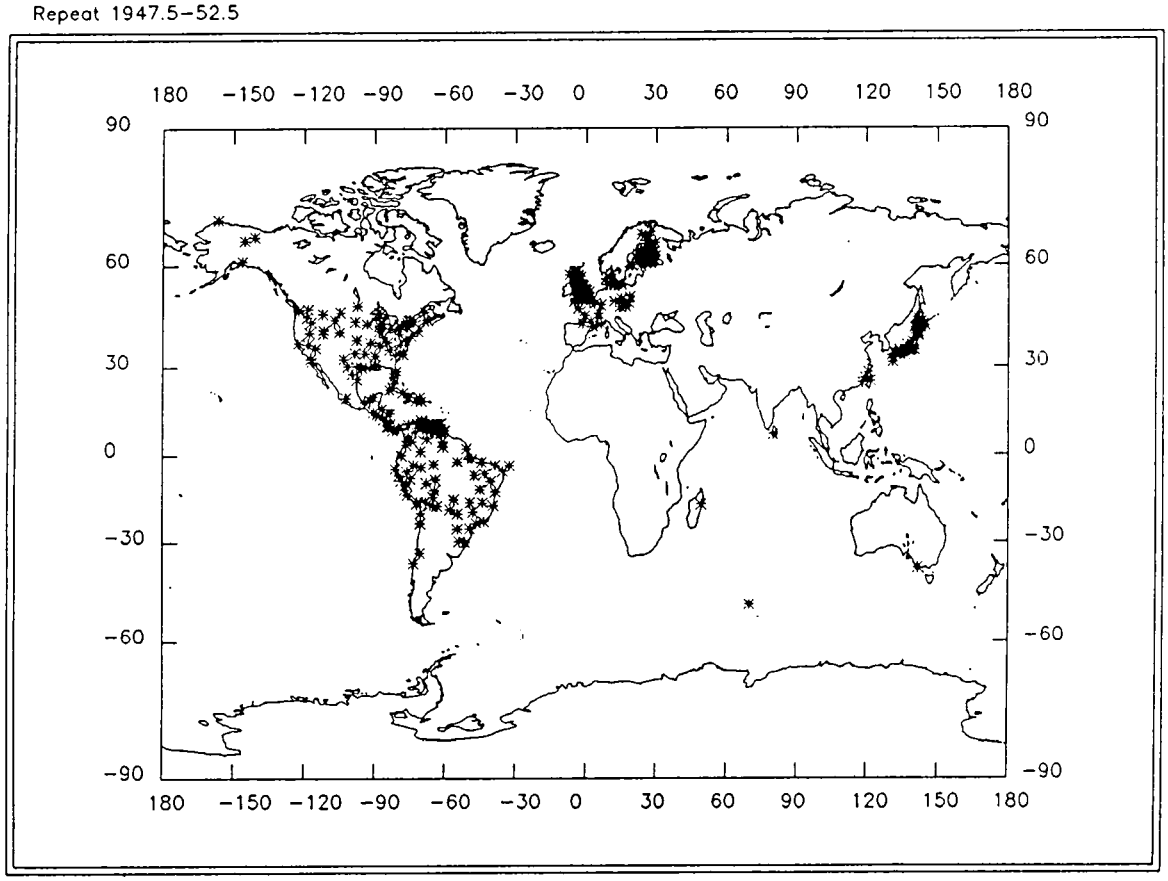

Figure 7 continued... (i) 1942.5 - 1947.5, and (j) 1947.5 - 1952.5

Repeat 1952.5–57.5

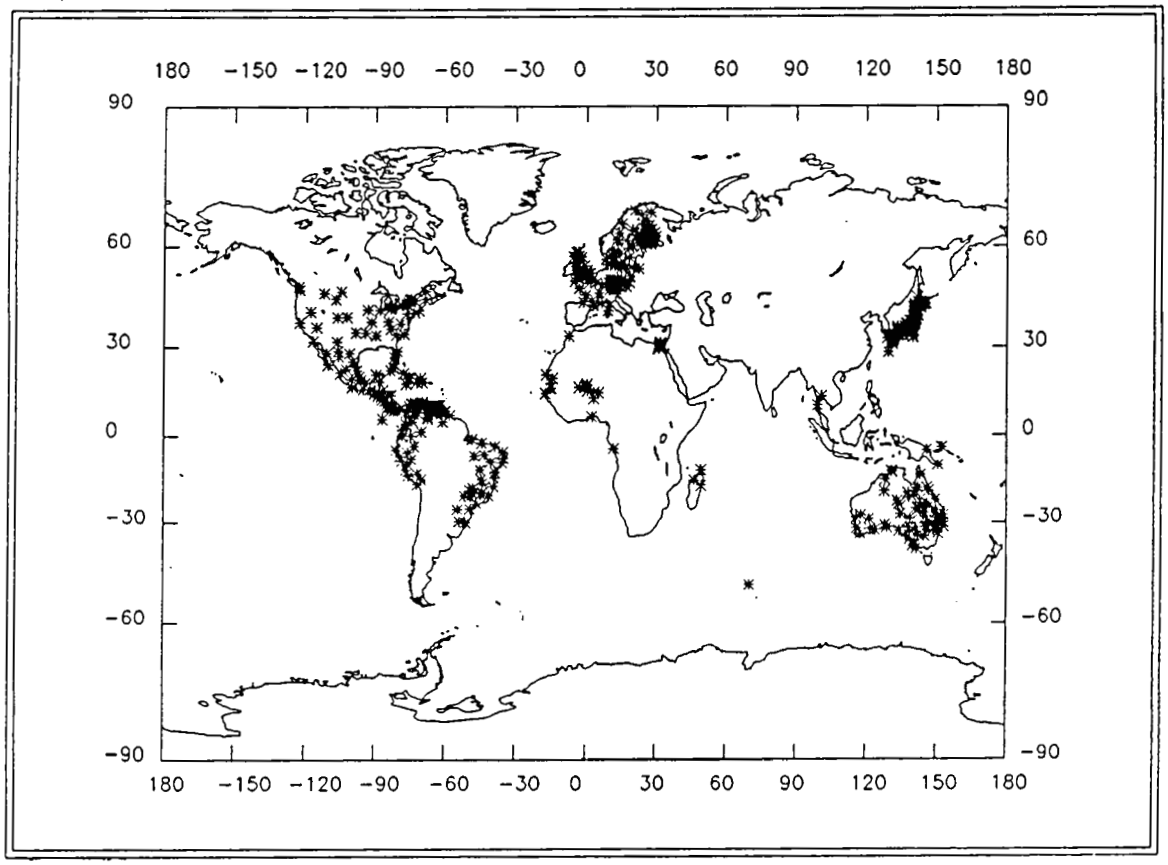

Repeat 1957.5–62.5

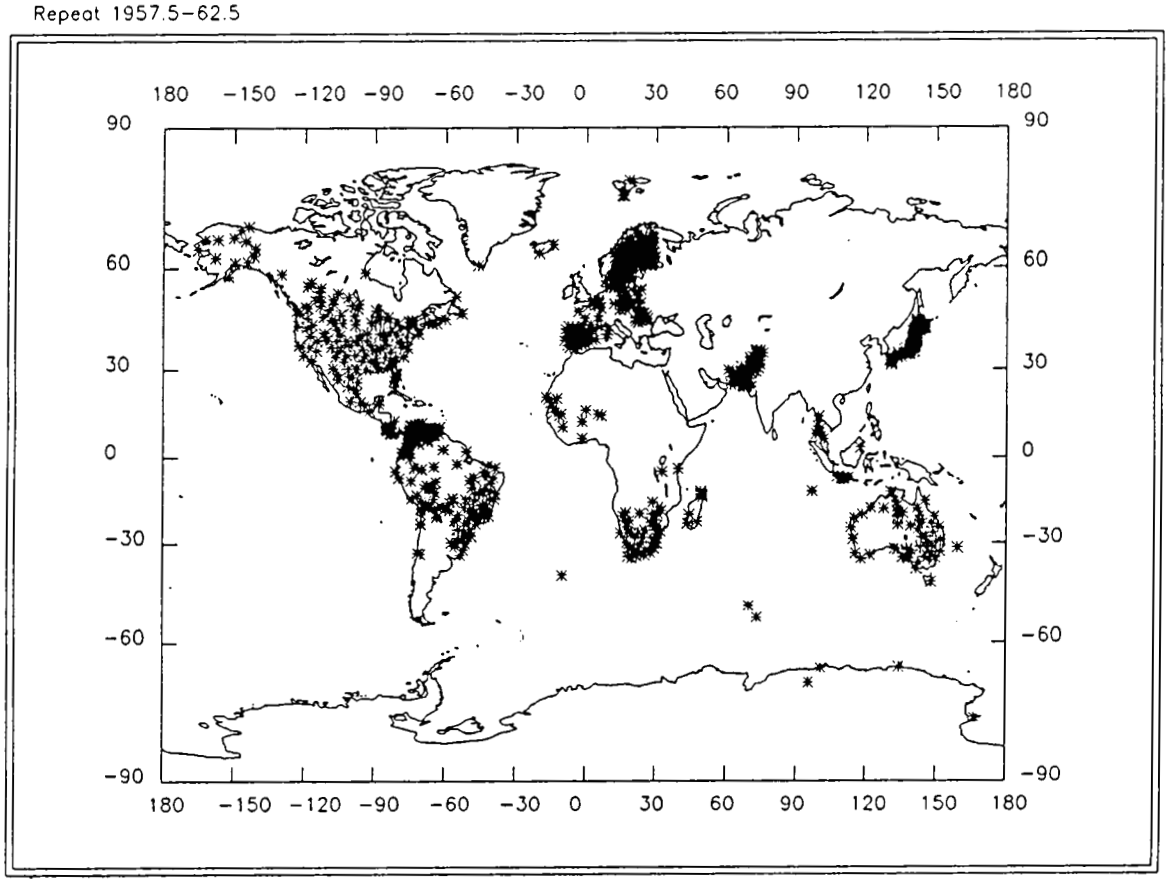

Figure 7 continued... **(k)** 1952.5 - 1957.5, and **(l)** 1957.5 - 1962.5

Repeat 1962.5–67.5

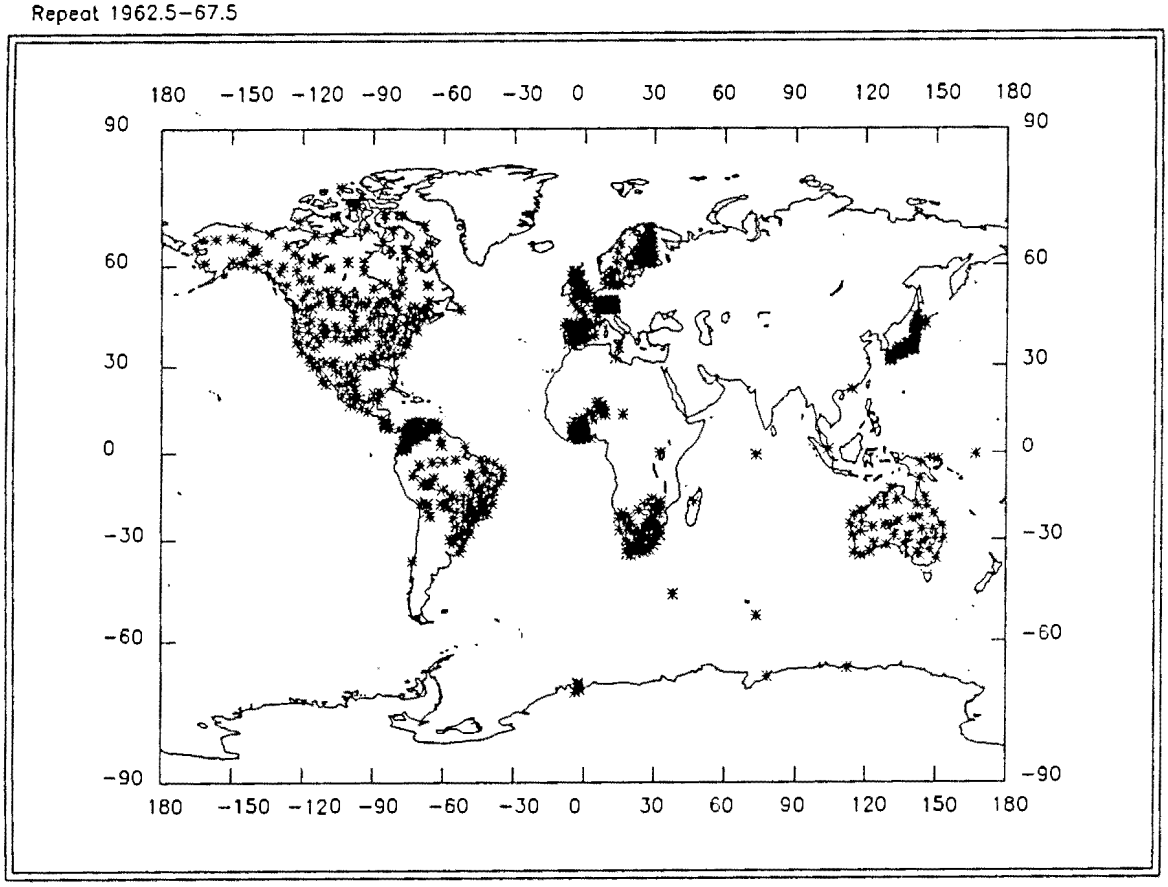

Repeat 1967.5–72.5

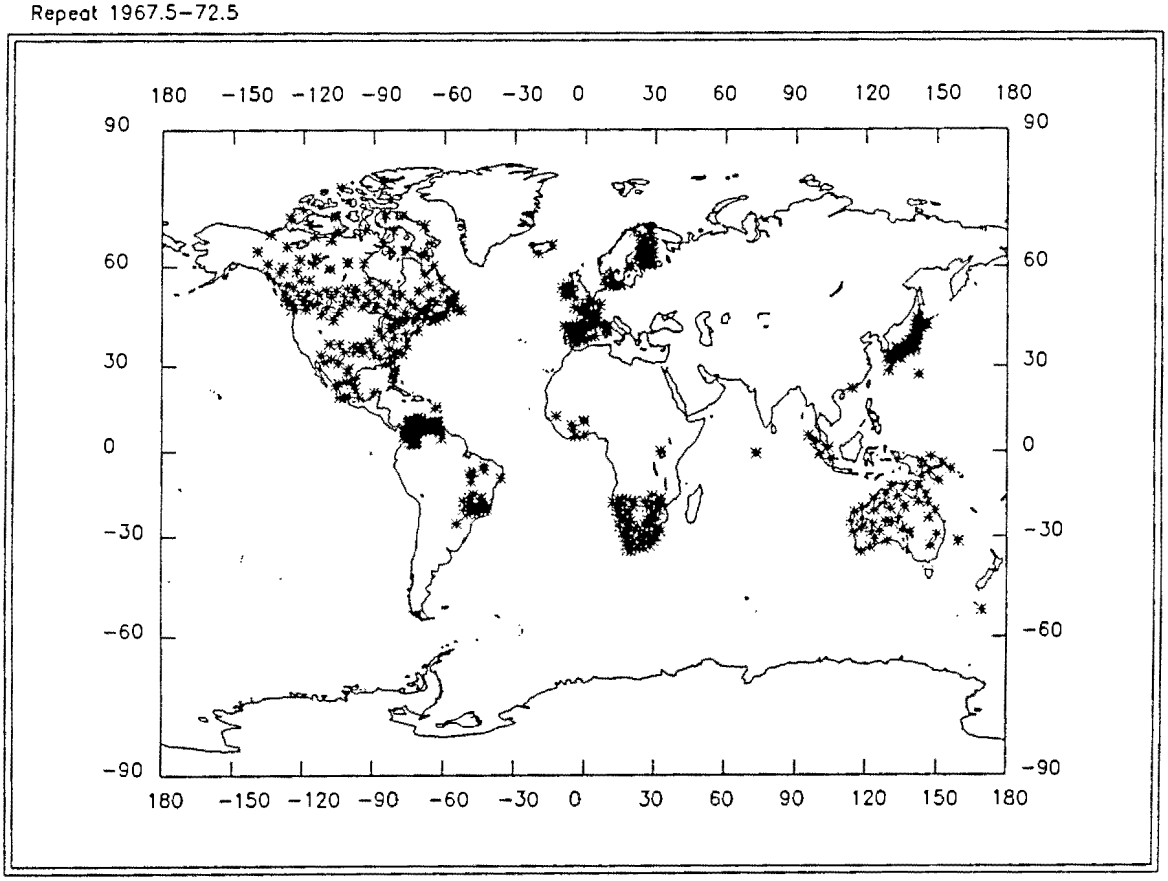

Figure 7 continued... **(m)** 1962.5 - 1967.5, and **(n)** 1967.5 - 1972.5

Repeat 1972.5–77.5

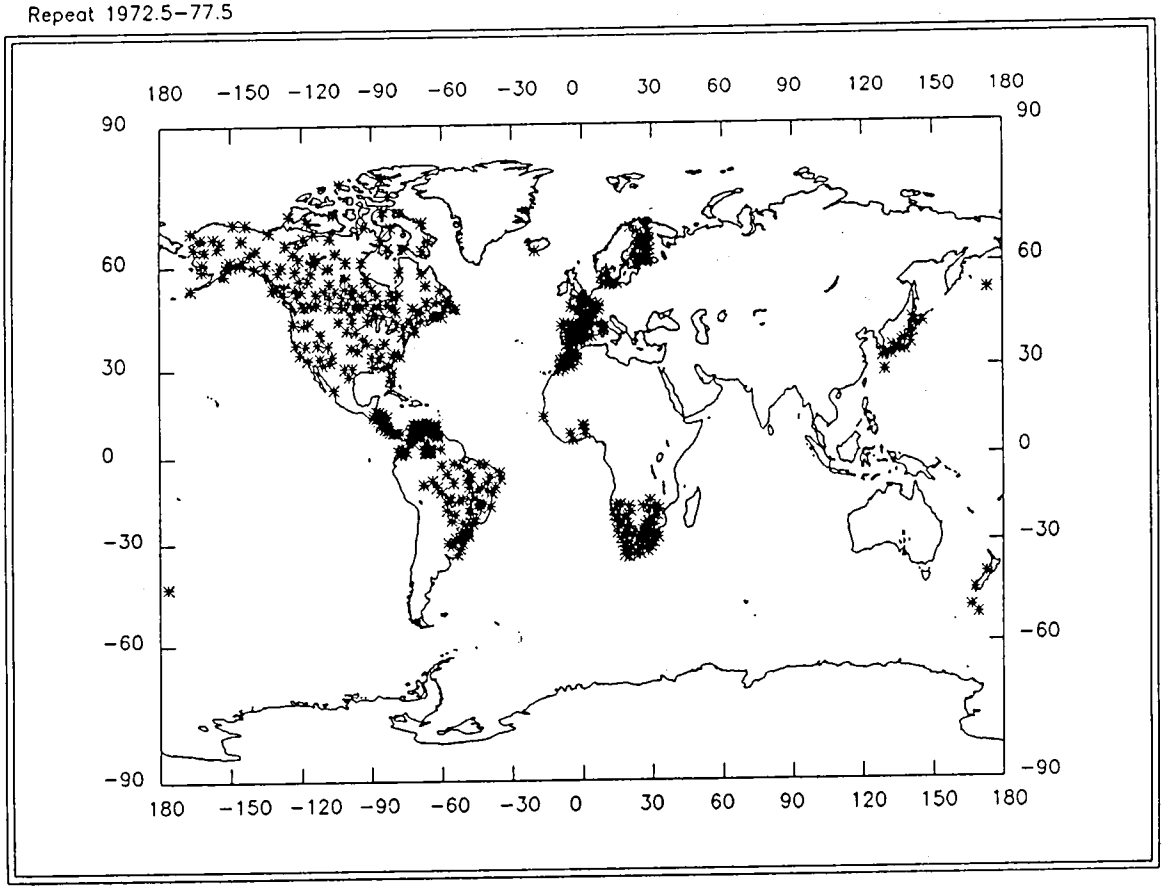

Repeat 1977.5–82.5

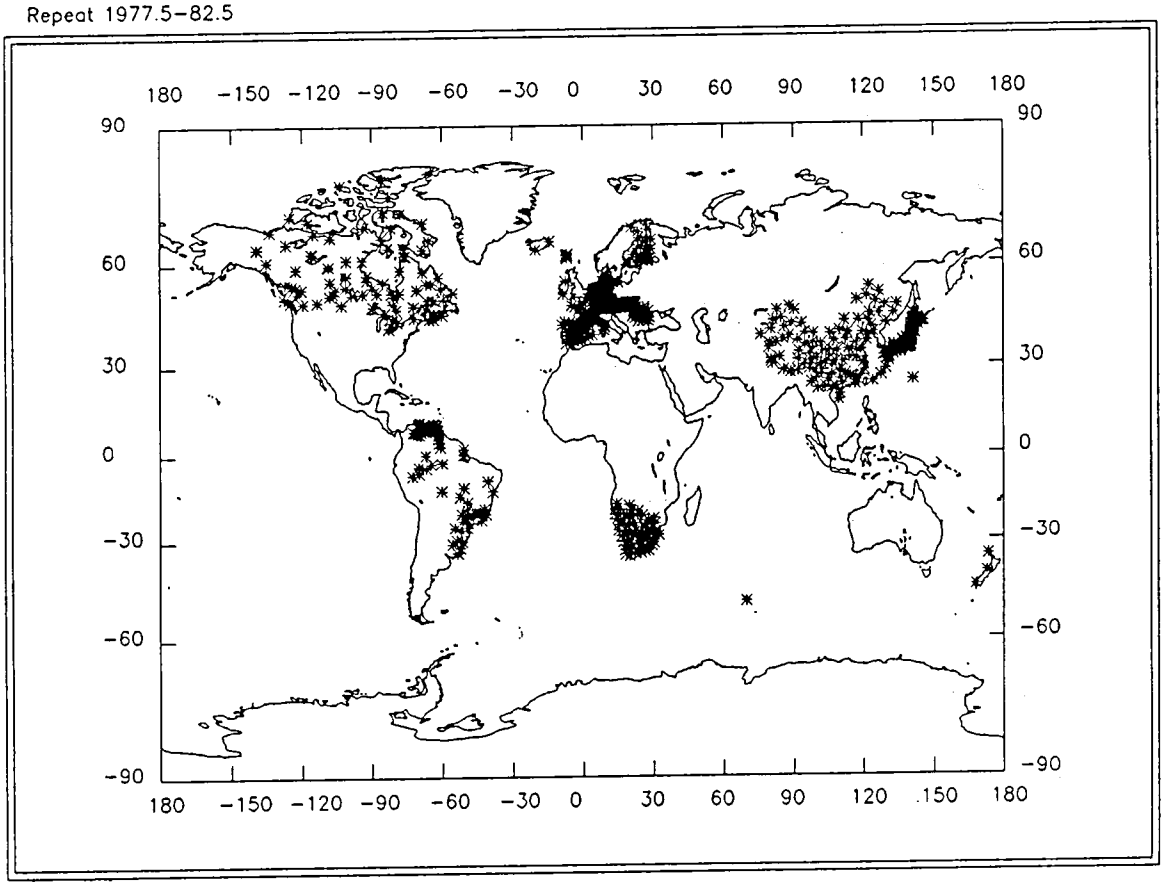

Figure 7 continued... **(o)** 1972.5 - 1977.5, and **(p)** 1977.5 - 1982.5

Repeat 1982.5–87.5

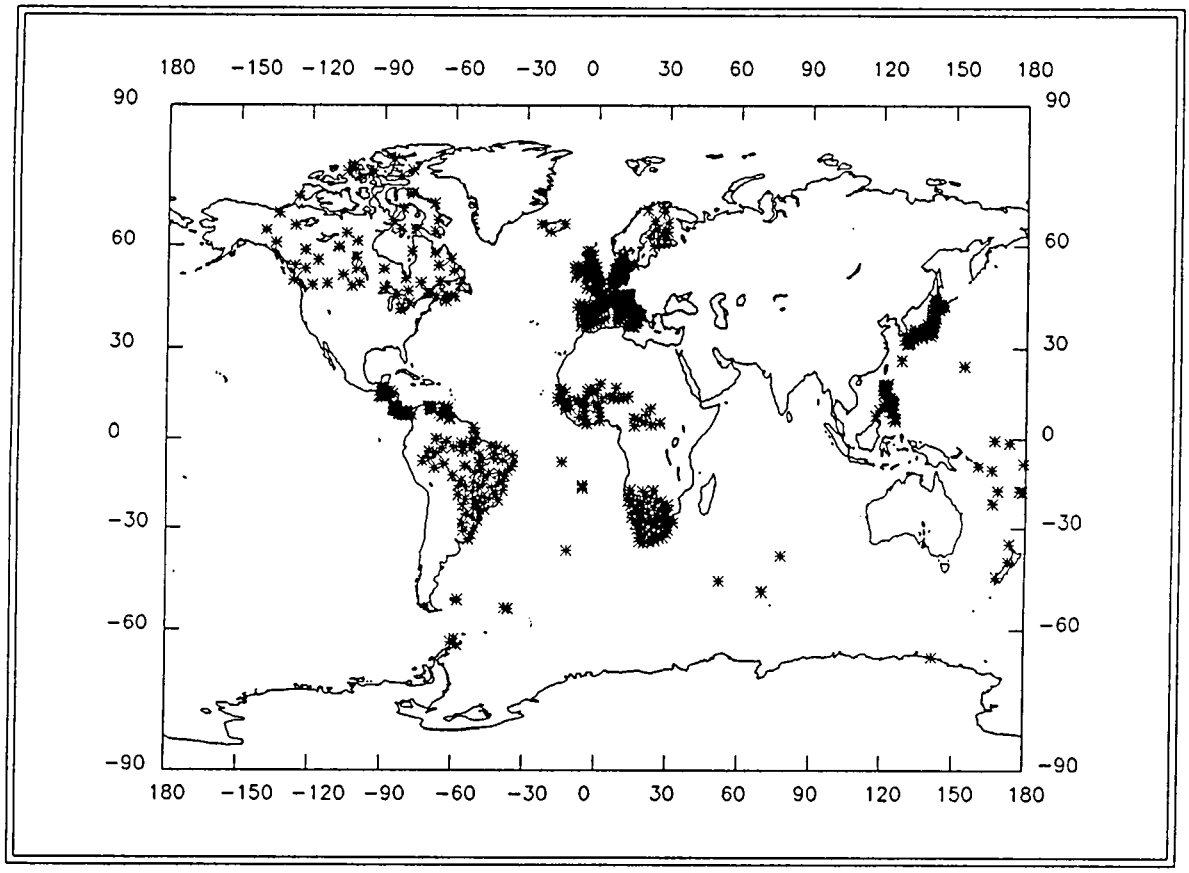

Repeat 1987.5 onwards

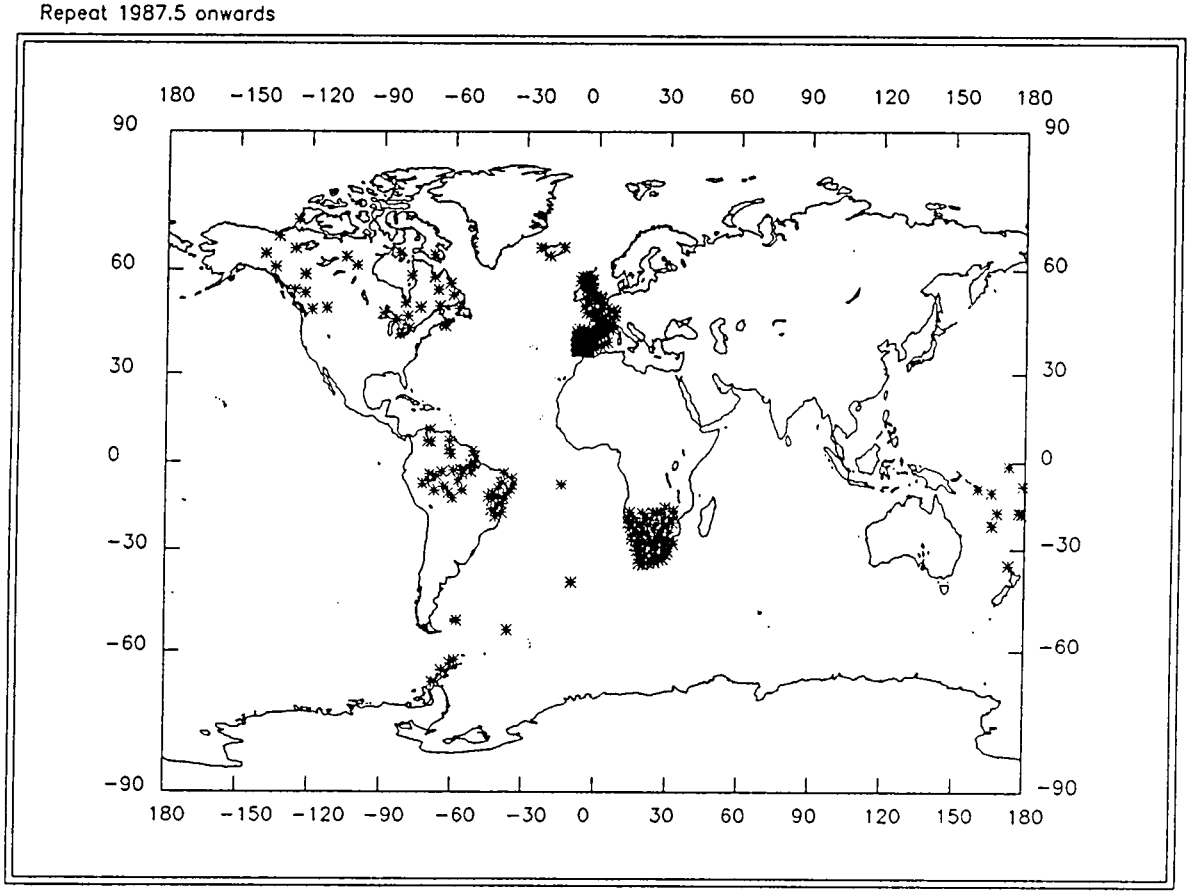

Figure 7 continued... (q) 1982.5 - 1987.5, and (r) 1987.5 +

Conclusion

Repeat station data are a valuable supplement to secular variation information provided by permanent magnetic observatories. The most difficult problem is to make an adequate correction for external field effects, particularly long-term transient effects on the night-time value of the field. We must rely on neighbouring permanent magnetic observatories to complete the corrections, even when a variometer is deployed on-site. Consequently repeat data are never truly independent.

To date, repeat station information has been used almost exclusively for regional field modelling. When good observational procedures are employed, and appropriate corrections are made for external field effects, then repeat data are sufficiently accurate to be used for global models of the secular variation (e.g. IGRF). No doubt we will see this happen as more countries use the new IAGA scheme for reporting and classifying repeat station data.

The distinction between magnetic survey stations and magnetic repeat stations has become blurred. In several regions the initial surveys have not been followed by reoccupations of the stations, for example in Iran,Afghanistan and Pakistan - Figure 7l, and in China - Figure 7p). Also, several of the repeat station data holdings in the WDC's are too large to be credible for repeat stations that could be reoccupied on a regular 5-yearly, or even 10-yearly basis. It is both unfortunate and inefficient when this happens because the value of the repeat data is then little greater than for ordinary magnetic survey measurements (yet the time and effort involved in making a proper repeat station measurement is 2 orders of magnitude greater).

It is important to strike a balance between the number of stations that are occupied, the frequency of occupation and the accuracy of the data that can be obtained from each station. The appropriate balance will depend on local conditions (e.g. the availability of reference observatories, the nature of inductive problems, and the magnetic latitude) and the magnitude of the secular variation signal being measured. However, there is often a tendency to occupy a large number of stations in order to get "good coverage" of a region at the expense of accuracy. Provided good observational practices are used, and appropriate steps are taken to correct for external field effects, then there is not much to be gained by increasing the duration of each station occupation. The best way to improve accuracy is to increase the frequency of station occupations. This was the rationale behind IAGA's recommendation that the interval between repeat station occupations should be 2 years. Observations should always be made under the most quiet magnetic conditions possible, even when the daily variation of the field is accurately known.

A question we should now ask is, if we are interested only in determining the secular variation, what are the minimum observational requirements at a station in order to achieve an accuracy that is comparable to that obtained from permanent observatories? The question is pertinent (i) when a restricted observatory schedule is necessary to save money, (ii) at polar stations that can be manned only during the summer, and (iii) for ocean-bottom observatories with limited data handling capabilities.

Acknowledgements

David Barraclough kindly provided Figures 6 and 7. I thank Larry Newitt, Daniel Gilbert, Jacques Bitterly and Andrew McEwin for their advice and suggestions. This paper is published with the permission of the Director, BMR Geology and Geophysics.

References

Bloxham, Gubbins and Jackson (1989). Geomagnetic secular variation. Phil. Trans. R. Soc. Lond., **A329**, 415-502.

Chamalaun, F.H. and P. Cunneen (1990). The Canning Basin geomagnetic induction anomaly. Aust. J. Earth Sci., **37**, 401-408.

Courtillot, V. and J.-L. Le Mouël (1978). Geomagnetic secular variation impulse. Nature, **311**, 709-716.

IAGA Working Group V-4, C.E. Barton ed. (1991). National repeat station network descriptions (IAGA magnetic repeat station reporting scheme), Bureau of Mineral Resources Geology and Geophysics, Canberra, Australia, Record No. 1991/72,

IAGA Working Group V-8, R.A. Langel, Chairman (in press). International Geomagnetic Reference Field, 1991 revision. Geophysics, PAGEOPH, Geophys. J. Int., J. Geomag. Geoelectr., Geomag. Aeronomy, Phys. Earth Planet. Int., EOS Trans. Am. Geophys. Un.

Fischer, G., P.-A. Schnegg and J. Sesiano (1979). A new geomagnetic survey of Switzerland. Géophysique no. 19, Commission Suisse de Géophysique.

Gilbert, D. and J. Bitterly (1988). Guide pour les campagnes de mesures faites dans les stations des reseau magnetiques de repetition français. Unpublished set of instructions, Bureau Central de Magnetisme Terrestre, Institut de Physique du Globe, Paris.

Molina, F., E. Armando, R. Balia, O. Battelli, E. Bozzo, G. Budetta, G. Caneva, M. Ciminale, N. De Florentiis, A. De Santis, G. Dominici, M. Donnaloia, A. Elena, V. Iliceto, R. Lanza, M. Loddo, A. Meloni, E. Pinna, G. Santarato and R. Zambrano (1985). Geomagnetic survey of Italy. Repeat station network and magnetic maps: a short report. Annales Geophysicicae, **3**, 365-368.

Mundt, W. (1980). Geomagnetic secular variation of the territory of the GDR. Gerlands Beitr. Geophysik, **89**, 467-476.

Newitt, L.R., C.E. Barton, D. Gilbert and J. Bitterly (in preparation). IAGA guide for magnetic repeat station surveys. To be published through IUGG.

Scheepers, G.L.M. (1969). Geomagnetic secular variation in South Africa, 1939-1966. M.Sc. Thesis, Department of Physics, University of Natal, Hermanus.

Vestine, E.H. (1961). Instruction manual on world magnetic survey. IUGG-IAGA Monogram No. 11.

APPENDIX-1

IAGA reporting and station classification scheme - explanatory notes

Each agency conducting repeat station surveys is asked to submit to WDC-A, Colorado *a Regional Magnetic Repeat Station Network Description* giving general details about the network, a *Regional Magnetic Repeat Station Record sheet* for each occupation of a station giving an alpha-numeric classification code and a summary of the main results and a *Computer File* listing the main results of one or more surveys.

Magnetic repeat station network description

This is short document summarizing the characteristics of a regional network of magnetic repeat stations, the instruments and observational procedures employed, the data reduction methods used, and a list of the models and charts produced. A diagram showing the locations of the stations, and a list of related publications may also be included. An example of regional magnetic repeat station network description is given in Appendix 2. One copy should be sent to WDC–A and another copy to the Chairman of Working Group V-4. An example from Japan is given in Appendix 2. Network descriptions are all prepared in a similar format and should be updated as necessary.

Magnetic repeat station record sheets

A blank record sheet is shown in Appendix-3. In many cases it may not be possible to fill in all the information specified - please complete as much as possible on every record sheet, including details (such as country) that will be repeated on a set of sheets. Record sheets should be prepared for old surveys as well as new ones. If possible, a summary of results should be provided in the form of an ASCII computer file as specified below.

Station name

Do not use the same name for different station markers at the same locality. For example use names such as Station-A, Station-B etc. to denote different sub-stations. Ensure that names agrees exactly with those given on previous record sheets and data files.

Station coordinates should be given in geodetic coordinates, i.e. on a spheroidal Earth. The distinction between coordinates on different spheroids is unimportant. However, the distinction between geodetic coordinates and geocentric coordinates (on a spherical Earth) is important. Coordinates should be in decimal degrees; latitude positive north, negative south; longitude positive east of the Greenwich meridian. If the height above mean sea level is not known accurately please enter an approximate value (to the nearest few hundred metres), and indicate that it is approximate.

Results

(Enter "N/A", if a particular result is not available, or is not applicable).

Mid-date of station occupation is the date about which the observations are centred, given either in decimal years or as year,month,day (yyyy mm dd) - e.g. 1989 06 23 for 23rd

June 1989.

Duration of station occupation is the time interval spanned by the run of absolute/variometer observations - rounded to the nearest day or hour as appropriate.

Uncertainty in station relocation - **this information is very important.** Errors in relocating the absolute instruments between successive occupations may vary from less than 1 cm up to many metres.

Record the average horizontal gradient of **F** (e.g. the mean of N-S and E-W values) and the vertical gradient of **F** at the point where the absolute instruments are placed at the repeat station.

Field elements

(a) List the three field elements observed and enter your best estimate of the 'night-time' values of the field. If four elements are observed then enter the three most accurate ones. 'Night-time' refers to the time when diurnal effects are at a minimum, although the field may still be disturbed. Enter approximate errors for the results, e.g. the standard deviation of a set of night-time field determinations (it may only be possible to make a guess, taking into consideration the accuracy of the instrumental and data reduction corrections applied). Conventions are: +X northwards, +Y eastwards, +Z downwards, +D east of north, +I downwards. Enter angles (D & I) in decimal degrees, to three decimal places if possible, and field strengths in nanotesla.

(b) Enter values for the three field elements after a correction has been made to get an estimate of the truly undisturbed value of the field. This correction is important unless it is known that observations were made during extremely quiet conditions. If data are reduced to get an equivalent annual mean value for the repeat station, using neighbouring observatory records for reference, then give the appropriate epoch in decimal years. Enter estimates (guesses if necessary) of the errors in determining the undisturbed field/annual mean values.

Annual change estimates: *(It is not essential to complete this section)*

Enter the values previously determined for the annual change in each field element at the last 5-year epoch, e.g. 1990.0, and your new estimates for the next 5-year epoch, e.g. 1995.0. Record the epochs concerned. Estimates might be based on simple differences between corrected observations at successive station occupations, or on the gradient of an appropriate curve fitted to a time-series of observations at the repeat station.

Magnetic disturbance

Give information from the one or two nearest magnetic observatories (or recording stations, possibly the magnetic repeat station itself) to show the typical level of magnetic disturbance for the period during which results were obtained. Daily range values are convenient, but any commonly used index or indicator of geomagnetic disturbance is acceptable.

Station classification (Please pay special attention to this question)

Assign a classification letter and number (in the range 1 to 3) to the results for each station. If an intermediate classification best describes your results, then assign an appropriate decimal value.

Classification 1 - applies to results when considerable care has been taken to correct fully for external fields, and associated induction effects, to get an undisturbed night-time value of the field. In most cases this requires that on-site continuous variometer, or nearby magnetic observatory, records are available. Unless observations were made under very quiet magnetic conditions, a correction for the long-term after-effects of magnetic storms and other transients may also be necessary.

Classification 2 - applies to results when an approximate correction has been made for the effects of external fields. For example, if absolute observations have been made throughout the day then an approximate diurnal correction can be made. 'Night-time' observations made under magnetically quiet conditions would qualify for a "2" classification, or possibly "1" if the observer has reason to believe that the completely undisturbed field was measured.

Classification 3 - is appropriate for spot measurements of the vector field made during relatively low levels of magnetic disturbance. (Spot observations made under disturbed conditions are not suitable for deriving secular variation information).

The classification number should be prefixed by one of the following classification letters to denote the type of diurnal control applied:

V - an on-site variometer was used
M - one or more magnetic observatories were used as a reference standard
A - absolute observations at the repeat station alone were used.

Examples of classifications

V 1 Day-time absolutes used to provide baselines to calibrate an on-site variometer; observations made on magnetically quiet days only.

V 1.3 As above, except that observations are made under moderately disturbed conditions and only an approximate correction is possible, based on observatory records, to obtain the undisturbed night-time value of the field.

M 1.1 Morning and evening absolutes, corrected by means of a neighbouring reference observatory to obtain equivalent annual mean values. The classification number could be anywhere between 1 and 2 depending on how accurately the reference observatory represents the diurnal variation at the repeat station.

A 1.2 Sets of absolute measurements made in the middle of the night on a magnetically quiet day.

A 2 A good spread of day-time absolute observations, including early morning and late evening. The nearest reference observatory is too far away to provide any improvement in diurnal control.

A 3 Spot measurement of the field made early in the morning on a fairly quiet day.

Note the important distinction between the "night-time" value, i.e. the field in the middle of the night when the diurnal variation and disturbances are at a minimum, and the "undisturbed night-time" value which represents only the main core field (including crustal remanence and main field-induced contributions) with no external field contributions or associated induction effects. It may be necessary to undertake a special study to establish how accurately records at the nearest observatory represent the diurnal signal at a repeat station. This is

particularly important if either site is suspected of being under the influence of crustal or coastal induction effects.

Computer files

If possible, provide a computer file summarizing the results of your repeat station surveys. This should be done in addition to completing a regional magnetic repeat station record sheet for each re-occupation of each station. The computer file can be either a **Survey File** of the results from a particular survey, and/or a **Master File** containing a compilation of results from several re-occupations of the same stations. It will usually be assumed that any new revision of a master file replaces earlier versions, unless stated otherwise in the header line(s) of the file.

Files should be written in ASCII and recorded on any commonly used medium (preferably IBM diskette). Files should have the following format:

```
HEADER
*STATION   LATITUDE   LONGITUDE   ELEVATION   ESTABLISHED
CLASS   DATE/YEAR   ELT1  ELT2  ELT3    EPOCH  dELT1  dELT2  dELT3
CLASS   DATE/YEAR   ELT1  ELT2  ELT3    EPOCH  dELT1  dELT2  dELT3
  etc....
*STATION   LATITUDE   LONGITUDE   ELEVATION   ESTABLISHED
CLASS   DATE/YEAR   ELT1  ELT2  ELT3    EPOCH  dELT1  dELT2  dELT3
  etc....
```

where

HEADER = descriptive header including the revision date, occupying as many lines as you wish

*STATION = name of the repeat station, preceded by an asterisk, spaces are not allowed

LATITUDE = latitude of station in decimal degrees; positive north, negative south

LONGITUDE = longitude of station in decimal degrees; positive east of Greenwich

ELEVATION = height of station above mean sea level in metres

ESTABLISHED = year when station was first used (optional)

CLASS = a 10-character code: R EEE Lm.n (include the spaces)

R = D if data are reduced to undisturbed values for a particular day
= Y if data are reduced to an annual mean value

EEE = any three of X,Y,Z,H,F,D,I to designate the elements reported

L = V if on-site variometer control was used
= M if a reference magnetic observatory was used to obtain undisturbed night-time or annual means values of the field
= A if absolute observations alone were used
= ? if the type of diurnal control is not identified

m.n = classification number for the results, e.g. 1.0, 1.5, 2.0, ...

DATE/YEAR = yyyymmdd for data reduced to a particular day (code D above), e.g. 19890717 for 17 July 1989.
Enter a pair of 9's if the day or month are unknown

= yyyy.y for data reduced to an annual mean (code Y above), e.g. 1989.5

ELT1,...3 = values of the three field elements, reduced to undisturbed night-time or annual mean values. Angles in decimal degrees; fields in nT

EPOCH= the epoch (i.e. decimal year) for the annual change estimates

dELT1,...3 = best estimates of the annual change in each element at the epoch specified. Angles in decimal degrees per year; field strengths in nT per year.

Notes

- Upper or lower case lettering is acceptable.
- There is no restriction on the number of characters per line, or the number of characters per data-field, but each field should be the same size throughout the file.
- Station names must be unique and match exactly those on corresponding record sheets and data files.
- Data-fields should be separated by one or more spaces, or a comma, or a tab character.
- Enter a string of 9's in the appropriate data-field to denote missing values.
- Angles (latitude, longitude, **D**, **I**) should be in decimal degrees.
- As a general rule the three elements measured should be entered in the file. However, any three elements defining the field vector may be specified, e.g. **D,H,Z** or **X,Y,Z**. If a combination such as **D,H,F** is used, which does not specify the sign of **Z**, then **F** should be give the sign of **Z**.
- Comments relating to a result can be appended to the end of the line.
- For master files it will be assumed that the annual change estimates are the original (usually prospective) ones made at the time of each survey. If the annual change values in a master file have been recalculated retrospectively, then add a note of explanation to the file header, and/or onto the end of the appropriate lines of results.

Example of a Survey File

```
BMR Australia, Repeat station survey 1986-1989      Rev: 17 December 1990
This file contains data from continental Australia, surrounding islands, Papua
New Guinea and SW Pacific Islands.  No Antarctic data
--------------------------------------------------------------------------------
*Albany_C          -34.945   117.805   075   1965
D DHZ V1.1  19870413  -3.083   21433  -56195   1990.0  0.042  -13.4  -1.9
*AliceSprings_B    -23.807   133.897   500   1942       (approx.elevation)
D DHZ V1.1  19891206   5.070   29941  -44697   1990.0  0.027  - 3.0   0.1
*AyersRock_A       -25.348   131.062   560   1947
D DHZ V1.1  19891225   4.322   28877  -46751   1990.0  0.026  -09.7   0.6
....etc.....
```

In this example, variometer control was used to make a diurnal correction, and a subsequent adjustment for night-time disturbance was applied. However, observations were not made strictly under magnetically quiet conditions - hence a classification of V1.1 has been used instead of V1.0. Absolute observations of D,I,F were made, but the results have been expressed as D,H,Z throughout to be consistent with earlier results. A comment about the approximate elevation for Alice Springs has been added to the station line.

Example of a Master File

```
BMR Australia, Repeat station masterfile 1969-1989   Rev: 25 December 1990
This file contains data from continental Australia, surrounding islands, Papua
New Guinea and SW Pacific Islands.  No Antarctic data.  Annual changes are the
original forward estimates, not recalculated.
--------------------------------------------------------------------------------
*Albany_C         -34.945   117.805   075   1965
D DHF A2.0  19780627  -3.015  21722  -60184   1980.0 -0.016 9999.9   3.6
D DHZ V1.1  19831002  -3.099  21548  -56231   1985.0  0.022  -15.6 -11.5
D DHZ V1.1  19870413  -3.083  21433  -56195   1990.0  0.042  -13.4  -1.9
*AliceSprings_B  -23.807   133.897   590   1942
D DHZ V1.5  19690803   4.720  30463  -44232   1970.0  0.008  -21.6  -5.3
....etc.....
```

In this example, the Albany 1978 results are specified for **D,H,F** so the sign of **Z** has been transferred to **F**. The annual change in **H** at 1980.0 is missing.

Archival And Retrieval of Repeat Station Information

World Data Center-A in Boulder, Colorado, U.S.A. acts as the primary center for accumulating and disseminating repeat station information. If you send data to any other World Data Center then please indicate that copies should be forwarded to WDC-A. Please send completed record sheets and computer files to:

Geomagnetism Services
WDC-A Solid Earth Geophysics
325 Broadway
Boulder, CO 80303-3328 U.S.A. fax: +1-303-4976513

Up-to-date copies of your repeat station network description should be also be lodged with WDC-A, and a copy sent to IAGA Working Group V-4. The responsible officer is currently Charles Barton, BMR Geology & Geophysics, PO Box 378, Canberra ACT 2601, Australia. (tel: +61-6-2499111; fax: +61-6-2576041).

IAGA Working Group V-4 can also be contacted through the current chairman:
Dr Jacques Bitterly, Service des Observatoires Magnétiques, Institut de Physique du Globe, 5 rue René Descartes, 67084 Strasbourg Cedex, France.
(tel: +33-88-416367; fax: +33-88-616747).

Requests for repeat station data should be addressed to WDC-A. Requests for repeat station network descriptions can be addressed to either WDC-A, or to IAGA Working Group V-4. Enquiries and comments concerning the IAGA reporting scheme should be addressed to IAGA Working Group V-4.

APPENDIX-2

Example of a magnetic repeat station network description

Country JAPAN **Revised:** 18 December 1990

Contact Director, Geodetic Department
Attention Masaru Kaidzu
Geographical Survey Institute
Ministry of Construction
Kitasato -1, Tsukuba-Shi
Ibaraki-Ken 305

Tel: +81-298-64 1111 ext 431
Fax: +81-298-64 1802

NETWORK CONFIGURATION

Stations	Reoccupation Interval
105 first-order stations	2 to 4 years
850 second-order stations	

Observatories

Kakioka	36°13'45"N,	140°11'23"E	(1913 +)
Kanoya	31°25'14"N,	130°52'56"E	(1958 +)
Kanozan	35°15'11"N,	139°57'32"E	(1961 +)
Memambetsu	43°54'30"N,	144°11'35"E	(1952 +)
Mizusawa	39°06'32"N,	141°12'25"E	(1970 +)

Repeat station surveys were started by the Geographical Survey Institute (GSI) in 1949.
Station density: one first-order station every 3,600 km^2
First-order stations occupied: 1983 (37 stations) , 1984 (29), 1985 (31), 1986 (29)

Station markers: a granite pillar of 15 cm square head and 70 cm length is laid upon the ground. It's head is about 10 cm above ground level. The precise position of the station is marked by a "O" at the centre of the pillar head.

Auxiliary stations: nil

Logistics

Access:	most stations are accessible by road
Fieldwork:	approximately 3 to 4 months per year
Staff:	1 skilled observer plus 1 assistant per party

OBSERVATIONAL PROCEDURES

Absolute Instruments

D, I	GSI type precise magnetometer (fluxgate theodolite, 0.1' precision)
F	Geometrics G856 proton precession magnetometer
Polaris obs.	GSI type precise magnetometer

Variometer

D,H,Z	triaxial fluxgate magnetometer (MB-162)

T	temperature of fluxgate sensors (coefficient 0.1 nT/°C)
Recording	**H** is recorded continuously on a chart recorder
	D, H & Z are digitized every minute and recorded onto cassette tape.

Frequency and Duration of Observations

Variometers are operated for 24 hours from 0^h to 24^h UT on a calm day of magnetic activity.

Absolute observations are performed simultaneously at four times (0^h, 4^h, 8^h and 24^h UT) to determine the baseline values of the variometers used.

At each of these four times 3 sets of observations of **F, D, I** are made.

If for any reason the variometer cannot be operated (e.g. topographical constraints) absolute observations of **D, I, F** are conducted at hourly interval from 21^h UT to 13^h UT the next day.

Polaris observations are made to check the azimuths of reference marks.

Comments

In addition to the above first-order stations, 850 second-order stations have been established. Data from these second-order stations are used for preparing magnetic charts.

DATA REDUCTION PROCEDURES

The variometer records are digitized at 1-minute intervals; these data are averaged at hourly and daily intervals.

The absolute observations are used to calibrate the digitized variometer data to produce mean daily absolute values of **D, H, Z** and **F**.

The station variations are compared with data from a reference station and adjusted to eliminate atypical disturbance effects in the field; the reference station is the Kakioka Geomagnetic Observatory.

Adjusted station values for **D, H, Z** and **F** near local midnight are considered to represent the long-term undisturbed field at the station for the epoch of occupation.

Station values are later updated to a common epoch using appropriate plots or models of the secular variation.

MODELS & CHARTS

Isomagnetic charts are prepared from geomagnetic survey and reference station data.

1952+	Charts of **D, I, H, Z & F** (hand-contoured)
1985	Charts for 7 components by polynomial least squares

REFERENCES

Geographical Survey Institute: Results of the first order magnetic survey, Bull. G.S.I., vol XXV - part 1 (1981).

Tanaka, M., K. Hiroishi & S. Matsumura (1984), J. Geomag. Geoelectr., **36**, 463-470.

Geomagnetic observations at Mizusawa and Kanozan 1988, First order geomagentic stations 1979-1988, G.S.I. publication B4 - No.8, March 1990.

APPENDIX-3
REGIONAL MAGNETIC REPEAT STATION RECORD SHEET
(Revised: November 1991)

For information on how to complete record sheets refer to the document "Regional Magnetic Repeat Station Records - Explanatory Notes" issued by IAGA Working Group V-4. If the information requested below is inappropriate, please modify the form to suit your situation. Return record sheets to: Geomagnetism Services, WDC-A Solid Earth Geophysics, 325 Broadway, Boulder, CO 80303-3328, U.S.A. Fax: +1-303-4976513

STATION NAME : COUNTRY :

Latitude : Is this a new station: No/Yes*

Longitude : Is this an exact re-occupation: Yes/No*

Height above sea level (m) : Year of previous occupation:

RESULTS CLASSIFICATION (see notes)

Mid-date of station occupation: ..... | | |

Duration of station occupation: ..... days/hours* | _____ |

Total number of sets of absolutes: ..... Sequence of elements per set: .....

	Uncertainty in instrument relocation		Gradient of total field at station
Horizontal:	m	:	nT/m
Vertical :	m	:	nT/m

Element	(a) Mean night-time value and estimated uncertainty		(b) Undisturbed night-time/annual mean value* @ epoch†=..... estimated uncertainty
1 :	±	:	±
2 :	±	:	±
3 :	±	:	±

Estimated annual change

Element	@ previous epoch = ...		@ new epoch = ...
1 :		:	
2 :		:	
3 :		:	

MAGNETIC DISTURBANCE

Observatory name	Distance from repeat station		Disturbance indicator (state what)
1.	: km	:	.....
2.	: km	:	.....

---

*circle one † if annual mean is quoted then give mid-year epoch

NOTES (continue on reverse side if necessary)

Geomagnetic Data from the U.S. Magnetic Observatory Network

Donald C. Herzog

U.S. Geological Survey
Denver Federal Center
MS 968 Box 25046
Denver, Colorado 80225-0046 (U.S.A.)

Abstract. The United States operates a network of, at present, 13 ground-based magnetic observatories. Continuous, one-minute digital vector and scalar geomagnetic field values have been recorded for the last decade, and extend about five years further back for several stations. Periodic, 3-component absolute measurements of the magnetic field are made to provide baseline reference data with which to determine calibrated field values at all intervals. These data are now being made available on CD-ROM. The quality of the data depends upon a number of factors, including the types of instrumentation used to monitor and measure the field, the procedures and equipment used to collect and process the data, and the quality controls employed to check the data for erroneous values. These various factors are described here for the U.S. digital geomagnetic observatory data. The observatories have been undergoing an evolution over the last 15 years that will continue to significantly improve the accuracy, precision, and availability of geomagnetic data.

1. Introduction

The National Geomagnetic Information Center (NGIC), located in Golden, Colorado, currently operates a network of 13 magnetic observatories under the auspicies of the United States Geological Survey (USGS). At these observatories, the Earth's magnetic field is continuously monitored, regular measurements of the absolute vector values of the field are made, and baseline reference data are maintained to provide calibration data files. Figure 1 shows a map of the locations of these observatories as indicated by their IAGA 3-letter identification (ID) code. Table 1 provides additional information about these stations. Three of these stations are located in Alaska, one each is in Hawaii, Guam, and Puerto Rico, and the remainder are in the continental United States. In the late 1970's, the USGS began converting from analog data collection in the form of traces on photographic paper (known as magnetograms), to digital systems that used saturable-core fluxgate magnetometers and data loggers to store 10-second samples on magnetic tape that were then processed into 1-minute field values. However, only five observatories (Barrow, Boulder, College, Sitka, and Tucson) were provided with digital equipment, and a variety of problems prevented the successful collection of a great deal of data from these first attempts.

In the early 1980's, the USGS began providing all observatories with digital data capabilities, even though some stations continue to record data on magnetograms. Incidentally, these photographic records have continued to be a valuable tool in identifying problems with data from the digital systems. Each observatory is equipped with separate vector and scalar magnetometers, and a data acquisition system for the collection,

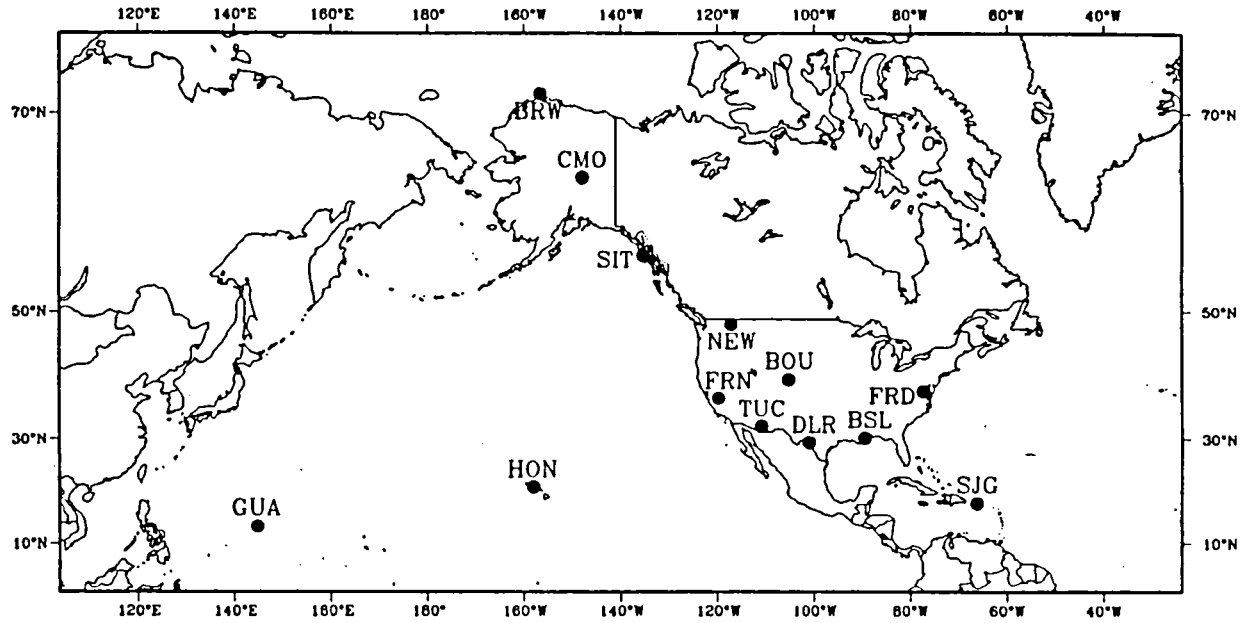

Fig. 1. Locations of the U.S. Magnetic Observatories, as identified by their 3-letter ID code. See Table 1 for the key to these codes and additional information about the stations.

storage, and transmission of geomagnetic field values. Also provided are an analog chart recorder to give an on-site indication of the output of the magnetometers, a modem for telephone communications, a monitor for on-site access to the data acquisition system, a printer, and an uninterruptable power supply (UPS) to sustain temporary operation during power outages. Each observatory is queried three times per week via telephone to check the status of the station and to dump out the data stored in memory.

The NGIC is currently undergoing an upgrade in their magnetic observatory systems that will allow near-real time (every 12 minutes) data acquisition via satellite, and provide preliminary on-line field values (as opposed to variation data) using a self-biasing ring-core magnetometer with quasi-absolute calibration control. When completed, the NGIC stations will comprise the contribution of the United States to INTERMAGNET, an international, cooperative program designed to make a global network of real-time geomagnetic observatory data available to the scientific community (Green, 1991). This paper describes the types of instrumentation used at the U.S. magnetic observatories, discusses the methods and procedures used in processing the data, and indicates some of the quality controls employed to eliminate erroneous values in the data.

2. Observatory Instrumentation

The vector magnetometers at the observatories are triaxial, cylindrical core saturable fluxgates like those described by Trigg, et. al. (1971). They have a nominal output of 10 millivolts (mV) per nanotesla (nT), and a dynamic range of +/- 1000 nT. For high latitude stations, the output is modified to 2.5 mV/nT with a dynamic range of +/- 4000 nT. At the NGIC observatories, the orthogonal sensors are oriented with the X and Z sensors in the magnetic meridian plane so that the Y sensor is normal to the horizontal north-south direction of the Earth's magnetic field, giving a declination (D), horizontal intensity (H), and vertical intensity (Z)

TABLE 1. Magnetic Observatory Information

	ID	Lat. (deg.)	Long. (deg.)	Digital (mo/yr)	OMIS (mo/yr)	DCP (mo/yr)	Manned Station
Barrow, AK	BRW	71.30	203.38	05/75	06/84	A	D
Boulder, CO	BOU	40.14	254.76	01/78	06/81	B	G
Bay St. Louis, MS	BSL	30.40	270.36	C	06/86	A	F,G
College, AK	CMO	64.86	212.16	09/75	06/84	A	Yes
Del Rio, TX	DLR	29.49	259.08	C	09/82	A	F,G
Fresno, CA	FRN	37.09	240.28	C	06/82	11/90	F,G
Fredericksburg, VA	FRD	38.21	282.63	C	11/82	07/89	Yes
Guam, M.I.	GUA	13.58	144.87	C	12/82	A	Yes
Honolulu, HI	HON	21.32	202.00	C	12/82	04/91	E
Newport, WA	NEW	48.26	242.88	C	10/82	09/90	F,G
San Juan, PR	SJG	18.11	293.85	C	01/83	A	Yes
Sitka, AK	SIT	57.06	224.68	01/78	12/83	10/91	F,G
Tucson, AZ	TUC	32.25	249.17	01/78	10/82	A	Yes

LEGEND

A : DCP has not yet been installed
B : DCP is installed, but satellite transmission is not permitted on observatory grounds. Data are retrieved by dedicated phone line.
C : Station was not equipped with digital data capabilities initially.
D : Station is serviced by personnel from College observatory
E : Station is operated by personnel at the Pacific Tsunami Warning Center, NOAA
F : Station has contract person on-site to perform emergency repairs.
G : Station is serviced by personnel from NGIC in Golden, CO.

orientation. Bias circuits are used to null out most of the H and Z fields, and the fluxgate provides a continuous bipolar output (in volts) that is proportional to the intensity of the ambient field about the zero (nulled) level.

Periodic absolute measurements of the magnetic field are made to provide a baseline reference (the zero level) to use in determining field values at all times. Some stations make scale value measurements, but where this is not possible, the nominal scale value is used. The baselines and scale values comprise the calibration data that are used to convert variation data in electrical units into magnetic field values. Wienert (1970) provides a description of the procedures followed in standard observatory practices.

Although some temperature compensation is built into the electronic circuitry, fluxgate magnetometers are quite sensitive to temperature variations and tilt. Trigg et. al. found nominal temperature factors of about 3 nT/°C for the Z component, and less than 1 nT/°C for D and H. The fluxgates at U.S. observatories are in somewhat thermally controlled environments, and generally mounted on massive marble tables, but no compensations for temperature or tilt, per se, are made in processing the data. The fluxgate

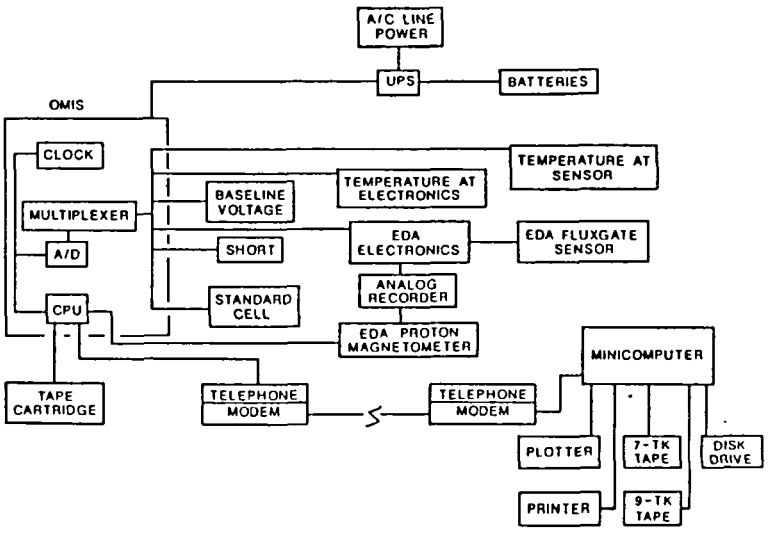

Fig. 2. Block diagram of an OMIS data collection system, with the accompanying peripherals and connections to the data processing center.

sensors are leveled using bubble levels mounted on the sensor bases.

The scalar magnetometer is a proton precession magnetometer that outputs the scalar value of the total field intensity (F) with a resolution of 0.1 nT. This instrument provides an independent measurement system with which to compare the field values obtained from the vector instrument. Also, because it is not particularly sensitive to temperature or orientation, it is used to perform quality control tests on the vector data. However, because of the large polarizing current required for operation, and the relatively long decay times involved, the sampling rate is restricted to 20 second intervals.

The data acquisition equipment, termed an Observatory Magnetometer Interface System (OMIS), employs a microprocessor-based (Z-80) data collection, manipulation, and storage system. Figure 2 shows a block diagram of an OMIS system. Nine analog input channels are available with 14-bit analog-to-digital (A/D) conversion and a dynamic range of +/- 10 volts. The three fluxgate components are sampled 40 times per second and averaged into one-minute values centered on the minute. The on-site software is stored in four EPROMs (Erasable Programmable Read Only Memory), and 64 kilobytes (Kb) of RAM are used to store up to 3 1/2 days of data. A 1600 bpi tape cartridge is also used, and the data from memory is written to tape every 105 minutes. The OMIS also computes and stores mean hourly values (MHVs), temperatures at both the sensor and electronics, flags that give error alerts, and reference values that are used to check the A/D converter and diagnose the status of the on-site system. All stations are queried three times per week by phone to check their status, and the data are dumped by phone from memory to serve as a backup for the tape cartridges that are changed approximately once a month and sent to the NGIC data processing center.

The new NGIC data acquisition systems, termed Data Collection Platforms (DCPs), have the capability of numerical filtering to prevent aliasing of the data, and satellite transmission on 12-minute intervals, primarily by means of the GOES-East and GOES-West satellites. It uses a 16-bit CMOS microprocessor with 16 A/D input channels, two serial

(RS-232) I/O ports, and 27 digital inputs. Although there are no magnetic tape storage capabilities, there are 256 Kb of RAM to allow almost two weeks of data storage and, in the event of a power failure, the system can continue to operate for that time on just two car batteries. It requires less than three watts of power to operate in the wake mode, and only 10% of that in the sleep mode. The system is also capable of 1-second and/or 5-second data collection and storage. In addition to the vector and scalar data, the DCPs also store 1-hour and 3-hour range indices, component baseline reference measurements, and four environmental parameters.

The new vector magnetometers are triaxial ring-core fluxgates, that are self-biasing in increments (bins) of a fixed value (usually 327 or 654 nT) with a range of +/- 80,000 nT, and a resolution limit of 0.01 nT in each axis. Once the bin constants are known, along with the zero-level offsets, magnetic field values can be obtained directly using a conversion factor of 100 nT/volt. The ring-core fluxgates have a much better temperature stability, nominally 0.1 nT/°C, and require less than 2 watts of power for operation.

A system for obtaining vector absolute magnetic field values using a proton magnetometer mounted within a pair of orthogonal Helmholz coils was originally suggested by Bacon (1955), and later expanded upon by Alldredge (1960) and Alldredge and Saldukas (1964). L.R. Wilson (1986, private communication) suggested that such systems be used at unmanned observatories to obtain frequent calibration data. Herzog (1990) tested such a system at a mid-latitude observatory (Boulder) and obtained very encouraging results. These quasi-absolute coil systems, now referred to as DIDD (Deflected-Inclination-Deflected-Declination) systems, will eventually be installed at all NGIC observatories.

Once in place, the new systems will provide near-real time calibrated magnetic field values from the entire network of NGIC observatories. A telephone dial-in service is being developed and installed at NGIC that will allow users to access these data directly over phone lines or through electronic mail.

3. Data Processing

The processing of observatory data requires the assimilation of raw field data values from a variety of sources; the adoption of calibration data files to be used in the conversion of data from electrical units into magnetic units; the application of quality control checks to identify timeshifts, clean out bad values, and cross-check adopted field values; and the formatting and archiving of the data for dissemination. These procedures themselves have undergone an evolution in the conversion from the analog photographic magnetograms to the digital recording systems, but the present discussion will be limited to the procedures followed in processing the OMIS digital data.

After the first of each month, where possible, the OMIS tape cartridge is unloaded and sent into the NGIC data processing center. For some unmanned stations, like Barrow, the delay in receiving the tape can be as much as several months. When the data is read off the tape satisfactorily, the hourly values are stripped off and stored in separate files from the one-minute data. The one-minute variation data are then merged into monthly files and stored on 9-track magnetic tape. Missing data are filled in from the tri-weekly phone dumps. The data are then plotted to obtain a hard copy to check for timeshifts, spikes, and other problems.

Calibration files are also maintained that contain the absolute measurements, scale values, and the adopted baseline values. Tests on scale value measurements showed that they remained quite stable and, except for Barrow and College, all stations use the nominal scale value of 10 mV/nT. Ordinate values are converted from electrical units (mVs) into magnetic units (nT and minutes of arc) using the scale values, and added onto the baselines to give magnetic field values for all 3 components. A computer algorithm is used to obtain a running least-squares fit of line segments to the adopted baseline values. These line segments become the baselines used in obtaining the final one-minute magnetic field data. Figure 3 shows an example of the baseline values and adopted line segments for D, H, and Z at the San Juan observatory for 1986. The points mark the computed baseline values, and the line segments are the adopted baselines themselves.

Once the data have been cleaned and corrected, and converted to magnetic field values, several quality control checks are performed. First, the field values derived with the calibration data are compared to the absolutes obtained from the actual field observations over the interval of the measurements. Differences between the computed D, H, and Z values, and those obtained during absolute measurements of the field itself, are output for each interval of observation. The distribution of differences should be more or less random about a near-zero value. Any large or consistently different differences are then a sign of a problem between the adopted field values and the absolute field measurements.

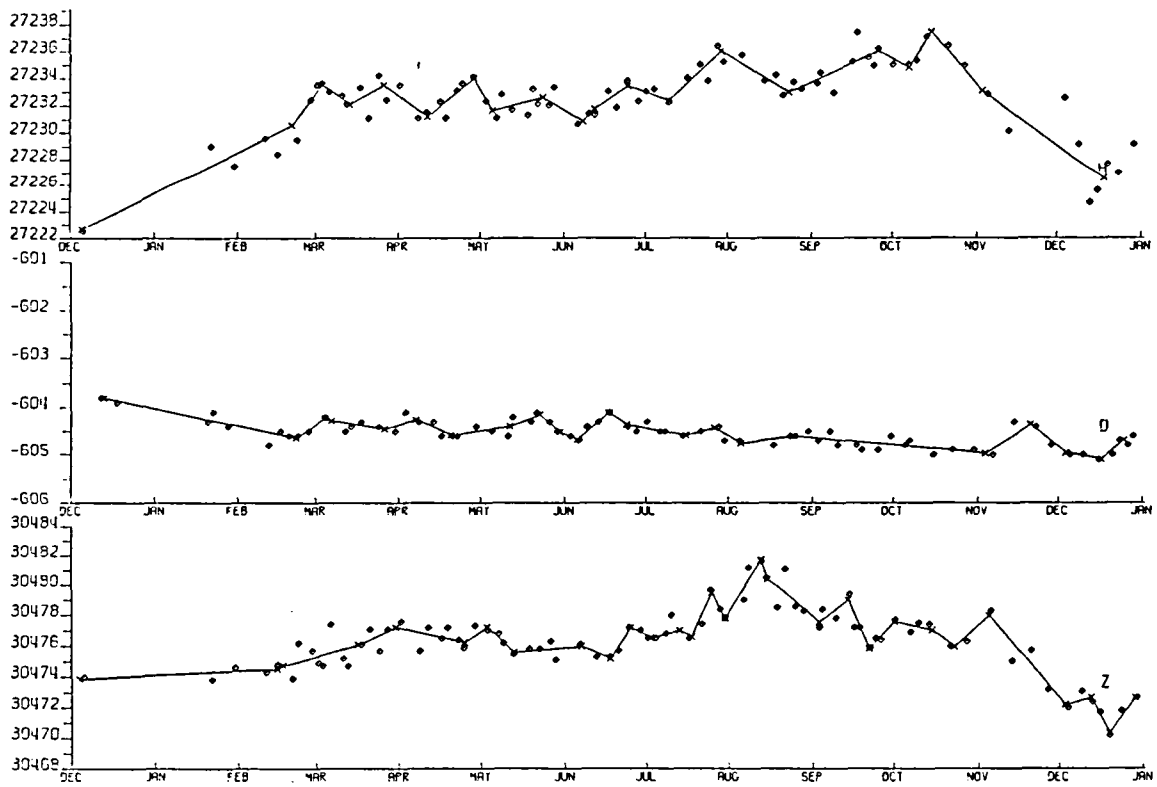

Fig. 3. Baseline observations and adopted line segments for San Juan observatory about the year 1986. The top plot is for horizontal intensity (H), the center for declination(D), and the bottom plot is for vertical intensity (Z). Negative declination values indicate West declination.

A second check consists in comparing the mean hourly values of the total field intensity (F) computed from the derived H and Z values with the values obtained with the proton magnetometer. One would expect an even distribution of these differences about some mean value that represents a pier difference between the proton and fluxgate sensor locations. Departures from a normal distribution about this pier difference indicate the presence of systematic influences.

After the data have passed these two quality controls, final plots are made, examined, and kept on file. The data are then written to magnetic tape as monthly files. A new program is now in operation whereby the data are re-formatted and archived onto a CD-ROM, along with hourly, daily, and monthly means, K-Indices, and other geomagnetic data. At present, one-minute data is available on CD-ROM for the years 1985 thru 1989, and for 1990. Each year, a 1-year CD-ROM will be produced for the previous year of data until five years are available, and then a separate CD-ROM of those five years will be made and distributed.

With the introduction of the DCPs, an extensive revision of the data processing procedures is underway. Incoming data for each station, in the form of magnetic field units, will be updated every 12 minutes and made available immediately as *Reported* data. Multiplexed phone lines will enable users to call in and obtain stack plots of the field components, output ASCII values to their terminal, or have data files transferred by phone or electronic mail to their location. After plotting the values for the previous day, doing any necessary cleaning and adjustments, and applying the baseline reference measurements using the DIDD systems, the corrected data will then be made available 1-3 days later as *Adjusted* data. Finally, after a complete review, making all corrections and performing the quality control checks, the data will be made available as *Definitive* data and then processed for CD-ROM production.

4. Data Accuracy

The accuracy of geomagnetic data is dependent upon the quality and methods for adopting calibration data, the accuracy of the monitoring and recording instruments, and the quality controls used in identifying and correcting errors in the data. Absolute measurements at nearly all U.S. observatories are made with a Declination/Inclination Magnetometer (DIM), with a resolution of 1 nT. These instruments employ essentially the same sensors and electronics as the cylindrical-core fluxgates used in field monitoring, and are restricted in current observatory applications by the resolution of the theodolite used in measuring the angles of rotation. The conversion to DIMs was made in the late 1980's. Prior to that, absolutes were generally made using Quartz Horizontal Magnetometers (QHMs), proton magnetometers, and a Ruska magnetometer for measuring D.

The frequency of observation varies from several times per week at some manned stations, to approximately once every two months at Barrow. Figure 4 shows a relative plot of the H-baselines for 7 observatories. The actual base values have been adjusted to allow comparison on a single plot. The standard error of the data points about each adopted line segment is computed and then averaged together to provide a measure of the distribution of baseline measurements about the adopted values. Table 2 shows the average standard errors of the D, H, and Z adopted baselines for 7 observatories for 1989.

Herzog and Wilson (1987) studied

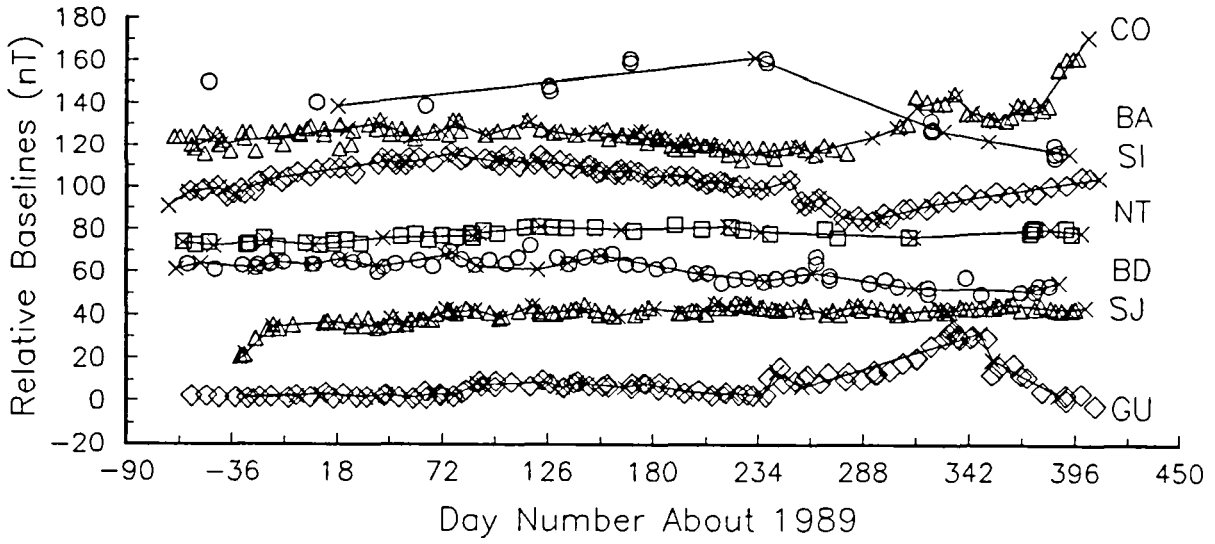

Fig. 4. Relative baselines for a selection of 7 observatories. Actual baselines for each station have been subtracted to allow the plots to be placed on the same scale.

the effect of observation frequency at a low latitude station (San Juan) on the adopted baselines by successively deleting every other observation from a calibration file and comparing the new baselines to the original set. They found that the frequency of observations on the order of a week made surprisingly little difference in the resulting baselines, even after reducing the original number of 75 observations to only 9 for the year. It is thought that the weekly observation frequency, assuming no baseline jumps or equipment problems, primarily compensates for only long-term or seasonal influences on the baselines.

Herzog (1990) compared the baselines at Boulder over a 6-month period obtained from using the standard weekly procedures, with those from a DIDD system that was programmed to provide absolutes on a twice-daily basis. Figure 5 shows the results of these two procedures for the Z-component. At the time of these tests, weekly absolute measurements were made using a QHM,

TABLE 2. - Average Standard Errors of Adopted Baselines for 1989 at 7 stations. Values are in nT for H and Z, and minutes of arc for D.

	Barrow	Boulder	College	Guam	Newport	San Juan	Sitka
H	5.3	3.0	5.2	3.2	2.0	2.4	2.5
D	0.8	0.3	0.95	0.2	0.4	0.2	0.3
Z	3.8	3.2	3.4	3.3	2.0	1.1	0.9

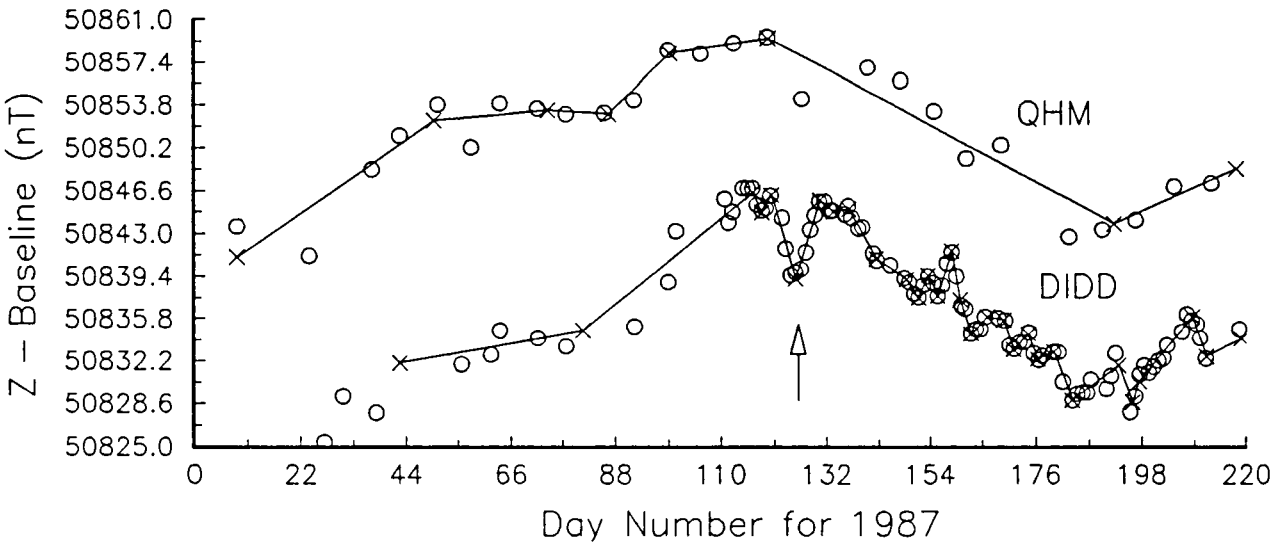

Fig. 5. Comparison of Z-baseline at Boulder between weekly observations (QHM) and twice-daily observations using a DIDD system. Note the large excursion about day 125 (indicated by the arrow) that the DIDD system baseline compensated for, but the QHM system did not.

and is referred to as the QHM system in the figure. A fine structure is clearly evident in the DIDD observations that does not appear in the adopted baseline segments derived from the weekly (QHM) measurements, even though the general (longer-term) character of the adopted baselines are the same. In particular, on about day 125 (as noted by the arrow), the DIDD system detects a clear drop in the Z-baseline, followed by a return to its original level, that the baselines from the QHM observations interprets as simply an outlying value. This excursion in the Z-baseline represents a +/- 7 nT change in the calibration data that could have only been detected by the frequent observations provided by the DIDD system. While the weekly observations are able to account for the long-term baseline variations, observations on the order of a day or less are required to correct for the short-term fluctuations, which can be significant. The use of DIDD systems at the observatories can obviously help improve the accuracy and precision of magnetic observatory data.

A comparison of the MHV's of total intensity, computed from H and Z, with the proton values, reveals another measure (delta-F) of how well the derived field components compare with those obtained from a separate measurement system. Figure 6 shows three observatory-month plots of these delta-F differences. The horizontal axes are divided into 12-hour intervals for the month. The vertical axes are in 0.1 nT, and are divided into increments corresponding to one-half a standard error value of the distribution about the mean difference for that station and month. Thus, if the standard error for a delta-F distribution were 2.0, the vertical axis would be separated into units of 10 tenth-nT. The numbers along the vertical axis indicate one standard error value. The numbers within the distribution indicate how many MHV's fell within a given half-standard error range for a given 12-hour interval. An asterisk (*) indicates that 10 or more values fell within that interval. The columns of numbers to the right of the plot gives the number of observed values in each standard error interval (left

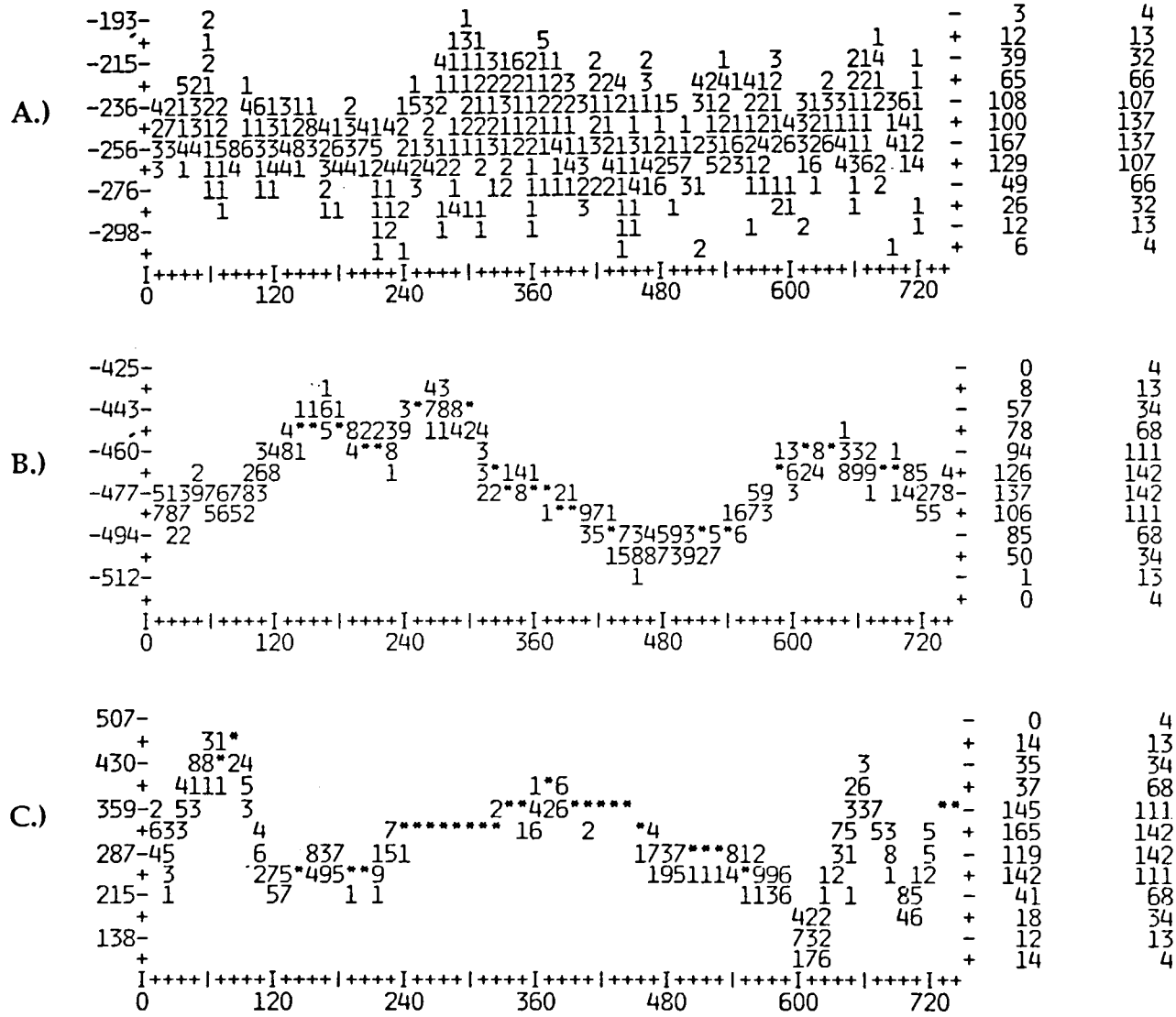

Fig. 6. Three plots of hourly mean differences of total intensity (F) computed from H and Z versus those from the proton magnetometer. The top plot (A) is for College in April of 1986, the center plot (B) is for Tucson in October of 1986, and the bottom plot (C) is for Barrow in January of 1986. The horizontal axes are in hours of the month, and the vertical axes are in tenth-nT increments of one-half standard error for the particular distribution of differences. The columns to the right give the actual (left) and expected (right) frequency distribution of delta-F differences. Refer to the text for further details.

column), and the number one would expect for a normal distribution of differences (right column).

Figure 6A shows a fairly well distributed set of differences at College for April, 1986. The mean difference was -24.6 nT with a standard error of 2.04 nT. This mean difference should represent a pier difference due to the different locations of the fluxgate and proton sensors. Although the distribution of differences appears to be spread evenly throughout the month, a chi-square test indicated that the data were not normally distributed at the 5% level of confidence. Very few chi-square tests of these differences are ever normally distributed.

Figure 6B shows the monthly distribution at Tucson for October, 1986, with a mean difference of -46.9 nT and a standard error of 1.69 nT. There is an obvious periodicity in this distribution that often appears in these delta-F plots. This one has a period of about 19 days

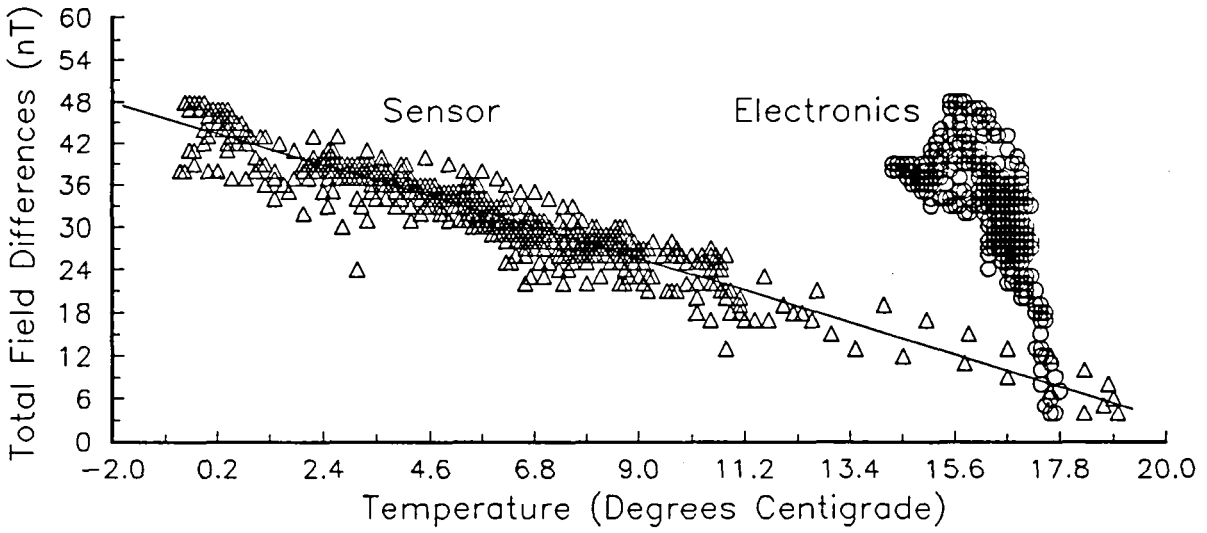

Fig. 7. Plot of total field differences (delta-F) versus temperatures at the sensor and electronics, for Barrow during January, 1986.

(456 hours). The cause of these periodicities is not well understood, although temperature variations are suspected since the fluxgates are very temperature sensitive while the proton magnetometers are not.

Figure 6C shows a distribution at Barrow for January, 1986, with a mean difference of 32.3 nT and a standard error of 7.16 nT. Here, we see a combination of periodic intervals (of varying length), as well as intervals in which the differences are fairly constant. Figure 7 shows a plot of these differences against the temperatures at the sensor and electronics, and supports the notion that temperature is largely responsible for the variation in differences. The delta-F differences are strongly correlated with the sensor temperature, while much less so with the temperature at the electronics. The slope of this line is about -2.2 nT/°C, which is consistent with the values found for the fluxgate sensors. This result led us to test other stations and observatory-months to see if the relationship would hold consistently. It did not, though, and the more cases we studied, the more diverse were the results. Some stations showed almost no relationship of delta-F differences to temperature, and some showed an inverse relationship to the one shown here. Although it needs further study, these results were included to demonstrate how much the accuracy of geomagnetic data can vary, at least on some occasions.

5. Summary and Conclusions

Geomagnetic data from the U.S. magnetic observatory network have been undergoing an evolution in improvement for more than two decades. The transition from fiber-suspension variometers that produced analog magnetograms, to fluxgate magnetometers with digital recording and data collection systems, allowed the development of computer data processing algorithms and procedures that, in turn, resulted in a reproducible methodology for determining baseline calibration data, the ability to make quality control checks to detect and eliminate erroneous data values, the capability of deriving quantitative

estimates of the accuracy and precision of geomagnetic data, and the opportunity to make massive quantities of data available to everyone on a low-cost, high-density storage medium. Five years of one-minute data for four elements (D, H, Z, and F) for 13 observatories (over 550 megabytes) are now available on a single CD-ROM.

We have described here some of the instrumentation currently in operation at those observatories, as well as the data processing procedures used to reduce the raw data and absolute measurements to final geomagnetic field values. The next generation of observatory operations promises to further improve the accuracy, precision, and availability of these data. Self-biasing ring-core magnetometers, having minimum power requirements, with greater resolution, better stability, and better thermal characteristics, will provide more precision to the recorded data and output it directly in calibrated magnetic field units. The DIDD coils will improve the accuracy of the data by taking more frequent absolute measurements and thereby compensating for the short-term influences on the calibration data. The data collection platforms, that also have very low power requirements, will provide numerical filtering of the data to reduce aliasing effects, allow for 1-second, 5-second, and 1-minute data recording modes, and transmit the data via satellite every 12 minutes directly to Geomagnetic Information Nodes (GINs) where they will be made immediately available to users. These observatories will also participate in INTERMAGNET's program to provide a global network of magnetic observatory data in near-real time. At the time of this writing, the NGIC had five observatories (FRN, FRD, HON, NEW, and SIT) operating these new systems in conjunction with the OMIS systems.

REFERENCES

Alldredge, L.R., 1960. A proposed automatic standard magnetic observatory, J. Geophys. Res., 65: 3777-3786.

Alldredge, L.R. and Saldukas, I., 1964. An automatic standard magnetic observatory. J. Geophys. Res. 69: 1963-1970.

Bacon, F. W., 1955. Adaptation of a free precession magnetometer to measurements of declination. Master's Thesis, U.S. Naval Postgraduate School, Monterey, CA.

Green, A.W. , Jr., 1991. Global real-time geomagnetic data sets for INTERMAGNET. Proceedings of the International Symposium., Heinrich-Hertz-Institute für Atmosphärenforschung und Geomagnetismus. No. 22.

Herzog, D.C. and Wilson, L.R., 1987. The precision of digital magnetic data from U.S. magnetic observatories [abs.]: IUGG XIX General Assembly Abstracts, p.674.

Herzog, D.C., 1990. An evaluation of the accuracy of geomagnetic data obtained from an unattended, automated, quasi-absolute station. Phys. Earth Planet. Inter., 59: 112-118.

Trigg, D.F., Serson, P.H., and Camfield, P.A., 1971. A solid-state electrical recording magnetometer, Department of Energy, Mines, and Resources, Vol. 41, No. 5, Ottawa, Canada.

Wienert, K.A., 1970. Notes on geomagnetic observatory and survey practice. UNESCO, Van Buggenhoudt Press, Brussels.

Magnetic and electromagnetic induction effects in the annual means of geomagnetic elements

CRIŞAN DEMETRESCU and MARIA ANDREESCU

Institute of Geodynamics, 19-21 J.L.Calderon St., Bucharest 37,Romania

The solar-cycle-related (SC) variation in the annual means of the horizontal and vertical components of the geomagnetic field at European observatories is used to infer information on the magnetic and electric properties of the interior, characteristic to the observatory location, by identifying and analysing the magnetic induction component and respectively the electromagnetic induction component of the SC variation. The obtained results and the method can be used to better constrain the anomaly bias in main field modelling and to improve the reliability of secular variation models beyond the time interval covered by data.

1.Introduction

It is a well established fact that in the annual means of the geomagnetic elements recorded at observatories (Chapman and Bartels, 1940; Yukutake, 1965; Alldredge, 1976; Courtillot and Le Mouël, 1976; Alldredge et al.,1979; Yukutake and Cain, 1979; Demetrescu et al.,1988) as well as in the annual values recorded at repeat stations (Atanasiu et al.,1976; Anghel and Demetrescu,1980; Galdeano et al.,1980; Demetrescu et al.,1985) a solar-cycle-related (SC) variation is present. Since the secular variation models rely on observatory and repeat station data, the SC variation might cause difficulties in predicting the secular variation beyond the time interval covered by data. On the other hand, main field models which include observatory data have to take into account the so-called anomaly bias (Langel and Estes,1985) which is related to the fields from crustal anomalies at observatory locations.

In this report we show, on data sets from the European observatories, how the SC variation present in the annual means of geomagnetic elements can be used to better describe individual observatories as regards the magnetic and electric properties of the interior, characteristic to the site, with possible consequences in improving the secular variation and main field models.

2. Data and method

The input data are the annual means of the horizontal and vertical components at European observatories (Golovkov et al.,1983). Two sets of data were analysed: annual

means from 22 observatories in the time interval 1952.5 - 1980.5 and annual means from 42 observatories in the time interval 1961.5 - 1977.5. The distribution of the observatories is shown in Fig.1.

Data were processed to show the SC variation by modelling the variation of the core field with a sum of sinusoids (see for details Demetrescu et al.,1988; Demetrescu and Andreescu, 1992). The SC variation for the set of data from 22 observatories is presented in the upper (H_S) and middle (Z_S) plots of Fig.2, together with the sunspot numbers (lower plot). Curves for individual observatories were superimposed to show, on one hand, the coherency of this variation, suggesting a common source, and, on the other hand, differences in amplitude and phase, reflecting peculiarities of the site. The fact that H_S, Z_S, $\dot{H}_S$, $\dot{Z}_S$ are station dependent can be accounted for by the magnetic and electric structure of the subsurface material, as the variable external solar-cycle-related magnetic field induces variable internal magnetic fields by magnetic and electromagnetic induction.

As in Demetrescu et al.(1988) and Demetrescu and Andreescu (1992), we fit H_S and Z_S data to a model of pure magnetic induction, obtaining both the magnetic induction component, as the calculated values of the model, and the electromagnetic induction component, as residuals. In the following we shall briefly review the principles used in the two papers mentioned above.

In case of pure magnetic induction, the temporal variation of H_S and Z_S at a given observing point is a linear combination of the components of the magnetic force. As estimates of the latter, we took the components of the field produced by external sources, as calculated from the external spherical harmonic coefficients of Yukutake and Cain (1979, table 4b) using the following equations (Chapman and Bartels, 1940):

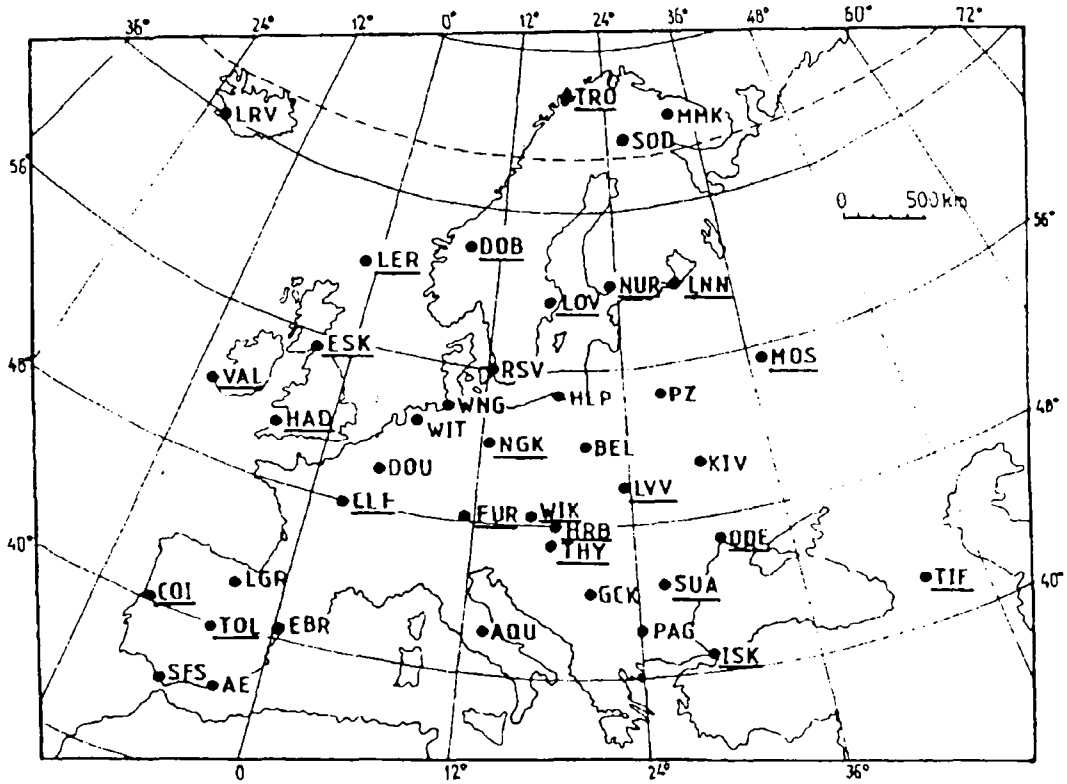

Fig 1. Distribution of the observatories used for analysis. Underlined symbols: set of 22 observatories with longer series of data.

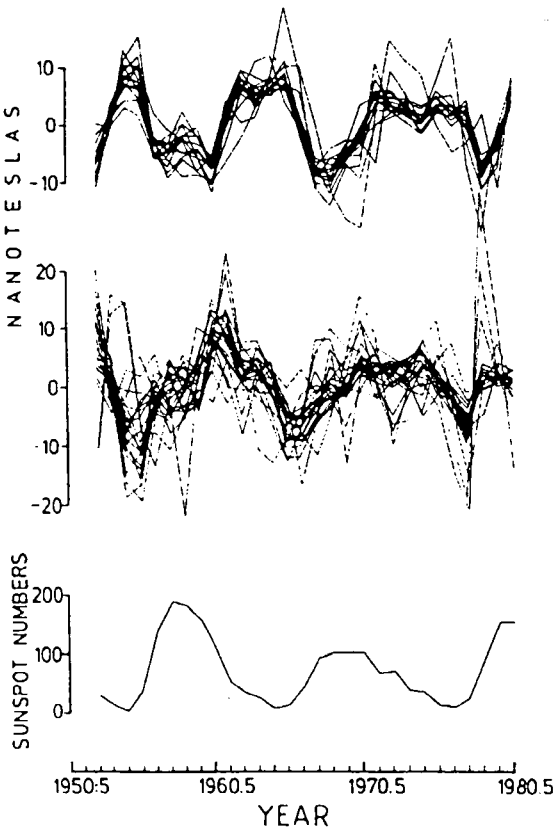

Fig. 2. Solar-cycle-related variations of the horizontal (upper plot) and vertical (midle plot) components and sunspot numbers (lower plot) between 1952.5 and 1980.5

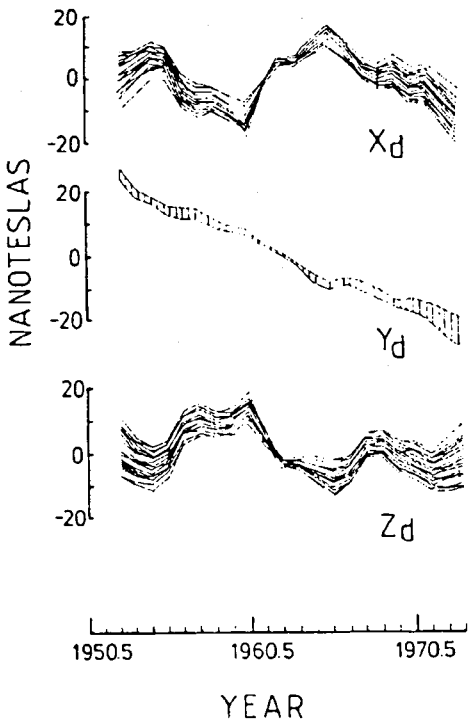

Fig. 3. Variation of the components of the external dipole field betwen 1952.5 and 1980.5.

$$X_d = -g_{10}\sin\theta + \cos\theta(g_{11}\cos\phi + h_{11}\sin\phi)$$

$$Y_d = g_{11}\sin\phi - h_{11}\cos\phi \qquad (1)$$

$$Z_d = g_{10}\cos\theta + \sin\theta(g_{11}\cos\phi + h_{11}\sin\phi)$$

where g_{10}, g_{11}, h_{11} are the external first degree coefficients, θ the colatitude, and φ the longitude of the given observatory. The time evolution of X_d , Y_d and Z_d is displayed in Fig.3.

For each observatory and field component, we have at time t

$$\Delta \begin{matrix} H_S \\ Z_S \end{matrix} (t) = \begin{matrix} \alpha_X \\ \beta_X \end{matrix} \Delta X_d(t) + \begin{matrix} \alpha_Y \\ \beta_Y \end{matrix} \Delta Y_d(t) + \begin{matrix} \alpha_Z \\ \beta_Z \end{matrix} \Delta Z_d(t) \qquad (2)$$

where Δ denotes variations about temporal averages for the considered time interval. The coefficients α and β depend on the effective magnetic permeability, which in turn depends on the position of the observing point. They can be calculated by a least squares procedure.

Then the calculated ΔH_S and ΔZ_S of eq.2 contain the contribution of the magnetic induction and the residuals, $REZ_H = \Delta H_S - \Delta H_S$ (calc.) and $REZ_Z = \Delta Z_S - \Delta Z_S$ (calc.), contain the contribution of the electromagnetic induction to the observed field. The residuals might also contain internal signals of periods less than 20 years (20 years was the smallest period used in modelling the core field with a sum of sinusoids) and /or external components, related or not to the solar cycle, but not present in the external field of eq.1.

3. Results and discussion

The analysis of the longer series of data (1952.5 - 1980.5, from 22 observatories) was extended only to 1973.5, the last epoch with available external first degree coefficients (Yukutake and Cain, 1979). The results are displayed in Fig.4, the calculated values, and Fig.5, the residuals.

3.1. Magnetic induction effects

It appears from Figs.4 and 5 that: (a) the contribution of the magnetic induction to the SC variation depends on the site, as would be expected if magnetic properties of rocks beneath the observing point were different; and (b) in case of the horizontal component the magnetic induction accounts for the largest part of the SC variation, while in case of the vertical component the contribution of the magnetic induction is comparatively weak.

The lateral variation of the coefficients α and β can be mapped, resulting in images of the lateral variation of the magnetic properties of the lithosphere. In Figs.6 and 7 we give the results for the second set of data (1961.5 - 1977.5, from 42 observatories). For a discussion on the effect the shorter time series and, consequently, the smaller number of sinusoids in the core field model have on the calculated coefficients, as well as for a discussion on the pattern and resolution of the maps, see Demetrescu et al. (1988) and Demetrescu and Andreescu (1992). Here we only point out that the information given by

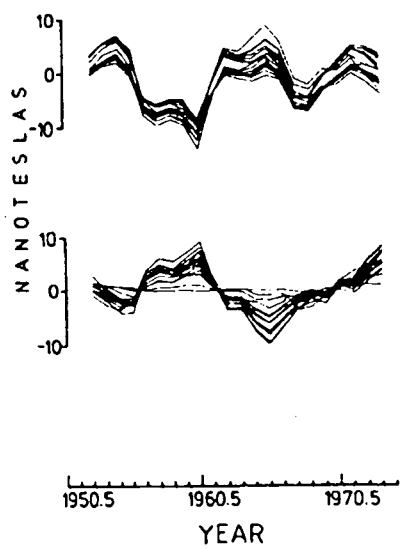

Fig. 4. Induction model. Calculated ΔH_S and ΔZ_S.

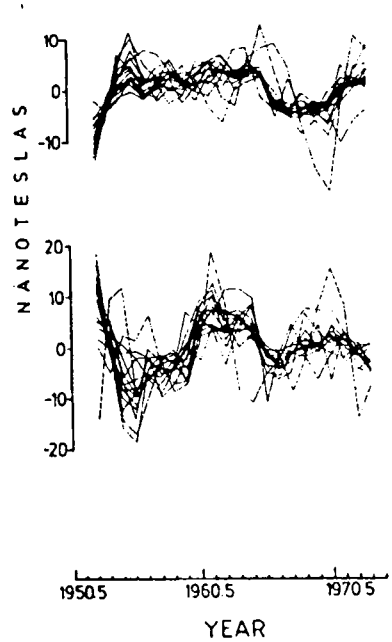

Fig. 5. Induction model. Reziduals.

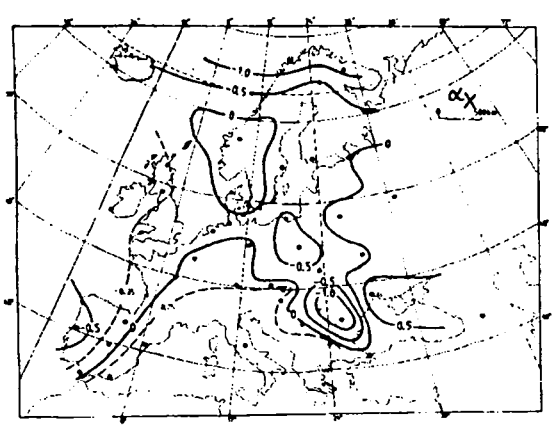

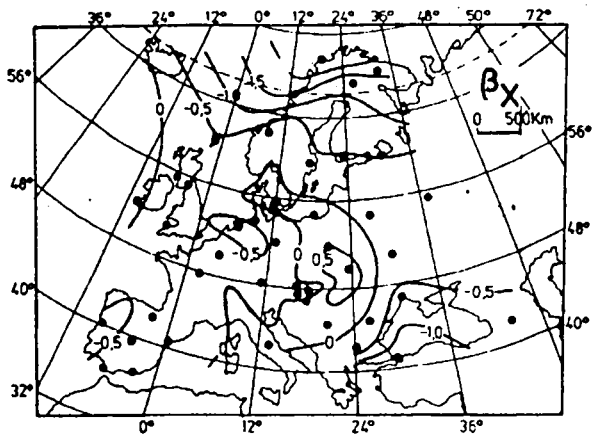

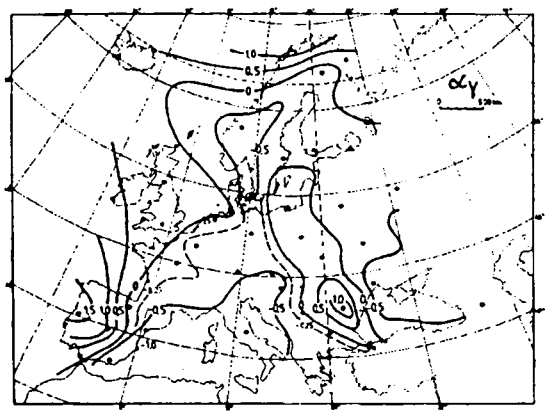

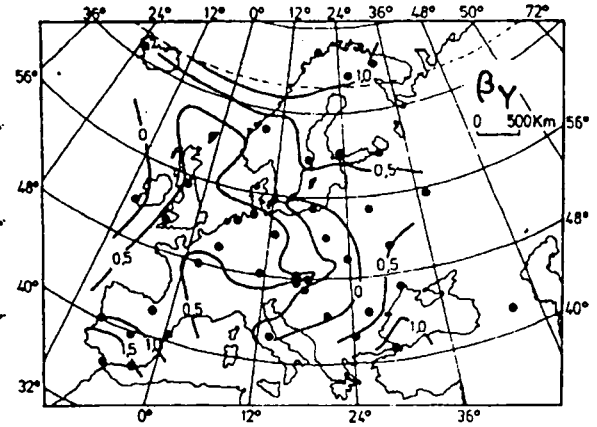

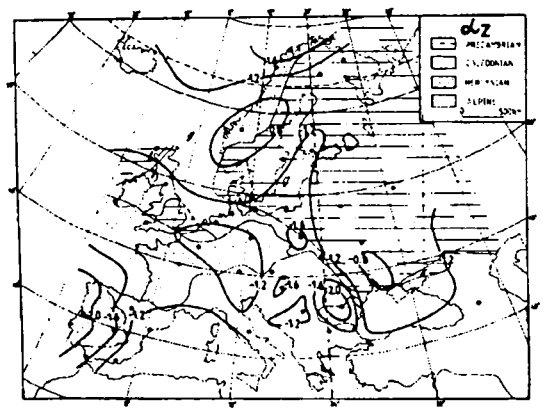

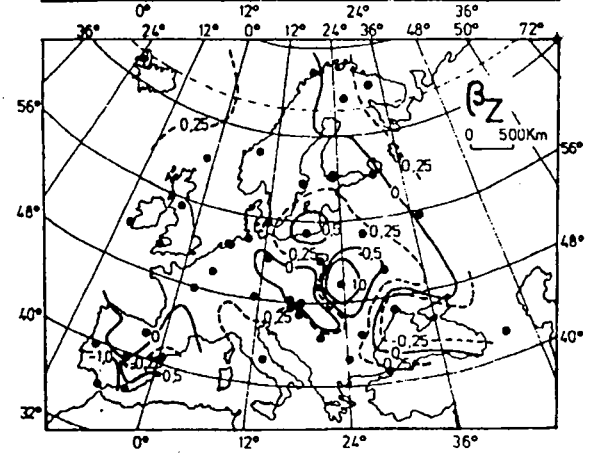

Fig. 6. Distribution of the coefficients α.

Fig. 7. Distribution of the coefficients β.

Full circles = magnetic observatories.

the α and β coefficients averages a volume of magnetic material going down to the Curie isotherm and that the maps in Figs.6 and 7 display magnetic permeability contrasts rather than actual permeabilities.

3.2. Electromagnetic induction effects

The residuals, Fig.5, should contain the contribution of the electromagnetic induction to the observed field. If any, this contribution in the horizontal component is small and/or masked by noise or other causes, such as: internal signals of periods less than 20 years and/or external components, related or not to the solar cycle, but not present in the dipole field we have chosen to represent the inductive force (Demetrescu et al., 1988). On the contrary, in case of the vertical component the residuals account for a large part of the SC variation, being more important than calculated ΔZ_S.

The low efficiency of the electromagnetic induction in the case of the horizontal component and the more pronounced electromagnetically induced response of the Earth in the case of the vertical component might be explained by the layered structure of the Earth. In the first case, this structure prevents induced currents of enough vertical extent to develop, favouring vertical loops of elongated horizontal extent producing small resultant horizontal magnetic field; in the second case, it favours horizontal induced currents producing comparatively larger resultant vertical magnetic fields. The behaviour of the magnetically induced components is compatible with this explanation too.

That the residuals describe the electromagnetic induction component was shown by Demetrescu and Andreescu (1992) for the vertical component. The noise in the initial data propagate in Z_S, in ΔZ_S(calc.), and residuals, being more important in the latter. However, in spite of the rather large noise, the residuals show a systematic behaviour, with lows at arround 1955.5 and 1966.5 and highs at arround 1961.5 and 1970.5. The residuals corelate well with $-\dot{Z}_d$ (Fig.8), which should be the case if the residuals were the effect of the electromagnetic induction produced by the varying external field Z_d, since the induction electromotive force is given by the negative time derivative of the magnetic flux of the inducing field.

In terms of loops of current flowing in the more conductive layers (Demetrescu and Andreescu, in preparation), having in view that the magnetic field B produced in the center of a circular loop of radius a by a current of intensity I is given by

$$B = 2\pi k \frac{I}{a} \tag{3}$$

where $k = 10^{-7}$ WbA^{-1}m^{-1}, the residuals could be viewed as a measure of the intensity of the current in an equivalent circular loop of radius unity surrounding the point of observation. This allows us to estimate the inductance L and the resistance R of the equivalent circuit, based on the relation between the instantaneous values of tension, u, and intensity, i, in a R-L circuit:

$$u = L\frac{di}{dt} + Ri \tag{4}$$

which, with the above established equivalents reads

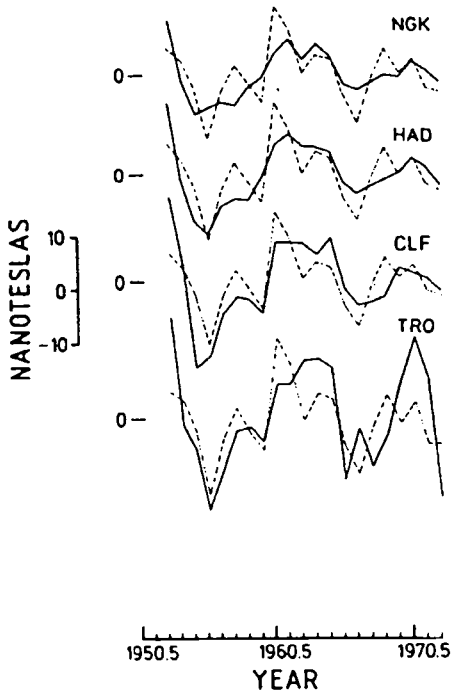

Fig. 8. Correlation of the residuals in the case of the vertical component (full line) with $-\dot{Z}_d$ (broken line).

$$-\dot{Z}_d(t) = L \cdot \dot{REZ}(t) + R \cdot REZ(t) \qquad (5)$$

L and R can be evaluated for each observatory for the given time interval by a least squares procedure. The lateral distribution of L and R can be mapped, resulting in images of the lateral variation of the electric properties of rocks beneath the observing points. Such maps can not be presented for the moment due to the bad geographical coverage of the longer set of data (only 22 observatories) and bad temporal coverage of the shorter one.

The study in preparation mentioned above also points out that the variable external source of the electromagnetically induced component seems to correlate with the solar activity in a way that makes the sunspot number and its first derivative useful indicators in attempts to estimate (predict) this component both in H and Z.

4. Conclusion

The solar-cycle-related variation present in the annual means of the horizontal and vertical components of the geomagnetic field at European observatories was analysed to obtain information on the magnetic and electric properties of the interior, characteristic to the observatory location.

The calculated values of the magnetic induction model fitted to the data estimate the contribution of the pure magnetic induction to the observed SC variation, while the residuals correspond to the electromagnetic induction component. It appears that, on one hand, the magnetic induction accounts for a large part of the observed SC variation in H, being comparatively small in Z; on the other hand, the electromagnetically induced response of the Earth is well present in the vertical component and weak or

masked by noise or other causes in the horizontal component.

The parameters related to the magnetic permeability of rocks and to the inductance and resistance of current loops in the Earth, derived for each observatory, can be used to constrain the anomaly bias in main field modelling, as well as to improve the secular variation models.

References

Alldredge, L.R., 1976. Effects of solar activity on annual means of geomagnetic components. J. Geophys. Res., 81: 2990-2996.

Alldredge, L.R., Stearns, C.O. and Sugiura, M., 1979. Solar cycle variation in geomagnetic external spherical harmonic coefficients. J. Geomagn. Geoelectr., 31: 495-508.

Anghel, M. and Demetrescu, C., 1980. The effect of solar activity on the secular variation of the geomagnetic field in Romania.Phys. Earth Planet. Inter., 22: 53-59.

Atanasiu, G., Neştianu, T., Demetrescu, C. and Anghel, M., 1976. Some aspects of the secular variation of the geomagnetic elements H, Z and F between 1958 and 1974 in Romania. Phys. Earth Planet.Inter., 12: P11-P17.

Chapman, S. and Bartels, J., 1940. Geomagnetism. Clarendon Press Oxford, 1049 pp.

Courtillot, V. and Le Mouël, J.-L., 1976. On the long period variations of the Earth's magnetic field from 2 months to 20 years. J.Geophys. Res., 81: 2941-2950.

Demetrescu, C. and Andreescu, M., 1992. Magnetic and electromagnetic induction effects in the annual means of the vertical component of the geomagnetic field at European observatories. Submitted to Phys. Earth Planet. Inter.

Demetrescu, C., Andreescu, M. and Neştianu, T., 1988. Induction model for the secular variation of the geomagnetic field in Europe. Phys. Earth Planet. Inter., 50: 261-271.

Demetrescu, C., Andreescu, M., Neştianu, T. and Ene, M., 1985.Characteristics of the secular variation of the geomagnetic field between 1964 and 1981 in Romania. Phys. Earth Planet. Inter., 37: 46-51.

Galdeano, A., Courtillot, V. and Le Mouël, J.-L., 1980. La cartografie magnétique de la France au 1er juillet 1978.Ann.Geophys., 36: 85-106.

Golovkov, V.P., Kolomijtzeva, G.I., Konyashchenko, L.P. and Semyonova, G.M., 1983. The summary of the annual mean values of magnetic elements at the world magnetic observatories. IZMIRAN, Moscow, 351 pp.

Langel, R.A. and Estes, R.H., 1985. The near-Earth magnetic field at 1980 determined from Magsat data. J.Geophys.Res., 90: 2495 - 2509.

Yukutake, T., 1965. The solar cycle contribution to the secular change in the geomagnetic field. J. Geomagn. Geoelectr., 17: 287-309.

Yukutake, T. and Cain, J.C., 1979. Solar cycle variations of the first-degree spherical harmonic components of the geomagnetic field. J.Geomagn.Geoelectr., 31: 509-544.

INDEPENDENT CONSTITUENTS IN OBSERVATORY TIME SERIES IN CHARACTERIZING THE SECULAR VARIATION

W. Webers
Central Institute for Physics of the Earth
Telegrafenberg, D-1561
Potsdam, Germany

Summary

By an ansatz of a finite set of N superimposed oscillations, observatory time series are fitted. This start model is optimized for the independence of the used 2N-dimensional functional system as a criterion. Here, the contributions of each of the dimensions to the volume of the corresponding 2N-dimensional parallelepiped of the functional space is to be evaluated. Independence and an equal standard for the constituents are achieved by the optimizing procedure varying the start values of frequencies in the fitting ansatz when quotients of successively constructed Gram-determinants are beyond a definite threshold and of nearly the same numerical value. Results for globally distributed observatories characterize the secular variation.

Introduction

As a reflection of the physical processes in the Earth's body and its surrounding space, the time series of the geomagnetic field represent essential subjects of geophysical research for different aspects. For the study of numerous geophysical processes, especially periodic ones, this seems to be of special importance. Consequently, geophysicists try to separate the first of all periodic constituents in the recordings. This is of special interest when independent and stable periodic constituents in the time series of the magnetic elements recorded at geomagnetic observatories can be used as global characteristics of the secular variation.

The results presented here are based on annual means of the records of some observatories. The method used does not contain any restrictions from the data bases or from any other source. Therefore, it can be applied without modifications to any other kind of data series where oscillating constituents in time or in space are to be determined.

This method is more general than the Fourier analysis where an internal dependence as harmonics is supposed.

On the Method

In the given time interval, the linearly trend-corrected time series f(t) is modeled deterministically as a supposed ansatz by a finite set of superimposed oscillations which are assumed to be stationary.

$$f(t) \approx g(t) = \sum_{i=1}^{N} \left(a_i \sin \frac{2\pi}{T_i} t + b_i \cos \frac{2\pi}{T_i} t \right) \qquad (1)$$

The coefficients a_1 and b_1 of eq. (1) are determined by the method of least squares where the used functional system f_j, j = 1, ..., 2N formed by the sine and cosine terms is to be linearly independent.

$$F_j(t) = \sin \frac{2\pi}{T_i} t \qquad \text{for } j = 2i-1 \qquad (2a)$$

$$F_j(t) = \cos \frac{2\pi}{T_i} t \qquad \text{for } j = 2i \qquad (2b)$$

$$j = 1, ..., N$$

The start tupel of periodicities T_i used in Eq. (1) are taken from spectral analytical investigations of the time series f(t) as well as from physical knowledge about possible sources of the processes. In general, T_i derived this way are in most cases, roughly estimated values being insufficient for a physical theory. As is well known, all the spectral analytical methods are of limited efficiency (De Meyer and De Vuyst, 1982; Saito, 1978; Kane and Trivedi, 1982; and Webers, 1985).

For such a set of periodicities T_i (i = 1, ..., N) given in this way, the coefficients a_1 and b_1 of Eq. (1) determined by the method of least squares result in related amplitudes A_1 and phases φ_i calculated by

$$A_1 = (a_i^2 + b_i^2)^{1/2} \qquad (3)$$

$$j_i = \arctan \frac{b_i}{a_i} \qquad (4)$$

Because of the fact that the used T_i in the start tupel are only roughly estimated values and quite possibly, some of them are relatively doubtful from the spectrum, it is becomes necessary to precisely determine them. This refers to the number N of the used T_i as well as to their definite value.

Consequently, the computer program includes an

-- optimizing procedure for the approximation quality m_0 of g(t) for f(t) by varying the start tupel of T_i, and an

-- optimizing procedure for the independence of the used 2N-dimensional functional system of the ansatz (1) as optimizing criterion by varying the start tupel of T_i within a given interval ΔT_i (Webers, 1987; 1991).

Here, the functions F_j (t), j = 1, 2, ..., 2N are interpreted as 2N vectors forming a 2N-dimensional vector space, and their independence is proved by calculating the volume of the corresponding parallelepiped given by the 2N coordinate axes with directions of these 2N vectors $\xi_j = f_j(t)$.

The quality of independence of the functions F_j (t), i.e., of the vectors ξ_j, is given by their contribution to the volume of the 2N-dimensional parallelepiped that they build up. Consequently, the corresponding contribution of every F_j, j = 1, ..., 2N can be evaluated numerically when the related volumina are compared in constructing the 2N-dimensional space step by step with j = 1, 2, ..., 2N.

The volume of the parallelepiped is calculated by the Gram-determinant

$$G_j = \det(\xi_k, \xi_l); \qquad \begin{matrix} k = 1, 2, ..., j \\ l = 1, 2, ..., j \\ j = 1, 2, ..., 2N \end{matrix} \qquad (5)$$

where its elements consist of scalar products of the vectors ξ_j. The procedure is essentially simplified when the functions $F_j(t) = \varphi_j$ are orthogonolized before the method of least squares is applied. As a consequence, final amplitudes and phases are calculated independently of the number of periodicities T_j used and the Gram-determinant G_j is given by the product of its elements in the principal diagonal.

Furthermore, the orthogonalization of the functional system enables an improvement to the approximation quality by enlarging the fitting ansatz (1). Every dimension, i.e., functional term of an oscillating constituent in the time series f(t) can only give an essential contribution in representing the 2N-dimensional space of modelling f(t) when the relation of successive Gram-determinants

$$H_j = \frac{G_j + 1}{G_j} \quad ; j = 1, 2, ..., 2N \qquad (6)$$

is beyond a definite threshold, moreover when they all are nearly of the same value. In this sense, the oscillating constituents of the ansatz (1) are of the same quality of independence in modelling the time series f(t). Consequently, this mathematical criterion is therefore also of physical importance.

Evaluating hereby the linear independence and the significance of the functional system is not influenced in any way by the different amounts of the corresponding amplitudes and phases.

On the other hand, there is a definite value for the relation of successive Gram-determinants being a numerical characteristic for the time series under investigation. Numerical instability of the fitting ansatz is indicated by

-- essentially varying amplitudes within the optimizing procedure; and
-- very different quotients H_j of the Gram determinants.

Results

Tables 1 through 6 show the results for the geomagnetic component X of some observatories. Figure 1 presents a comparison of Niemegk X time series f(t) (trend corrected), and its modelling g(t) where

T_i: 120; 66; 50; 40; 30; 22; 18.6; 13[yr] and the residual curve 4(t).

There is a good approximation quality given by m_o. The corresponding amplitudes and phases are shown in Table 1. Table 2 demonstrates that the approximation quality is significantly worse when a long-period constituent of about $T \approx 120/130$ years is neglected. This holds despite the fact that the time series is not long enough (cf. Webers, 1985). By the relation of the Gram determinants H_j, Table 3 shows that a model gives a good approximation for f(t) but does not guarantee that the oscillating constituents it uses are of the same quality

for the independence from each other. Therefore, they do not have the same significance. By optimizing the used start tupel of T_i (Table 3), independence and more significance could be achieved (Table 4). Table 4 also shows the way in which the model of the ansatz is improved when more significant constituents are added by enlarging Eq. (1) to higher N. Table 5 shows the results for the X-component at Chambon-la-Foret observatory.

Because of the fact that each of the oscillating constituents is represented in Eq. (1) by two terms; i.e., by functions based on a sine and a cosine expression of the same T_i, the more interesting sizes H_j are those with reference to the same T_i. In Tables 2 through 5, only those H_j are given. In general, all the other H_j describing the interrelation between the relevant functions of different T_i are also of importance as well as of evidence.

Table 6 shows a comparison of the optimized models for the X component of the following observatories: Oslo (1820-1948), Niemegk (1890-1989), Hartland (1849-1984), Chambon-la-Foret (1883-1986), Choimbra (1867-1985), Tangerang/Batavia (1884-1983, and Alibag (1848-1987). In general, the published observatory data (annual means) are used for the presented calculations without detailed evaluation; the data bases having been supposed as essentially correct. Only for the Oslo X component between 1917 and 1919 has an obviously erroneous spike in the data been smoothed (Webers, 1985). Differences of the models in essential parts seem to be caused by physical effects, but on the other hand, there are obvious influences arising from different data quality.

In general, the analysis of the observatory data series by the presented method results in significant and numerically stable constituents that are global characteristics of the secular variation.

References

De Meyer, F. and A. De Vuyst, 1982, "The geomagnetic line spectrum at one station (Dourbes)," *Ann. Geophys.*, **38**, 1, pp. 61-73.

Kane, R.P. and N.B. Trivedi, 1982, "Comparison of maximum entropy spectral analysis (MESA) and least-squares linear prediction (LSLP) method for artificial samples," *Geophysics*, **47**, 12, pp. 1731-1736.

Saito, M., 1978, "Possible instability in the Burg maximum entropy method," *J. Phys. Earth*, **26**, pp. 123-128.

Webers, W., 1981, "On spectral analyzing the time series of the geomagnetic field," Veröffentl. d. Zentralinstituts f. Physik d. Erde, Potsdam, Nr. 70, pp. 99-113.

Webers, W., 1985, "On analyzing the time series of the recent geomagnetic field," *Geod. Geoph. Veröff*, d. NKGG d. DDR, RIII, H 53 (1985), pp. 120-131.

Webers, 1987, "Geomagnetic time series--mathematical model and physical content," HHI-Report No. 21 (1987), Berlin, pp. 71-74.

Webers, W., 1991, "On independent constituents in geomagnetic observatory time series and their global distribution," HHI-Report No. 22 (1991), Berlin, pp. 75-86.

Table 1. Niemegk, X, 1890-1985, linearly trend-corrected annual means, range 450.5 nT.

T_i [yr]	A_i [nT]	φ_i [°]
120	117.4	172.7
66	304.7	-65.8
50	228.3	0.6
40	98.4	70.4
30	14.3	126.4
22	13.6	128.8
18.6	12.8	175.9
13	7.0	155.5
	m_o = 16.98	

Table 2. Niemegk, X, 1890-1985.

T_i [yr]	T_i [yr]	T_i [yr]	T_i [yr]
		120	120
64	64	64	66
			50
	42	42	40
	32	32	30
			22
			18.6
10	10	10	13
3.8	3.8	3.8	
2.8	2.8	2.8	
m_o = 62.6	m_o = 43.7	m_o = 18.9	m_o = 16.98

Table 3. Niemegk, X, 1890-1985.

T_i [yr]	A_i [nT]	H_j	T_i	A_i [nT]	H_j
130	75.5	47.0	130	160.3	47.0
			80	314.2	25.7
64	229.2	46.6	64	138.1	13.9
50	97.0	10.3			
35	23.5	46.2	35	27.4	28.2
24	10.0	46.5	24	11.7	46.0
18.6	8.0	47.1	18.6	8.8	46.0
13	6.2	47.0	13	6.5	46.5
8.8	1.0	47.3	8.8	1.6	46.6
m_o = 16.94			m_o = 16.94		

Table 4. Niemegk X 1890-1989, range 450.5 nT

T_i	A_i	H_j	T_i	A_i	H_j	T_i	A_i	H_j
140	74.1	50.6	138	74.8	49.9	138	62.2	49.9
65	166.4	50.8	66	162.9	49.6	66	173.3	49.6
						40	50.1	49.9
			32	21.4	49.1	29	15.6	48.8
24	19.7	50.2	24	19.5	50.0	23	7.9	47.3
						18.6	8.5	48.8
11	7.7	50.5	13	7.4	49.8	13	6.2	48.7
						8.8	0.7	49.6
						5.6	0.1	49.7
m_o = 42.36			m_o = 36.80			m_o = 17.04		

Table 5. Chambon-la-Foret X 1883-1986, range 316.9 nT

T_i	A_i	H_j	T_i	A_i	H_j
142	55.7	51.3	142	52.9	51.3
67	119.4	53.1	67	120.3	53.1
			41	37.8	52.7
			29	7.0	52.8
23	6.9	52.2	23	6.2	52.1
			18.6	5.6	52.4
12	5.2	52.5	12	4.5	52.4
			8.8	1.7	51.7
			3.6	0.5	52.2
	$m_o = 31.15$			$m_o = 13.70$	

Table 6. Optimized models (cp. Eq. 1) for X component.

	T_i [yr]									m_o [nT]
Oslo	127	82	52	30	23	16.6	11	7.9		22.81
Niemegk	138	66	40	29	23	18.6	13	8.8	5.6	17.04
Hartland	129	69	45	34	22	18.6	13	8.8	6.0	20.85
Chambon/ la-Foret	142	67	41	29	23	18.6	12	8.8	3.6	13.70
Choimbra	120	68	45	33	24	18.6	13	8.8	4.6	30.35
Tangerang/ Batavia	104	64	40	30	24	18.6	12	8.8	5.6	45.43
Alibag	122	67	43	33	22	18.6	13	8.8	5.6	102.47

*U.S. GOVERNMENT PRINTING OFFICE: 1992-627-150/60001

REPORT DOCUMENTATION PAGE

Form Approved
OMB No. 0704-0188

1. AGENCY USE ONLY *(Leave blank)*	2. REPORT DATE	3. REPORT TYPE AND DATES COVERED
	June 1992	Conference Publication

4. TITLE AND SUBTITLE
Types and Characteristics of Data for Geomagnetic Field Modeling

5. FUNDING NUMBERS

6. AUTHOR(S)

R.A. Langel and R.T. Baldwin, Editors

7. PERFORMING ORGANIZATION NAME(S) AND ADDRESS(ES)

NASA-Goddard Space Flight Center
Greenbelt, Maryland 20771

8. PERFORMING ORGANIZATION REPORT NUMBER

92B00061; Code 921

9. SPONSORING/MONITORING AGENCY NAME(S) AND ADDRESS(ES)

National Aeronautics and Space Administration
Washington, D.C. 20546-0001

10. SPONSORING/MONITORING AGENCY REPORT NUMBER

NASA CP-3153

11. SUPPLEMENTARY NOTES

R.A. Langel, Laboratory for Terrestrial Physics, NASA GSFC, Greenbelt, Maryland, 20771.
R.T. Baldwin, Hughes STX Corporation, Lanham, Maryland, 20706.

12a. DISTRIBUTION/AVAILABILITY STATEMENT

Unclassified - Unlimited
Subject Category 39

12b. DISTRIBUTION CODE

13. ABSTRACT *(Maximum 200 words)*

This publication contains material presented at a symposium convened on Friday, August 23, 1991, at the General Assembly of the International Union of Geodesy and Geophysics (IUGG) held in Vienna, Austria.

Models of the geomagnetic field are only as good as the data upon which they are based, and depend upon correct understanding of data characteristics such as accuracy, correlations, systematic errors and general statistical properties. This symposium was intended to expose and illuminate these data characteristics. Papers were included which discussed the properties and availability of the various kinds of data.

14. SUBJECT TERMS

Geomagnetic Field, Earth, Terrestrial Magnetism, Modeling, Data Reduction

15. NUMBER OF PAGES
360

16. PRICE CODE
A16

17. SECURITY CLASSIFICATION OF REPORT	18. SECURITY CLASSIFICATION OF THIS PAGE	19. SECURITY CLASSIFICATION OF ABSTRACT	20. LIMITATION OF ABSTRACT
Unclassified	Unclassified	Unclassified	Unlimited

National Aeronautics and
Space Administration
Code JTT
Washington, D.C.
20546-0001

Official Business

Penalty for Private Use, $300

NASA

POSTMASTER: If Undeliverable (Section 158 Postal Manual) Do Not Return